

University of Strathclyde
Department of Pure and Applied Chemistry

Increasing the Saturation of BET Inhibitors

Joseph Edward Dixon

Doctor of Philosophy

2018



This thesis is the result of the author's original research. It has been composed by the author and has not been previously submitted for examination which has led to the award of a degree.

The copyright of this thesis belongs to GSK in accordance with the author's contract of engagement with GSK under the terms of the United Kingdom Copyright Acts. Due acknowledgement must always be made of the use of any material contained in, or derived from, this thesis.

Signed:

Date:

Abstract

Bromodomains are epigenetic reader modules that are found as part of multidomain proteins. They recognise acetylated lysine residues on histone tails in order to regulate gene expression. Bromodomain and extra-terminal domain (BET) proteins are a family of bromodomain-containing proteins that consist of BRD2, BRD3, BRD4 and BRDT. Each of these contains the tandem bromodomain modules, BD1 and BD2. BET proteins are an interesting target for drug discovery that has emerged in recent years, with numerous pan-BET inhibitors being reported to have anti-inflammatory and anti-proliferative properties.

A chemoinformatic analysis has demonstrated that, compared to approved drugs, reported BET inhibitors had relatively low three-dimensional character.¹ In other words, they are highly unsaturated, flat molecules. The relevance of this is explained in the “Escape from Flatland” papers, wherein empirical analysis demonstrated that drug candidates with a higher degree of saturation are likely to be less promiscuous, more soluble and overall be more likely to succeed to market.^{2,3}

This research set out to develop a series of pan-BET inhibitors with an increased degree of saturation to those existing in the literature. The approach taken involved replacing a phenyl ring in a well-established inhibitor fragment with a saturated analogue, and exploring the vectors produced. During this process a molecule was discovered that had unexpected selectivity for the BD2 domain of BRD4 over the BD1 domain.

There are very few published examples of BD2-selective BET inhibitors, and as a result there is limited understanding of how the biological roles of BD2 domains differ from their BD1 counterparts. Therefore, the direction of this project was altered in order to try and understand the source of this observed selectivity, and rationally improve upon it. Target compounds were designed to probe which amino acid residue differences were responsible for the selectivity, and from this a hypothesis was generated. The end result was a lead compound with three stereocentres around a piperidine framework, sub-micromolar potency, and over twice the level of BD2-selectivity at BRD4 of any compounds reported to date. This compound, and the approach taken to discover it, represents an important contribution to the art and provides a basis for further investigations in this scientific field.

Acknowledgements

First and foremost, I would like to thank my industrial supervisor, Chris Wellaway. For Chris, the word “supervisor” doesn’t quite cut it; “mentor” gets a bit closer; and “therapist” isn’t far from the truth. His guidance has been invaluable over the past three years, and our conversations have frequently left me feeling calmer and more focussed when I didn’t even realise I was stressed. He has helped me develop my practical chemistry skills, but more importantly, he has helped me develop confidence in those skills, and confidence in the work I have produced, to the extent where I will now proudly profess to be an “alright chemist”. I’m endlessly grateful for the hours he has spent poring over my reports, and his meticulous proofreading skills have made me come across as a far more accurate writer than I should truly have taken credit for.

I would also like to thank my academic supervisor, Allan Watson, whose advice and input along the way has helped sculpt this document into something I will admit to being very proud of. The encouragement that both Allan and Chris have offered me in relation to my reports has been instrumental in helping me realise how much I enjoy the writing process, and making the difficult decision to leave the lab behind me and pursue this interest further.

Next, I would like to thank Harry Kelly and Billy Kerr for their work setting up this programme, and their continued support throughout. I would also like to thank Andrea Malley and the other administrative staff at GSK and Strathclyde for everything they do to keep things running smoothly. Harry needs to get an additional thank you for running the Residential Chemistry Training Experience, which I attended back in 2013, and without which I may not have had the same eagerness to apply for this programme.

The collective knowledge housed within GSK is astonishing, and I’d like to thank everyone I’ve worked alongside for their contribution, conversation, and company: Vipul Patel and everyone who was in the FDU while I worked there; Diane Coe and the AI DPU where I have been for the past two years; and our neighbours in the rest of the SmartLab, who have made it such a pleasant place to work. Special thanks need to go to anyone who has shared a fume hood with me, notably Rishi Shah, Craig Robertson and Sam Holman. They have borne the brunt of my incessant talking, and have helped me work through problems in my work, as well as key career decisions. Also, to Jonny Spencer, Rob Griffiths and Matt Gray, who have listened to me witter on about a whole range of other nonsense every lunch time.

Outside of my lab, I'd like to thank everyone who has contributed to this work with assays, purification, physchem analysis, crystallography, and presumably many other tasks which I have been too privileged a chemist to think of here. Special thanks need to go to Katherine Wheelhouse, who has gone out of her way to help with my chemistry, and is always good to catch up with on the train. Also, to Richard Horan, who has continually attended our PhD meetings and pushed us to be better. He also interviewed me for a GSK summer placement while I was an undergraduate, which I didn't get, and that experience gave me the kick I needed to actually prepare for my PhD interview the following year. I would also like to thank the rest of my fellow PhD students, past and present, for the sense of camaraderie that has been a comfort throughout this process.

I would like to thank my parents, who have helped keep me grounded throughout my studies, and have an ability to completely deplete me of stress when I see them. Without their encouragement and constant belief in me I would never have made it to this stage. My friends have been vital for keeping me from going too crazy. They have generally been accepting when I've decided I'm too busy to see them, and at other times have helped take my mind off work with the aid of kayaks, bikes, board games, and gin. A special mention needs to go to my housemate, Sophie Mitchell, who I can thank for a good portion of my sanity. I don't underestimate how important it has been to come home to someone who understands what I've been doing. We've been able to share our individual PhD successes, and commiserate in each other's problems. Ignoring the short period where she nearly succeeded in turning me into an alcoholic, I will greatly miss us living together after we have each graduated.

Finally, and with a level of sincerity with which I even surprise myself, I would like to thank John Scalzi, Orson Scott Card, Joe Haldeman, Cassandra Clare, Dan Simmons, Douglas Adams, and Isaac Asimov. These are the authors who have aided in the important task of turning my brain off from chemistry. At the end of every day I have been very grateful for the escapism they have provided, and they have done their very best to stop me dreaming about isoxazoles!

Contents

Declaration.....	i
Abstract.....	ii
Acknowledgements.....	iii
Contents.....	v
Abbreviations.....	vii
1. Epigenetics.....	1
2. BET Proteins.....	9
2.1 Role in Disease.....	10
2.2 Existing BET Inhibitors.....	12
2.3 Determining the Roles of Individual BET Bromodomains.....	15
2.4 Features of the BET Binding Site.....	18
3. Saturation.....	21
3.1 Saturation of BET Inhibitors.....	21
3.2 Saturation of Drug Molecules.....	22
4. Aim and Objectives.....	25
5. Substituted Isoxazole Synthesis.....	30
6. Results and Discussion.....	38
6.1 Disconnections.....	38
6.1.1 Cross-Coupling Reactions.....	38
6.1.2 Saturated Ring Formation.....	41
6.1.3 Isoxazole Formation.....	42
6.2 Core Fragment Synthesis.....	48
6.2.1 Five-Membered Rings.....	48
6.2.2 Six-Membered Rings.....	50
6.2.3 Seven-Membered Rings.....	53
6.3 Prioritisation of Core.....	56
6.4 Extension to the WPF Shelf.....	60
6.5 Exploration of the ZA Channel.....	72
6.5.1 Synthesis of Amides.....	75
6.6 Alternative Linkers.....	81
6.6.1 Synthesis of Hydroxymethylene Linked Compound.....	81
6.6.2 Synthesis of Amine and Ether Linked Compounds.....	82
6.6.3 Evaluation of Linkers.....	84

6.6.4	Confirming the Effect of Saturation on BD2 Selectivity.....	88
6.7	Mechanisms behind BD2 Selectivity.....	91
6.8	Explorations to Improve BD2-Selectivity	97
6.8.1	Reinvestigation of Linker Length.....	97
6.8.2	Shelf-Binding Group Investigation.....	100
6.9	Disubstituted Piperidines.....	108
6.9.1	3,5-Disubstitution	110
6.9.2	2,3-Disubstitution	118
6.9.3	Further Data	128
6.10	Trisubstituted Piperidine	130
6.10.1	Reductive Amination.....	133
6.10.2	Acylation	139
6.10.3	Reduction.....	142
6.10.4	Final Steps and Epimerisation	148
6.10.5	Final Data.....	152
7.	Conclusion	158
8.	Future Work.....	163
9.	Experimental	166
9.1	General Information.....	166
9.2	Synthetic Procedures and Compound Characterisation.....	169
9.3	Supplementary Protocols	254
10.	References.....	258

Abbreviations

Å	Ångstroms
Ac	Acetyl
AcOH	Acetic Acid
Ala/A	Alanine
AMP	Artificial Membrane Permeability
AP	Aromatic Proportion
Arg/R	Arginine
Asn/N	Asparagine
Asp/D	Aspartate
ATP	Adenosine Triphosphate
BCP	Bromodomain-containing Protein
BD	Bromodomain
BET	Bromodomain and Extra-terminal Domain
BPTF	Bromodomain PHD Finger Transcription Factor
Boc	<i>tert</i> -Butyloxycarbonyl
bp	Base Pair(s)
Bu	Butyl
^t Bu	<i>tert</i> -Butyl
C	Celsius
CAN	Cerium Ammonium Nitrate
cAMP	Cyclic Adenosine Monophosphate
Cbz	Carboxybenzyl
chromLogD _{pH7.4}	Chromatographic LogD at pH 7.4
CLND	Chemiluminescent Nitrogen Detection
CoA	Coenzyme A
CBP	CREB-Binding Protein (also see CREBBP)
conc.	Concentrated
CREB	cAMP Response-Element Binding Protein
CREBBP	CREB-Binding Protein (also see CBP)
CTD	C-Terminal Domain
CYP	Cytochrome P450
CYPinh	Cytochrome P450 Inhibition
Cys/C	Cysteine

dba	Dibenzylideneacetone
DBU	1,8-Diazabicycloundec-7-ene
DCM	Dichloromethane
DIPEA	<i>N,N</i> -Diisopropylethylamine
DMA	<i>N,N</i> -Dimethylacetamide
DMAP	4-Dimethylaminopyridine
DMF	<i>N,N</i> -Dimethylformamide
DMSO	Dimethyl Sulfoxide
DNA	Deoxyribonucleic Acid
DNMT	DNA Methyltransferase
dtbpf	1,1'-Bis(di- <i>tert</i> -butylphosphino)ferrocene
ET	Extra-terminal
Et	Ethyl
eq.	Equivalents
FaSSIF	Fasted State Simulated Intestinal Fluid
Fchiral	Fraction chiral
Fsp ³	Fraction sp ³
g	Grams
Gln/Q	Glutamine
Glu/E	Glutamate
Gly/G	Glycine
GRAS	Generally Regarded as Safe
h	Hours
HAC	Heavy Atom Count
HAT	Histone Acetyltransferase
HDAC	Histone Deacetylase
HFIP	Hexafluoroisopropanol
His/H	Histidine
HPLC	High Performance Liquid Chromatography
HRMS	High Resolution Mass Spectrometry
Hz	Hertz
Ile/I	Isoleucine
Imp	Impurity
IPA	Isopropanol
IR	Infrared
ITC	Isothermal Titration Calorimetry

KAc	Acetyl-lysine
LCMS	Liquid Chromatography Mass Spectrometry
LDA	Lithium Diisopropylamide
LE	Ligand Efficiency
Leu/L	Leucine
LLE	Lipophilic Ligand Efficiency
LLE _{AT}	LLE adjusted for Heavy Atom Count
LiHMDS	Lithium Bis(trimethylsilyl)amide
LPS	Lipoprotein Polysaccharide
Lys/K	Lysine
M	Molar
MCP1	Monocyte Chemoattractant Protein 1
MDAP	Mass Directed Auto Preparation
Me	Methyl
MeCN	Acetonitrile
Met/M	Methionine
MeOH	Methanol
MHz	Megahertz
min	Minutes
mg	Milligram
mL	Millilitres
mM	Millimolar
mmol	Millimoles
MOE	Molecular Operating Environment
mol	Moles
Ms	Mesyl
MW	Molecular Weight
NaHMDS	Sodium Bis(trimethylsilyl)amide
NBS	<i>N</i> -Bromosuccinimide
nm	Nanometres
nM	Nanomolar
NMC	NUT Midline Carcinoma
NMR	Nuclear Magnetic Resonance
NURF	Nucleosome Remodelling Factor
NUT	Nuclear Protein in Testis
PBMC	Peripheral Blood Mononuclear Cells

P	Product
PCAF	p300/CBP-Associated Factor
PEPPSI	Pyridine-Enhanced Precatalyst Preparation Stabilisation and Initiation
PFI	Property Forecast Index
Ph	Phenyl
Phe/F	Phenylalanine
Pic-BH ₃	α-Picoline Borane
PMHS	Polymethylhydrosiloxane
ⁱ Pr	Isopropyl
Pro/P	Proline
pTEFb	Positive Transcription Elongation Factor b
PTM	Post-translational Modification
RNA	Ribonucleic Acid
RT	Room Temperature
s	Seconds
SAR	Structure Activity Relationship
Ser/S	Serine
SM	Starting Material
TBD	1,5,7-Triazabicyclo[4.4.0]dec-5-ene
TEG	Triethylene Glycol
TFA	Trifluoroacetic Acid
TFIID	Transcription Factor II D
THF	Tetrahydrofuran
Thr/T	Threonine
TLC	Thin-layer Chromatography
TMS	Tetramethylsilane
Trp/W	Tryptophan
Ts	Tosyl
Tyr/Y	Tyrosine
UV	Ultraviolet
Val/V	Valine
v/v	Volume/Volume
μg	Microgram
μL	Microlitre
μM	Micromolar
μmol	Micromoles

“Either this is madness or it is Hell.”

“It is neither,” calmly replied the voice of the Sphere,

“it is Knowledge; it is Three Dimensions”

— Flatland: A Romance in Many Dimensions

1. Epigenetics

Within eukaryotic cells genomic Deoxyribonucleic Acid (DNA) is hierarchically packaged by histone proteins into chromatin.^{4,5} The term chromatin was coined by the pioneer of mitosis research, Walther Flemming, in 1882, literally meaning ‘stainable material’.⁶ Chromatin is built of repeating units called nucleosomes. These consist of two copies each of the histone proteins H2A, H2B, H3 and H4, assembled into octamers with 145–147 base pairs (bp) of DNA wrapped around to form the nucleosome core.⁷ Histones are highly basic due to around a fifth of their sequence being composed of either arginine or lysine residues.⁸ This means that at physiological pH they carry a positive charge which interacts strongly with the negatively charged DNA. Extended, a 146-bp stretch of DNA would be approximately 500 Å long, while a nucleosome is approximately 100 Å across, decreasing the length by a factor of 5.^{5,9} Under an electron microscope, extended chromatin has the appearance of beads on a string (Figure 1).¹⁰

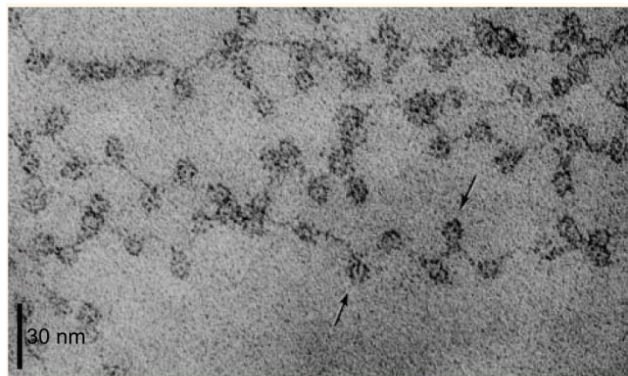


Figure 1. Electron micrograph image of chromatin at low ionic-strength, which results in an extended conformation. Arrows mark individual nucleosomes, which appear as ‘beads on a string’. Image reproduced with permission from Macmillan Publishers Ltd.¹⁰

The repeating nucleosome units further assemble, with the aid of linker histone proteins H1 and H5 into chromatin fibres, approximately 300 Å in diameter. There is still debate over the structure of these fibres, with two helical models proposed, based on a solenoid or a zig-zag form, each with around six nucleosomes per turn.⁵ These chromatin fibres can become further compacted and the extreme of this occurs during metaphase of mitosis when DNA is compacted by a factor of 10^4 and forms the classical four arm structure that is visible under a light microscope, consisting of a pair of sister chromatids (Figure 2).¹¹ Sister chromatids are identical copies of a chromosome, replicated before mitosis starts and held together by a centromere. The chromatids get pulled apart during anaphase and end up in separate daughter cells.¹²

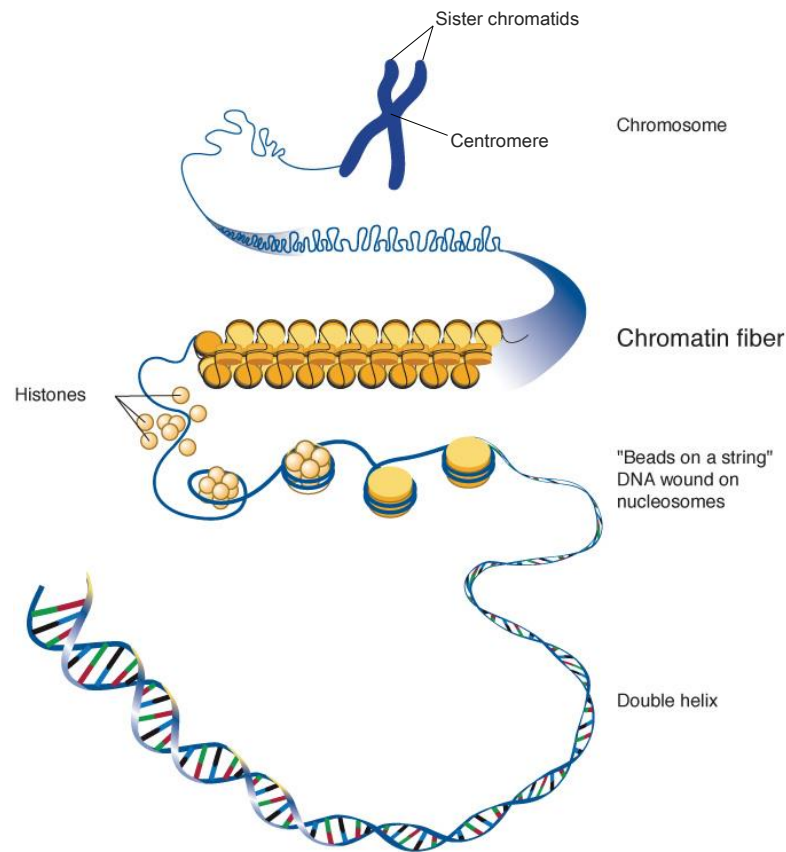


Figure 2. The packaging of DNA into chromatin.
Image courtesy of the National Human Genome Research Institute.¹³

While every cell in the human body contains the full complement of DNA, and all the information held within its sequence, different cell types express a different range of genes. Whether or not a gene is expressed is, in part, determined by how well-packed that section of DNA is.^{14,15} Put simply, if a gene is tightly packaged (heterochromatin) then transcription factors cannot bind to it and transcription is silenced. But if a gene is loosely packaged (euchromatin) then the transcription machinery can be recruited. Chromatin can be remodelled between these states to change the transcriptome of the cell in response to environmental cues.^{16,17} We say that each cell is genetically identical, but epigenetically different.

The term epigenetics (meaning 'above genetics') refers to the heritable changes in gene expression or phenotype that are stable between cell divisions, and sometimes between generations, but do not involve changes in the underlying DNA sequence.¹⁸ These heritable changes take the form of covalent modifications of both DNA itself and the histone proteins.¹⁹ The combination of all the modifications is known as the epigenome.

Modifications of DNA include methylation and hydroxymethylation of the 5' position of cytosine, which does not affect the hydrogen bonding of cytosine with guanine and hence

the DNA sequence is unaffected (Figure 3).^{20,21} DNA methylation is commonly associated with transcriptional repression. This can either be mediated by a direct interference with the binding of transcription factors or, more importantly, by recruiting methyl DNA-binding proteins and repressive complexes.²²

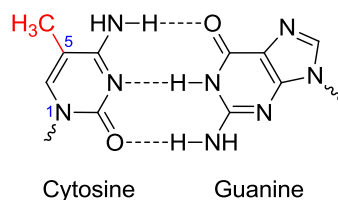


Figure 3. Methylation at the 5-position of cytosine (red) does not affect the hydrogen bonding pattern (dotted lines) with guanine. Wavy lines represent bonds to the deoxyribose moiety of the nucleotide.

The histone proteins that form nucleosomes have amino-terminal tails that extend from the core globular structure.⁷ Post-translational modifications (PTMs) of these tails, particularly at lysine and arginine residues, play a major role in the regulation of gene expression. Histone PTMs include phosphorylation and ubiquitylation, but the most abundant and most widely studied are acetylation and methylation.^{18,23}

There are several protein families involved in regulating the epigenome.¹⁸ These are broadly categorised as ‘writers’, which add PTMs, ‘readers’, which interact with the PTMs, and ‘erasers’, which remove the modifying groups (Figure 4). These protein families are summarised in Table 1.

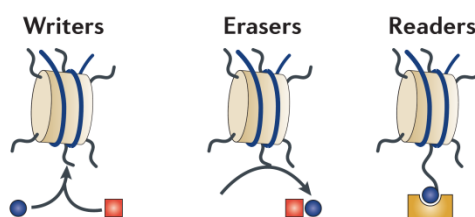


Figure 4. Post-translational modification of histone tails.
Image reproduced with permission from Macmillan Publishers Ltd.¹⁸

Family	Activity	Number of domains
<i>Writers</i>		
Histone acetyltransferases	K → K- Ac	18
Protein methyltransferases	K → K- Me R → R- Me	60
<i>Erasers</i>		
Histone deacetylases	K- Ac → K	17
Lysine demethylases	K- Me → K	25
<i>Readers</i>		
Bromodomain-containing proteins	K- Ac	61
Methyl-lysine- and/or methyl-arginine-binding domain-containing proteins (such as Tudor domains, MBT domains, chromodomains and PWWP domains)	K- Me R- Me	95
PHD-containing proteins	K- Ac K- Me R- Me K	104

Table 1. Summary of the major protein families that regulate the epigenome, including proteins that deposit PTMs (writers), remove PTMs (erasers) or bind to PTMs (readers). The PTMs involved are either acetyl groups (red) or methyl groups (blue) on lysine (K) or arginine (R) side chains. The number of separate examples of each domain found in the human genome is given. Abbreviations: MBT, malignant brain tumour; PWWP, Pro-Trp-Trp-Pro; PHD, plant homeodomain.¹⁸

Histone acetylation on lysine residues can activate transcription through a combination of three mechanisms.⁴ Firstly, lysine bears a positively charged ammonium group at physiological pH, while the acetylation of lysine forms an uncharged amide (Figure 5). This reduces the affinity of the histone tail for the negatively charged DNA and results in a loosening of the complex.^{4,24}

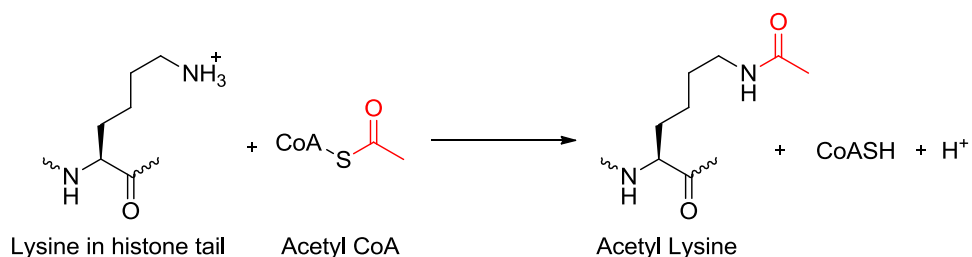


Figure 5. Addition of an acetyl group (red) to a lysine residue using acetyl coenzyme A (CoA), as catalysed by histone acetyltransferases (HATs).

Acetyl-lysine (KAc) groups can interact with a domain present in many proteins that regulate eukaryotic transcription, called a bromodomain, and these proteins are responsible for the other two mechanisms.²⁵

Firstly, bromodomains have been shown to be necessary for the binding of certain transcription factors to DNA, thus aiding in the recruitment of the transcription machinery to particular genes.²⁶ For example, it has been shown that the recruitment of Transcription Factor II D (TFIID), to the promoter of the human Interferon- β gene relies upon its double bromodomain-containing subunit, Transcription Initiation Factor TFIID subunit 1, to be bound to histone H3.²⁷

Secondly, bromodomain-containing proteins (BCPs) are found as part of chromatin remodelling complexes. These complexes use Adenosine Triphosphate (ATP) hydrolysis to provide energy to shift the position of nucleosomes along DNA, potentially exposing binding sites for other protein factors.²⁶ For example, Bromodomain PHD Finger Transcription Factor (BPTF) is one of the components of Nucleosome Remodelling Factor (NURF), and is necessary for anchoring the complex to DNA *via* KAc recognition sites.²⁸

Somewhat confusingly, bromodomains do not contain, nor do they interact with, bromine. Instead they are named after the *brahma* gene from *Drosophila melanogaster*.²⁹ The rationale behind naming the *Drosophila* gene after the Hindu god of creation was not explicitly stated by Kennison and Tamkun when they identified it in 1988.³⁰ However, it was discovered as part of a screen for genes that were involved in the determination of segmental identity, and they named all the genetic loci they found along the general theme of fate. Other genes in the set include *devenir* (French for “to become”), *kismet* (a Turkish term for destiny) and *verthandi* (one of the Norns of Norse mythology, who rule the fates of men).

Bromodomains are small domains consisting of ~110 amino acids. The human genome contains 61 bromodomains, in 42 different proteins.¹⁸ This means that there are some proteins that contain more than one bromodomain, and an extreme case of this is human polybromo1, which contains six.³¹ These domains are evolutionarily and structurally conserved and share a common fold consisting of four antiparallel α -helices (α Z- α A- α B- α C) arranged in a left-handed twist. The linkers between the helices are known as the ZA, AB and BC loops (Figure 6).

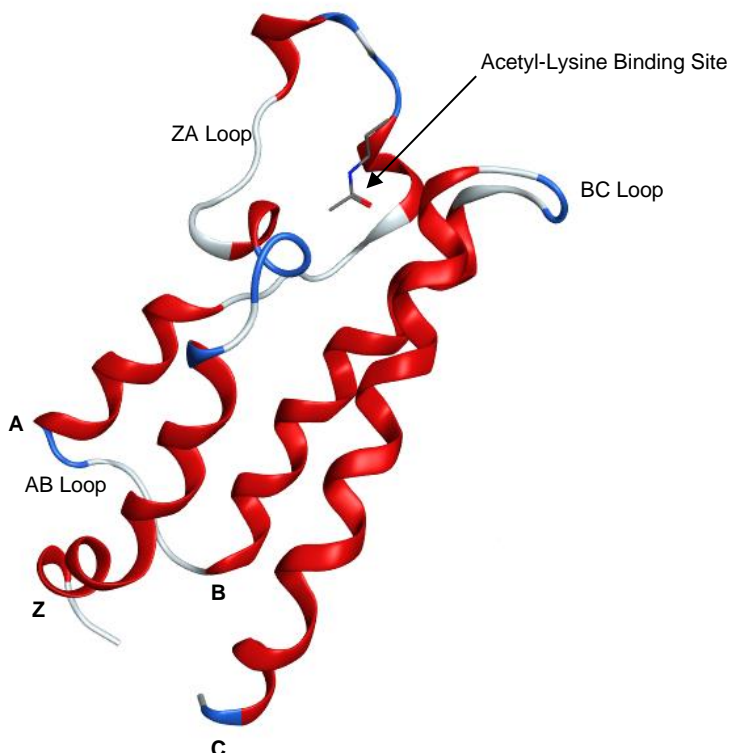


Figure 6. Structure of the bromodomain of CREBBP* bound to an acetylated amine (PDB: 3P1C).³²
*CREBBP, CREB-binding protein; CREB, cAMP response element binding; cAMP, cyclic adenosine monophosphate.

The KAc binding site lies at one end of the four-helix bundle and is flanked by the ZA and BC loops, which are responsible for the affinity and specificity for the target peptide. At the bottom of the binding pocket are located conserved arginine and tyrosine residues which form key interactions with acetylated lysine residues (Figure 7).

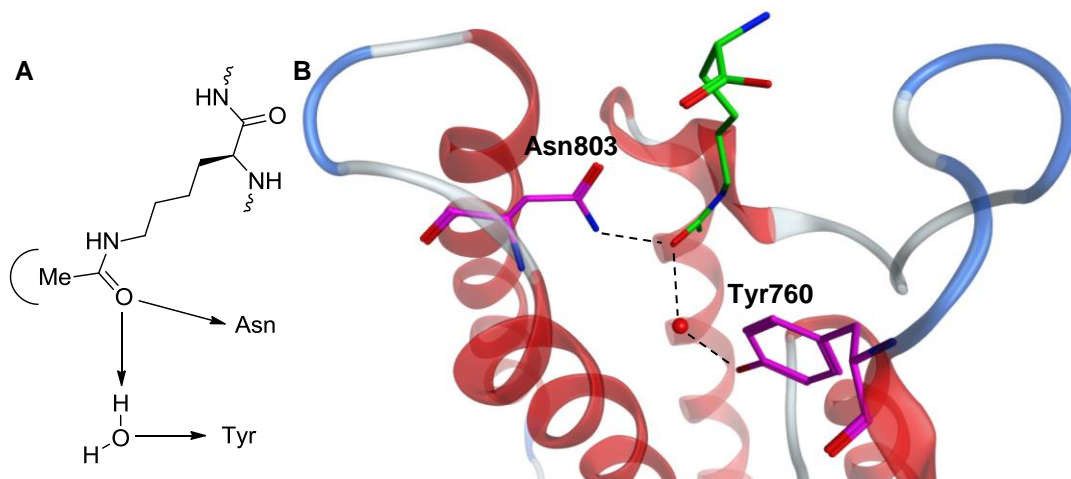


Figure 7. A) Schematic of the interactions formed by acetylated lysine residues in a bromodomain binding site.³³ The arrows represent hydrogen bonds to a conserved asparagine residue, and a tyrosine residue, *via* a bridging water molecule. The curved line indicates a lipophilic pocket. B) X-ray crystal structure of acetyl lysine (green) bound to the bromodomain of PCAF* (PDB: 5FE0). Tyr760 and Asn803 are shown in bold (magenta). Dashed lines are shown, representing the hydrogen bonds from the ligand to Asn803 and *via* the bridging water molecule (red) to Tyr760. All other residues and water molecules have been removed for clarity. *PCAF, p300/CBP-associated factor; CBP, CREB-binding protein; p300, histone acetyltransferase p300.

The oxygen of the acetyl carbonyl forms two hydrogen bonding interactions: one directly with the conserved asparagine residue, and another *via* a bridging water molecule with the conserved tyrosine residue. The methyl group occupies an adjacent lipophilic pocket.³³ While other features of the binding site may vary, these key interactions are common to all bromodomains.

Bromodomains are an interesting new target for drug discovery that has received a lot of attention in recent years. Human genetic data implicates BCPs in a broad range of disease areas,³⁴ and there are existing precedents for successfully drugging the epigenome. There are four drugs currently on the market that seek to rebalance an aberrant lysine acetylation profile: Vorinostat, Romidepsin, Belinostat and Panobinostat.³⁵⁻³⁷ All of these are inhibitors of histone deacetylases (HDACs) and are used to treat either T-cell lymphoma or multiple myeloma. They demonstrate the viability of modifying disease by interacting with cellular acetylation signals.³⁸

As bromodomains are mediators of protein-protein interactions, they were initially perceived to be poorly tractable to small-molecule intervention, unlike the enzymatic epigenetic proteins.³³ However, the interfaces provided by bromodomains are not flat and featureless, but have a pocket for acetyl-lysine binding that can accommodate small molecules.

Currently, the majority of research has focussed on a family of BCPs known as the BET (bromodomain and extra-terminal domain) proteins due to the well-established links with disease.³⁹

2. BET Proteins

BET proteins are a family of BCPs, consisting of BRD2, BRD3, BRD4 and BRDT. Each protein contains two bromodomains, BD1 and BD2 (sometimes referred to as *N*-terminal and *C*-terminal bromodomains, respectively).^{40,41} The bromodomains of the BET family are highly evolutionarily conserved (Figure 8). BET proteins also contain an extra-terminal domain (ET) which functions as a protein-protein interaction module for recruiting effectors to regulate transcriptional activity.⁴² As well as these, BRD4 and BRDT also contain *C*-terminal domains (CTDs), which are not present in the other BET proteins. In BRD4, this has been shown to recruit positive transcription elongation factor b (pTEFb), thereby stimulating the transcription of primary response genes.⁴²

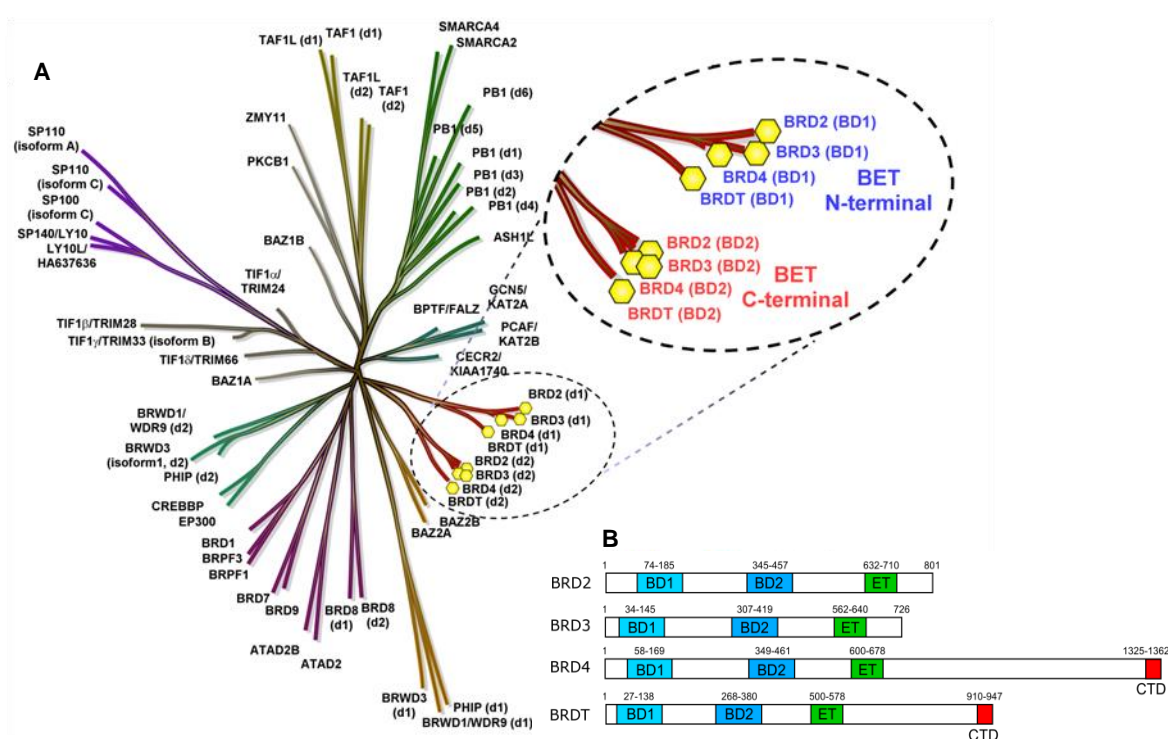


Figure 8. A) Phylogenetic tree of human bromodomains based on sequence alignments; the BET bromodomains are highlighted.⁴³ Image courtesy of Paul Bamborough. B) The positions of the domains within the BET protein sequences. Image reproduced with permission from Elsevier.⁴⁴

BET proteins have been shown to be vital for key aspects of cell cycle control, with early studies demonstrating the involvement of BRD4 in the onset of mitosis.⁴⁵ Their clear importance in the normal cell cycle has made it difficult to elucidate their precise roles through standard genetic deletion experiments: knockouts of *BRD2* and *BRD4* are lethal in multiple species, and mice with only one functioning *BRD4* allele have severe defects in differentiation and organogenesis.⁴⁶ While it is believed that the BET proteins may have similar roles and some functional redundancy between them, this redundancy is

clearly not sufficient to allow for the complete absence of one family member.⁴⁷ BET proteins have been implicated in various disease areas and it is the biology of these states that has been more widely studied, some examples of which will now be presented.

2.1 Role in Disease

Oncology

Irregular activity of BET proteins has been associated with a number of cancers.⁴⁰ A recurrent chromosomal translocation from chromosome 15 to chromosome 19 results in the fusion of BRD4 with the nuclear protein in testis (NUT) gene (Figure 9) and gives rise to the severe and aggressive cancer NUT midline carcinoma (NMC), which can manifest in any organ or tissue type.^{41,48} RNA-silencing of the BRD4-NUT chimaera arrests the cell cycle and prompts differentiation of the cells, suggesting that a BRD4 inhibitor would be beneficial in NMC.

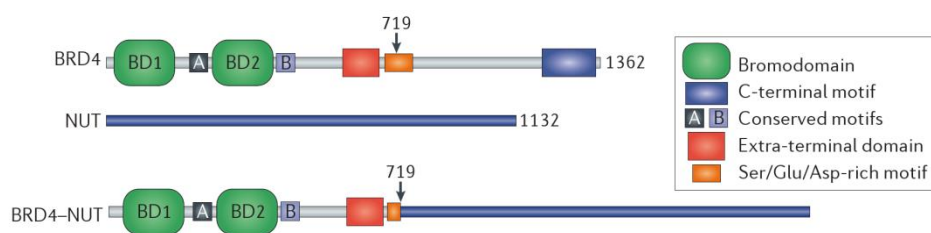


Figure 9. A single chromosomal translocation whereby the majority of the NUT protein is fused to the bromodomain-containing end of BRD4. The arrow indicates the breakpoint in BRD4 where the fusion occurs. This is observed in many cases of NMC. *Image reproduced with permission from Macmillan Publishers Ltd.*²⁹

Overexpression of BRDT is often seen in non-small-cell lung cancer, among other cancers, but the functional consequences of this are not understood.^{49,50} BRD4 has been identified in breast cancer as an inherited susceptibility gene for disease progression and its expression levels have been associated with patient survival.⁵¹

BRD4 and BRD2, unlike non-BET bromodomain proteins, remain bound to chromatin during mitosis and it is thought that this property is important for the maintenance of epigenetic memory.⁴⁶ This provides an opportunity for the transmission of tumour-causing viruses during cell division, by providing an anchor that allows the viral episome (closed circular DNA molecule) to attach to the host's chromatin.⁴⁰ An example of this is Kaposi's sarcoma, which is a tumour caused by infection with human herpes virus 8.⁵² During the latent viral infection stage, transmission of viral genomes to daughter cells in mitosis is mediated by latency-associated nuclear antigen 1, which associates with BRD4

in order to become tethered to chromatin. Papilloma viruses, linked to cervical cancers, and Epstein-Barr viruses also associate with BRD4 for similar purposes.^{53,54}

Inflammation

BET proteins have been associated with inflammation in a number of cases. Studies to investigate individuals who are metabolically healthy but obese, have shown that these people also have a favourable inflammation profile.⁵⁵ A mouse model has been developed that appears to mimic this state by whole-body disruption of *Brd2*.⁵⁶ The mice became severely obese on a normal diet, but also displayed ablated inflammatory responses, suggesting that BRD2 is involved in inflammatory signal transduction. Furthermore, single-nucleotide polymorphisms at three sites in human *BRD2* have been linked to rheumatoid arthritis.⁵⁷

Male Fertility

While BRD2, 3 and 4 are ubiquitously expressed, BRDT is only found in the testes and ovaries.⁵⁸ While all of the BET family are expressed at unique times during spermatogenesis, BRDT is particularly important.⁵⁹ Studies have found links between single-nucleotide polymorphisms in human BRDT BD1 and male infertility, with complete knockout resulting in incomplete sperm elongation and severe morphological defects.^{59,60}

The development of small-molecule BET inhibitors has led to further discoveries about the role these proteins play in disease states.

2.2 Existing BET Inhibitors

In December 2010, two papers were published which pioneered the inhibition of bromodomains as a new method for treating human disease.^{41,61} Both reported structurally related molecules, JQ1 **1** from groups in Oxford and Harvard⁴¹ and I-BET762 **2** from GSK and Rockefeller University (Figure 10).⁶¹ These molecules were shown to inhibit both bromodomains of all four BET proteins.

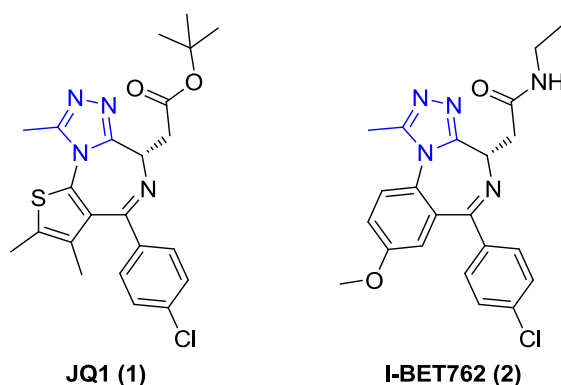


Figure 10. Structures of JQ1 **1** and I-BET762 **2**. The KAc mimetics are highlighted in blue.

In recent years, a number of BET inhibitors have been published in the literature, including several from GSK laboratories (Figure 11). These compounds generally possess a moiety that acts as an acetyl-lysine mimetic by forming the same hydrogen bonds as the natural ligand, and placing a lipophilic group into the methyl pocket. The KAc mimetic is sometimes referred to as the warhead, and in Figure 11 these moieties have been highlighted.⁶²

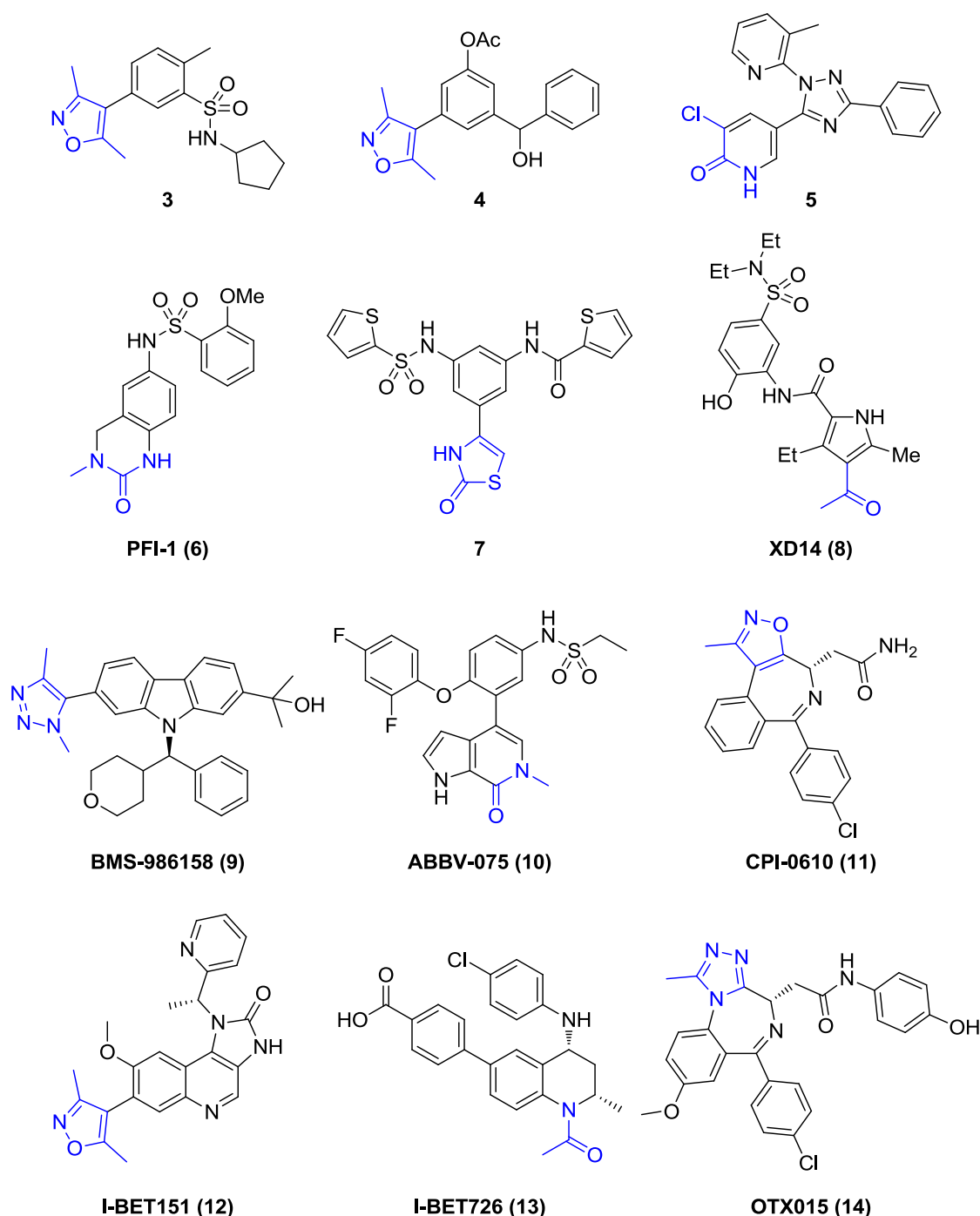


Figure 11. Selection of molecules identified as BET bromodomain inhibitors, including molecules from GSK laboratories.^{62–73} The KAC mimetics are highlighted in blue. Where an X-ray crystal structure is not available the KAC mimetic has been identified by analogy with similar inhibitors.

Inhibitors such as these have helped further our understanding of the role of BET proteins in normal function, and particularly in disease states, and have been demonstrated to have anti-inflammatory and anti-proliferative properties.⁴⁶ A number of BET inhibitors are currently in clinical trials for oncology indications, including I-BET762 **2**, BMS-986158 **9**, ABBV-075 **10**, CPI-0610 **11**, and OTX015 **14**.⁷⁴

The first clinical trial to be initiated was with I-BET762 **2** in 2012 for NUT midline carcinoma, with the sound rationale based on the BRD4 gene translocation that has previously been discussed (Figure 9, Section 2.1), and this study is still ongoing. Following this, many further trials were set up for a range of other solid tumours and haematological malignancies.⁴⁷

The justification for some of these trials is based on observations that BET inhibitors downregulate expression of MYC.^{47,75} MYC (often termed c-MYC, short for cellular MYC, to distinguish it from the viral homologue, v-Myc, and the related proteins N-MYC and L-MYC) is a transcription factor that is believed to be involved in the regulation of 15% of all genes in the body.⁷⁶ As a proto-oncogene, *MYC* is commonly found in mutated, oncogenic form in many cancers, and overexpression and gene translocations have been established as impact factors in tumour progression.⁷⁷⁻⁷⁹ BET inhibitors have been shown to have anti-tumour activity in cancer models where aberrant MYC activity is known to be a factor.⁸⁰

However, with these potential drugs inhibiting all of the bromodomains within the BET family there is high potential for side-effects. Some of these potential issues have been highlighted in the literature: for example, JQ1 **1** and OTX015 **14** have been demonstrated to reactivate latent HIV infections.^{73,81} The HIV transcription factor Tat competes with host BRD4 to bind to pTEFb, a transcription factor involved in the expression of viral proteins.⁸² In cells harbouring a latent infection, these interactions are at an equilibrium and it is believed that the disruption of this by BRD4 inhibition leads to the reactivation of the virus.⁸¹ This, in combination with antiretroviral therapy, has the potential to aid in the complete eradication of HIV from the body, but could also cause extra complications with HIV-positive cancer sufferers.^{47,81}

With information such as this already available, it is clear that inhibiting all eight bromodomains within the BET family, while offering promising clinical advantages, has the potential for widespread and unforeseen side-effects. Further investigations into the biological functions of the individual proteins, and each of the two bromodomains contained within, are vital for developing new and safer medicines.

2.3 Determining the Roles of Individual BET Bromodomains

The majority of BET inhibitors published to date, including all those exemplified on the previous pages, have been pan-BET selective, meaning they had shown little or no selectivity between the eight separate bromodomains found within the four proteins of the BET family.⁸³ Therefore, it is difficult to attribute phenotypic data collected from experiments with these inhibitors to the action on any specific bromodomain. The development of more specific inhibitors would help decouple these pharmacological effects from each other, and may lead to clinical advantages such as narrowed disease scope.

One of the challenges with developing selective probe molecules is that the sequence homology between the BET bromodomains is very high.⁴¹ However, while the sequence identity between the four BD1 domains and between the four BD2 domains is over 75%, the sequence identity between the BD1 and BD2 domains within individual BET proteins is on average only 38%.⁸³ This suggests that the two domains had distinct evolutionary ancestors, and that their functions may be just as distinct. It also suggests that the development of inhibitors that are selective between BD1 and BD2 domains across the BET family is more easily achieved than one that is selective for the bromodomains of an individual BET protein (Figure 12). The development of a single-domain inhibitor would be even more challenging.

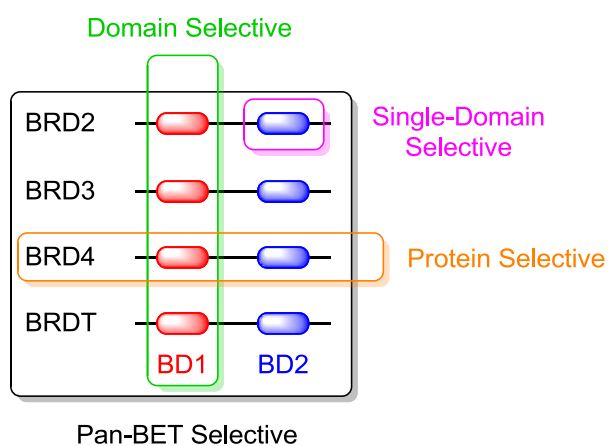


Figure 12. Potential selectivities of BET inhibitors.

A small body of evidence has begun to emerge to suggest that the two bromodomains have different biological functions.⁸³ A study by Filippakopoulos *et al.* into the affinity of individual BET bromodomains for specific acetyl lysine sequences on Histone H3 and Histone H4 revealed that BRD4 BD1 had particular affinity for the H4 tail, while BRD4 BD2 was more likely to recognise multiply acetylated marks on H3.³² A difference in

substrate specificity is also shown for non-histone proteins. For example, Gamsjaeger *et al.* demonstrate that two acetylated lysines in the hematopoietic transcription factor GATA 1 are recognised by the BD1 domain of BRD3, but that the BD2 domain does not form a significant interaction.⁸⁴ It stands to reason that if the natural substrates of the different domains are different then it should be possible to inhibit them separately.

A method has been developed by Baud *et al.* to artificially probe the function of an individual BET bromodomain using chemical biology and genetics, known as a “bump-and-hole” approach.^{85,86} Using sequence alignments and structural analysis the authors identified a residue that was universally conserved across all eight BET bromodomains, a leucine residue in the ZA Loop. Using site-directed mutagenesis this residue was switched with alanine which, being smaller, created a “hole” in the protein. This did not significantly affect the protein stability or natural functionality. An inhibitor **15** was developed, based on a methyl ester analogue of I-BET762 **2**, with the addition of an ethyl group as a “bump” to occupy the “hole” in the mutant protein (Figure 13).

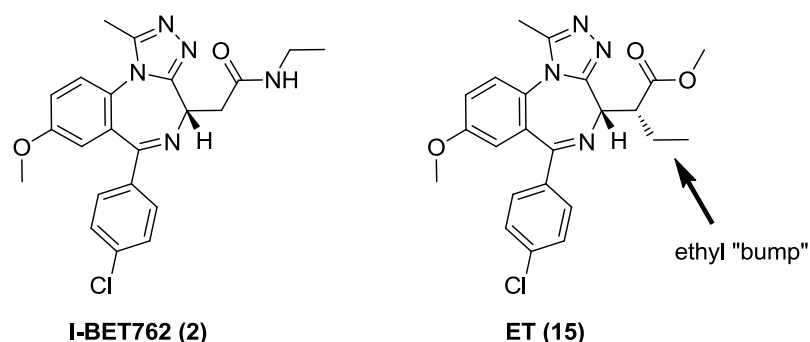


Figure 13. I-BET762 **2** and its analogue, ET **15**, containing an ethyl group designed as a “bump” to form engineered shape complementarity with the “hole” created in a mutant BET bromodomain.

Binding affinities were measured between this compound **15** (termed ET) and all eight BET bromodomains, both in wild-type form, and with the “hole” mutation. ET **15** was shown to bind all mutant domains with nanomolar affinities, but only bind to the wild-type domains with single- to double- digit micromolar affinities.⁸⁵ Selectivities of no less than 30-fold, and as much as 540-fold were reported across the BET family.

Following on from this, ET **15** was exposed to cells containing BRD4, with and without the “hole” mutation in the BD1 domain.⁸⁵ The authors used this to demonstrate that chromatin binding of BRD4 could be displaced by inhibition of BRD4 BD1 only. No further biological data has been published from this technique, but this is good evidence that selective inhibition of bromodomains will create a different pharmacological profile to pan-BET inhibition.

A handful of inhibitors with a bias towards BD1 or BD2 have been developed, and the BD2-selective examples shall be discussed in detail in Section 6.7, along with the rationale behind their selectivity. However, only one inhibitor has been developed with sufficient selectivity for one set of the domains such that biological conclusions may be drawn.

Olinone **16** is a weak inhibitor of BET BD1 domains that does not show any measurable affinity for BD2 (Figure 14).⁸⁷

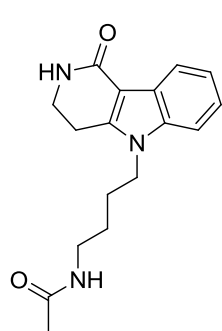
 Olinone (16)	Bromodomain	K_d / μ M
	BRD2 BD1	8.6
BRD2 BD2	>300	
BRD3 BD1	3.7	
BRD3 BD2	>300	
BRD4 BD1	3.3	
BRD4 BD2	>300	

Figure 14. Structure of Olinone 16 and K_d values derived from isothermal titration calorimetry.⁸⁷

Studies with Olinone **16** showed that the selective inhibition of BET BD1 domains enhanced the progression of differentiation of oligodendrocytes in mice, while a pan-BET inhibitor hindered this differentiation. This definitely lends credence to the idea that the roles of the two domains differ, but would be more convincing with a more potent inhibitor for which the degree of selectivity could be better defined. Development of more potent inhibitors with meaningful domain selectivity would be a significant contribution to the field. In addition, it has yet to be demonstrated that once selectivity has been achieved, it can be rationally optimised, especially from low molecular weight fragments. This would also contribute to the field, and the matter is discussed further in Section 6.7.

2.4 Features of the BET Binding Site

As has been discussed previously (Section 2.2), BET inhibitors tend to have a moiety that acts as a KAc mimetic. A common example that is found in a number of reported BET inhibitors, such as I-BET151 **12**, is the 3,5-dimethylisoxazole moiety. Figure 15 shows an overlay of I-BET151 **12** bound to BRD2 BD1, with an acetylated lysine residue, also bound to BRD2 BD1.

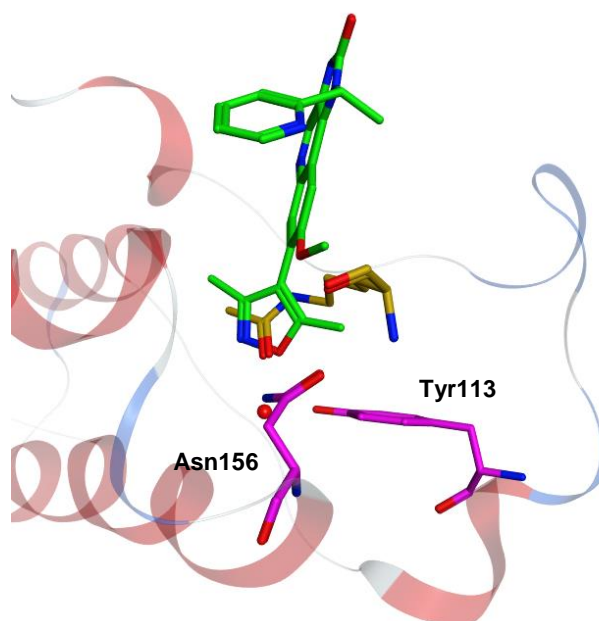


Figure 15. X-ray crystal structure of I-BET151 **12** (green) bound to BRD2 BD1 (PDB: 4ALG). The residues involved in acetyl lysine binding, Tyr113 and Asn156, are shown in bold (magenta) along with the bridging water molecule (red). All other residues and water molecules have been removed for clarity. Structure is superposed with that of BRD2 BD1 bound to an acetylated lysine residue (orange) on histone H4 (PDB: 3UVX). Other H4 residues have been removed for clarity.

The nitrogen and oxygen of the isoxazole group of I-BET151 **12** overlay with the carbonyl oxygen of the acetyl-lysine, forming hydrogen bonds with the conserved asparagine, and with the conserved tyrosine *via* a water molecule.⁷¹ One of the methyl groups occupies the lipophilic region where the acetyl methyl is normally located, and the other extends in a similar direction to the ϵ -CH₂ group of the KAc side-chain.

Around the KAc pocket there is a shapely binding site containing two areas that are commonly targeted to achieve high potency.⁸⁸ The first is the ZA channel, which is formed by residues in the loop region between the Z and A helices. This area has a number of polar residues and is generally occupied by water molecules, as part of a conserved water network that stretches down into the base of the binding site (Figure 16).

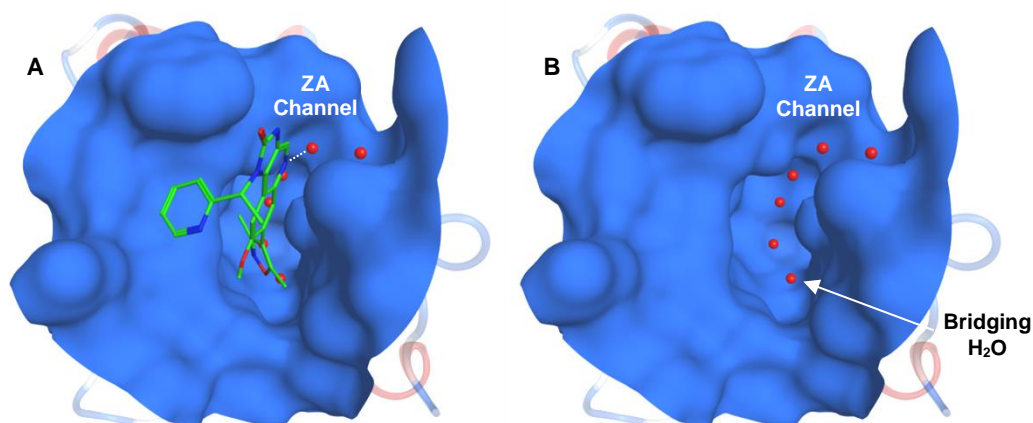


Figure 16. A) X-ray crystal structure of I-BET151 **12** (green) bound to BRD2 BD1 (blue surface, PDB: 4ALG). Image includes six water molecules in the binding pocket (red). The dotted line represents a hydrogen bond between the quinoline nitrogen and a water molecule in the ZA channel. All other water molecules have been removed for clarity. B) The same image with I-BET151 **12** removed. The water molecule that bridges the KAc mimetic and Tyr113 is labelled.

Figure 16 shows I-BET151 **12** bound to BRD2 BD1. At the base of the binding site is the water molecule that is involved in the hydrogen bonding between the KAc mimetic and the conserved tyrosine. A network of five more water molecules can be seen from this water, up through the ZA channel. The nitrogen atom in the quinoline ring of I-BET151 **12** is projected into the ZA channel and forms a hydrogen bond with one of these water molecules.

The second area commonly targeted is known as the WPF shelf. This is a shallow hydrophobic groove formed by conserved tryptophan (W), proline (P) and phenylalanine (F) residues (Figure 17).

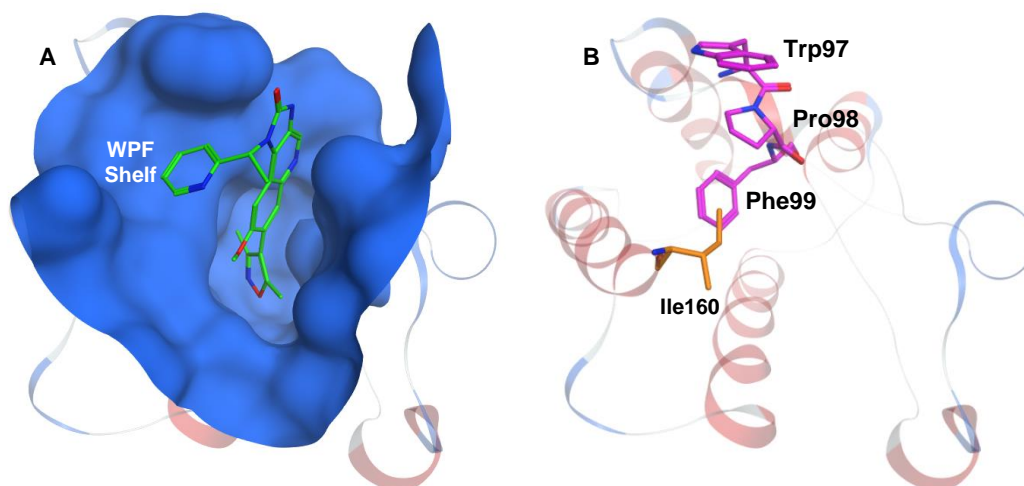


Figure 17. A) X-ray crystal structure of I-BET151 **12** (green) bound to BRD2 BD1 (blue surface, PDB: 4ALG). Water molecules have been excluded from the image for clarity. B) The same image with I-BET151 **12** and the protein surface removed. The residues that flank the WPF shelf are shown in bold (magenta): Trp97, Pro98 and Phe99. The gatekeeper residue, Ile160, is also shown in bold (orange). All other residues have been removed for clarity.

At the edge of this region is a residue that is often termed the “gatekeeper”, as its size determines whether binding onto the WPF shelf is possible with small molecule inhibitors.⁸⁹ While this residue is large in some BCPs, in BET bromodomains it is relatively small (an isoleucine in BD1 domains) so the WPF shelf is accessible.⁸⁸ This area generally forms favourable interactions with lipophilic “shelf-binding” groups, such as the pyridine moiety in I-BET151 **12**.

When designing new BET inhibitors, both of these areas present good opportunities to build potency. Pleasingly, the inclination of the ZA channel to accommodate polar groups provides an opportunity to balance out the lipophilicity that is required for interaction with the WPF shelf, helping to attain favourable overall physicochemical properties. It can aid lead optimisation programmes if considerations such as this are made at an early stage in drug development, and if favourable physical properties are built into molecular scaffolds this may ease the levels of attrition in clinical drug development in the future.⁹⁰

The positioning of the WPF shelf and ZA channel around the KAc pocket define a natural curvature in the BET binding site, which one may expect to be apparent in the design of inhibitors with similar three-dimensional character.

3. Saturation

3.1 Saturation of BET Inhibitors

Visual inspection of the selection of structures in Figure 11 highlights the striking prevalence of flat, aromatic structure in BET inhibitors, despite the shapely nature of the binding site. An analysis of the chemical space occupied by BET inhibitors was performed by Prieto-Martinez *et al.*¹ using structures taken from ChEMBL⁹¹ and Binding Database.⁹² In total around 2000 compounds were downloaded, which was curated down to 207 unique molecules. Chemoinformatic analysis was used to compare the physicochemical properties, structural diversity and coverage of chemical space of this set against similar sets generated for HDAC inhibitors, DNA methyltransferase (DNMT) inhibitors, approved drugs, compounds in clinical trials, molecules that are ‘generally recognised as safe’ (GRAS), and two commercial screening libraries, one general and one focussed on epigenetic targets.

Of particular note in this study were comparisons made using two metrics of molecular complexity: F_{sp^3} and F_{chiral} . F_{sp^3} refers to the fraction of the number of carbons in a molecule which are sp^3 hybridised, and thus is a measure of how saturated a molecule is, with flatter, more saturated compounds giving lower F_{sp^3} values (Equation 1).

$$F_{sp^3} = \frac{\text{number of } sp^3 \text{ hybridised carbons}}{\text{total number of carbons}}$$

Equation 1.

Similarly, F_{chiral} refers to the fraction of the number of carbons in a molecule which are chiral centres, and is used as a measure of stereochemical complexity (Equation 2).

$$F_{chiral} = \frac{\text{number of chiral carbons}}{\text{total number of carbons}}$$

Equation 2.

The mean F_{sp^3} calculated for the set of bromodomain inhibitors was the lowest of the eight datasets, at 0.245.⁹³ In comparison, the average for approved drugs was 0.458 and for the general screening library was 0.326. The mean F_{chiral} for the bromodomain inhibitors was also the lowest of the eight datasets, at 0.024, while the approved drugs averaged 0.107, and the general screening library averaged 0.048. This suggests that reported bromodomain inhibitors have less stereochemical complexity and are more flat than currently approved drugs. The potential implications of this are now discussed.

3.2 Saturation of Drug Molecules

In 2009, Lovering *et al.* published the first of two “Escape from Flatland” papers. This comprised of an empirical study that investigated whether there was a link between complexity of molecules and success in the transition from discovery, to clinical trials, to marketed drugs.² For this they utilised two descriptors. The first was F_{sp^3} , which has previously been discussed (Equation 1), and the second was simply whether a chiral centre was present or not.

Their rationale for conducting this analysis was that there are many more isomers available to a saturated molecule compared to its unsaturated counterpart, with only a very small increase in molecular weight (Figure 18), which allows for the exploration of more diverse chemical space.

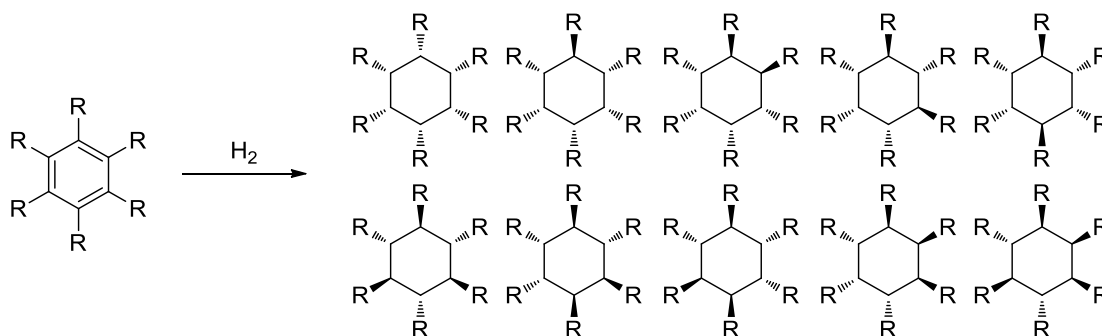


Figure 18. A uniformly hexasubstituted benzene moiety has a 10-fold increase in the number of possible stereoisomers upon full hydrogenation.

Saturated molecules have a more three-dimensional structure which might allow particular moieties of the compound to be better positioned within an active site, in a way which may not be possible for the flat, aromatic equivalent.

In this analysis, molecules were taken from the GVK Bio database (an online database that collates data on clinical trial outcomes from publicly available sources).² The furthest stage of development of the compounds (discovery, phase I, II, III, or marketed drugs) was compared with F_{sp^3} . It was found that there was a consistent increase in saturation when moving to later stages, with an average F_{sp^3} value of 0.36 for discovery compounds and 0.47 for marketed drugs. This suggested that compounds with greater saturation are more likely to succeed to market.

A similar comparison was made for the percentage of compounds at each stage that contained one or more stereocentres.² A similar trend was seen, with an increase from 53% of discovery compounds to 64% of marketed drugs.

However, these derived properties did not just correlate with success, but with physical properties such as aqueous solubility and melting point.² Using a literature set of solubility data for 1202 compounds they found that average Fsp³ increased proportionally with solubility. Furthermore, a literature set of melting point data for 4432 compounds was used to show a clear downward trend in melting point as Fsp³ decreased. Lovering did not find this surprising. Firstly, a link between saturation and melting point was known, demonstrated by the impact of hydrogenation on the melting point of oils,⁹⁴ and general equations have been derived where solubility can be estimated from melting point and log P.^{95,96}

This finding is supported by a model developed by Lamanna *et al.* for discarding insoluble compounds that only uses molecular weight (MW) and aromatic proportion (AP) as molecular descriptors.⁹⁷ AP is the fraction of heavy atoms in a molecule that are aromatic (Equation 3). The practical difference between AP and Fsp³ is that AP is low for saturated compounds, while Fsp³ is high.

$$AP = \frac{\text{number of aromatic atoms}}{\text{total number of heavy atoms}}$$

Equation 3.

Their AP model answers the simple question ‘Is this compound likely to be soluble?’ with ‘yes’ or ‘no’, based on a straightforward flow chart.⁹⁷ They claim an accuracy of this model of 81% (defined as the percentage of results that were true from a test set of 1200 compounds).

Further work by Lovering in 2013 investigated links between the descriptors of complexity, Fsp³ and number of chiral centres, with promiscuity.³ In this case, the hypothesis was that increased complexity would increase target selectivity, and minimise toxicity due to off-target effects. Lovering analysed the activity of 7098 compounds against a set of 15 assays selected from the Cerep panel, which is used to assess off-target activity. Promiscuity was defined as the fraction of targets inhibited to greater than 50% at a test compound concentration of 10 mM. The compounds examined had to be split into groups, with and without ionisable amines (aminergic and non-aminergic), as aminergic compounds were shown to be more promiscuous and have higher Fsp³, so these factors needed decoupling from each other.

Lovering showed that promiscuity decreased as a function of Fsp³. For non-aminergic compounds the average promiscuity for an Fsp³ of 0–0.2 was 0.075, which steadily

trended downwards and was reduced by 59% to 0.031 for an Fsp³ of 0.8–1.0. Aminergic compounds produced a similar trend, starting at a promiscuity of 0.27 for an Fsp³ of 0–0.2 and reducing by 89%, giving a value of 0.031 for an Fsp³ of 0.8–1.0.

A similar analysis was performed based on number of chiral centres, and a downward trend in promiscuity was seen as the number increased.³ Again, the trend was more pronounced in the aminergic compounds which possessed an average promiscuity of 0.31 with no chiral centres, which reduced by 58% for compounds with >2 centres. Non-aminergic compounds started at 0.066 and reduced by 48%.

Promiscuity was also analysed by examining inhibition of cytochrome P450 (CYP) isozymes (termed CYPinh). CYPinh was defined as the percentage of CYP isozymes inhibited to greater than 30% at a test compound concentration of 3 µM. CYPinh was found not to be affected by the presence of an ionisable amine. A downward trend in CYPinh was seen as Fsp³ increased. CYPinh for an Fsp³ of 0–0.2 was 0.19, which steadily trended downwards and was reduced by 77% for an Fsp³ of 0.8–1.0. No trend was observed between CYPinh and the number of chiral centres.

In conclusion, Lovering has empirically shown that drug candidates with a higher degree of saturation are more likely to have higher aqueous solubility, lower promiscuity, and overall, a higher chance of succeeding to market.^{2,3} This makes the inclusion of saturation early on in a drug development programme a highly attractive strategy for exploring new areas of chemical space.

4. Aim and Objectives

In the previous section two important studies were discussed which underpin the aim and objectives of this research programme. The chemoinformatic analysis performed by Prieto-Martinez *et al.* demonstrated that, compared to approved drugs, reported BET inhibitors had relatively low three-dimensional character.¹ Studies by Lovering *et al.* illustrated the potential benefits of designing molecules with an increased level of saturation, such as lower promiscuity, and higher chance of succeeding to market.^{2,3} Taken together, it was clear that there was scope to design and synthesise BET inhibitors with an increased degree of saturation, which would allow the exploration of new areas of chemical space. This formed the basis of this research, and the compounds produced would be evaluated against their similar, highly unsaturated counterparts.

There were two main options for how to approach this aim. The first was in a top-down manner, taking existing BET inhibitors and replacing aromatic rings with saturated variants (Figure 19). However, this severely limited the chemical space that could be explored, and changing the three-dimensional structure of a molecule already optimised for the binding pocket was very likely to detract from its potency.

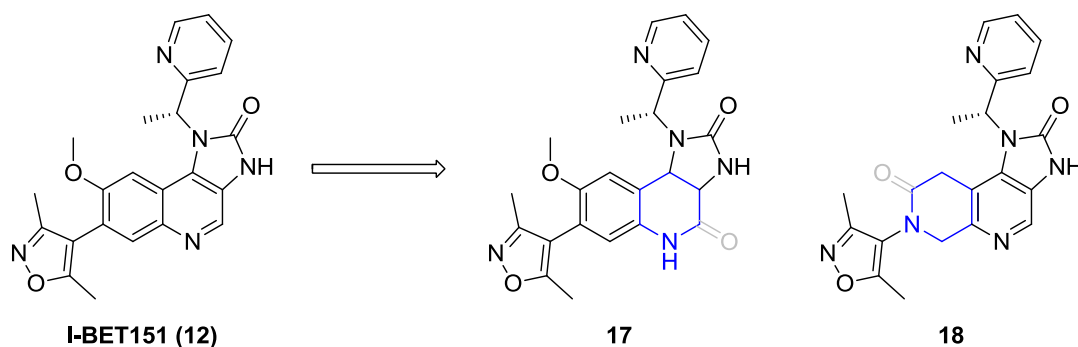


Figure 19. Top-down approach to increasing saturation of BET inhibitors, using I-BET151 12 as an example.

A more promising way to approach the aim was in a bottom-up manner. This involved starting with an established acetyl-lysine mimetic, and building fragments to be screened. This *de novo* design promised novel and more efficient exploration of vectors for growth.

3,5-Dimethylisoxazole is a well-established KAc mimetic that has been utilised in a number of published fragment-based drug discovery papers.^{64,71,98,99} These mostly focus around a phenylisoxazole fragment hit **19** and elaborate out from there.

The first aim of this project was to synthesise a range of fragments in which the phenyl ring of the phenylisoxazole **19** was replaced by a saturated ring, in order to prioritise a core structure to further elaborate. It was acknowledged that the atom used to link the saturated rings with the isoxazole would have a large effect on the conformation of the saturated rings. In order to focus synthetic efforts, it was decided that it was best to choose between having a nitrogen or carbon atom at this position. Therefore, conformational analysis was carried out to compare phenylisoxazole **19** with its cyclohexane **20** and piperidine **21** analogues (Figure 20).

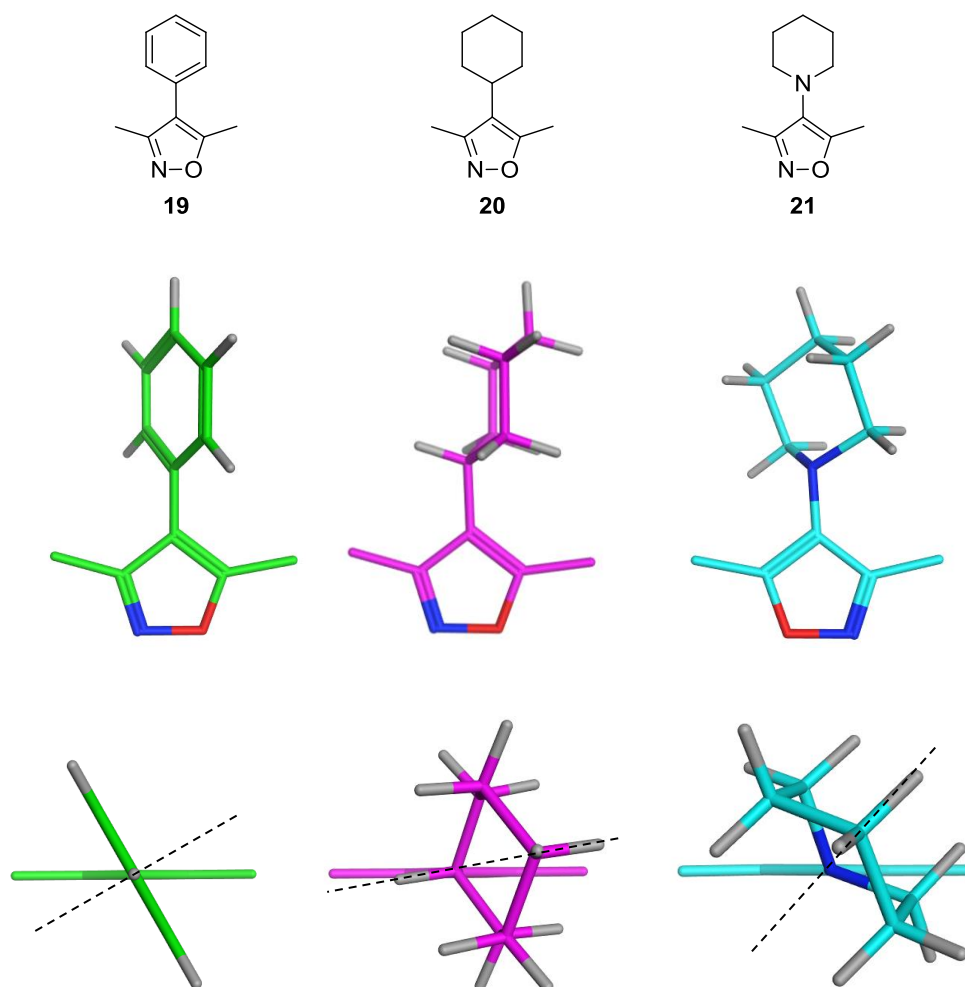


Figure 20. Lowest energy conformations of phenyl **19**, cyclohexyl **20** and piperidine **21** isoxazole systems. The dotted lines represent the plane of a perpendicular bisection of the second ring.¹⁰⁰

The lowest energy conformations were computed using Molecular Operating Environment (MOE).¹⁰⁰ In order to perform these calculations it has been assumed that the nitrogen atom of the piperidine system **21** is not sufficiently basic to become protonated at physiological pH, which would significantly affect the conformation. The most basic atom is predicted to be the isoxazole nitrogen rather than the piperidine, with

a pK_{aH} of 1.35,¹⁰¹ suggesting that the molecule would indeed be unprotonated at physiological pH. The actual pK_{aH} value of the piperidine isoxazole fragment **21** was later measured to be 3.93. While being significantly higher than predicted, this is still low enough to draw the same conclusion.

Figure 20 depicts the lowest energy conformation of these systems, from both a face-on viewpoint and down the plane of the bond between the isoxazole and the second ring. The importance of dihedral ring angle has been discussed in the literature for the phenylisoxazole system, so this property was inspected for these systems.^{98,99} As two of the rings are not flat the most appropriate value to compare is the angle between the isoxazole and a perpendicular bisection of the second ring, passing through the linking bond. This is represented by the dotted lines in Figure 20. By this measure, the torsion angles were measured as follows: 30° in the phenyl system **19**; 9° in the cyclohexyl system **20**; 47° in the piperidine system **21**. The almost perpendicular conformation adopted by the cyclohexane isoxazole **20** can be rationalised in terms of avoidance of clash with the methyl groups on the isoxazole. This factor also plays a role in the conformation of the phenyl and piperidine rings. However, both of these would benefit energetically from being in the same plane as the isoxazole, due to conjugation with either the aromatic system of the benzene ring, or the lone pair of the nitrogen, and therefore, the angles observed were a compromise between conjugation and avoidance of steric clash.

It was decided that the torsion angle provided by having a nitrogen linked ring would better mimic the phenylisoxazole **19** and be more likely to provide suitable vectors to explore. Therefore, a range of saturated rings were chosen as initial targets for synthesis, including five-, six- and seven-membered rings (Figure 21).

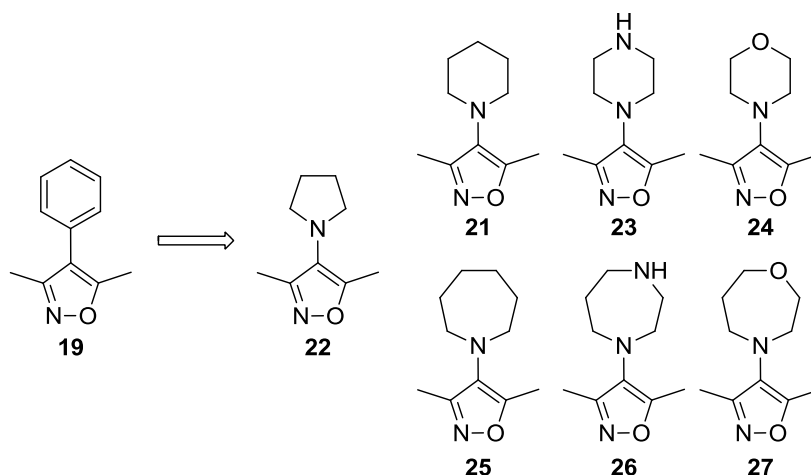


Figure 21. Replacement of phenyl ring in the phenylisoxazole fragment 19 with a range of saturated rings.

It was anticipated that high concentration screening would be used to identify which of the rings was preferred and, if crystallisation attempts were successful, X-ray crystal structures could be used to select the best vectors for elaboration. At this stage, groups would then be added to probe for interactions with the WPF shelf and/or the ZA channel, which are areas of the binding site commonly targeted for potency increases, as was discussed in Section 2.4. Inspiration would be taken from published BET inhibitors, with the aim to also find novel groups, using modelling for guidance.

The ultimate aim of this project was to produce a molecule that would be suitable for entering into lead optimisation, with a similar potency to published lead molecules, but with a greater degree of saturation. Such a molecule would need to be in a novel area of chemical space and display suitable vectors for future exploration, with evidence that they could be exploited to modulate both potency and physicochemical properties. This molecule should also demonstrate a reasonable level of selectivity over other BCPs.

Two compounds were selected from the literature to be used as standards to compare against (Figure 22). Both were based around the phenylisoxazole chemotype and had been identified as potential lead compounds by the authors.

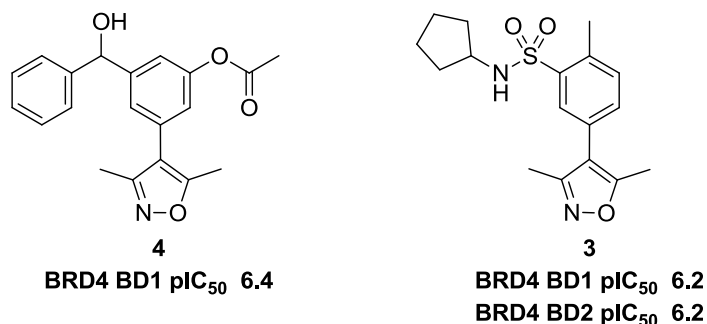


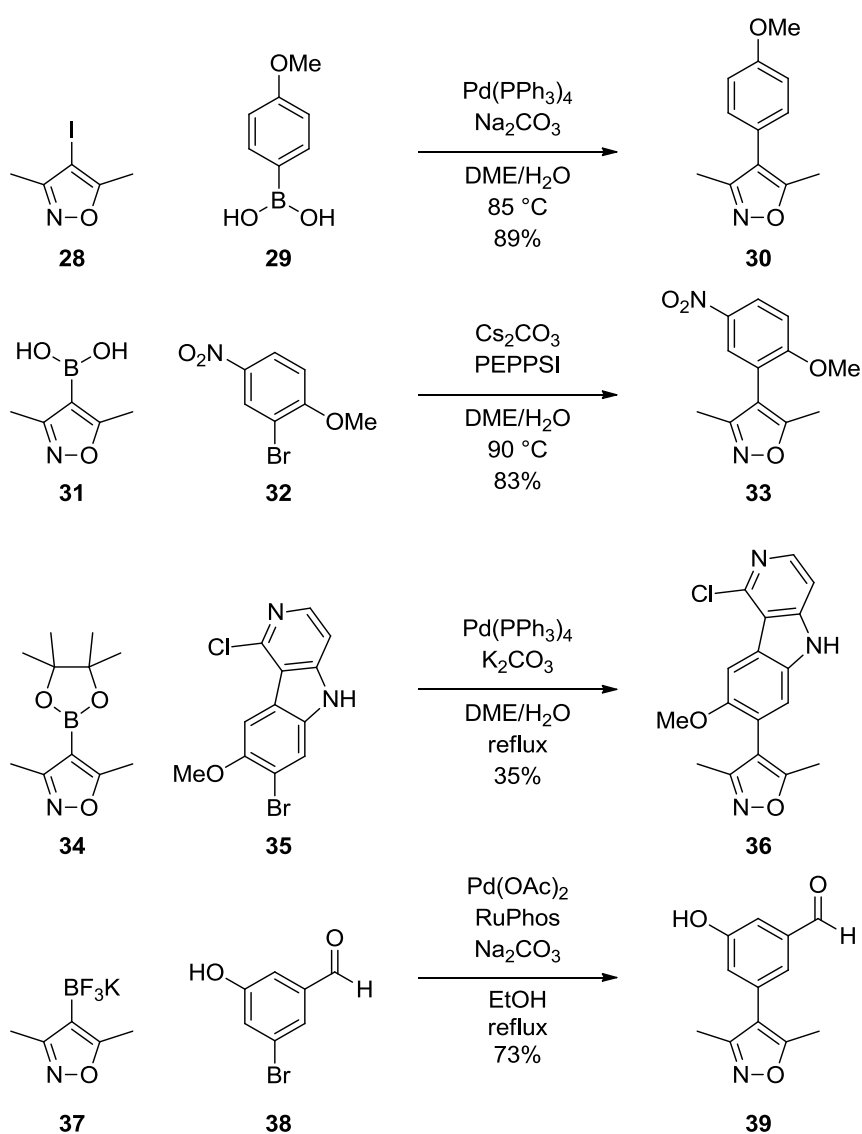
Figure 22. Literature comparator compounds.^{64,99}

Firstly, a molecule published by Hewings *et al.* **4** was selected.⁶⁴ This compound contains a phenyl moiety that binds on the WPF shelf, and an acetate moiety that points towards the ZA channel. The reported IC₅₀ of this compound against BRD4 BD1 was 371 nM (in an AlphaScreen assay), which equates to a pIC₅₀ of 6.4. Secondly, a sulfonamide **3** was identified, published by Bamborough *et al.* from within GSK laboratories.⁹⁹ This molecule has been tested in the same assay system that was to be used for this project and returned pIC₅₀ values of 6.2 at both BRD4 BD1 and BD2. Therefore, the target pIC₅₀ for this project was set at greater than or equal to 6.0, which corresponded to an IC₅₀ of less than or equal to 1 μM. Additionally, guidelines for lead-likeness suggested that compounds should not be too large, and that a molecular weight of less than 350 Da was desirable.¹⁰²

5. Substituted Isoxazole Synthesis

Before embarking on practical synthetic investigations into the synthesis of 4-amino-substituted 3,5-dimethylisoxazole compounds (Figure 21), a comprehensive examination of relevant published syntheses was performed. This commenced with an inspection of how isoxazoles had been installed into BET inhibitors in the past.

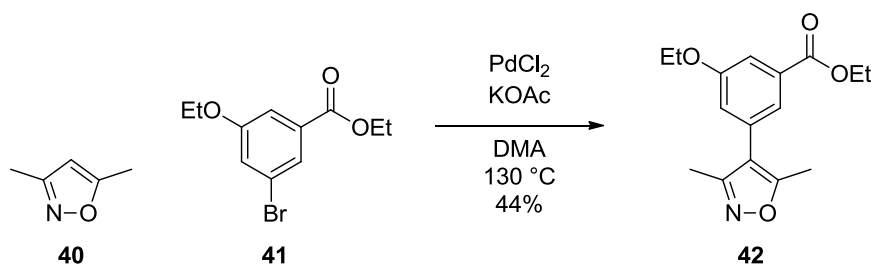
In the majority of examples where an isoxazole has been used as the KAc mimetic of a BET inhibitor, the heterocycle has been installed using a Suzuki-Miyaura coupling. Scheme 1 shows representative examples of conditions from across multiple medicinal chemistry programmes.



Scheme 1. Isoxazole-installation step of published BET inhibitors.^{64,99,103,104}

It can be seen that this particular Suzuki coupling is fairly versatile, and has been performed in the presence of potentially problematic functionality, such as aldehydes, amines and other halides. The isoxazole has been used as both the halide and the boron species coupling partner, and in the case of the latter, the boronic acid **31**, pinacol ester **34** and trifluoroborate **37** have all been used successfully. This was seen as a promising sign that metal-catalysed C-N cross couplings with this substrate may be possible, despite the marked lack of literature precedent.

The only other reaction type that has been published for these compounds is a direct arylation of 3,5-dimethylisoxazole **40**, without the aid of a functional handle (Scheme 2).⁹⁸

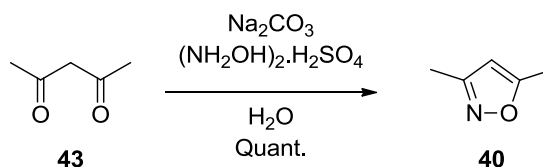


Scheme 2. Direct arylation of 3,5-dimethylisoxazole **40**.⁹⁸

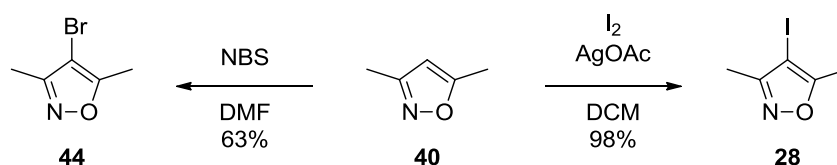
This ligand-free, palladium-catalysed arylation procedure has been used to isolate a small number of examples, but in the instance shown here it was abandoned in favour of Suzuki chemistry due to low yields.^{98,105,106} Indeed, the researchers who originally developed the protocol comment on how reactivity is greatly reduced by electron-withdrawing substituents on the aryl bromide.¹⁰⁷

The above examples all use starting materials where the isoxazole is preformed, mostly with a synthetic handle, and all of these building blocks are currently commercially available. The routes used to isolate these were examined, to see if they would provide inspiration for disconnections, as well as to identify other potentially useful starting materials that were available.

3,5-Dimethylisoxazole **40** appears to be the common intermediate from which all the functionalised building blocks are formed. This simple heterocycle can be formed by condensing acetylacetone **43** with hydroxylamine (Scheme 3). For example, a quantitative yield can be achieved using hydroxylamine sulfate in water, with sodium carbonate as a base.¹⁰⁸

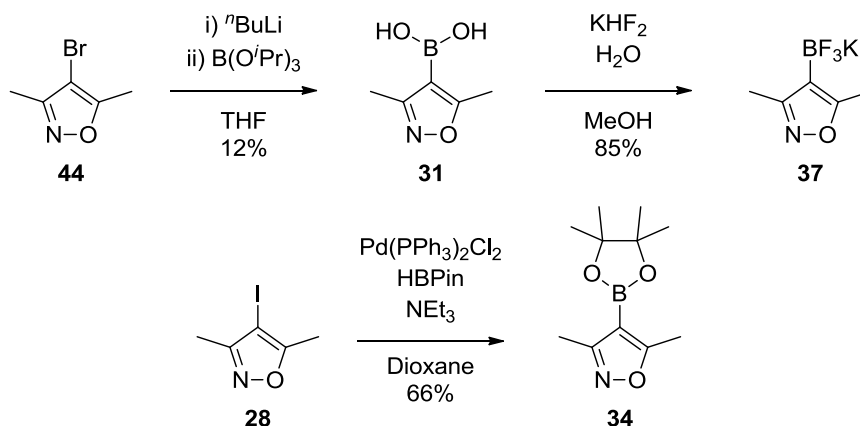
Scheme 3. Synthesis of 3,5-dimethylisoxazole **40**.¹⁰⁸

This species is sufficiently electron-rich to allow electrophilic aromatic substitution to occur at the 4-position. In this manner, halogenated products can be formed (Scheme 4).

Scheme 4. Halogenation of 3,5-dimethylisoxazole **40**.^{109,110}

Literature examples of this include bromination using *N*-bromosuccinimide, and iodination in excellent yield using molecular iodine and silver acetate.^{109,110}

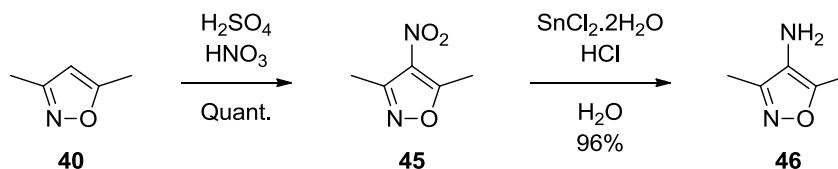
As well as being useful building blocks in their own right, the bromoisoxazole **44** and iodoisoxazole **28** can be used to isolate the three commercially available boron derivatives (Scheme 5).

Scheme 5. Synthesis of 3,5-dimethylisoxazole boron derivatives.^{98,110,111}

The bromoisoxazole **44** may undergo lithium-halogen exchange with ⁿBuLi to form a lithiated intermediate. To this is added triisopropyl borate, and the resulting borate ester is hydrolysed on workup to provide the boronic acid **31**. The published example shown provides a very poor yield of only 12%.¹¹⁰ The trifluoroborate salt **37** may be formed from this boronic acid **31** using potassium hydrogenfluoride in a good yield of 85%.⁹⁸ A number of publications demonstrate the formation of the boronic acid pinacol ester **34**

in different ways, with the example shown here using iodoisoxazole **28**, pinacolborane and a palladium catalyst.¹¹¹

As well as halogenation, nitration at the 4-position is also achievable, and the nitroisoxazole **45** can be formed in quantitative yield using the conventional sulfuric/nitric acid conditions (Scheme 6).

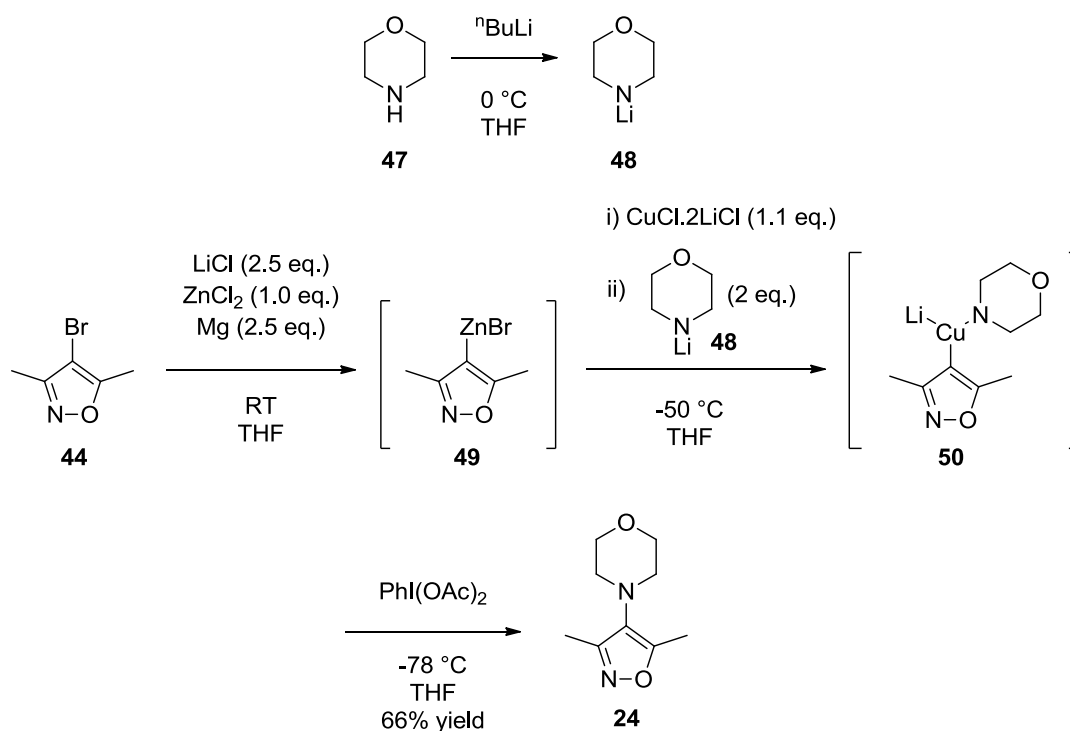


Scheme 6. Synthesis of 4-amino-3,5-dimethylisoxazole **46**.^{108,112}

Through reduction of the nitro species **45**, an aminoisoxazole **46** is accessible. This aminoisoxazole **46** has the potential to be incredibly useful in this piece of research; lending itself to alkylation chemistry to form the saturated heterocyclic targets.

Following on from this, examples of the synthesis of 4-amino-substituted isoxazoles were sought. Unsurprisingly, alkylation of the primary amine **46** is preceded and shall not be discussed further here.

Of the initial targets, it was found that the morpholine example **24** is a known compound that has previously been isolated by the group of Prof. Paul Knochel using an approach involving the oxidative amination of zinc reagents (Scheme 7).¹¹³

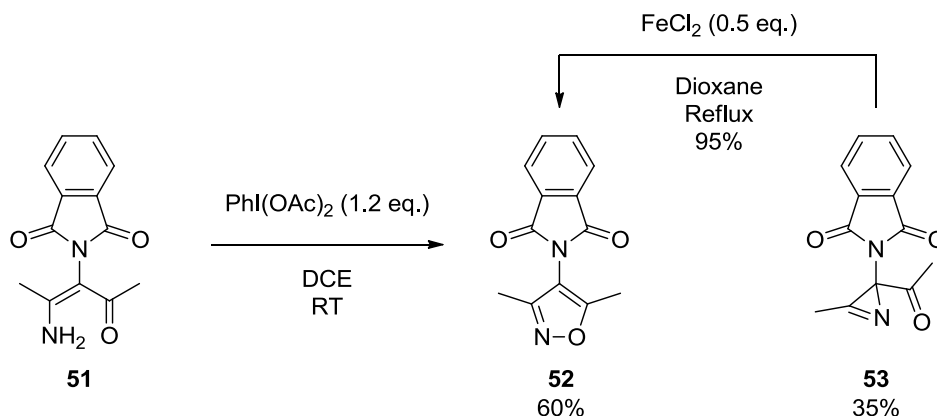


Scheme 7. Synthesis of morphine isoxazole **24 by metalation of bromoisoxazole **44** followed by oxidative amination.¹¹³**

The procedure begins with magnesium insertion into the heterocyclic bromide **44** in the presence of lithium chloride and zinc chloride, resulting in an organometallic zinc reagent **49**. This intermediate is then transmetalated with copper (I) chloride bis(lithium chloride) complex before the addition of lithiated morpholine **48** to provide an amidocuprate **50**. Oxidation of this species with PhI(OAc)_2 then leads to the morpholine isoxazole product **24** in a reasonable 66% yield.

While it was reassuring to see that it was possible to isolate one of the initial target compounds, it was not felt that this methodology would be suitable for a medicinal chemistry programme. Contributing factors to this decision included the apparent necessity for rigorous exclusion of water from the multiple metals in the experimental procedure, the requirement to lithiate the amine coupling partner, and the generally complex nature of the process as a whole. It was envisioned that methodology could be developed that was simpler, more amenable to high-throughput, and more likely to be tolerant to additional functionality on the amine.

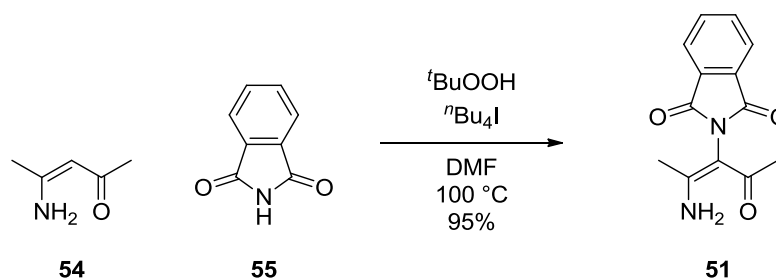
Two examples were found in which the isoxazole was formed as part of the methodology, with a nitrogen substituent at the 4-position. The first of these involved cyclisation of an enamine **51** to form a dimethylisoxazole with a phthalamide group at the 4-position **52** (Scheme 8).¹¹⁴



Scheme 8. Cyclisation of enamine **51** to form phthalimide-substituted isoxazole **52**.¹¹⁴

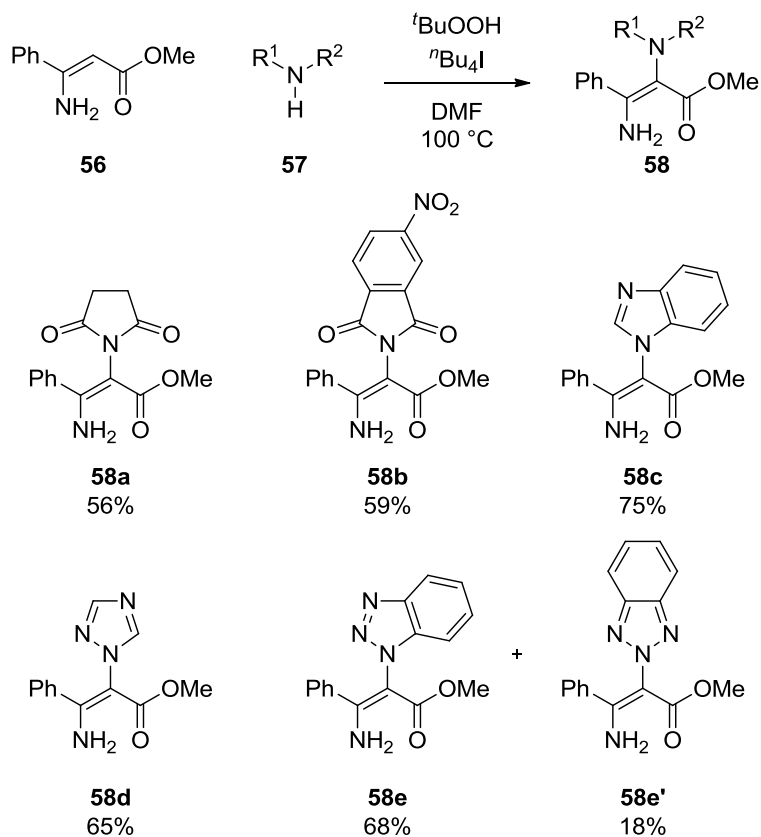
The cyclisation process, mediated by $\text{PhI}(\text{OAc})_2$, mostly produced the isoxazole **52**, but also a separable azirine byproduct **53**. Conveniently, this byproduct could be converted to the desired product **52** by heating with an iron catalyst.

The starting material in this reaction was generated through an oxidative coupling of acetylacetone-derived enamine **54** and phthalimide **55** (Scheme 9).



Scheme 9. Generation of phthalimide-substituted isoxazole precursor **51**.¹¹⁴

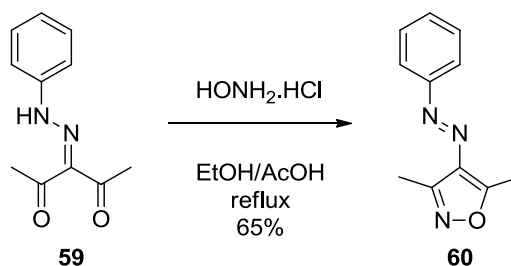
Of course, the phthalimide product **52** is of limited utility in this research as deprotection would provide the commercially available primary amine **46**. Therefore, the coupling would need to be applicable to a range of amines, and ideally the saturated cyclic amines chosen as targets. However, the authors of the work state that only electron-deficient amines may be used, and provide a very limited substrate scope (Scheme 10).

Scheme 10. Amine substrate scope of oxidative C-N coupling of enamine **56**.¹¹⁴

They also provide a short list of amines that provided no product, including saccharin, diphenylamine, aniline, and dibenzylamine, the last of these being the key to suggesting this procedure would not be applicable to saturated cyclic amines. A literature search did not find any suitable alternative processes for isolating such enamines. It was acknowledged that reduction of the carbonyls in compounds such as succinimide **58a** could provide access to some target compounds. However, this line of enquiry was not pursued as it was expected to have limited scope: the requirement for two different oxidising agents may cause problems if and when further substituents were added to the amine rings, the carbonyls effectively block off two potential sites for vector exploration, and there was no evidence that the methodology would be applicable to larger ring sizes. To allow steady progression of medicinal chemistry, more broadly applicable methodologies were desirable.

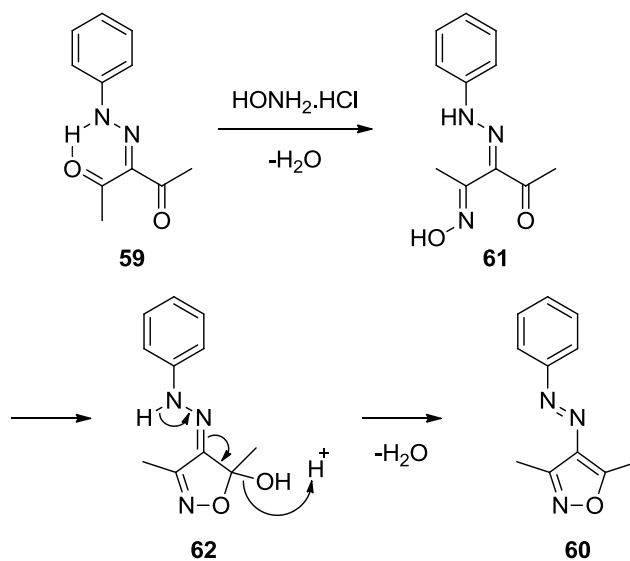
The second example of the formation of an isoxazole with a nitrogenous substituent at the 4-position used a 1,3-diketone, rather than an enamine, as the starting material. The

authors performed a double condensation reaction with hydroxylamine to provide a diazene-substituted isoxazole product **60** (Scheme 11).^{115,116}



Scheme 11. Synthesis of diazene-substituted isoxazole 60.¹¹⁶

The proposed mechanism involves an initial condensation of one of the ketones, which it was noted could form an internal hydrogen bond with the hydrazone, with hydroxylamine to form an oxime **61** (Scheme 12). The oxygen of this oxime could then attack the remaining ketone carbonyl. The hydrazone is then deprotonated to form a diazene and a second molecule of water is eliminated, forming the aromatic ring system. It is presumably this step that is encouraged by the acidic reaction conditions.



Scheme 12. Proposed mechanism for synthesis of diazene-substituted isoxazole 61.¹¹⁶

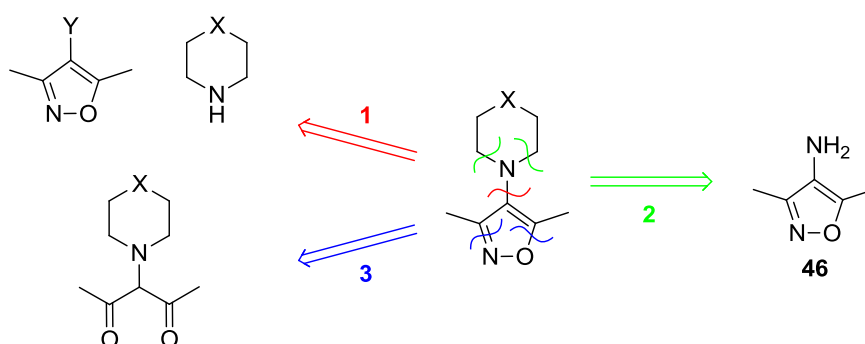
While the exact details of this mechanism were not applicable to the target compounds in this research, which would not have a hydrazone to take part in the condensation process, the method of isoxazole formation from a diketone with hydroxylamine certainly showed promise. Indeed, it was identified as one of three key disconnections to be explored.

6. Results and Discussion

6.1 Disconnections

In order to gain access to the initial target molecules, three disconnections were identified (Scheme 13), which shall be discussed in the following order:

1. Cross-coupling reaction between a dimethylisoxazole and secondary, cyclic amines.
2. Alkylation of the aminoisoxazole **46** to form the saturated ring.
3. Formation of the isoxazole by cyclisation of a 1,3-dicarbonyl species.



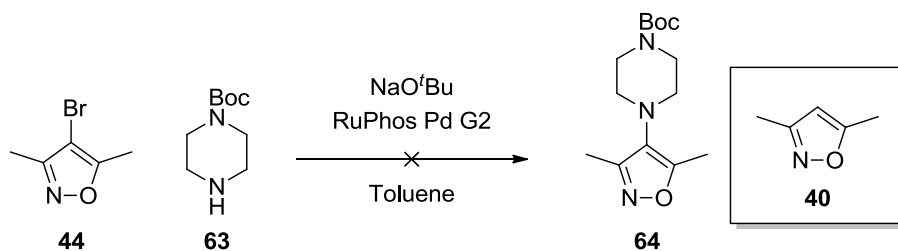
Scheme 13. Disconnections explored to access target molecules.

6.1.1 Cross-Coupling Reactions

Cross-coupling to form a C-N bond is a very attractive method for the synthesis of these molecules as it would provide quick access to a large range of analogues due to the wide availability of secondary cyclic amines.

6.1.1.1 Buchwald-Hartwig Coupling

Buchwald-Hartwig conditions were the first to be investigated. In Surry and Buchwald's 'user's guide' to Pd-catalyzed amination, five-membered heteroaryl halides are described as 'recalcitrant substrates', which was not a promising starting point.¹¹⁷ The aforementioned text recommends RuPhos as a good, general ligand for couplings with secondary amines, and thus a trial reaction was performed using 2nd Generation RuPhos Precatalyst (Scheme 14).

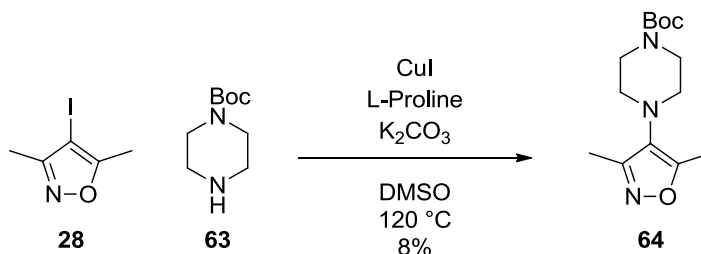


Scheme 14. Initial Buchwald-Hartwig trial.

Unfortunately, no product was observed in this reaction. However, a peak was observed in the LCMS trace which was consistent with the formation of the protodebrominated isoxazole **40**, suggesting that oxidative addition into the C-Br bond was occurring. Two rounds of screening were performed to see if an example of productive catalysis could be found (data not shown). Ten ligands were screened in total, including a range of monodentate and bidentate phosphines, along with two *N*-heterocyclic carbenes. The only ligand to achieve any conversion to product was PEPPSI™-IPent, with sodium *tert*-butoxide in toluene, for which a 3% product peak was observed by HPLC for the coupling of the bromoisoxazole **44** with morpholine. This was sufficient evidence that suitable Buchwald-Hartwig conditions were unlikely to be found, so further investigation was ceased and alternative coupling methodologies were explored.

6.1.1.2 Modified Ullmann Coupling

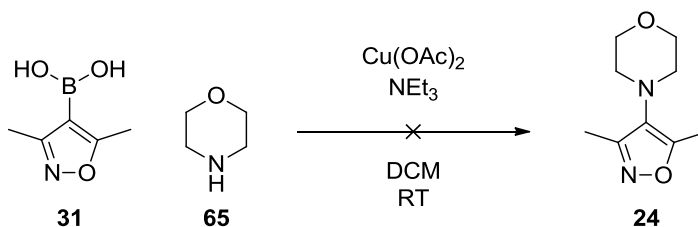
The modified Ullmann coupling is a C-N bond forming methodology that utilises copper salts and stabilising ligands, such as diamines, amino-acids, diols and 1,10-phenanthrolines. A small screen was performed that identified conditions using copper iodide, proline and potassium carbonate in DMSO that could successfully catalyse the coupling of the iodoisoxazole **28** with *N*-Boc piperazine **63** (data not shown).^{118,119} However, after optimisation, the greatest isolated yield achieved was 8% (Scheme 15). While this yield was very low, and not synthetically useful, it was still a significant improvement over the minimal conversions observed for Buchwald-Hartwig conditions.



Scheme 15. Highest yielding modified Ullmann coupling conditions.

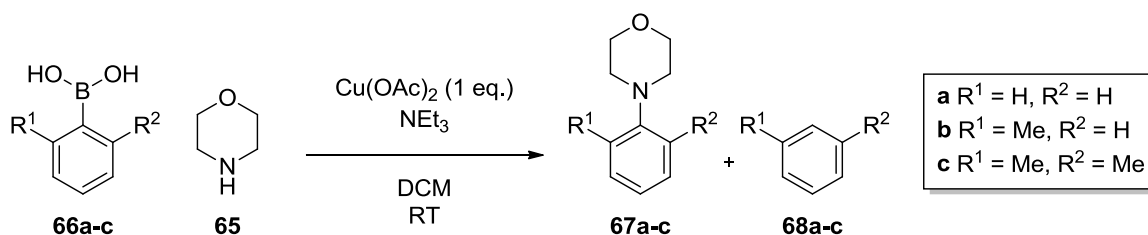
6.1.1.3 Chan-Lam Coupling

Finally, Chan-Lam conditions were investigated, which utilises copper catalysis to couple boronic acids with amines.¹²⁰ Literature conditions for coupling phenylboronic acid, with stoichiometric copper (II) acetate, were applied to the isoxazole boronic acid **31** (Scheme 16).¹²¹



Scheme 16. Trialled Chan-Lam amination conditions.

The reaction was unsuccessful, and complete protodeboronation of the starting material was observed. Based on this result, further substrates were subjected to these Chan-Lam conditions in order to understand the requirements for successful cross-coupling. Firstly, the non-heteroaromatic system, phenylboronic acid **66a**, was investigated to evaluate electronic effects (Scheme 17), and this resulted in excellent conversion (Table 2).



Scheme 17. Confirmation of the efficacy of the Chan-Lam coupling conditions and investigation into the effect of neighbouring methyl groups.

Secondly, the effect of neighbouring methyl groups was probed using *o*-tolylboronic acid **66b** and (2,6-dimethylphenyl)boronic acid **66c**. It was found that a single *ortho* methyl group slightly decreased the conversion to product and increased the amount of protodeboronation occurring. A second *ortho* methyl group ablated cross-coupling, with no product being detectable after 24 h. This is good evidence that steric hindrance caused by the neighbouring methyl groups of the dimethylisoxazoleboronic acid **31** are, at least in part, responsible for the failure of the amination of this substrate.

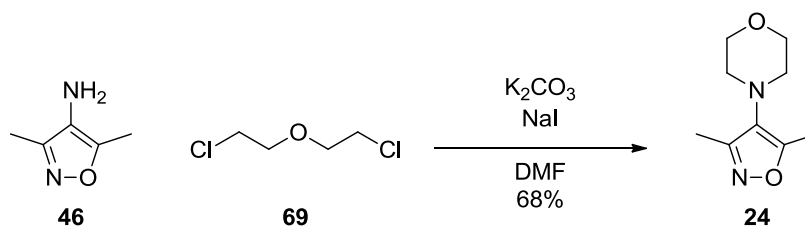
Methyl Groups	66 / %	68 / %	67 / %
0 (a)	4	9	74
1 (b)	2	20	63
2 (c)	37	15	-

Table 2. Results of LCMS analysis of Chan-Lam reactions of morpholine 65 with phenylboronic acid 66a and its methyl 66b and dimethyl 66c derivatives, after 24 h. Values are given as a percentage of the LCMS UV trace.

In conclusion, a body of evidence has been collected that strongly suggests that cross-coupling methodologies are unsuitable for the formation of the C-N bond in question. While it is acknowledged that only a small fraction of the vast range of published conditions have been applied to this system,¹²² efforts were focussed on investigating alternative disconnections to increase the chance of successfully forming the target compounds.

6.1.2 Saturated Ring Formation

The second disconnection that was explored for the synthesis of target compounds was the formation of the saturated ring by alkylation of the commercially available 4-amino-3,5-dimethylisoxazole **46**. Suitable reagents for this alkylation were identified as dihalides. Literature conditions were adapted from a similar reaction with 2,4,6-dimethylaniline, as it was thought that this amine would suitably emulate the steric environment of the aminoisoxazole **46**.¹²³ Using the commercially available dichloride **69**, sodium iodide, and potassium carbonate, the morpholine derivative **24** was prepared (Scheme 18).

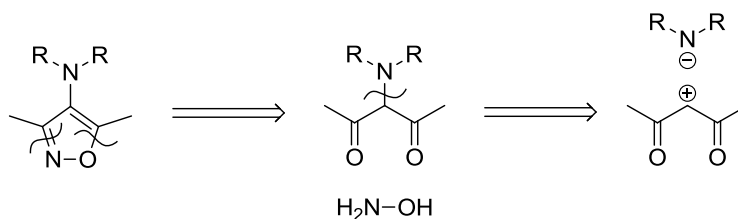


Scheme 18. Synthesis of morpholine isoxazole 24 by alkylation of aminoisoxazole 46.

The first attempt at this reaction gave a disappointing yield of 19%. However, it was discovered that this was, at least in part, due to volatility of the product. Repetition of the reaction with careful handling greatly improved the yield to 68%. This result demonstrated the potential for using this disconnection to synthesise a range of analogues.

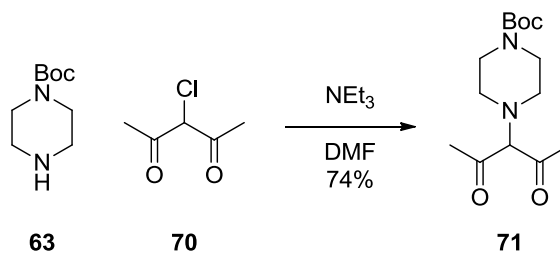
6.1.3 Isoxazole Formation

While the formation of the saturated ring seemed highly promising, there were target molecules that were not easily accessible *via* this route. Therefore, a final disconnection was explored: the formation of the isoxazole ring itself. Retrosynthetically, it was envisioned that this could be achieved from a 1,3-dicarbonyl species, which could be formed by an S_N2 reaction of an amine with a suitable alkylating agent (Scheme 19).



Scheme 19. Retrosynthetic analysis of 4-amino-3,5-dimethylisoxazoles.

The first step of the forward synthesis was performed using *N*-Boc piperazine **63**, with 3-chloro-2,4-pentanedione **70** as the alkylating agent. Conditions were adapted from a published synthesis that used an alternative piperazine,¹²⁴ and a good yield of 74% was achieved (Scheme 20).

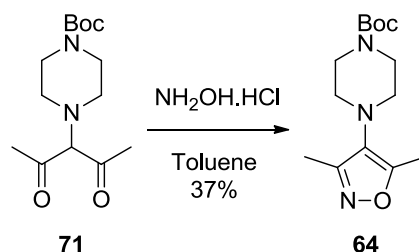


Scheme 20. Synthesis of 1,3-dicarbonyl piperazine derivative 71.

The formation of the isoxazole proved more challenging. The majority of literature syntheses have been performed in ethanol with hydroxylamine hydrochloride. This reaction was attempted and the product **64** was isolated in only a 7% yield, so attempts were made to improve this yield (Scheme 21).

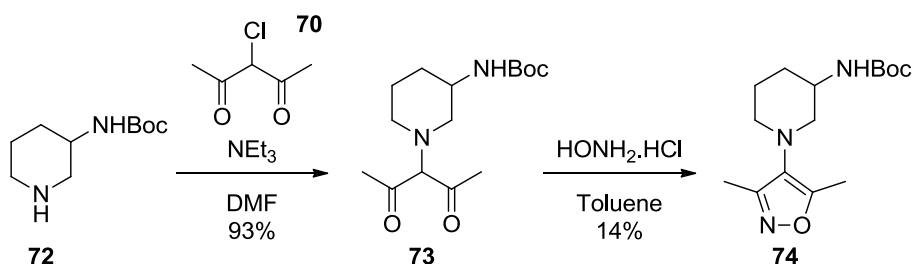
Working with the hypothesis that the final dehydration step was problematic, the addition of acetic acid and sodium acetate were trialled, the former of which was included in the conditions for synthesising the diazene-substituted isoxazoles discussed in Section 5 (Scheme 11, p37). Unfortunately, neither of these additives improved the observed yield. The addition of molecular sieves had the greatest effect, increasing the yield to 16%. This supported the hypothesis that aiding dehydration was important. Therefore, the reaction was performed in toluene using Dean-Stark apparatus. Although

the hydroxylamine hydrochloride was insoluble in the solvent, a large excess provided conversion to product. Through this method, an improved yield of 37% was achieved, and while this yield was not ideal, it was high enough to provide access to useful amounts of product (Scheme 21).



Scheme 21. Formation of *N*-Boc piperazine isoxazole **64 from its 1,3-dicarbonyl precursor **71**.**

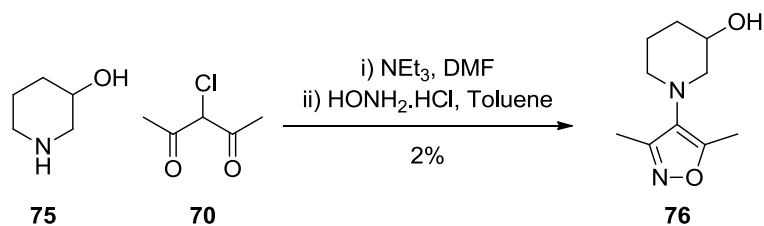
This methodology was used to isolate a number of analogues and allowed progress to be made on this research programme. However, a stage was reached when a large batch of intermediate was required and the yield provided *via* this route was insufficient (Scheme 22).



Scheme 22. Synthesis of Boc protected 3-aminopiperidine isoxazole **74.**

While the 13% yield over the two steps was acceptable when the aminopiperidine **74** was being taken through to a single product (see Section 6.6.2), plans to diversify after this point (see Section 6.8.2) would have been hindered. Therefore, efforts were directed towards improving this process.

An opportunity for improvement presented itself when 3-piperidinol **75** was subjected to the existing conditions, in an attempt to form an analogue of the piperidine compounds with an alcohol at the 3-position. In this case the dicarbonyl intermediate **73** was very polar and proved difficult to extract from the aqueous phase during workup. Instead, the aqueous layer was evaporated and the intermediate was telescoped into the second step, resulting in a very poor yield of 2% over the two steps (Scheme 23).



Scheme 23. First attempt at synthesis of 3-piperidinol isoxazole 76.

While the yield of this reaction was not promising, telescoping the chemistry had potential to streamline the process. However, the use of DMF as the solvent in the first step was not ideal as it was difficult to remove from the polar intermediate and significant amounts were taken through to the subsequent cyclisation step. Therefore, a small solvent screen was performed to determine if another, more volatile, solvent could take its place (Table 3).

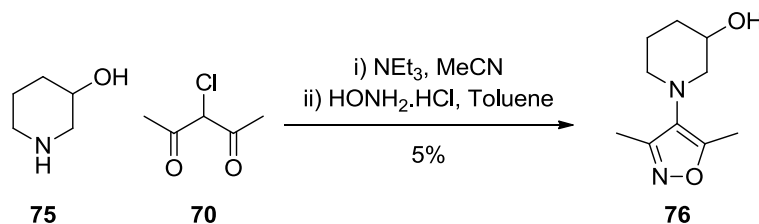
Solvent	Concentration / M	LCMS Trace Integration of 77 / %
Acetone	0.5	91
Acetonitrile	0.5	94
Ethanol	1	100
Ethyl Acetate	0.3	94*

Table 3. Alkylation solvent screen: 3-piperidinol 75 (100 mg, 1 mmol), NEt₃ (1.1 eq.) and 3-chloropentane-2,4-dione 70 (1.2 eq.) in the specified solvent were stirred at RT under nitrogen for 24 h and aliquots were analysed by LCMS. *Value adjusted to discount ethyl acetate peak.

Four polar solvents were chosen: acetone, acetonitrile, ethanol and ethyl acetate, and the reactions run for 24 h at room temperature. The reaction mixtures were then analysed by LCMS. It should be noted that the amine starting material was not UV active, so conversion could not be determined by this method alone. Therefore, LCMS was only being used to estimate how cleanly product was formed. The alkylating agent 70, however, was UV active so extent of the reaction was judged to a degree by its depletion over time.

At first glance, ethanol appeared to give the cleanest product. However, the absorption in the UV trace was much weaker than for the other solvents, and alkylating agent 70 had been consumed. Inspection of the literature showed multiple examples of alkylation of phenols and carboxylic acids with this reagent, so it is highly likely that it was reacting with ethanol, and therefore this result was discounted.^{125,126}

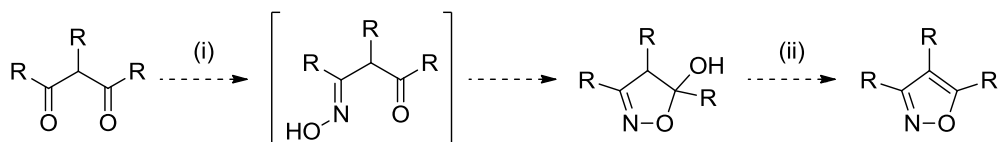
Ethyl acetate was discarded due to poor solubility of the amine, and acetonitrile was chosen over acetone due to marginally cleaner conversion. Acetonitrile was then applied to the isoxazole formation process, and was removed with ease after the alkylation. In place of an aqueous workup this residue was dissolved in ethyl acetate and filtered to remove the insoluble triethylamine hydrochloride, before being telescoped into the isoxazole cyclisation step (Scheme 24).



Scheme 24. Second attempt at synthesis of 3-piperidinol isoxazole 76.

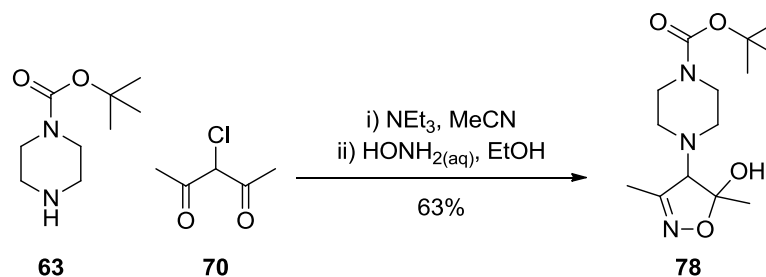
This second attempt at synthesising the 3-piperidinol congener **76** proceeded with a 5% overall yield. This minimal improvement (3% increase over the first attempt) still resulted in an impractical yield; therefore, the second step of the process was reinvestigated.

While previous attempts had been focussed on forming the isoxazole from the 1,3-dicarbonyl with one set of conditions, further examination of the literature showed a number of examples where a two-step approach was used, whereby, after the oxime formation and cyclisation, a change in conditions was required for the elimination of the second molecule of water (Scheme 25).^{127–131}



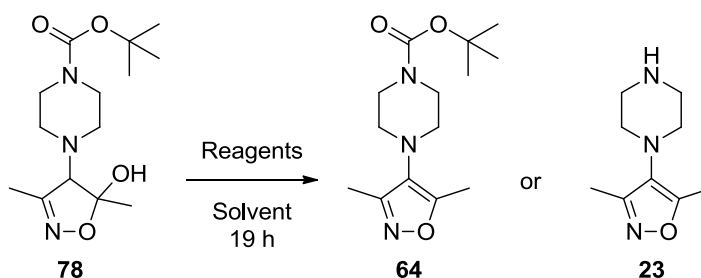
Scheme 25. Two step approach to the formation of an isoxazole from a 1,3-dicarbonyl.

During initial investigations, a set of conditions had been trialled in which a 1,3-dicarbonyl was heated in ethanol with aqueous hydroxylamine. LCMS analysis provided a mass ion which was consistent with the intermediate under discussion, in which the second water molecule had not been eliminated. This line of enquiry was not pursued at the time as hydroxylamine hydrochloride was found to form the isoxazole in one step, albeit in poor yield. This experiment was reperformed in order to isolate this intermediate **78** (Scheme 26).

Scheme 26. Formation of hydroxydihydroisoxazole **78**.

The new conditions for dicarbonyl formation were applied, which was telescoped into the next step. The residue was heated to reflux in ethanol with an excess of aqueous hydroxylamine until all the dicarbonyl was consumed. The hydroxydihydroisoxazole **78** was isolated in a good yield of 63% (Scheme 26). NMR analysis was consistent with the suggested structure, with two diastereomers of the dihydroisoxazole moiety distinguishable in both the ^1H and ^{13}C spectra, in a roughly 4:3 ratio.

In order to eliminate water and form the aromatic system, five sets of literature conditions were screened in parallel. These included acidic conditions with sulfuric acid or TFA, basic conditions with sodium carbonate, and conditions that activated the alcohol as a leaving group with either mesyl chloride or tosyl chloride (Table 4).¹²⁷⁻¹³¹



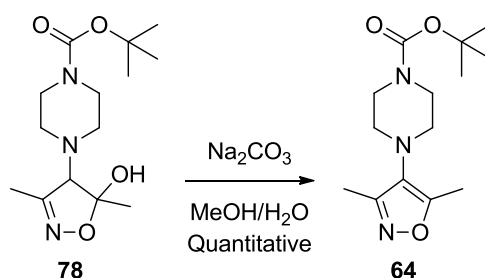
Reagent	Solvent	Temp.	LCMS Trace Integration / %			
			64	23		
1 Sulfuric acid	1 mL	-	-	96		
2 TFA	1 mL	DCM	2 mL	RT	-	100
3 Na ₂ CO ₃	2 eq.	1:1 MeOH:H ₂ O	4 mL	70 °C	100	-
4 MsCl, NET ₃	1.5 eq., 1.5 eq.	DCM	2 mL	RT	100	-
5 TsCl, NET ₃ , DMAP	1.0 eq., 2.0 eq., 0.1 eq.	MeCN	2 mL	RT	56*	-

Table 4. Elimination conditions screen: hydroxydihydroisoxazole **78** (100 mg, 0.33 mmol) was subjected to each set of conditions for 19 h. *Adjusted to exclude peaks known to correspond to tosic acid and DMAP.

The reactions were followed by LCMS, using the retention times of previously synthesised samples of product for reference. Both acidic conditions successfully

mediated the elimination to isoxazole, and, as expected, also removed the Boc group to give the unprotected piperazine product **23**. The sulfuric acid conditions resulted in minor side-product formation, while the TFA conditions showed clean conversion. The basic, sodium carbonate-mediated conditions also proceeded cleanly to product **64**, without the loss of the Boc group. The activation of the alcohol as a leaving group with mesyl chloride was successful, with full conversion observed. However, the tosyl chloride and catalytic DMAP strategy did not result in complete conversion and starting material was still present in the reaction mixture.

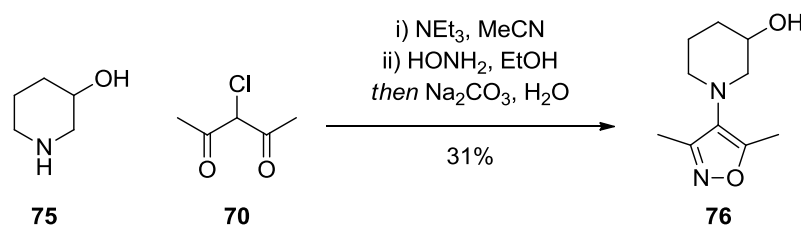
Of the successful conditions, sodium carbonate was chosen as the most convenient. The conditions were applied to 1.5 mmol of the hydroxydihydroisoxazole **78** and were found to proceed with quantitative yield, with no need for purification after workup (Scheme 27).



Scheme 27. Formation of isoxazole **64** from hydroxydihydroisoxazole **78**.

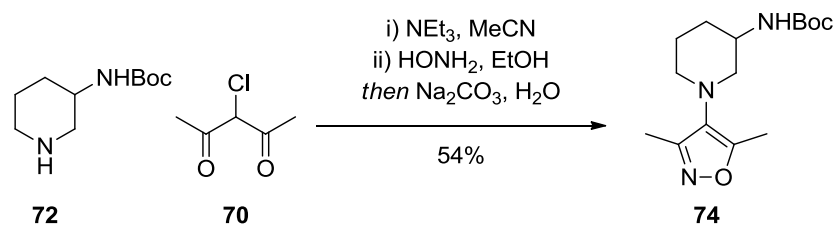
As the first step of the isoxazole cyclisation was performed in ethanol, it was envisioned that there would be no need for a solvent swap and sodium carbonate solution could be added once the intermediate had fully formed. A trial reaction was performed in order to confirm that ethanol could be used in place of methanol in the elimination, and LCMS analysis suggested full consumption of starting material.

This newly developed process was applied in full to the 3-piperidinol system and the product was isolated in a 31% yield (Scheme 28). This is a large improvement on the 2% and 5% achieved previously.



Scheme 28. Third attempt at synthesis of 3-piperidinol isoxazole **76**.

Subsequently, the conditions were applied to the 3-amino system in order to provide a sufficient batch of the desired intermediate **74** (Scheme 29).



Scheme 29. Large scale synthesis of Boc-protected 3-amino piperidine isoxazole **74**.

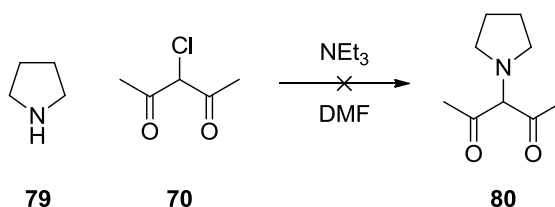
Gratifyingly, from 8.5 g of piperidine starting material **72** 6.8 g of the isoxazole-substituted piperidine product **74** were isolated, corresponding to a 54% yield. This is a vast improvement on the 13% yield achieved by the previous methodology (Scheme 22). Additionally, only one round of chromatography was performed, rather than two, and the reaction setup was simplified as the need for Dean-Stark apparatus had been removed. This new process represented a truly viable method for forming secondary cyclic amine-substituted dimethylisoxazole compounds on a useful scale.

With these two disconnection strategies established (isoxazole formation and amine alkylation), the synthesis of target compounds was carried out. For each target compound the merits of both disconnection were analysed and the most appropriate option chosen, based on the availability and reactivity of suitable starting materials. The routes to the core fragments shall now be presented, organised by ring size, starting with five-membered rings.

6.2 Core Fragment Synthesis

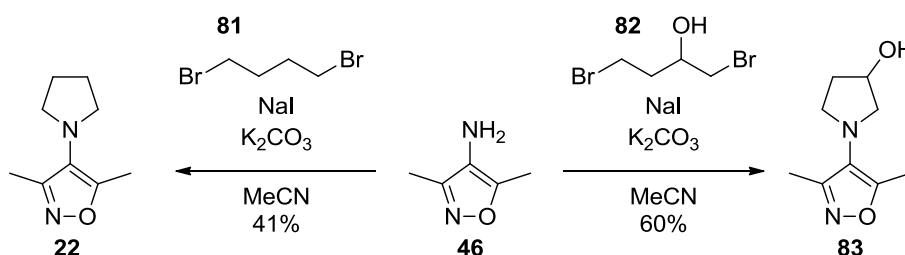
6.2.1 Five-Membered Rings

In order to synthesise pyrrolidine isoxazole analogue the cyclodehydration route was trialled first. However, pyrrolidine **79** was found not to react as expected with 3-chloro-2,4-pentanedione **70** in the first step of the synthetic sequence (Scheme 30). Instead, a multitude of products were formed, presumably *via* the formation of enamines and subsequent polymerisation.



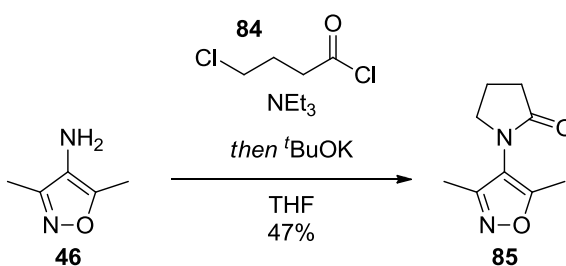
Scheme 30. Failed alkylation of pyrrolidine **79** to the 1,3-dicarbonyl derivative **80**.

Therefore, formation of the saturated ring was established as the most appropriate route. Two commercially available alkyl dihalides were identified to provide pyrrolidine **22** and 3-pyrrolidinol **83** analogues (Scheme 31).



Scheme 31. Synthesis of pyrrolidine **22** and 3-pyrrolidinol analogues **83**.

4-Chlorobutanoyl chloride **84** was also identified as a suitable alkylating agent, which contains both an acyl chloride and an alkyl chloride, and was used to form a 2-pyrrolidinone derivative **85** (Scheme 32).

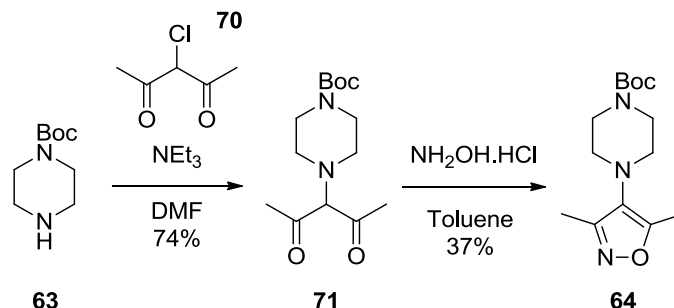


Scheme 32. Synthesis of 2-pyrrolidinone analogue **85**.

This reaction occurred in two stages. First the aminoisoxazole **46** was reacted with the acyl chloride moiety, using triethylamine as a base. Once this stage was complete, potassium *tert*-butoxide was added to mediate the displacement of the second chloride and form the product **85**.

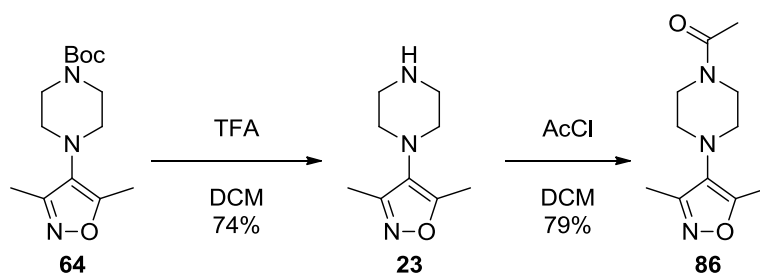
6.2.2 Six-Membered Rings

As has previously been shown, an *N*-Boc piperazine analogue **64** was synthesised *via* the isoxazole formation route (Scheme 33).



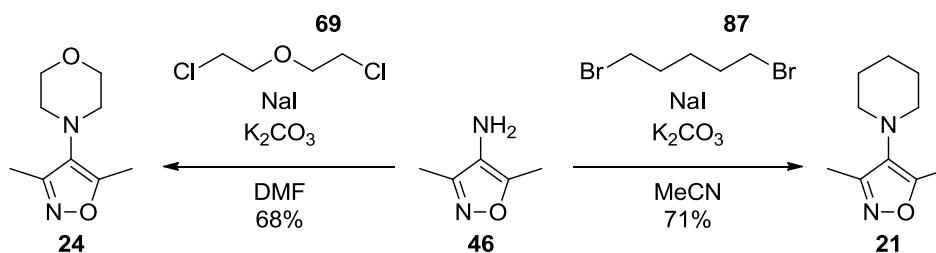
Scheme 33. Synthesis of *N*-Boc piperazine analogue **64**.

This analogue was subsequently deprotected to provide the free base piperazine **23**, which was acylated to provide an acetyl piperazine analogue **86** (Scheme 34).



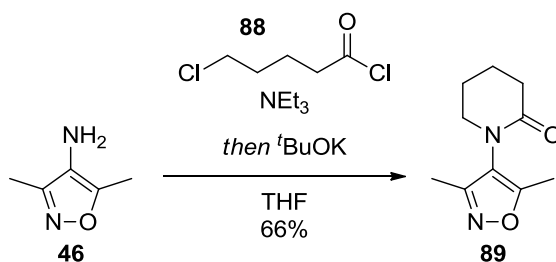
Scheme 34. Synthesis of free base **23** and acetyl **86** piperazine analogues.

The rest of the six-membered derivatives were synthesised *via* saturated ring formation. Along with the morpholine **24** previously shown, the piperidine **21** was also formed by reaction with an alkyl dihalide **87** (Scheme 35).

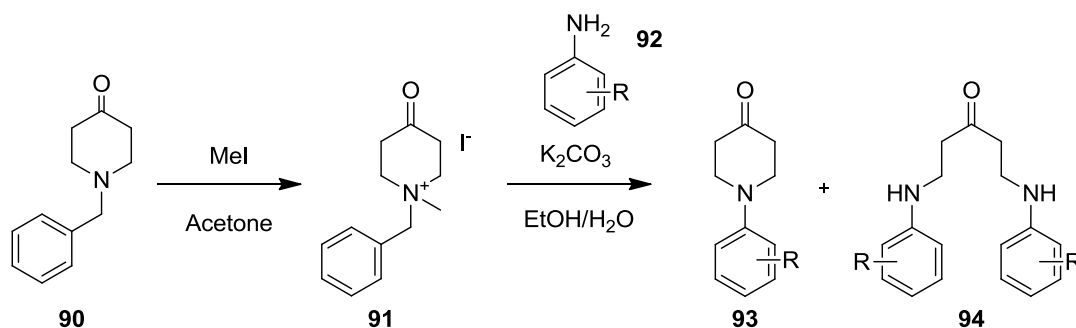


Scheme 35. Synthesis of morpholine **24** and piperidine **21** analogues.

As with the five-membered system, an alkylating agent **88** was available for synthesising a six-membered lactam. The 2-piperidinone **89** was formed in the same two-stage reaction process as used previously (Scheme 36).

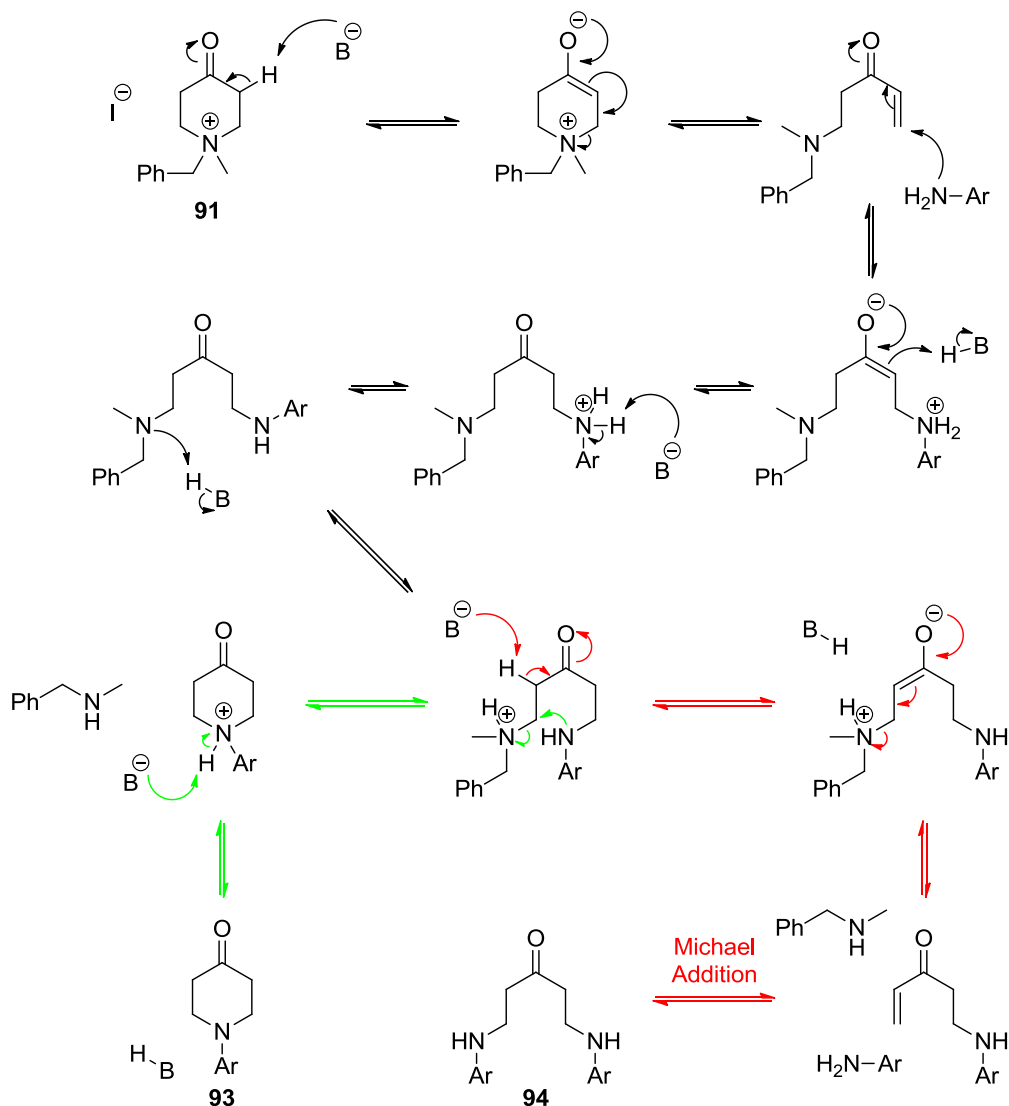
Scheme 36. Synthesis of the piperidin-2-one analogue **89**.

In efforts to seek alternative pathways to target compounds, a literature search revealed an unusual electrophile to react with aminoisoxazole **46**. An interesting method published by Tortolani and Poss describes the synthesis of *N*-aryl 4-piperidinones **93** (Scheme 37).¹³²

Scheme 37. Published synthesis of *N*-aryl 4-piperidinones **93**.

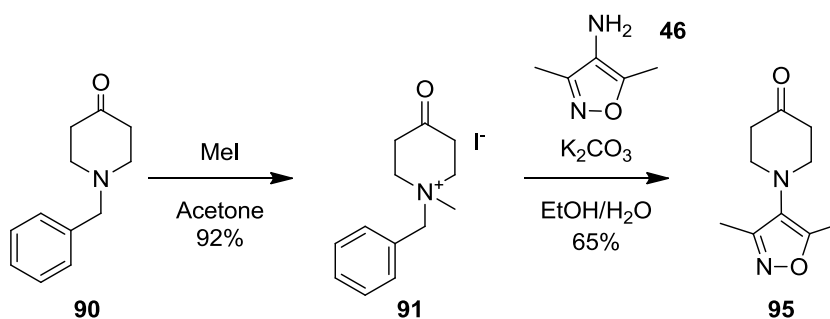
The authors added iodomethane to *N*-benzylpiperidone **90** to form a quaternary ammonium salt **91**. They then reacted this with various substituted anilines **92** in the presence of a base, to give *N*-aryl-substituted 4-piperidinones **93**, and in some cases a side-product **94**.

The reaction is thought to proceed *via* a base-catalysed Hofmann elimination to form a transient Michael acceptor, which is attacked by the amine (Scheme 38).¹³² The resulting secondary amine then displaces benzylmethylamine to give the tertiary aniline **93**. In some cases, the cyclisation does not occur before a second Hofmann elimination and amine addition, which results in the formation of bis secondary aniline **94**. This side-product was mainly observed when the substituted aniline was of an electron-deficient nature, or sterically hindered.¹³²



Scheme 38. Putative mechanism for the formation of 4-piperidinones **93** (green route) and the observed side product **94** (red route). B represents a base.

The reaction conditions were applied to the aminoisoxazole **46** and were found to be successful (Scheme 39).

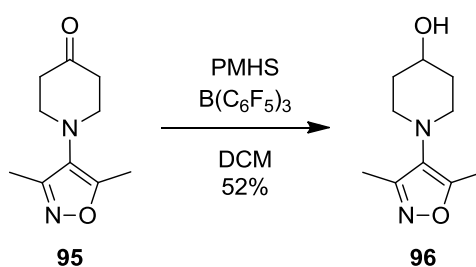


Scheme 39. Synthesis of the 4-piperidinone analogue **95**.

The published conditions had to be adapted to improve the yield with this system. Using the suggested 1.5 equivalents of quaternary ammonium salt **91** only provided a 38%

yield, with unreacted amine remaining in the reaction mixture. Therefore, the reaction was conducted with 3 equivalents, which provided an improved 65% yield, with respect to the amine **46**. This process had the potential to be highly useful as the ketone functionality could provide a handle for introducing substituents to the ring.

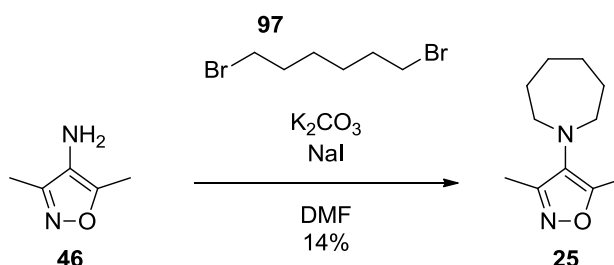
A final six-membered analogue was isolated by reducing the ketone of the above piperidinone **95** to an alcohol, providing the 4-piperidinol **96** (Scheme 40). This product was formed during an attempt to reduce the ketone to a methylene using a combination of polymethylhydrosiloxane (PMHS) and $B(C_6F_5)_3$.¹³³



Scheme 40. Reduction of 4-piperidinone **95** to 4-piperidinol **96**.

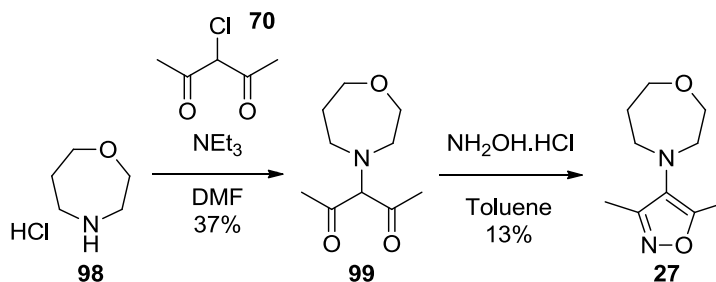
6.2.3 Seven-Membered Rings

The first seven-membered analogue was synthesised by formation of the saturated ring using a straight chain alkyl dihalide **97**, providing the azepane analogue **25** (Scheme 41).

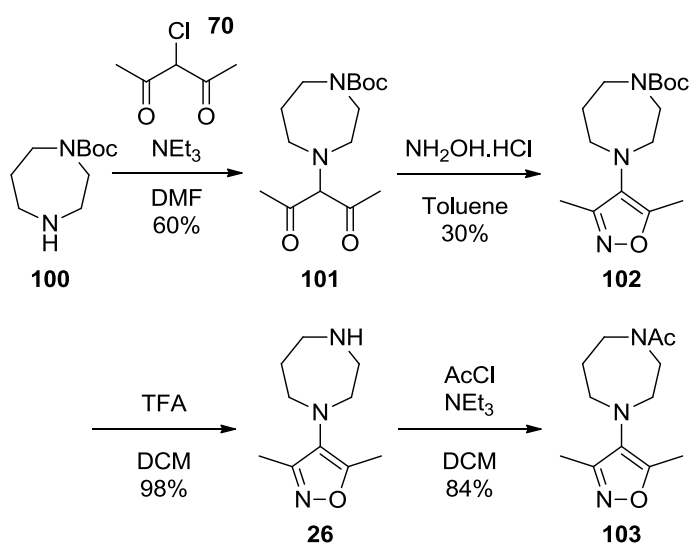


Scheme 41. Synthesis of the azepane analogue **25**.

Suitable dihalide reagents for the synthesis of the homomorpholine **27** (Scheme 42) and homopiperazine **26** (Scheme 43) targets were not readily available. Therefore, the isoxazole formation route was applied, firstly to homomorpholine hydrochloride **98** to provide the homomorpholine analogue **27** (Scheme 42).

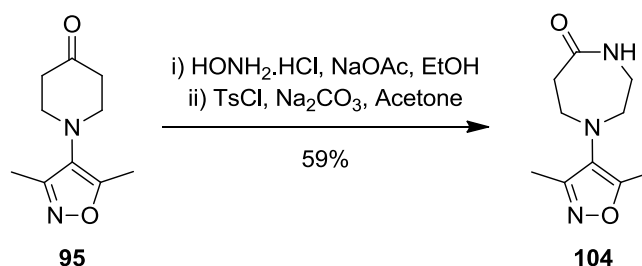
Scheme 42. Synthesis of the homomorpholine analogue **27**.

As with the synthesis of the piperazines, an *N*-Boc protected homopiperazine **100** was used (Scheme 43). The product **102** was subsequently deprotected to the free base **26** and acylated to provide the acetyl homopiperazine **103**.



Scheme 43. Synthesis of the homopiperazine analogues.

A final seven-membered analogue was formed by ring expansion of the versatile 4-piperidinone compound **95** (Scheme 44).

Scheme 44. Synthesis of a lactam analogue **104** by ring expansion of the 4-piperidinone **95**.

An oxime was formed with hydroxylamine hydrochloride, in the presence of a base. The oxime was then tosylated, providing a good leaving group and triggering a Beckmann rearrangement to provide a lactam analogue **104**.

Using a range of chemistry, centred on the two key disconnection strategies identified as being practicable, all the desired fragments were synthesised and isolated. As well as those molecules originally targeted, a number of fragments were prepared based on the opportunistic use of available starting materials and interesting synthetic procedures. Among these was a versatile ketone **95**, and the synthetic procedure to isolate this was optimised to improve the yield as it was envisaged that it would be a useful intermediate at a later stage of research. These additional fragments resulted in a larger set of data to support the decision of which framework to investigate further. This decision was aided by a combination of biological data, X-ray crystallography and synthetic considerations.

6.3 Prioritisation of Core

The core fragments were submitted for screening in the biological assays for BRD4 BD1 and BD2. While the regular assays have a lower pIC₅₀ limit of 4.3 it was expected that these compounds would have low affinity due to their small size, hence they were run in a modified assay with a higher concentration of compound, giving a lower pIC₅₀ limit of 3.3. The phenylisoxazole fragment **19** was also tested, for comparison, and all of the results are displayed in Figure 23.

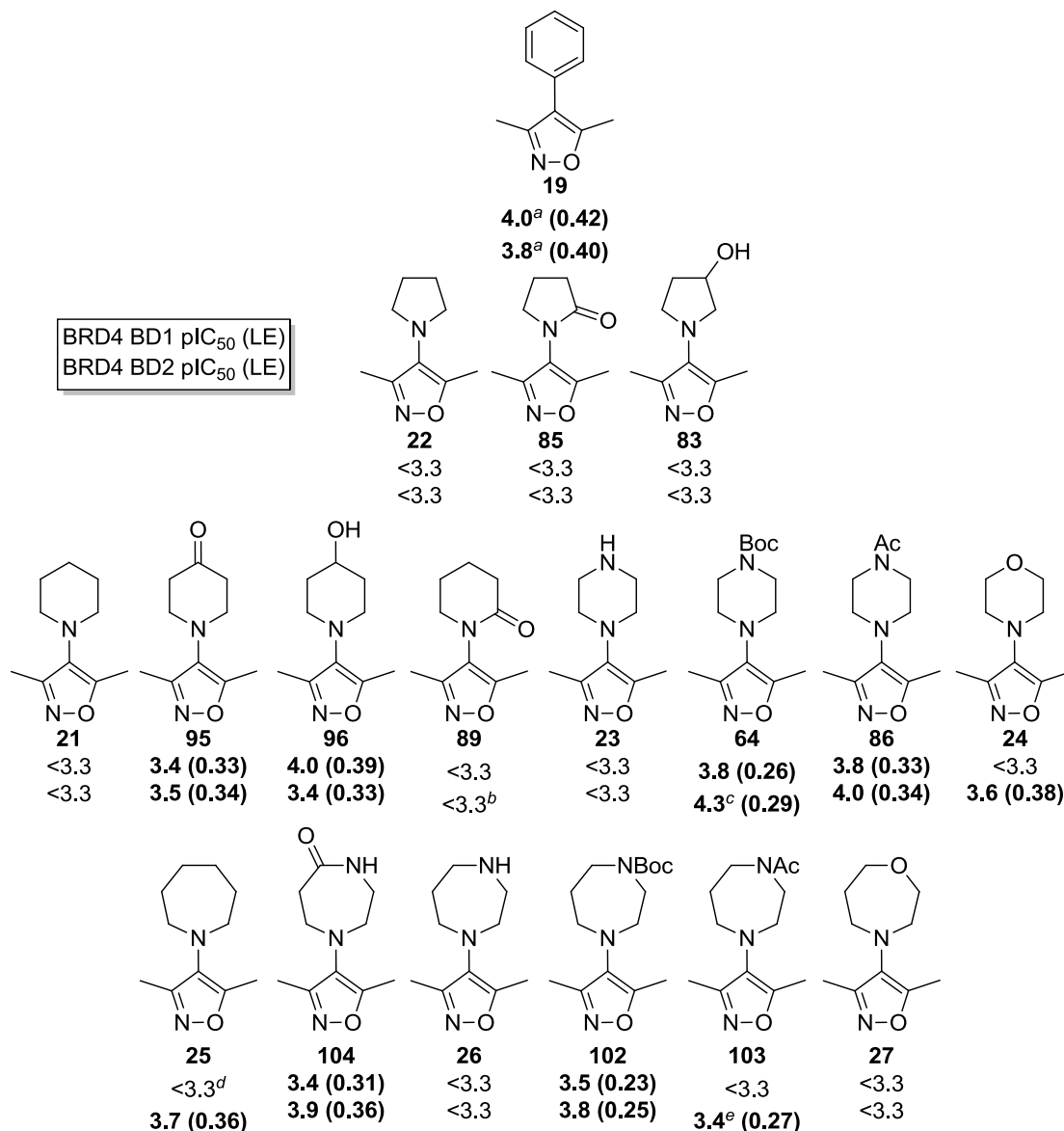


Figure 23. Assay data and calculated ligand efficiency (LE) for core fragments. ^aValue based on two high concentration test occasions, rather than three or more. ^bA pIC₅₀ value of 3.5 was determined on one test occasion of out three and was excluded from the reported value. ^cA pIC₅₀ value of <4.3 was determined on one test occasion out of 6 and was excluded from the reported mean value. ^dpIC₅₀ values of 3.5 and 3.7 were determined on two test occasions out of five and were excluded from the reported value. ^eA pIC₅₀ value of <3.3 was determined on one test occasion out of three and was excluded from the reported mean value.

Included in Figure 23 is a calculated value called ligand efficiency (LE). LE is a ligand metric derived as the Gibbs free energy of binding per heavy atom, calculated as the pIC_{50} divided by the Heavy Atom Count (HAC), multiplied by a constant (Equation 4).¹³⁴

$$\text{LE} = \frac{1.37 \times \text{pIC}_{50}}{\text{HAC}}$$

Equation 4.

LE is a useful guide through drug development to help assess whether increases in molecular size are delivering reasonable increases in target potency, thus preventing medicinal chemists from designing needlessly large molecules which could have unfavourable physicochemical properties. It is also useful in assessing whether small, weakly binding fragments are actually providing a good degree of potency in proportion to their size.¹³⁴ Generally, LE values greater than 0.30 are deemed acceptable for drug candidates, with lead compounds having values in this region or higher, such that favourable values can be maintained through lead optimisation.^{90,134} Of course, LE is only a tool and should not be the sole factor considered;¹³⁵ once higher potencies were achieved in this research programme other properties were also examined.

Pleasingly, a number of the fragments register on the assay and have comparable potency to the phenylisoxazole comparator **19** (Figure 23), which returned pIC_{50} values of 4.0 and 3.8 at BRD4 BD1 and BD2, respectively. At this stage, the ring sizes needed to be ranked in order to decide which system to progress.

None of the five-membered rings registered on the high concentration assay. As the potencies achieved by analogues with larger ring sizes were very close to the lower limit of the assay this did not necessarily mean that the five-membered rings were not binding, but it did not provide any assurance that elaboration of this ring size would be a successful endeavour. This, in combination with the fact that only one of the two disconnections could be utilised for five-membered ring systems made them the least attractive for progression, and therefore no further work was performed on them.

On the other hand, examples of both the six- and seven-membered ring systems both displayed similar or higher potencies to the phenylisoxazole **19**. X-ray crystal structures were obtained in the binding site of BRD2 BD2, and those for the morpholine **24** and homomorpholine **27** are shown in Figure 24A and B, respectively.

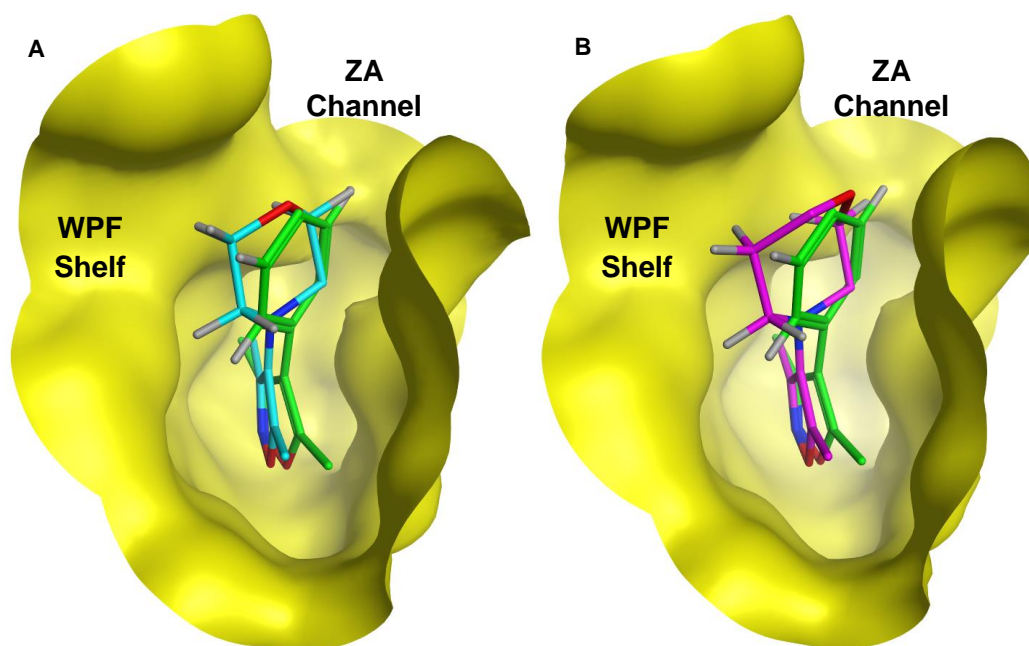


Figure 24. A) X-ray crystal structure of the morpholine analogue **24** (cyan) bound to BRD2 BD2 (yellow). The WPF shelf and ZA channel are marked. The dimethylisoxazole moiety is bound as expected, with hydrogen bonds to Asn429 and *via* water to Tyr386 (not shown). The image is superposed with the structure of phenyl isoxazole **19** (green) bound to BRD2 BD1. For clarity BRD2 BD1 and water molecules have been removed from the image. B) A similar image with homomorpholine analogue **27** (magenta) bound to BRD2 BD2, superposed with phenylisoxazole **19** (green) bound to BRD2 BD1.

The binding mode of the isoxazole in both cases was as expected, with hydrogen bonds to the asparagine and *via* water to the tyrosine. Both images have been superposed with the X-ray crystal structure of the phenylisoxazole comparator **19** bound to BRD2 BD1. Hydrogen atoms on the rings have been shown in order to demonstrate the potential vectors for substitution, and that those offered by the saturated rings are different to those offered by the phenyl ring, allowing for exploration of subtly different areas of space in the binding site.

Figure 25 shows a view from above the binding site, with the structures of the morpholine **24** and homomorpholine **27** analogues superposed in order to compare the vectors.

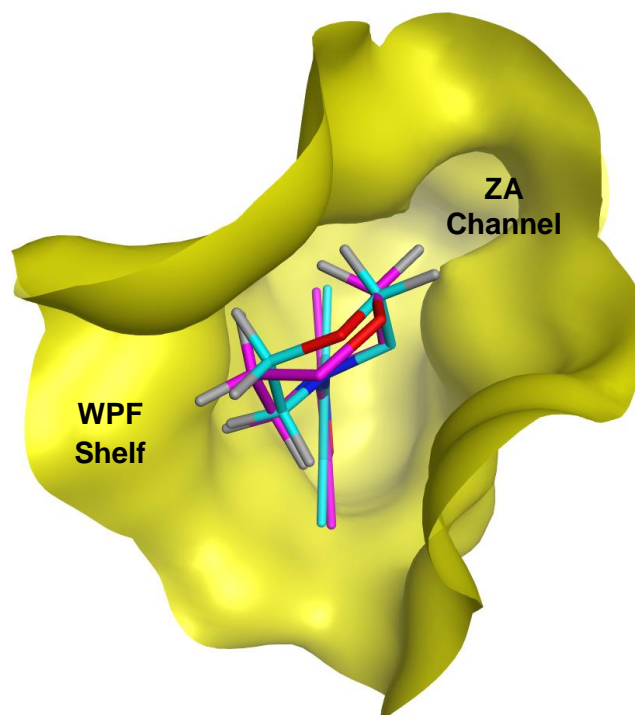


Figure 25. X-ray crystal structure of the morpholine analogue **24** (cyan) bound to BRD2 BD2 (yellow). The WPF shelf and ZA channel are marked. The image is superposed with the structure of the homomorpholine analogue **27** (magenta) also bound to BRD2 BD2. For clarity, water molecules have been removed from the image.

Both saturated rings offered similar vectors in the region of the WPF shelf, which is the area where the most potency was expected to be gained. The vectors directed towards the ZA channel were also similar. Taken together with the biological assay data, the structural information could not distinguish between the six- and seven-membered ring sizes. Therefore, the decision was made from a practical perspective: six-membered, nitrogen-containing, saturated heterocycles are more readily available than their seven-membered counterparts, and the chemistry surrounding them has been more widely published, therefore this ring size was pursued. This left the option open to return to seven-membered rings should an adequate potency level not be achieved.

At this juncture, structural information was analysed to help prioritise which particular six-membered core to progress. Alongside the morpholine **24**, X-ray crystal structures were obtained for the 4-piperidinone **95** and the *N*-acetyl piperazine **86**. These are shown together in Figure 26.

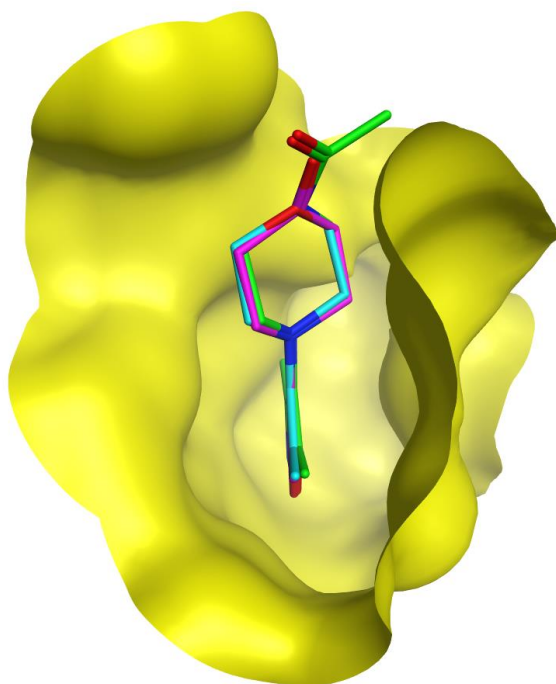


Figure 26. X-ray crystal structure of the morpholine analogue **24** (cyan) bound to BRD2 BD2 (yellow). The image is superposed with the structures of the 4-piperidinone analogue **95** (magenta) and the *N*-acetyl piperazine analogue **86** (green), also bound to BRD2 BD2. For clarity, water molecules have been removed from the image.

From this superposition, it was clear that the binding modes of the different heterorings were identical and, therefore, could not be differentiated for further exploration. The most potent compounds in the biological assay were the *N*-Boc **64** and *N*-acetyl **86** piperazines, and the crystal structure suggests that this may be due to an edge-to-face π -interaction between the face of the carbonyl and the edge of the adjacent tryptophan (W of the WPF shelf). However, the functional handle provided by the ketone moiety of the 4-piperidinone compound **95** allowed a plausible way to synthesise analogues to probe for the WPF shelf, after which the ketone could be reduced to a methylene group. Therefore, a piperidine framework was pursued, with the expectation that SARs generated with this heteroring could be applied to the piperazines at a later date.

6.4 Extension to the WPF Shelf

The X-ray crystal structures solved for the unsubstituted six-membered heterorings (Figure 26) indicated that the vector from the 3-position would best provide access to the WPF shelf. Accordingly, a set of target molecules containing substituents at the piperidine 3-position were devised with the aim of gaining potency (Figure 27).

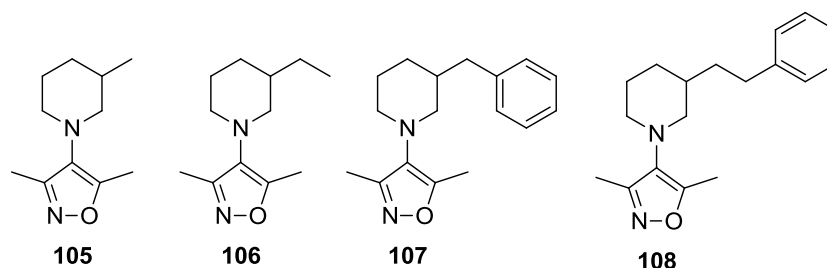
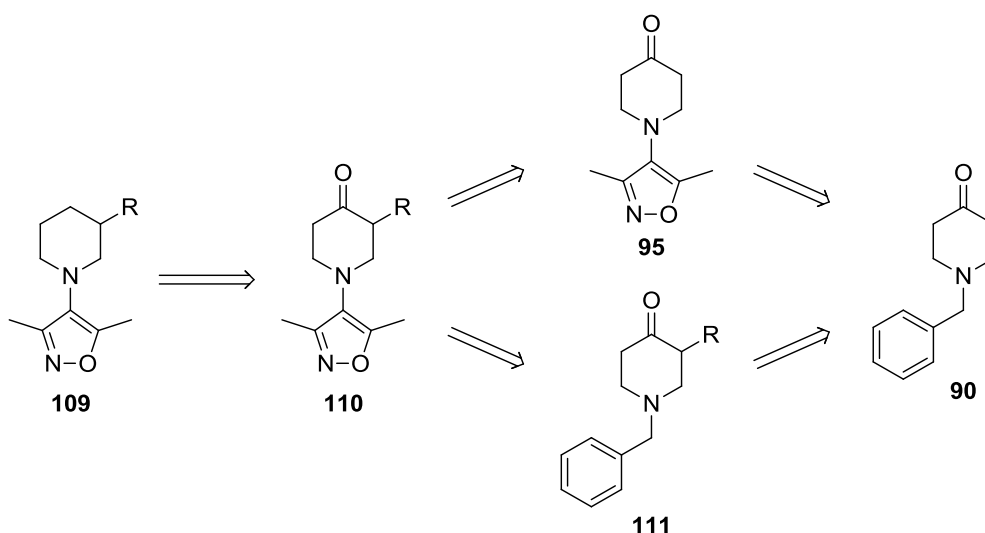


Figure 27. Target compounds to probe for the WPF shelf.

Groups of incrementally increasing size were selected in order to give a better understanding of the Structure-Activity Relationship (SAR) data generated. These included a methyl **105** and an ethyl **106** group, which were not expected to result in a significant interaction with the shelf, as well as benzyl **107** and phenethyl **108** groups. The phenyl ring of these compounds was intended to occupy the WPF shelf, with either a one or two carbon linker from the piperidine 3-position. Docking experiments performed within our laboratories indicated that either of these linker lengths was capable of placing the phenyl group on the shelf, but a three carbon chain would be unnecessarily long and result in poor binding.¹³⁶

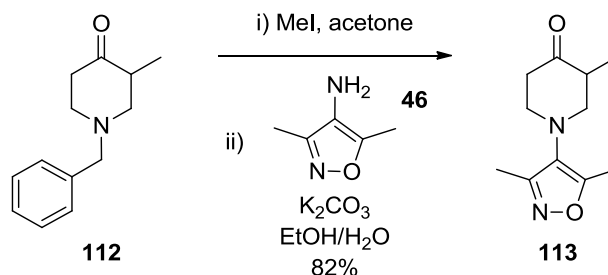
The planned synthetic routes to these compounds utilised the 4-piperidinone compound **95** that was previously isolated, which itself derived from *N*-benzyl 4-piperidinone **90** (Scheme 45).



Scheme 45. Retrosynthesis of 3-substituted piperidine isoxazoles 109.

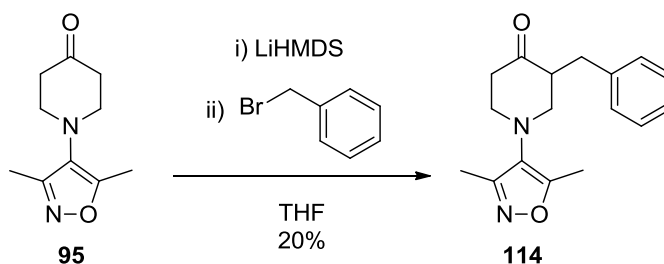
Enolate alkylation chemistry could be used to append the desired group α to the ketone, either before or after the substitution of the isoxazole. From there the reduction of the carbonyl to a methylene would provide the target compounds **109**.

To synthesise the methyl congener **105**, advantage was taken of the commercial availability of the appropriate *N*-benzyl 4-piperidinone **112** (Scheme 46). The piperidone was alkylated with iodomethane to provide the intermediate ammonium salt, which was taken into the second step without purification. The reaction with the aminoisoxazole **46** in the presence of base provided the desired product **113** in an 82% yield.



Scheme 46. Synthesis of methyl-substituted piperidinone **113**.

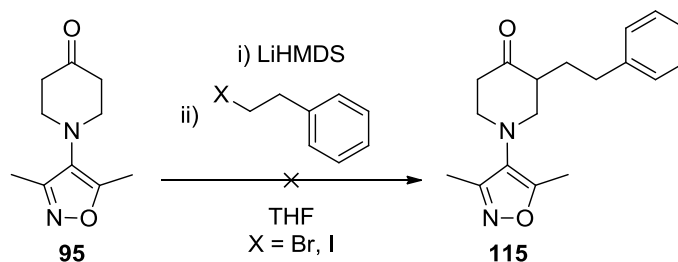
The benzyl piperidinone **114** was synthesised *via* lithium enolate chemistry from the unsubstituted piperidinone **95** (Scheme 47). Initially, LDA was used as the base to form the lithium enolate, and alkylation appeared to be successful. However, after purification the ¹H NMR showed a complex mixture of products. It was thought that LDA, with a pK_{aH} of 36,¹³⁷ was too strong a base and was deprotonating one of the methyl groups on the isoxazole ring, which have a predicted pK_a of 35.¹⁰¹ To avoid this, the base was replaced with LiHMDS which has a lower pK_{aH} of 26,¹³⁷ which is still sufficient to deprotonate the position α to the ketone, which possessed a calculated pK_a of 19.¹⁰¹



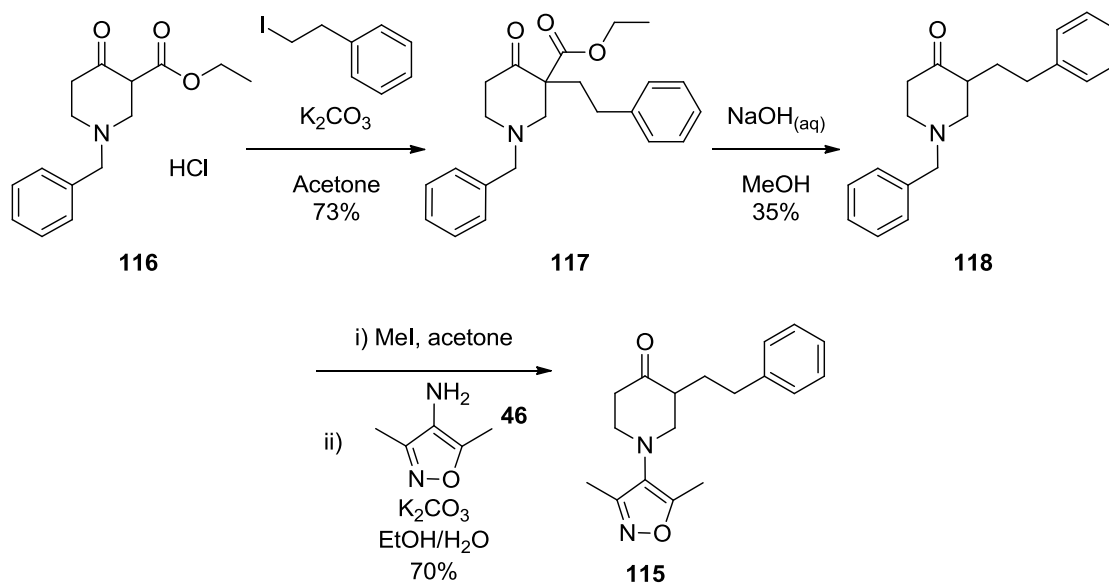
Scheme 47. Synthesis of benzyl-substituted piperidinone **114**.

By this method, the benzyl piperidinone **114** was isolated in a low yield (20%). The remainder of the mass balance consisted largely of the bis- and tris-polyalkylation byproducts, and unreacted starting material, according to LCMS analysis of the reaction mixture.

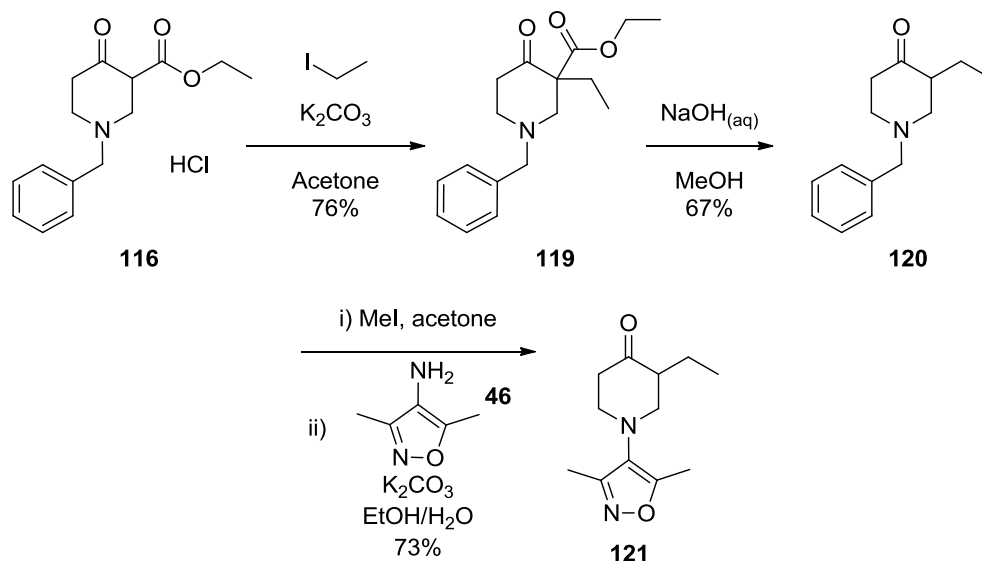
Attempts to apply this methodology to prepare the phenethyl congener **115** were unsuccessful. Neither phenethyl bromide nor iodide were sufficiently reactive electrophiles to allow reaction with the lithium enolate to occur (Scheme 48).

Scheme 48. Failed synthesis of phenethyl piperidinone **115**.

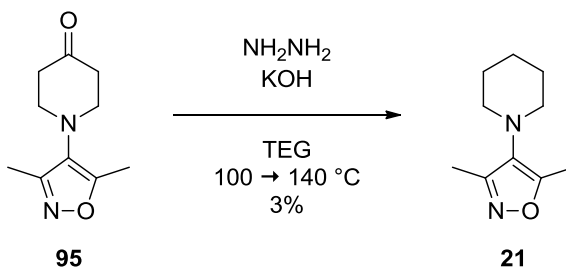
An alternative route to this compound was designed, using the commercially available β -keto ester **116** as a precursor and installing the isoxazole as the final step (Scheme 49).

Scheme 49. Synthesis of phenethyl piperidinone isoxazole **115**.

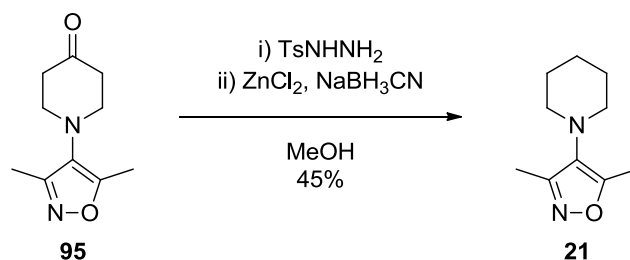
The β -keto ester functionality allowed for selective monoalkylation with phenethyl iodide, with the aid of a mild base, to provide alkylation product **117** an isolated yield of 73%. The ester was then hydrolysed in a sodium hydroxide solution, with subsequent decarboxylation, to provide phenethyl-substituted *N*-benzyl piperidinone **118** in 35% yield. The aminoisoxazole **46** was then alkylated with the quaternary ammonium salt of **118**, offering phenethyl **115** in a 70% yield. This route was also applied to the synthesis of the ethyl-substituted derivative **121**, where similar yields were obtained for the two alkylation steps, but with a greater yield for the decarboxylation step of 67% (Scheme 50).

Scheme 50. Synthesis of ethyl-substituted piperidinone **121**.

In order to reduce the carbonyl group out of these compounds, conditions were first trialled on the unsubstituted piperidinone **95** (Scheme 51). Initially, standard Wolff-Kishner conditions were applied, but alongside the product **21**, multiple other species were formed, possibly due to the high temperatures and strong base used. After complete consumption of the starting material, the product was only isolated in a 3% yield.

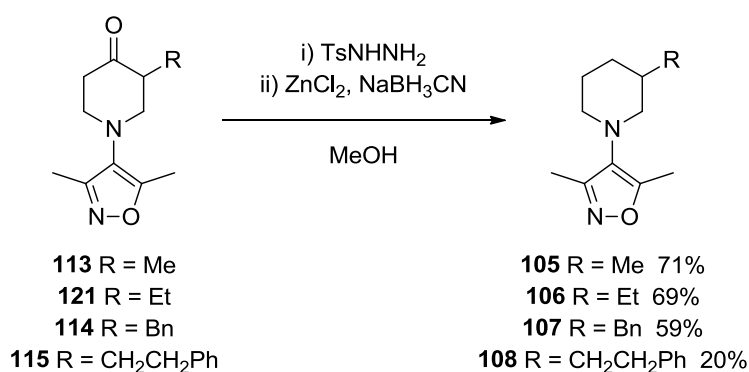
Scheme 51. Wolff-Kishner conditions for the reduction of piperidinone **95** to piperidine **21**.

Such forcing reduction conditions were suspected to be the cause of the low isolated yield, so the literature was consulted for a milder method. A modified version of the Wolff-Kishner reduction was published by Kim *et al.* which involved the formation of a tosylhydrazone followed by reduction with a mixture of zinc chloride and sodium cyanoborohydride.¹³⁸ When applied to the piperidinone **95**, these milder conditions provided the piperidine **21** in an isolated yield of 45% (Scheme 52).



Scheme 52. Reduction of piperidinone 95 to piperidine 21 using modified Wolff-Kishner conditions.

Using these conditions, the four substituted piperidinone compounds were reduced to the associated piperidines (Scheme 53). Yields were moderate to good, other than the phenethyl congener **108** which was only isolated in a 20% yield.



Scheme 53. Reduction of substituted piperidinones to substituted piperidines.

The substituted piperidines were submitted for biological screening and the results are shown in Figure 28.

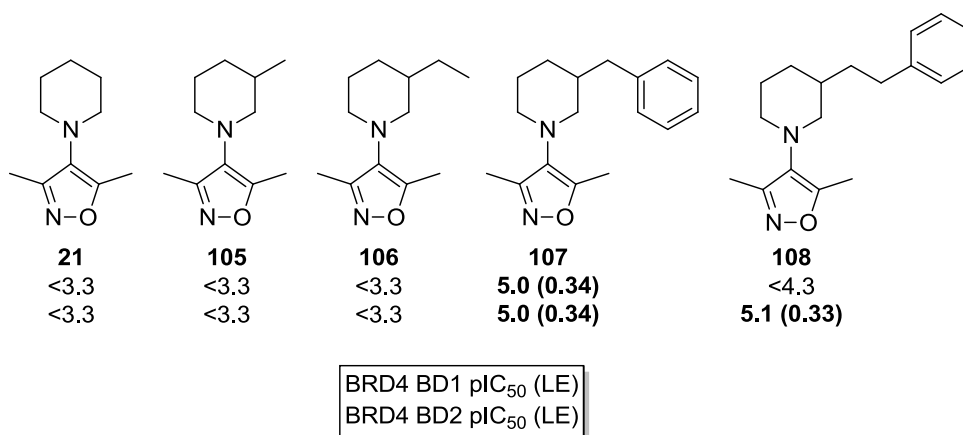


Figure 28. Assay data and ligand efficiencies for the piperidine analogues.

Neither the methyl nor ethyl groups provided any measurable boost in potency over the unsubstituted piperidine, but this was unsurprising as neither substituent was sufficiently long to interact with the WPF shelf, according to initial modelling. The two phenyl ring-containing compounds **107/108**, on the other hand, both displayed activity. The benzyl compound **107** displayed the same activity (pIC₅₀ = 5.0) at both BRD4 BD1

and BD2, which equated to LE values of 0.34, which is above the accepted lower limit of 0.30. The phenethyl compound showed a similar potency at BD2, with a pIC_{50} of 5.1, but does not register above $pIC_{50} = 4.3$ at BD1. The greater activity observed at BRD4 BD2 over BD1 was an interesting result, but at that time in the research project this was not pursued further due to the focus on targeting pan-BET inhibition. However, these data were re-evaluated at a later stage of the research when their significance became clearer.

It was evident from these data that a one-atom linker was sufficient to place the phenyl group onto the WPF shelf. This was corroborated by the X-ray crystal structure that was obtained of the benzyl piperidine **107** in the binding site of BRD2 BD2 which confirmed that the group was indeed bound to the shelf (Figure 29).

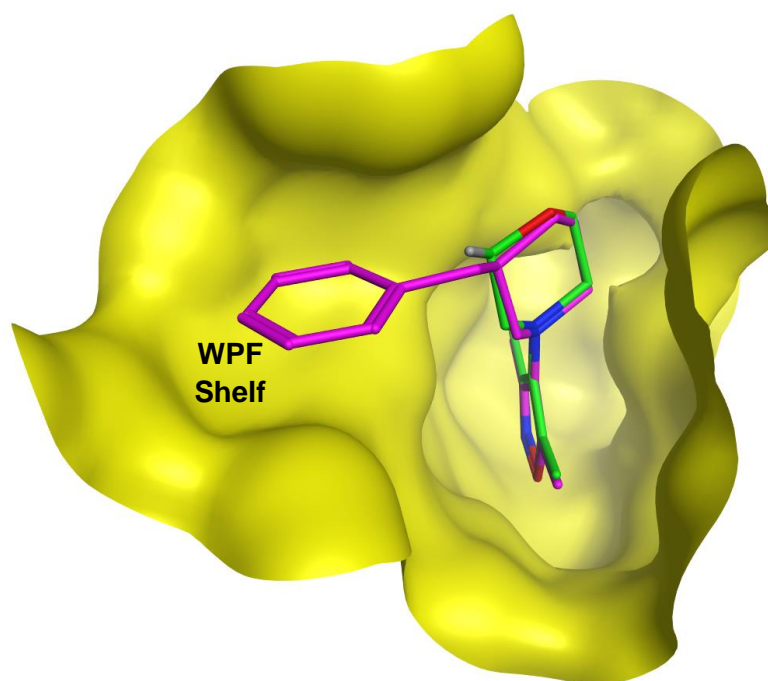
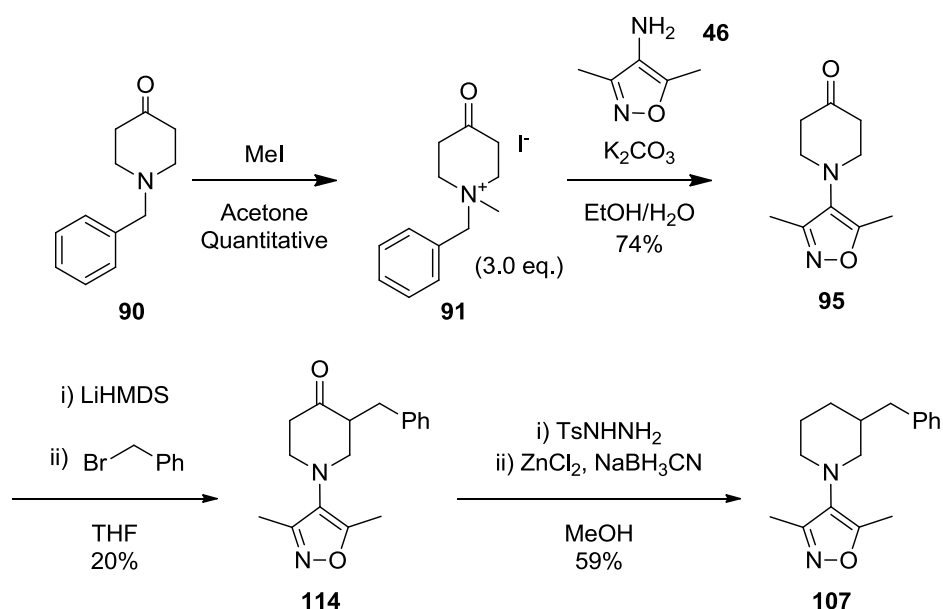


Figure 29. X-ray crystal structure of the benzyl piperidine **107** (magenta) bound to BRD2 BD2 (yellow). The image is superposed with the structures of the morpholine analogue **24** (green), also bound to BRD2 BD2. For clarity, water molecules have been removed from the image.

The crystal structure of the morpholine analogue **24** was superposed over that of the benzyl piperidine **107** and highlighted the similar binding mode of the isoxazoles and conformation of the saturated rings. It was clear from the overlay that binding of the phenyl ring to the WPF shelf did not necessitate a change from either the chair conformation of the piperidine ring or the torsion angle between the piperidine and isoxazole rings.

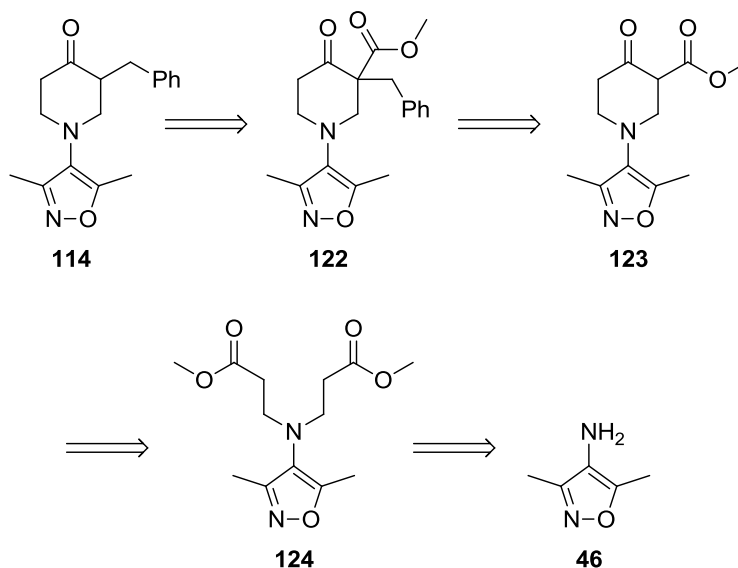
The X-ray crystal structure solved for the benzyl piperidine **107** (Figure 29) resulted from soaks of a racemic mixture. However, density was observed only for the *R*-enantiomer, which suggested that this isomer was more potent than the *S*-enantiomer.

Therefore, separation of the racemate was sought, to determine the activities of the individual enantiomers. This required a resynthesis to obtain sufficient material, which was taken as an opportunity to improve the synthetic route, which is detailed in Scheme 54.



Scheme 54. Full synthesis of benzyl piperidine 107.

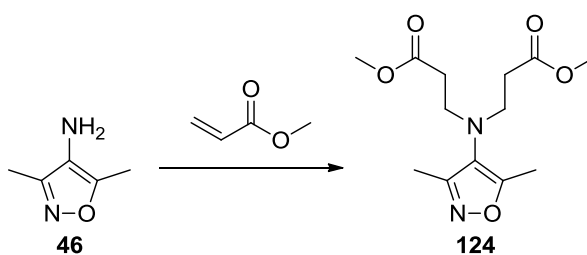
The two main drawbacks of this route are the requirement for three equivalents of the ammonium salt in order to achieve an acceptable yield, with respect to the aminoisoxazole **46**, and the poor yield of the enolate alkylation step, which was due to polyalkylation. A positive aspect of the route was the late-stage installation of the benzyl group, which was a potential area for introducing variability. Accordingly, a new route was devised to the benzyl piperidinone **114**, aiming to avoid these issues while retaining the ability to variably functionalise the 3-position later in the synthetic sequence (Scheme 55).



Scheme 55. Retrosynthesis of benzyl piperidinone 114 via an isoxazole-containing β -keto ester intermediate 123.

Inspiration was taken from the previous use of the β -keto ester functionality to promote high yielding monoalkylation (Scheme 49, p63). It was envisioned that this could be installed in a compound already containing the isoxazole, to avoid the losses associated with the benzyl ammonium salt route, by alkylating the aminoisoxazole **46** and performing a Dieckmann condensation.

A range of conditions were trialled to elicit the bis-alkylation of the aminoisoxazole **46** with methyl acrylate, and these are summarised in Table 5.



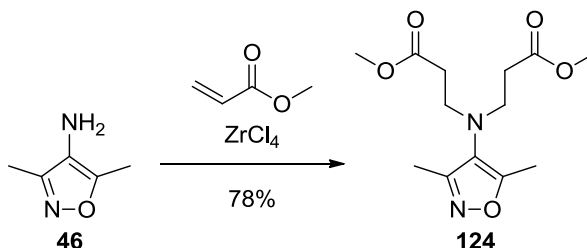
Methyl Acrylate / eq.	Solvent	Conc. / M	Catalyst (25 mol%)	Temp. / °C	Time / h	46 / %	Intermediate / %	124 / %
20	AcOH	0.38	-	120	96	16	52	27
22	AcOH	0.33	CuCl	100	2	17	44	0
13	HFIP	0.46	-	60	48	90	10	0
22	-	0.50	CAN	80	70	14	27	48
22	-	0.50	ZrCl ₄	80	3	0	0	85

Table 5. Conditions screened for the bis-alkylation of aminoisoxazole 46 with methyl acrylate. Values for reaction components are given as a percentage of the LCMS UV trace, with the peak corresponding to methyl acrylate discounted.

A species was detected in the LCMS traces of these reactions with a mass ion consistent with a mono-alkylated intermediate, and this peak has also been reported in Table 5.

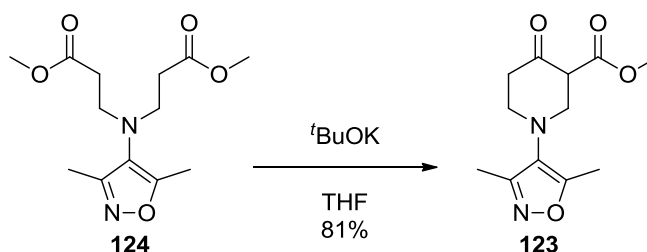
Heating with a large excess of acrylate and acetic acid afforded a small amount of product formation after 4 days, but with many unidentified side-products also formed.¹³⁹ The inclusion of copper (I) chloride as a catalyst increased the rate of the monoalkylation but did not prevent these side-products being formed so was abandoned after 2 h.¹⁴⁰ A method published by De *et al.* suggested that the use of hexafluoroisopropyl alcohol (HFIP) as a solvent promoted double aza-Michael addition to aromatic amines.¹⁴¹ However, after 2 days these conditions only provided a small conversion to the monoalkylated product, although there were no other detectable side-products. Finally, cerium ammonium nitrate (CAN) and zirconium (IV) chloride were trialed as Lewis acid promoters.^{142,143} The use of CAN gave some conversion to product, with the monoalkylation product also being present, along with unreacted amine, and some side-product formation. However, ZrCl₄ provided excellent conversion to product in only 3 h, with no amine or intermediate detected by LCMS.

The ZrCl₄-catalysed alkylation, was performed on a 1 g scale and was found to proceed at room temperature, rather than the 80 °C used in the trial reaction, to provide a 78% isolated yield (Scheme 56).



Scheme 56. Bis-alkylation of aminoisoxazole 46 with methyl acrylate.

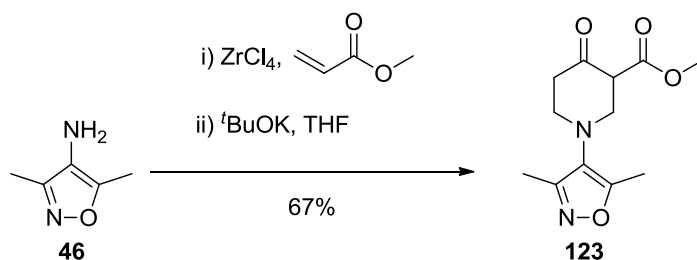
Following from this, the Dieckmann condensation was trialed using sodium methoxide as a base, but no product formation was observed.¹⁴⁴ However, the reaction proceeded smoothly when the stronger base, potassium *tert*-butoxide, was used instead, resulting in an 81% isolated yield (Scheme 57).¹⁴⁵



Scheme 57. Dieckmann condensation to form the isoxazole-containing β -keto ester species 123.

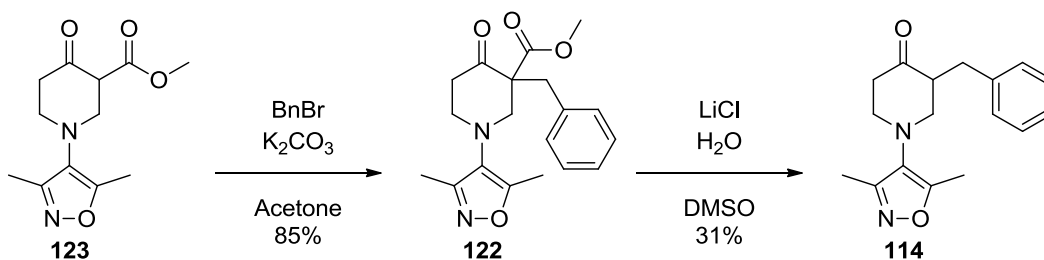
These two reactions were further scaled up, without the purification of the diester intermediate **124** to provide 14.4 g of β -keto ester **123** from 9.6 g of aminoisoxazole **46**

(Scheme 58). A small improvement in percentage yield was gained from telescoping these reactions, from 63% over two steps, to 67%.



Scheme 58. Large scale synthesis of β -keto ester 123.

The β -keto ester **123** was alkylated with benzyl bromide in very good yield (Scheme 59). The decarboxylation, however, did not prove straightforward. Previously, decarboxylations to α -alkylated products **118** and **120** were achieved by heating the esters **117/119** in a sodium hydroxide solution (Scheme 49 and Scheme 50), but these conditions did not result in successful product formation in this situation. Acidic conditions were also unsuccessful. Fortunately, the use of the methyl ester allowed the application of Krapcho conditions, to provide an acceptable yield (31%) of the decarboxylated product **114**.



Scheme 59. Alkylation of β -keto ester 123 with benzyl bromide, and subsequent Krapcho decarboxylation.

The reduction of the benzyl piperidinone **114** to the piperidine **107** was conducted as before (Scheme 53, p65) and over 200 mg of product was isolated, which was ample for chiral separation. This route represents an overall yield of 10% over five steps from the aminoisoxazole **46**, which is only a marginal improvement on the previous synthesis that gave a 9% yield over three steps from the same amine. However, this route allowed for a higher yielding alkylation step, which was the step where further derivatisation was expected to be conducted in future investigations.

After separation of racemate **107** by chiral chromatography, the enantiomers were submitted for biological screening, and the results are shown in Figure 30.

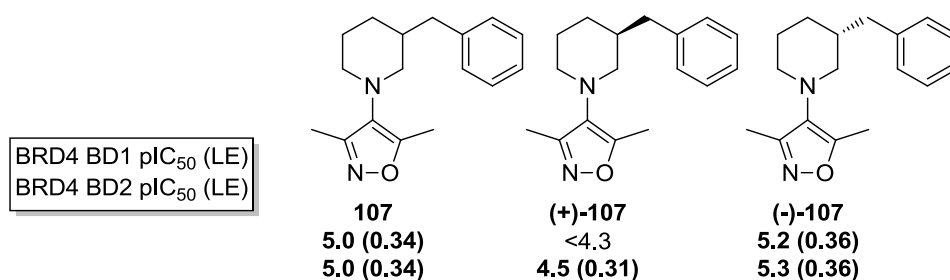
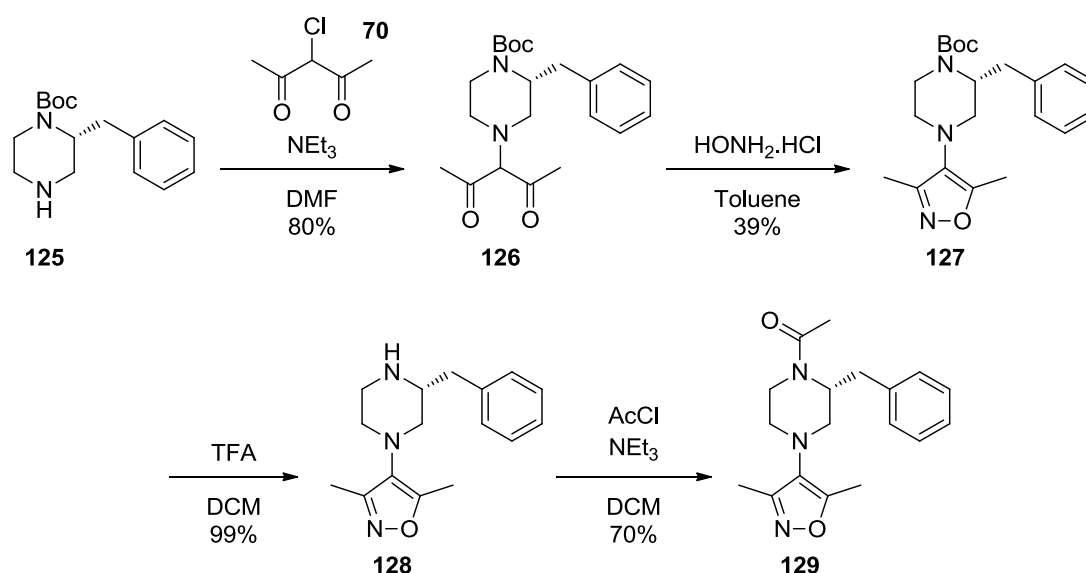


Figure 30. Assay data and calculated ligand efficiencies for benzyl piperidine **107** as the racemate and separated enantiomers. Configurations have been assigned by comparison with the X-ray crystal structure gained from the racemate in BRD2 BD2 and the assumption that enantiomer seen is the more potent of the two.

From these data, the assumption was made that the (-)-enantiomer possessed the *R*-stereochemistry observed in the X-ray crystal structure and was able to place the phenyl group on the WPF shelf, while the (+)-enantiomer could not place the group on the shelf without adopting an alternative, higher energy conformation and hence has reduced affinity for the binding site.

With this information in hand, a small investigation was performed to determine whether SAR from the piperidine compounds could be directly applied to a piperazine core. The *N*-Boc **64** and *N*-acetyl **86** piperazine fragments were the most potent of those tested (Figure 23, p56), and this was thought to be due to the carbonyl group gaining extra contact with the protein. Therefore, a benzyl-substituted piperazine was synthesised to determine whether it was possible to interact with the WPF shelf in the same way from this core (Scheme 60).



Scheme 60. Synthesis of benzyl-substituted piperazine analogues.

The enantiomerically pure *N*-Boc protected benzyl-substituted piperazine **125**, with the optimal *R*-configuration, was commercially available and so was used as the starting

point. This amine was alkylated and cyclised to form the isoxazole, producing the *N*-Boc product **127** in 31% over two steps. This was then deprotected to provide the free base **128** and acylated to provide the acetyl product **129**. These compounds were submitted for biological screening and the results are shown in Figure 31.

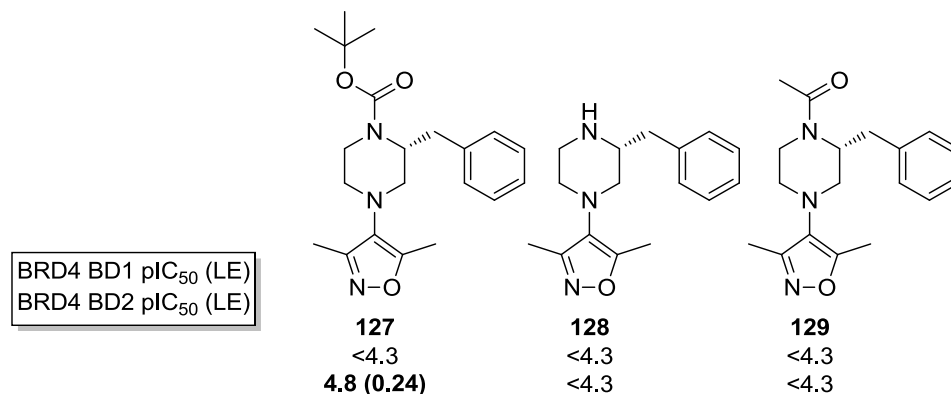


Figure 31. Assay data and calculated ligand efficiencies for benzyl-substituted piperazines.

In the most part, these compounds did not register in the assay above the lower pIC₅₀ limit of 4.3. Some activity was recorded at BRD4 BD2 for the *N*-Boc analogue **127**, with a pIC₅₀ of 4.8, which was only a 0.5 log unit increase over the unsubstituted *N*-Boc compound **64** for that bromodomain, and less potent than the benzyl piperidine **107**. This provided clear evidence that the SAR data collected for the piperidine systems did not apply to the piperazine core.

In conclusion, it has been demonstrated that it is possible to gain an increase in potency from the piperidine core by placing a phenyl group onto the WPF shelf *via* a one atom linker (**-**)-**107**. This represented the most potent compound achieved to this point in the research programme. The same interaction could not be adequately gained from the piperazine core with this linker length. Through X-ray crystallography and chiral chromatography, it has been shown that there is a preferred enantiomer and the desired configuration of the chiral centre has been identified. In parallel to investigations of WPF shelf-binding groups, an exploration of the ZA channel was conducted and is now described in detail.

6.5 Exploration of the ZA Channel

Having demonstrated the potential of interacting with the WPF shelf from the piperidine core, a similar investigation was undertaken aiming to probe for an interaction with the ZA channel. As was discussed in the introduction, and illustrated with X-ray crystal structures (Figure 16, p19), this is an area of the protein binding site which contains a

number of conserved water molecules, and generally tolerates polar groups, such as amides¹⁴⁶ and esters.⁶⁴

The reasons that this area was explored were two-fold. Firstly, there was the opportunity to gain potency benefits through polar interactions with water molecules or polar residues. Secondly, the physical properties of the molecule would benefit from the inclusion of a hydrophilic group, to balance the need for a lipophilic WPF shelf-binding group. For example, the benzyl piperidine **107** has a chromatographic LogD value at pH 7.4 (chromLogD_{pH7.4}) of 8.2. For a lead-like compound this value should ideally be at least as low as 3.0.¹⁰² If a methyl amide were to be appended to this molecule, giving a disubstituted compound **130** (Figure 32), the chromLogD_{pH7.4} is calculated to reduce to 4.3. While more work would still be required to further reduce the lipophilicity, the inclusion of an amide group would be a large step towards a favourable property space.

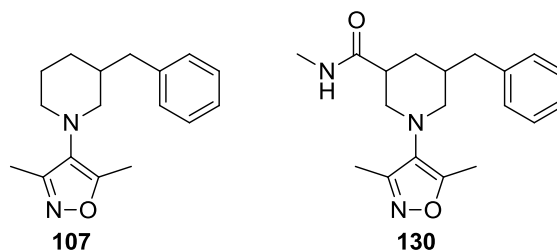
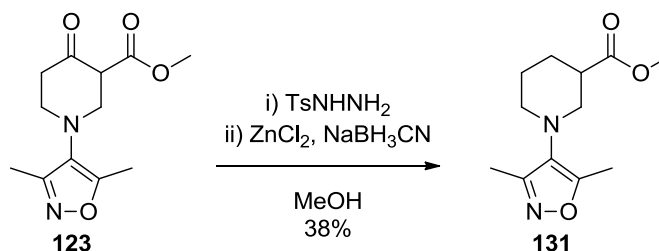


Figure 32. Benzyl piperidine **107** and a disubstituted analogue with a methyl amide appendage **130**.

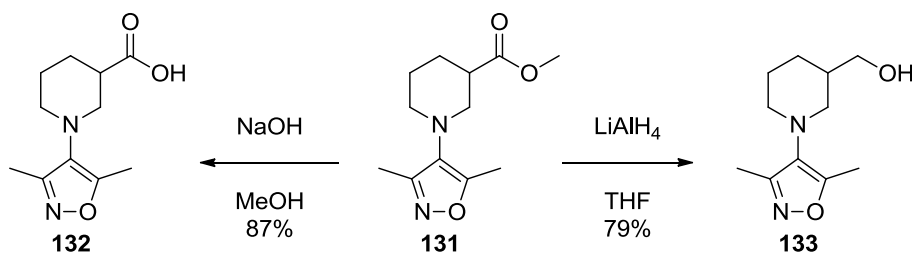
Therefore, an ester group was identified as a useful synthetic handle allowing access to target molecules containing polar groups, such as amides and an alcohol. The ester was accessed from the β -keto ester **123** previously prepared (Scheme 58, p70) *via* a modified Wolff-Kishner reaction (Scheme 61).



Scheme 61. Reduction of β -keto ester **123** to ester **131**.

These conditions were selected for this system with the rationale that the hydrazone would preferentially form with the more electrophilic ketone carbonyl rather than the ester, and that the ester would then be stable to cyanoborohydride reduction. Pleasingly this reduction was successful, providing an ester-substituted piperidine **131** in an acceptable yield (38%).

Initial derivatisations of this compound were made by hydrolysis to the carboxylic acid **132**, and reduction to the alcohol **133** (Scheme 62).



Scheme 62. Hydrolysis and reduction of ester-substituted piperidine **131**.

These three compounds were submitted for biological screening and the results are shown in Figure 33.

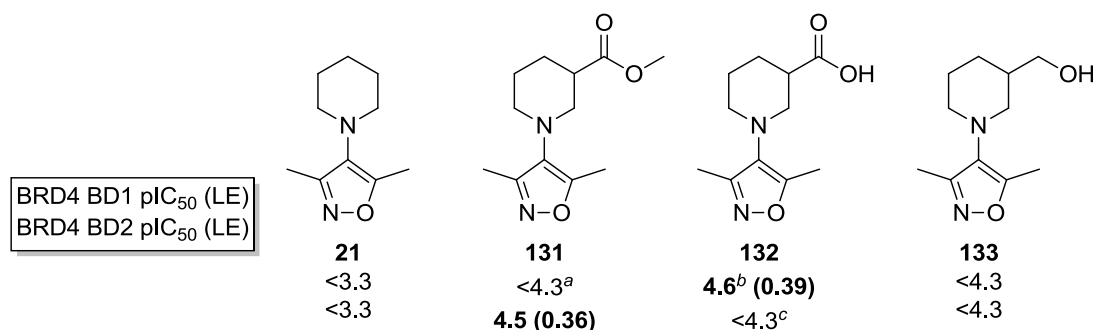


Figure 33. Assay data and calculated ligand efficiencies for ester-substituted piperidine **131** and its derivatives. ^apIC₅₀ values of 3.9 and 4.3 were determined on two out of six test occasions and were excluded from the reported value. ^bA pIC₅₀ value of <3.3 was determined on one test occasion out of four and was excluded from the reported value. ^cA pIC₅₀ value of 3.5 was determined on one test occasion out of four and was excluded from the reported value.

Both the ester **131** and the acid **132** display activity in the assay, with ligand efficiencies of 0.30 or above. This represented a notable improvement of activity over the unsubstituted piperidine **21**, which did not register any activity despite being tested in a high concentration assay format. To explore any potential interactions formed by these functional groups, a series of amides were targeted for synthesis (Figure 34).

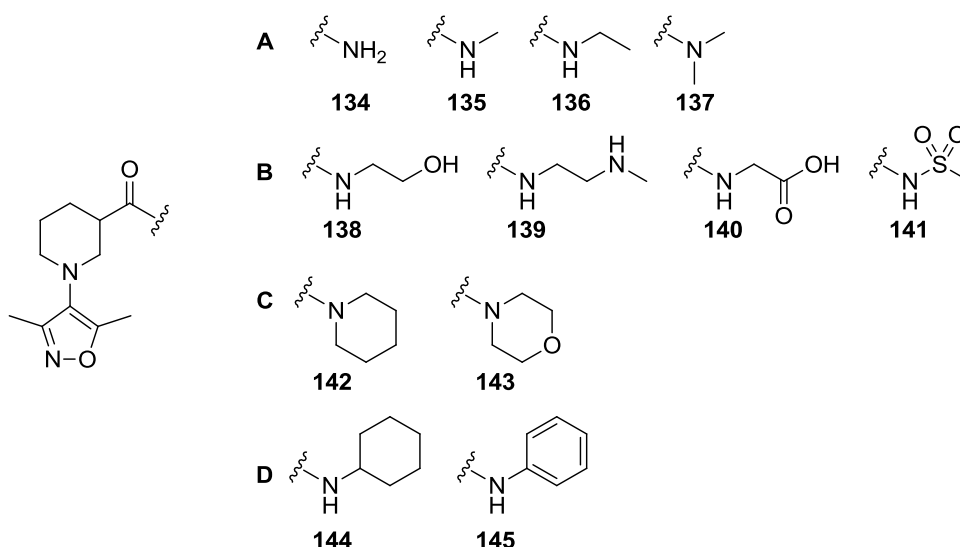


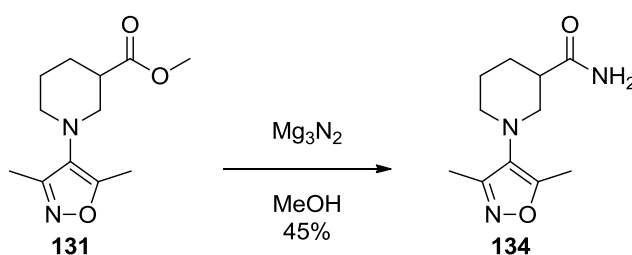
Figure 34. Amide target compounds.

The amides were carefully selected to answer specific questions. To determine if similar activity to the methyl ester could be achieved, four baseline compounds were selected: the primary **134**, methyl **135**, ethyl **136** and dimethyl **137** amides (Figure 34A). The ZA channel contains conserved water molecules which could form interactions with, or be displaced by, polar groups. To this end, some polar amides were selected with an alcohol **138**, amine **139** or carboxylic acid **140** group attached (Figure 34B). A sulfonamide derivative **141** was also selected as a way to provide a polar group with a shorter linker length.

It was speculated that a large, lipophilic group could cause the ring to flip round and place the amide towards the WPF shelf. This was investigated with two different linker lengths: firstly, with tertiary amides derived from piperidine **142** and morpholine **143** (Figure 34C), and also with secondary amides containing a cyclohexyl **144** or phenyl **145** moiety (Figure 34D).

6.5.1 Synthesis of Amides

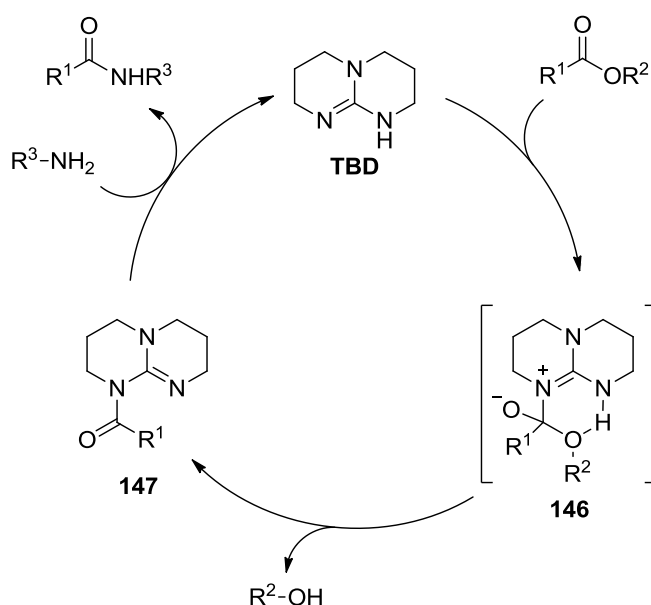
Firstly, the primary amide was synthesised from the ester using magnesium nitride in methanol (Scheme 63).¹⁴⁷

Scheme 63. Conversion of ester **131** to primary amide **134**.

This process is reported to involve the *in situ* generation of ammonia from the reaction of magnesium nitride with methanol, with magnesium methoxide as the byproduct.¹⁴⁷ Veitch *et al.* demonstrate that commercial solutions of ammonia are not as effective as their conditions, concluding that the magnesium salts are catalysing the conversion. These conditions provided the primary amide in a 45% yield.

In order to synthesise the remainder of the amides, a general process was sought that could supply all the desired products. The majority of commercially available coupling reagents react carboxylic acids with amines.¹⁴⁸ However, in this case it would be more convenient to couple directly from the ester and avoid the need to hydrolyse first.

1,5,7-Triazabicyclo[4.4.0]dec-5-ene (TBD) is a bicyclic guanidine that has been reported by Sabot *et al.* as an organocatalyst for coupling esters with amines.¹⁴⁹ In the first step of the proposed mechanism TBD acts as a nucleophile and attacks the ester (Scheme 64).

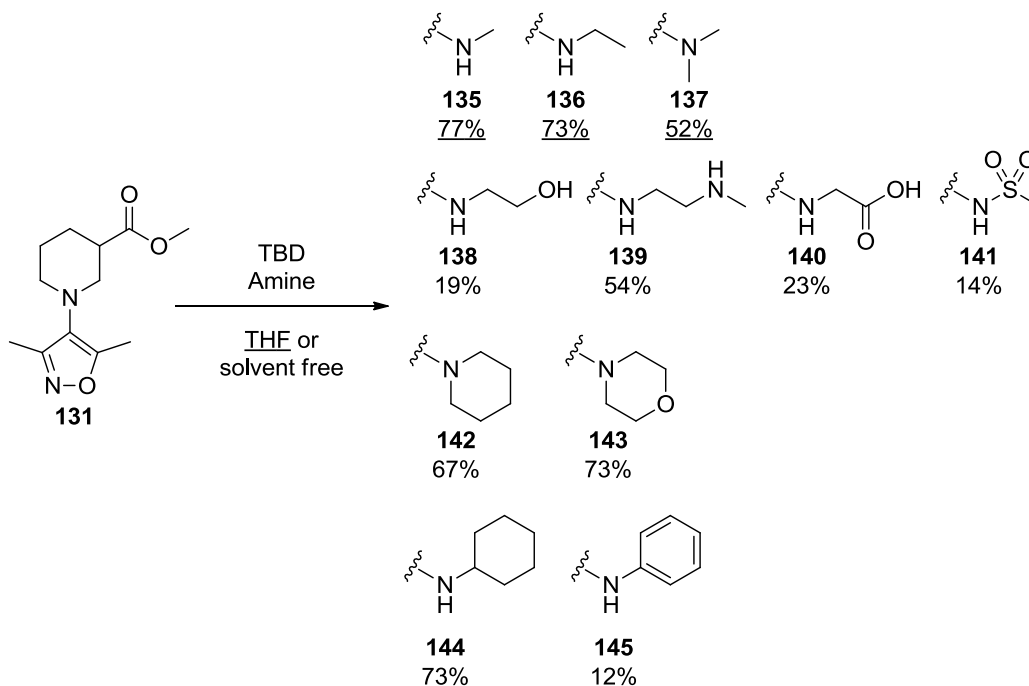


Scheme 64. Proposed mechanism for ester to amide conversion catalysed by TBD.¹⁴⁹

This forms an intermediate **146** in which a protonated nitrogen is well positioned to facilitate proton transfer to the alcohol leaving group, resulting in a TBD amide **147**. The amine then attacks this amide, TBD acts as a good leaving group, and the desired amide is formed.

The reaction was reported with a 30 mol% loading of the organocatalyst, 1.2 equivalents of amine, and solvent-free conditions. While many polar solvents reduced the efficiency of conversion, THF was tolerated.¹⁴⁹ This finding by the authors was of interest for this research as a number of low molecular weight amines to be investigated were volatile and were commercially available as solutions in THF. Also, the authors indicated that the

reaction mixture could be subjected to chromatography without any need for workup. Overall this made for a very convenient process, which was successfully applied to the ester-substituted piperidine system (Scheme 65).



Scheme 65. Synthesis of amides from the ester-substituted piperidine **131 using TBD. Underlined yields indicate that the reaction took place in THF rather than in solvent free conditions.**

All the desired amide targets were isolated *via* this method, with yields ranging from 12 to 77%. The low molecular weight, volatile amines were used as solutions in THF, corroborating the observations by Sabot *et al.* that this solvent would be tolerated.¹⁴⁹ Low yields were obtained in cases where the amine was a weak nucleophile, such as aniline used to make the phenyl amide **145**. Amines containing polar groups also have poor yields, due to poor conversions rather than side reactions, with unreacted ester **131** still detected in the reaction mixtures by LCMS.

Two of the results were particularly pleasing. Firstly, the reaction with *N*-methylethylenediamine proceeds exclusively from the primary amine to form the desired amide **139** with a secondary amine side-chain. This is in accordance with the literature and the regioselectivity was confirmed by the presence of an amide proton peak in the ¹H NMR spectrum.¹⁴⁹ The second pleasing result was the successful coupling with glycine, to provide the amide containing a carboxylic acid group **140**. It is not surprising that the catalytic system selectively couples the ester, as the organic base would deprotonate the carboxylic acid rather than attack the carbonyl, but it is pleasing that the presence of an acid does not render the basic catalyst completely protonated and unavailable for reaction. Partial protonation would, however, explain the poor

conversion. While the possibility was not alluded to by Sabot *et al.*,¹⁴⁹ this route provides a product in one step that may otherwise have taken three (hydrolysis of the ester-substituted piperidine, amide coupling to a glycine ester and a final ester hydrolysis step).

The amides were submitted for biological screening and the results are shown in Table 6. The methyl ester **131** has also been included for comparison.

		BRD4 BD1		BRD4 BD2	
		pIC ₅₀	LE	pIC ₅₀	LE
131		<4.3 ^a	-	4.5	0.36
134		3.7	0.32	4.4	0.38
135		<3.3 ^b	-	3.9	0.31
136		<3.3 ^c	-	3.9	0.30
137		3.8	0.29	4.5	0.34
138		<4.3	-	<4.3	-
139		<3.3 ^d	-	4.7^e	0.32
140		<4.2	-	<4.2	-
141		<4.3	-	<4.3	-
142		4.5	0.29	4.9	0.32
143		3.9	0.25	4.6	0.30
144		<3.3	-	<3.3 ^f	-
145		<4.3 ^g	-	<4.3 ^h	-

Table 6. Assay data and calculated ligand efficiencies for amide-substituted piperidines. The methyl ester **131** has been included for comparison. ^apIC₅₀ values of 3.9 and 4.3 were determined on two out of six test occasions and were excluded from the reported value. ^bA pIC₅₀ value of 3.4 was determined on one high concentration test occasion out of three and was excluded from the reported value. ^cA pIC₅₀ value of 3.8 was determined on one high concentration test occasion out of four and was excluded from the reported value. ^dValue based on two high concentration test occasions, rather than three or more. ^eA pIC₅₀ value of <3.3 was determined on one test occasion out of four and was excluded from the reported value. ^fA pIC₅₀ value of <3.8 was determined on one high concentration test occasion out of three and was excluded from the reported value. ^gpIC₅₀ values of 4.1 and <3.3 were determined on two test occasions out of five and were excluded from the reported value. ^hA pIC₅₀ value of 3.6 was determined on one test occasion out of four and was excluded from the reported value.

Both the primary **134** and dimethyl **137** amides displayed a similar BRD4 BD2 activity to the methyl ester **131**, with the same selectivity bias over BRD4 BD1. Of the four amides

with polar groups only the amine **139** showed any BRD4 BD2 activity. Interestingly this compound displayed a selectivity for BRD4 BD2 of at least 25-fold over BD1. Of the lipophilic amides, which were expected to bind onto the WPF shelf, appreciable activity was seen for the secondary amides, which were nearing pIC₅₀ values of 5 at BD2, but the secondary amides were significantly weaker ligands.

After the completion of this screen, an X-ray crystal structure of the methyl ester **131** bound to BRD2 BD2 was solved (Figure 35).

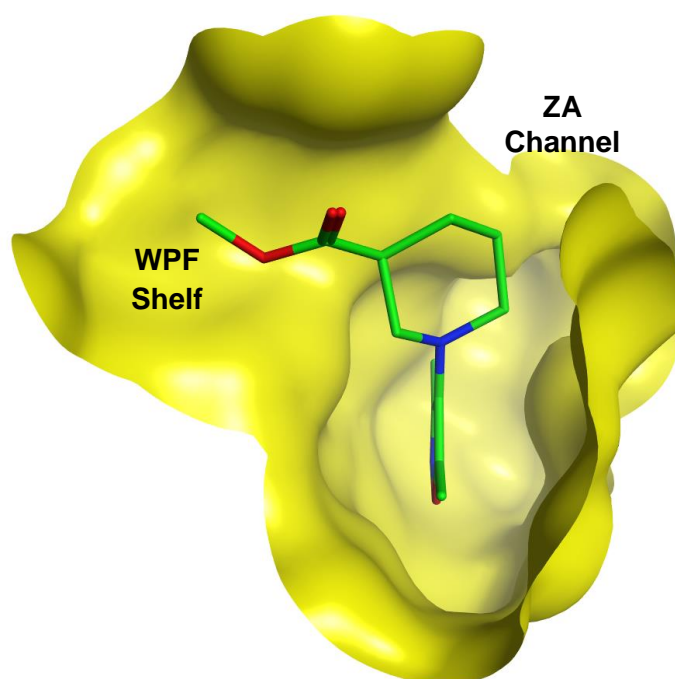


Figure 35. X-ray crystal structure of methyl ester-substituted piperidine **131 (green) bound to BRD2 BD2 (yellow). Water molecules have been removed from the image for clarity.**

The crystal structure shown resulted from soaks of the racemic mixture **131**, and interestingly, only the *S*-enantiomer was crystallised. Contrary to the original hypothesis, the crystal structure showed the ester directed towards the WPF shelf rather than the ZA channel, which made interpretation of the SAR more difficult. However, the design of the targets was carried out with the possibility of the alternative binding modes and it is worth noting that X-ray crystallography provides an image of a point in time and does not entirely discount the presence of multiple binding modes. In order to truly probe the ZA channel in this manner it was realised that it was necessary to synthesise disubstituted piperidine compounds that interacted strongly with the WPF shelf, to ensure amide groups don't bind in this region. This was the subject of later work, after an optimisation of the interaction with the WPF shelf was undertaken.

6.6 Alternative Linkers

Research to this point had established that a one-atom linker at the piperidine 3-position was sufficient to place a phenyl group onto the WPF shelf. Thus far, only a methylene had been evaluated, so an investigation was undertaken to see if an alternative linker could better position the phenyl group on the shelf for further potency gains. In this regard, three linkers were targeted for synthesis (Figure 36).

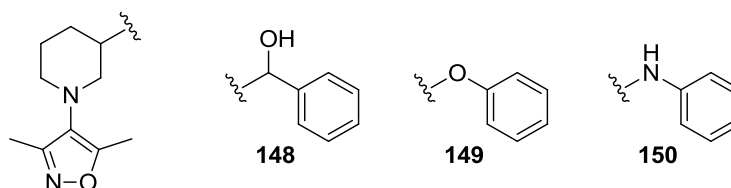
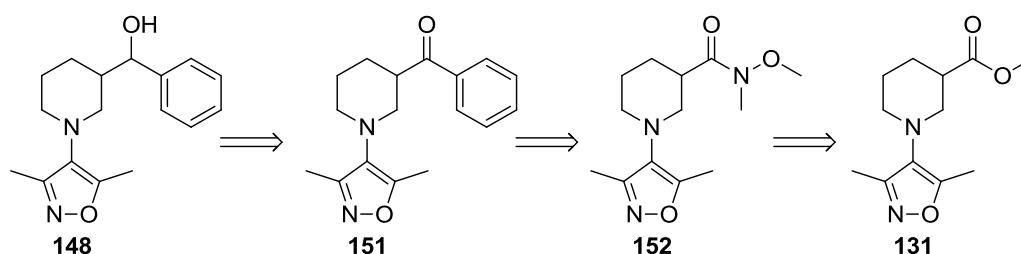


Figure 36. Target molecules with alternative linkers to place phenyl groups onto the WPF shelf.

Firstly, inspiration was taken from the literature: the BET inhibitors published by Hewings *et al.*⁶⁴ utilise a hydroxymethylene linker to place a phenyl group on the WPF shelf from a phenylisoxazole core. Hewings' rationale for retaining the hydroxyl is not explicitly stated, and comparators with an unsubstituted methylene linker were not published, therefore the effect on the potency is unclear. It may be that the hydroxyl was simply a remnant of the synthetic strategy, or desirable for improved solubility, but it seemed prudent to investigate its effect on this series. Secondly, the effect of changing the linking atom itself from carbon to oxygen or nitrogen was investigated in order to probe alternative conformations.

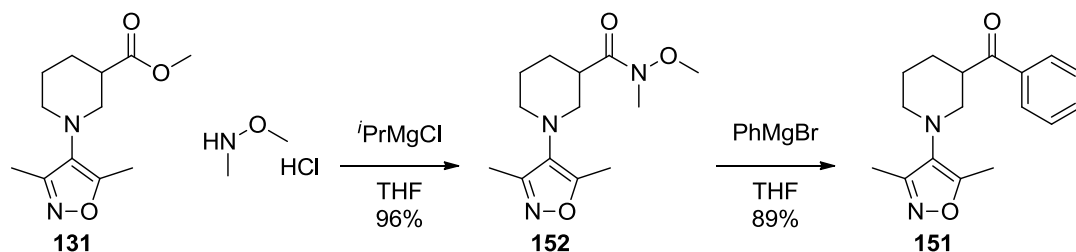
6.6.1 Synthesis of Hydroxymethylene Linked Compound

It was realised that that hydroxymethylene target compound **148** could be disconnected to the methyl ester compound **131** that had been prepared previously in this research, via a Weinreb amide (Scheme 66).



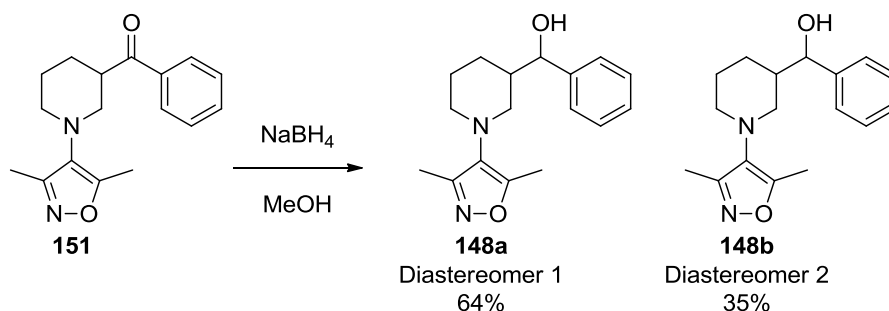
Scheme 66. Retrosynthesis of hydroxymethylene compound 148.

The Weinreb amide **152** was formed in excellent yield from the ester **131** using *N,O*-dimethylhydroxylamine hydrochloride, and isopropylmagnesium chloride as a base (Scheme 67).¹⁵⁰



Scheme 67. Formation of Weinreb amide **152** and subsequent reaction with phenylmagnesium bromide.

The Weinreb amide **152** was then treated with excess phenylmagnesium bromide to form the ketone **151** in very good yield. This ketone **151** was reduced using sodium borohydride to provide diastereomeric products in a roughly 2:1 ratio, and these diastereomers were separated (Scheme 68).

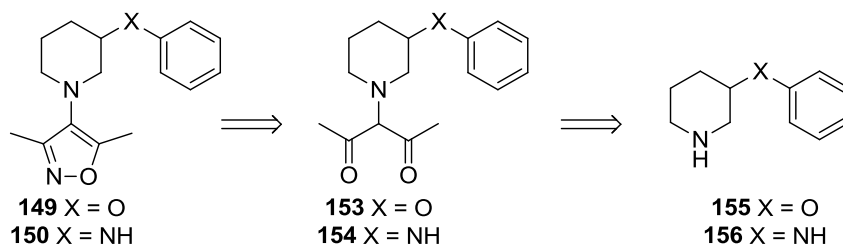


Scheme 68. Reduction of ketone **151** to the two diastereomers of the hydroxymethylene linked target compound **148**.

The relative stereochemistries were not identifiable by ¹H NMR, but this could potentially be achieved by X-ray crystallography if either diastereomer displayed promising activity (biological results reported later in Table 7).

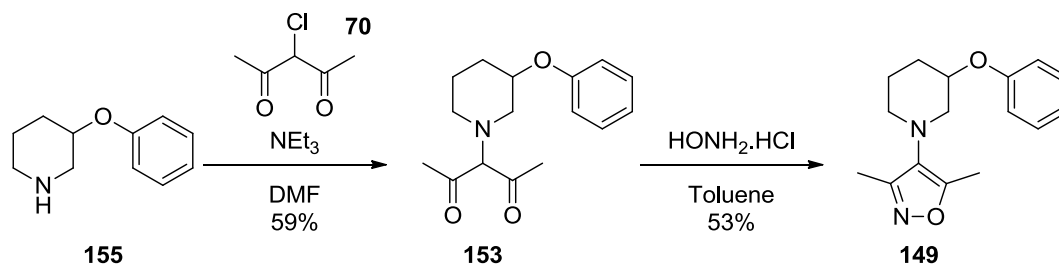
6.6.2 Synthesis of Amine and Ether Linked Compounds

In order to synthesise the ether **149** and amine **150** linked compounds, the isoxazole formation route was utilised (Scheme 69).



Scheme 69. Retrosynthesis of ether **149 and amine **150** linked compounds using isoxazole formation chemistry.**

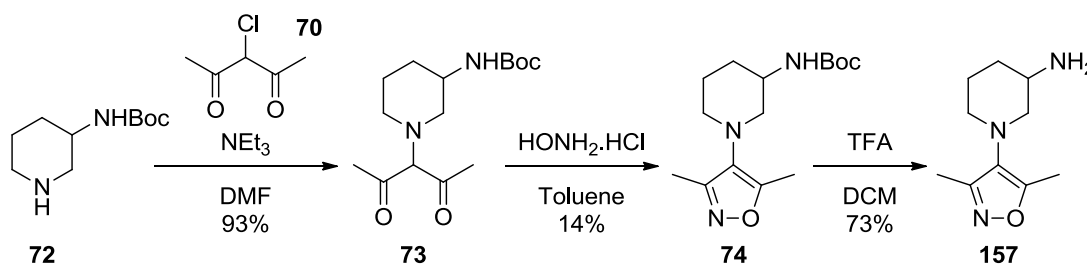
To form the ether linked compound **149** it was found that 3-phenoxy piperidine **155** was commercially available, so a synthesis was initiated from this starting material (Scheme 70).



Scheme 70. Synthesis of ether linked compound **149.**

Formation of the dicarbonyl intermediate **153** by alkylation of the phenoxy piperidine **155** proceeded smoothly in acceptable yield. The isoxazole formation, which utilised excess hydroxylamine hydrochloride in toluene with Dean-Stark apparatus, provided the target compound **149** in 53% yield, which was one of the best yields achieved with this method at this stage in the research programme.

The corresponding aniline starting material was not readily available, so instead Boc-protected 3-aminopiperidine **72** was used (Scheme 71).

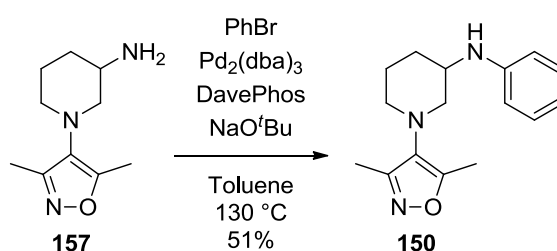


Scheme 71. Synthesis of 3-aminopiperidine isoxazole **157.**

The alkylation of the piperidine starting material **72** proceeded with excellent yield. The isoxazole formation was successful, but only provided product in a poor, 14% yield. This compound was subsequently deprotected to provide the free base amine **157**.

The last step in this synthesis was the incorporation of the phenyl group *via* C-N cross coupling. A literature search for conditions used on similar systems revealed work by

Jean *et al.* investigating coupling of 3-aminopyridines and 3-aminopyrrolidines.¹⁵¹ After preliminary experiments to discover an appropriate transition metal catalyst, the authors' attention focussed on the Buchwald-Hartwig coupling. They investigated five main substrates, the relevant two to this work being *N*-benzyl- and *N*-Boc-3-aminopiperidine. Sodium *tert*-butoxide was chosen as the base after an initial screen in which other bases were trialled and found ineffective. A range of ligands were screened and it was found that DavePhos consistently achieved yields over 70%. In a number of cases with monophosphine ligands a strong temperature dependency was observed, with effective coupling occurring at 130 °C but not at 100 °C. The optimal conditions from this work were applied to the system at hand (Scheme 72).



Scheme 72. Buchwald-Hartwig coupling of 3-aminopiperidine **157** with bromobenzene to form the amine linked target compound **150**.

Pleasingly the reaction was successful, and the desired product **150** was isolated in 51% yield.

6.6.3 Evaluation of Linkers

The collection of compounds with alternative linkers between the piperidine and the shelf-binding phenyl ring were submitted for biological screening and the results are presented in Table 7.

		BRD4 BD1		BRD4 BD2		BD2 – BD1
		pIC ₅₀	LE	pIC ₅₀	LE	
107		5.0	0.34	5.0	0.34	0.0
151		4.8	0.31	5.5	0.36	0.7
148a		4.5	0.29	4.7	0.31	0.2
	Diastereomer 1					
148b		4.6	0.30	4.8	0.31	0.2
	Diastereomer 2					
149		4.6^a	0.32	5.4	0.37	0.8
150		4.7	0.32	5.7	0.39	1.0

Table 7. Assay data and calculated ligand efficiencies for compounds containing varying linkers to place a phenyl group onto the WPF shelf. BD2 selectivity is also given, as a difference in pIC₅₀ values between BRD4 BD2 and BD1. ^aA pIC₅₀ value of <4.3 was determined on one test occasion out of four and was excluded from the reported value.

Neither of the diastereomers of the hydroxymethylene linked compound displayed an improved potency with respect to the methylene linked compound **107**, which has been included in Table 7 for comparison. However, the precursor ketone linked compound **151** was also tested and, interestingly, had an increased potency at BRD4 BD2, with a pIC₅₀ of 5.5, and 5-fold selectivity over BD1. This was noteworthy given that BD2 selectivity had been observed in a number of compounds prior to this point but had not previously been associated with increased potency. Both the ether linked **149** and amine linked **150** compounds shared this attribute, and the effect was most profound for the amine **150** which displayed a pIC₅₀ at BRD4 BD2 of 5.7 and 10-fold selectivity over BD1.

In an attempt to understand the selectivity for BD2, X-ray crystal structures were solved for both the ether linked **149** and amine linked **150** compounds in the binding site of BRD2 BD2 (Figure 37).

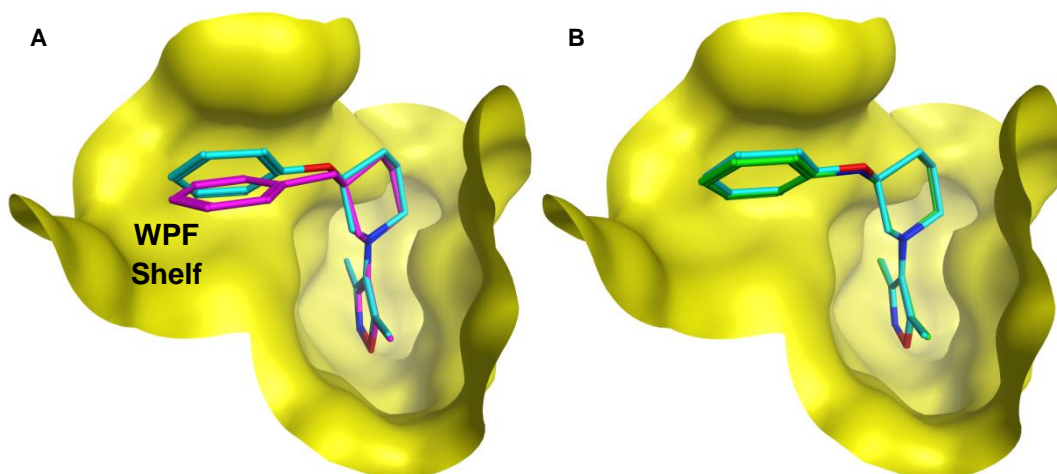


Figure 37. A) X-ray crystal structure of ether linked compound **149** (cyan) bound to BRD2 BD2 (yellow) with benzyl piperidine **107** (magenta) superposed. B) The same image with amine linked compound **150** (green) superposed instead. Water molecules have been removed from both images for clarity.

In Figure 37A the X-ray crystal structure of the ether linked compound **149** is shown with that of the methylene linked congener **107** overlaid. It can be seen that the binding mode of the isoxazole and piperidine core are very similar and the main difference is the orientation of the phenyl ring on the WPF shelf, which could be the reason for the difference in activity at BD2 *versus* BD1 as several residue differences are apparent in this region (*vide infra*). Figure 37B shows the ether linked **149** and amine linked **150** compounds overlaid, demonstrating their almost identical conformations.

The crystal structures of each of these compounds were prepared from soaks of the racemates, and, in each case, density was only seen for the single enantiomers. Given the amine linked compound **150** displayed the highest potency seen in this series so far, it was desirable to confirm the preference for binding of one stereoisomer over the other, in a similar manner to that carried out for the methylene linked compound **107** (Figure 30, p71). Therefore, the individual enantiomers were separated by chiral chromatography and submitted for screening, the results of which are shown in Figure 38.

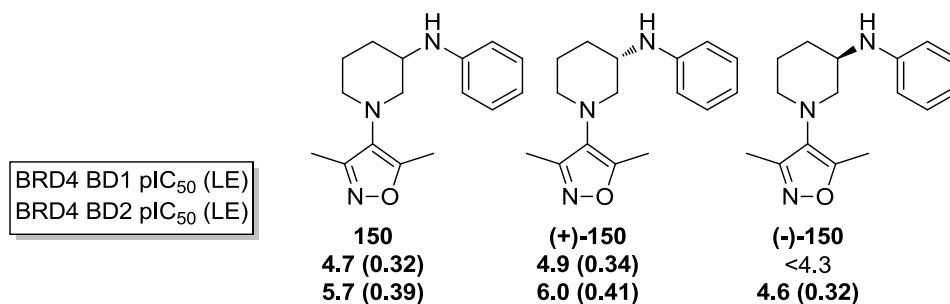


Figure 38. Assay data and calculated ligand efficiencies for amine linked compound **150** as the racemate and separated enantiomers. Configurations have been assigned by comparison with the X-ray crystal structure solved in BRD2 BD2 from the racemic mixture and the assumption that the observed stereoisomer was the more potent of the two.

The (+)-enantiomer displayed significantly higher activity than the (-)-enantiomer, with a pIC₅₀ of 6.0 at BRD4 BD2, and 13-fold selectivity over BD1. It was implied from the X-ray crystal structure that this was the (*S*)-enantiomer (Figure 37).

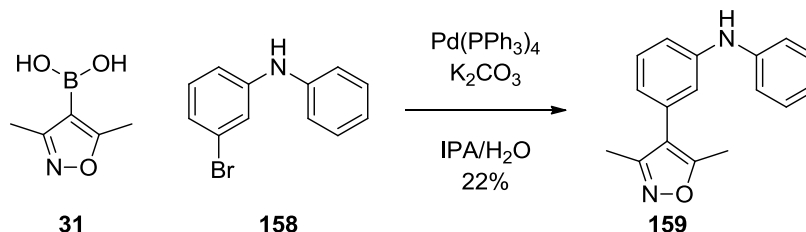
This result represents a significant milestone in this research. Up until this stage only modest potency had been observed. Prior to this investigation into alternative linkers the highest potency that had been achieved was for the *R*-enantiomer of the methylene-linked compound **107**, with a pIC₅₀ of 5.4 at BRD4 BD2 (Figure 30). An extensive exploration of potential interactions with the ZA channel was undertaken, during which an ester, a range of amides, a carboxylic acid and an alcohol were synthesised but no pIC₅₀ values greater than 4.9 were gained. However, after an X-ray crystal structure was obtained which showed the methyl ester group directed away from the ZA channel it was concluded that the investigation of this area would best be carried out with disubstituted compounds to reduce the potential for multiple binding modes and the resulting complication for SAR interpretation.

This amine linked compound **(+)-150** achieved the target pIC₅₀ of greater than or equal to 6.0 that was set at the start of this research. It also exhibited a ligand efficiency of 0.41 at BRD4 BD2, which was higher than those seen for the published phenylisoxazole compounds being used as comparators (Figure 22, p29, 0.35 for the Hewings compound **4** and 0.37 for the Bamborough compound **3**).^{64,99}

Of particular interest was the fact that the ‘increasing saturation’ approach appeared to have provided an interesting avenue to pursue in terms of BD2 selectivity, warranting further investigation.

6.6.4 Confirming the Effect of Saturation on BD2 Selectivity

To confirm that the saturation approach was the key feature affording BD2 selectivity, a comparator compound was required with the same amine linker, but with a saturated core. To this end, an aniline-substituted phenylisoxazole **159** compound was synthesised (Scheme 73).



Scheme 73. Synthesis of the aniline-substituted phenylisoxazole **159**.

A suitable aryl bromide **158** was commercially available so was used in a Suzuki coupling with the isoxazole boronic acid **31**. Suzuki conditions were used that have previously been effective in coupling this particular boronic acid with aryl bromides within GSK laboratories.¹⁵² The unsaturated analogue was submitted for biological screening and the data is shown in Figure 39.

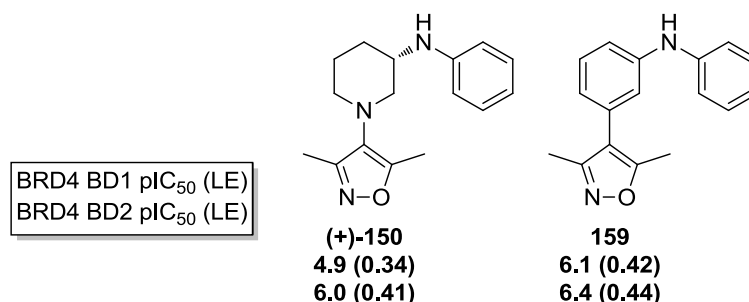


Figure 39. Assay data and calculated ligand efficiencies for the preferred enantiomer of amine linked piperidine compound **150** and its unsaturated analogue **159**.

Strikingly, there was a notably lower degree of selectivity seen for the unsaturated compound **159** than the piperidine **150**. This suggested that there was something key about the shape of piperidine and the vector it provided for accessing the WPF shelf that allowed this preferential binding at BD2.

It was also noted that the unsaturated molecule **159** displayed slightly higher potency, with a pIC₅₀ of 6.4 at BRD4 BD2, compared to 6.0 for the piperidine **(+)-150**. It was hypothesised that the addition of some degree of unsaturation into the piperidine core may increase the potency of the molecule and would also provide further insight into the requirements for BD2 selectivity. Therefore, a target molecule was designed that

included a carbon-carbon double bond in the core, in the only position in which it would not be in conjugation with an amine (Figure 40).

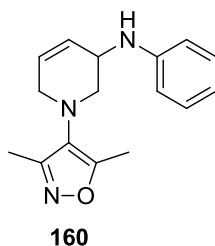
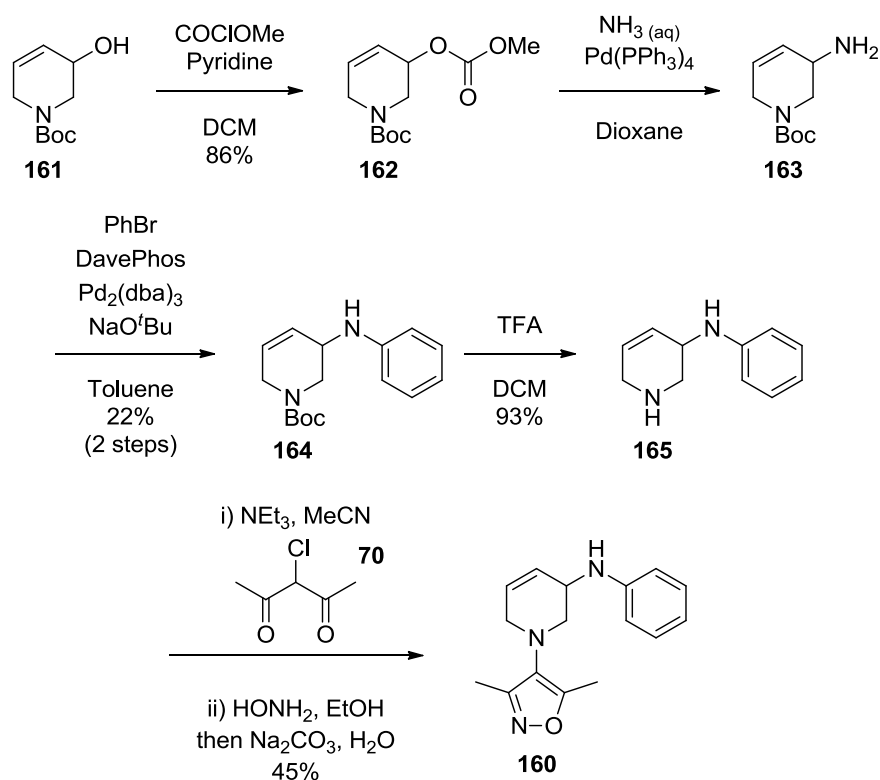


Figure 40. Tetrahydropyridine target molecule 160.

In order to provide access to the tetrahydropyridine target molecule **160**, a suitable starting material was identified, in the form of an *N*-Boc protected tetrahydropyridinol **161** (Scheme 74).



Scheme 74. Synthesis of aniline-substituted tetrahydropyridine 160.

The tetrahydropyridinol **161** starting material was converted to the carbonate **162** with methyl chloroformate in a good yield.¹⁵³ This intermediate was then subjected to a Tsuji-Trost style allylic amination using aqueous ammonia in the presence of catalytic palladium (0), to provide the allylic primary amine **163**.¹⁵⁴

The shelf-binding phenyl group was installed onto the allylic amine using the Buchwald-Hartwig conditions previously identified within this research, providing the anilinic product **164** in a yield of 22% over the two steps.¹⁵¹ The *N*-Boc protecting group was

subsequently removed using TFA to provide the free base tetrahydropyridine **165**. The isoxazole was installed using the improved alkylation and cyclisation process in which the two condensation steps required to form the aromatic ring occur under separate conditions (see Section 6.1.3). This provided the target compound in an overall yield of 11% over five steps.

The semi-unsaturated analogue **160** was submitted for biological screening, and the results are shown in Figure 41.

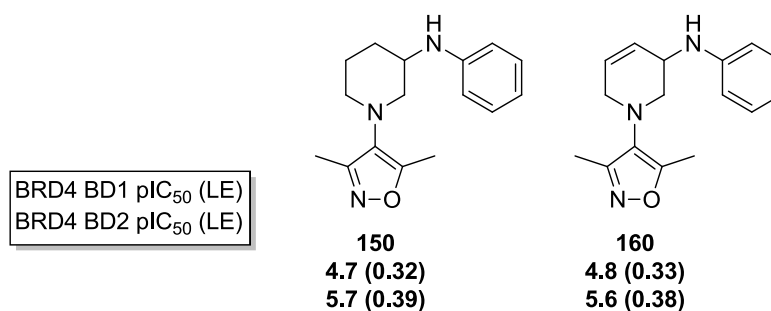


Figure 41. Assay data for amine linked piperidine compound **150 and its semi-unsaturated analogue **160**.**

The assay results for this analogue **160** were very similar to those obtained for the fully saturated piperidine analogue **150**. While this may not fully elucidate the origins of the BD2 selectivity, the fact that similar levels of selectivity were replicated in a close analogue gave confidence that this was a real phenomenon. Therefore, the remainder of this research was directed at trying to understand how this selectivity was being achieved and whether such an understanding could be used to rationally design more selective compounds. To achieve this, an examination of what is currently known about BD2 selectivity was undertaken, which shall now be discussed.

6.7 Mechanisms behind BD2 Selectivity

As was discussed in Section 2.3, the majority of BET-inhibitors published to date have been pan-BET selective; having little or no variation in potency across the eight bromodomains of the BET family. A body of evidence has been collected to suggest that the two bromodomains contained within each BET protein, BD1 and BD2, have different biological functions, and domain-selective inhibitors could create a different pharmacological profile to their pan-BET comparators.

Despite high sequence homology, there are some notable differences between BD1 and BD2 binding sites that could be exploited to gain selectivity. Sequence alignments of the eight BET bromodomains were used to identify these differences (Figure 42).⁴¹



Figure 42. Sequence alignments of the eight human bromodomains contained within the BET family. Conserved residues are highlighted in red. Residues consistently different between BD1 and BD2 domains are highlighted in green. Residues with a consistent difference between domains in three out of four of the BET proteins are highlighted in yellow. The boxed residues show differences located near the KAc binding pocket.⁴¹

In Figure 42, residues have been highlighted in red if they are completely conserved between all eight BET bromodomains. Residues have been highlighted in green if they show a consistent difference between BD1 and BD2 domains. Those highlighted in yellow have a difference between domains that is consistent for three out of the four BET proteins. The residues contained within the boxes show differences that are located near the KAc binding pocket and could, therefore, be exploited to gain selectivity by small molecules. The X-ray crystal structures of BRD4 BD1 and BD2 have been used to show the locations of these residues (Figure 43).

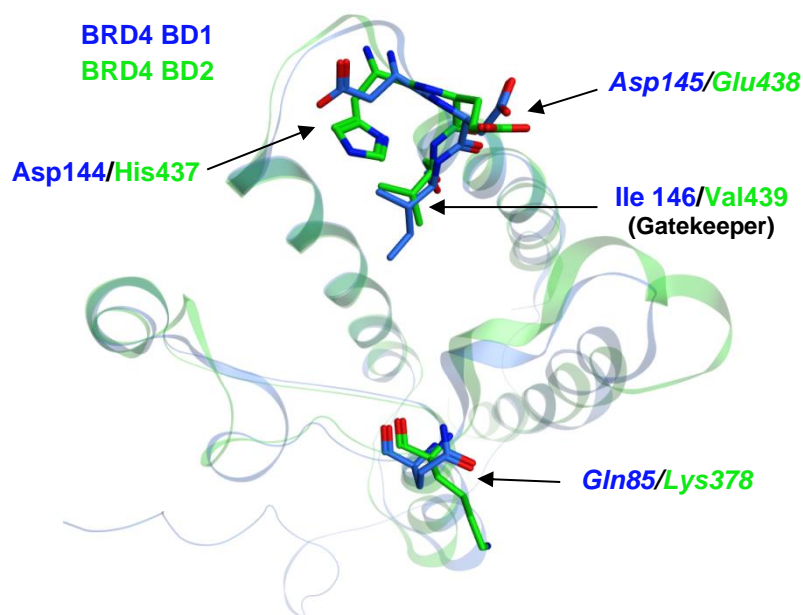


Figure 43. X-ray crystal structures comparing BRD4 BD1 (blue, PDB: 2OSS) and BRD4 BD2 (green, PDB: 2DWW). Differing residues adjacent to the binding pocket are shown in bold. Italicised labels refer to differences that only apply to three out of four BET proteins (see text for details). Other residues and water molecules have been omitted for clarity.

Firstly, there is a residue change at the base of the ZA channel, with a glutamine in BD1 replaced by a lysine in BD2. This is not true of BRDT which has an arginine and asparagine at BD1 and BD2, respectively. The other three changes are concentrated around the WPF shelf region. The residue that restricts access to the WPF shelf is termed the “gatekeeper” and is an isoleucine in BD1, but a valine in BD2. The next residue in the sequence is an aspartate in BD1 but a glutamate in BD2, apart from in BRD2 where they are both aspartates. Finally, the following residue in the sequence shows perhaps the biggest difference, being an aspartate in BD1 and a histidine in BD2. Thereby switching from a smaller, potentially negatively charged group in one domain, to a larger, aromatic, potentially positively charged group in the other.

From this structural information, two strategies present themselves for achieving BD2 selectivity. The size difference in the gatekeeper residue could be exploited by creating a ligand that clashes with the extra methyl group of the isoleucine in BD1, but forms good contact with the smaller valine in BD2. Alternatively, a ligand could be used that forms interactions with the histidine residue in BD2, which has the potential to form π -interactions, hydrogen bonds or ionic bonds. The same interactions would not be possible with the aspartate of BD1. These strategies have yet to have been exploited in the rational design of BD2-selective inhibitors but have been cited upon retrospective analysis of the very few BD2-selective molecules disclosed to date (Figure 44).

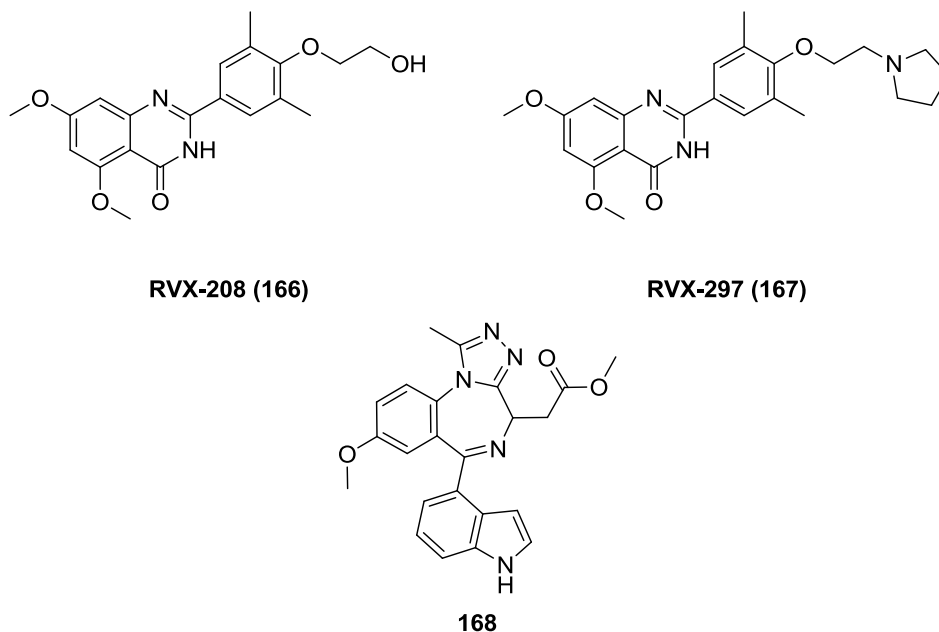


Figure 44. Published BD2-selective BET inhibitors.

The first BD2 selective inhibitor to be reported was RVX-208 **166**, which was developed by Resverlogix Corp. and is currently in Phase III clinical trials for cardiovascular diseases associated with diabetes and atherosclerosis.^{155,156} RVX-208 **166** was discovered through a phenotypic screen for compounds that enhanced mRNA expression of ApoA-I, the upregulation of which is associated with increased cholesterol efflux.¹⁵⁶ It was subsequently discovered to be a BET inhibitor with a bias for BD2 domains. Two papers have published binding affinities of this molecule as measured by isothermal titration calorimetry (ITC), with some discrepancy, which probably reflects the differing conditions used in the experiments. Picaud *et al.* measured the BD2 selectivity as 23-fold at BRD2 and 8-fold at BRD4,¹⁵⁵ while McLure *et al.* measure the selectivity as 82-fold at BRD2 and 30-fold at BRD4.¹⁵⁶

The X-ray crystal structures of RVX-208 **166** in the binding sites of BRD4 BD1 and BRD2 BD2 were used by the authors to post-rationalise the selectivities for the BD2 domains (Figure 45).¹⁵⁵

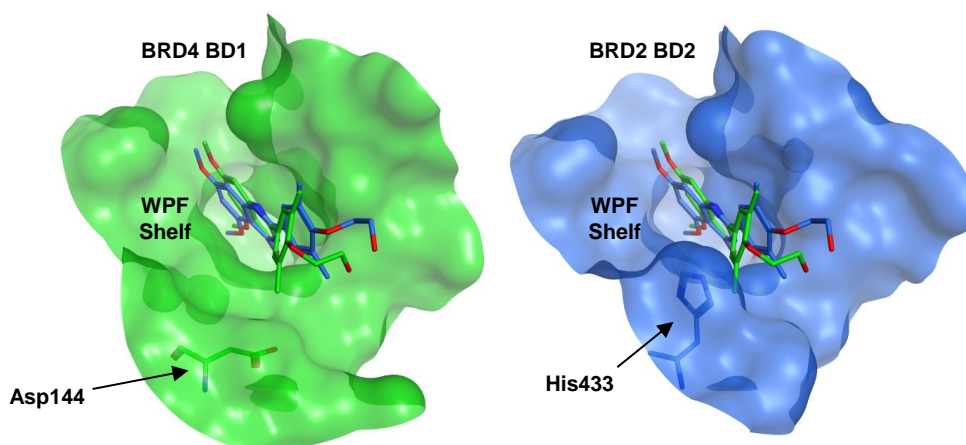


Figure 45. X-ray crystal structures of RVX-208 166 bound to BRD4 BD1 (green, left, PDB: 4J3I) superposed with the same molecule bound to BRD2 BD2 (blue, right, PDB: 4J1P). In the left-hand image, the BRD4 BD1 surface and Asp 144 (green) are shown and the BRD2 BD2 surface and His433 (blue) are shown on the right.

The authors reached the hypothesis that the BD2 selectivity derives from a face-on packing interaction between the dimethylphenol ring of the ligand and the histidine that is only present in the BD2 domains (Figure 45).¹⁵⁵ In BD1 domains this interaction can't be made and the dimethylphenol ring sits at a different angle. Similar differences are seen in the structurally related molecule RVX-297 167, for which 8-fold BD2 selectivity at BRD4 is reported.¹⁵⁷

A recent computational study simulated the binding modes of RVX-208 166 in BD1 and BD2 and identified the importance of a hydrogen bond between a conserved tyrosine on the BC loop and a conserved aspartate on the ZA loop, which is located close to the hydroxyethyl end of bound RX-208 166 (Figure 46).¹⁵⁸

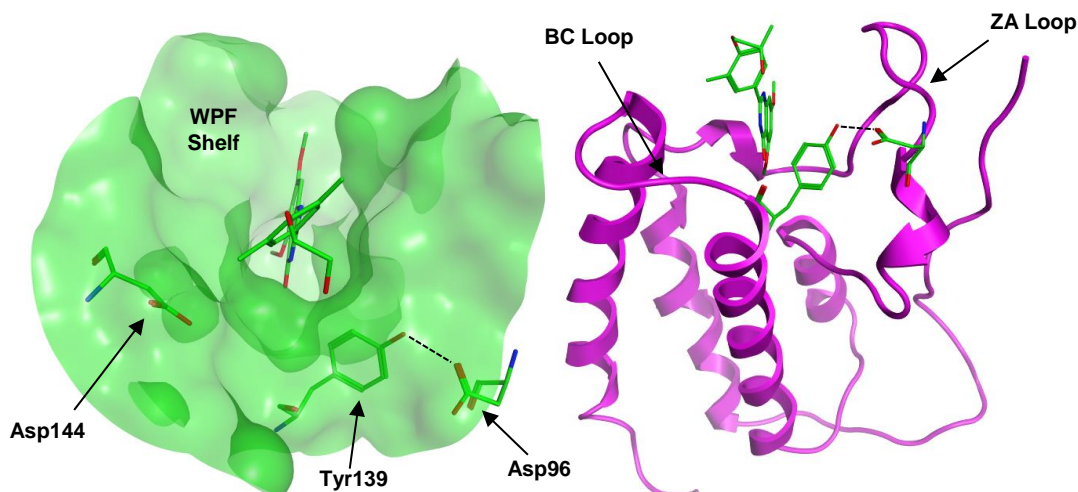


Figure 46. X-ray crystal structures of RVX-208 166 (green) bound to BRD4 BD1 (PDB: 4J3I). In the left-hand image the BD1-specific aspartate (Asp144) and protein surface (green) is shown for perspective. The right-hand image shows the protein ribbon (magenta) and the relevant loops are labelled. The hydrogen bond between the conserved tyrosine and aspartate (Asp96 and Tyr139 in BRD4 BD1) is shown with a dashed line.

The simulations suggested that this hydrogen bond anchored an “in” conformation of the ZA loop, and when not present the ZA loop adopted an alternative “out” state. They calculated that the “in” conformation provided a greater average energy of binding for RVX-208 **166** than the “out” state. Simulations of the dynamic binding mode of RVX-208 **166** in BD1 showed the hydroxyl group at the end of the ethyl chain disrupting this hydrogen bond by interacting with the aspartate, and thus stabilising the “out” state of the ZA loop and weakening the affinity of BD1 for RVX-208 **166**. Conversely, in BD2 the hydroxyl group remained distant from the aspartate, allowing the “in” conformation to persist. They concluded that the difference in positioning was due to the π - π stacking interaction between the phenol ring and the BD2-specific histidine holding the molecule in place, as well as providing added binding affinity.

Interestingly, their simulations showed that the pyrrolidine in RVX-297 **167** that replaces the hydroxy group of RVX-208 **166** does not interact in the same way with the aspartate, which explains the lower level of BD2 selectivity observed for this molecule.

Interestingly, it is also this Asp/His difference which is responsible for the BD1-selectivity of Olinone **16** (Figure 47). This molecule, while only a weak inhibitor, is at least 100-fold selective for BD1.⁸³

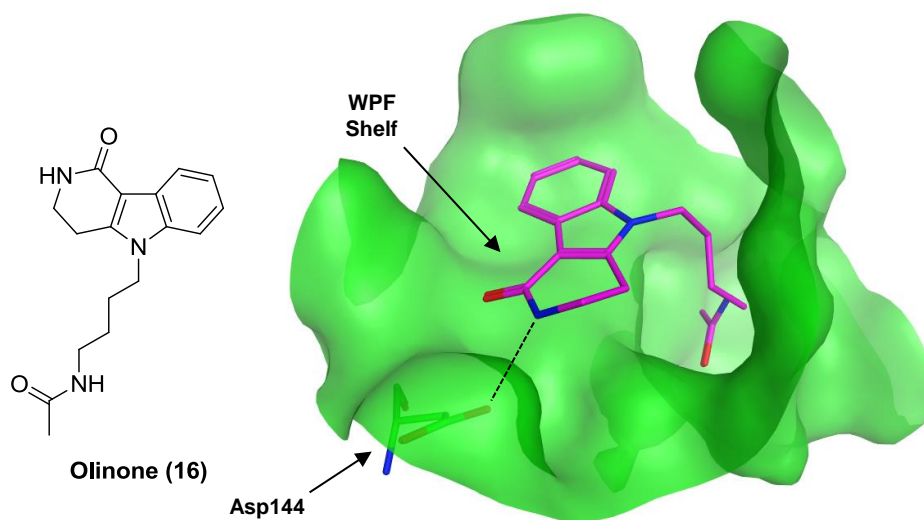


Figure 47. The structure of the BD1-selective inhibitor, Olinone **16** (left) and an X-ray crystal structure of Olinone (magenta) bound to BRD4 BD1 (right, green, PDB: 4QB3). The BD1-specific aspartate (Asp144 in BRD4 BD1) and WPF shelf are labelled. The hydrogen bond between the Olinone shelf-binding group and Asp144 is shown with a dashed line.

Olinone **16** consists of an acetyl amine which serves as the KAc mimetic, connected by an alkyl chain to a tricyclic tetrahydropyrido indole, which occupies the WPF shelf. This large ring system forms a hydrogen bond with the aspartate specific to BD1 domains, but

would clash with the histidine found in BD2 domains, and hence no binding has been detected with the latter.

During the development of the ET ligand **15** for the “bump-and-hole” approach described previously (Section 2.3), Baud *et al.* synthesised an indole analogue **168** of I-BET762 **2** (Figure 44) which displayed 17-fold BD2 selectivity at BRD2 and 10-fold selectivity at BRD4.⁸⁶ An X-ray crystal structure of this indole compound **168** was obtained in a BRD2 BD2 mutant (possessing a phenylalanine in place of the tryptophan of the WPF shelf) and compared this with a similar structure obtained with I-BET762 **2** (Figure 48).

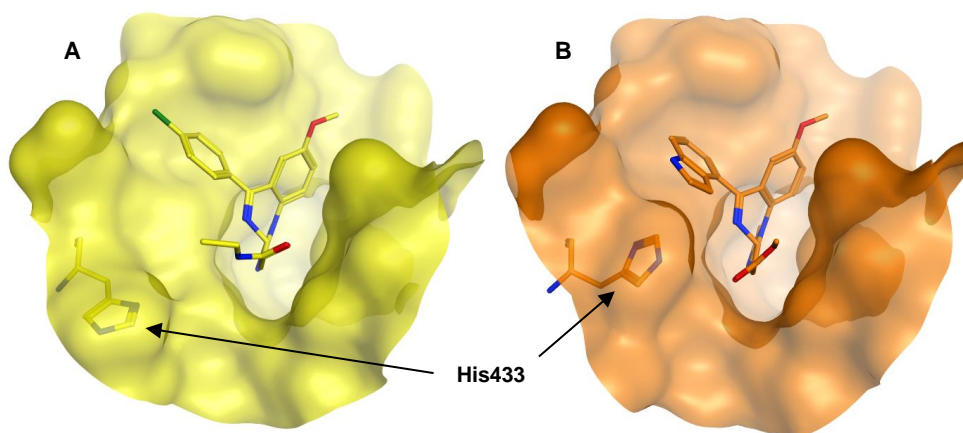


Figure 48. A) X-ray crystal structures of I-BET762 **2** (yellow) bound to BRD2 BD2_{W370F} (PDB: 5DFC). His433 is shown in bold. B) X-ray structure of I-BET762 indole analogue **168** (orange) bound to BRD2 BD2_{W370F} (orange, PDB: 5DFD). His433 is shown in bold. Water molecules have been removed from both images for clarity.

The authors note that in the structure of I-BET762 **2** the BD2-specific histidine sits in an “open” conformation, swung away from the chlorophenyl shelf-binding group.⁸⁶ The structure of the indole compound **168** superposes very well with I-BET762 **2**, with the indole and chlorophenyl groups being almost coplanar. In this structure the histidine is swung into a “closed” conformation, forming an edge-to-face interaction with the indole, which the BD2 selectivity is attributed to. These “open” and “closed” conformations have also been observed in crystal structures of the wild type BET proteins (e.g. PDB codes 2E3K and 5BT5 for BRD2, and 2O01 and 3S92 for BRD3), suggesting that the interaction formed by the indole group was not specific to the BRD2 mutant, and that stabilisation of the “closed” conformation of the histidine is a strategy by which BD2 selectivity could be gained in other molecules.

In conclusion, the development of domain selectivity is a promising pathway of enquiry within the field of bromodomain inhibition, which could help elucidate the separate biological roles of these proteins and ultimately lead to more targeted medicines. Two

chemotypes have been reported that achieve a degree of BD2 selectivity, with claims of up to 82-fold at BRD2 and 30-fold at BRD4.¹⁵⁶ At this stage in this research, 13-fold selectivity at BRD4 had been observed. Both of the examples of BD2 selectivity disclosed have been rationalised in terms of interactions with the histidine residue that is found in BD2 domains only. The discovery of a new chemotype that exhibits rationally improved BD2-selectivity, developed with an understanding of the mechanism by which the selectivity is gained would be a significant contribution to the art.

6.8 Explorations to Improve BD2-Selectivity

At this point in the research programme, an amine linked piperidine compound **(+)-150** had been identified as a potent small molecule BET inhibitor possessing a high ligand efficiency and 13-fold selectivity for the second bromodomain of BRD4 over the first (Figure 49).

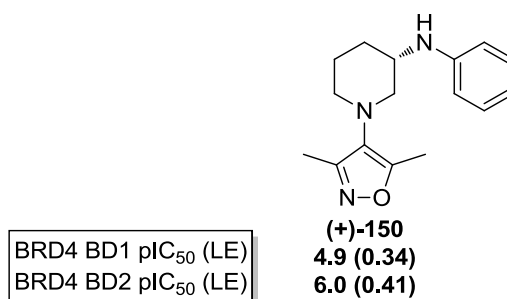


Figure 49. Assay data and calculated ligand efficiency for the preferred enantiomer of the amine linked piperidine compound (+)-150.

Initial investigations had established that the saturation of the core was key to the BD2-selectivity, but the mechanism behind this was unclear. In order to understand the source of the selectivity a series of investigations were subsequently undertaken to elucidate which particular aspect of the compound was important. Hypotheses developed through examining the residue differences in the binding sites of BET BD1 and BD2 domains were used to help design these investigations. The aim was to identify the source of selectivity and synthesise analogues that enhance the effect.

6.8.1 Reinvestigation of Linker Length

From the data collected up to this point, a number of analogues had reproducibly displayed modest, but notable, selectivity for BRD4 BD2 over BD1. One such example, discovered during investigations into linker length in the early stages of this research was the phenethyl piperidine compound **108**, with a two-carbon linker to a phenyl group (Figure 50).

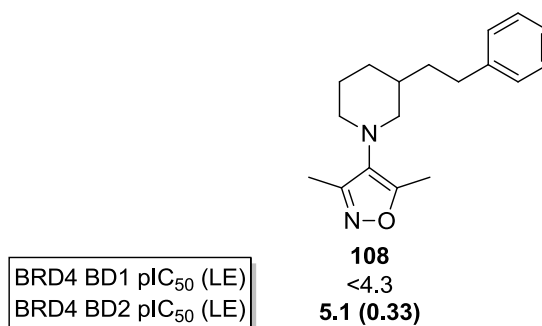


Figure 50. Assay data and calculated ligand efficiency for the phenethyl-substituted piperidine **108**.

It was noted that this compound **108** displayed at least 6-fold selectivity for BD2; the precise level could not be determined as the activity at BRD4 BD1 was below the level of the assay. The significance of this result was not realised at the time.

It was hypothesised that it may be possible to combine the potency and selectivity of the amine-linked compound **150** with the selectivity also present in the phenethyl compound **108**. Therefore, two targets were selected for synthesis, each containing a two atom linker with one carbon and one nitrogen atom, in both available positions.

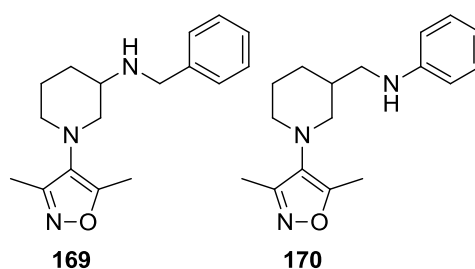
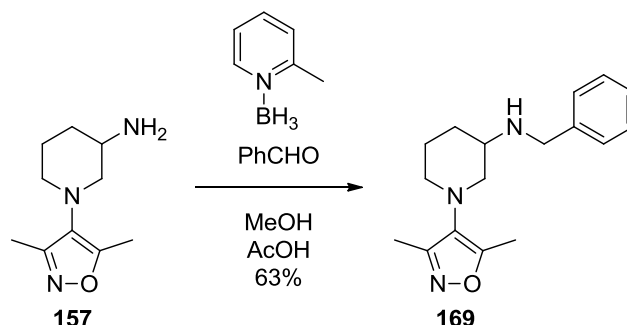


Figure 51. Target compounds with two-atom amine linkers.

The compound with the nitrogen adjacent to the piperidine **169** was synthesised by reductive amination of the previously isolated 3-aminopiperidine intermediate **157** with benzaldehyde (Scheme 75).

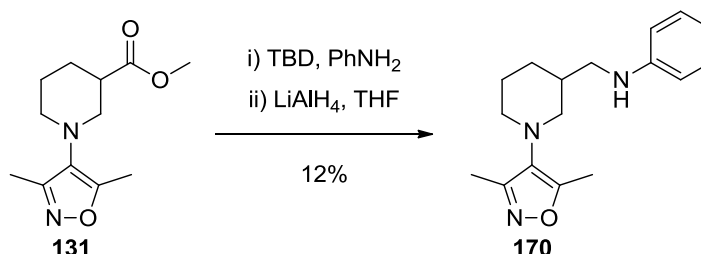


Scheme 75. Reductive amination of 3-aminopiperidine **157** with benzaldehyde.

To mediate this reaction, α -picoline-borane (Pic-BH₃) was identified as a suitable reducing agent.¹⁵⁹ Pic-BH₃ allows reductive amination to be carried out in one-pot, without the need to pre-form the imine, due to its selectivity for imines over carbonyls.

Using equimolar quantities of the amine **157** and benzaldehyde, in a methanol/acetic acid solvent system, the desired product **169** was isolated in 63% yield.

The anilinic congener **170** was synthesised by reducing the corresponding amide (Scheme 76).



Scheme 76. Amide coupling of methyl ester-substituted piperidine **131** with aniline and subsequent reduction to amine **170**.

The phenyl amide intermediate **145** has previously been synthesised using TBD (Section 6.5.1, p75). This procedure was repeated, but rather than isolate the amide, excess amine (both aniline and TBD) was removed by trapping on an acidic ion exchange cartridge, and the remainder of the reaction mixture reduced with lithium aluminium hydride. The desired product **170** was then separated from the alcohol byproduct resulting from the reduction of the ester not fully consumed in the first step.

These amine analogues were submitted for biological screening and the results are shown in Figure 52.

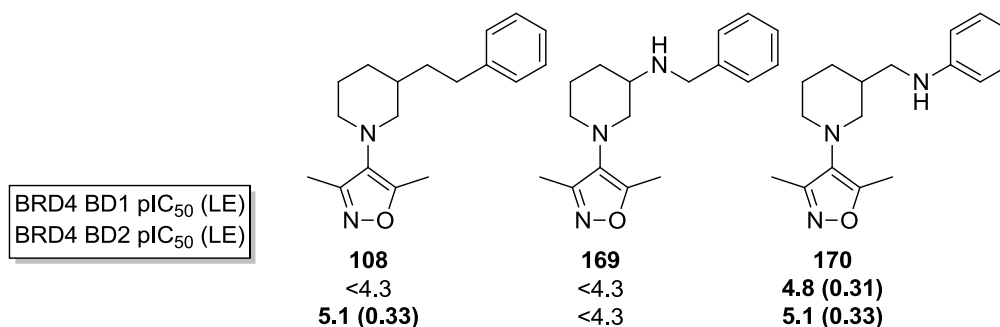


Figure 52. Assay data and calculated ligand efficiencies for two-atom amine linked compounds.

While the anilinic congener **170** displayed similar activity to the phenethyl compound **108**, it provided a reduced degree of selectivity. The benzylamine congener **169**, on the other hand did not register on the assay at all. This may be because the alkyl amine would be protonated at physiological pH, having a calculated pK_{aH} of 9.4,¹⁰¹ which would significantly affect the shape of the linker and unfavourably place a charged species in a lipophilic area of the binding site. Therefore, it was concluded that it was necessary to have only one atom in the linker for the amine to provide the potency and selectivity seen.

6.8.2 Shelf-Binding Group Investigation

Both of the BD2-selective chemotypes disclosed to date have their selectivity rationalised in terms of an interaction with the histidine found only in BD2 domains. Therefore, it was hypothesised that a similar interaction was either already involved in the observed selectivity of the amine linked compound **150**, or could be exploited in order to improve it. It was noted that the main observable difference between the X-ray crystal structures of the methylene linked compound **107**, and the ether **149** and amine **150** linked compounds, was the orientation of the phenyl group on the WPF shelf, with the latter two being almost coplanar (Figure 37, p86). It was hypothesised that this difference in orientation could be resulting in an improved edge-to-face interaction with the BD2-specific histidine residue. Therefore, an investigation was undertaken, varying the steric and electronic properties of the shelf-binding group, to determine whether this would modulate the BD2-selectivity.

Shelf-binding groups to include in this investigation were chosen based on two aims, with the primary aim being the optimisation of potency and selectivity. The secondary consideration was the reduction of lipophilicity. The unsubstituted anilinic starting point **150** possessed a high lipophilicity, with a chromatographic LogD at pH 7.4 (chromLogD_{pH7.4}) of 6.5. Current candidate quality guidelines at GSK use the composite measure of lipophilicity called the property forecast index (PFI) which is calculated as a sum of the chromLogD_{pH7.4} and the number of aromatic rings (Equation 5).^{160,161}

$$PFI = \text{chromLogD}_{\text{pH}7.4} + \#Ar$$

Equation 5.

Guidelines suggest that a PFI value less than 6 is desirable to ensure good solubility and minimal non-specific off-target activity (e.g. CYP inhibition).¹⁶⁰ These molecules have two aromatic rings, and thus the aim was to lower the chromLogD_{pH7.4} to less than 4. The target compounds selected for synthesis are shown in Figure 53.

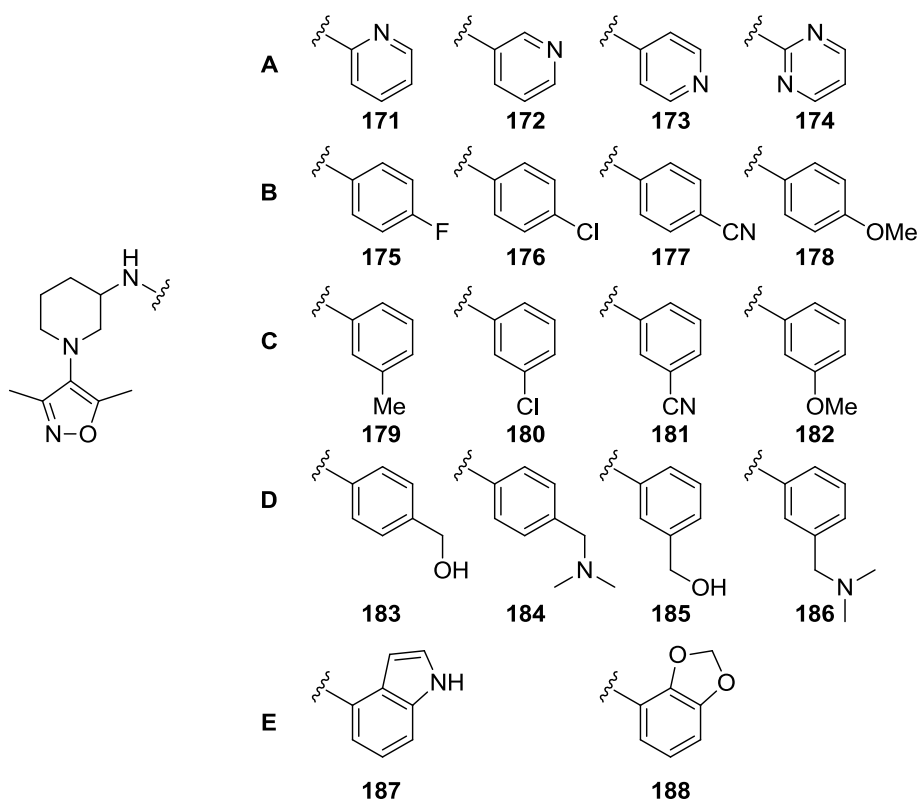


Figure 53. WPF shelf-binding group selection.

Firstly, six-membered heterocycles containing nitrogen atoms were selected (Figure 53A). The nitrogen atoms would significantly alter the electronic distribution of the rings, potentially affecting the interaction with histidine in BD2, and also act to reduce the lipophilicity of the compounds.

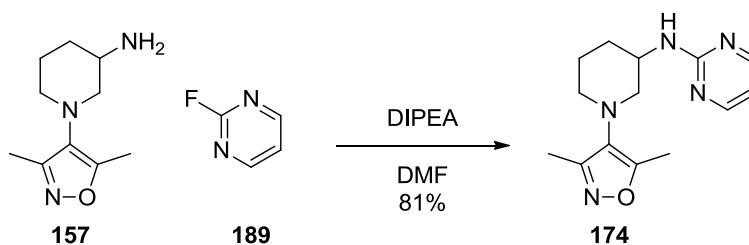
Through examination of the X-ray crystal structure of the unsubstituted compound **150** (Figure 37, p86), the 3- and 4-positions of the phenyl ring were identified as positions where groups would be tolerated, and furthermore could result in increased contact with the protein surface. Therefore, a small set of 3- and 4-substituted phenyl rings were selected (Figure 53B/C). Rings with pendant alcohol and amine groups at the 3- and 4-positions were also selected, with the reduction of lipophilicity in mind (Figure 53D).

Finally, an indole target **187** was identified in an attempt to mimic the selectivity of the I-BET762 indole analogue **168** described by Baud *et al.*,⁸⁶ along with a benzodioxole group **188** that has been used to enhance BD2 selectivity within GSK laboratories (Figure 53E).¹⁶²

It has been recognised that certain anilines are known to exhibit genotoxic effects.¹⁶³ This did not affect the choice of shelf-binding groups at this stage, but would need to be a consideration if any of these compounds were taken on to lead optimisation studies.

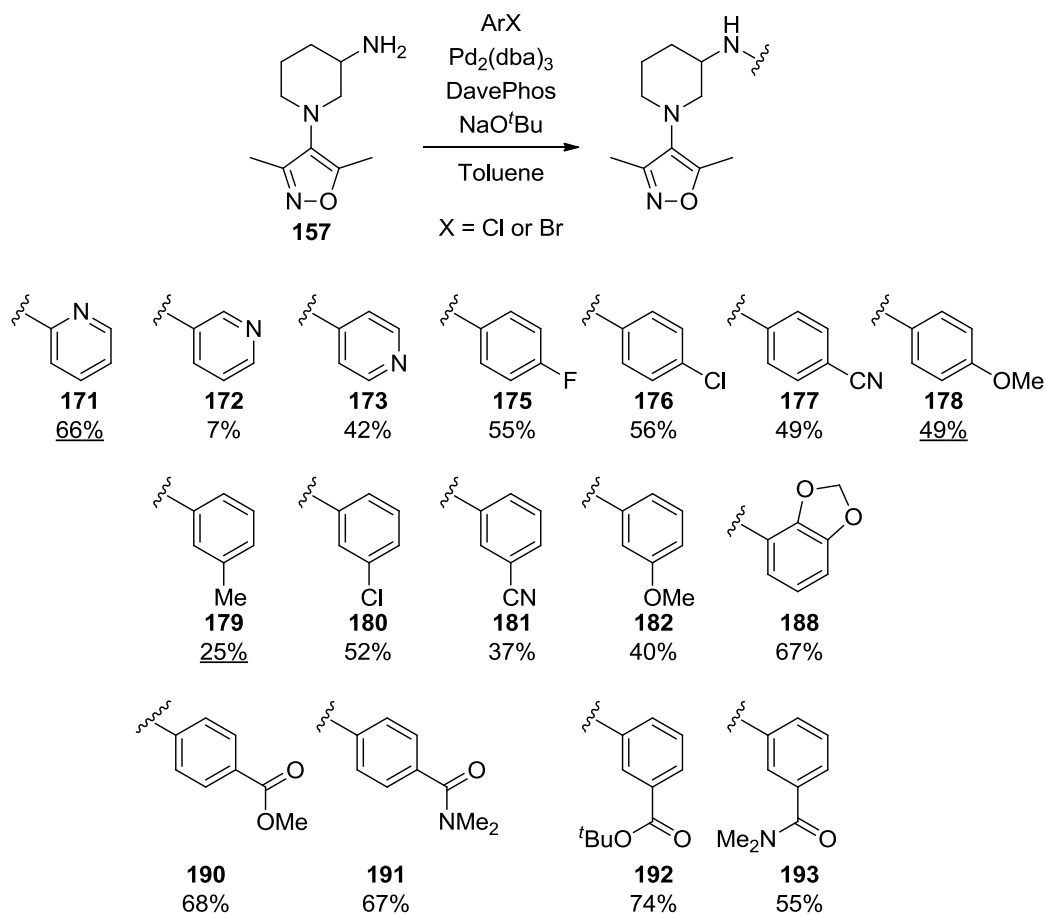
The synthetic route to these analogues was based on the chemistry used to prepare the baseline anilinic compound **150**. Therefore, a large batch of the primary amine intermediate **157** was required. This triggered the reinvestigation of the isoxazole formation route, which is described in Section 6.1.3, to improve the yield and allow sufficient material to be isolated in order to synthesise all of the desired target compounds.

Firstly, S_NAr chemistry was used to access the pyrimidine derivative **174** (Scheme 77). Using DIPEA as a base, the reaction between the amine **157** and 2-fluoropyrimidine **189** proceeded rapidly under microwave irradiation and the desired product was isolated in a very good yield of 81%.



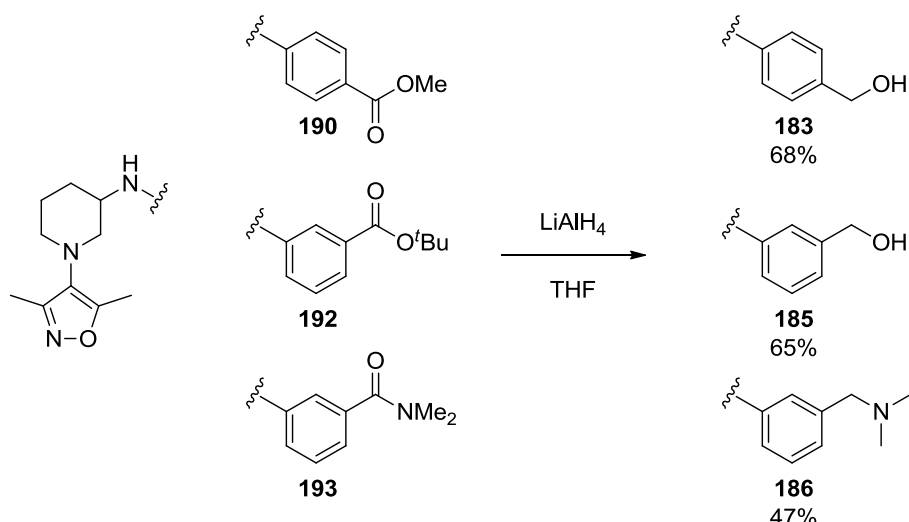
Scheme 77. Synthesis of the pyrimidine derivative 174.

For the remainder of the target compounds, Buchwald-Hartwig chemistry was used. The conditions previously identified, using $Pd_2(dba)_3$, DavePhos and NaO^tBu in toluene, were found to be applicable to the majority of substrates (Scheme 78).



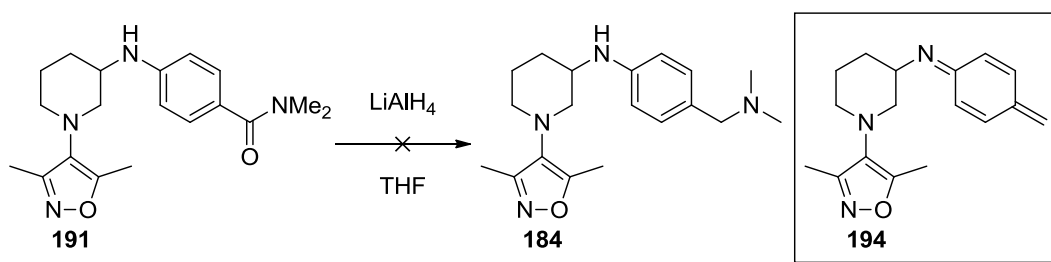
Scheme 78. Synthesis of the majority of the WPF shelf-binding group array. Underlined yields indicate to the use of the aryl chloride in the reaction. All other products were synthesised using an aryl bromide.

Yields were generally acceptable, with the activated 2-pyridine **171** being notably good. In order to synthesise the pendant alcohol and amine analogues, appropriate esters and amides were used for the amination step. These compounds were subsequently subjected to reduction conditions (Scheme 79).



Scheme 79. Reduction of ester and amide analogues to their pendant alcohol and amine derivatives.

While three of the four pendant amine and alcohol compounds were isolated, the fourth reaction did not provide the desired product (Scheme 80).

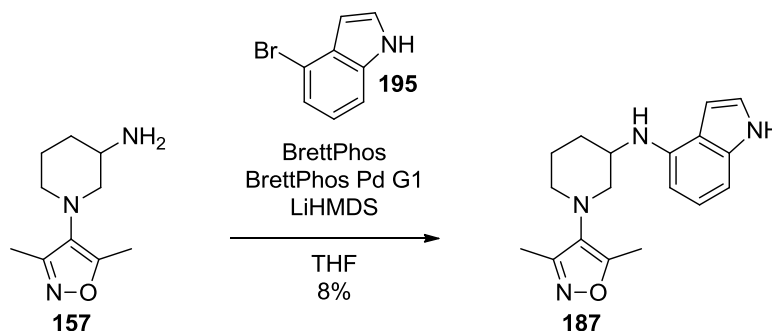


Scheme 80. Attempted reduction of 4-substituted amide analogue **191**.

LCMS analysis of the reaction mixture of the reduction of the 4-amide analogue **191** with lithium aluminium hydride showed complete consumption of starting material and two main products. The LCMS retention time and mass ion of the major product was consistent with that of the pendant alcohol congener **183**, which is presumed to form by elimination of dimethylamine and subsequent attack by water as the mass ion of the minor product was consistent with an azaquinone methide **194** that would be formed in this pathway.¹⁶⁴ This was taken as sufficient evidence that the product was unstable and no further attempts to isolate it were undertaken.

The final analogue to be synthesised was the indole compound **187** (Scheme 81). However, when the general conditions were applied to this analogue, multiple products were formed and a significant amount of unreacted starting material remained **157** in the reaction mixture. Attempts to purify the small amount of product formed were unsuccessful. A literature search for conditions to couple unprotected bromoindoles was conducted and revealed conditions published by Henderson and Buchwald which had been used to couple the indole in question with a range of primary amines, using

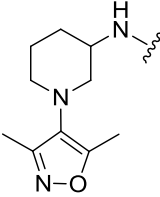
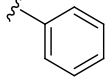
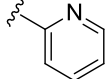
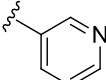
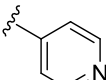
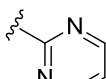
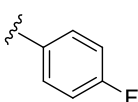
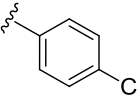
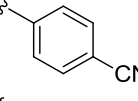
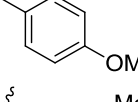
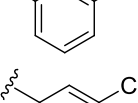
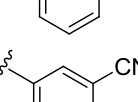
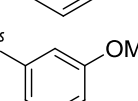
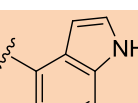
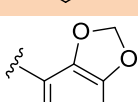
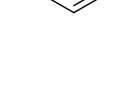
BrettPhos and LiHMDS.¹⁶⁵ These conditions were applied and were found to be successful (Scheme 81).



Scheme 81. Synthesis of the indole analogue 187.

While the reaction appeared to proceed with good conversion, it became apparent that the product was decomposing while the aqueous ammonium carbonate was being removed *in vacuo* after reverse phase purification. This significantly affected the purity of the material and explained the previous failure to isolate the product. A subsequent normal phase purification had to be performed, providing the desired compound in an 8% yield.

The compounds from the shelf-binding group array were submitted for biological screening and the data is presented in Table 8.

		BRD4 BD1		BRD4 BD2		BD2 – BD1	ChromLogD pH 7.4
		pIC ₅₀	LE	pIC ₅₀	LE		
150		4.7	0.32	5.7	0.39	1.0	6.5
171		<4.3	-	5.3	0.36	>1.0	4.7
172		<4.3	-	5.1	0.35	>0.8	3.9
173		<4.3	-	4.7	0.32	>0.4	1.7
174		4.6	0.32	5.3	0.36	0.7	3.9
175		4.6	0.30	5.4	0.35	0.8	6.4
176		4.7	0.31	5.5	0.36	0.8	7.2
177		4.6 ^a	0.29	5.4	0.34	0.8	5.6
178		4.5	0.28	5.1	0.32	0.6	6.0
179		4.5	0.29	5.5	0.36	1.0	7.0
180		4.7	0.31	5.7	0.37	1.0	7.2
181		4.4	0.27	5.3	0.33	0.9	6.0
182		4.5	0.28	5.6	0.35	1.1	6.2
187		4.9	0.29	6.1	0.36	1.2	5.7
188		4.5	0.27	5.6	0.33	1.1	6.4

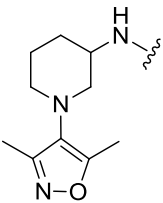
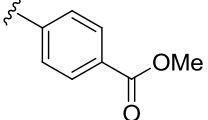
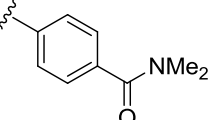
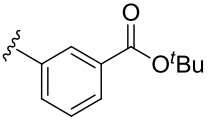
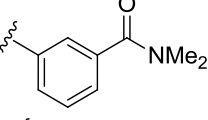
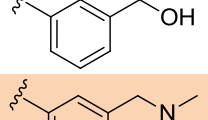
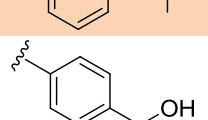
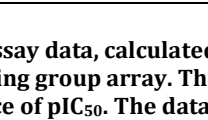
		BRD4 BD1		BRD4 BD2		BD2 – BD1	ChromLogD pH 7.4
		pIC ₅₀	LE	pIC ₅₀	LE		
190		4.5	0.26	5.3	0.30	0.8	5.9
191		5.0	0.27	5.0	0.27	0	4.3
192		<4.3	-	5.2	0.26	>0.9	7.8
193		4.4	0.24	5.4	0.30	1.0	4.5
185		4.4	0.27	5.6	0.35	1.2	4.2
186		4.6	0.26	5.9	0.34	1.3	3.2
183		4.5	0.28	5.1	0.32	0.6	4.1

Table 8. Assay data, calculated ligand efficiencies and ChromLogD at pH 7.4 for compounds from the shelf-binding group array. The selectivity of each compound for BRD4 BD2 over BD1 is expressed as a difference of pIC₅₀. The data for the unsubstituted, racemic aniline **150 has been included to allow direct comparison and compounds displaying an increased potency at BRD4 BD2 have been highlighted. ^aA pIC₅₀ value of <4.3 was determined on one test occasion out of four and was excluded from the reported value.**

The majority of these compounds returned lower potencies at BRD4 BD2 than the unsubstituted aniline **150**, which has a pIC₅₀ of 5.7 (data from the racemate has been used here to allow for direct comparison). The two exceptions are pendant amine **186** with a pIC₅₀ of 5.9, and the indole **187** with a pIC₅₀ of 6.1 (highlighted in Table 8). Though these increases are not vast, and within experimental error, the pendant amine **186** has the distinct advantage of greatly reducing the chromLogD_{pH7.4} versus the unsubstituted ring **150** (3.2 and 6.5, respectively).

The important observation made from these data was that the majority of the compounds displayed around a log unit of selectivity for BD2 over BD1. The exception was the 4-substituted amide analogue **191** which showed no domain selectivity, while the related ester **190** did. Even the indole compound **187**, which was selected due to its

precedent for displaying BD2 selectivity,⁸⁶ exhibited no significant increase in selectivity over the baseline aniline **150** (1.2 *versus* 1.0 log units, respectively). This was taken as good evidence that the selectivity does not originate exclusively from interactions on the WPF shelf.

Further evidence that the BD2-selectivity is governed from elsewhere within the molecules was gained from an X-ray crystal structure obtained from the semi-unsaturated amine linked analogue **160** (Figure 54).

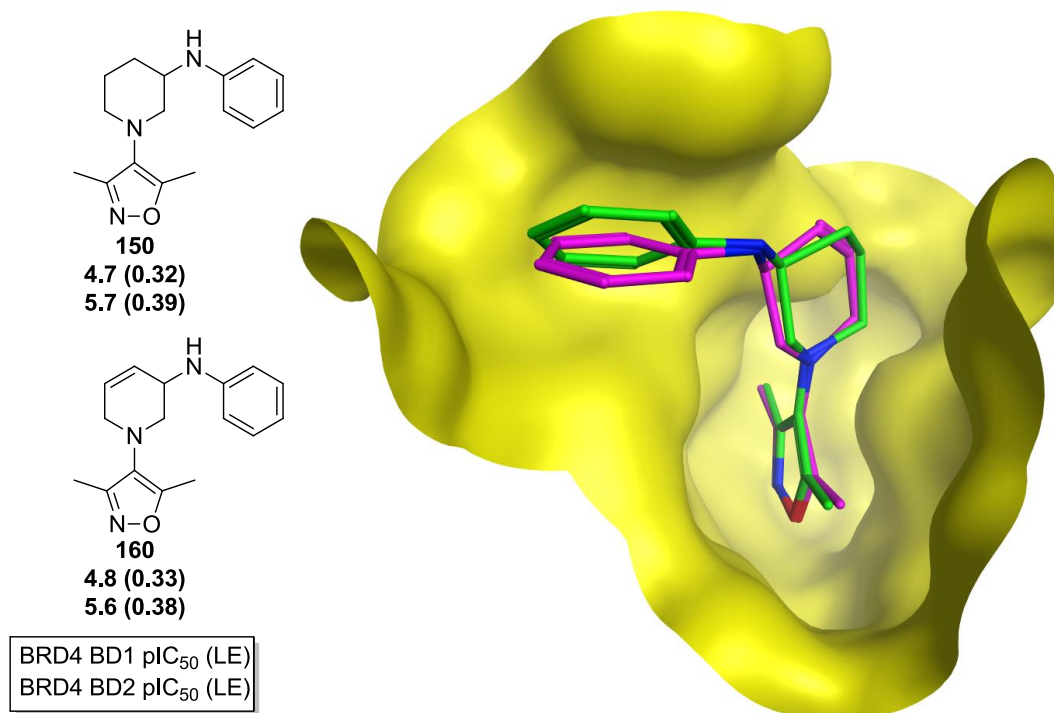


Figure 54. X-ray crystal structure of the semi-unsaturated amine linked analogue **160** (magenta) bound to BRD2 BD2 (yellow) with the saturated analogue **150** (green), also bound to BRD2 BD2, superposed. Water molecules have been removed from the image for clarity. The structures of both molecules are shown (left) along with their assay data and calculated ligand efficiencies.

The amine-linked piperidine **150** and its semi-unsaturated analogue **160** displayed similar activities, and therefore selectivities, at BRD4 BD1 and BD2. However, when their X-ray crystal structures were compared, the orientation of the phenyl groups on the WPF shelf were subtly different, while the core of both molecules overlaid very well. Therefore, it was hypothesised that the selectivity originated from an aspect of the conformation or placement of the core itself. Disubstituted piperidine targets were selected in order to probe this idea, and to identify further vectors for elaboration.

6.9 Disubstituted Piperidines

The next stage of this research was the design and synthesis of disubstituted piperidine compounds, in order to explore how the conformation of the molecules, and their

positioning within the binding site, was affected. The aims behind this were two-fold. Firstly, the selectivity observed with the amine-linked piperidine compound **150** may be connected with the shape and position of the piperidine core, so it was desirable to understand and potentially improve this phenomenon. Secondly, a viable lead compound requires opportunities for further elaboration; therefore, it was important to identify potential vectors to other areas of the binding site and determine whether or not they would provide any benefit in terms of activity and/or physicochemical properties. Based on this, two vectors were selected for exploration (Figure 55).

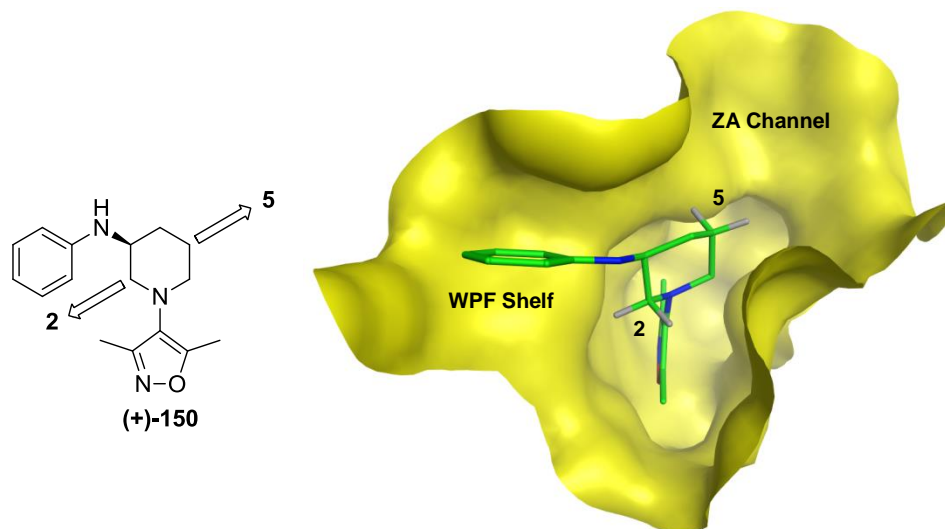


Figure 55. Selected vectors for exploration from the framework of monosubstituted piperidine (+)-150. X-ray crystal structure piperidine 150 (green) bound to BRD2 BD2 (yellow). The WPF shelf and the ZA channel are labelled and hydrogen atoms have been included at the labelled 2- and 5-positions to illustrate the vectors they provide. Water molecules have been removed from the image for clarity.

According to the X-ray crystal structure obtained from the 3-aniline **150** (Figure 55), the 5-position of the piperidine offered the potential to access the ZA channel. The previous attempt to explore an interaction with this area of the binding site was hindered by the ambiguity of the binding mode of the mono-substituted piperidine ester/amides, after an X-ray crystal structure was obtained showing a methyl ester moiety directed towards the WPF shelf (Figure 35, p80). However, with a 3-position WPF shelf-binding group already in place this was less of a concern.

The 2-position of the piperidine was also selected, as the axial vector was directed in such a way as to provide access to a groove adjacent to the BD2-specific histidine and, therefore, presented an opportunity to gain potency and selectivity in a lead optimisation programme. Furthermore, occupation of this groove was deemed important in rationalising the BD2-selectivity of RVX-208 **166** and RVX-297 **167** due to a face-on

packing interaction between the histidine and the dimethylphenol ring of the ligand (Figure 56).^{155,157}

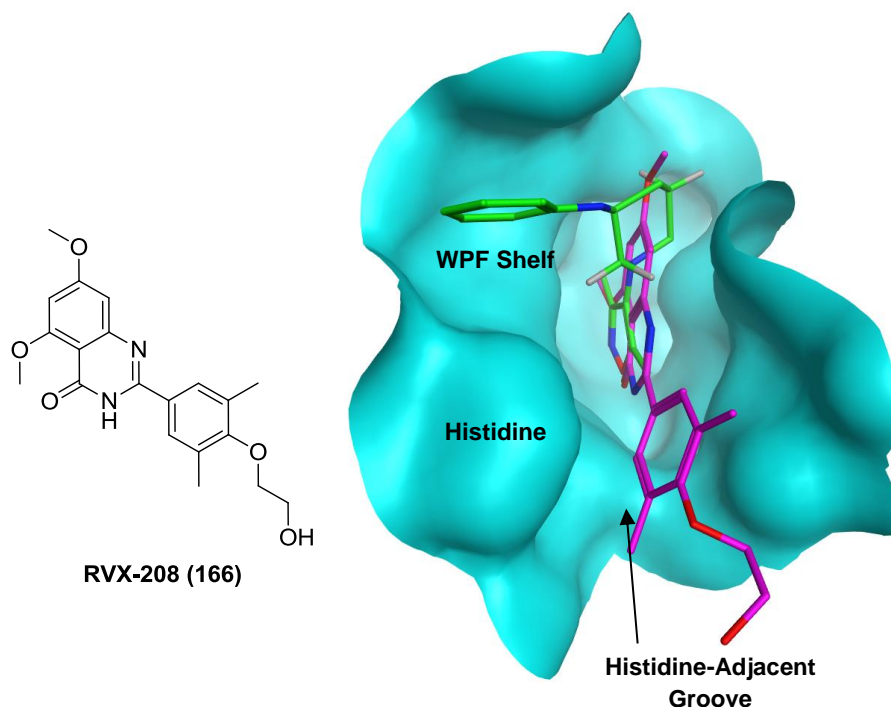
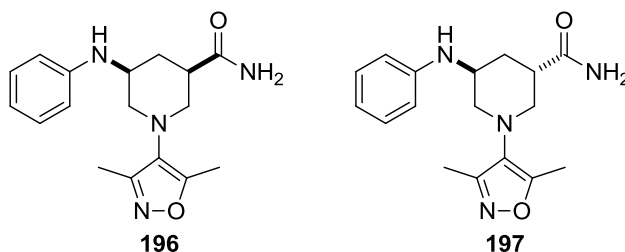


Figure 56. The structure of RVX-208 166.¹⁵⁵ X-ray crystal structure of RVX-208 166 (magenta) bound to BRD4 BD2 (cyan, PDB: 4J1P). The structure of monosubstituted piperidine 150 (green) bound to BRD2 BD2 has been superposed. The WPF shelf and the area of the molecular surface corresponding to the BD2-specific histidine have been labelled. The histidine-adjacent groove is occupied. Water molecules have been removed from the image for clarity.

6.9.1 3,5-Disubstitution

As before, an amide was chosen with which to probe for an interaction with the ZA channel. Rather than targeting an array of amides, a single example was chosen which had the highest likelihood of being tolerated in the binding site, namely a primary amide (Scheme 82).

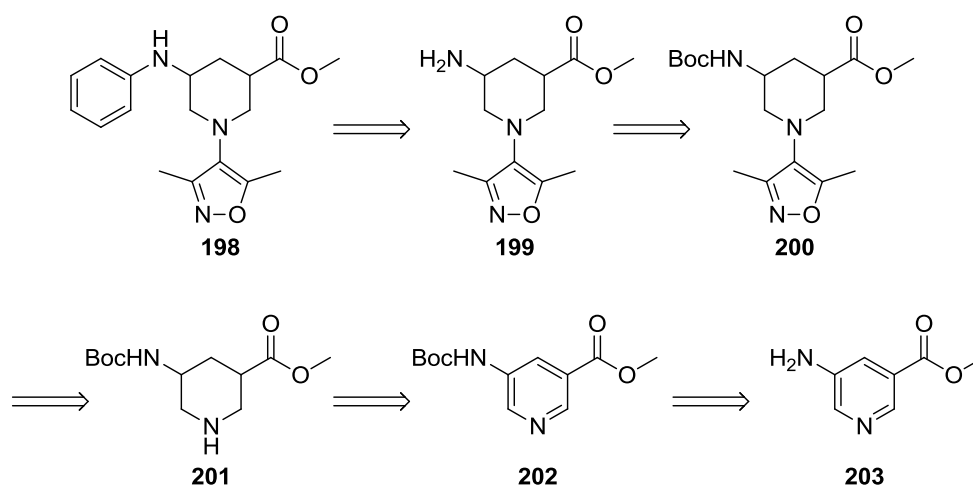


Scheme 82. 3,5-Disubstituted target compounds.

For this investigation, an unsubstituted phenyl shelf-binding group was used rather one of the groups from the shelf-binding array (Section 6.8.2) in order to decouple the SAR observations from one another. With this established, a lead optimisation programme could bring together favourable 3- and 5-position groups in one molecule.

Examination of the X-ray crystal structure of the monosubstituted amine-linked compound **150** suggested that the *cis* arrangement **196** was more likely to position the amide group favourably. However, if a synthesis were employed that also generated the *trans* diastereomer **197** then this hypothesis could be tested. The benefits being sought from these targets were an increase in potency and/or a reduction in lipophilicity. The latter point was important as the $\text{chromLogD}_{\text{pH}7.4}$ of the monosubstituted amine linked piperidine **150** was relatively high (6.5). The inclusion of the primary amide was calculated to reduce the $\text{chromLogD}_{\text{pH}7.4}$ to 3.4, which corresponds to a PFI value of 5.4, which falls within the desirable parameter of less than 6 for drug candidates.¹⁶⁰

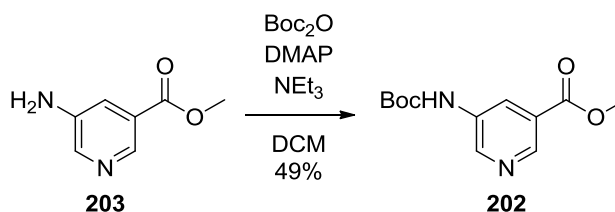
It was envisaged that these compounds could be isolated from a common, methyl ester intermediate **198** (Scheme 83).



Scheme 83. Retrosynthetic analysis of 3,5-disubstituted methyl ester common intermediate 198.

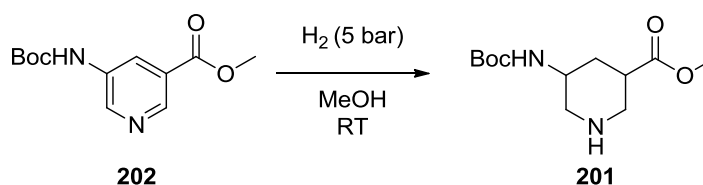
Isoxazole formation chemistry was to be used, with the appropriate piperidine **201** being synthesised by hydrogenation of pyridine **202**. *N*-Boc protection was required to avoid undesired product formation during the *N*-alkylation process. Therefore, the first step in the forward synthesis was the protection of the commercially available starting material, methyl 5-aminonicotinate **203**.

A search of procedures carried out within GSK laboratories revealed that the *N*-Boc protection had been performed previously on this exact substrate, so these conditions were replicated (Scheme 84).¹⁶⁶

Scheme 84. *N*-Boc protection of methyl 5-aminonicotinate **203**.

Using catalytic DMAP, triethylamine as a base, and 1.2 equivalent of Boc anhydride in DCM, the protected product was isolated in a 49% yield, which was comparable to the yield from the procedure being followed.¹⁶⁶

For the second step in the reaction sequence, a screen of hydrogenation catalysts was performed in order to find conditions that provided clean conversion to the piperidine product **201** (Table 9).



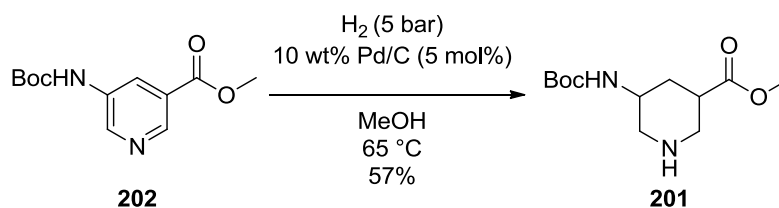
Catalyst	Loading / mol%				+ AcOH		
		202	Imp	201?	202	Imp	201?
Pd on C 5 wt%	5	66	34	✓	-	100	✓
Ru on C 5 wt%	5	100	-	✗	100	-	✗
Pt on C 5 wt%	5	87	13	✗	82	18	✓
Pd on C 10 wt%	10	-	100	✓	-	67	✓ (23%)
Rh on Al₂O₃ 5 wt%	5	79	21	✗	69	31	✓
PtO₂	5	89	11	✓	86	14	✓

Table 9. Pyridine **202** (20 mg, 79 μmol) and a catalyst in MeOH (0.75 mL), with or without AcOH (2 eq.) was stirred for 24 h under an atmosphere of hydrogen (5 bar). For each reaction, the percentage of the LCMS UV trace is given for the starting material **202** and a common impurity (Imp), thought to be an intermediate. The presence or absence of product **201** in the reaction mixture is indicated by a tick or a cross, respectively.

Six catalysts were included in the screen, including two commercial sources of palladium on carbon. Methanol was used due to the poor solubility of the pyridine in other solvents, and to avoid cross-esterification with other alcoholic solvents. All reactions were performed in duplicate, with or without two equivalents of acetic acid. The reactions were stirred at room temperature under a five bar atmosphere of hydrogen for 24 hours and the reaction mixtures analysed by LCMS. The product was only very weakly UV active, so LCMS analysis could only be used to determine if the mass of the product was present (denoted by ticks and cross in Table 9), but not to quantify it. LCMS was chiefly used to follow the depletion of the starting material, as well as an unidentified impurity

that was speculated to be a partially hydrogenated intermediate (shown as percentages of the UV trace in Table 9).

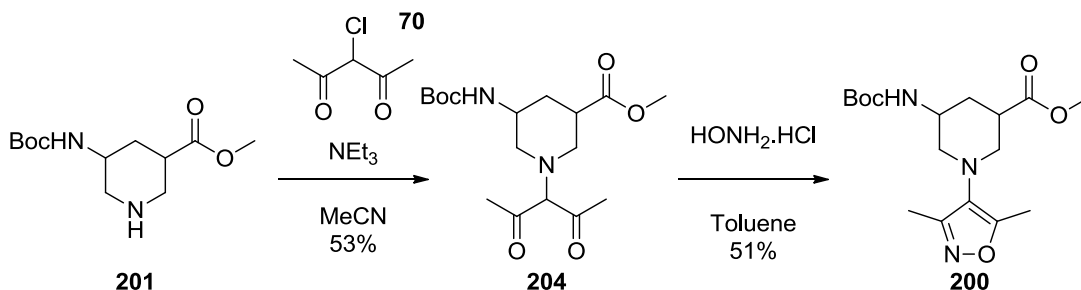
The only conditions that completely removed the starting material involved a palladium on carbon catalyst, and in one of those reactions there was enough product formed for it to be detectable on the LCMS UV trace. The 10 wt% palladium on carbon catalyst was selected for further investigation and it was found that if the temperature was increased to 65 °C then excellent conversion could be achieved, without the need for acetic acid (Scheme 85).



Scheme 85. Hydrogenation of *N*-Boc methyl ester pyridine **202.**

Using these conditions, 4.5 g of piperidine **201** was isolated from 7.7 g of pyridine **202**, representing a 57% yield. A significant portion of the remaining mass-balance was lost due to partial hydrolysis of the ester during reverse-phase chromatography. The acid impurity was removed by capture on a basic ion exchange cartridge. ¹H NMR analysis indicated that both diastereomers of the product were present in a 1:1 ratio, allowing both diastereomers of the product to be targeted.

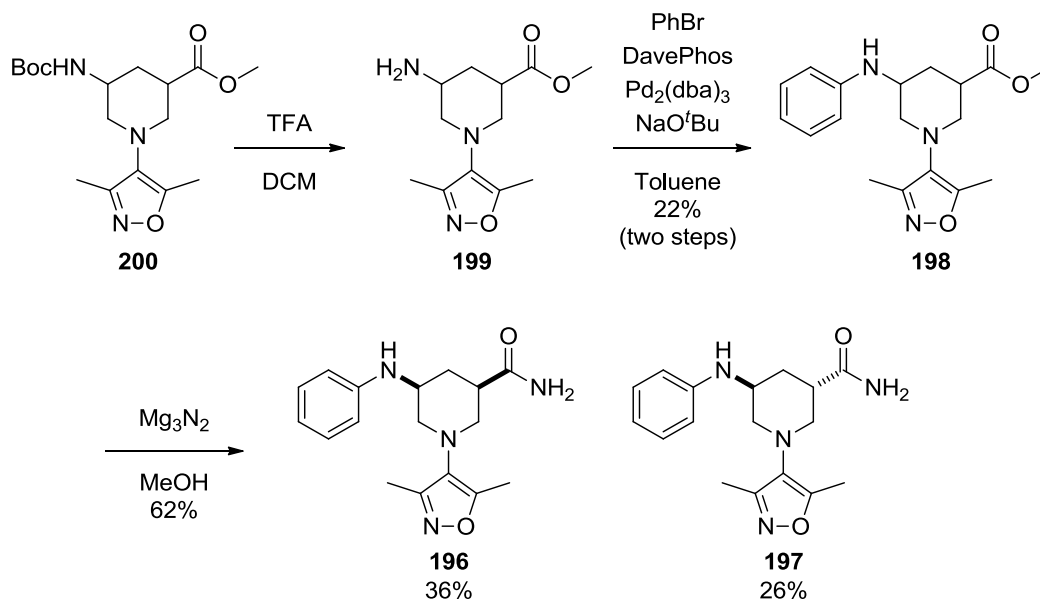
Unfortunately, when the optimised isoxazole formation conditions (HONH₂ in EtOH followed by Na₂CO₃ in H₂O) were applied to this piperidine **201**, multiple species were formed. The formation of the isoxazole product **200** was negligible, regardless of whether the dicarbonyl intermediate **204** was telescoped through to cyclisation or isolated first. Therefore, conditions were reverted to the Dean-Stark method used previously (Scheme 86).



Scheme 86. Isoxazole formation in the synthesis of 3,5-disubstituted piperidine targets.

The cyclisation step from the intermediate dicarbonyl **204** proceeded with an isolated yield of 51%, which was among the highest yields achieved with this method in this research.

Following from this, the Boc group was removed and the resulting amine intermediate **199** was subjected to the Buchwald-Hartwig amination conditions that have previously been used on this series (Scheme 87).



Scheme 87. Synthesis of 3,5-disubstituted primary amides.

The disubstituted methyl ester **198**, which remained as a mixture of diastereomers, was heated with magnesium nitride in methanol to convert the ester to a primary amide, with a yield of 62%. Pleasingly, at this final stage, the separation of the diastereomers, as observed by LCMS, was improved in comparison to the previous intermediates. This allowed for isolation of both diastereomers without significant losses being accrued in purification. These racemates were submitted for biological screening, and the data is shown in Figure 57.

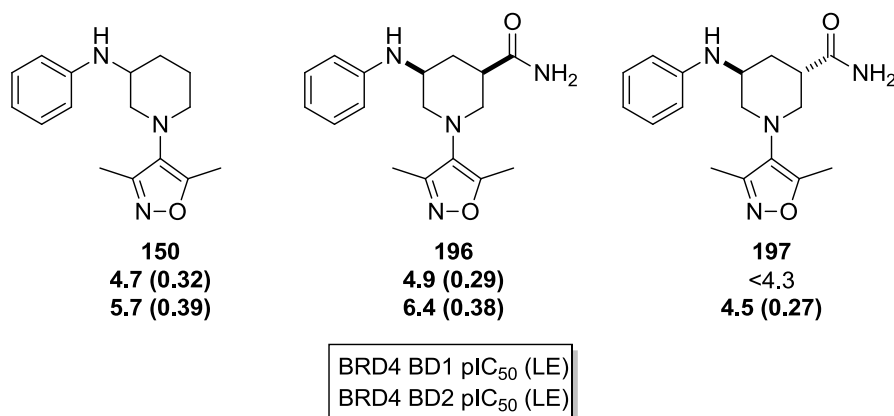


Figure 57. Assay data and calculated ligand efficiencies for 3,5-disubstituted piperidines. The racemic monosubstituted analogue **150** has been included for comparison.

As suspected, the *cis* diastereomer **196** was significantly more active than its *trans* counterpart **197**, which only just registered above the lower limit of the assay at BRD4 BD2. The *cis* substitution was not only tolerated, but resulted in over half a log unit potency increase at BD2 compared the racemic monosubstituted analogue **150**. This material was subsequently separated into the single enantiomers by chiral chromatography and the biological data associated with these is presented in Figure 58.

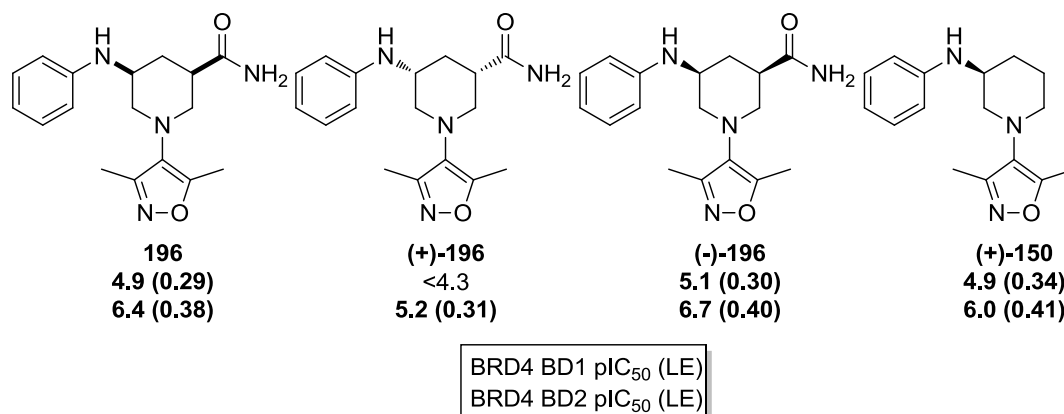


Figure 58. Assay data and calculated ligand efficiencies for *cis* 3,5-disubstituted piperidines. The enantiomerically pure monosubstituted analogue **(+)-150** has been included for comparison.

The (-)-enantiomer **(-)-196** displayed greater activity than the (+)-enantiomer **(+)-196** and from this, and the X-ray crystal structure obtained from the racemate (Figure 59), a 3*R*,5*S*-stereochemical assignment was inferred. In comparison to the enantiopure monosubstituted analogue **(+)-150** a 0.7 log unit increase in potency at BRD4 BD2 was achieved, but only a 0.3 log unit increase at BD1, and thus the selectivity was improved from 13-fold to 40-fold.

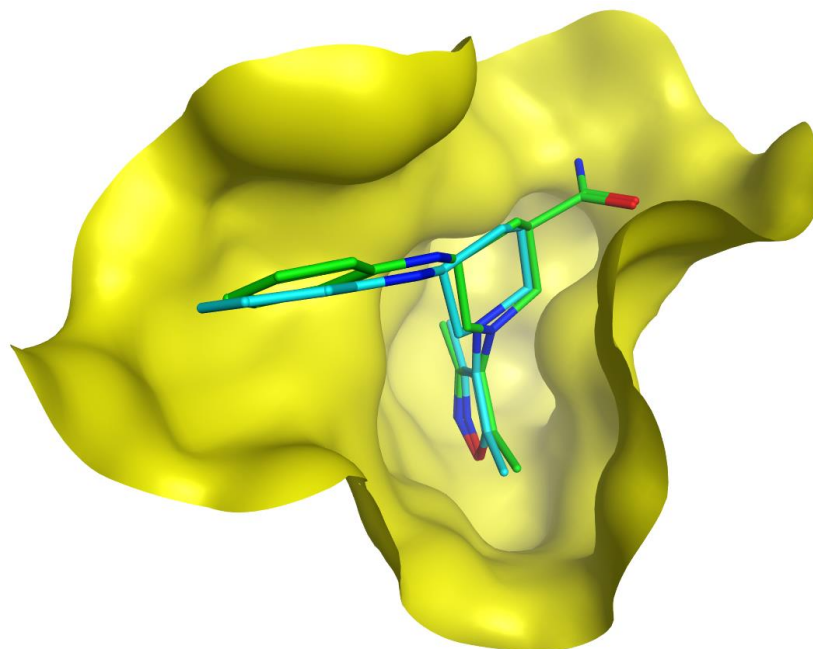


Figure 59. X-ray crystal structure of the *cis*-3,5-disubstituted piperidine **196** (green) bound to BRD2 BD2 (yellow) with the monosubstituted analogue **150** (cyan), also bound to BRD2 BD2, superposed. Water molecules have been removed from the image for clarity.

Figure 59 shows an X-ray crystal structure of the *cis*-disubstituted compound **196** bound to BRD2 BD2. As was expected, the primary amide was positioned at the bottom of the ZA channel, without significant movement of the piperidine core in comparison to the monosubstituted analogue **150**, which has been superposed on the image. The crystal structure suggested the presence of at least two hydrogen bonding interactions with the peptide backbone (Figure 60).

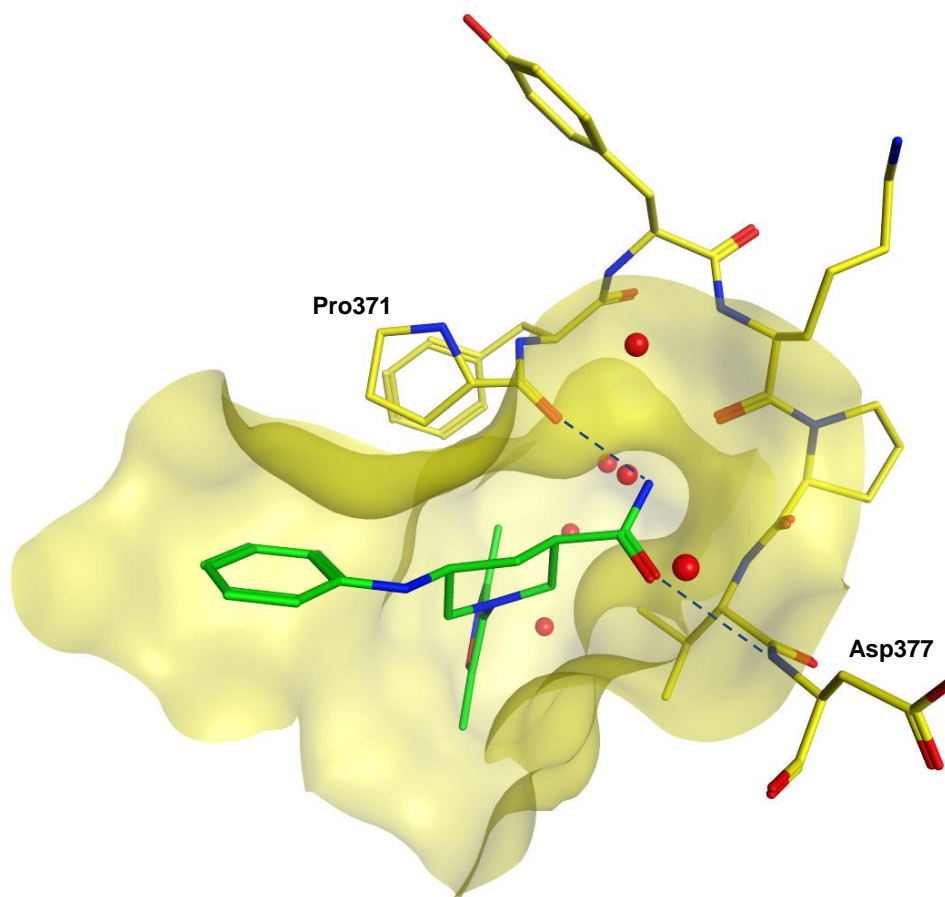


Figure 60. X-ray crystal structure of the *cis*-3,5-disubstituted piperidine 196 (green) bound to BRD2 BD2 (yellow). Water molecules (red) and peptide residues (yellow) in the vicinity of the primary amide have been highlighted, with all others removed for clarity. Dotted lines (blue) show atoms in close enough proximity for hydrogen bonding interactions to occur.

The NH₂ group of the primary amide formed a hydrogen bond with the backbone carbonyl of Pro371, which is the proline that constitutes the “P” in “WPF shelf”, while the amide carbonyl formed a hydrogen bond with the backbone NH of Asp377. It had been envisioned that this group would be able to form polar interactions of this type within this region of the protein, and they are likely to be responsible for the increased potency at BRD4 BD2. The lower potency increase at BRD4 BD1 may have been due to subtle repositioning of the piperidine core against the isoleucine gatekeeper residue of BRD4 BD1, and this hypothesis was further investigated by examining the effects of 2,3-disubstitution.

6.9.2 2,3-Disubstitution

To ascertain the viability of using the 2-position as a vector, methyl-substituted compounds, with both the possible arrangements, were targeted for synthesis (Figure 61).

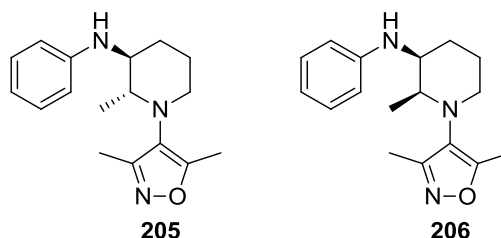
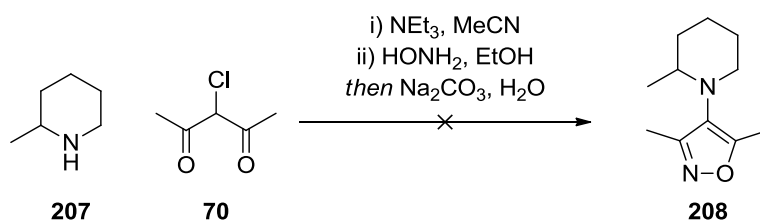


Figure 61. 2,3-Disubstituted target compounds.

Based on the X-ray crystal structure of the monosubstituted analogue **150**, the *cis*-diastereomer **206** would place the methyl in the position that could potentially be extended from to access the groove adjacent to the BD2-specific histidine residue, in a similar manner to RVX-208 (Figure 56, p110). The *trans*-diastereomer **205**, on the other hand, would place a methyl group in a position which was pointed directly at the protein; more specifically, at the valine gatekeeper residue which is specific to BD2 domains and is an isoleucine in BD1 domains. It was hypothesised that a clash with the isoleucine in BD1 domains may be the source of the BD2 selectivity seen in the amine linked piperidine **150**. It may also be the reason that the introduction of a primary amide at the 5-position resulted in a greater increase in potency at BRD4 BD2 than BD1, as the disubstituted compound had a reduced ability to manoeuvre away from the gatekeeper residue. It was envisaged that the methyl group of *trans*-diastereomer **205** could accentuate this clash and form improved lipophilic interactions with the valine of BD2 domains.

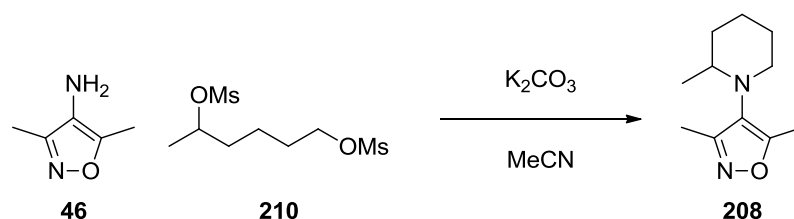
The initial route proposal to access these compounds was to synthesise the appropriate piperidines and then use the isoxazole formation chemistry. The viability of this approach was determined using 2-methylpiperidine **207** (Scheme 88).



Scheme 88. Attempted *N*-alkylation and isoxazole formation with 2-methylpiperidine **207**.

Unfortunately, no product could be isolated from this process. The *N*-alkylation step, which had proceeded cleanly for all other substrates prior to this point, produced multiple products in this case. Even when a sample of the dicarbonyl intermediate was isolated and then subjected to the cyclisation conditions, multiple product formation was again observed. Therefore, this disconnection was abandoned, and routes to form the target compounds *via* formation of the saturated ring were investigated.

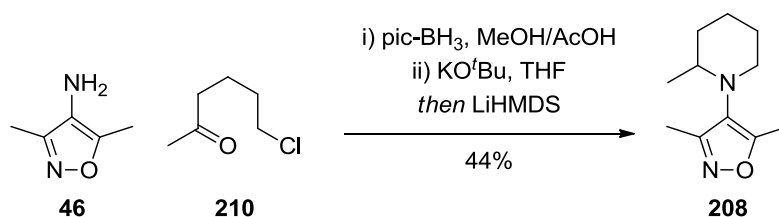
Again, validation of potential routes was carried out for the 2-methylpiperidine isoxazole **208**. The first proposed route involved the conditions previously used to alkylate the aminoisoxazole **46** with alkyl dihalides, applied to a mesylated diol **209** (Scheme 89).



Scheme 89. Attempted synthesis of 2-methylpiperidine isoxazole **208** using a mesylated diol **209**.

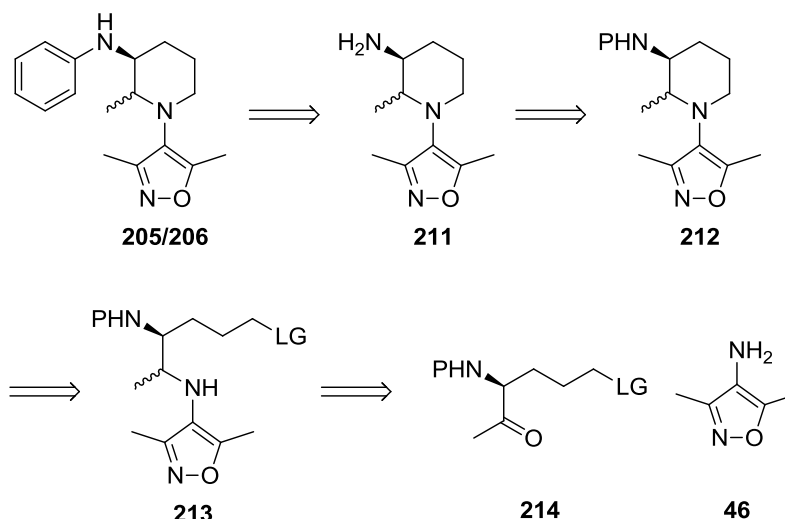
Some conversion was seen in this reaction by LCMS analysis, but it was not deemed sufficient to warrant purification, and alternative alkylations were investigated.

Secondly, a reductive amination approach was carried out between a ketone bearing an alkyl chloride **210** and the aminoisoxazole **46** using picoline borane as the reducing agent. Successful initial amine formation occurred and the subsequent cyclisation, mediated by LiHMDS, provided the desired product **208** in 44% yield (Scheme 90).



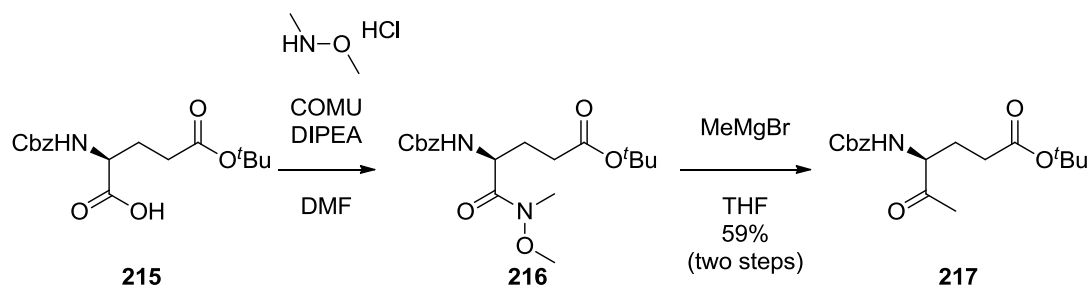
Scheme 90. Synthesis of 2-methylpiperidine isoxazole **208**.

Based on these results on the model substrate, a retrosynthesis of the 2,3-disubstituted piperidine derivatives was designed, with the key steps being a reductive amination and subsequent base-catalysed displacement of leaving group to form the ring (Scheme 91).



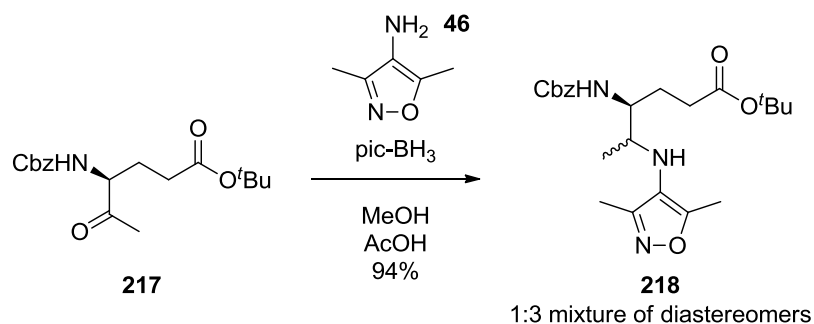
Scheme 91. Retrosynthetic analysis of 2,3-disubstituted piperidine analogues. P represents an appropriate amine protecting group and LG an appropriate leaving group.

The forward route associated with this retrosynthesis required a starting material containing a methyl ketone with a protected amine at the α -position, and an appropriate leaving group on the end of the alkyl chain **214**. A commercially available precursor was identified as a protected L-Glutamic acid **215** (Scheme 92).



Scheme 92. Synthesis of the methyl ketone derivative **217 of the protected L-Glutamic acid **215**.**

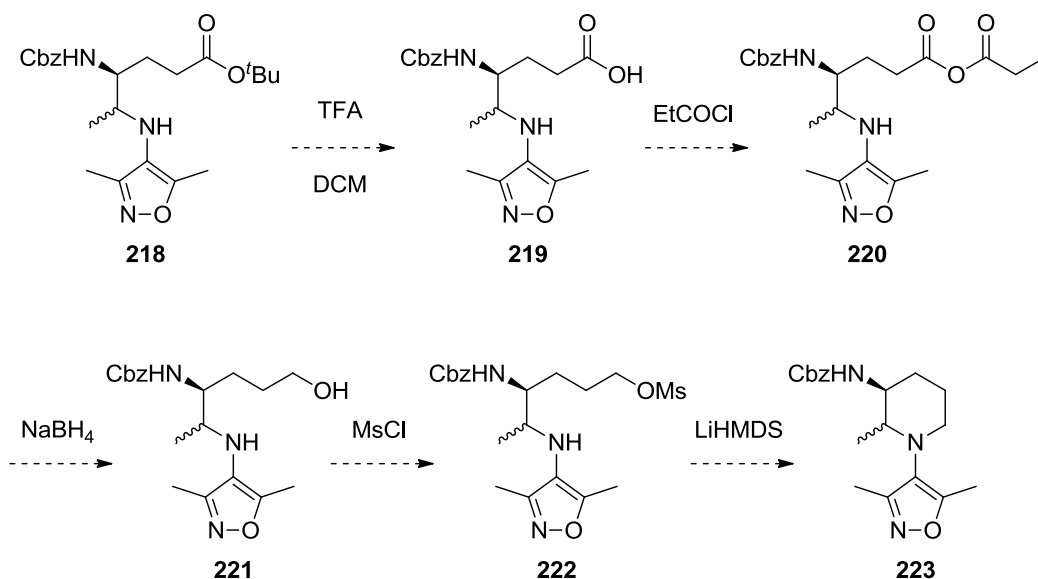
The L-glutamic acid derivative **215**, bearing Cbz protection on the amine and a *tert*-butyl ester in place of the side chain carboxylic acid, was converted to a Weinreb amide by amide coupling. The coupling agent used was COMU, which is reported to result in low to non-existent racemisation of α -amino acids.¹⁶⁷ The Weinreb amide **216** was used after workup, without purification, in the next step, in which it was subjected to an excess of methylmagnesium bromide. The Grignard reagent reacted selectively with the Weinreb amide, and not the *tert*-butyl ester or the carbamate protecting group, despite the use of three equivalents. This provided the methyl ketone **217** in 59% yield over two steps. This ketone **217** was then subjected to reductive amination conditions with the aminoisoxazole **46** (Scheme 93).



Scheme 93. Reductive amination of aminoisoxazole 46 with the methyl ketone glutamic acid derivative 217.

The reductive amination proceeded in an excellent yield of 94%. The product **218** was isolated as a 1:3 mixture of diastereomers, as determined by ¹H NMR. The diastereomers were not readily separable at this stage so the material was advanced through the synthetic route as a mixture.

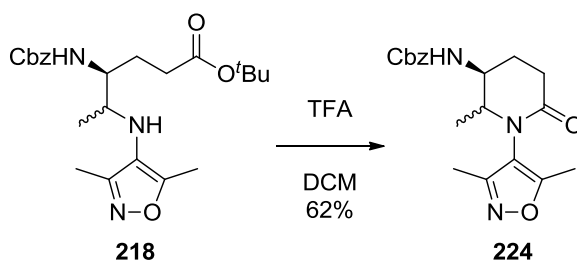
The intended method to form the piperidine ring was to reduce the ester group to an alcohol, which would then be mesylated (Scheme 94). A strong base would then be used to deprotonate the isoxazole amine and displace the mesylate leaving group.



Scheme 94. Intended cyclisation route.

It was recognised that lithium aluminium hydride could not be used to reduce the ester to an alcohol, as the carbamate protecting group on the amine would also be susceptible to reduction. To avoid this, the *tert*-butyl group was to be removed with TFA, the carboxylic acid acylated to form a mixed anhydride, and then sodium borohydride used to form the alcohol.¹⁶⁸ The *tert*-butyl removal proceeded cleanly, as determined by LCMS. Interestingly, after a test scale reaction, the TFA and DCM was removed under a stream of nitrogen at 40 °C, which resulted in complete conversion of the intermediate to a

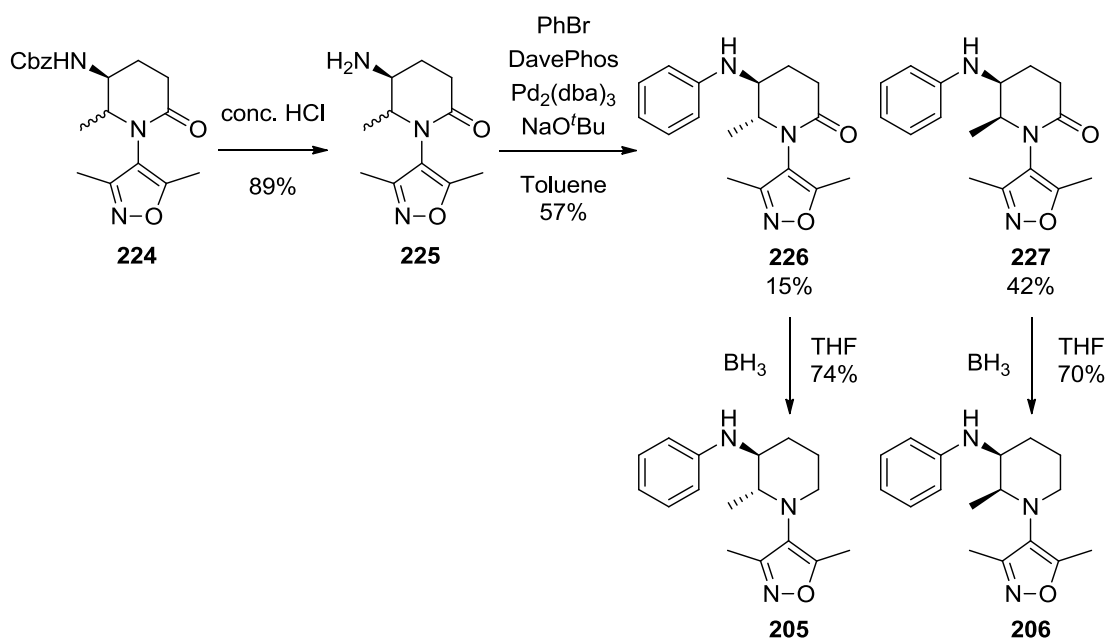
different species, as determined by LCMS. This product was identified as the lactam **224**, so the reaction was scaled up and heated to reflux to replicate the conditions (Scheme 95).



Scheme 95. Acid-catalysed lactamisation.

Gratifyingly, the lactamised product **224** was isolated in 62% yield, also as a 1:3 mixture of diastereomers. This greatly simplified the route and provided the possibility for accessing lactam analogues of the target compounds and screening their biological activity.

Following lactamisation, the Cbz group was removed using concentrated hydrochloric acid, and the free base amine **225** was isolated in a good yield (Scheme 96).



Scheme 96. Synthesis of 2,3-disubstituted piperidine targets.

The Buchwald-Hartwig conditions that have previously been used in this research on these systems were successfully applied to attach the phenyl group to the deprotected amine **225**, proceeding with a 57% yield. At this stage the diastereomers were separated to provide the *trans* **226** and *cis* **227** diastereomers in a 1:3 ratio. These separated diastereomers were then reduced with borane to provide the *trans* **205** and *cis* **206**

diastereomers of the 2,3-disubstituted piperidine targets, in overall yields of 3% and 9%, respectively, over seven steps.

The 2,3-disubstituted piperidines, and their lactam precursors, were submitted for biological screening and the results are shown in Figure 62.

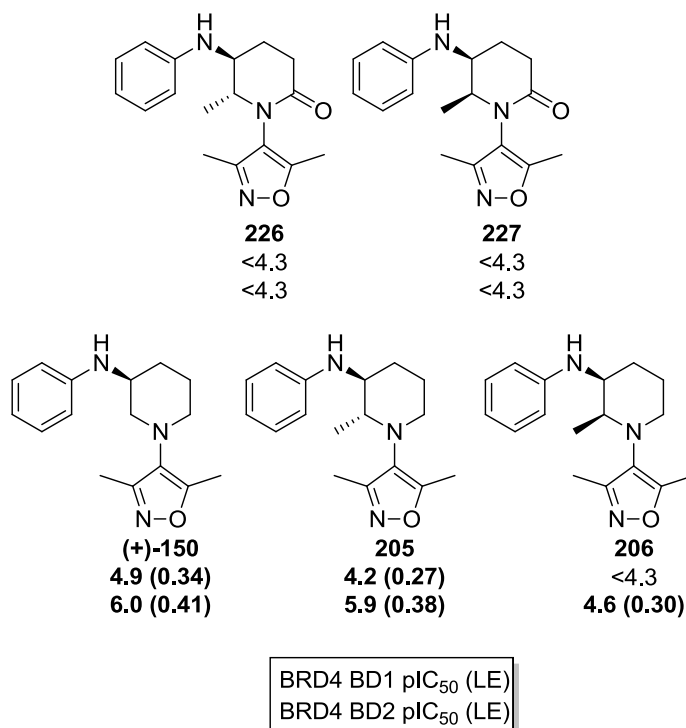


Figure 62. Assay data and calculated ligand efficiencies for 2,3-disubstituted piperidines and 2-piperidinones.

Neither of the lactam analogues displayed measurable activity in the assays, which may be due to a significant change in the conformation of the molecules with respect to the piperidines or because the oxygen of the lactam would be unfavourably placed in close proximity to a lipophilic valine residue (Val376 in BRD2 BD2).

The *cis*-substituted piperidine **206** exhibited much reduced potency in comparison to the monosubstituted analogue **(+)-150**, suggesting that access to the histidine-adjacent groove, while retaining potency from the shelf-binding interaction, is unlikely to be achievable using this vector. This may be due to the methyl group destabilising the desired ring conformation, which X-ray crystallography suggests requires the amine linker to be in an equatorial position in order to place the phenyl group on the WPF shelf. This would require the methyl group to occupy an unfavourable axial position, therefore the equilibrium of ring conformations is likely to have been significantly shifted, thus increasing the free energy cost of binding (Figure 63).

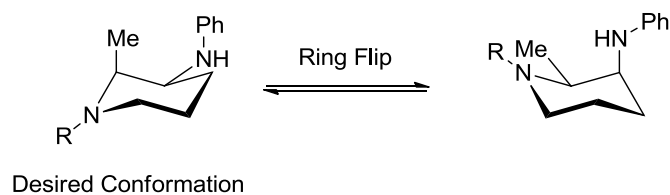
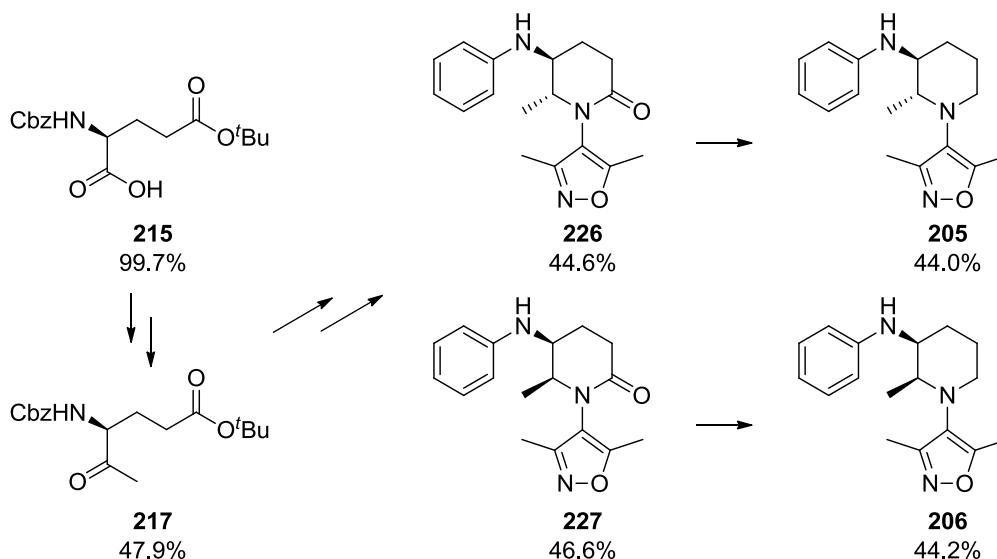


Figure 63. Possible ring conformations of 2,3-*cis*-disubstituted piperidine **206**. R represents the 3,5-dimethylisoxazole.

Gratifyingly, the *trans*-substituted piperidine **205** retained a similar activity ($pIC_{50} = 5.9$) at BRD4 BD2 as the monosubstituted analogue **(+)-150** ($pIC_{50} = 6.0$). The potency of *trans*-substituted piperidine **205** at BRD4 BD1 dropped below the lower limit of the normal assay ($pIC_{50} < 4.3$), but was measured in the high concentration assay at 4.2, which equated to BD2-selectivity of 50-fold; a notable increase upon that measured for mono-substituted piperidine **(+)-150** (13-fold).

The synthesis of these molecules utilised an enantiopure amino acid starting material **215**. To determine whether this optical purity was retained in the final products **205/206** the route was repeated from the opposite enantiomer of the starting material, a protected D-Glutamic acid, to provide reference material for analysis by chiral HPLC (compounds **228–235**, see Experimental). The measured enantiomeric excesses of the products, starting material and ketone intermediate are shown in Scheme 97.



Scheme 97. Measured enantiomeric purities of 2,3-disubstituted piperidines and relevant precursors, expressed as percentage enantiomeric excess.

Unfortunately, the enantiopurity of the material was diminished on conversion of the acid group **215** to a methyl ketone **217**. As the formation of the Weinreb amide with COMU is documented to proceed without racemisation of α -amino acids,¹⁶⁷ it is more likely that the partial racemisation occurred during the methyl Grignard step, caused by

deprotonation of the α -position by the organometallic reagent. Therefore, the *trans*-piperidine **205** was isolated in a 72:28 ratio of enantiomers. As advanced biological testing had already commenced for the enantioenriched sample **205**, it was deemed important that primary BD1-BD2 potency and selectivity data were comparable with an enantiopure batch of *trans*-piperidine **205a**. Accordingly, a small amount was separated by chiral chromatography and submitted to the biochemical assays (Figure 64).

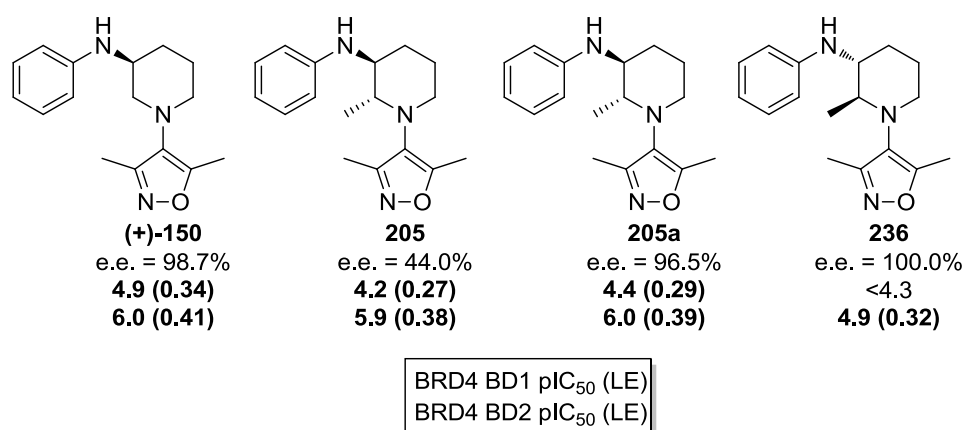


Figure 64. Assay data for *trans*-disubstituted piperidines as the separated enantiomers and as an enantioenriched mixture **205**. Data for the monosubstituted analogue (+)-150 is shown for reference.

The enantiopure sample **205a** displayed similar potencies at both BRD2 BD2 and BD1 as the enantioenriched sample **205**, suggesting that further biological profiling of the latter would provide an accurate representation of the properties of the molecule. The opposite enantiomer **236** was also isolated and displayed much reduced potency at both bromodomains, as was expected.

An X-ray crystal structure was solved for the 2,3-disubstituted compound **205** (Figure 65), which solely showed density for the desired *2R,3S*-enantiomer, and was inspected in order to rationalise the observed selectivity and the confirm the design hypothesis.

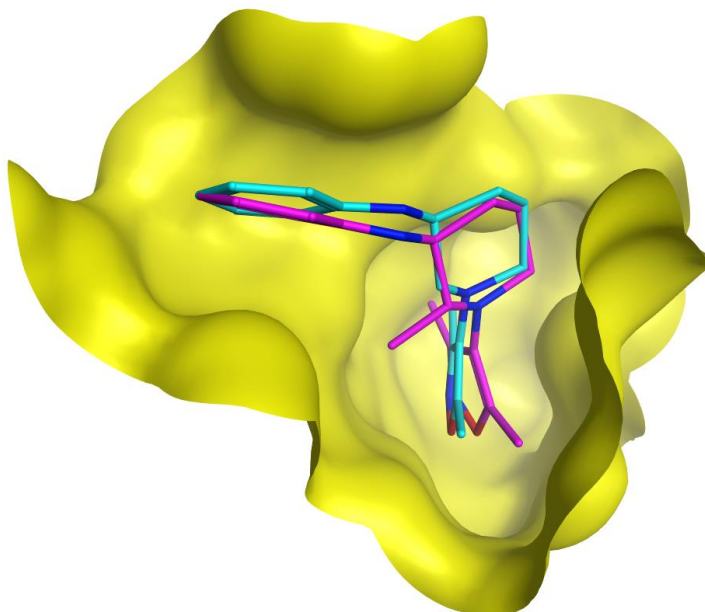


Figure 65. X-ray crystal structure of the *trans*-2,3-disubstituted piperidine **205** (magenta) bound to BRD2 BD2 (yellow) with the monosubstituted analogue **150** (cyan), also bound to BRD2 BD2, superposed. Water molecules have been removed from the image for clarity.

Compared to the monosubstituted analogue **150**, there was some small movement of the isoxazole warhead and piperidine core on substitution with the methyl group, but this did not appear to be significant in terms of potency at BD2. The methyl group was indeed directed towards the valine gatekeeper residue of BD2, as was envisioned.

In Figure 66 a surface has been generated for the ligand **205** (magenta, mesh) as well as the protein (yellow), and the gatekeeper residue is highlighted. This illustrates the close contact between the methyl group at the 2-position and the valine residue and the resulting shape complementarity.

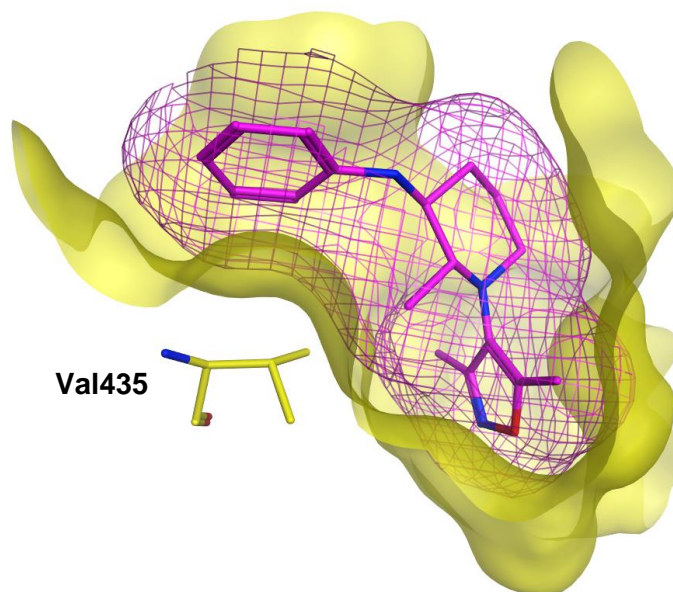


Figure 66. X-ray crystal structure of the *trans*-2,3-disubstituted piperidine **205** (magenta) bound to BRD2 BD2 (yellow). A molecular surface has been generated for the ligand (magenta, mesh) and the valine gatekeeper residue is highlighted (yellow). Water molecules have been removed from the image for clarity.

Figure 67 shows a similar image to Figure 66, with the addition of a superposed molecular surface generated for the monosubstituted analogue **150** (cyan). The surface of the additional methyl group can clearly be seen to occupy a previously empty space.

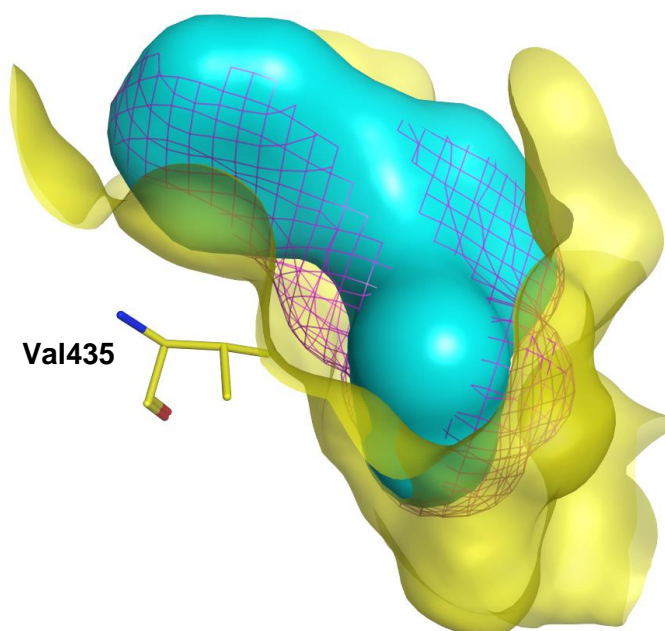


Figure 67. X-ray crystal structure of the *trans*-2,3-disubstituted piperidine **205** (magenta) bound to BRD2 BD2 (yellow). A molecular surface has been generated for the ligand (magenta, mesh) and the valine gatekeeper residue is highlighted (yellow). A molecular surface generated for the monosubstituted analogue **150** (cyan), also bound to BRD2 BD2, is superposed. Water molecules have been removed from the image for clarity.

The biological data, and the X-ray crystal structure, supported the hypothesis that the BD2-selectivity was governed by the different sizes of the gatekeeper residue in BD1 and

BD2. The shape complementarity observed between the 2,3-disubstituted piperidine **205** and the valine of BD2 is likely to be disrupted by the larger isoleucine residue of BD1 resulting in reduced potency. If correct, this result constitutes the first known example of a BET inhibitor that exploits the difference in the gatekeeper residue to gain BD2 selectivity.

6.9.3 Further Data

With the two disubstituted compounds in hand, supplementary data was acquired and examined (Table 10).

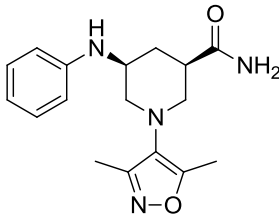
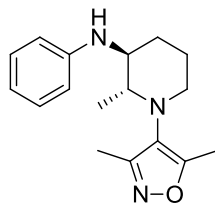
	 (-)-196	 205
BRD4 BD1 pIC ₅₀	5.1	4.2
BRD4 BD2 pIC ₅₀	6.7	5.9
BRD4 BD2 LE	0.40	0.38
Fold BD2-Selectivity	40	50
PBMC pIC ₅₀	6.9	5.9
AMP (nm/s)	310	405
CLND Solubility (μM)	≥409	125
FaSSIF Solubility (μg/mL)	309	-
ChromLogD _{pH7.4}	3.5	7.2
PFI	5.5	9.2

Table 10. Profile of disubstituted piperidine compounds.

The compounds were assayed in lipoprotein polysaccharide (LPS)-stimulated peripheral blood mononuclear cells (PBMCs) to determine the degree to which they inhibit the release of the proinflammatory cytokine monocyte chemoattractant protein 1 (MCP1), and both returned pIC₅₀ values very similar to their BRD4 BD2 potencies. This suggested that they were readily able to enter the cells and reach the site of action. This is corroborated by the artificial membrane permeability (AMP), which was high in both cases.

In terms of physicochemical properties, the introduction of the primary amide had the desired effect of lowering the ChromLogD_{pH7.4}, from 6.5 for the monosubstituted

analogue **150** to 3.5 for the amide **(-)-196**. This corresponded to a PFI of 5.5, which is below the guideline maximum of 6.¹⁶⁰ The introduction of the methyl group at the 2-position increased the chromLogD_{pH7.4}, but this was to be expected and this compound was designed as a tool to probe selectivity rather than to reduce lipophilicity. Therefore it was not concerning that the solubility of this compound **205**, as determined by CLND, was much lower than that of the amide compound **(-)-196**, which was above the top limit of the assay. The amide compound was isolated as a solid, while the other compound was an oil, so solubility in Fasted State Simulated Intestinal Fluid (FaSSIF) could be determined. Current candidate quality guidelines at GSK suggest that FaSSIF solubility of greater than 100 µg/mL is desirable.¹⁶⁰ The amide **(-)-196** greatly exceeded this and had a measured value of 309 µg/mL. It should be noted that this was recorded from an amorphous solid and would reduce if crystalline material were obtained, but it is nevertheless a pleasing result.

To determine the selectivity of this framework against a wider range of bromodomains, the 2,3-substituted analogue **205** was submitted to DiscoverRx's single shot BROMOscan™ assay. The compound was screened at a concentration of 100 µM against 32 bromodomains, including all 8 members of the BET family and the percent inhibition for each is displayed in Figure 68.

BRPF1	1	WDR9(2)	94 ^a
BRD9	29	TRIM33	0
BRD7	7	TRIM24	0
BRDT(2)	100	TAF1L(2)	22
BRDT(1)	43	TAF1(2)	71
BRD4(2)	100	SMARCA4	0
BRD4(1)	70	SMARCA2	9
BRD3(2)	100	PCAF	2
BRD3(1)	88	PBRM1(5)	0
BRD2(2)	100	PBRM1(2)	38
BRD2(1)	84	GCN5L2	0
BRD1	19	FALZ	13
BAZZB	0	EP300	40
BAZZA	42	CREBBP	57
ATAD2B	27	CECR2	16
ATAD2A	6	BRPF3	0

Figure 68. DiscoverRx BROMOscan™ one-shot selectivity data. The enantioenriched 2,3-disubstituted piperidine **205** was screened at 100 µM against a panel of 32 bromodomains, each in duplicate, with the average inhibition being reported. ^aDue to significant disparity between the two replicates, the lower value was invalidated and the higher value was reported.

Pleasingly, complete inhibition was seen at all four BET BD2 domains, and nowhere else. Some selectivity was observed over all of the BET BD1 domains, and this was particularly notable for BRDT BD1 which was only inhibited by 43% at this compound concentration. The selectivity over non-BET bromodomains is impressive considering the small size of

the molecule and the relatively high screening concentration, with only CREBBP and the second bromodomains of TAF1 and WDR9 being inhibited by more than 50%.

On the strength of these data, this piperidine isoxazole framework was a promising lead. With the increased selectivity provided by the methyl group at the 2-position, and the increased selectivity, potency and solubility provided by the amide at the 5-position, the obvious next step was to ascertain whether these effects could be compounded (Figure 69). Therefore, the trisubstituted piperidine **237**, which combined both the 2-Me and 5-amide features, was identified as a target compound for synthesis and test.

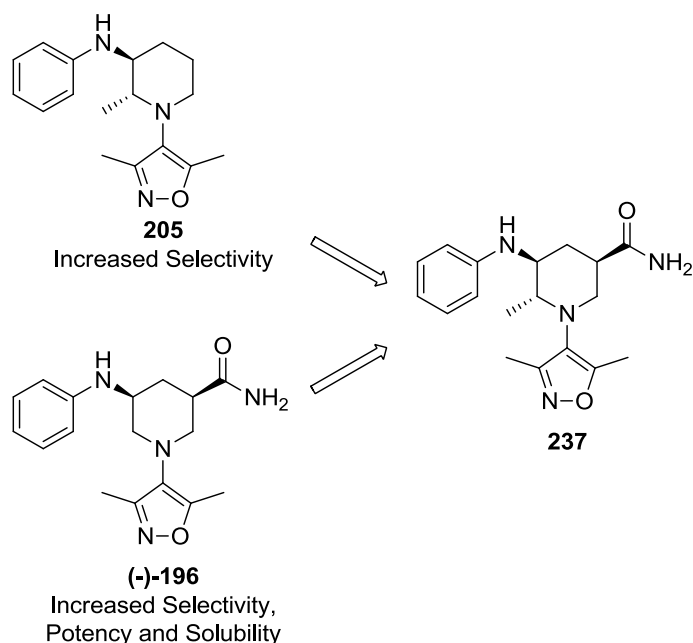
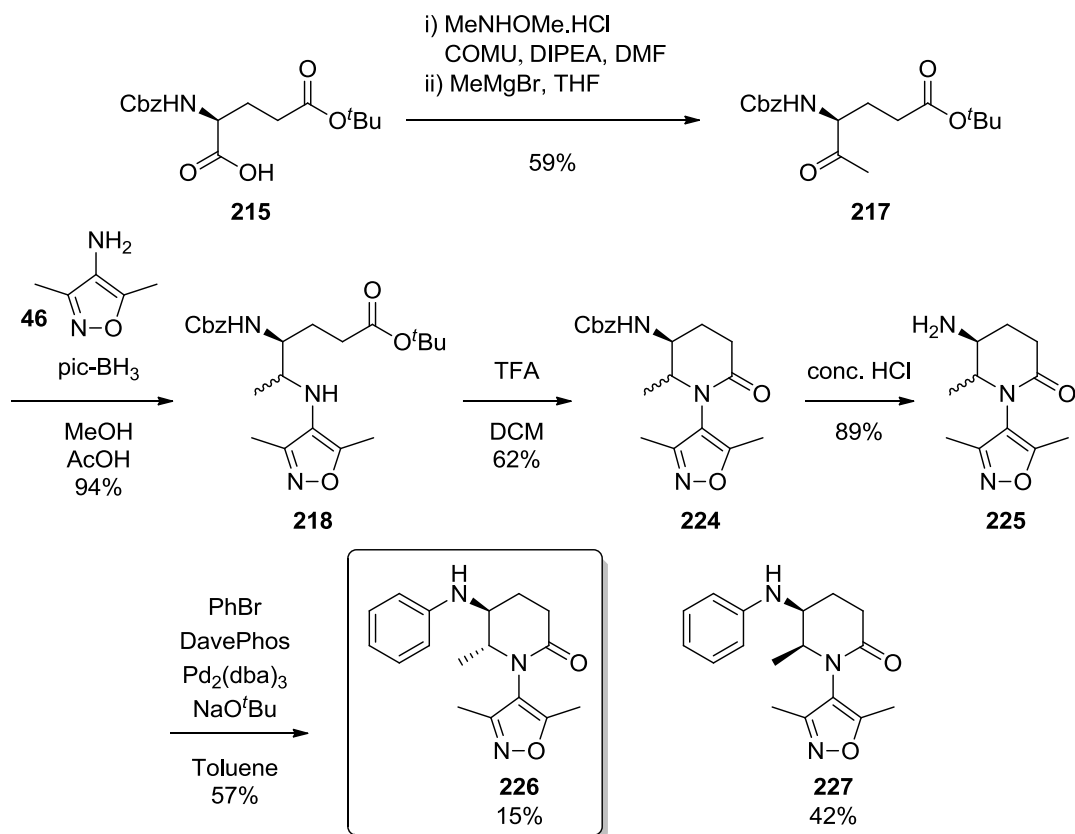


Figure 69. Combining the key features of the disubstituted piperidine compounds **205** & **(-)-196**.

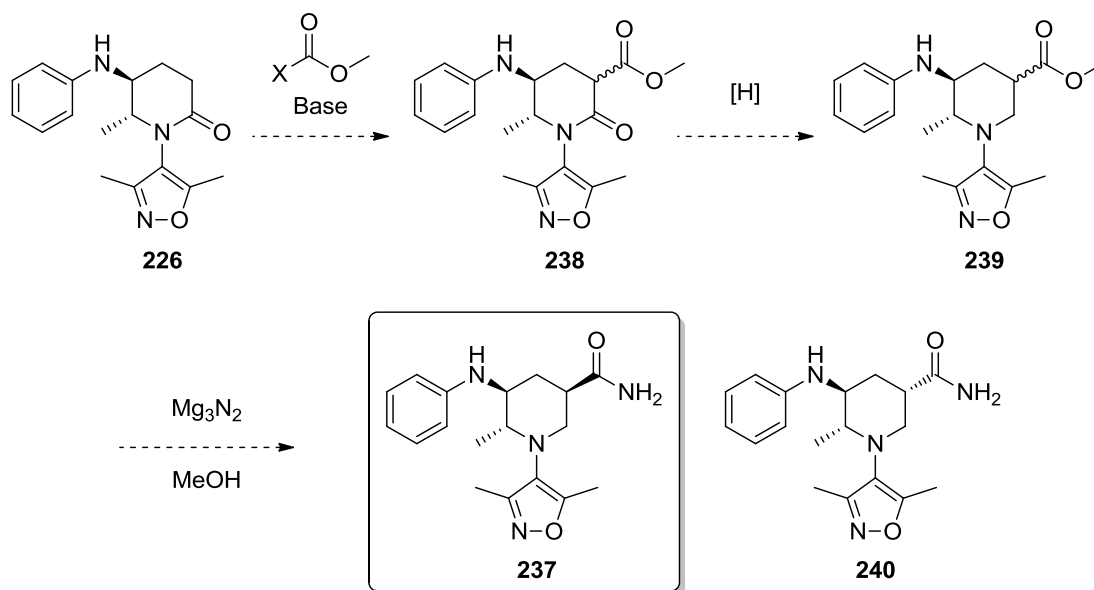
6.10 Trisubstituted Piperidine

When designing the synthetic route to the trisubstituted piperidine **237**, it was hoped that previous routes could be built upon in order to focus the investigations. The route to the 3,5-substituted piperidine **196** was not appropriate as it had already been shown that *N*-alkylation of a piperidine with a methyl group at the 2-position could not be accomplished (Scheme 88, p118). However, the route to the 2,3-substituted compound **205**, which proceeded *via* the lactam intermediate **226**, was identified as a plausible starting point for route design (Scheme 98).



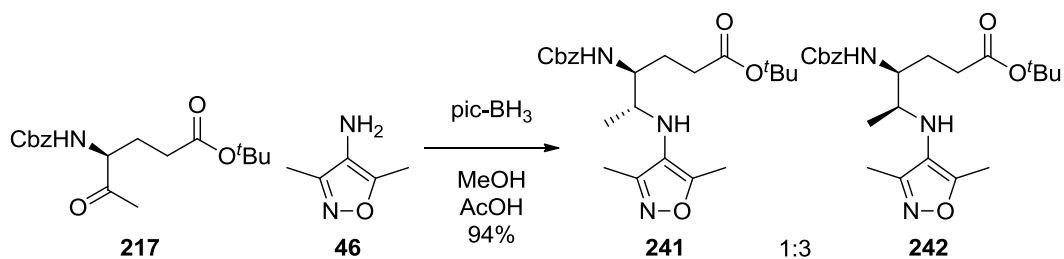
Scheme 98. Identifying the key intermediate 226 from the synthetic route to the 2,3-substituted piperidines.

It was envisioned that the position α to the lactam of the key intermediate **226** could be deprotonated with a suitable base, and acylated to provide a methyl ester **238** (Scheme 99). Selective reduction would then be employed to remove the lactam carbonyl and provide a methyl ester-substituted piperidine **239**, which could then be converted to the primary amide product **237** with the magnesium nitride conditions used previously.



Scheme 99. Proposed route outline from the key lactam intermediate **226** to the trisubstituted final compound **237**.

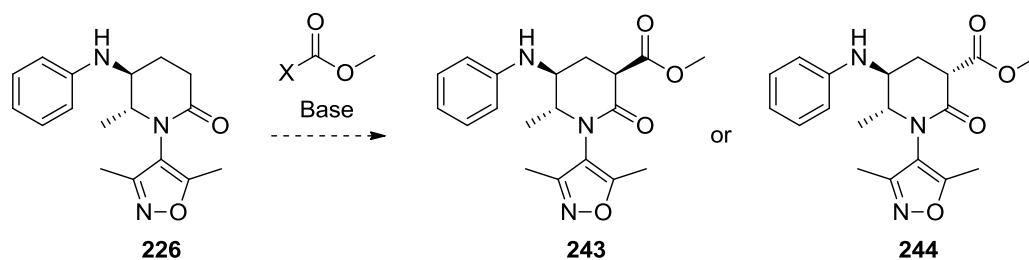
There were, of course, a number of issues that could arise with this route. Three major points were identified that required particular attention. Firstly, the route leading up to the key lactam intermediate **226** included a reductive amination step between the aminoisoxazole **46** and the glutamic acid-derived ketone **217** (Scheme 100).



Scheme 100. Reductive amination of aminoisoxazole **46** with glutamic acid-derived ketone **217**. Ratio of products is based on 1H NMR of the isolated mixture, and identities of diastereomers is based on piperidine products isolated further along the route.

This reductive amination, while high-yielding, was selective for the wrong diastereomer of the product; providing three times as much of the *cis*-amine **242** as the desired *trans*-isomer **241**. If sufficient quantities of important intermediates were to be isolated, this selectivity needed to be inverted.

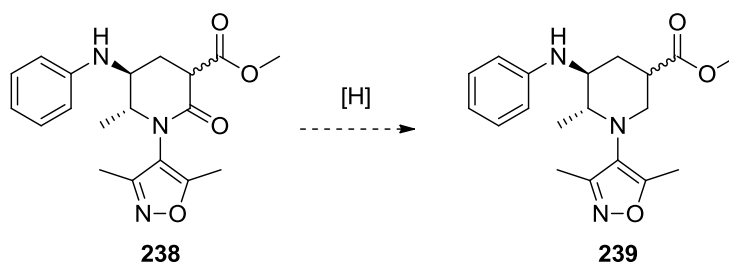
Secondly, the acylation step was identified as being potentially problematic. As well as issues of selectivity between the α -position and the anilinic nitrogen, there are two possible products depending on the stereoselectivity of the acylation (Scheme 101).



Scheme 101. Possible products of α -acylation of key lactam 226.

It was expected that the desired diastereomer **243**, with all substituents equatorial, would be the thermodynamic product, but it was acknowledged that the flattening of the ring caused by the sp^2 centres may alter the relative energies of the isomers in comparison with an idealised cyclohexyl ring system. If the undesired diastereomer **244** was the major product, then epimerisation of the α -stereocentre with methoxide may be required to access the desired diastereomer, after reduction of the lactam carbonyl.

Finally, the reduction of the lactam **238** to the piperidine **239** (Scheme 102) was expected to require exploration of a range of conditions in order to avoid reducing the ester, which one would expect to be the simpler of the two carbonyl functionalities to selectively reduce.

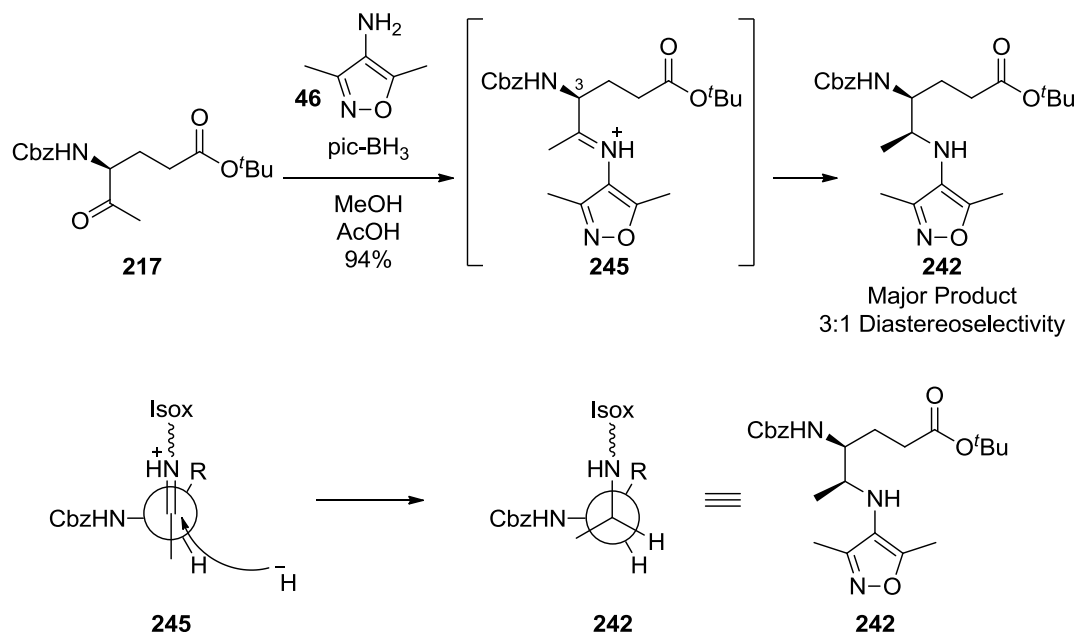


Scheme 102. Selective reduction of lactam 238 to piperidine 239 in the presence of a methyl ester.

Despite these potential difficulties, this route was prioritised for further investigation as it was expected that each of the issues could be overcome with the aid of in-depth literature searching and experimental work.

6.10.1 Reductive Amination

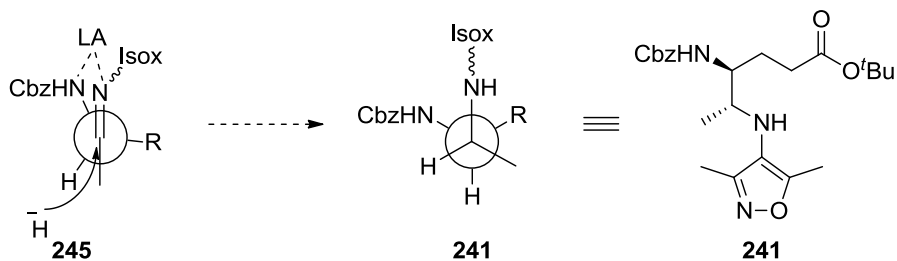
In order to determine how to invert the selectivity of the reductive amination step, it was necessary to first understand the mechanism behind the existing selectivity (Scheme 103).



Scheme 103. Felkin-Anh model to explain the observed selectivity in the reductive amination of aminoisoxazole **46** and glutamic acid-derived ketone **217**.

The ketone **217** and the amine **46** condense to form an iminium intermediate **245**, which can be reduced by the picoline borane when in the protonated state. The stereoselectivity observed can be explained by the Felkin-Anh model: the most reactive conformation of the iminium intermediate **245** is one in which the C3-N bond is perpendicular to the C=N imine bond, such that the σ^* orbital of the former can interact with the π^* of the latter to form a new, lower energy molecular orbital which is more susceptible to nucleophilic attack.¹⁶⁹ Of the two possibilities, the one shown above reacts faster as the reducing agent can attack unhindered past the hydrogen, rather than past the bulkier alkyl chain. The same selectivity with reductive amination of methyl α -amino ketones was reported by Reetz and Schmitz in 1999.¹⁷⁰

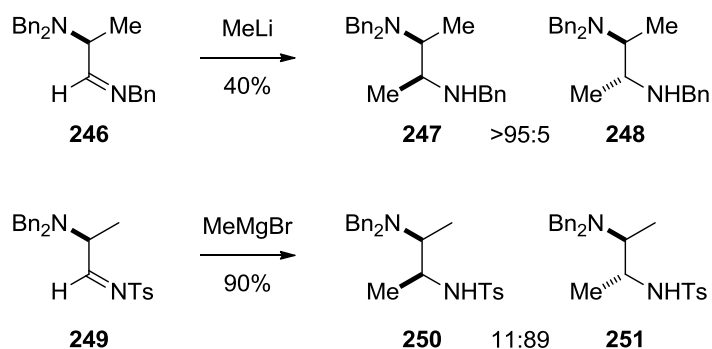
Based on this understanding of the mechanism, the logical solution to inverting the selectivity would be to employ chelation control (Scheme 104).



Scheme 104. Proposed chelation control method to invert the selectivity of the reductive amination and favour the *trans*-amine product **241**.

A suitable Lewis acid may be able to chelate both the amine and imine nitrogens, and change the conformation of the intermediate such that when the reducing agent attacks, with the unhindered approach past the hydrogen, it is attacking from the other side of the imine. This would result in the desired *trans*-diastereomer of the amine product **241**.

An effect similar to that being described was reported by Reetz *et al.* in 1991 for the addition of organometallic reagents to α -aminoaldimines, derived from α -aminoaldehydes and amines (Scheme 105).



Scheme 105. Stereoselective synthesis of vicinal diamines.¹⁷¹

The authors found that when the aldimines were made with benzylamine, alkyllithiums (used because Grignard reagents could not be made to react in this case) added to the aldimines with chelation control. However, if the aldimine was formed from an amine with an electron-withdrawing substituent, tosylamine, then Grignard reagents added to the aldimines without chelation control. It was concluded that in the second case the lone pair of the tosyl imine was not sufficiently available as to be chelated to the magnesium and held together with the amine.

This demonstrates the plausibility of controlling selectivity through the chelation of imines and amines, and this methodology had the potential to be applicable had the reductive amination work not been successful. However, there is a major drawback in that the selectivity here is under substrate-control rather than reagent-control, i.e. the amine, and consequent imine, must be non-chelating in order to obtain the desired diastereomer. Therefore, applying this approach in the current research programme, with the chelating aminoisoxazole **46** would be unsuccessful. Alternatively, it may be possible to change the *N*-Cbz protecting group on the aminoketone **217** to avoid chelation, but this would involve adding extra steps to the synthetic route, and it would be much more elegant to continue with the substrate protected in a manner that is commercially available.

Surprisingly, there is a relatively small amount of literature relating to chelation-controlled diastereoselective reductive amination, and no conditions were found to isolate 1,2-diamines in this manner.

In one example with potential relevance, Hughes *et al.* demonstrated a switch in stereoselectivity when reducing an imine **252** that contained an adjacent carboxylic acid, with sodium borohydride, with and without the addition of zinc chloride (Figure 70).¹⁷²

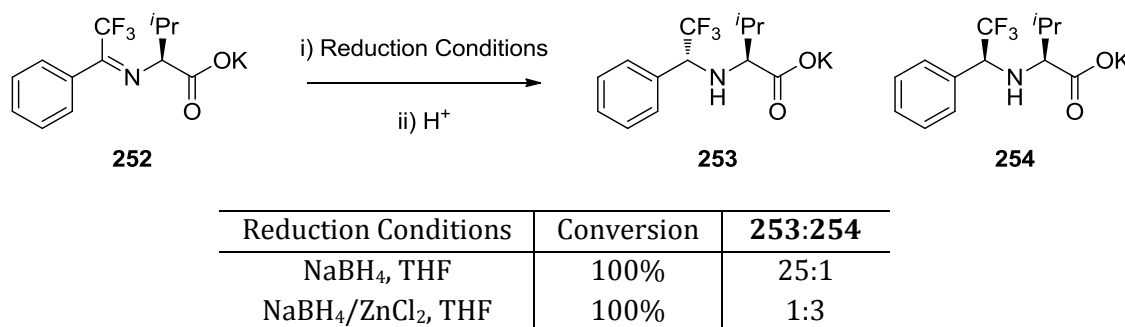
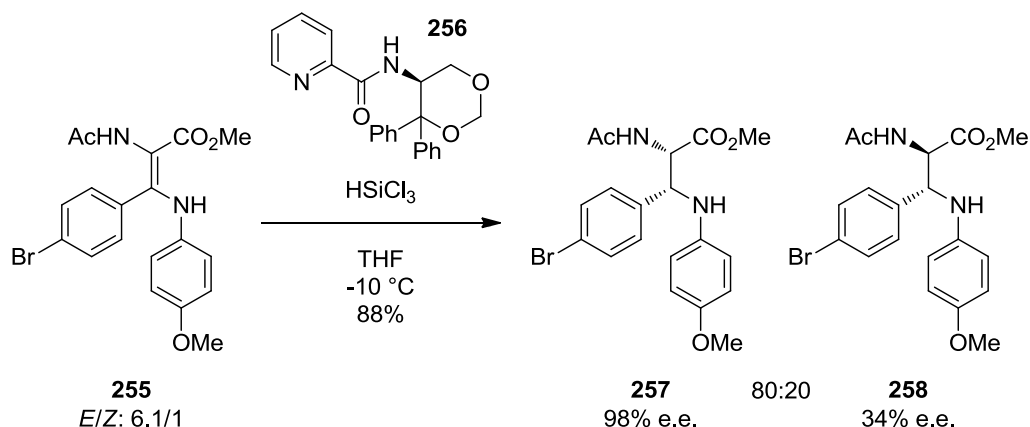


Figure 70. Diastereoselective reductive amination of aryl trifluoromethyl ketones and α -amino esters.¹⁷²

In this case the stereogenic centre is on what was the amine starting material, which differs from the system currently under investigation in which it is on the carbonyl-containing partner. The authors propose that the zinc chelates the imine and the carboxylic acid, and that the bulky ion blocks the face that would otherwise be the favourable side of attack, such that the borohydride approaches from the opposite direction. While this is not directly relevant to the system under consideration in this research programme, it does provide an example of coordination of a Lewis acid to an imine and another group in the same molecule.

Other literature methods for the synthesis of chiral 1,2-diamines were also investigated to see if there were any observations that may be relevant. A method published by Jiang *et al.* involves asymmetric hydrosilylation of α -acetamido- β -enamino esters (Scheme 106).¹⁷³

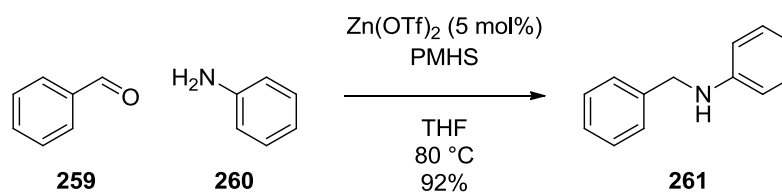


Scheme 106. Stereoselective Lewis base-catalysed asymmetric hydrosilylation of α -acetamido- β -enamino esters. A particularly selective example is shown.¹⁷³

The proposed mechanism for this reaction involves the formation of an imine with the anilinic nitrogen. To form the major product **257** this imine is held together with the ester carbonyl (not the amide nitrogen) by either coordination to silicon, or hydrogen bonding through a proton generated by the reaction of trichlorosilane with traces of water in the solvent. The amide additive **256** is proposed to activate the trichlorosilane and provide the enantioselectivity by only allowing the silane to attack from one side of the molecule. When the imine forms, the first sp^3 stereocenter is created (the upper one in Scheme 106). This imine formation is in equilibrium, and while one enantiomer interacts favourably with the chiral additive **256**, giving the major diastereomer **257** in good e.e., the other enantiomer interacts less favourably with the catalyst, providing a poor e.e. and a different diastereomer **258**. The authors suggest that the minor diastereomer **258** is the result of a conformation in which the imine is hydrogen bonded to the amide nitrogen. It is this second scenario, which forms the minor diastereomer **258**, that would be desirable to promote with the system in this research programme. However, the authors do not allude to any methods to invert the diastereoselectivity they observed.¹⁷³

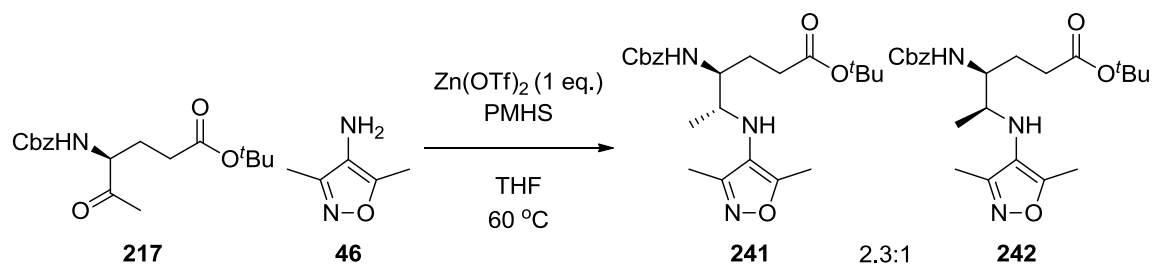
A set of trial reactions were carried out in an attempt to invert the selectivity, including the addition of cerium chloride to the picoline borane reaction mixture, and the use of the zinc chloride/sodium borohydride conditions discussed above (data not shown). Disappointingly, these were unsuccessful so it was decided that there would be a higher chance of success if conditions were used in which a Lewis acid was already integral to the reaction mechanism.

In 2011, Enthaler reported the reductive amination of a range of benzaldehydes with anilines to make secondary amines, using polymethylhydrosiloxane (PMHS) and zinc triflate (Scheme 107).¹⁷⁴



Scheme 107. Practical one-pot synthesis of secondary amines by zinc-catalysed reductive amination.¹⁷⁴

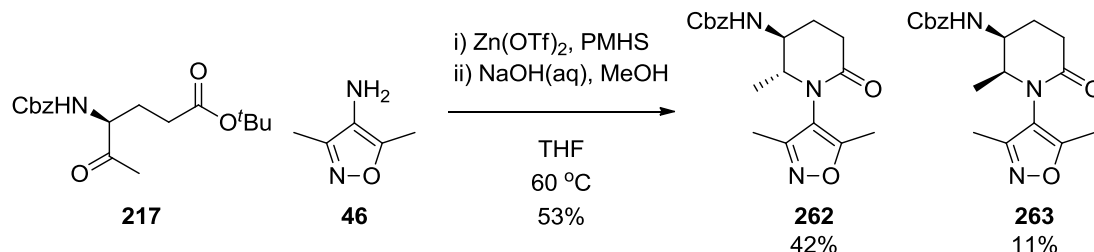
These conditions were applied to the ketone **217** system under investigation, using a whole equivalent of the zinc salt rather than 5 mol%, and were found to successfully invert the selectivity in favour of the desired *trans*-product **241** (Scheme 108).



Scheme 108. Initial trial of zinc-mediated reductive amination.

LCMS analysis of the trial reaction mixture provided a UV trace containing a peak relating to the desired product **241** with an area of 55%, and one relating to the undesired *cis*-product **242** with an area of 24%, giving an estimated selectivity of 2.3:1.

This reaction was scaled up, and when the siloxane was quenched with aqueous sodium hydroxide, partial hydrolysis of the *tert*-butyl ester occurred. To avoid unnecessary losses in purification it was decided to fully hydrolyse the ester and isolate the acid, which could then be cyclised under the acidic conditions used previously. However, it was found that cyclisation also occurred under these basic conditions (Scheme 109).



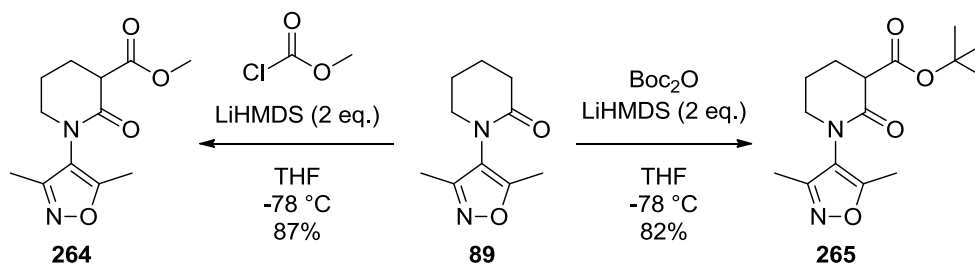
Scheme 109. Isolation of *trans*-substituted lactam **262** with zinc-mediated reductive amination conditions.

Through these conditions it was possible to isolate a clean batch of the desired diastereomer of the lactam **262** in a 42% yield, and only 11% of the undesired isomer **263**.

This yield and selectivity was sufficient to allow for a useful amount of the desired intermediate **262** to be isolated. Obtaining this diastereoselectivity is unprecedented in the literature and there are plans to further investigate and optimise the procedure, with non-proprietary molecules, with a view to publication.

6.10.2 Acylation

With the first of the key issues solved, attention was turned to the next important step: the acylation to form an ester-substituted lactam. To explore potential conditions, reactions were first trialled on the unsubstituted lactam **89** (Scheme 110).

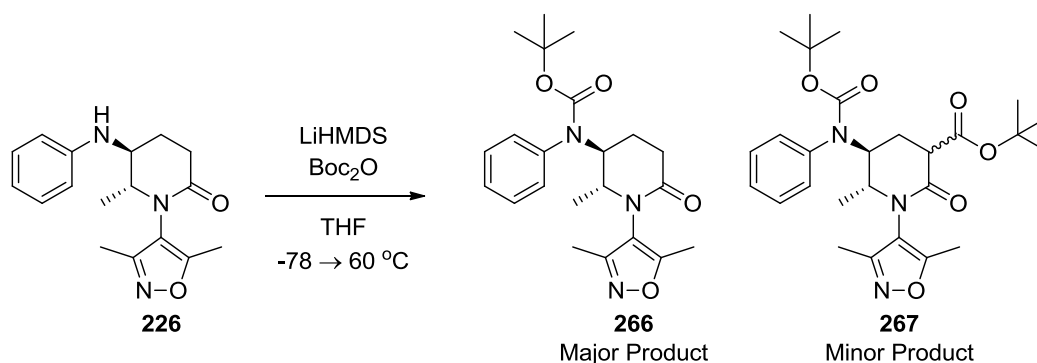


Scheme 110. Acylation of unsubstituted lactam **89** to form a methyl ester **264** and a *tert*-butyl ester **265**.

To form the methyl ester **264**, LiHMDS was identified as a suitable base, and methyl chloroformate as a suitable acylating agent.¹⁷⁵ It was also decided to investigate a *tert*-butyl ester **265** as it was thought that it may be easier to selectively reduce the lactam over the sterically hindered *tert*-butyl ester rather than the methyl ester analogue. For this transformation, Boc anhydride was identified as an appropriate acylating agent.¹⁷⁶ In both cases one equivalent of base resulted in roughly 50% conversion but, with two equivalents, the reactions went to near completion. This can be attributed to the fact that the product is more acidic than the starting material so, as it forms, it is deprotonated by the lithium enolate intermediate. The second equivalent of base prevents this from being an issue and gratifyingly, no overacylation was observed. Through this method, the *tert*-butyl ester **265** was isolated in an 82% yield, and the methyl ester **264**, the formation of which had a cleaner LCMS UV trace, was isolated in an 87% yield.

Next, these acylation conditions were applied to the fully substituted phenyl lactam **226** (Scheme 111). It was acknowledged that LiHMDS was a strong enough base to deprotonate two positions on this compound: the anilinic nitrogen as well as the lactam

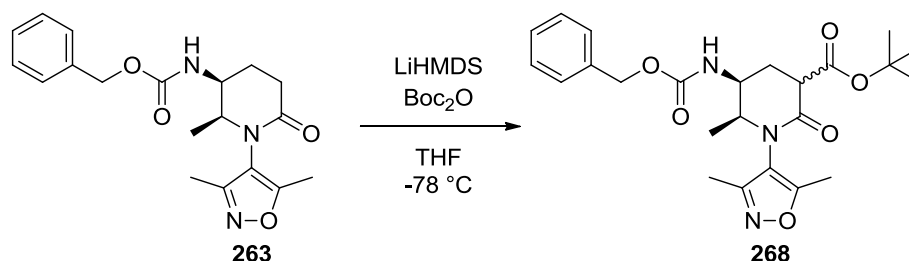
α -position. However, the anilinic nitrogen was expected to be the more acidic of the two and deprotonate first. The protons at the α -position were expected to be less acidic, and therefore the anion formed should be less stable and more reactive towards acylation. Initial attempts were performed with Boc anhydride as it should be possible to determine where the acylation had occurred from the mass fragmentation pattern of the products.



Scheme 111. Trial acylation of fully substituted phenyl lactam **226**.

Unfortunately, the major product of the reaction, as determined by LCMS, was the Boc-protected aniline **266**. It was thought that it may be possible to doubly acylate and then remove the *N*-Boc group afterwards, but heating of the reaction with excess base and acylating agent was only able to provide small amounts of a species with a mass ion consistent with this doubly acylated product **267**.

This could have potentially been a major barrier to the synthetic route, and thus the order of the steps was reconsidered. This inspired acylation attempts on the Cbz-protected amino lactam precursor **262**, and a trial reaction was first conducted on the unwanted diastereomer **263** in order to prove the concept without consuming valuable intermediate (Scheme 112).

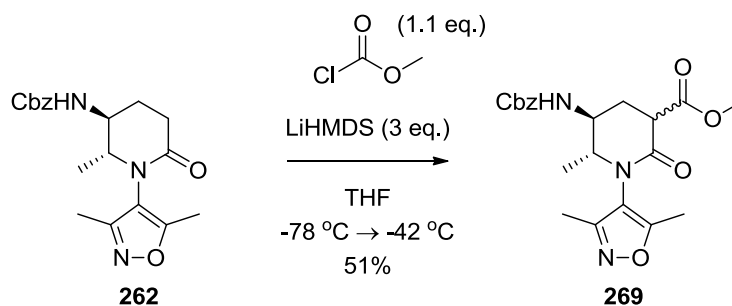


Scheme 112. Test reaction on the Cbz-protected *cis*-lactam **263** suggesting that acylation may be more achievable earlier in the synthetic route.

The LCMS UV trace of this reaction showed two close-running peaks with mass fragmentation patterns consistent with the desired acylation product **268**: an [M-

$C_4H_8+H]^+$ peak representing the cleavage of the *tert*-butyl group, but no $[M-CO_2-C_4H_8+H]^+$ peak, which would be the result of decarboxylation also occurring and is characteristic of *N*-Boc groups. The presence of two peaks would also be consistent with two diastereomers being formed.

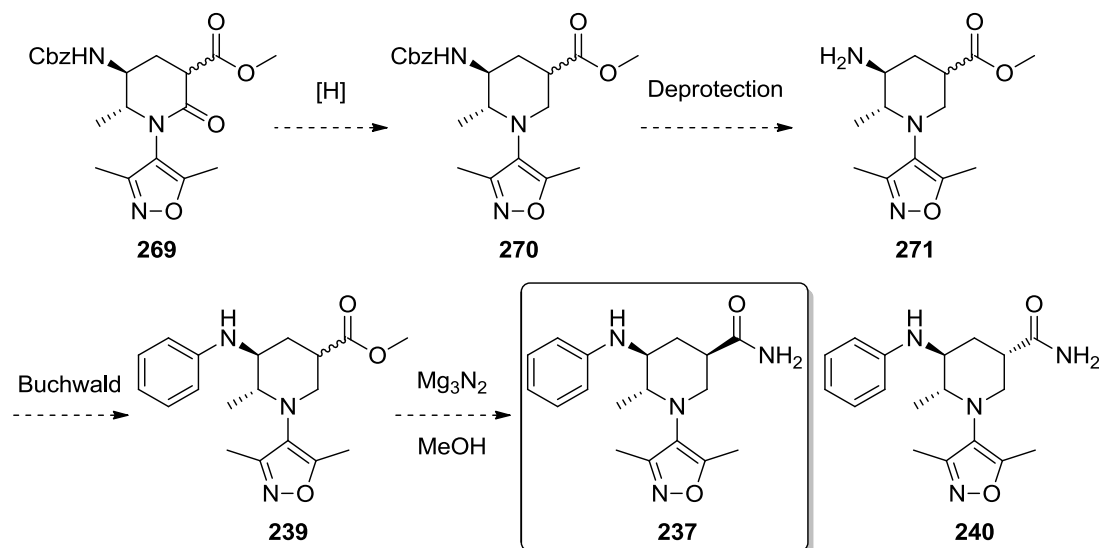
Following on from this promising result, the acylation was trialled on the correct diastereomer of the Cbz-protected lactam **262** (Scheme 113).



Scheme 113. Successful acylation to provide the methyl ester-substituted lactam 269.

At this point the acylating agent was switched from Boc anhydride to methyl chloroformate, as this had been seen to produce fewer minor byproducts when used on the unsubstituted lactam system **89**. Stirring the lactam **262** and base at -78 °C and then adding the electrophile resulted in poor conversion. But it was found that if the mixture was warmed to -42 °C for four hours to allow deprotonation to occur, and then cooled back down to -78 °C before adding the electrophile, much better conversion was observed. By this method, the methyl ester-substituted product **269** was isolated in a reasonable 51% yield. 1H NMR and LCMS of this material suggested that it was present as a roughly 2:1 mixture of diastereomers, but due to the presence of rotamers and overlapping peaks it was not feasible to assign them at this stage. The other major component in the reaction was starting material **262**, and significant quantities of this could be recovered, allowing for recycling and isolation of useful quantities of the product **269**.

As the acylation was performed at a different stage in the route than was originally planned, the route had to be redesigned to accommodate this change (Scheme 114).

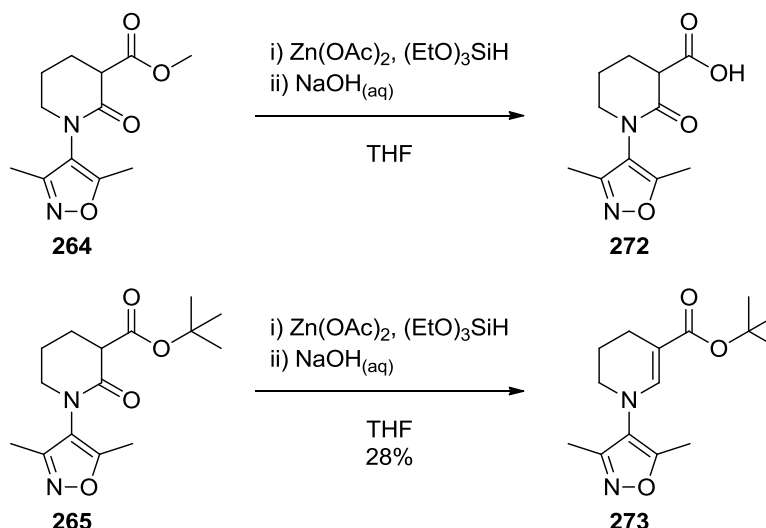


Scheme 114. Reordered route plan from Cbz-protected methyl ester-substituted lactam 269.

The plan was now to perform a selective lactam reduction before the phenyl group was installed. This meant that reduction conditions now had to be selective for the lactam over both an ester and a carbamate. New conditions for the deprotection of the Cbz group would also need to be found as the concentrated hydrochloric acid previously used would result in hydrolysis of the methyl ester. The Buchwald-Hartwig coupling had previously been performed on the 3,5-substituted system containing a methyl ester, so this was not considered a problem, and the final step to convert the methyl ester to a primary amide was the same as the original plan.

6.10.3 Reduction

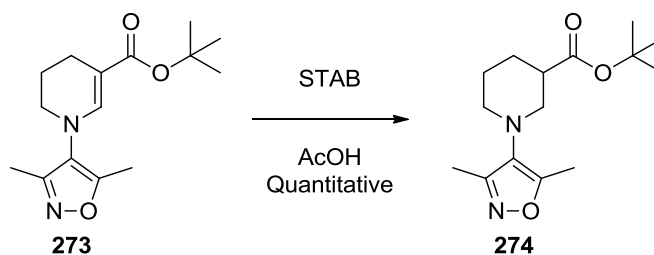
As with the acylation step, conditions for the selective reduction of the lactam carbonyl in the presence of the ester group were initially trialled on the simpler, less substituted lactam systems. To begin with, conditions were sought from the literature which demonstrated selective reduction of any amides in molecules also containing esters. This search revealed a procedure published by Das *et al.* that used zinc acetate and triethoxysilane to reduce a variety of amides to amines, one of which contained a methyl ester which remained intact.¹⁷⁷ These conditions were applied to both the methyl ester-**264** and *tert*-butyl ester-**265** substituted lactams (Scheme 115).



Scheme 115. Application of zinc-catalysed amide reduction conditions to methyl ester- **264** and *tert*-butyl ester- **265** substituted lactams.

In neither case did the reaction produce the expected product. With the methyl ester system, LCMS analysis suggested there was one major product, which had a mass ion consistent with hydrolysis of the ester to the carboxylic acid **272**, and this trial reaction was abandoned. In the case of the *tert*-butyl analogue **265**, complete reduction to the piperidine was not observed, and instead a conjugated enamine species **273** was isolated. When the reaction was performed on a small, 0.15 mmol scale, it appeared to have excellent conversion to product. However, when the reaction was scaled up to 1.4 mmol, much poorer conversion was seen, and only a 28% isolated yield was obtained. In fact, LCMS suggested that significant quantities of product reverted back to starting material after additional portions of triethoxysilane were added, and this was hypothesised to be due to water content of the silane reacting with an intermediate on the reaction pathway. An attempt to remedy this with the addition of molecular sieves greatly reduced the reactivity and resulted in very little conversion. It was therefore decided that this methodology was not robust enough, and higher yielding conditions were sought.

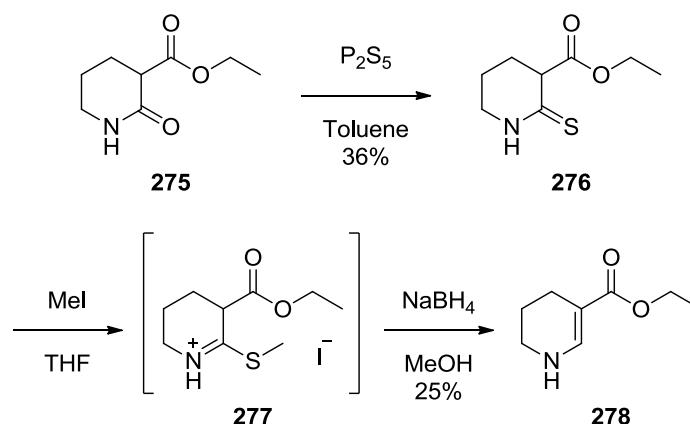
Despite the decision not to work with this zinc-catalysed reduction methodology, investigations into a method to reduce the carbon-carbon double-bond of the conjugated enamine product **273** had already been undertaken. An example of a similar reduction was found which used sodium cyanoborohydride.¹⁷⁸ Due to the toxicity of this reagent, the less toxic alternative, sodium triacetoxyborohydride (STAB) was trialled first (Scheme 116).



Scheme 116. Reduction of the conjugated enamine **273** to the piperidine **274** with sodium triacetoxyborohydride.

STAB in acetic acid was found to quickly, and cleanly, reduce the double bond of the conjugated enamine **273** to the piperidine **274**, which was isolated in quantitative yield after an aqueous workup, with no need for chromatography.

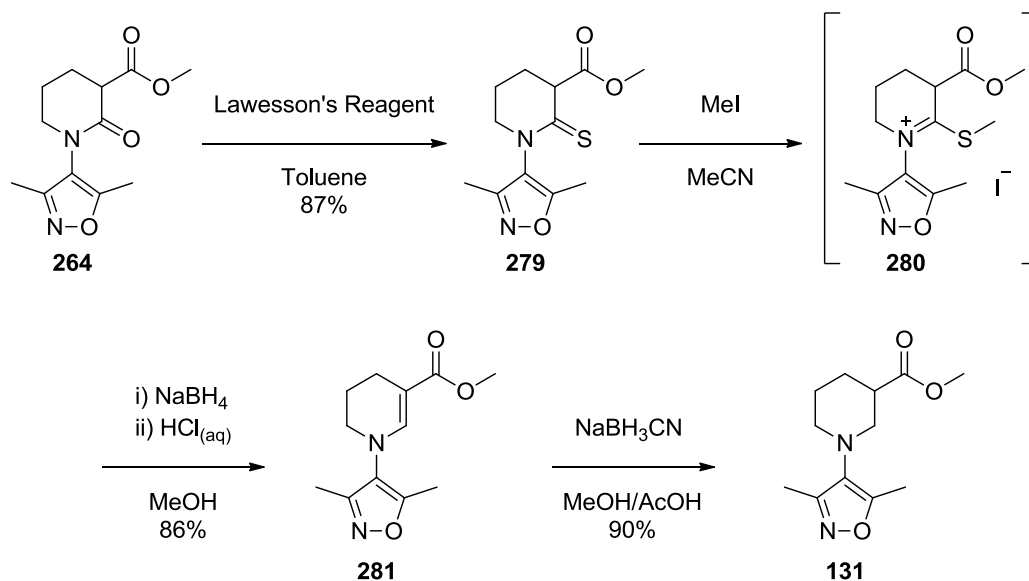
At this point, the search for conditions was narrowed to find methods applied specifically to ester-substituted lactam systems. Pleasingly, a procedure was found for a similar, ethyl ester-substituted lactam **275** that involved conversion to a thiolactam intermediate **276** followed by desulfurisation (Scheme 117).¹⁷⁹



Scheme 117. Selective reduction of an ester-substituted lactam **275** via a thiolactam intermediate **276**.¹⁷⁹

In this procedure, phosphorus pentasulfide was used to convert to lactam **275** to a thiolactam **276**. The sulfur atom was then methylated with iodomethane to form a thioiminium salt **277** which was then reduced with sodium borohydride to provide a conjugated enamine **278**. The yields in this example were particularly low, but with this route in mind, higher yielding methods to perform the same transformations could be sought.

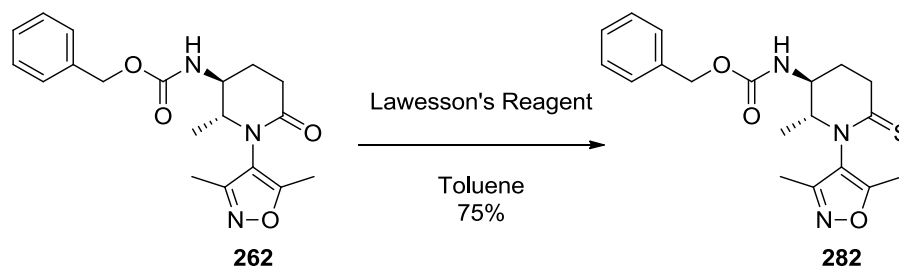
Once again, this route was first applied to the simpler, less substituted lactam system. Unlike the zinc-silane conditions used at the start of this section, this methodology did not appear to be restricted to base-hydrolysis-resistant esters. Therefore, the *tert*-butyl ester line of enquiry was discarded, and the methyl ester **264** focussed on (Scheme 118).



Scheme 118. Reduction of ester-substituted lactam **264** to ester-substituted piperidine **131** via a thiolactam intermediate **279**.

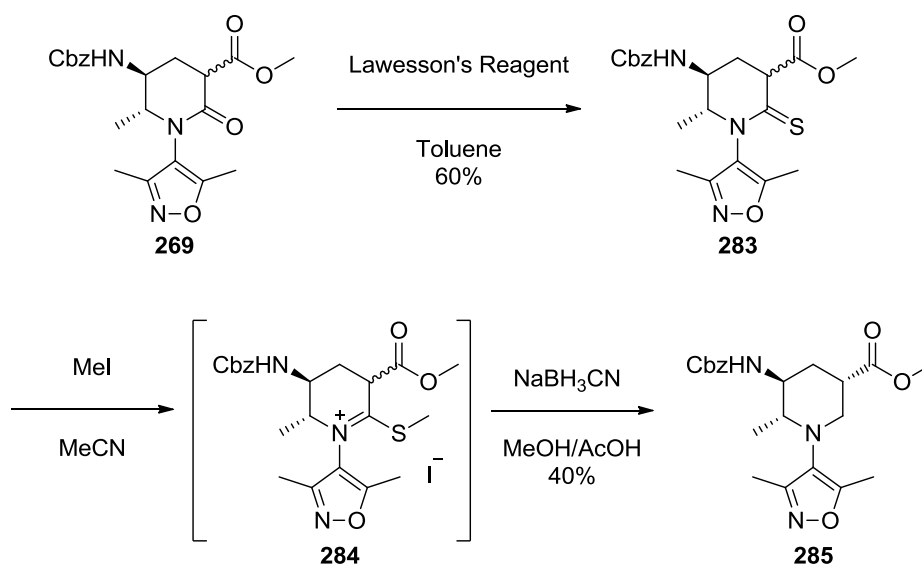
Instead of phosphorus pentasulfide, Lawesson's reagent was used, as this had been used to good effect in more recent examples,¹⁸⁰ and by this method the thiolactam **279** was isolated in an excellent 87% yield. The methylation step was trialled with a large excess of iodomethane in acetonitrile, DCM, THF, and acetone, and acetonitrile was found to provide the best conversion at room temperature (data not shown). This conversion was improved by heating the reaction in a sealed vessel at 40 °C. To avoid prolonged contact with atmospheric moisture, once the solvent had been removed from the reaction mixture, the hygroscopic thioiminium salt **280** was immediately dissolved in methanol and cooled to -78 °C before sodium borohydride was added. After an acidic workup, the conjugated enamine **281** was isolated in an excellent yield of 86%. From previous investigations (Scheme 116) it was known that this enamine could be easily reduced. However, in this case STAB in acetic acid was only found to result in minimal conversion and sodium cyanoborohydride had to be used instead, providing the piperidine **131** in a 90% yield.

There is literature precedent to suggest that Lawesson's Reagent is compatible with carbamates,^{181,182} but as a final check before applying these conditions to the fully elaborated system **269**, the reaction was tested on the Cbz-protected *trans*-lactam **263** (Scheme 119).



Scheme 119. Thiolactam formation with the Cbz-protected *trans*-substituted lactam **262**.

As expected, the carbamate proved not to be an issue and the thiolactam **282** was isolated in a good yield of 75%. The lactam **262** was also subjected to iodomethane in acetonitrile to ensure there would be no methylation of the amine, and no reaction was observed after stirring overnight at room temperature. With these checks complete, the methodology was applied to the fully elaborated system **269** (Scheme 120).

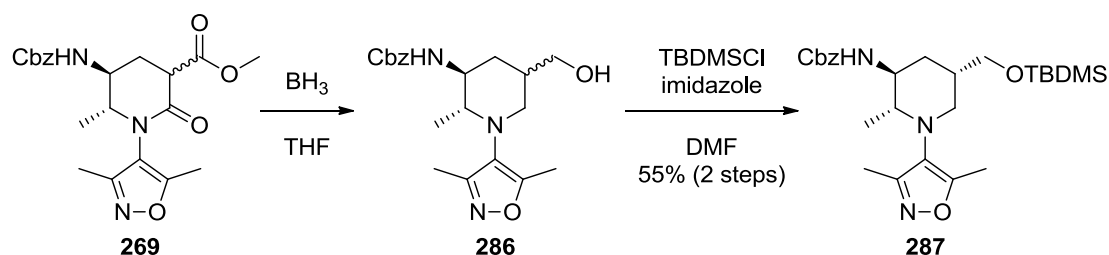


Scheme 120. Reduction of lactam carbonyl in the ester-substituted lactam **269**, *via* the thiolactam intermediate **283**.

The thiolactam **283** was isolated in a slightly reduced, but still acceptable yield of 60%, as a mixture of diastereomers. This intermediate was successfully methylated to form the thioiminium salt **284**, but when sodium borohydride was added very little reduction occurred. There was precedent in the literature for switching between sodium borohydride and sodium cyanoborohydride giving different results,¹⁷⁹ so sodium cyanoborohydride was added and found to facilitate the reduction of the thioiminium **284** directly to the piperidine **285** without the need to go *via* a conjugated enamine intermediate. With this method, the piperidine **285** was isolated in a 40% yield.

Interestingly, while the lactam **269** and thiolactam **283** were determined by LCMS and ¹H NMR to be mixtures of diastereomers, the reduced piperidine **285** was isolated as a

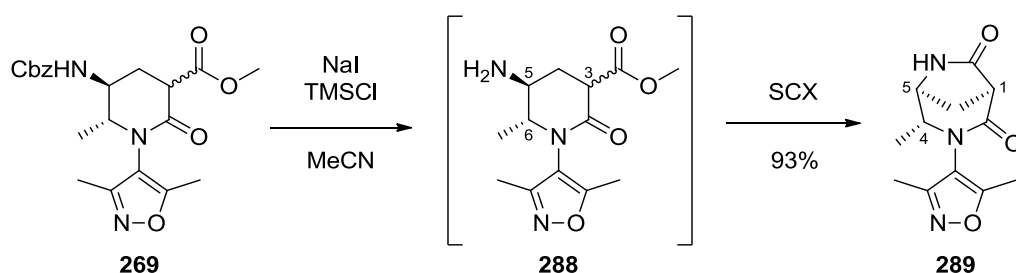
single diastereomer which, unfortunately, had the undesired stereochemistry with the ester *trans* to the amine. This phenomenon was also observed during an alternative route exploration in which both the lactam and ester were fully reduced, with the aim to reoxidise the resultant alcohol **286** at a later stage (Scheme 121). This alternative route, which is not discussed further in this manuscript, ultimately proved unproductive due to difficulties in cleanly oxidising the alcohol **286**.



Scheme 121. Borane reduction of methyl ester-substituted lactam **269**, with subsequent silyl protection of the alcohol intermediate **286**.

In the example shown, the ester-substituted lactam **269** was reduced with borane and the alcohol **286** was subsequently TBDMS protected. Only one diastereomer of the silyl protected product **287** was isolated, and, once again, this was determined to be of the undesired diastereomer with the silyl ether *trans* to the amine.

This raised the question of whether the analysis of the ester-substituted lactam **269** as being a mixture of two diastereomers was correct, or whether an impurity had been erroneously identified and there was not in fact any of the desired isomer going in to these reductions. However, a second observation from another alternative route exploration assuaged this concern (Scheme 122).



Scheme 122. *N*-Cbz deprotection of the methyl ester-substituted lactam **269** with subsequent cyclisation during ion exchange (SCX-2) chromatography.

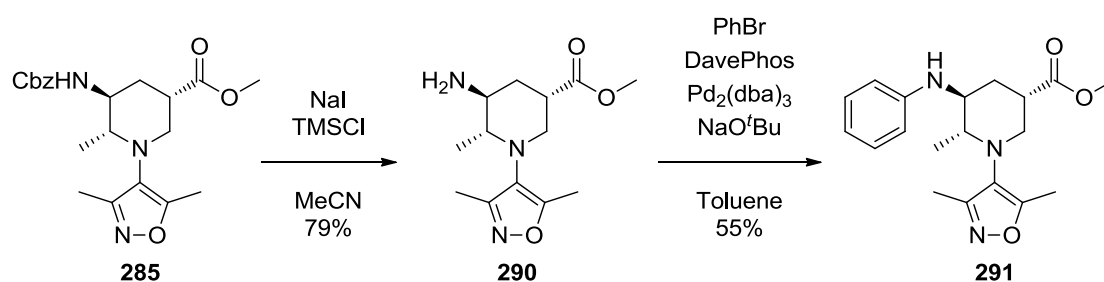
In this example, the possibility of reordering the steps such that Cbz deprotection and C-N cross-coupling occurred before the lactam reduction was investigated. Acidic conditions could not be used to remove the Cbz group due to the possibility of hydrolysing the methyl ester, while hydrogenation could not be used as this has previously been found to be incompatible with the isoxazole. A suitable procedure was

found that used TMS iodide, generated *in situ* from TMS chloride and sodium iodide.¹⁸³ This reaction was successful, and LCMS of the crude reaction mixture suggested excellent conversion to the deprotected amine **288**. However, when this amine was purified by ion exchange chromatography, the species that was eluted from the cartridge with ammonia in methanol was a bridged dilactam **289**. This product was clearly the result of cyclisation between the amine and the ester, but the important points to note are the high yield of 93% and the fact that cyclisation could only occur if the amine and ester were on the same side of the ring, in the desired *cis*-arrangement. This suggests that the 3-position, α to both the ester and the lactam, is readily epimerisable, and that one epimer was reacting significantly faster than the other, giving single diastereomer products. Reports from multiple sources suggest that this is a known issue with these lactam-ester systems, and epimerisation is stated to occur at neutral pH, with selective crystallisation being the main solution.^{184–186} The most tractable solution to the problem in this case was to epimerise the 3-position with methoxide at a later stage.

On a side note, the bridged dilactam **289** is a novel heterocycle. Syntheses to analogues with one or neither of the carbonyls have been published, but not with both in these positions, and none were found that included stereoselective substitution at the 4-position.^{187,188}

6.10.4 Final Steps and Epimerisation

The next two steps of the synthesis used chemistry that had already been established in this research (Scheme 123).

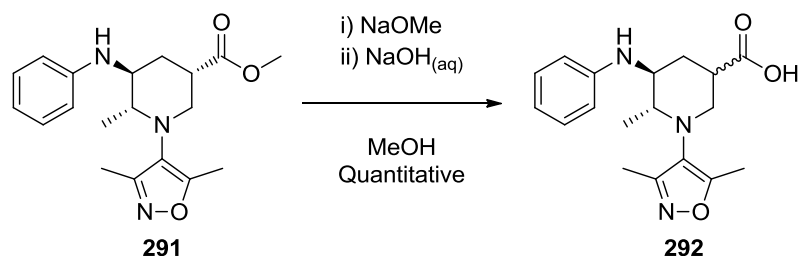


Scheme 123. Amine deprotection and Buchwald-Hartwig cross-coupling to form phenyl-substituted aminopiperidine 291.

First, the Cbz group was removed from the protected intermediate **285** using the TMS iodide conditions that had previously been used (Scheme 122), which theoretically should not hydrolyse the methyl ester.¹⁸³ This provided the free base amine **290** in a 79% yield. The Buchwald-Hartwig coupling conditions that have been successful

previously proved once again to be suitable, and a 55% yield of the phenyl product **291** was isolated.

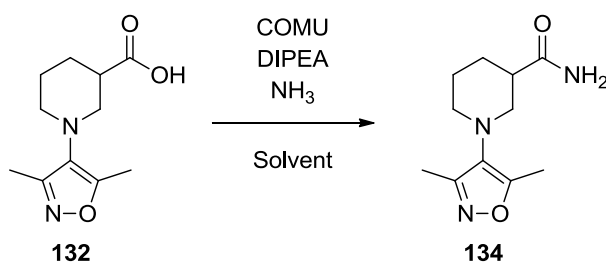
It was at this point that epimerisation of the ester α -position was performed (Scheme 124).



Scheme 124. Epimerisation and hydrolysis of the methyl ester-substituted piperidine 291.

The ester **291** was heated with sodium methoxide in methanol overnight. Given the small scale, even trace presence of water was likely to be significant, and it was not surprising that LCMS analysis showed significant hydrolysis to have occurred. Therefore, aqueous sodium hydroxide was added to complete the hydrolysis, and the carboxylic acid **292** was isolated in quantitative yield as a 1.4:1 mixture of diastereomers, with the desired isomer being the major component.

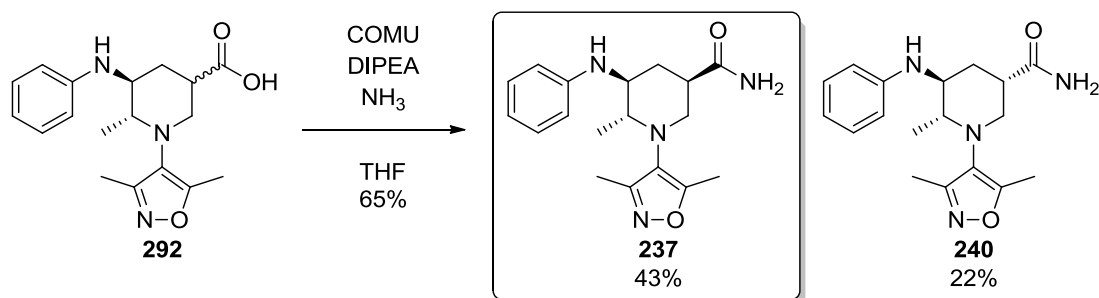
Originally, the plan for the final step was to use magnesium nitride to convert a methyl ester to a primary amide. However, as the final intermediate was now a carboxylic acid, amide coupling conditions needed to be optimised (Scheme 125).



Scheme 125. Solvent screen for amide coupling of carboxylic acid 132 with ammonia.

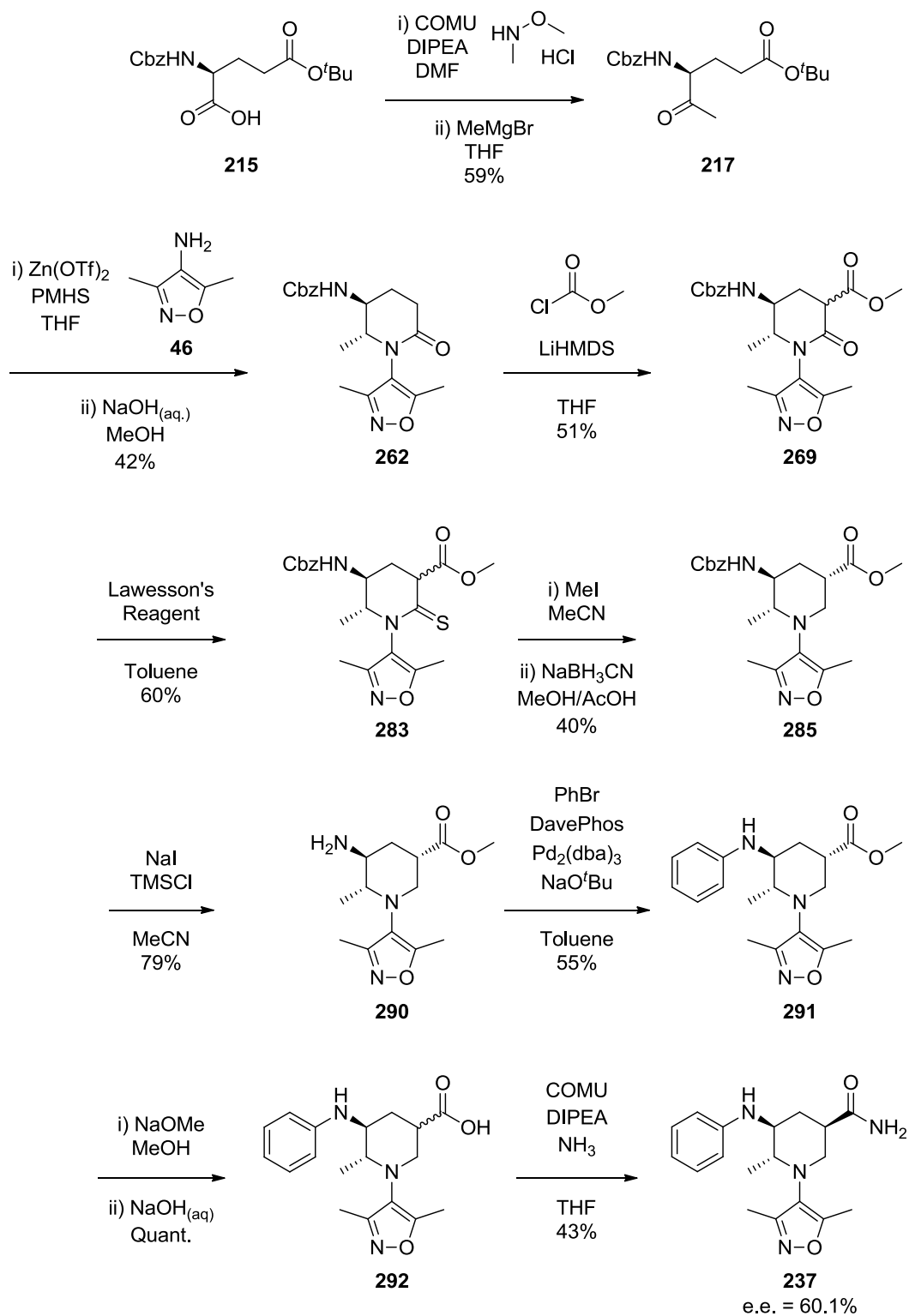
Using the less substituted carboxylic acid **132** as a test reactant, amide coupling with COMU was trialled with large excesses of ammonia. At the time, ammonia was available as solutions in water, dioxane and THF, so all of these were trialled. LCMS analysis of the reactions suggested that no product **134** was formed in the aqueous reaction; some conversion was seen in dioxane; but the best conversion was seen for THF, and after a second addition of COMU there was no longer any detectable starting material.

Finally, these amide coupling conditions were applied to the carboxylic acid intermediate **292** and complete conversion to primary amide, as determined by LCMS, was achieved (Scheme 126).



Scheme 126. Amide coupling to isolated the final trisubstituted primary amide compound 237.

After purification, the desired final product **237** was isolated in a 43% yield, with a 22% yield of the opposite diastereomer **240** also obtained. A total of 12 mg of this final compound **237** was isolated, which represented an overall yield of 0.56% over nine steps (Scheme 127).



Scheme 127. Full route to final trisubstituted piperidine isoxazole 237.

6.10.5 Final Data

The trisubstituted piperidine **237** was obtained as an 80:20 mixture of enantiomers, as determined by chiral HPLC. The reduction in enantiopurity, with respect to the amino acid starting material **215**, was also observed in the synthesis of the disubstituted 2-Me analogue **205**, and it was concluded that the epimerisation occurred during the Grignard attack on the Weinreb amide intermediate **216**. After separation of the stereoisomer mixture **237** by chiral chromatography, the desired enantiomer **237a** was isolated with an e.e. of 97.8%, alongside the less active enantiomer **293**, and both of these compounds were submitted for biological testing.

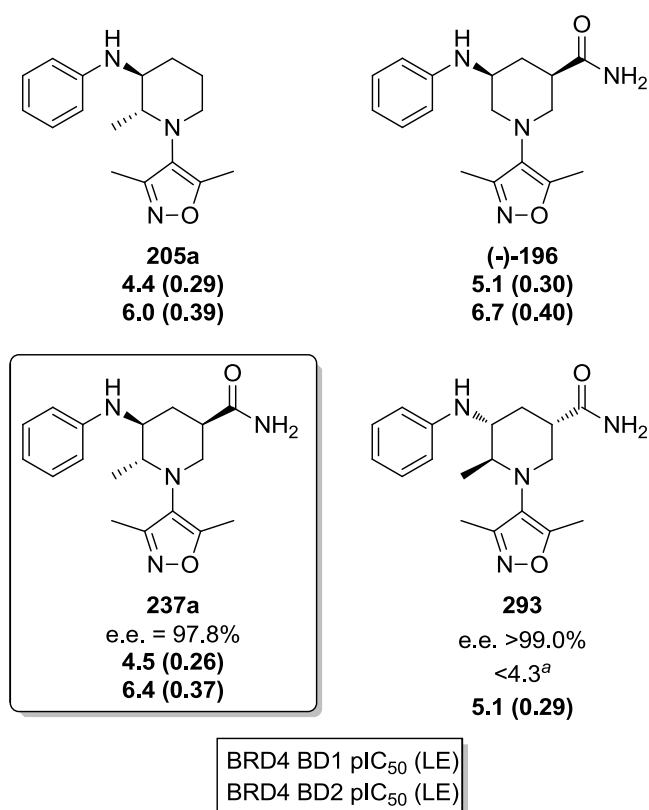


Figure 71. Assay data for the final trisubstituted piperidine **237a**, and its opposite enantiomer **293**. ^aA pIC₅₀ value of <4.8 was determined on one test occasion out of three and was excluded from the reported value.

The trisubstituted piperidine **237a** returned a pIC₅₀ at BRD4 BD2 of 6.4, which was a 0.4 log unit improvement over the disubstituted 2-Me analogue **205a**. While this was a slight reduction compared to the disubstituted 5-amide analogue **(-)-196**, which had a pIC₅₀ of 6.7, this result demonstrates the ability to interact with the ZA channel from this vector in the more elaborated system. Perhaps more importantly, the selectivity has increased from 40-fold, in both the disubstituted examples, to 79-fold. The largest BD2-selectivity claimed for BRD4 in the literature is only 30-fold, reported for RVX-208 **166**,¹⁵⁶ so this

result represented a significant improvement in the field. As expected, the undesired enantiomer **293** possessed significantly reduced activity relative to **237a**.

An X-ray crystal structure of the final compound **237a** in the binding site of BRD2 BD2 was solved and this is shown in Figure 72, with the structure of the 2,3-disubstituted analogue **205** superposed.

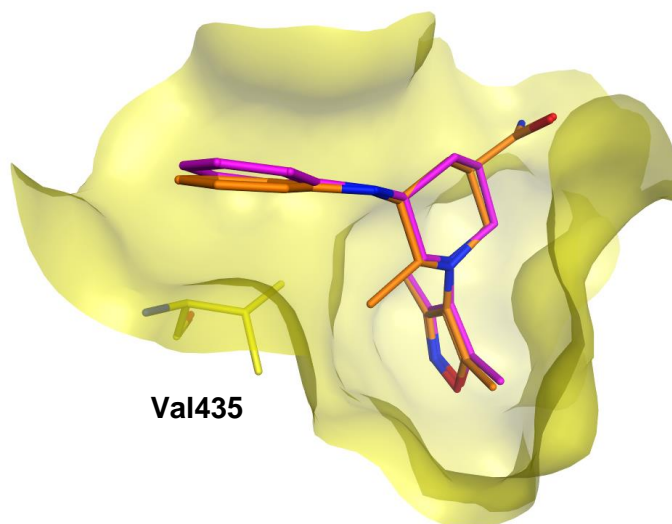


Figure 72. X-ray crystal structure of the trisubstituted piperidine **237a** (orange) bound to BRD2 BD2 (yellow) with the 2,3-disubstituted analogue **205** (magenta), also bound to BRD2 BD2, superposed. The valine gatekeeper residue has been highlighted (yellow). Water molecules have been removed from the image for clarity.

The binding mode of the trisubstituted piperidine **237a** overlaps well with the 2,3-disubstituted analogue **205**, with the methyl groups of both being directed towards the gatekeeper residue (see also Figure 66, p127). The boost in selectivity seen in both of these compounds, compared to the relevant analogues without the 2-Me group, further supports the hypothesis that the differing sizes of the gatekeeper residue in BD1 and BD2 domains is a key contributor to the BD2-selectivity.

As expected, the primary amide group was directed into the base of the ZA channel (Figure 73).

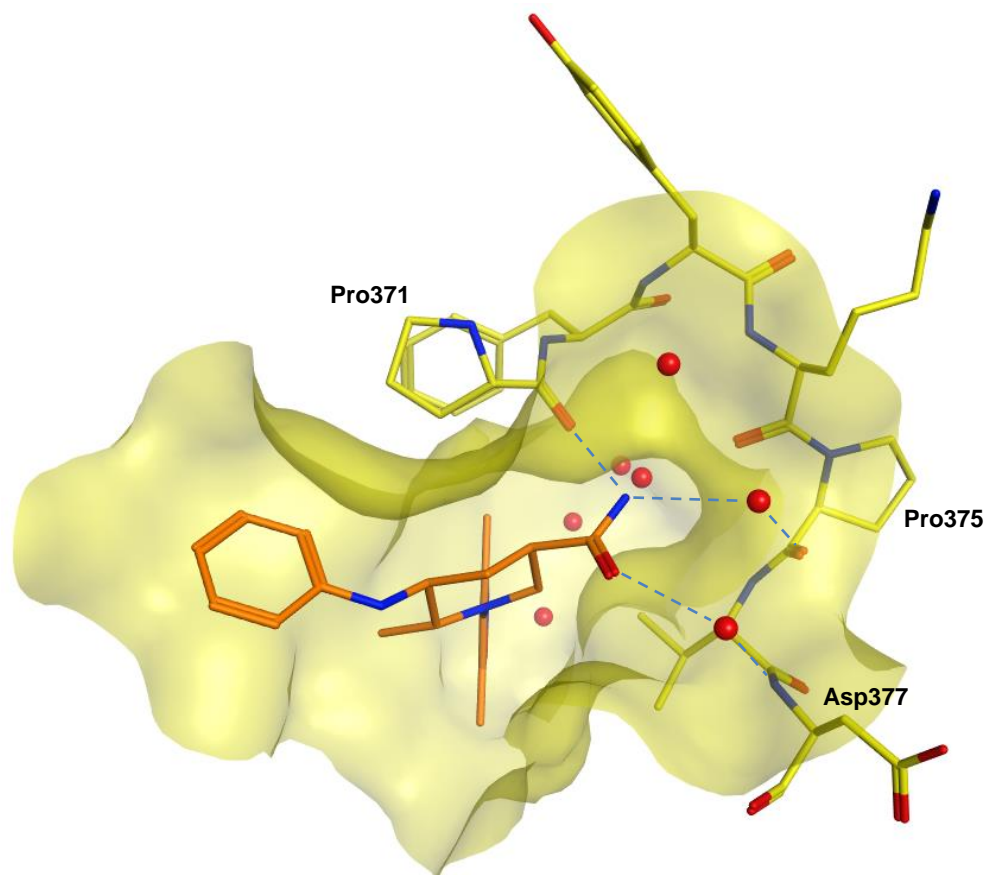


Figure 73. X-ray crystal structure of the trisubstituted piperidine **237a** (orange) bound to BRD2 BD2 (yellow). Water molecules (red) and peptide residues (yellow) in the vicinity of the primary amide have been highlighted, with all others removed for clarity. Dotted lines (blue) show atoms in close enough proximity for hydrogen bonding interactions to occur.

As with the 3,5-disubstituted analogue **196** (Figure 60, p117), the amide NH_2 group of the trisubstituted piperidine **237a** was seen to form a hydrogen bond with the backbone carbonyl of Pro371. Where the binding modes differ, however, is that the carbonyl oxygen of the former compound forms a hydrogen bond directly with the backbone NH of Asp377, while the latter makes this interaction *via* a bridging water molecule. Another hydrogen bonding interaction is also present between the NH_2 group of the primary amide and the backbone carbonyl of Pro375, *via* a second water molecule. These two water molecules are part of the conserved water network seen in BET bromodomain binding sites (Figure 16, p19), but neither molecule was present in the crystal structure of the 3,5-disubstituted piperidine **196**, suggesting that the primary amide displaced them in that case. Figure 74 shows an overlay of these two structures, and the conserved water molecules observed in each.

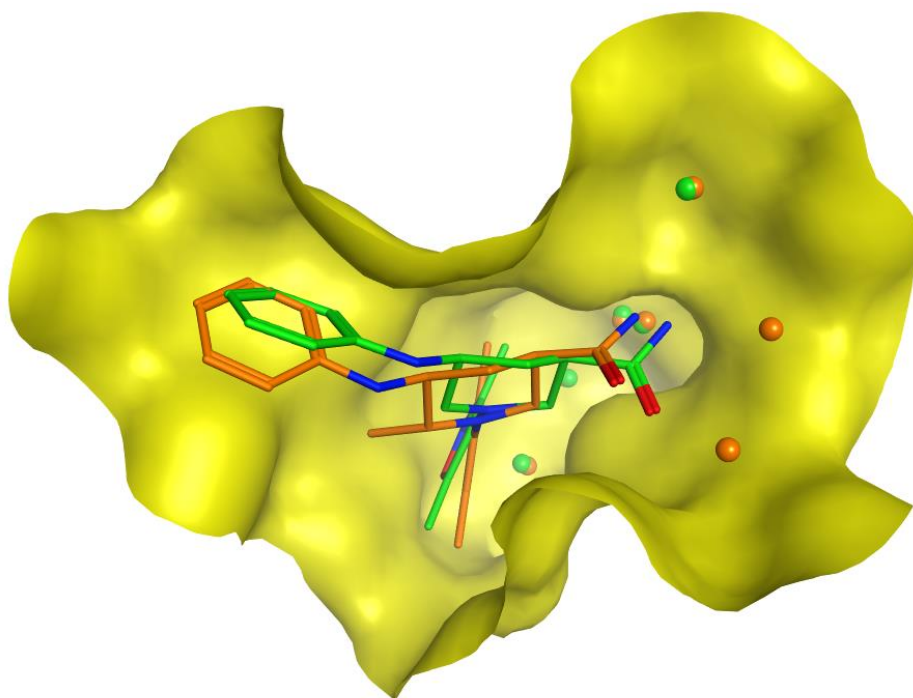


Figure 74. X-ray crystal structure of the trisubstituted piperidine **237a** (orange) bound to BRD2 BD2 (yellow) with the 3,5-disubstituted analogue **196** (green), also bound to BRD2 BD2, superposed. Water molecules in the vicinity of the primary amide and isoxazole of each compound have been shown in the same colour, while all others have been removed from the image for clarity.

Compared to the 3,5-disubstituted piperidine **196**, the trisubstituted piperidine **237a** was shifted towards the WPF shelf, taking up less space in the ZA channel and not displacing two of the conserved water molecules. This results in the different hydrogen bonding networks of the two molecules, and is likely to be the reason for the slightly reduced BRD4 BD2 potency of the trisubstituted piperidine **237a**.

Supplementary biological and physicochemical data was collected for the trisubstituted piperidine **237a** and is displayed in Table 11, with the 3,5-disubstituted compound (-)-**196** included for comparison.

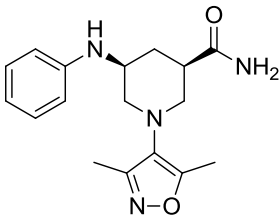
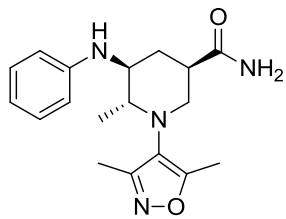
	 (-)-196	 237a
BRD4 BD1 pIC ₅₀	5.1	4.5
BRD4 BD2 pIC ₅₀	6.7	6.4
BRD4 BD2 LE	0.40	0.37
Fold BD2-Selectivity	40	79
PBMC pIC ₅₀	6.9	6.3 ^a
AMP (nm/s)	310	330
CLND Solubility (μM)	≥ 409	-
CAD Solubility (μM)	-	≥ 389
ChromLogD _{pH7.4}	3.5	4.0
PFI	5.5	6.0

Table 11. Profile of the trisubstituted piperidine 237 compared to the 3,5-disubstituted analogue (-)-196. ^aValue based on one test occasion only, while other PBMC pIC₅₀ values are based on four or more.

It can be seen that the final compound has retained its high artificial membrane permeability and solubility, and has a potency in the cell-based assay which is in line with the biochemical BRD4 BD2 data. In comparison to the 3,5-disubstituted example **(-)-196**, the addition of the methyl group to form the trisubstituted compound **237a** has increased the ChromLogD_{pH7.4} from 3.5 to 4.0. Adding the number of aromatic rings to this value gives the PFI as 6.0 (Equation 5, p100). Guidelines for small molecule oral candidates suggest that a PFI of less than or equal to 6 is desirable, which this compound fulfils without having been through a lead optimisation programme.¹⁶⁰

Overall, the data for this series has been very encouraging. A final compound **237a** has been generated with similar biochemical activity to published lead compounds, with the added advantage of 79-fold selectivity for the BRD4 BD2 domain over its BD1 counterpart. Furthermore, data has been collected for 2,3-disubstituted analogue **205** showing that this BD2-selectivity is also apparent at the other members of the BET family: BRD2, BRD3 and BRDT (Figure 68, p129). The same set of assays also showed this compound **205** to have excellent selectivity over a range of non-BET bromodomains, especially when the small size of the molecule is considered. The series has

demonstrated permeability in an artificial membrane assay and has displayed cell activity in line with the biochemical assays.

SAR data has been generated to show that there are two areas of the framework that are exploitable to modulate physicochemical properties: the substituents on the anilinic group at the piperidine 3-position can be varied, and an amide group can be included at the piperidine 5-position. Both of these areas can also be manipulated to increase potency. Collectively, these properties suggest that this piperidine-isoxazole framework would be suitable for a lead optimisation programme.

7. Conclusion

This research set out to produce BET inhibitors with an increased degree of saturation to those previously reported, in order to explore new areas of chemical space containing molecules with a greater three-dimensional character. The approach taken was to use a well-established fragment, a phenylisoxazole **19**, retain the dimethylisoxazole acetyl-lysine mimetic, and replace the phenyl ring with a saturated heterocycle. A number of fragments were synthesised, during which process two productive synthetic disconnections were identified which were utilised in the design of all later syntheses. A piperidine framework was prioritised for further exploration, based on structural information, biological assay data and chemical tractability (Figure 75).

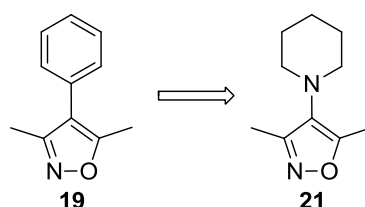


Figure 75. Overarching saturation approach from published phenylisoxazole **19**.

Investigations to probe for an interaction with the WPF shelf from this piperidine core established that a one-atom linker was sufficient to place a phenyl group onto the shelf from the piperidine 3-position and gain an appreciable boost in potency (Figure 76).

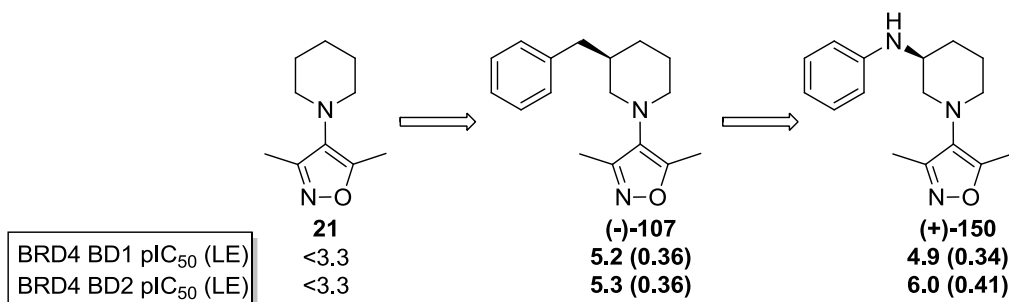


Figure 76. Extension from piperidine **21** to the WPF shelf, resulting in a BD2-selective amine (+)-**150**.

Analogs of this methylene linked compound **107** were synthesised in order to optimise the interaction with the WPF shelf and it was found that an amine-linked analogue **150** provided improved potency, as well as 13-fold selectivity for the second bromodomain of BRD4 over the first. This serendipitous discovery was investigated further and the purpose of this research turned towards understanding and improving this selectivity.

The synthesis and biological testing of an unsaturated analogue **159** of the aniline-substituted piperidine **(+)-150** confirmed that the saturation of the core was a necessary feature to provide the observed BD2-selectivity (Figure 77).

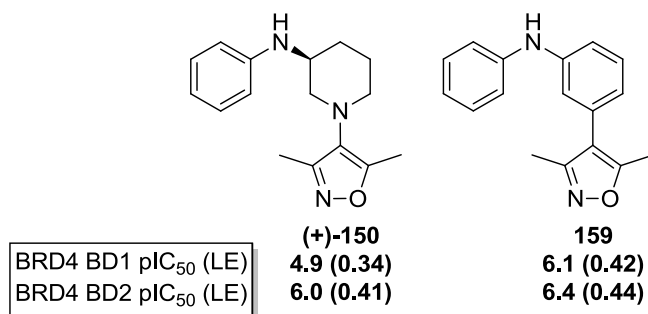


Figure 77. Comparison of the saturated BD2-selective piperidine **(+)-150** with an unsaturated analogue **159**.

A range of congeners of the aniline-substituted piperidine **150** were prepared with altered shelf-binding groups, and while the potency varied, the level of selectivity remained roughly constant. These modifications also demonstrated the ability to modulate lipophilicity from this area of the molecule.

In order to improve potency, selectivity and physicochemical properties, the inclusion of additional, carefully selected substituents on the piperidine ring was investigated (Figure 78).

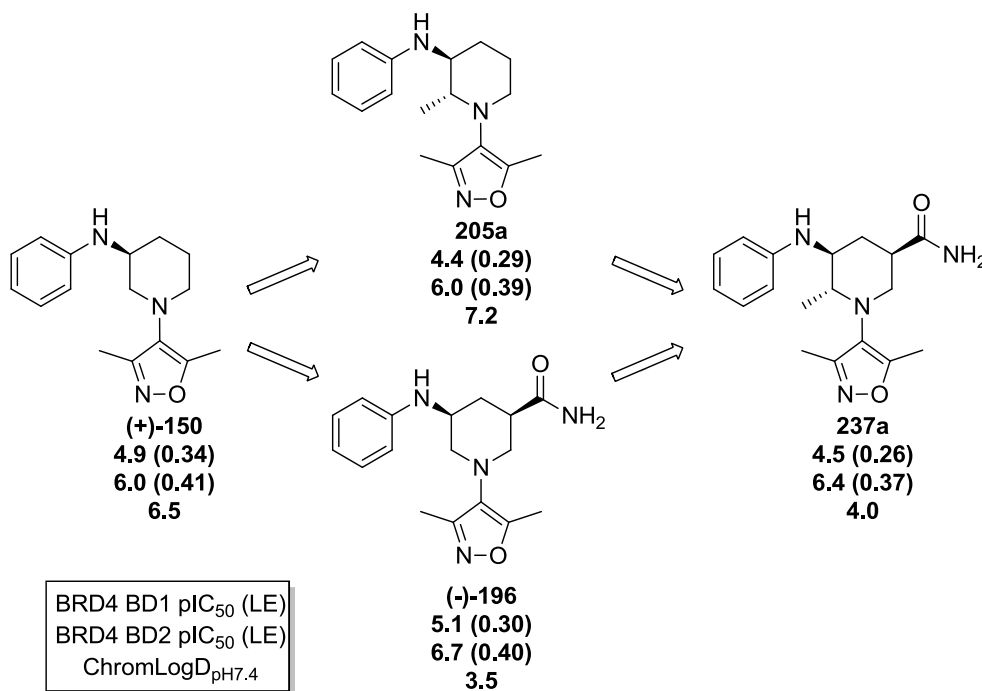


Figure 78. Elaboration of the monosubstituted, amine-linked, BD2-selective piperidine **(+)-150** to investigate methods for improving potency, selectivity and physicochemical properties, resulting in a trisubstituted example **237a**.

A residue difference between BD1 and BD2 domains was postulated as contributing towards the BD2 selectivity observed. This residue, termed the gatekeeper, restricts access to the WPF shelf and in BD2 domains it is a valine, but it is a slightly larger isoleucine residue in BD1 domains. It was hypothesised that a methyl group at the piperidine 2-position could further accentuate a clash with the isoleucine of BD1 domains, while being tolerated by the BD2 domains. Gratifyingly, the biological data for the 2,3-disubstituted piperidine **205a** supported this hypothesis, retaining a high pIC_{50} of 6.0 at BRD4 BD2, with increased selectivity over BD1 to 50-fold.

The use of the piperidine 5-position as a vector to gain increased potency and improved physicochemical properties was explored with a primary amide. The *cis*-substituted analogue **(-)-196** indeed achieved these goals, with a 3 log unit decrease in $ChromLogD_{pH7.4}$ and a 0.7 log unit increase in potency at BRD4 BD2, compared to the monosubstituted analogue **(+)-150**.

Given the benefits gained from each of these substituents, a trisubstituted compound **237** was targeted that incorporated both of these elements. The resultant compound **237a** displayed an increased selectivity of 79-fold, an improvement on the 40-fold seen for both disubstituted examples. The pIC_{50} at BRD2 BD2 was 6.4, which is not as high as the 6.7 observed for the 5-amide analogue **(-)-196**, but is still a 0.4 log unit boost over the 2-Me analogue **(+)-150**. The $ChromLogD_{pH7.4}$ of this final compound **237a** was 4.0, which corresponds to a PFI of 6.0 (Equation 5, p57). Therefore, prior to any lead optimisation efforts, this metric falls within the PFI guidelines for small molecule oral candidates of less than or equal to 6.¹⁶⁰

At the outset of this research, two literature compounds were chosen as comparators (Figure 79).

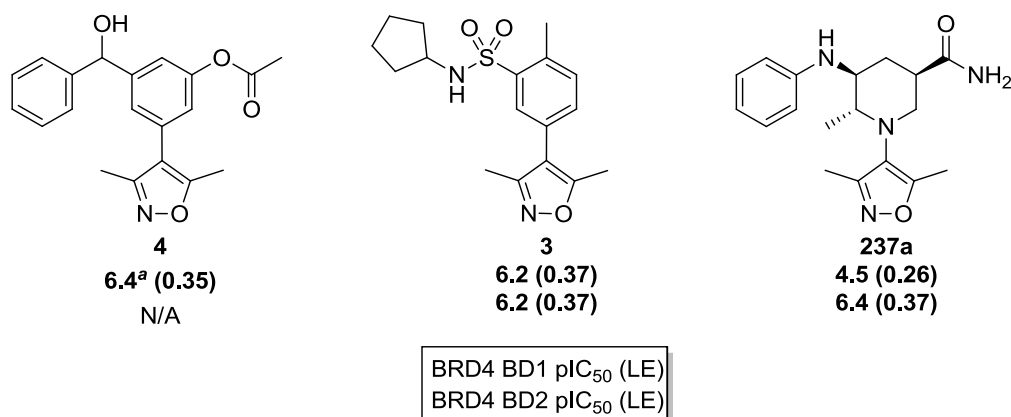


Figure 79. Literature comparator compounds and their measured potencies alongside the trisubstituted piperidine compound **237a**. ^aData from external AlphaScreen assay.⁶⁴

The sulfonamide compound **3**⁹⁹ has been screened in the same BRD4 FRET assay system as the compounds in this research so data can be directly compared, and the trisubstituted piperidine **237a** can be seen to have similar potency and ligand efficiency at BRD4 BD2, but has the distinct advantage of selectivity over BD1.

Two criteria that were set at the start of this programme for a suitable lead molecule were a pIC₅₀ above 6.0 and a molecular weight below 350 Da. This compound **237a** has a pIC₅₀ of 6.4 and molecular weight of 328, satisfying these stipulations. It also has an Fsp³ of 0.444, which is significantly larger than the average value calculated for BET inhibitors by Prieto-Martinez *et al.* of 0.245,¹ and investigations have shown the possibility of modulating the potency and selectivity by altering the substituents on the phenyl ring. Therefore, this compound was deemed suitable as a potential lead compound.

This piperidine framework represents a new chemotype of BD2-selective BET inhibitors. There is a standing hypothesis to explain how this selectivity has been gained, which was used to rationally reduce the BD1 potency, in contrast to the post-rationalisation used with reported examples.^{86,155} These published examples reference a major residue difference, while this work exploits a more subtle change that is located closer to the KAc interaction site. Differential interaction with this “gatekeeper” residue could only feasibly be enacted by optimising the shape of the core of the inhibitor molecule, and hence this work has demonstrated the benefits of exploring new chemical space by increasing three-dimensional character with more highly saturated molecules.

However, with their relative ease of synthesis, it is understandable that medicinal chemistry has tended towards flat, aromatic systems. The wealth of sp² cross-coupling methodologies that have been reported means that it is often possible to quickly and efficiently synthesise and screen large numbers of compounds. Introducing complexity in target compounds, in the form of saturation, often introduces complexity in synthesis. This may mean that seemingly small alterations in target molecules can result in the need for bespoke synthetic strategies, an issue that arose in this research programme with the two disubstituted piperidine compounds each requiring drastically different syntheses. Fortunately, this issue had been foreseen and two distinct disconnection strategies were pursued from an early stage, which hinged on the formation of either the saturated ring or the isoxazole warhead as part of the route. Moreover, further complications arose when it was decided to combine the features of these molecules and synthesise the trisubstituted compound **237**, basing the route on the synthesis of the 2,3-disubstituted

analogue **205**. Methodology did not exist to selectively form the desired diastereomer from reductive amination of α -aminoketones and, therefore, suitable conditions had to be investigated, and were successfully developed.

In an ideal future, synthetic organic methodology will have advanced such that medicinal chemists can investigate wide-ranging three-dimensional scaffolds on a reasonable time-scale. Prior to this, however, there remains the question of whether it is a better use of time to isolate large numbers of flatter compounds and screen them, or to make a relatively small number of more complex molecules. This work is evidence of what can be achieved with the latter approach.

8. Future Work

The trisubstituted piperidine **237** has been proposed as a potential lead compound. Were this to be taken up as part of a lead optimisation programme then there are a number of lines of enquiry that could be explored, some of which are shown in Figure 80, separated into changes at the 2-, 3- and 5-positions.

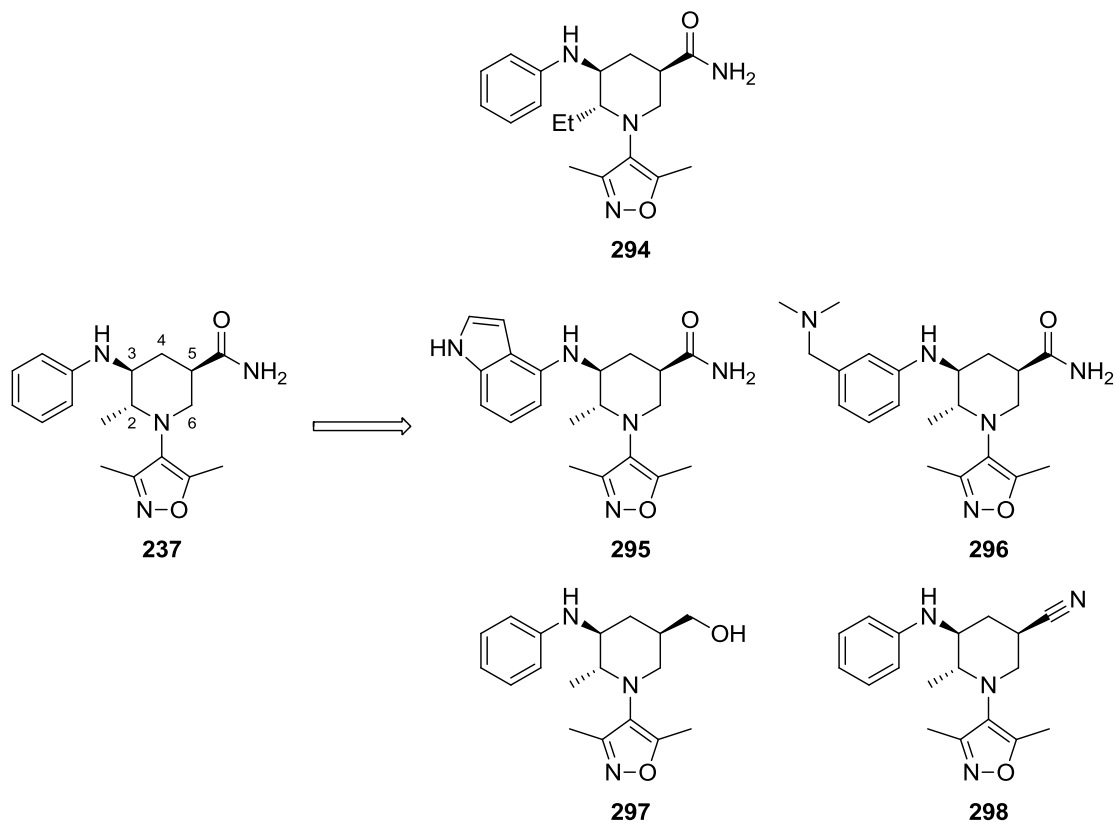


Figure 80. Potential lines of enquiry for a lead optimisation programme, using trisubstituted piperidine **237** as a starting point, including explorations at the 2-, 3- and 5-positions.

At the 2-position, only a methyl group has been installed thus far. Larger groups may further improve selectivity, and X-ray crystal structure information does not rule out the possibility of using this part of the molecule as a vector for further growth. An ethyl analogue **294** would be a good initial target to determine the viability of this approach.

During investigations into the shelf binding group attached at the 3-position (see Section 6.8.2), it was shown that it was possible, to an extent, to modulate the potency and lipophilicity of this series by adding substituents to the ring. Determining whether these improvements would translate to the more elaborated system by synthesising the indole **295** and pendant amine **296** analogues would be a good start. Furthermore, it may also be necessary to vary this group to avoid the potential mutagenic risk associated with anilines.

At the 5-position, only a primary amide has been trialled in compounds also containing a shelf-binding group. Analogues with other hydrophilic groups, such as an alcohol **297** or a nitrile **298**, could be synthesised to determine if potency could be improved.

Neither the 4- nor 6-positions have not been probed in this research, but their potential use could be examined in a lead optimisation programme. For example, a group at the 4-position could be used to boost potency by forming an interaction with the edge of the nearby tryptophan (W of the WPF shelf), as was posited to be occurring with the *N*-Boc **64** and *N*-acetyl **104** piperazine fragments (Figure 25, p59).

Early investigations in this research explored the possibility of using five- and seven-membered rings as the core. Five-membered rings were discounted due to lack of biological potency and X-ray crystallography data, but seven-membered rings showed similar promise to their six-membered analogues, with the latter mainly being prioritised due to chemical tractability. It may be interesting to revisit seven-membered cores to determine if the BD2-selective traits would still be present, or even enhanced, with the larger ring. A lactam core would be of particular interest due to the intrinsic polarity it would provide and the potential to use the amide nitrogen as a vector to access the ZA channel (Figure 81).

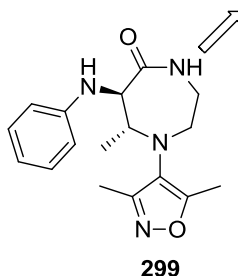


Figure 81. Exploration of seven-membered cores. A potentially useful vector to access the ZA channel is marked.

Finally, the lessons learnt from this series could be applied to alternative chemotypes. In the first instance, alternative warheads could be substituted for the isoxazole, although it is possible that this would cause a repositioning in the binding site, removing the beneficial effects on selectivity seen here. Saturation could be applied to larger BET inhibitor scaffolds to manoeuvre vectors towards the gatekeeper residue in order to engineer a clash. This is effectively the top-down approach that was initially rejected in this project (Figure 19, p25) as it would be likely to change the shape of the rest of the molecule significantly, and necessitate extensive reoptimisation. This argument still applies, but the idea seems more attractive now that the possible benefits have been demonstrated. However, the consideration of more saturated moieties early on in drug

development programmes, with less of a focus on flat fragments in screening libraries, would allow benefits such as this to be discovered on a more regular basis.

9. Experimental

9.1 General Information

Solvents and reagents. Magnetic stirrer bars were stirred vigorously using stirrer hot plates. Solvents and reagents were purchased from commercial suppliers and used as received. Reactions were monitored by thin layer chromatography (TLC) or liquid chromatography-mass spectroscopy (LCMS). Heating was conducted using hotplates with DrySyn adaptors.

Chromatography. Thin layer chromatography (TLC) was carried out using polyester-backed precoated silica plates (particle size 0.2 mm). Spots were visualised by ultraviolet (UV) light ($\lambda_{\text{max}} = 254 \text{ nm}$ or 365 nm) and then stained with potassium permanganate solution followed by gentle heating. Flash column chromatography was carried out using the Teledyne ISCO CombiFlash® Rf+ apparatus with RediSep® or GraceResolv™ silica cartridges.

Liquid Chromatography Mass Spectrometry. LCMS analysis was carried out on a Waters Acquity UPLC instrument equipped with a BEH column (50 mm x 2.1 mm, 1.7 μm packing diameter) and Waters Micromass ZQ MS using alternate-scan positive and negative electrospray. Analytes were detected as a summed UV wavelength of 210–350 nm. Two liquid phase methods were used:

Formic: 40 °C, 1 mL/min flow rate, using a gradient elution with the mobile phases as (A) H₂O containing 0.1% volume/volume (v/v) formic acid and (B) acetonitrile containing 0.1% (v/v) formic acid. Gradient conditions were initially 1% B, increasing linearly to 97% B over 1.5 min, remaining at 97% B for 0.4 min then increasing to 100% B over 0.1 min.

High pH: 40 °C, 1 mL/min flow rate, using a gradient elution with the mobile phases as (A) 10 mM aqueous ammonium bicarbonate solution, adjusted to pH 10 with 0.88 M aqueous ammonia and (B) acetonitrile. Gradient conditions were initially 1% B, increasing linearly to 97% B over 1.5 min, remaining at 97% B for 0.4 min then increasing to 100% B over 0.1 min.

Nuclear Magnetic Resonance (NMR) Spectroscopy. Proton (¹H), carbon (¹³C) and fluorine (¹⁹F) spectra were recorded in deuterated solvents at ambient temperature (unless otherwise stated) using standard pulse methods on any of the following spectrometers and signal frequencies: Bruker AV-400 (¹H = 400 MHz, ¹³C = 101 MHz, ¹⁹F

= 376 MHz), Bruker AV-500 (^1H = 500 MHz, ^{13}C = 126 MHz), or Bruker AV-600 (^1H = 600 MHz, ^{13}C = 150 MHz). Chemical shifts are reported in ppm and are referenced to tetramethylsilane (TMS) or the following solvent peaks: CDCl_3 (^1H = 7.27 ppm, ^{13}C = 77.0 ppm), $\text{DMSO-}d_6$ (^1H = 2.50 ppm, ^{13}C = 39.5 ppm), CD_3OD (^1H = 3.31 ppm, ^{13}C = 49.0 ppm) or CD_3CN (^1H = 1.94 ppm, ^{13}C = 118.7 ppm). Peak assignments were made on the basis of chemical shifts, integrations, and coupling constants, using COSY, DEPT, HSQC and HMBC where appropriate. Coupling constants are quoted to the nearest 0.1 Hz and multiplicities are described as singlet (s), doublet (d), triplet (t), quartet (q), quintet (quin), sextet (sxt), septet (sept), broad (br.) and multiplet (m).

Infrared (IR) Spectroscopy. Infrared spectra were recorded using a Perkin Elmer Spectrum 1 or Spectrum 2 machine. Absorption maxima (ν_{max}) are reported in wavenumbers (cm^{-1}) and are described as strong (s), medium (m), weak (w) and broad (br.).

High-Resolution Mass Spectrometry (HRMS). High-resolution mass spectra were recorded on one of two systems:

System A – Micromass Q-ToF Ultima hybrid quadrupole time-of-flight mass spectrometer, with analytes separated on an Agilent 1100 Liquid Chromatograph equipped with a Phenomenex Luna C_{18} (2) reversed phase column (100 mm x 2.1 mm, 3 μm packing diameter). LC conditions were 0.5 mL/min flow rate, 35 $^\circ\text{C}$, injection volume 2–5 μL , using a gradient elution with (A) H_2O containing 0.1% (v/v) formic acid and (B) acetonitrile containing 0.1% (v/v) formic acid. Gradient conditions were initially 5% B, increasing linearly to 100% B over 6 min, remaining at 100% B for 2.5 min then decreasing linearly to 5% B over 1 min followed by an equilibration period of 2.5 min prior to the next injection.

System B – Waters XEVO G2-XS quadrupole time-of-flight mass spectrometer, with analytes separated on an Acquity UPLC CSH C_{18} column (100 mm x 2.1 mm, 1.7 μm packing diameter). LC conditions were 0.8 mL/min flow rate, 50 $^\circ\text{C}$, injection volume 0.2 μL , using a gradient elution with (A) H_2O containing 0.1% (v/v) formic acid and (B) acetonitrile containing 0.1% (v/v) formic acid. Gradient conditions were initially 3% B, increasing linearly to 100% B over 8.5 min, remaining at 100% B for 0.5 min then decreasing linearly to 3% B over 0.5 min followed by an equilibration period of 0.5 min prior to the next injection.

Mass to charge ratios (m/z) are reported in Daltons.

Melting points. Melting points were recorded on either Stuart SMP10 or Stuart SMP40 melting point apparatus.

Mass Directed Auto Preparation (MDAP). Mass-directed automatic purification was carried out using a Waters ZQ MS using alternate scan positive and negative electrospray and a summed UV wavelength of 210–350 nm. Two liquid phase methods were used:

Formic – Sunfire C₁₈ column (100 mm x 19 mm, 5 µm packing diameter, 20 mL/min flow rate) or Sunfire C₁₈ column (150 mm x 30 mm, 5 µm packing diameter, 40 mL/min flow rate), using a gradient elution at ambient temperature with the mobile phases as (A) H₂O containing 0.1% volume/volume (v/v) formic acid and (B) acetonitrile containing 0.1% (v/v) formic acid.

High pH – Xbridge C₁₈ column (100 mm x 19 mm, 5 µm packing diameter, 20 mL/min flow rate) or Xbridge C₁₈ column (150 mm x 30 mm, 5 µm packing diameter, 40 mL/min flow rate), using a gradient elution at ambient temperature with the mobile phases as (A) 10 mM aqueous ammonium bicarbonate solution, adjusted to pH 10 with 0.88 M aqueous ammonia and (B) acetonitrile.

Hydrophobic frit cartridges by ISOLUTE® contain a frit which is selectively permeable to organic solutions. These are separated from aqueous phase under gravity. Various cartridge sizes were used.

SCX-2 cartridges by ISOLUTE® contain a silica (50 µm) based sorbent with a chemically bonded propylsulfonic acid group. Various cartridge sizes were used for catch and release and scavenging SPE protocols.

Aminopropyl cartridges by ISOLUTE® contain a silica (50 µm) based sorbent with a chemically bonded aminopropyl group. Various cartridge sizes were used for catch and release and scavenging SPE protocols.

9.2 Synthetic Procedures and Compound Characterisation

General Procedure A – Amide Coupling

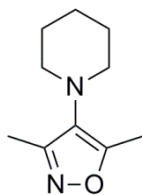
A vial was charged with methyl 1-(3,5-dimethylisoxazol-4-yl)piperidine-3-carboxylate **131** (100 mg, 0.42 mmol), TBD (18 mg, 0.13 mmol) and the relevant amine. The vial was sealed, and put under a nitrogen atmosphere before being heated to 75 °C for 4 h. The reaction mixture was allowed to cool before being dissolved in 1:1 MeOH:DMSO (2 mL) and purified by MDAP (Formic) to provide the amide product.

General Procedure B – Buchwald-Hartwig Coupling

A vial was charged with Pd₂(dba)₃ (12 mg, 0.013 mmol), DavePhos (8 mg, 0.02 mmol), NaO^tBu (35 mg, 0.36 mmol) and toluene (0.5 mL). The vial was sealed and evacuated and purged with nitrogen. To this was added a solution of 1-(3,5-dimethylisoxazol-4-yl)piperidin-3-amine **157** (50 mg, 0.26 mmol) and aryl halide (0.26 mmol) in toluene (0.5 mL), and the sealed vial was heated to 130 °C for 4 h or 15 h. This was allowed to cool and the solvent was removed under a stream of nitrogen. The residue was taken up into EtOAc (5 mL) and filtered through Celite (2.5 g), and flushed through with further EtOAc (3 x 10 mL). The combined organics were concentrated *in vacuo* and the residue was dissolved in 1:1 MeOH:DMSO (1 mL) and purified by MDAP (High pH) to provide aryl amine product.

General Procedure C – Buchwald-Hartwig Coupling

A vial was charged with Pd₂(dba)₃ (23 mg, 0.026 mmol), DavePhos (15 mg, 0.038 mmol), NaO^tBu (69 mg, 0.72 mmol) and toluene (1 mL). The vial was sealed and evacuated and purged with nitrogen. To this was added a solution of 1-(3,5-dimethylisoxazol-4-yl)piperidin-3-amine **157** (100 mg, 0.51 mmol) and aryl halide (0.51 mmol) in toluene (1 mL), and the sealed vial was heated to 130 °C for 4 h or 15 h. This was allowed to cool and the solvent was removed under a stream of nitrogen. The residue was taken up into EtOAc (5 mL) and filtered through Celite (2.5 g), and flushed through with further EtOAc (3 x 10 mL). The combined organics were concentrated *in vacuo* and the residue was dissolved in 1:1 MeOH:DMSO (2 mL) and purified by MDAP (High pH) to provide aryl amine product.

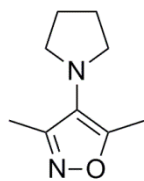
3,5-Dimethyl-4-(piperidin-1-yl)isoxazole (21)

a) *Via* alkylation of amine **46**

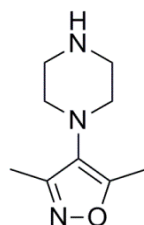
4-Amino-3,5-dimethylisoxazole **46** (500 mg, 4.46 mmol), 1,5-dibromopentane **87** (1.22 mL, 8.92 mmol), K_2CO_3 (1.36 g, 9.81 mmol) and NaI (1.47 g, 9.81 mmol) in MeCN (15 mL) were stirred for 20 h at 85 °C, under atmospheric conditions. The reaction was allowed to cool and Et_2O (100 mL) was added. The mixture was filtered and the precipitate washed on the filter with Et_2O (3 x 20 mL). The combined organics were concentrated *in vacuo* and the residue was taken up into DCM (2 mL) and purified by normal phase column chromatography (EtOAc in cyclohexane, 0 → 50%, 80 g SiO_2) to provide a sample of product containing small impurities. This sample was taken up into DCM (2 mL) and repurified by the same method shown above, to provide the titled compound as an orange oil (568 mg, 71% yield). ν_{max} ($CDCl_3$): 2934(s), 2852(w), 2806(w), 1627(w) cm^{-1} ; 1H NMR (400 MHz, $CDCl_3$) δ = 2.89 (t, J = 5.4 Hz, 4H), 2.36 (s, 3H), 2.22 (s, 3H), 1.67 - 1.60 (m, 4H), 1.56 - 1.48 (m, 2H); ^{13}C NMR (101 MHz, $CDCl_3$) δ = 160.1, 158.4, 128.7, 53.2 (2C), 26.8 (2C), 24.1, 11.6, 10.4; LCMS (Formic): t_R = 1.02 min, $[M+H]^+$ = 181, (100% purity); HRMS: ($C_{10}H_{16}N_2O$) $[M+H]^+$ requires 181.1341, found $[M+H]^+$ 181.1339.

b) *Via* reduction of piperidinone **95** with zinc-modified cyanoborohydride

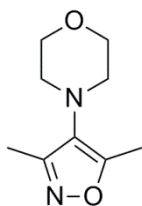
A solution of 1-(3,5-dimethylisoxazol-4-yl)piperidin-4-one **95** (50 mg, 0.26 mmol) and tosylhydrazide (72 mg, 0.39 mmol) in MeOH (2 mL) was stirred at RT for 2 h under a nitrogen atmosphere. To this was added a solution of $ZnCl_2$, 1.9 M in 2-MeTHF (0.10 mL, 0.19 mmol) and $NaBH_3CN$ (25 mg, 0.40 mmol) in MeOH (1 mL). The reaction mixture was heated to reflux under a nitrogen atmosphere for 17 h. The reaction mixture was allowed to cool and was diluted with EtOAc (20 mL). The product was extracted with 1 M HCl (aq, 20 mL). The aqueous phase was basified with 1 M NaOH (aq, 10 mL) and extracted with DCM (3 x 15 mL). The combined organics were washed with sat. $NaHCO_3$ (aq, 20 mL), brine (20 mL), passed through a hydrophobic frit and the solvent removed *in vacuo*. The residue was taken up into DCM (1 mL) and purified by normal phase column chromatography (EtOAc in cyclohexane, 0 → 50%, 12 g SiO_2) to provide the titled compound as a colourless oil (21 mg, 45% yield). 1H NMR (400 MHz, $CDCl_3$) δ = 2.91 (t, J = 5.4 Hz, 4H), 2.38 (s, 3H), 2.24 (s, 3H), 1.70 - 1.62 (m, 4H), 1.58 - 1.49 (m, 2H); LCMS (Formic): t_R = 1.00 min, $[M+H]^+$ = 181, (95% purity).

3,5-Dimethyl-4-(pyrrolidin-1-yl)isoxazole (22)

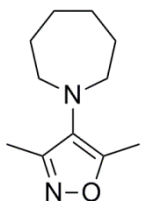
4-Amino-3,5-dimethylisoxazole **46** (105 mg, 0.936 mmol), 1,4-dibromobutane **81** (112 μ L, 0.936 mmol), K_2CO_3 (285 mg, 2.06 mmol) and NaI (309 mg, 2.06 mmol) in MeCN (2.5 mL) were stirred for 42 h at 85 $^\circ$ C under atmospheric conditions. Two further portions of 1,4-dibromobutane **81** (56 μ L, 0.47 mmol) were added at 21 h and 26 h. The reaction was allowed to cool and Et_2O (40 mL) was added. The mixture was filtered and the precipitate washed on the filter with Et_2O (3 x 10 mL). The organics were combined and passed through a hydrophobic frit. The solvent was removed *in vacuo* and the residue was taken up into in 1:1 MeOH:DMSO (0.8 mL) and purified by MDAP (High pH). The desired fractions were combined and concentrated *in vacuo*, before the product was extracted with DCM (3 x 20 mL). The combined organics were washed with brine (20 mL) and passed through a hydrophobic frit. The solvent was removed *in vacuo* to give the titled compound as an orange oil (64 mg, 41% yield). ν_{max} (neat): 2968(w), 2874(w), 2824(w), 1631(w) cm^{-1} ; 1H NMR (400 MHz, $CDCl_3$) δ = 3.20 - 3.07 (m, 4H), 2.39 (s, 3H), 2.26 (s, 3H), 2.06 - 1.88 (m, 4H); ^{13}C NMR (101 MHz, $CDCl_3$) δ = 158.5, 157.6, 125.6, 51.9 (2C), 25.0 (2C), 11.8, 11.2; LCMS (High pH): t_R = 0.92 min, $[M+H]^+$ = 167, (100% purity); HRMS: ($C_9H_{14}N_2O$) $[M+H]^+$ requires 167.1179, found $[M+H]^+$ 167.1181.

3,5-Dimethyl-4-(piperazin-1-yl)isoxazole (23)

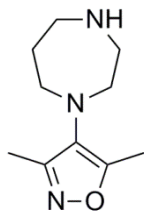
A solution of *tert*-butyl 4-(3,5-dimethylisoxazol-4-yl)piperazine-1-carboxylate **64** (300 mg, 1.07 mmol) in DCM (4 mL) was treated with TFA (82 μ L, 1.1 mmol) using ice water for external cooling. The mixture was then allowed to warm to RT and stirred under atmospheric conditions for 2 h. The reaction mixture was carefully quenched with sat. $NaHCO_3$ (aq, 20 mL) and extracted with DCM (5 x 20 mL). The combined organics were passed through a hydrophobic frit, and the solvent removed *in vacuo*. The residue was taken up into MeOH (2 mL) and loaded onto a pre-equilibrated SCX-2 cartridge (5 g). After 10 minutes the column was flushed with MeOH (4 CV) followed by 2 M NH_3 in MeOH (2 CV). The desired fractions were combined and the solvent removed *in vacuo* to give the titled compound as a pale brown oil (143 mg, 74% yield). ν_{max} ($CDCl_3$): 3302(br.), 2943(m), 2824(m), 1629(w) cm^{-1} ; 1H NMR (400 MHz, $DMSO-d_6$) δ = 2.84 - 2.79 (m, 4H), 2.78 - 2.73 (m, 4H), 2.34 (s, 3H), 2.14 (s, 3H); ^{13}C NMR (101 MHz, $CDCl_3$) δ = 160.9, 158.3, 127.8, 52.8 (2C), 46.7 (2C), 11.5, 10.5; LCMS (High pH): t_R = 0.61 min, $[M+H]^+$ = 182, (100% purity); HRMS: ($C_9H_{15}N_3O$) $[M+H]^+$ requires 182.1293, found $[M+H]^+$ 182.1297.

4-(3,5-Dimethylisoxazol-4-yl)morpholine (24)

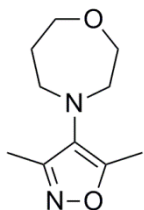
4-Amino-3,5-dimethylisoxazole **46** (500 mg, 4.46 mmol), 2-chloroethyl ether **69** (1045 μ L, 8.92 mmol), K_2CO_3 (1.36 g, 9.81 mmol) and NaI (1.47 g, 9.81 mmol) in DMF (15 mL) were stirred at 100 °C under a nitrogen atmosphere. After 4 h further 2-chloroethyl ether **69** (523 μ L, 4.46 mmol) was added and the mixture heated for a further 8 h. The reaction was allowed to cool and Et_2O (50 mL) was added. The mixture was filtered and the precipitate washed on the filter with Et_2O (3 x 20 mL). The organics were combined and passed through a hydrophobic frit. The solvent was removed *in vacuo* and the residue was taken up into cyclohexane (2 mL) and purified by normal phase column chromatography (EtOAc in cyclohexane, 0 \rightarrow 50%, 80 g SiO_2) to provide the titled compound as a yellow oil (552 mg, 68% yield). ν_{max} (neat): 2959(w), 2854(w), 1636(w) cm^{-1} ; 1H NMR (400 MHz, $CDCl_3$) δ = 3.79 (t, J = 4.6 Hz, 4H), 2.97 (t, J = 4.6 Hz, 4H), 2.40 (s, 3H), 2.27 (s, 3H); ^{13}C NMR (101 MHz, $CDCl_3$) δ = 161.3, 158.2, 127.3, 67.6 (2C), 52.0 (2C), 11.5, 10.5; LCMS (High pH): t_R = 0.74 min, $[M+H]^+$ = 183, (99% purity); HRMS: ($C_9H_{14}N_2O_2$) $[M+H]^+$ requires 183.1128, found $[M+H]^+$ 183.1127.

4-(Azepan-1-yl)-3,5-dimethylisoxazole (25)

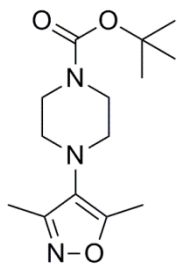
4-Amino-3,5-dimethylisoxazole **46** (105 mg, 0.936 mmol), 1,6-dibromohexane **97** (144 μ L, 0.936 mmol), K_2CO_3 (285 mg, 2.06 mmol) and NaI (309 mg, 2.06 mmol) in DMF (2.5 mL) were stirred for 24 h at 85 °C. The reaction was allowed to cool and Et_2O (30 mL) was added. The mixture was filtered and the precipitate washed on the filter with Et_2O (3 x 10 mL). The combined organics were washed with 5% LiCl (aq, 3 x 20 mL) and passed through a hydrophobic frit. The solvent was removed *in vacuo* and the residue was dissolved in 1:1 MeOH:DMSO (1.8 mL) and purified by MDAP (Formic). The desired fractions were combined and extracted with DCM (3 x 20 mL). The combined organics were washed with brine (20 mL) and passed through a hydrophobic frit. The solvent was removed *in vacuo* to give the titled compound as an orange oil (25 mg, 14% yield). ν_{max} (neat): 2925(s), 2853(m), 1725(w), 1673(w), 1638(w) cm^{-1} ; 1H NMR (400 MHz, $CDCl_3$) δ = 3.09 - 3.02 (m, 4H), 2.34 (s, 3H), 2.23 (s, 3H), 1.70 (m, 8H); ^{13}C NMR (101 MHz, $CDCl_3$) δ = 161.2, 158.8, 130.4, 55.0 (2C), 30.5 (2C), 27.4 (2C), 11.1, 10.4; LCMS (Formic): t_R = 1.24 min, $[M+H]^+$ = 195, (100% purity); HRMS: ($C_{11}H_{18}N_2O$) $[M+H]^+$ requires 195.1492, found $[M+H]^+$ 195.1495.

4-(1,4-Diazepan-1-yl)-3,5-dimethylisoxazole (26)

A solution of *tert*-butyl 4-(3,5-dimethylisoxazol-4-yl)-1,4-diazepane-1-carboxylate **102** (215 mg, 0.728 mmol) in DCM (2 mL) was treated with TFA (2.00 mL, 26.0 mmol) using ice water for external cooling. The mixture was then allowed to warm to RT and stirred under atmospheric conditions for 3 h. The solvent was removed *in vacuo* and the residue was dissolved in H₂O (2 mL) and 2 M NaOH (aq, 2 mL) was added. The product was extracted with DCM (3 x 15 mL). The combined organics were passed through a hydrophobic frit, and the solvent removed *in vacuo* to give the titled compound as a brown oil (139 mg, 98% yield). ν_{\max} (neat): 2930(m), 2840(w), 1663(w), 1627(w) cm⁻¹; ¹H NMR (400 MHz, DMSO-*d*₆, 120 °C) δ = 3.29 (br. s, 1H), 3.15 - 3.09 (m, 4H), 2.98 (t, *J* = 5.9 Hz, 2H), 2.93 - 2.88 (m, 2H), 2.33 (s, 3H), 2.17 (s, 3H), 1.84 - 1.76 (m, 2H); ¹³C NMR (101 MHz, DMSO-*d*₆, 120 °C) δ = 160.6, 158.1, 130.1, 57.2, 54.2, 50.5, 47.6, 31.5, 11.2, 10.2; LCMS (High pH): t_R = 0.65 min, [M+H]⁺ = 196, (100% purity); HRMS: (C₁₀H₁₇N₃O) [M+H]⁺ requires 196.1444, found [M+H]⁺ 196.1440.

4-(3,5-Dimethylisoxazol-4-yl)-1,4-oxazepane (27)

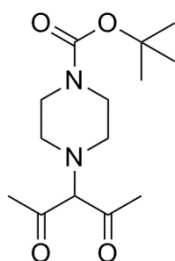
A solution of 3-(1,4-oxazepan-4-yl)pentane-2,4-dione **99** (144 mg, 0.723 mmol) and hydroxylamine hydrochloride (753 mg, 10.8 mmol) in toluene (20 mL) was heated to reflux using Dean Stark apparatus for 29 h. Further portions of hydroxylamine hydrochloride (301 mg, 4.34 mmol) were added at 5 h, 21 h and 27 h. The reaction mixture was allowed to cool and H₂O (40 mL) was added. The mixture was adjusted to approximately pH 7 by the addition of 1 M NaOH (aq, ~4 mL) and was extracted with EtOAc (3 x 30 mL). The combined organics were washed with brine (30 mL), passed through a hydrophobic frit, and the solvent was removed *in vacuo*. The residue was dissolved in 1:1 MeOH:DMSO (9 mL) and purified by MDAP (High pH). The desired fractions were combined and concentrated *in vacuo*, then extracted with DCM (3 x 30 mL). The combined organics were passed through a hydrophobic frit and the solvent was removed *in vacuo* to give the titled compound as an orange oil (19 mg, 13% yield). ν_{\max} (neat): 3503(br.), 2939(w), 2855(w), 1628(w) cm⁻¹; ¹H NMR (400 MHz, CDCl₃) δ = 3.92 (t, *J* = 5.9 Hz, 2H), 3.82 - 3.74 (m, 2H), 3.21 - 3.13 (m, 4H), 2.37 (s, 3H), 2.26 (s, 3H), 1.98 (quin, *J* = 5.9 Hz, 2H); ¹³C NMR (101 MHz, CDCl₃) δ = 161.3, 158.4, 129.6, 71.6, 69.4, 57.7, 53.7, 31.7, 11.2, 10.4; LCMS (High pH): t_R = 0.83 min, [M+H]⁺ = 197, (100% purity); HRMS: (C₁₀H₁₆N₂O₂) [M+H]⁺ requires 197.1285, found [M+H]⁺ 197.1282.

tert*-Butyl 4-(3,5-dimethylisoxazol-4-yl)piperazine-1-carboxylate (64)****a) From dicarbonyl **71*

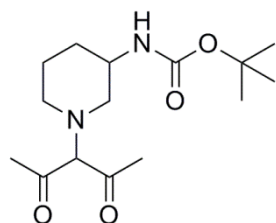
A solution of *tert*-butyl 4-(2,4-dioxopentan-3-yl)piperazine-1-carboxylate **71** (330 mg, 1.16 mmol) and hydroxylamine hydrochloride (1.21 g, 17.4 mmol) in toluene (20 mL) was heated to reflux using Dean Stark apparatus for 19 h. A further portion of hydroxylamine hydrochloride (242 mg, 3.48 mmol) was added after 16 h. The reaction mixture was allowed to cool and the solvent was removed *in vacuo*. The residue was dissolved in H₂O (40 mL). The mixture was adjusted to approximately pH 7 by the addition of 1 M NaOH (aq, ~4 mL) and was extracted with EtOAc (3 x 30 mL). The combined organics were washed with brine (30 mL), passed through a hydrophobic frit, and the solvent removed *in vacuo*. The residue was taken up into 1:1 MeOH:DMSO (4 mL) and purified by reverse phase column chromatography (MeCN + 0.1% HCO₂H in H₂O + 0.1% HCO₂H, 5 → 95%, 60 g C₁₈). The desired fractions were combined and concentrated *in vacuo*. The product was extracted with DCM (6 x 20 mL). The organics were combined, passed through a hydrophobic frit and the solvent was removed *in vacuo* to provide the titled compound as an off-white solid (121 mg, 37% yield). M.pt.: 91–97 °C; ν_{\max} (neat): 2981(w), 2892(w), 2841(w), 1686(s) cm⁻¹; ¹H NMR (400 MHz, DMSO-*d*₆) δ = 3.40 (t, *J* = 4.9 Hz, 4H), 2.87 (t, *J* = 4.9 Hz, 4H), 2.35 (s, 3H), 2.16 (s, 3H), 1.42 (s, 9H); ¹³C NMR (101 MHz, CDCl₃) δ = 161.2, 158.2, 154.7, 127.4, 79.9, 51.7 (4C), 28.4 (3C), 11.5, 10.5; LCMS (Formic): *t*_R = 1.12 min, [M+H]⁺ = 282.46, (100% purity); HRMS: (C₁₄H₂₃N₃O₃) [M+H]⁺ requires 282.1812, found [M+H]⁺ 282.1811.

b) From hydroxydihydroisoxazole **78**

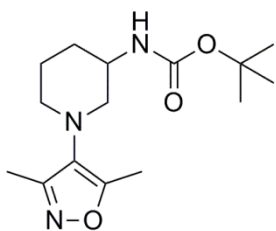
To a solution of *tert*-butyl 4-(5-hydroxy-3,5-dimethyl-4,5-dihydroisoxazol-4-yl)piperazine-1-carboxylate **78** (450 mg, 1.50 mmol) in MeOH (10 mL) was added a solution of Na₂CO₃ (319 mg, 3.01 mmol) in H₂O (10 mL). The resulting solution was heated to reflux for 2 h, under atmospheric conditions. To this was added EtOAc (40 mL) and the organic phase washed with H₂O (20 mL). The aqueous layer was neutralised with 2 M HCl (aq, 1.5 mL) and further extracted with EtOAc (40 mL). The combined organics were passed through a hydrophobic frit and the solvent removed *in vacuo* to give the titled compound as an off-white solid (427 mg, quantitative yield). ¹H NMR (400 MHz, CDCl₃) δ = 3.50 (t, *J* = 4.8 Hz, 4H), 2.90 (t, *J* = 4.8 Hz, 4H), 2.36 (s, 3H), 2.23 (s, 3H), 1.49 (s, 9H); LCMS (High pH): *t*_R = 1.16 min, [M+H]⁺ = 282, (100% purity).

***tert*-Butyl 4-(2,4-dioxopentan-3-yl)piperazine-1-carboxylate (71)**

A solution of *N*-Boc piperazine **63** (3.22 g, 17.3 mmol) in DMF (12 mL) was stirred at RT under a nitrogen atmosphere. 3-Chloro-2,4-pentanedione **70** (839 μ L, 7.43 mmol) was added and the resulting solution stirred at RT for 5 h under a nitrogen atmosphere. At this point NEt_3 (2.5 mL, 18 mmol) and further 3-chloro-2,4-pentanedione **70** (839 μ L, 7.43 mmol) was added and the reaction mixture stirred for a further 17 h. The reaction mixture was poured into H_2O (50 mL) and the resulting mixture extracted with EtOAc (3 x 25 mL). The combined organics were washed with brine (25 mL), and passed through a hydrophobic frit. The solvent was removed *in vacuo* and the residue was taken up into DCM (2 mL) and purified by normal phase column chromatography (EtOAc in cyclohexane, 0 \rightarrow 70%, 120 g SiO_2) to provide the titled compound as an orange gum (3.14 g, 74% yield). NMR analysis indicates that the product exists in equilibrium between keto and enol forms. In $\text{DMSO}-d_6$ the ratio was roughly 1:1. ^1H NMR (400 MHz, $\text{DMSO}-d_6$) δ = 15.93 (s, 0.5H), 4.39 (s, 0.5H), 3.36 (t, J = 4.9 Hz, 2H), 2.80 (t, J = 4.9 Hz, 2H), 2.57 (t, J = 4.9 Hz, 2H), 2.24 - 2.11 (m, 6H), 1.41 (s, 9H), (1 x methylene obscured by H_2O peak); LCMS (Formic): t_{R} = 1.01 min, $[\text{M}+\text{H}]^+$ = 285, (100% purity).

***tert*-Butyl (1-(2,4-dioxopentan-3-yl)piperidin-3-yl)carbamate (73)**

A solution of *tert*-butyl piperidin-3-ylcarbamate **72** (5.00 g, 25.0 mmol) and NEt_3 (4.18 mL, 30.0 mmol) in DMF (25 mL) was stirred at RT under a nitrogen atmosphere. 3-Chloropentane-2,4-dione **70** (3.10 mL, 27.5 mmol) was added and the resulting solution stirred at RT under a nitrogen atmosphere for 22 h. The reaction was poured into H_2O (200 mL) and the resulting mixture extracted with EtOAc (3 x 100 mL). The combined organics were washed with 5% LiCl (aq, 3 x 50 mL) and brine (50 mL), and passed through a hydrophobic frit. The solvent was removed *in vacuo* and the residue was taken up into cyclohexane (5 mL) and purified by normal phase column chromatography (EtOAc in cyclohexane, 0 \rightarrow 70%, 120 g SiO_2) to provide the titled compound as an orange oil (6.91 g, 93% yield). NMR in CDCl_3 showed the product to exist mainly in an enol form. ^1H NMR (400 MHz, CDCl_3) δ = 15.87 (s, 1H), 4.62 (br. s, 1H), 3.69 (br. s, 1H), 3.18 - 3.10 (m, 1H), 2.84 - 2.79 (m, 2H), 2.66 - 2.59 (m, 1H), 2.26 - 2.09 (m, 6H), 1.94 - 1.84 (m, 1H), 1.79 - 1.58 (m, 2H), 1.46 (s, 9H), 1.35 - 1.24 (m, 1H); LCMS (Formic): t_{R} = 0.87 min, $[\text{M}+\text{H}]^+$ = 299, (100% purity).

***tert*-Butyl (1-(3,5-dimethylisoxazol-4-yl)piperidin-3-yl)carbamate (74)**a) *Via* 1,3-dicarbonyl **73**

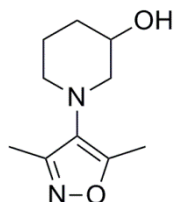
A solution of *tert*-butyl (1-(2,4-dioxopentan-3-yl)piperidin-3-yl)carbamate **73** (6.78 g, 22.7 mmol) and hydroxylamine hydrochloride (15.8 g, 227 mmol) in toluene (90 mL) was heated to reflux using Dean Stark apparatus for 16 h under atmospheric conditions. The reaction mixture was allowed to cool, and was filtered and washed through with EtOAc (3 x 25 mL). The organics were combined and the solvent was removed *in vacuo*. The residue was taken up into DCM (3 mL) and purified by normal phase column chromatography (EtOAc in cyclohexane, 0 → 50%, 80 g SiO₂) to provide a crude residue which was taken up into DMSO (3 mL) and purified by reverse phase column chromatography (MeCN + 0.1% HCO₂H in H₂O + 0.1% HCO₂H, 30 → 85%, 40 g C₁₈) to provide the titled compound as an orange solid (943 mg, 14% yield). M.pt.: 85–90 °C; ν_{\max} (neat): 3355(m), 2933(w), 1677(s) cm⁻¹; ¹H NMR (400 MHz, DMSO-*d*₆) δ = 6.76 (d, *J* = 7.6 Hz, 1H), 3.43 (br. s., 1H), 3.02 - 2.94 (m, 1H), 2.90 - 2.82 (m, 1H), 2.78 - 2.69 (m, 1H), 2.65 - 2.56 (m, 1H), 2.33 (s, 3H), 2.14 (s, 3H), 1.81 - 1.67 (m, 2H), 1.58 - 1.46 (m, 1H), 1.38 (s, 9H), 1.32 - 1.20 (m, 1H); ¹³C NMR (101 MHz, CDCl₃) δ = 160.8, 158.2, 155.2, 127.7, 79.4, 57.7, 52.6, 46.7, 29.5, 28.4 (3C), 23.4, 11.5, 10.5; LCMS (Formic): *t*_R = 1.14 min, [M+H]⁺ = 296, (100% purity); HRMS: (C₁₅H₂₅N₃O₃) [M+H]⁺ requires 296.1969, found [M+H]⁺ 296.1958.

b) Direct from amine **72**

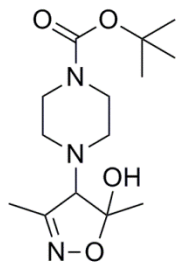
A solution of *tert*-butyl piperidin-3-ylcarbamate **72** (8.50 g, 42.4 mmol) and NEt₃ (7.10 mL, 50.9 mmol) in MeCN (120 mL) was stirred at RT under a nitrogen atmosphere. 3-Chloropentane-2,4-dione **70** (6.70 mL, 59.4 mmol) was added and the resulting solution stirred at RT for 19 h. The solvent was removed *in vacuo* and the residue was taken up into EtOAc (100 mL), filtered, and washed through with EtOAc (3 x 50 mL). The organics were combined and concentrated *in vacuo*. The residue was redissolved in EtOH (150 mL), and hydroxylamine, 50 wt% in H₂O (3.90 mL, 63.7 mmol) was added. The reaction mixture heated to reflux for 8 h, under atmospheric conditions. At this point a solution of Na₂CO₃ (9.0 g, 85 mmol) in H₂O (150 mL) was added and the mixture heated for a further 5 h. The reaction mixture was allowed to cool and was concentrated *in vacuo* before being neutralised with 2 M HCl (aq, ~40 mL) and extracted with EtOAc (3 x 100 mL). The combined organics were passed through a hydrophobic frit, and the solvent was removed *in vacuo*. The residue was taken up into 1:1 MeOH:DMSO (10 mL) and

purified by reverse phase column chromatography (MeCN + 0.1% HCO₂H in H₂O + 0.1% HCO₂H, 10 → 70%, 400 g C₁₈) to provide the titled as an orange gum (6.82 g, 54% yield). LCMS (Formic): t_R = 1.13 min, [M+H]⁺ = 296, (100% purity).

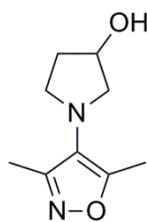
1-(3,5-Dimethylisoxazol-4-yl)piperidin-3-ol (76)



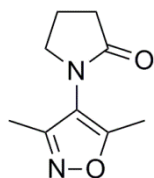
A solution of piperidin-3-ol **75** (2.00 g, 19.8 mmol) and NEt₃ (3.31 mL, 23.7 mmol) in MeCN (75 mL) was stirred at RT under a nitrogen atmosphere. 3-Chloropentane-2,4-dione **70** (3.12 mL, 27.7 mmol) was added and the resulting solution stirred at RT under a nitrogen atmosphere for 19 h. The solvent was removed *in vacuo* and the residue was taken up into EtOAc (50 mL) and filtered. The precipitate was washed with further EtOAc (3 x 25 mL). The organics were combined and the solvent was removed *in vacuo*. The residue was redissolved in EtOH (75 mL), and hydroxylamine, 50 wt% in H₂O (1.82 mL, 29.7 mmol) was added. The reaction mixture heated to reflux for 16 h, under atmospheric conditions. At this point a solution of Na₂CO₃ (4.19 g, 39.5 mmol) in H₂O (75 mL) was added and the mixture heated to reflux for 4 h. The reaction mixture was allowed to cool and was concentrated *in vacuo* before being neutralised with 2 M HCl (aq, ~20 mL) and extracted with EtOAc (3 x 100 mL). The combined organics were washed with brine (50 mL) and passed through a hydrophobic frit, before the solvent was removed *in vacuo*. The residue was taken up into 1:1 MeOH:DMSO (5 mL) and purified by reverse phase column chromatography (MeCN in H₂O + 0.1% (NH₄)₂CO₃, 10 → 50%, 120 g C₁₈) to provide the titled compound as an orange oil (1.19 g, 31% yield). ν_{max} (neat): 3378(br.), 2938(m), 2858(w), 2809(w), 1629(w) cm⁻¹; ¹H NMR (400 MHz, DMSO-*d*₆) δ = 4.69 (d, *J* = 4.6 Hz, 1H), 3.59 - 3.48 (m, 1H), 3.00 (dd, *J* = 3.9, 10.5 Hz, 1H), 2.87 - 2.79 (m, 1H), 2.72 (dt, *J* = 2.4, 10.9 Hz, 1H), 2.59 (t, *J* = 9.7 Hz, 1H), 2.33 (s, 3H), 2.14 (s, 3H), 1.90 - 1.81 (m, 1H), 1.74 - 1.65 (m, 1H), 1.56 - 1.43 (m, 1H), 1.26 - 1.14 (m, 1H); ¹³C NMR (101 MHz, DMSO-*d*₆) δ = 159.9, 158.0, 128.1, 66.7, 60.1, 52.1, 33.3, 24.5, 11.7, 10.4; LCMS (Formic): t_R = 0.71 min, [M+H]⁺ = 197, (100% purity); HRMS: (C₁₀H₁₆N₂O₂) [M+H]⁺ requires 197.1285, found [M+H]⁺ 197.1282.

***tert*-Butyl 4-(5-hydroxy-3,5-dimethyl-4,5-dihydroisoxazol-4-yl)piperazine-1-carboxylate (78)**

A solution of *tert*-butyl piperazine-1-carboxylate **63** (3.00 g, 16.1 mmol) and NEt₃ (2.69 mL, 19.3 mmol) in MeCN (25 mL) was stirred at RT under a nitrogen atmosphere. 3-Chloropentane-2,4-dione **70** (2.55 mL, 22.6 mmol) was added and the resulting solution stirred at RT under a nitrogen atmosphere for 24 h. The solvent was removed *in vacuo* and the residue was taken up into EtOAc (50 mL) and filtered. The precipitate was washed with further EtOAc (3 x 50 mL). The organics were combined and the solvent removed *in vacuo* to give an orange solid. This was dissolved in EtOH (50 mL) and hydroxylamine, 50 wt% in H₂O (1.18 mL, 19.3 mmol) was added. The mixture was heated to 60 °C for 16 h. Another portion of hydroxylamine, 50 wt% in H₂O (1.18 mL, 19.3 mmol) was added and the mixture heated to reflux for a further 3 h. The reaction mixture was allowed to cool and the solvent was removed *in vacuo*. The residue was taken up into EtOAc (100 mL) and washed with H₂O (30 mL) and brine (30 mL). The organic phase was passed through a hydrophobic frit and the solvent was removed *in vacuo*. The residue was taken up into DCM (5 mL) purified by normal phase column chromatography (EtOAc in cyclohexane, 0 → 100%, 24 g SiO₂) to provide a crude residue which was taken up into DMSO (4 mL) and purified by reverse phase column chromatography (MeCN + 0.1% HCO₂H in H₂O + 0.1% HCO₂H, 15 → 55%, 120 g C₁₈) to provide the titled compound as an orange gum (3.03 g, 63% yield). NMR analysis indicated that two isomers were present in a ratio of 4:3. ν_{\max} (neat): 3365(br.), 2977(w), 2930(w), 2860(w), 1692(s), 1670(s) cm⁻¹; Major: ¹H NMR (500 MHz, CD₃CN) δ = 3.56 (s, 1H), 3.48 - 3.32 (m, 4H), 2.93 - 2.51 (m, 4H), 2.02 (s, 3H), 1.49 (s, 3H), 1.44 (s, 9H); ¹³C NMR (126 MHz, CD₃CN) δ = 157.1, 154.5, 105.5, 79.9, 79.0, 49.6 (br. s, 2C), 44.2 (br. s, 2C), 27.5 (3C), 19.5, 13.5; Minor: ¹H NMR (500 MHz, CD₃CN) δ = 3.50 (s, 1H), 3.48 - 3.32 (m, 4H), 2.93 - 2.51 (m, 4H), 2.01 (s, 3H), 1.45 (s, 9H), 1.41 (s, 3H); ¹³C NMR (126 MHz, CD₃CN) δ = 156.1, 154.4, 104.9, 79.1, 75.7, 49.6 (br. s, 2C), 44.2 (br. s, 2C), 27.5 (3C), 19.5, 13.7; LCMS (High pH): t_R = 0.93 min, [M+H]⁺ = 300, (96% purity); HRMS: (C₁₄H₂₅N₃O₄) [M+H]⁺ requires 300.1918, found [M+H]⁺ 300.1907.

1-(3,5-Dimethylisoxazol-4-yl)pyrrolidin-3-ol (83)

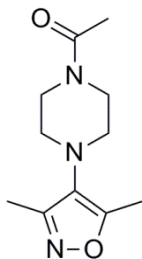
4-Amino-3,5-dimethylisoxazole **46** (200 mg, 1.78 mmol), 1,4-dibromobutan-2-ol **82** (620 μ L, 5.35 mmol), K_2CO_3 (542 mg, 3.92 mmol) and NaI (588 mg, 3.92 mmol) in MeCN (15 mL) were stirred at 85 °C under a nitrogen atmosphere for 24 h. After 16 h further 1,4-dibromobutan-2-ol **82** (620 μ L, 5.35 mmol) was added. The reaction was allowed to cool and Et_2O (50 mL) was added. The mixture was filtered and washed through with Et_2O (2 x 50 mL). The organics were combined and passed through a hydrophobic frit. The solvent was removed *in vacuo* and the residue was taken up into DCM (2 mL) and purified by normal phase column chromatography ($EtOAc$ in cyclohexane, 0 \rightarrow 100%, 24 g SiO_2) to provide the titled compound a brown oil (195 mg, 60% yield). ν_{max} (neat): 3380(br.), 2928(m), 2854(m), 1631(m) cm^{-1} ; 1H NMR (400 MHz, $DMSO-d_6$) δ = 4.85 (d, J = 4.0 Hz, 1H), 4.33 - 4.27 (m, 1H), 3.33 - 3.28 (m, 1H), 3.23 (q, J = 7.7 Hz, 1H), 3.05 (dt, J = 4.5, 8.2 Hz, 1H), 2.92 - 2.87 (m, 1H), 2.35 (s, 3H), 2.17 (s, 3H), 2.04 - 1.95 (m, 1H), 1.77 - 1.68 (m, 1H); ^{13}C NMR (101 MHz, $DMSO-d_6$) δ = 157.9, 157.3, 125.9, 70.1, 60.7, 50.5, 35.3, 11.9, 11.1; LCMS (Formic): t_R = 0.52 min, $[M+H]^+$ = 183, (100% purity); HRMS: ($C_9H_{14}N_2O_2$) $[M+H]^+$ requires 183.1128, found $[M+H]^+$ 183.1127.

1-(3,5-Dimethylisoxazol-4-yl)pyrrolidin-2-one (85)

To a solution of 4-amino-3,5-dimethylisoxazole **46** (500 mg, 4.46 mmol) and NEt_3 (1.24 mL, 8.92 mmol) in THF (10 mL), cooled to 0 °C, was added a solution of 4-chlorobutanoyl chloride **84** (624 μ L, 5.57 mmol) in THF (10 mL). The reaction mixture was allowed to warm to RT and stirred for 16 h, under a nitrogen atmosphere. This mixture was cooled to 0 °C and $tBuOK$, 1 M in THF (12.3 mL, 12.3 mmol) was added. The reaction mixture was allowed to warm to RT and stirred for a further 4 h. The solvent was removed *in vacuo* and the residue was redissolved in $EtOAc$ (100 mL) and H_2O (25 mL) and the layers separated. The aqueous layer was further extracted with DCM (3 x 50 mL) and the combined organics were washed with H_2O (30 mL) and brine (20 mL) before being passed through a hydrophobic frit and the solvent being removed *in vacuo*. The residue was taken up into 1:1 $MeOH:DMSO$ (8 mL) and purified by MDAP (High pH) to provide the titled compound as an orange oil (374 mg, 47% yield). ν_{max} (neat): 2974(w), 1695(s), 1647(m) cm^{-1} ; 1H NMR (400 MHz, $CDCl_3$) δ = 3.65 (t, J = 6.9 Hz, 2H), 2.56 (t, J = 8.0 Hz, 2H), 2.33 (s, 3H), 2.21 (s, 3H), 2.28 - 2.19 (m, 2H); ^{13}C NMR (101 MHz, $CDCl_3$) δ = 174.9, 164.3, 157.5, 115.3, 49.7,

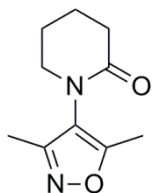
30.5, 19.0, 11.3, 10.1; LCMS (Formic): $t_R = 0.53$ min, $[M+H]^+ = 181$, (100% purity); HRMS: $(C_9H_{12}N_2O_2)$ $[M+H]^+$ requires 181.0972, found $[M+H]^+ 181.0963$.

1-(4-(3,5-Dimethylisoxazol-4-yl)piperazin-1-yl)ethanone (86)



A solution of 3,5-dimethyl-4-(piperazin-1-yl)isoxazole **23** (40 mg, 0.22 mmol) and NEt_3 (77 μ L, 0.55 mmol) in DCM (5 mL) was treated with acetyl chloride (19 μ L, 0.27 mmol), and the reaction mixture stirred at RT for 2 h, before the solvent was removed *in vacuo*. The residue was dissolved in 1:1 MeOH:DMSO (1.6 mL) and purified by MDAP (Formic) to provide the titled compound as a brown oil (39 mg, 79% yield). ν_{max} (neat): 3487(br.), 2925(w), 2827(w), 1627(s) cm^{-1} ; 1H NMR (400 MHz, $DMSO-d_6$) $\delta = 3.58 - 3.44$ (m, 4H), 2.92 (t, $J = 5.0$ Hz, 2H), 2.85 (t, $J = 5.0$ Hz, 2H), 2.35 (s, 3H), 2.17 (s, 3H), 2.03 (s, 3H); 1H NMR (400 MHz, $DMSO-d_6$, 120 $^\circ C$) $\delta = 3.55$ (t, $J = 5.0$ Hz, 4H), 2.93 (t, $J = 5.0$ Hz, 4H), 2.35 (s, 3H), 2.18 (s, 3H), 2.04 (s, 3H); ^{13}C NMR (101 MHz, $DMSO-d_6$) $\delta = 168.7, 160.6, 158.0, 127.5, 51.8, 51.6, 47.0, 42.0, 21.7, 11.7, 10.4$; ^{13}C NMR (101 MHz, $DMSO-d_6$, 120 $^\circ C$) $\delta = 168.8, 160.7, 157.8, 127.5, 51.8$ (4C), 21.3, 11.5, 10.2; LCMS (Formic): $t_R = 0.63$ min, $[M+H]^+ = 224$, (100% purity); HRMS: $(C_{11}H_{17}N_3O_2)$ $[M+H]^+$ requires 224.1394, found $[M+H]^+ 224.1388$.

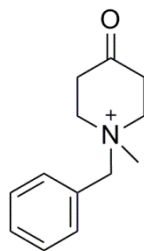
1-(3,5-Dimethylisoxazol-4-yl)piperidin-2-one (89)



To a solution of 4-amino-3,5-dimethylisoxazole **46** (500 mg, 4.46 mmol) and NEt_3 (1.24 mL, 8.92 mmol) in THF (10 mL), cooled to 0 $^\circ C$, was added a solution of 5-chloropentanoyl chloride **88** (720 μ L, 5.57 mmol) in THF (10 mL). The reaction mixture was allowed to warm to RT and stirred, under a nitrogen atmosphere, for 16 h. This mixture was cooled to 0 $^\circ C$ and $tBuOK$, 1 M in THF (12.3 mL, 12.3 mmol) was added. The reaction mixture was allowed to warm to RT and stirred for a further 4 h, under a nitrogen atmosphere. The solvent was removed *in vacuo* and the residue was redissolved in EtOAc (50 mL) and H_2O (50 mL) and the layers separated. The aqueous layer was further extracted with EtOAc (4 x 50 mL) and DCM (2 x 50 mL) and the combined organics were washed with H_2O (30 mL) and brine (20 mL) before being passed through a hydrophobic frit and the solvent being removed *in vacuo*. The residue was taken up into 1:1 MeOH:DMSO (8 mL) and purified by MDAP (High pH) to provide the titled compound as an orange oil (570 mg, 66%

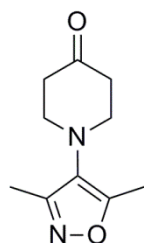
yield). ν_{\max} (neat): 2949(w), 1661(s), 1642(s) cm^{-1} ; $^1\text{H NMR}$ (400 MHz, CDCl_3) δ = 3.49 - 3.44 (m, 2H), 2.59 - 2.54 (m, 2H), 2.31 (s, 3H), 2.18 (s, 3H), 1.99 - 1.93 (m, 4H); $^{13}\text{C NMR}$ (101 MHz, CDCl_3) δ = 170.1, 163.7, 157.7, 119.7, 51.3, 32.5, 23.5, 21.4, 11.0, 9.8; LCMS (Formic): t_{R} = 0.58 min, $[\text{M}+\text{H}]^+$ = 195, (100% purity); HRMS: ($\text{C}_{10}\text{H}_{14}\text{N}_2\text{O}_2$) $[\text{M}+\text{H}]^+$ requires 195.1128, found $[\text{M}+\text{H}]^+$ 195.1119.

***N*-Methyl-*N*-benzyl-4-oxopiperidinium iodide (91)**



MeI (2.00 mL, 32.0 mmol) was slowly added to a solution of *N*-benzylpiperidone **90** (1.50 g, 7.90 mmol) in acetone (10 mL). The mixture was stirred at RT for 4 h in a stoppered flask, at which point further MeI (1.00 mL, 16.0 mmol) was added, and the mixture stirred for a further 24 h. A final portion of MeI was added (3.30 mL, 52.8 mmol) and the reaction mixture sat for 16 h. The product was collected by vacuum filtration and washed with ice-cold acetone (3 x 30 mL). The product was dried under high vacuum to give the titled compound as a white solid (2.41 g, 92% yield). M.pt.: 172–174 °C; ν_{\max} (neat): 2983(w), 2937(w), 1722(s) cm^{-1} ; $^1\text{H NMR}$ (400 MHz, $\text{DMSO}-d_6$) δ = 7.62 - 7.51 (m, 5H), 4.77 (s, 2H), 3.84 - 3.74 (m, 2H), 3.74 - 3.64 (m, 2H), 3.16 (s, 3H), 2.92 - 2.80 (m, 2H), 2.71 (td, J = 4.4, 17.4 Hz, 2H); $^{13}\text{C NMR}$ (101 MHz, $\text{DMSO}-d_6$) δ = 201.5, 133.0 (2C), 130.4, 128.9 (2C), 127.5, 66.5, 57.8 (2C), 46.1, 34.9 (2C); LCMS (High pH): t_{R} = 0.52 min, $[\text{M}]^+$ = 204, $[\text{M}+\text{H}_2\text{O}]^+$ = 222, (100% purity); HRMS: ($\text{C}_{13}\text{H}_{18}\text{NO}$) $[\text{M}+\text{H}_2\text{O}]^+$ requires 222.1494, found $[\text{M}]^+$ 222.1505. Major mass ion is believed to correspond to carbonyl hydrate, which forms under the LC conditions. This is consistent with a published report that compounds of this form exist exclusively as a hemiacetal in MeOH at RT.¹⁸⁹

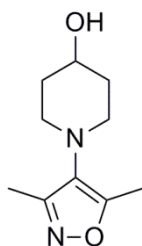
1-(3,5-Dimethylisoxazol-4-yl)piperidin-4-one (95)



4-Amino-3,5-dimethylisoxazole **46** (210 mg, 1.87 mmol) and K_2CO_3 (65 mg, 0.47 mmol) in EtOH (10 mL) and H_2O (10 mL) was stirred at RT for 10 min and then heated to 85 °C. *N*-methyl-*N*-benzyl-4-oxopiperidinium iodide **91** (1.86 g, 5.62 mmol) was added portionwise over 30 min and the reaction heated at 85 °C for 26 h. The reaction mixture was allowed to cool and H_2O (25 mL) was added. The product was extracted with DCM (4 x 25 mL). The extracts were combined and passed through a hydrophobic frit, and the solvent was removed *in vacuo*. The residue was taken up into DCM (5 mL) and purified by normal phase column chromatography (EtOAc in cyclohexane, 0 → 100%, 40 g SiO_2) to provide

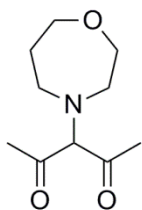
the titled compound as a yellow solid (235 mg, 65% yield). ν_{\max} (CDCl_3): 2964(w), 2821(w), 1715(s), 1635(w) cm^{-1} ; ^1H NMR (400 MHz, CDCl_3) δ = 3.27 (t, J = 6.0 Hz, 4H), 2.55 (t, J = 6.0 Hz, 4H), 2.39 (s, 3H), 2.27 (s, 3H); ^{13}C NMR (101 MHz, CDCl_3) δ = 207.7, 161.2, 158.0, 126.9, 52.1 (2C), 42.4 (2C), 11.5, 10.4; LCMS (Formic): t_{R} = 0.72 min, $[\text{M}+\text{H}]^+$ = 195, (96% purity); HRMS: ($\text{C}_{10}\text{H}_{14}\text{N}_2\text{O}_2$) $[\text{M}+\text{H}]^+$ requires 195.1134, found $[\text{M}+\text{H}]^+$ 195.1140.

1-(3,5-Dimethylisoxazol-4-yl)piperidin-4-ol (96)



To a solution of 1-(3,5-dimethylisoxazol-4-yl)piperidin-4-one **95** (50 mg, 0.26 mmol) and tris(pentafluorophenyl)borane (140 mg, 0.27 mmol) in DCM (2 mL), under a nitrogen atmosphere, was slowly added polymethylhydrosiloxane (350 μL , 0.77 mmol) and the mixture stirred at RT for 1 h. At this point the solvent was removed *in vacuo* and the residue was dissolved in 1:1 MeOH:DMSO (1 mL) and purified by MDAP (Formic). The desired fractions were combined and concentrated *in vacuo* and the product was extracted with DCM (3 x 20 mL). The combined organics were washed with brine (20 mL) and passed through a hydrophobic frit before the solvent was removed *in vacuo* to give the titled compound as an orange oil (26 mg, 52% yield). ν_{\max} (neat): 3380(br.), 2943(m), 2821(w), 1632(w) cm^{-1} ; ^1H NMR (400 MHz, CDCl_3) δ = 3.88 - 3.78 (m, 1H), 3.14 - 3.04 (m, 2H), 2.94 - 2.85 (m, 2H), 2.38 (s, 3H), 2.24 (s, 3H), 2.03 - 1.93 (m, 2H), 1.74 - 1.63 (m, 2H), 1.52 (br. s., 1H); ^{13}C NMR (101 MHz, CDCl_3) δ = 160.5, 158.3, 127.9, 67.4, 49.6 (2C), 35.3 (2C), 11.6, 10.4; LCMS (High pH): t_{R} = 0.64 min, $[\text{M}+\text{H}]^+$ = 197, (100% purity); HRMS: ($\text{C}_{10}\text{H}_{16}\text{N}_2\text{O}_2$) $[\text{M}+\text{H}]^+$ requires 197.1285, found $[\text{M}+\text{H}]^+$ 197.1280.

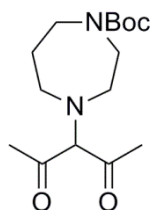
3-(1,4-Oxazepan-4-yl)pentane-2,4-dione (99)



A solution of homomorpholine hydrochloride **98** (360 mg, 2.62 mmol) and NEt_3 (729 μL , 5.23 mmol) in DMF (3 mL) was stirred at RT under a nitrogen atmosphere. 3-Chloropentane-2,4-dione **70** (268 μL , 2.38 mmol) was added and the resulting solution stirred at RT under a nitrogen atmosphere for 19 h. The reaction mixture was poured into H_2O (25 mL) and the resulting mixture extracted with EtOAc (8 x 25 mL). The combined organics were washed with brine (30 mL), and passed through a hydrophobic frit. The solvent was removed *in vacuo* and the residue was taken up into cyclohexane (5 mL) and purified by normal phase column chromatography (EtOAc in cyclohexane, 0 \rightarrow 70%, 80 g SiO_2) to provide the titled compound as an orange oil (176 mg, 37% yield). NMR analysis

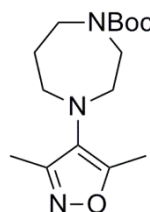
indicated that the product existed in equilibrium between keto and enol forms. In DMSO- d_6 the ratio was roughly 1:3. ^1H NMR (400 MHz, DMSO- d_6) δ = 15.82 (s, 0.75H), 4.58 (s, 0.25H), 3.76 (t, J = 5.4 Hz, 1.5H), 3.70 (t, J = 5.9 Hz, 0.5H), 3.66 - 3.61 (m, 1.5H), 3.56 (t, J = 4.9 Hz, 0.5H), 3.07 - 2.99 (m, 3H), 2.88 - 2.80 (m, 0.5H), 2.51 (quin, J = 1.9 Hz, 0.5H), 2.16 (s, 6H), 1.87 - 1.72 (m, 2H); LCMS (Formic): t_{R} = 0.44 min, $[\text{M}+\text{H}]^+$ = 200, (100% purity).

***tert*-Butyl 4-(2,4-dioxopentan-3-yl)-1,4-diazepane-1-carboxylate (101)**



A solution of 1-Boc-hexahydro-1,4-diazepine **100** (516 μL , 2.62 mmol) and NEt_3 (398 μL , 2.85 mmol) in DMF (3 mL) was stirred at RT under a nitrogen atmosphere. 3-Chloropentane-2,4-dione **70** (268 μL , 2.38 mmol) was added and the resulting solution stirred at RT under a nitrogen atmosphere for 19 h. The reaction was poured into H_2O (25 mL) and the resulting mixture extracted with EtOAc (3 x 20 mL). The combined organics were washed with brine (20 mL) and passed through a hydrophobic frit. The solvent was removed *in vacuo* and the residue was taken up into cyclohexane (5 mL) and purified by normal phase column chromatography (EtOAc in cyclohexane, 0 \rightarrow 70%, 80 g SiO_2) to provide the titled compound as an orange oil (428 mg, 60% yield). NMR analysis indicated that the product existed in equilibrium between keto and enol forms. In DMSO- d_6 the ratio was roughly 1:3. ^1H NMR (400 MHz, DMSO- d_6) δ = 15.81 (s, 0.75H), 4.61 - 4.57 (m, 0.25H), 3.44 - 3.32 (m, 4H), 3.01 - 2.71 (m, 4H), 2.11 (s, 6H), 1.75 - 1.53 (m, 2H), 1.40 (s, 9H); LCMS (Formic): t_{R} = 1.03 min, $[\text{M}+\text{H}]^+$ = 299, (100% purity).

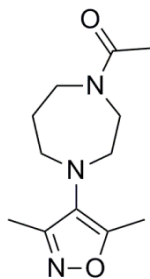
***tert*-Butyl 4-(3,5-dimethylisoxazol-4-yl)-1,4-diazepane-1-carboxylate (102)**



A solution of *tert*-butyl 4-(2,4-dioxopentan-3-yl)-1,4-diazepane-1-carboxylate **101** (2000 mg, 6.70 mmol) and hydroxylamine hydrochloride (6.9 g, 99 mmol) in toluene (40 mL) was heated to reflux using Dean-Stark apparatus for 24 h. Further portions of hydroxylamine hydrochloride were added after 16 h (6.9 g, 99 mmol) and 22 h (1.4 g, 20 mmol). The reaction mixture was allowed to cool to RT, filtered and washed through with toluene (3 x 20 mL) and EtOAc (3 x 20 mL). The organics were combined and the solvent was removed *in vacuo*. The residue was taken up into 1:1 MeOH:DMSO (5 mL) and purified by MDAP (Formic) to provide the titled compound as an orange oil (588 mg, 30% yield). ν_{max} (neat): 2933(w), 2973(w), 1687(s) cm^{-1} ; ^1H NMR (400 MHz, DMSO- d_6 , 120 $^\circ\text{C}$) δ = 3.52 - 3.45 (m, 4H), 3.12 - 3.05 (m, 4H), 2.31 (s, 3H), 2.15 (s, 3H), 1.82 - 1.74 (m, 2H), 1.46 (s, 9H); ^{13}C NMR (101 MHz, DMSO- d_6 , 120 $^\circ\text{C}$) δ = 160.9, 158.0, 155.1, 130.0, 79.0, 55.2,

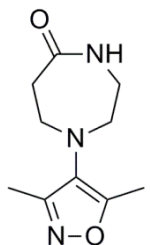
54.7, 48.5, 46.2, 30.0, 28.7 (3C), 11.1, 10.0; LCMS (Formic): t_R = 1.14 min, $[M+H]^+$ = 296, (97% purity); HRMS: ($C_{15}H_{25}N_3O_3$) $[M+H]^+$ requires 296.1969, found $[M+H]^+$ 296.1963.

1-(4-(3,5-Dimethylisoxazol-4-yl)-1,4-diazepan-1-yl)ethanone (103)



A solution of 3,5-dimethyl-4-(3-methylpiperazin-1-yl)isoxazole **26** (72 mg, 0.37 mmol) and NEt_3 (130 μ L, 0.92 mmol) in DCM (3 mL) was treated with acetyl chloride (26 μ L, 0.37 mmol). The reaction mixture was stirred at RT for 3 h, under atmospheric conditions, before the solvent was removed *in vacuo*. The residue was dissolved in 1:1 MeOH:DMSO (1.6 mL) and purified by MDAP (Formic) to provide the titled compound as a colourless oil (51 mg, 84% yield). ν_{max} (neat): 2938(w), 2823(w), 1623(s) cm^{-1} ; 1H NMR (400 MHz, $DMSO-d_6$, 120 $^\circ C$) δ = 3.63 - 3.56 (m, 4H), 3.11 - 3.06 (m, 4H), 2.31 (s, 3H), 2.15 (s, 3H), 2.04 (s, 3H), 1.81 (br. s, 2H); ^{13}C NMR (101 MHz, $DMSO-d_6$, 120 $^\circ C$) δ = 169.6, 161.0, 158.1, 129.9, 54.8, 54.6, 47.9, 47.1, 30.3, 21.5, 11.1, 10.0; LCMS (Formic): t_R = 0.72 min, $[M+H]^+$ = 238, (100% purity); HRMS: ($C_{12}H_{19}N_3O_2$) $[M+H]^+$ requires 238.1550, found $[M+H]^+$ 238.1547.

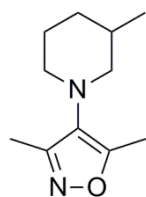
1-(3,5-Dimethylisoxazol-4-yl)-1,4-diazepan-5-one (104)



1-(3,5-Dimethylisoxazol-4-yl)piperidin-4-one **95** (118 mg, 0.608 mmol) was dissolved in EtOH (2 mL). Hydroxylamine hydrochloride (84 mg, 1.2 mmol) and NaOAc (100 mg, 1.215 mmol) were added, and the mixture was stirred at 100 $^\circ C$ under atmospheric conditions for 6 h before being allowed to cool to RT. The reaction mixture was filtered and washed through with EtOH (3 x 2 mL), and the filtrate was concentrated *in vacuo*. H_2O (10 mL) was added, and the mixture was extracted with EtOAc (3 x 25 mL). The combined organics were washed with sat. $NaHCO_3$ (aq, 10 mL) and brine (10 mL), before being passed through a hydrophobic frit. The solvent was removed *in vacuo* and the residue was dissolved in acetone (2 mL) and was treated with Na_2CO_3 (193 mg, 1.82 mmol) in H_2O (4 mL), and the mixture stirred at RT for 5 min. A solution of tosyl chloride (174 mg, 0.911 mmol) in acetone (2 mL) was slowly added, and the mixture stirred at RT under atmospheric conditions for 4 h. The reaction mixture was concentrated *in vacuo*, and partitioned between H_2O (20 mL) and DCM (20 mL). The aqueous phase was further extracted with DCM (2 x 20 mL), and the combined extracts were washed with brine (40 mL) and passed through a hydrophobic frit. The solvent was removed *in vacuo* and the residue taken up into DCM (1 mL) and purified by normal phase column chromatography

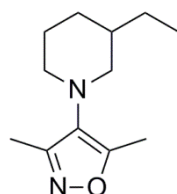
(TBME in cyclohexane, 0 → 100%, MeOH in TBME, 0 → 20%, 12 g SiO₂) to provide the titled compound as a white solid (75 mg, 59% yield). M.pt.: 143–146 °C; ν_{\max} (neat): 3207(w), 2823(w), 1674(s) cm⁻¹; ¹H NMR (400 MHz, CDCl₃) δ = 6.29 (br. s., 1H), 3.43 - 3.37 (m, 2H), 3.18 - 3.06 (m, 4H), 2.76 - 2.71 (m, 2H), 2.37 (s, 3H), 2.25 (s, 3H); ¹³C NMR (101 MHz, CDCl₃) δ = 177.3, 161.6, 158.0, 128.9, 56.8, 50.4, 44.2, 39.7, 11.3, 10.4; LCMS (High pH): t_R = 0.58 min, [M+H]⁺ = 210, (99% purity); HRMS: (C₁₀H₁₅N₃O₂) [M+H]⁺ requires 210.1237, found [M+H]⁺ 210.1236.

3,5-Dimethyl-4-(3-methylpiperidin-1-yl)isoxazole (105)



A solution of 1-(3,5-dimethylisoxazol-4-yl)-3-methylpiperidin-4-one **113** (156 mg, 0.749 mmol) and tosylhydrazide (209 mg, 1.12 mmol) in MeOH (4 mL) was stirred at RT for 2 h under a nitrogen atmosphere. To this was added a solution of ZnCl₂, 1.9 M in 2-MeTHF (300 μ L, 0.56 mmol) and NaBH₃CN (71 mg, 1.1 mmol) in MeOH (2 mL). The reaction mixture was heated to reflux under a nitrogen atmosphere for 17 h before being allowed to cool. The reaction mixture was diluted with EtOAc (20 mL) and washed with H₂O (20 mL), sat. NaHCO₃ (aq, 20 mL) and brine (20 mL) before being passed through a hydrophobic frit and the solvent being removed *in vacuo*. The residue was taken up into DCM (1 mL) and purified by normal phase column chromatography (EtOAc in cyclohexane, 0 → 50%, 12 g SiO₂) to provide the titled compound as a yellow oil (103 mg, 71% yield). ν_{\max} (neat): 2928(m), 2851(w), 2804(w), 1728(w), 1627(w) cm⁻¹; ¹H NMR (400 MHz, CDCl₃) δ = 2.97 - 2.89 (m, 2H), 2.84 - 2.74 (m, 1H), 2.53 - 2.44 (m, 1H), 2.37 (s, 3H), 2.23 (s, 3H), 1.80 - 1.59 (m, 4H), 1.06 - 0.95 (m, 1H), 0.92 (d, J = 6.6 Hz, 3H); ¹³C NMR (101 MHz, CDCl₃) δ = 160.3, 158.5, 128.4, 60.4, 52.7, 32.6, 31.8, 26.1, 19.2, 11.6, 10.4; LCMS (Formic): t_R = 1.19 min, [M+H]⁺ = 195, (100% purity); HRMS: (C₁₁H₁₈N₂O) [M+H]⁺ requires 195.1492, found [M+H]⁺ 195.1484.

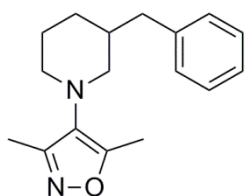
4-(3-Ethylpiperidin-1-yl)-3,5-dimethylisoxazole (106)



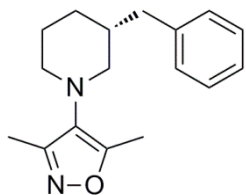
A solution of 1-(3,5-dimethylisoxazol-4-yl)-3-ethylpiperidin-4-one **121** (130 mg, 0.585 mmol) and tosylhydrazide (163 mg, 0.877 mmol) in MeOH (4 mL) was stirred at RT for 2 h under a nitrogen atmosphere. To this was added a solution of ZnCl₂, 1.9 M in 2-MeTHF (230 μ L, 0.44 mmol) and NaBH₃CN (55 mg, 0.88 mmol) in MeOH (2 mL). The reaction mixture was heated to reflux under a nitrogen atmosphere for 17 h before being allowed to cool. The reaction mixture was diluted with EtOAc (20 mL) and washed with H₂O (20 mL), 0.1 M NaOH (aq, 20 mL), sat. NaHCO₃ (aq, 20 mL) and brine (20 mL) before being passed

through a hydrophobic frit and the solvent being removed *in vacuo*. The residue was taken up into DCM (1 mL) and purified by normal phase column chromatography (EtOAc in cyclohexane, 0 → 50%, 12 g SiO₂) to provide the titled compound as a colourless oil (84 mg, 69% yield). ν_{\max} (neat): 2931(s), 2854(m), 2802(w), 1726(w), 1691(w), 1629(w) cm⁻¹; ¹H NMR (400 MHz, CDCl₃) δ = 3.01 - 2.91 (m, 2H), 2.81 (dt, J = 2.9, 10.9 Hz, 1H), 2.50 (dd, J = 9.8, 10.8 Hz, 1H), 2.37 (s, 3H), 2.24 (s, 3H), 1.87 - 1.80 (m, 1H), 1.76 - 1.68 (m, 1H), 1.67 - 1.58 (m, 1H), 1.57 - 1.46 (m, 1H), 1.33 - 1.24 (m, 2H), 1.05 - 0.95 (m, 1H), 0.92 (t, J = 7.5 Hz, 3H); ¹³C NMR (101 MHz, CDCl₃) δ = 160.2, 158.5, 128.5, 58.6, 53.0, 38.6, 30.3, 26.8, 26.1, 11.6, 11.4, 10.5; LCMS (High pH): t_R = 1.34 min, [M+H]⁺ = 209, (98% purity); HRMS: (C₁₂H₂₀N₂O) [M+H]⁺ requires 209.1648, found [M+H]⁺ 209.1644.

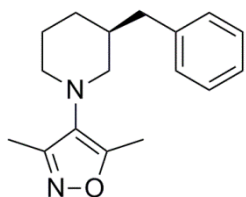
4-(3-Benzylpiperidin-1-yl)-3,5-dimethylisoxazole (107)



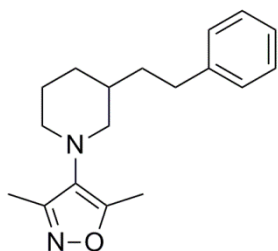
A solution of 3-benzyl-1-(3,5-dimethylisoxazol-4-yl)piperidin-4-one **114** (160 mg, 0.563 mmol) and tosylhydrazide (157 mg, 0.844 mmol) in MeOH (4 mL) was stirred at RT for 2 h under a nitrogen atmosphere. To this was added a solution of ZnCl₂, 1.9 M in 2-MeTHF (220 μ L, 0.42 mmol) and NaBH₃CN (53 mg, 0.84 mmol) in MeOH (2 mL). The reaction mixture was heated to reflux under a nitrogen atmosphere for 5 h before being allowed to cool to RT. The reaction mixture was diluted with EtOAc (20 mL) and washed with H₂O (20 mL), 0.1 M NaOH (aq, 20 mL), sat. NaHCO₃ (aq, 20 mL) and brine (20 mL) before being passed through a hydrophobic frit and the solvent being removed *in vacuo*. The residue was taken up into 1:1 MeOH:DMSO and purified by MDAP (High pH). The desired fractions were combined and concentrated under a stream on nitrogen. The product was extracted with DCM (3 x 25 mL) and the combined organics were passed through a hydrophobic frit before the solvent was removed *in vacuo*, to give the titled compound as a colourless oil (89 mg, 59% yield). ν_{\max} (neat): 3026(w), 2929(m), 2850(w), 2803(w), 1630(w), 1603(w) cm⁻¹; ¹H NMR (400 MHz, CDCl₃) δ = 7.32 - 7.26 (m, 2H), 7.24 - 7.14 (m, 3H), 2.97 - 2.91 (m, 2H), 2.83 (dt, J = 2.7, 10.8 Hz, 1H), 2.65 - 2.51 (m, 3H), 2.35 (s, 3H), 2.19 (s, 3H), 1.99 - 1.88 (m, 1H), 1.84 - 1.71 (m, 2H), 1.65 - 1.57 (m, 1H), 1.16 - 1.05 (m, 1H); ¹³C NMR (101 MHz, CDCl₃) δ = 160.2, 158.4, 140.3, 129.0 (2C), 128.4, 128.3 (2C), 125.9, 58.3, 53.0, 40.5, 38.7, 30.4, 25.9, 11.6, 10.5; LCMS (High pH): t_R = 1.41 min, [M+H]⁺ = 271, (100% purity); HRMS: (C₁₇H₂₂N₂O) [M+H]⁺ requires 271.1805, found [M+H]⁺ 271.1804.

(-)-4-(3-Benzylpiperidin-1-yl)-3,5-dimethylisoxazole ((-)-107)

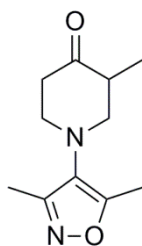
4-(3-Benzylpiperidin-1-yl)-3,5-dimethylisoxazole **107** (192 mg) was dissolved in EtOH and separated on a 30 mm x 25 cm Chiralcel OJ-H (5 μ m) column, eluting with 5% EtOH in heptane to provide the (+)-enantiomer **(+)-107** (see below) and the titled compound as a colourless oil (80 mg). Configuration has been assigned by comparison of biological assay and crystallographic data. e.e. = 99.5%; $[\alpha]_D^{25}$ -32.1° (c 0.50, CDCl_3); ν_{max} (neat): 3026(w), 2929(m), 2850(w), 2803(w), 1629(w), 1603(w) cm^{-1} ; ^1H NMR (400 MHz, CDCl_3) δ = 7.33 - 7.27 (m, 2H), 7.24 - 7.15 (m, 3H), 2.98 - 2.91 (m, 2H), 2.83 (dt, J = 2.5, 11.1 Hz, 1H), 2.62 - 2.55 (m, 3H), 2.36 (s, 3H), 2.20 (s, 3H), 2.00 - 1.89 (m, 1H), 1.84 - 1.71 (m, 2H), 1.68 - 1.55 (m, 1H), 1.16 - 1.05 (m, 1H); ^{13}C NMR (101 MHz, CDCl_3) δ = 160.2, 158.3, 140.2, 129.0 (2C), 128.3 (2C), 125.9, 58.3, 53.0, 40.5, 38.7, 30.4, 25.9, 11.6, 10.5. Quaternary ^{13}C peak, seen at 128.4 ppm in racemate **107**, not observed in this sample; LCMS (Formic): t_{R} = 1.43 min, $[\text{M}+\text{H}]^+$ = 271, (100% purity); HRMS: ($\text{C}_{17}\text{H}_{22}\text{N}_2\text{O}$) $[\text{M}+\text{H}]^+$ requires 271.1810, found $[\text{M}+\text{H}]^+$ 271.1821.

(+)-4-(3-Benzylpiperidin-1-yl)-3,5-dimethylisoxazole ((+)-107)

The titled compound was isolated as per the above protocol, as a colourless oil (74 mg). Configuration has been assigned by comparison of biological assay and crystallographic data. e.e. = 98.6%; $[\alpha]_D^{25}$ $+40.1^\circ$ (c 0.50, CDCl_3); ν_{max} (neat): 3026(w), 2929(m), 2850(w), 2802(w), 1629(w), 1603(w) cm^{-1} ; ^1H NMR (400 MHz, CDCl_3) δ = 7.33 - 7.27 (m, 2H), 7.24 - 7.14 (m, 3H), 2.98 - 2.91 (m, 2H), 2.83 (dt, J = 2.4, 11.1 Hz, 1H), 2.62 - 2.55 (m, 3H), 2.35 (s, 3H), 2.19 (s, 3H), 2.00 - 1.88 (m, 1H), 1.84 - 1.71 (m, 2H), 1.67 - 1.55 (m, 1H), 1.16 - 1.05 (m, 1H); ^{13}C NMR (101 MHz, CDCl_3) δ = 160.2, 158.4, 140.3, 128.9 (2C), 128.3 (2C), 125.9, 58.3, 53.0, 40.5, 38.7, 30.4, 25.9, 11.6, 10.5. Quaternary ^{13}C peak, seen at 128.4 ppm in racemate **107**, not observed in this sample; LCMS (Formic): t_{R} = 1.42 min, $[\text{M}+\text{H}]^+$ = 271, (100% purity); HRMS: ($\text{C}_{17}\text{H}_{22}\text{N}_2\text{O}$) $[\text{M}+\text{H}]^+$ requires 271.1810, found $[\text{M}+\text{H}]^+$ 271.1821.

3,5-Dimethyl-4-(3-phenethylpiperidin-1-yl)isoxazole (108)

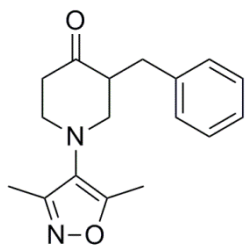
A solution of 1-(3,5-dimethylisoxazol-4-yl)-3-phenethylpiperidin-4-one **115** (67 mg, 0.23 mmol) and tosylhydrazide (63 mg, 0.34 mmol) in MeOH (4 mL) was stirred at RT for 2 h under a nitrogen atmosphere. To this was added a solution of ZnCl₂, 1.9 M in 2-MeTHF (89 μL, 0.17 mmol) and NaBH₃CN (21 mg, 0.34 mmol) in MeOH (2 mL). The reaction mixture was heated to reflux under a nitrogen atmosphere for 17 h before being allowed to cool to RT. The reaction mixture was diluted with EtOAc (20 mL) and washed with H₂O (20 mL), sat. NaHCO₃ (aq, 20 mL) and brine (20 mL) before being passed through a hydrophobic frit and the solvent being removed *in vacuo*. The residue was taken up into 1:1 MeOH:DMSO (1 mL) and purified by MDAP (High pH). The desired fractions were combined and concentrated *in vacuo*, and the product was extracted with DCM (3 x 15 mL). The combined organics were washed with brine (15 mL) and passed through a hydrophobic frit, before the solvent was removed *in vacuo* to give the titled compound as a colourless oil (13 mg, 20% yield). ν_{\max} (neat): 3026(w), 2926(m), 2852(w), 1688(w), 1640(w), 1603(w) cm⁻¹; ¹H NMR (400 MHz, CDCl₃) δ = 7.34 - 7.27 (m, 2H), 7.24 - 7.18 (m, 3H), 3.05 - 2.99 (m, 1H), 2.98 - 2.91 (m, 1H), 2.83 (dt, J = 2.9, 10.9 Hz, 1H), 2.70 - 2.61 (m, 2H), 2.57 (dd, J = 9.3, 10.9 Hz, 1H), 2.37 (s, 3H), 2.24 (s, 3H), 1.92 - 1.84 (m, 1H), 1.79 - 1.54 (m, 5H), 1.14 - 1.03 (m, 1H); ¹³C NMR (101 MHz, CDCl₃) δ = 160.4, 158.5, 142.5, 128.4, 128.3 (2C), 128.3 (2C), 125.8, 58.7, 53.0, 36.5, 35.8, 33.2, 30.6, 25.9, 11.6, 10.5; LCMS (High pH): t_R = 1.48 min, [M+H]⁺ = 285, (98% purity); HRMS: (C₁₈H₂₄N₂O) [M+H]⁺ requires 285.1961, found [M+H]⁺ 285.1965.

1-(3,5-Dimethylisoxazol-4-yl)-3-methylpiperidin-4-one (113)

MeI (2.00 mL, 32.0 mmol) was slowly added to a solution of 1-benzyl-3-methylpiperidin-4-one **112** (1.65 g, 8.12 mmol) in acetone (10 mL) and the reaction mixture stirred in a stoppered flask for 2 days. The solvent was removed *in vacuo* and the resulting solid was redissolved in EtOH (10 mL) and H₂O (10 mL). To this was added 4-amino-3,5-dimethylisoxazole **46** (320 mg, 2.85 mmol) and K₂CO₃ (99 mg, 0.71 mmol) and the reaction mixture was heated to 90 °C for 24 h. The reaction mixture was allowed to cool and water (30 mL)

was added. The product was extracted with DCM (3 x 25 mL). The extracts were combined and passed through a hydrophobic frit, and the solvent was removed *in vacuo*. The residue was taken up into DCM (6 mL) and purified by normal phase column chromatography (EtOAc in cyclohexane, 0 → 100%, 80 g SiO₂) to provide the titled compound as an orange oil (487 mg, 82% yield). ν_{\max} (neat): 2969(w), 2933(w), 2816(w) cm⁻¹; ¹H NMR (400 MHz, CDCl₃) δ = 3.35 - 3.24 (m, 3H), 2.96 (dd, J = 10.3, 11.0 Hz, 1H), 2.80 - 2.62 (m, 2H), 2.48 (td, J = 3.4, 13.9 Hz, 1H), 2.40 (s, 3H), 2.28 (s, 3H), 1.09 (d, J = 6.6 Hz, 3H); ¹³C NMR (101 MHz, CDCl₃) δ = 209.7, 161.3, 158.0, 126.8, 59.5, 52.8, 45.7, 41.9, 11.9, 11.5, 10.5; LCMS (High pH): t_R = 0.83 min, [M+H]⁺ = 209, (100% purity); HRMS: (C₁₁H₁₆N₂O₂) [M+H]⁺ requires 209.1285, found [M+H]⁺ 209.1284.

3-Benzyl-1-(3,5-dimethylisoxazol-4-yl)piperidin-4-one (114)



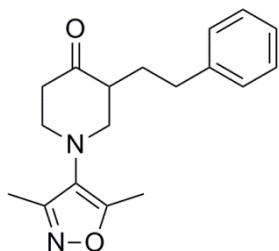
a) From piperidinone **95**

1-(3,5-Dimethylisoxazol-4-yl)piperidin-4-one **95** (189 mg, 0.973 mmol) was dissolved in THF (2 mL) and cooled to 0 °C under a nitrogen atmosphere. LiHMDS, 1.0 M in THF (1.2 mL, 1.2 mmol) was added and the mixture stirred at 0 °C for 1 h. To this was added benzyl bromide (139 μ L, 1.17 mmol) in THF (2 mL) and the reaction was stirred at 0 °C for 2 h before being allowed to warm to RT. The reaction mixture was partitioned between 1 M NH₄Cl (aq, 10 mL) and EtOAc (30 mL). The aqueous phase was washed with EtOAc (30 mL), and the combined organics were washed with brine (15 mL), passed through a hydrophobic frit, and the solvent was removed *in vacuo*. The residue was dissolved in 1:1 MeOH:DMSO (0.6 mL) and purified by MDAP (Formic). The desired fractions were combined and concentrated *in vacuo*, before the product was extracted with DCM (3 x 20 mL). The combined organics were passed through a hydrophobic frit and the solvent was removed *in vacuo* to give the titled compound as a colourless oil (56 mg, 20% yield). ν_{\max} (neat): 3027(w), 2962(w), 2925(w), 2817(w), 1712(s), 1634(w), 1604(w) cm⁻¹; ¹H NMR (400 MHz, CDCl₃) δ = 7.31 - 7.14 (m, 5H), 3.29 - 3.20 (m, 2H), 3.15 - 3.05 (m, 2H), 3.02 - 2.95 (m, 1H), 2.94 - 2.84 (m, 1H), 2.73 - 2.59 (m, 1H), 2.55 (s, 1H), 2.42 (td, J = 4.0, 13.9 Hz, 1H), 2.33 (s, 3H), 2.13 (s, 3H); ¹³C NMR (101 MHz, DMSO-*d*₆) δ = 209.0, 160.5, 157.9, 140.0, 129.3 (2C), 128.7 (2C), 127.2, 126.5, 56.7, 52.4, 52.2, 41.9, 33.2, 11.6, 10.3; LCMS (Formic) t_R = 1.14 min, [M+H]⁺ = 285, (100% purity); HRMS: (C₁₇H₂₀N₂O₂) [M+H]⁺ requires 285.1598, found [M+H]⁺ 285.1598.

b) From benzylated β -keto ester **122**

Methyl 3-benzyl-1-(3,5-dimethylisoxazol-4-yl)-4-oxopiperidine-3-carboxylate **122** (1.90 g, 5.55 mmol), LiCl (235 mg, 5.55 mmol), and H₂O (2.75 mL, 153 mmol) were mixed in DMSO (27 mL) and heated to 160 °C for 10 h under atmospheric conditions. The reaction mixture was allowed to cool and was concentrated under a stream of nitrogen overnight. The residue was partitioned between H₂O (400 mL) and Et₂O (100 mL). The aqueous phase was further extracted with Et₂O (3 x 100 mL) and the combined organics were washed with H₂O (2 x 50 mL) and brine (2 x 50 mL) before being passed through a hydrophobic frit. The solvent was removed *in vacuo* and the residue was taken up into DCM (3 mL) and purified by normal phase column chromatography (EtOAc in cyclohexane, 0 → 30%, 40 g SiO₂) to provide the titled compound as an orange oil (487 mg, 31% yield). LCMS (Formic): t_R = 1.15 min, [M+H]⁺ = 285, (92% purity).

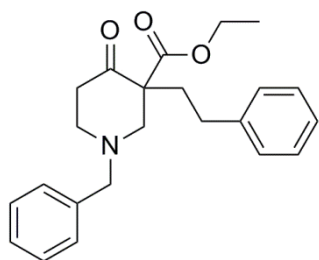
1-(3,5-Dimethylisoxazol-4-yl)-3-phenethylpiperidin-4-one (**115**)



MeI (368 μ L, 5.89 mmol) was slowly added to a solution of 1-benzyl-3-phenethylpiperidin-4-one **118** (400 mg, 1.36 mmol) in acetone (5 mL) and the reaction mixture stirred in a stoppered flask at RT for 22 h. Further portions of MeI (92 μ L, 1.5 mmol) were added after 4 h, 5 h and 6 h. The solvent was removed *in vacuo* and the resulting yellow solid was redissolved in EtOH (3 mL) and H₂O (3 mL). To this was added 4-amino-3,5-dimethylisoxazole **46** (55 mg, 0.49 mmol) and K₂CO₃ (17 mg, 0.12 mmol), and the reaction mixture stirred at 90 °C for 22 h, before being allowed to cool. H₂O (20 mL) was added and the product extracted with DCM (3 x 20 mL). The combined organics were washed with brine (20 mL) and passed through a hydrophobic frit, before the solvent was removed *in vacuo*. The residue was dissolved in 1:1 MeOH:DMSO (2 mL) and purified by MDAP (Formic). The desired fractions were combined and concentrated *in vacuo*. The product was extracted with DCM (5 x 20 mL). The combined organics were washed with brine (20 mL), passed through a hydrophobic frit, and the solvent was removed *in vacuo* to give the titled compound as a yellow oil (103 mg, 70% yield). ν_{\max} (neat): 3027(w), 2927(w), 2817(w), 1711(s), 1632(w), 1603(w) cm⁻¹; ¹H NMR (400 MHz, CDCl₃) δ = 7.34 - 7.28 (m, 2H), 7.25 - 7.17 (m, 3H), 3.37 - 3.31 (m, 1H), 3.31 - 3.26 (m, 2H), 3.00 (dd, J = 9.2, 11.1 Hz, 1H), 2.70 - 2.57 (m, 4H), 2.52 (td, J = 4.4, 13.9 Hz, 1H), 2.39 (s, 3H), 2.32 - 2.18 (m, 4H), 1.70 - 1.57 (m, 1H); ¹³C NMR (101 MHz, CDCl₃) δ = 209.4, 161.3, 158.0, 141.4, 128.5 (2C), 128.3 (2C), 126.8, 126.1, 57.8, 52.8, 50.4, 42.0, 33.2, 28.9, 11.5, 10.5; LCMS (High pH): t_R = 1.21 min, [M+H]⁺ = 299,

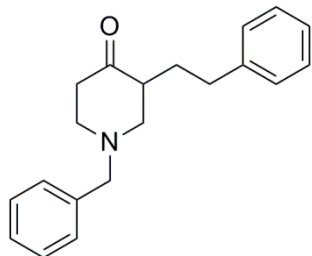
(100% purity); HRMS: (C₁₈H₂₂N₂O₂) [M+H]⁺ requires 299.1754, found [M+H]⁺ 299.1756.

Ethyl 1-benzyl-4-oxo-3-phenethylpiperidine-3-carboxylate (117)



Ethyl 1-benzyl-4-oxopiperidine-3-carboxylate hydrochloride **116** (750 mg, 2.52 mmol) and K₂CO₃ (1.74 g, 12.6 mmol) were suspended in acetone (15 mL) and stirred at RT for 30 min and heated to reflux for a further 30 min. At this point phenethyl iodide (1.09 mL, 7.56 mmol) was added and the reaction mixture heated to reflux for 28 h, before being allowed to cool. The reaction mixture was filtered and the solvent removed *in vacuo*. The residue was partitioned between H₂O (20 mL) and DCM (20 mL). The aqueous phase was further extracted with DCM (20 mL) and the combined organics were washed with brine (20 mL), passed through a hydrophobic frit and the solvent was removed *in vacuo*. The residue was taken up into DCM (4 mL) and purified by normal phase column chromatography (EtOAc in cyclohexane, 0 → 30%, 120 g SiO₂) to provide the titled compound as a colourless oil (668 mg, 73% yield). ν_{\max} (neat): 3028(w), 2962(w), 2807(w), 1716(s), 1603(w) cm⁻¹; ¹H NMR (400 MHz, CDCl₃) δ = 7.39 - 7.25 (m, 7H), 7.23 - 7.17 (m, 3H), 4.30 (qd, *J* = 7.1, 10.8 Hz, 1H), 4.22 (qd, *J* = 7.1, 10.8 Hz, 1H), 3.62 (s, 2H), 3.46 (dd, *J* = 2.7, 11.5 Hz, 1H), 3.09 - 3.01 (m, 1H), 3.00 - 2.89 (m, 1H), 2.76 (dt, *J* = 4.6, 12.8 Hz, 1H), 2.52 - 2.36 (m, 3H), 2.31 (d, *J* = 11.5 Hz, 1H), 2.15 - 2.05 (m, 1H), 1.90 - 1.80 (m, 1H), 1.30 (t, *J* = 7.1 Hz, 3H); ¹³C NMR (101 MHz, CDCl₃) δ = 206.3, 171.6, 141.9, 137.9, 128.8 (2C), 128.4 (4C), 128.3 (2C), 127.3, 125.9, 61.9, 61.2 (2C), 61.2, 53.7, 40.6, 34.3, 31.0, 14.2; LCMS (High pH): *t*_R = 1.46 min, [M+H]⁺ = 366, (99% purity); HRMS: (C₂₃H₂₇NO₃) [M+H]⁺ requires 366.2064, found [M+H]⁺ 366.2065.

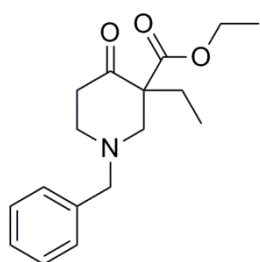
1-Benzyl-3-phenethylpiperidin-4-one (118)



Ethyl 1-benzyl-4-oxo-3-phenethylpiperidine-3-carboxylate **117** (620 mg, 1.70 mmol) was dissolved in MeOH (15 mL). 2 M NaOH (aq, 2.00 mL, 4.00 mmol) was added and the mixture was heated to reflux for 6 h. The solution was allowed to cool and 2 M HCl (aq, 2.00 mL, 4.00 mmol) was added. The reaction mixture was concentrated *in vacuo*. H₂O (20 mL) was added and the product was extracted with DCM (3 x 20 mL). The combined organics were washed with brine (20 mL), passed through a hydrophobic frit, and the solvent was removed *in vacuo*. The residue was taken up into DCM (5 mL) and purified by normal phase column chromatography (EtOAc in cyclohexane, 0 → 30%, 12 g SiO₂) to provide the titled

compound as a colourless oil (174 mg, 35% yield). ν_{\max} (neat): 3027(w), 2915(w), 2801(w), 1712(s), 1603(w) cm^{-1} ; $^1\text{H NMR}$ (400 MHz, CDCl_3) δ = 7.40 - 7.26 (m, 7H), 7.23 - 7.13 (m, 3H), 3.66 (d, J = 13.2 Hz, 1H), 3.60 (d, J = 13.2 Hz, 1H), 3.10 - 2.97 (m, 2H), 2.64 - 2.49 (m, 5H), 2.47 - 2.37 (m, 1H), 2.29 (dd, J = 9.8, 11.0 Hz, 1H), 2.21 - 2.11 (m, 1H), 1.62 - 1.52 (m, 1H); $^{13}\text{C NMR}$ (101 MHz, CDCl_3) δ = 210.8, 141.8, 138.2, 128.9 (2C), 128.4 (4C), 128.4 (2C), 127.3, 125.9, 61.9, 58.6, 53.8, 49.0, 41.0, 33.2, 29.2; LCMS (High pH): t_{R} = 1.36 min, $[\text{M}+\text{H}]^+$ = 294, (100% purity); HRMS: ($\text{C}_{20}\text{H}_{23}\text{NO}$) $[\text{M}+\text{H}]^+$ requires 294.1852, found $[\text{M}+\text{H}]^+$ 294.1852.

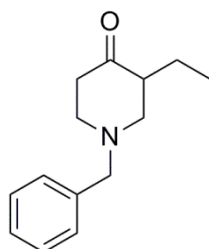
Ethyl 1-benzyl-3-ethyl-4-oxopiperidine-3-carboxylate (119)



A slurry of ethyl 1-benzyl-4-oxopiperidine-3-carboxylate hydrochloride **116** (1.55 g, 5.21 mmol) and K_2CO_3 (3.50 g, 25.3 mmol) in acetone (30 mL) was stirred for 1 h at RT and 1 h at reflux. At this point EtI (1.255 mL, 15.62 mmol) was added and the solution heated to reflux for 16 h before being allowed to cool.

The reaction mixture was filtered and the solvent removed *in vacuo*. The residue was partitioned between H_2O (20 mL) and DCM (20 mL). The aqueous phase was further extracted with DCM (20 mL). The combined organics were washed with brine (20 mL) and passed through a hydrophobic frit, before the solvent was removed *in vacuo*. The residue was taken up into DCM (4 mL) and purified by normal phase column chromatography (EtOAc in cyclohexane, 0 \rightarrow 30%, 120 g SiO_2) to provide the titled compound as a colourless oil (1.15 g, 76% yield). ν_{\max} (neat): 2968(w), 2807(w), 1715(s) cm^{-1} ; $^1\text{H NMR}$ (400 MHz, CDCl_3) δ = 7.40 - 7.26 (m, 5H), 4.33 - 4.16 (m, 2H), 3.66 - 3.55 (m, 2H), 3.43 (dd, J = 2.7, 11.5 Hz, 1H), 3.07 - 2.98 (m, 1H), 2.94 - 2.84 (m, 1H), 2.49 - 2.36 (m, 2H), 2.24 (d, J = 11.5 Hz, 1H), 1.93 - 1.83 (m, 1H), 1.66 - 1.54 (m, 1H), 1.28 (t, J = 7.1 Hz, 3H), 0.89 (t, J = 7.5 Hz, 3H); $^{13}\text{C NMR}$ (101 MHz, CDCl_3) δ = 206.5, 171.6, 138.0, 128.8 (2C), 128.3 (2C), 127.3, 61.9, 61.5, 61.1 (2C), 53.6, 40.7, 25.2, 14.2, 9.1; LCMS (High pH): t_{R} = 1.29 min, $[\text{M}+\text{H}]^+$ = 290, (100% purity); HRMS: ($\text{C}_{17}\text{H}_{23}\text{NO}_3$) $[\text{M}+\text{H}]^+$ requires 290.1751, found $[\text{M}+\text{H}]^+$ 290.1760.

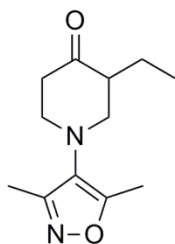
1-Benzyl-3-ethylpiperidin-4-one (120)



Ethyl 1-benzyl-3-ethyl-4-oxopiperidine-3-carboxylate **119** (1.05 g, 3.64 mmol) was dissolved in MeOH (30 mL). 2 M NaOH (aq, 4.00 mL, 8.00 mmol) was added and the mixture was heated to reflux for 18 h. The solution was allowed to cool and 2 M HCl (aq, 4.00 mL, 8.00 mmol) was added. The reaction mixture was concentrated *in vacuo*.

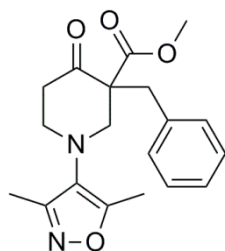
H₂O (20 mL) was added and the product was extracted with DCM (3 x 20 mL). The combined organics were washed with brine (20 mL), passed through a hydrophobic frit, and the solvent was removed *in vacuo*. The residue was taken up into DCM (3 mL) and purified by normal phase column chromatography (EtOAc in cyclohexane, 0 → 40%, 40 g SiO₂) to provide the titled compound as a colourless oil (531 mg, 67% yield). ν_{\max} (neat): 2962(w), 2876(w), 2800(w), 1713(s) cm⁻¹; ¹H NMR (400 MHz, CDCl₃) δ = 7.40 - 7.28 (m, 5H), 3.69 (d, *J* = 13.2 Hz, 1H), 3.59 (d, *J* = 13.2 Hz, 1H), 3.08 - 3.02 (m, 1H), 3.01 - 2.94 (m, 1H), 2.60 - 2.36 (m, 4H), 2.28 (dd, *J* = 9.7, 11.1 Hz, 1H), 1.91 - 1.79 (m, 1H), 1.41 - 1.25 (m, 1H), 0.90 (t, *J* = 7.5 Hz, 3H); ¹³C NMR (101 MHz, CDCl₃) δ = 211.0, 138.2, 128.9 (2C), 128.4 (2C), 127.3, 61.9, 58.5, 53.6, 51.4, 40.9, 20.7, 11.7; LCMS (High pH): *t_R* = 1.14 min, [M+H]⁺ = 218, (100% purity); HRMS: (C₁₄H₁₉NO) [M+H]⁺ requires 218.1539, found [M+H]⁺ 218.1545.

1-(3,5-Dimethylisoxazol-4-yl)-3-ethylpiperidin-4-one (121)



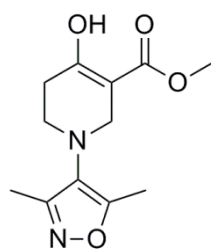
MeI (580 μ L, 9.28 mmol) was slowly added to a solution of 1-benzyl-3-ethylpiperidin-4-one **120** (500 mg, 2.30 mmol) in acetone (5 mL) and the reaction mixture stirred in a stoppered flask for 3 days. The solvent was removed *in vacuo* and the resulting yellow oil redissolved in EtOH (3 mL) and H₂O (3 mL). To this was added 4-amino-3,5-dimethylisoxazole **46** (140 mg, 1.25 mmol) and K₂CO₃ (43 mg, 0.31 mmol), and the reaction mixture stirred at 90 °C for 23 h. The mixture was allowed to cool and H₂O (20 mL) was added. The product was extracted with DCM (3 x 20 mL). The combined organics were washed with brine (20 mL), passed through a hydrophobic frit, and the solvent was removed *in vacuo*. The residue was dissolved in 1:1 MeOH:DMSO (3 mL) and purified by MDAP (High pH). The desired fractions were combined and concentrated *in vacuo*. The product was extracted with DCM (3 x 20 mL). The combined organics were washed with brine (20 mL), passed through a hydrophobic frit, and the solvent removed *in vacuo* to give the titled compound as a yellow oil (203 mg, 73% yield). ν_{\max} (neat): 2965(m), 2929(w), 2879(w), 2850(w), 1706(s), 1645(w), 1621(w) cm⁻¹; ¹H NMR (400 MHz, CDCl₃) δ = 3.38 - 3.32 (m, 1H), 3.31 - 3.25 (m, 2H), 2.98 (dd, *J* = 8.6, 11.2 Hz, 1H), 2.67 - 2.57 (m, 1H), 2.56 - 2.44 (m, 2H), 2.41 (s, 3H), 2.28 (s, 3H), 1.98 - 1.87 (m, 1H), 1.47 - 1.34 (m, 1H), 0.95 (t, *J* = 7.5 Hz, 3H); ¹³C NMR (101 MHz, CDCl₃) δ = 209.7, 161.3, 158.0, 126.9, 57.4, 52.8 (2C), 41.8, 20.6, 11.7, 11.5, 10.5; LCMS (Formic): *t_R* = 0.95 min, [M+H]⁺ = 223, (98% purity); HRMS: (C₁₂H₁₈N₂O₂) [M+H]⁺ requires 223.1441, found [M+H]⁺ 223.1433.

Methyl 3-benzyl-1-(3,5-dimethylisoxazol-4-yl)-4-oxopiperidine-3-carboxylate (122)



Methyl 1-(3,5-dimethylisoxazol-4-yl)-4-oxopiperidine-3-carboxylate **123** (2.16 g, 8.56 mmol) and K_2CO_3 (5.92 g, 42.8 mmol) were suspended in acetone (30 mL). Benzyl bromide (3.06 mL, 25.7 mmol) was added and the reaction mixture was heated to reflux, under atmospheric conditions, for 16 h. The cooled reaction mixture was filtered, washed through with acetone (3 x 20 mL) and then the combined organics were concentrated *in vacuo*. The residue was partitioned between H_2O (40 mL) and EtOAc (40 mL). The aqueous phase was extracted with EtOAc (2 x 40 mL). The combined organics were washed with brine (40 mL) and passed through a hydrophobic frit, before the solvent was removed *in vacuo*. The residue was taken up into DCM (2 mL) and purified by normal phase column chromatography (EtOAc in cyclohexane, 0 → 30%, 120 g SiO_2) to provide the titled compound as a white solid (2.50 g, 85% yield). ν_{max} ($CDCl_3$): 2931(w), 1718(s), 1623(w) cm^{-1} ; 1H NMR (400 MHz, $CDCl_3$) δ = 7.28 - 7.20 (m, 3H), 7.18 - 7.10 (m, 2H), 3.66 (s, 3H), 3.65 - 3.60 (m, 1H), 3.35 - 3.27 (m, 2H), 3.25 - 3.17 (m, 1H), 3.05 (d, J = 11.9 Hz, 1H), 2.99 - 2.89 (m, 2H), 2.54 (td, J = 2.9, 14.0 Hz, 1H), 2.34 (s, 3H), 2.23 (s, 3H); ^{13}C NMR (101 MHz, $CDCl_3$) δ = 204.1, 170.8, 162.4, 158.1, 135.7, 130.2 (2C), 128.2 (2C), 126.9, 126.4, 63.3, 60.2, 52.8, 52.2, 41.6, 37.3, 11.3, 10.5; LCMS (Formic): t_R = 1.17 min, $[M+H]^+$ = 343, (100% purity); HRMS: ($C_{19}H_{22}N_2O_4$) $[M+H]^+$ requires 343.1652, found $[M+H]^+$ 343.1645.

Methyl 1-(3,5-dimethylisoxazol-4-yl)-4-oxopiperidine-3-carboxylate (123)



a) From alkylated amine intermediate **124**

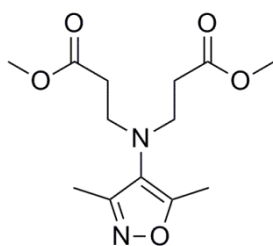
To a solution of dimethyl 3,3'-((3,5-dimethylisoxazol-4-yl)azanediyl)dipropionate **124** (1410 mg, 4.97 mmol) in THF (10 mL) was added $tBuOK$, 1.0 M in THF (10.9 mL, 10.9 mmol) and the resulting solution was heated to reflux for 2 h under a nitrogen atmosphere. The reaction mixture was allowed to cool and H_2O (40 mL) was added. The solution was adjusted to approximately pH 7 with 2 M HCl (aq, 6 mL), and extracted with EtOAc (3 x 40 mL). The combined organics were passed through a hydrophobic frit and the solvent removed *in vacuo*. The residue was taken up into DCM (4 mL) and purified by normal phase column chromatography (EtOAc in cyclohexane, 0 → 50%, 80 g SiO_2) to provide the titled compound as a white solid (1.01 g, 81% yield). NMR analysis indicates that the product exists in equilibrium between enol and keto forms. In $CDCl_3$ ratio is roughly 10:1. ν_{max}

(neat): 2956(w), 2837(w), 1661(s), 1623(s) cm⁻¹; Enol: ¹H NMR (400 MHz, CDCl₃) δ = 12.00 (s, 1H), 3.78 (s, 3H), 3.63 (t, *J* = 1.7 Hz, 2H), 3.18 (t, *J* = 5.7 Hz, 2H), 2.49 (tt, *J* = 1.7, 5.7 Hz, 2H), 2.38 (s, 3H), 2.26 (s, 3H); Keto: ¹H NMR (400 MHz, CDCl₃) δ = 3.81 (s, 3H), 3.71 - 3.66 (m, 1H), 3.54 - 3.50 (m, 1H), 3.40 (dd, *J* = 4.4, 11.5 Hz, 1H), 3.32 (t, *J* = 5.9 Hz, 2H), 2.85 - 2.76 (m, 1H), 2.61 (dtd, *J* = 1.5, 5.6, 14.2 Hz, 1H), 2.40 (s, 3H), 2.28 (s, 3H); Enol: ¹³C NMR (101 MHz, CDCl₃) δ = 171.1, 170.2, 161.5, 158.2, 127.0, 97.1, 51.5, 48.3, 48.2, 30.2, 11.4, 10.5; Keto: Not observed in ¹³C NMR spectrum; LCMS (Formic): *t*_R = 0.78 min, [M+H]⁺ = 253, (11% purity), *t*_R = 1.00 min, [M+H]⁺ = 253, (89% purity); HRMS: (C₁₂H₁₆N₂O₄) [M+H]⁺ requires 253.1183, found [M+H]⁺ 253.1185.

b) Directly from aminoisoxazole **46**

4-Amino-3,5-dimethylisoxazole **46** (9.6 g, 86 mmol) was dissolved in methyl acrylate (47 mL, 520 mmol) and ZrCl₄ (5.0 g, 21 mmol) was added slowly, using ice water for external cooling. The resulting solution was stirred at RT under atmospheric conditions for 6.5 h. The reaction mixture was diluted with EtOAc (100 mL) and washed with H₂O (2 x 70 mL). The aqueous phase was extracted with EtOAc (100 mL) and the combined organics were washed with brine (2 x 40 mL) before being passed through a hydrophobic frit and the solvent being removed *in vacuo*. The residue was dissolved in THF (80 mL). The solution was evacuated and purged with nitrogen and ^tBuOK, 1.0 M in THF (130 mL, 130 mmol) was added. The resulting solution was heated to reflux under a nitrogen atmosphere for 1.5 h. The reaction mixture was allowed to cool and H₂O (200 mL) was added. The solution was adjusted to approximately pH 7 with 2 M HCl (aq, 65 mL) and extracted with EtOAc (3 x 200 mL). The combined organics were washed with brine (100 mL) and the solvent was removed *in vacuo*. The residue was taken up into DCM (5 mL) and purified by normal phase column chromatography (EtOAc in cyclohexane, 0 → 50%, 340 g SiO₂) to provide the titled compound as a white solid (14.4 g, 67% yield). LCMS (Formic): *t*_R = 0.83 min, [M+H]⁺ = 253, (7% purity), *t*_R = 1.05 min, [M+H]⁺ = 253, (93% purity).

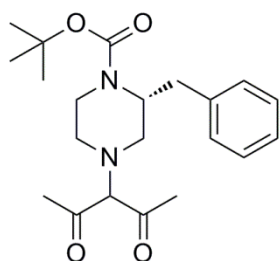
Dimethyl 3,3'-((3,5-dimethylisoxazol-4-yl)azanediyl)dipropionate (**124**)



4-Amino-3,5-dimethylisoxazole **46** (1.00 g, 8.92 mmol) and ZrCl₄ (416 mg, 1.78 mmol) were dissolved in methyl acrylate (10 mL, 110 mmol), and the mixture was stirred at RT under atmospheric conditions for 2.5 h. The reaction mixture was concentrated *in vacuo* and the residue was dissolved in H₂O (30

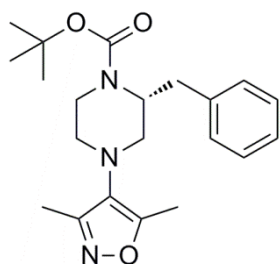
mL) and extracted with DCM (4 x 30 mL). The combined organics were passed through a hydrophobic frit and the solvent was removed *in vacuo*. The residue was taken up into DCM (4 mL) and purified by normal phase column chromatography (TBME in cyclohexane, 0 → 70%, 120 g SiO₂) to provide the titled compound as a colourless oil (1.97 g, 78% yield). ν_{\max} (neat): 2954(w), 2856(w), 1733(s), 1638(w) cm⁻¹; ¹H NMR (400 MHz, CDCl₃) δ = 3.65 (s, 6H), 3.25 (t, *J* = 6.8 Hz, 4H), 2.38 (t, *J* = 6.8 Hz, 4H), 2.23 (s, 3H), 2.28 (s, 3H); ¹³C NMR (101 MHz, CDCl₃) δ = 172.3 (2C), 165.2, 158.9, 123.4, 51.6 (2C), 50.7 (2C), 33.9 (2C), 10.9, 10.6; LCMS (High pH): *t*_R = 0.88 min, [M+H]⁺ = 285, (98% purity); HRMS: (C₁₃H₂₀N₂O₅) [M+H]⁺ requires 285.1445, found [M+H]⁺ 285.1436.

(R)-tert-Butyl 2-benzyl-4-(2,4-dioxopentan-3-yl)piperazine-1-carboxylate (126)



A solution of (*R*)-*tert*-butyl 2-benzylpiperazine-1-carboxylate **125** (1.00 g, 3.62 mmol) and NEt₃ (605 μ L, 4.34 mmol) in DMF (6 mL) was stirred at RT under a nitrogen atmosphere. 3-Chloropentane-2,4-dione **70** (449 μ L, 3.98 mmol) was added and the resulting solution stirred at RT for 24 h. The reaction was poured into H₂O (100 mL) and the resulting mixture extracted with EtOAc (3 x 50 mL). The combined organics were washed with 5% LiCl (aq, 3 x 40 mL) and brine (20 mL), and passed through a hydrophobic frit. The solvent was removed *in vacuo* and the residue was taken up into DCM (4 mL) and purified by normal phase column chromatography (EtOAc in cyclohexane, 0 → 30%, 80 g SiO₂) to provide the titled compound as an orange oil (1.08 g, 80% yield). NMR analysis indicates that the product exists mainly in an enol form in CDCl₃. ¹H NMR (400 MHz, CDCl₃) δ = 16.15 (s, 1H), 7.34 - 7.17 (m, 5H), 4.33 (br. s., 1H), 4.02 (d, *J* = 11.1 Hz, 1H), 3.26 (dt, *J* = 3.5, 12.4 Hz, 1H), 3.17 (dd, *J* = 3.9, 11.7 Hz, 1H), 3.12 - 3.00 (m, 3H), 2.84 - 2.73 (m, 1H), 2.73 - 2.64 (m, 1H), 2.45 - 2.40 (m, 3H), 2.10 (s, 3H), 1.37 (s, 9H); LCMS (Formic): *t*_R = 1.36 min, [M+H]⁺ = 375, (95% purity).

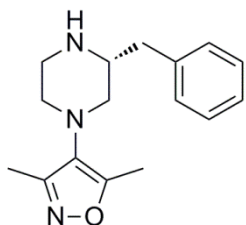
(R)-tert-Butyl 2-benzyl-4-(3,5-dimethylisoxazol-4-yl)piperazine-1-carboxylate (127)



A solution of (*R*)-*tert*-butyl 2-benzyl-4-(2,4-dioxopentan-3-yl)piperazine-1-carboxylate **126** (860 mg, 2.30 mmol) and hydroxylamine hydrochloride (2.39 g, 34.4 mmol) in toluene (30 mL) was heated to reflux using Dean Stark apparatus under atmospheric conditions for 8 h. The reaction mixture was allowed to cool to RT, filtered and washed through the filter with EtOAc (3 x 25 mL). The

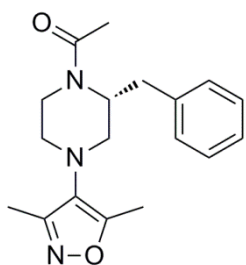
organics were combined and the solvent was removed *in vacuo*. The residue was taken up into DCM (3 mL) and purified by normal phase column chromatography (EtOAc in cyclohexane, 0 → 30%, 80 g SiO₂) to provide the titled compound as a colourless oil (331 mg, 39% yield). $[\alpha]_D^{20}$ -3.0° (c 0.10, MeOH); ν_{\max} (neat): 2987(w), 2962(w), 2936(w), 2844(w), 1684(s), 1626(w), 1602(w) cm⁻¹; ¹H NMR (400 MHz, CDCl₃) δ = 7.33 - 7.15 (m, 5H), 4.35 (br. s., 1H), 4.12 - 3.96 (m, 1H), 3.31 (dt, *J* = 3.5, 12.5 Hz, 1H), 3.20 - 2.97 (m, 4H), 2.96 - 2.89 (m, 1H), 2.78 (td, *J* = 1.5, 11.4 Hz, 1H), 2.41 (s, 3H), 2.29 (s, 3H), 1.41 (s, 9H); ¹³C NMR (101 MHz, CDCl₃) δ = 161.8, 158.3, 154.6, 138.8, 129.3 (2C), 128.5 (2C), 127.3, 126.4, 79.9 (br.), 53.2 (3C), 52.1, 35.6, 28.3 (3C), 11.5, 10.7; LCMS (Formic): *t_R* = 1.39 min, [M+H]⁺ = 372, (98% purity); HRMS: (C₂₁H₂₉N₃O₃) [M+H]⁺ requires 372.2282, found [M+H]⁺ 372.2270.

(R)-4-(3-Benzylpiperazin-1-yl)-3,5-dimethylisoxazole (128)



A solution of (*R*)-*tert*-butyl 2-benzyl-4-(3,5-dimethylisoxazol-4-yl)piperazine-1-carboxylate **127** (222 mg, 0.598 mmol) in DCM (4 mL) was treated with TFA (2.00 mL, 26.0 mmol), using ice water for external cooling. The mixture was then allowed to warm to RT and stirred under atmospheric conditions for 3 h. The reaction mixture was concentrated *in vacuo*, and the residue was dissolved in H₂O (10 mL). 2 M NaOH (aq, 11 mL) was added and the product was extracted with DCM (10 x 25 mL). The combined organics were passed through a hydrophobic frit, and the solvent removed *in vacuo* to give the titled compound as a brown oil (160 mg, 99% yield). $[\alpha]_D^{20}$ -15.0° (c 0.25, MeOH); ν_{\max} (neat): 3027(w), 2939(w), 2817(w), 1632(w), 1602(w) cm⁻¹; ¹H NMR (400 MHz, DMSO-*d*₆) δ = 7.33 - 7.25 (m, 2H), 7.24 - 7.18 (m, 3H), 2.92 - 2.81 (m, 3H), 2.79 - 2.56 (m, 7H), 2.31 (s, 3H), 2.10 (s, 3H); ¹³C NMR (101 MHz, CDCl₃) δ = 161.0, 158.3, 138.2, 129.2 (2C), 128.6 (2C), 127.6, 126.5, 58.0, 57.1, 52.2, 46.5, 40.5, 11.5, 10.5; LCMS (High pH): *t_R* = 1.02 min, [M+H]⁺ = 272, (100% purity); HRMS: (C₁₆H₂₁N₃O) [M+H]⁺ requires 272.1757, found [M+H]⁺ 272.1745.

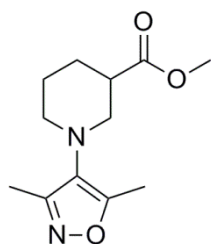
(R)-1-(2-Benzyl-4-(3,5-dimethylisoxazol-4-yl)piperazin-1-yl)ethanone (129)



A solution of (*R*)-4-(3-benzylpiperazin-1-yl)-3,5-dimethylisoxazole **128** (81 mg, 0.30 mmol) and triethylamine (104 μ L, 0.746 mmol) in DCM (3 mL) was treated with acetyl chloride (25 μ L, 0.36 mmol). The reaction mixture was stirred at RT for 17 h under atmospheric conditions. The solvent was removed *in vacuo* and the residue was dissolved in 1:1 MeOH:DMSO (1.6 mL) and

purified by MDAP (Formic) to provide the titled compound as a colourless oil (61 mg, 70% yield). $[\alpha]_D^{20} +5.4^\circ$ (c 0.25, MeOH); ν_{\max} (neat): 2927(w), 2824(w), 1721(w), 1636(s) cm^{-1} ; $^1\text{H NMR}$ (400 MHz, DMSO- d_6) $\delta = 7.34 - 7.16$ (m, 5H), 4.78 - 3.45 (m, 3H), 3.21 - 2.81 (m, 6H), 2.38 (s, 3H), 2.21 (s, 3H), 2.06 - 1.54 (m, 3H); $^{13}\text{C NMR}$ (101 MHz, DMSO- d_6) $\delta = 168.8, 161.3, 158.0, 139.4, 129.5$ (2C), 128.7 (2C), 127.5, 126.6, 52.2 (4C), 35.8, 21.2, 11.5, 10.3; LCMS (Formic): $t_R = 1.00$ min, $[\text{M}+\text{H}]^+ = 314$, (100% purity); HRMS: ($\text{C}_{18}\text{H}_{23}\text{N}_3\text{O}_2$) $[\text{M}+\text{H}]^+$ requires 314.1863, found $[\text{M}+\text{H}]^+ 314.1858$.

Methyl 1-(3,5-dimethylisoxazol-4-yl)piperidine-3-carboxylate (**131**)



a) From β -keto ester **123**

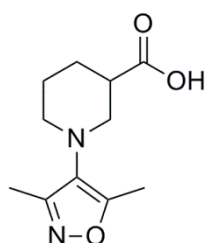
A solution of methyl 1-(3,5-dimethylisoxazol-4-yl)-4-oxopiperidine-3-carboxylate **123** (100 mg, 0.396 mmol) and tosylhydrazide (111 mg, 0.595 mmol) in MeOH (2 mL) was heated to reflux under a nitrogen atmosphere for 2 h. To this was added a solution of ZnCl_2 , 1.9 M in 2-MeTHF (160 μL , 0.30 mmol) and NaBH_3CN (38 mg, 0.61 mmol) in MeOH (2 mL), and the mixture was heated to reflux under a nitrogen atmosphere for 24 h. The reaction mixture was allowed to cool and was diluted with EtOAc (20 mL) before being washed with H_2O (20 mL), sat. NaHCO_3 (aq, 20 mL), brine (20 mL), passed through a hydrophobic frit and the solvent removed *in vacuo*. The residue was taken up into DCM (1 mL) and purified by normal phase column chromatography (EtOAc in cyclohexane, 0 \rightarrow 50%, 12 g SiO_2) to provide a crude residue, which was taken up into 1:1 MeOH:DMSO and purified by MDAP (Formic) to provide the titled compound as a colourless oil (36 mg, 38% yield). ν_{\max} (neat): 2950(w), 2815(w), 1731(s), 1629(w) cm^{-1} ; $^1\text{H NMR}$ (400 MHz, CDCl_3) $\delta = 3.71$ (s, 3H), 3.19 - 3.13 (m, 1H), 3.10 - 3.04 (m, 1H), 2.98 - 2.91 (m, 1H), 2.90 - 2.83 (m, 1H), 2.70 - 2.61 (m, 1H), 2.36 (s, 3H), 2.23 (s, 3H), 2.00 - 1.92 (m, 1H), 1.87 - 1.76 (m, 1H), 1.70 - 1.61 (m, 2H); $^{13}\text{C NMR}$ (101 MHz, CDCl_3) $\delta = 174.1, 161.1, 158.3, 127.9, 54.3, 52.5, 51.6, 42.3, 26.3, 25.1, 11.5, 10.4$; LCMS (Formic): $t_R = 0.98$ min, $[\text{M}+\text{H}]^+ = 239$, (100% purity); HRMS: ($\text{C}_{12}\text{H}_{18}\text{N}_2\text{O}_3$) $[\text{M}+\text{H}]^+$ requires 239.1390, found $[\text{M}+\text{H}]^+ 239.1385$.

b) From conjugated enamine **281**

To a solution of methyl 1-(3,5-dimethylisoxazol-4-yl)-1,4,5,6-tetrahydropyridine-3-d carboxylate **281** (31 mg, 0.13 mmol) in MeOH (0.5 mL) and AcOH (0.500 mL) was added NaBH_3CN (25 mg, 0.39 mmol), and the mixture was stirred at RT for 1 h before being slowly transferred to a flask containing sat. NaHCO_3 (aq, 40 mL). Once effervescence had

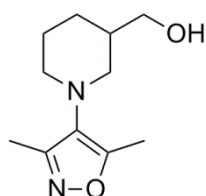
diminished (~15 min) the mixture was extracted with DCM (3 x 30 mL). The combined organics were washed with brine (20 mL), before being passed through a hydrophobic frit and the solvent being removed *in vacuo*. The residue was taken up into DCM (2 mL) and purified by normal phase column chromatography (EtOAc in cyclohexane, 0 → 50%, 12 g SiO₂) to provide the titled compound as a colourless oil (28 mg, 90% yield). ¹H NMR (400 MHz, CDCl₃) δ = 3.70 (s, 3H), 3.18 - 3.12 (m, 1H), 3.06 (dd, *J* = 8.8, 11.2 Hz, 1H), 2.97 - 2.90 (m, 1H), 2.89 - 2.82 (m, 1H), 2.70 - 2.61 (m, 1H), 2.36 (s, 3H), 2.22 (s, 3H), 2.00 - 1.91 (m, 1H), 1.86 - 1.76 (m, 1H), 1.71 - 1.61 (m, 2H); LCMS (Formic): *t_R* = 0.98 min, [M+H]⁺ = 239, (100% purity).

1-(3,5-Dimethylisoxazol-4-yl)piperidine-3-carboxylic acid (132)



To a solution of methyl 1-(3,5-dimethylisoxazol-4-yl)piperidine-3-carboxylate **131** (130 mg, 0.56 mmol) in MeOH (4 mL) was added 2 M NaOH (aq, 0.50 mL, 1.0 mmol) and the mixture heated to reflux for 4 h under atmospheric conditions. The reaction mixture was allowed to cool before H₂O (20 mL) was added, and the solution was acidified with 2 M HCl (aq, 1 mL). The product was extracted with DCM (3 x 10 mL) and the combined organics were washed with brine (10 mL) before being passed through a hydrophobic frit. The solvent was removed *in vacuo* and the residue was taken up into 1:1 MeOH:DMSO (1 mL) and purified by MDAP (Formic) to provide the titled compound as a brown oil (107 mg, 87% yield). *v*_{max} (neat): 2944(w), 2815(w), 1704(s), 1630(w) cm⁻¹; ¹H NMR (400 MHz, CDCl₃) δ = 3.23 - 3.10 (m, 2H), 3.01 - 2.89 (m, 2H), 2.77 - 2.69 (m, 1H), 2.39 (s, 3H), 2.26 (s, 3H), 1.99 - 1.63 (m, 4H). Carboxylic acid proton not observed; ¹³C NMR (101 MHz, CDCl₃) δ = 178.1, 161.4, 158.1, 127.5, 54.1, 52.7, 41.7, 26.1, 24.5, 11.5, 10.5; LCMS (Formic): *t_R* = 0.80 min, [M+H]⁺ = 225, (98% purity); HRMS: (C₁₁H₁₆N₂O₃) [M+H]⁺ requires 225.1234, found [M+H]⁺ 225.1227.

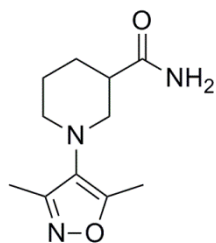
(1-(3,5-Dimethylisoxazol-4-yl)piperidin-3-yl)methanol (133)



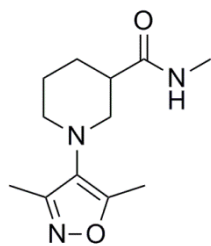
A solution of methyl 1-(3,5-dimethylisoxazol-4-yl)piperidine-3-carboxylate **131** (203 mg, 0.852 mmol) in THF (2 mL) was added dropwise to LiAlH₄, 2.0 M in THF (4.26 mL, 8.52 mmol) in THF (2 mL) cooled to 0 °C under a nitrogen atmosphere. The resulting solution was stirred at 0 °C for 1 h. The reaction mixture was quenched with dropwise addition of H₂O (1 mL), followed by 2 M NaOH (aq, 2 mL) and then further H₂O (3 mL). The resulting mixture was filtered and washed through the filter with EtOAc (20 mL). H₂O (20 mL) was added to the filtrate and the phases were separated. The aqueous phase was

extracted with further EtOAc (2 x 20 mL). The combined organics were washed with brine (20 mL), passed through a hydrophobic frit, and the solvent was removed *in vacuo*. The residue was taken up into DCM (2.5 mL) and purified by normal phase column chromatography (EtOAc in cyclohexane, 0 → 100%, 12 g SiO₂) to provide the titled compound as a colourless oil (141 mg, 79% yield). ν_{\max} (neat): 3404(br.), 2928(m), 2853(w), 2806(w), 1628(w) cm⁻¹; ¹H NMR (400 MHz, DMSO-*d*₆) δ = 4.42 (t, *J* = 5.4 Hz, 1H), 3.38 - 3.25 (m, 2H), 3.05 - 2.99 (m, 1H), 2.94 - 2.87 (m, 1H), 2.78 (dt, *J* = 2.4, 10.8 Hz, 1H), 2.57 (dd, *J* = 9.3, 11.0 Hz, 1H), 2.34 (s, 3H), 2.14 (s, 3H), 1.74 - 1.62 (m, 3H), 1.57 - 1.45 (m, 1H), 1.12 - 1.00 (m, 1H); ¹³C NMR (101 MHz, DMSO-*d*₆) δ = 159.8, 158.1, 128.6, 64.2, 56.0, 52.9, 39.9, 26.9, 25.6, 11.8, 10.4; LCMS (Formic): *t*_R = 0.70 min, [M+H]⁺ = 211, (100% purity); HRMS: (C₁₁H₁₈N₂O₂) [M+H]⁺ requires 211.1441, found [M+H]⁺ 211.1434.

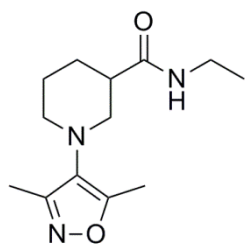
1-(3,5-Dimethylisoxazol-4-yl)piperidine-3-carboxamide (134)



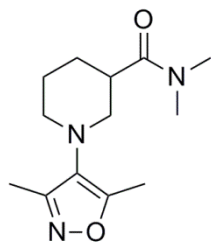
A vial was charged with methyl 1-(3,5-dimethylisoxazol-4-yl)piperidine-3-carboxylate **131** (100 mg, 0.420 mmol) and MeOH (1.5 mL) and was cooled to 0 °C, with stirring. Magnesium nitride (212 mg, 2.10 mmol) was added in one portion, and the vial was sealed immediately. The reaction was allowed to warm to RT and after 1 h it was heated to 75 °C for 24 h. The reaction mixture was allowed to cool and DCM (25 mL) and H₂O (25 mL) were added. The aqueous layer was acidified with 2 M HCl (aq, 1 mL) and the layers were separated. The aqueous layer was further extracted with DCM (2 x 25 mL) and the combined organics were passed through a hydrophobic frit before the solvent was removed *in vacuo*. The residue was taken up into 1:1 MeOH:DMSO (2 mL) and purified by MDAP (Formic) to provide the titled compound as a white solid (42 mg, 45% yield). M.pt.: 169–170 °C; ν_{\max} (neat): 3359(m), 3173(m), 2940(w), 2804(w), 1684(s), 1640(w) cm⁻¹; ¹H NMR (400 MHz, CDCl₃) δ = 6.45 (br. s., 1H), 5.70 (br. s., 1H), 3.20 - 3.09 (m, 2H), 2.98 - 2.89 (m, 2H), 2.60 - 2.52 (m, 1H), 2.39 (s, 3H), 2.25 (s, 3H), 1.92 - 1.76 (m, 3H), 1.75 - 1.62 (m, 1H); ¹³C NMR (101 MHz, CDCl₃) δ = 176.5, 161.2, 158.0, 127.7, 54.3, 52.9, 43.0, 26.9, 24.4, 11.7, 10.6; LCMS (Formic): *t*_R = 0.63 min, [M+H]⁺ = 224, (100% purity); HRMS: (C₁₁H₁₇N₃O₂) [M+H]⁺ requires 224.1394, found [M+H]⁺ 224.1392.

1-(3,5-Dimethylisoxazol-4-yl)-N-methylpiperidine-3-carboxamide (135)

The reaction was performed using General Procedure A, with methylamine, 2 M in THF (250 μ L, 0.500 mmol), providing the titled compound as a white solid (77 mg, 77% yield). M.pt.: 90–92 $^{\circ}$ C; ν_{\max} (neat): 3324(m), 2933(w), 2831(w), 1639(s), 1560(m) cm^{-1} ; ^1H NMR (400 MHz, CDCl_3) δ = 6.61 (br. s., 1H), 3.13 (d, J = 5.3 Hz, 2H), 2.96 - 2.91 (m, 2H), 2.86 (d, J = 5.1 Hz, 3H), 2.56 - 2.48 (m, 1H), 2.39 (s, 3H), 2.26 (s, 3H), 1.87 - 1.78 (m, 3H), 1.73 - 1.61 (m, 1H); ^{13}C NMR (101 MHz, CDCl_3) δ = 174.7, 161.1, 158.0, 127.6, 54.4, 52.9, 43.3, 26.8, 26.0, 24.4, 11.7, 10.6; LCMS (Formic): t_{R} = 0.68 min, $[\text{M}+\text{H}]^+$ = 238, (100% purity); HRMS: ($\text{C}_{12}\text{H}_{19}\text{N}_3\text{O}_2$) $[\text{M}+\text{H}]^+$ requires 238.1550, found $[\text{M}+\text{H}]^+$ 238.1537.

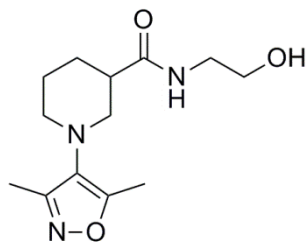
1-(3,5-Dimethylisoxazol-4-yl)-N-ethylpiperidine-3-carboxamide (136)

The reaction was performed using General Procedure A, with ethanamine, 2 M in THF (252 μ L, 0.504 mmol), providing the titled compound as a white solid (77 mg, 73% yield). M.pt.: 122–124 $^{\circ}$ C; ν_{\max} (neat): 3290(m), 2946(w), 1639(s), 1553(s) cm^{-1} ; ^1H NMR (400 MHz, CDCl_3) δ = 6.51 (br. s., 1H), 3.42 - 3.24 (m, 2H), 3.13 (d, J = 5.6 Hz, 2H), 2.97 - 2.87 (m, 2H), 2.49 (quin, J = 5.6 Hz, 1H), 2.39 (s, 3H), 2.25 (s, 3H), 1.86 - 1.77 (m, 3H), 1.71 - 1.60 (m, 1H), 1.17 (t, J = 7.2 Hz, 3H); ^{13}C NMR (101 MHz, CDCl_3) δ = 173.8, 161.1, 158.0, 127.7, 54.3, 53.0, 43.4, 34.1, 26.9, 24.4, 15.0, 11.7, 10.6; LCMS (Formic): t_{R} = 0.76 min, $[\text{M}+\text{H}]^+$ = 252, (100% purity); HRMS: ($\text{C}_{13}\text{H}_{21}\text{N}_3\text{O}_2$) $[\text{M}+\text{H}]^+$ requires 252.1707, found $[\text{M}+\text{H}]^+$ 252.1699.

1-(3,5-Dimethylisoxazol-4-yl)-N,N-dimethylpiperidine-3-carboxamide (137)

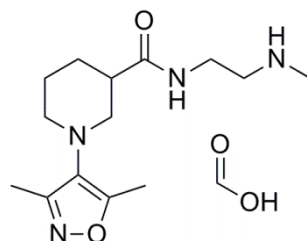
The reaction was performed using General Procedure A, with dimethylamine, 2 M in THF (252 μ L, 0.504 mmol), providing the titled compound as an orange oil (55 mg, 52% yield). ν_{\max} (neat): 3489(br.), 2938(m), 2855(w), 1721(w), 1634(s) cm^{-1} ; ^1H NMR (400 MHz, CDCl_3) δ = 3.16 - 3.11 (m, 1H), 3.10 (s, 3H), 3.02 - 2.92 (m, 5H), 2.91 - 2.80 (m, 2H), 2.38 (s, 3H), 2.24 (s, 3H), 1.93 - 1.86 (m, 1H), 1.85 - 1.78 (m, 1H), 1.75 - 1.55 (m, 2H); ^{13}C NMR (101 MHz, CDCl_3) δ = 173.7, 160.7, 158.3, 128.1, 54.7, 52.7, 40.6, 37.1, 35.5, 27.1, 25.8, 11.6, 10.4; LCMS (Formic): t_{R} = 0.76 min, $[\text{M}+\text{H}]^+$ = 252, (100% purity); HRMS: ($\text{C}_{13}\text{H}_{21}\text{N}_3\text{O}_2$) $[\text{M}+\text{H}]^+$ requires 252.1707, found $[\text{M}+\text{H}]^+$ 252.1700.

1-(3,5-Dimethylisoxazol-4-yl)-N-(2-hydroxyethyl)piperidine-3-carboxamide (138)



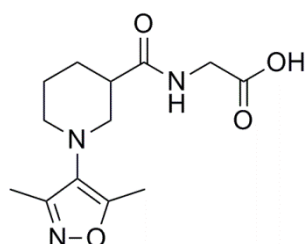
The reaction was performed using General Procedure A, with 2-aminoethanol (30 μ L, 0.50 mmol), providing the titled compound as a white solid (21 mg, 19% yield). M.pt.: 93–94 $^{\circ}$ C; ν_{max} (neat): 3278(m), 2930(m), 2822(w), 1619(s), 1554(s) cm^{-1} ; ^1H NMR (400 MHz, $\text{DMSO}-d_6$) δ = 7.81 (t, J = 5.4 Hz, 1H), 4.61 (t, J = 5.3 Hz, 1H), 3.41 - 3.35 (m, 2H), 3.11 (q, J = 6.0 Hz, 2H), 3.00 - 2.94 (m, 1H), 2.93 - 2.85 (m, 2H), 2.84 - 2.76 (m, 1H), 2.47 - 2.38 (m, 1H), 2.34 (s, 3H), 2.15 (s, 3H), 1.80 - 1.68 (m, 2H), 1.59 - 1.44 (m, 2H); ^{13}C NMR (101 MHz, CDCl_3) δ = 175.4, 161.2, 158.0, 127.6, 62.5, 54.2, 53.0, 43.2, 42.2, 26.8, 24.3, 11.7, 10.6; LCMS (Formic): t_{R} = 0.61 min, $[\text{M}+\text{H}]^+$ = 268, (100% purity); HRMS: ($\text{C}_{13}\text{H}_{21}\text{N}_3\text{O}_3$) $[\text{M}+\text{H}]^+$ requires 268.1661, found $[\text{M}+\text{H}]^+$ 268.1672.

1-(3,5-Dimethylisoxazol-4-yl)-N-(2-(methylamino)ethyl)piperidine-3-carboxamide, formic acid salt (139)



The reaction was performed using General Procedure A, with *N*-methylethylenediamine (44 μ L, 0.50 mmol), providing an impure sample of product. The residue was taken up into 1:1 MeOH:DMSO (1 mL) and purified by MDAP (Formic) to provide the titled compound as an orange oil (74 mg, 54% yield). ν_{max} (neat): 3286(br.), 2938(w), 2816(w), 1651(s), 1546(s) cm^{-1} ; ^1H NMR (400 MHz, CDCl_3) δ = 8.44 (br. s., 1H), 8.03 (t, J = 5.3 Hz, 1H), 7.71 - 7.43 (m, 2H), 3.62 - 3.55 (m, 2H), 3.13 - 3.00 (m, 4H), 2.95 - 2.82 (m, 2H), 2.64 (s, 3H), 2.56 - 2.45 (m, 1H), 2.36 (s, 3H), 2.23 (s, 3H), 1.95 - 1.86 (m, 1H), 1.84 - 1.72 (m, 1H), 1.71 - 1.55 (m, 2H); ^{13}C NMR (101 MHz, CDCl_3) δ = 175.3, 168.2, 161.1, 158.3, 127.9, 54.6, 52.5, 49.3, 44.0, 36.0, 33.0, 26.9, 25.2, 11.5, 10.4; LCMS (Formic): t_{R} = 0.42 min, $[\text{M}+\text{H}]^+$ = 281, (96% purity); HRMS: ($\text{C}_{14}\text{H}_{24}\text{N}_4\text{O}_2$) $[\text{M}+\text{H}]^+$ requires 281.1972, found $[\text{M}+\text{H}]^+$ 281.1970.

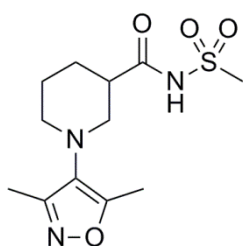
2-(1-(3,5-Dimethylisoxazol-4-yl)piperidine-3-carboxamido)acetic acid (140)



The reaction was performed using a variation on General Procedure A: THF (0.3 mL) was added as a solvent, and before being taken up into 1:1 MeOH:DMSO the reaction mixture was concentrated under a stream of nitrogen. Glycine (32 mg, 0.42 mmol) was used, and the procedure provided the titled

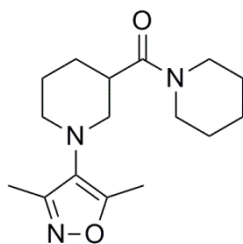
compound as an orange oil (27 mg, 23% yield). ν_{\max} (CDCl₃): 3303(br.), 2940(s), 1740(s), 1642(s), 1548(s) cm⁻¹; ¹H NMR (400 MHz, CDCl₃) δ = 7.59 (br. s., 1H), 4.20 - 4.07 (m, 1H), 4.03 - 3.92 (m, 1H), 3.15 (d, J = 4.4 Hz, 2H), 3.00 - 2.84 (m, 2H), 2.67 - 2.58 (m, 1H), 2.38 (s, 3H), 2.25 (s, 3H), 1.95 - 1.77 (m, 3H), 1.72 - 1.60 (m, 1H). Carboxylic acid proton not observed; ¹³C NMR (101 MHz, CDCl₃) δ = 175.4, 172.7, 161.2, 158.1, 127.6, 53.9, 53.0, 42.6, 41.4, 26.6, 24.0, 11.8, 10.6; LCMS (Formic): t_R = 0.66 min, [M+H]⁺ = 282, (97% purity); HRMS: (C₁₃H₁₉N₃O₄) [M+H]⁺ requires 282.1448, found [M+H]⁺ 282.1438.

1-(3,5-Dimethylisoxazol-4-yl)-N-(methylsulfonyl)piperidine-3-carboxamide (141)

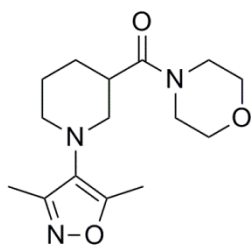


The reaction was performed using a variation on General Procedure A: THF (0.3 mL) was added as a solvent, and before being taken up into 1:1 MeOH:DMSO the reaction mixture was concentrated under a stream of nitrogen. Methanesulfonamide (48 mg, 0.50 mmol) was used, and the procedure provided the titled compound as a colourless oil (18 mg, 14% yield). ν_{\max} (CDCl₃): 3238(br.), 2940(m), 2855(w), 1712(s), 1631(w) cm⁻¹; ¹H NMR (400 MHz, CDCl₃) δ = 10.81 (br. s, 1H), 3.33 (s, 3H), 3.25 (d, J = 3.4 Hz, 2H), 3.09 (td, J = 3.7, 11.4 Hz, 1H), 2.96 - 2.87 (m, 1H), 2.78 - 2.70 (m, 1H), 2.45 (s, 3H), 2.33 (s, 3H), 2.12 - 2.02 (m, 1H), 1.99 - 1.72 (m, 3H); ¹³C NMR (101 MHz, CDCl₃) δ = 173.6, 162.0, 157.5, 126.5, 53.6, 52.7, 42.0, 41.7, 26.2, 22.7, 11.9, 11.1; LCMS (Formic): t_R = 0.77 min, [M+H]⁺ = 302, (100% purity); HRMS: (C₁₂H₁₉N₃O₄S) [M+H]⁺ requires 302.1169, found [M+H]⁺ 302.1164.

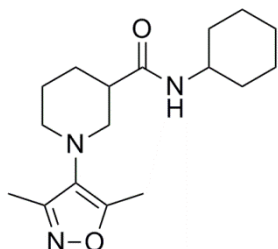
(1-(3,5-Dimethylisoxazol-4-yl)piperidin-3-yl)(piperidin-1-yl)methanone (142)



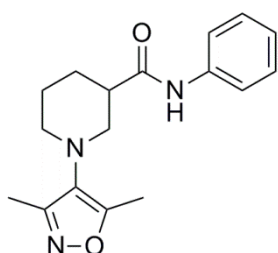
The reaction was performed using General Procedure A, with piperidine (42 μ L, 0.42 mmol), providing the titled compound as a white solid (82 mg, 67% yield). M.pt.: 62–65 °C; ν_{\max} (neat): 2949(m), 2920(m), 2854(m), 1726(w), 1633(s), 1571(w) cm⁻¹; ¹H NMR (400 MHz, CDCl₃) δ = 3.63 - 3.44 (m, 4H), 3.13 (t, J = 10.9 Hz, 1H), 3.01 - 2.91 (m, 2H), 2.91 - 2.77 (m, 2H), 2.38 (s, 3H), 2.24 (s, 3H), 1.90 - 1.77 (m, 2H), 1.72 - 1.51 (m, 8H); ¹³C NMR (101 MHz, CDCl₃) δ = 172.0, 160.6, 158.3, 128.1, 55.0, 52.7, 46.5, 42.7, 40.3, 27.4, 26.9, 25.9, 25.6, 24.6, 11.6, 10.4; LCMS (Formic): t_R = 0.98 min, [M+H]⁺ = 292, (100% purity); HRMS: (C₁₆H₂₅N₃O₂) [M+H]⁺ requires 292.202, found [M+H]⁺ 292.2009.

(1-(3,5-Dimethylisoxazol-4-yl)piperidin-3-yl)(morpholino)methanone (143)

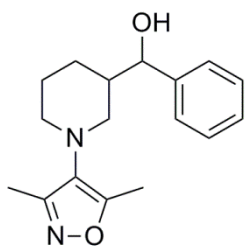
The reaction was performed using General Procedure A, with morpholine (37 μ L, 0.420 mmol), providing the titled compound as a colourless oil (90 mg, 73% yield). ν_{\max} (neat): 3490(br.), 2936(w), 2854(w), 1634(s) cm^{-1} ; ^1H NMR (400 MHz, CDCl_3) δ = 3.73 - 3.51 (m, 8H), 3.15 (t, J = 11.0 Hz, 1H), 3.01 - 2.90 (m, 2H), 2.90 - 2.82 (m, 1H), 2.82 - 2.73 (m, 1H), 2.37 (s, 3H), 2.22 (s, 3H), 1.89 - 1.78 (m, 2H), 1.72 - 1.56 (m, 2H); ^{13}C NMR (101 MHz, CDCl_3) δ = 172.3, 160.8, 158.2, 128.0, 66.9, 66.8, 54.7, 52.7, 46.0, 41.9, 40.1, 27.4, 25.8, 11.6, 10.4; LCMS (Formic): t_{R} = 0.76 min, $[\text{M}+\text{H}]^+$ = 294, (100% purity); HRMS: ($\text{C}_{15}\text{H}_{23}\text{N}_3\text{O}_3$) $[\text{M}+\text{H}]^+$ requires 294.1812, found $[\text{M}+\text{H}]^+$ 294.1808.

***N*-Cyclohexyl-1-(3,5-dimethylisoxazol-4-yl)piperidine-3-carboxamide (144)**

The reaction was performed using General Procedure A, with cyclohexanamine (58 μ L, 0.50 mmol), providing the titled compound as a white solid (94 mg, 73% yield). ν_{\max} (neat): 3289(m), 2926(m), 2853(m), 1636(s), 1542(s) cm^{-1} ; ^1H NMR (400 MHz, CDCl_3) δ = 6.28 (br. s., 1H), 3.87 - 3.75 (m, 1H), 3.13 (d, J = 5.6 Hz, 2H), 2.97 - 2.84 (m, 2H), 2.46 (quin, J = 5.6 Hz, 1H), 2.40 (s, 3H), 2.26 (s, 3H), 2.00 - 1.89 (m, 2H), 1.87 - 1.60 (m, 7H), 1.46 - 1.32 (m, 2H), 1.23 - 1.06 (m, 3H); ^{13}C NMR (101 MHz, CDCl_3) δ = 173.0, 160.9, 158.0, 127.8, 54.2, 53.1, 48.0, 43.5, 33.5, 33.4, 27.0, 25.6, 25.0, 25.0, 24.4, 11.8, 10.7; LCMS (Formic): t_{R} = 1.05 min, $[\text{M}+\text{H}]^+$ = 306, (100% purity); HRMS: ($\text{C}_{17}\text{H}_{27}\text{N}_3\text{O}_2$) $[\text{M}+\text{H}]^+$ requires 306.2176, found $[\text{M}+\text{H}]^+$ 306.2165.

1-(3,5-Dimethylisoxazol-4-yl)-*N*-phenylpiperidine-3-carboxamide (145)

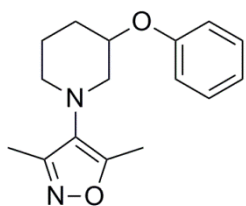
The reaction was performed using General Procedure A, with aniline (46 μ L, 0.50 mmol), providing the titled compound as a colourless oil (15 mg, 12% yield). ν_{\max} (DCM): 3302(br.), 2939(w), 2817(w), 1662(s), 1599(s) cm^{-1} ; ^1H NMR (400 MHz, CDCl_3) δ = 8.70 (br. s., 1H), 7.56 - 7.50 (m, 2H), 7.38 - 7.32 (m, 2H), 7.17 - 7.11 (m, 1H), 3.33 - 3.21 (m, 2H), 3.08 - 3.00 (m, 1H), 2.99 - 2.91 (m, 1H), 2.73 - 2.66 (m, 1H), 2.43 (s, 3H), 2.30 (s, 3H), 2.04 - 1.86 (m, 3H), 1.79 - 1.67 (m, 1H); ^{13}C NMR (101 MHz, CDCl_3) δ = 172.5, 161.0, 157.8, 137.7, 129.1 (2C), 127.5, 124.4, 120.2 (2C), 54.1, 53.3, 43.8, 26.9, 24.1, 11.9, 10.8; LCMS (Formic): t_{R} = 1.05 min, $[\text{M}+\text{H}]^+$ = 300, (100% purity); HRMS: ($\text{C}_{17}\text{H}_{21}\text{N}_3\text{O}_2$) $[\text{M}+\text{H}]^+$ requires 300.1707, found $[\text{M}+\text{H}]^+$ 300.1698.

(1-(3,5-Dimethylisoxazol-4-yl)piperidin-3-yl)(phenyl)methanol (148)

A solution of (1-(3,5-dimethylisoxazol-4-yl)piperidin-3-yl)(phenyl)methanone **151** (215 mg, 0.756 mmol) in MeOH (3.5 mL) was cooled to 0 °C. To this was added NaBH₄ (57 mg, 1.5 mmol) and the mixture was stirred for 2 h at 0 °C, under atmospheric conditions. The reaction mixture was concentrated *in vacuo* and the residue diluted with Et₂O (35 mL) and H₂O (15 mL). The aqueous phase was acidified with 2 M HCl (aq, 5 mL) and the layers were separated. The organic phase was washed with sat. NaHCO₃ (aq, 10 mL) and brine (10 mL), passed through a hydrophobic frit, and the solvent was removed *in vacuo*. The residue was taken up into 1:1 MeOH:DMSO (2 mL) and purified by MDAP (Formic) to provide separated diastereomers of the titled compound. Diastereomer 1 **148a** was isolated as an orange oil (138 mg, 64% yield) and diastereomer 2 **148b** as a white solid (76 mg, 35% yield).

Diastereomer 1 **148a**: ν_{\max} (neat): 3385(br.), 2934(w), 2851(w), 1630(w) cm⁻¹; ¹H NMR (400 MHz, DMSO-*d*₆) δ = 7.34 - 7.27 (m, 4H), 7.26 - 7.19 (m, 1H), 5.20 (br. s., 1H), 4.39 (d, *J* = 6.8 Hz, 1H), 2.91 - 2.84 (m, 1H), 2.72 (dt, *J* = 2.8, 11.1 Hz, 1H), 2.63 - 2.54 (m, 2H), 2.27 (s, 3H), 2.03 (s, 3H), 1.90 - 1.67 (m, 3H), 1.53 - 1.40 (m, 1H), 1.25 - 1.14 (m, 1H); ¹³C NMR (101 MHz, DMSO-*d*₆) δ = 159.4, 157.8, 145.0, 128.6, 128.3 (2C), 127.2, 126.8 (2C), 75.0, 55.5, 52.8, 44.6, 26.0, 25.9, 11.8, 10.3; LCMS (Formic): *t*_R = 1.07 min, [M+H]⁺ = 287, (100% purity); HRMS: (C₁₇H₂₂N₂O₂) [M+H]⁺ requires 287.17600, found [M+H]⁺ 287.1770.

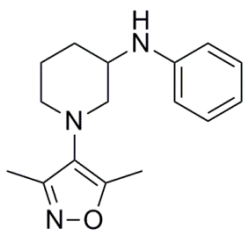
Diastereomer 2 **148b**: M.pt.: 116–119 °C; ν_{\max} (neat): 3429(br.), 2946(w), 2913(w), 1638(w) cm⁻¹; ¹H NMR (400MHz, DMSO-*d*₆) δ = 7.37 - 7.28 (m, 4H), 7.27 - 7.21 (m, 1H), 5.20 (d, *J* = 4.0 Hz, 1H), 4.34 (dd, *J* = 4.0, 7.8 Hz, 1H), 3.20 - 3.12 (m, 1H), 2.92 - 2.85 (m, 1H), 2.80 - 2.70 (m, 2H), 2.34 (s, 3H), 2.12 (s, 3H), 1.83 - 1.72 (m, 1H), 1.66 - 1.57 (m, 1H), 1.47 - 1.34 (m, 1H), 1.31 - 1.22 (m, 1H), 1.07 - 0.94 (m, 1H); ¹³C NMR (101 MHz, DMSO-*d*₆) δ = 159.6, 158.0, 145.1, 128.7, 128.4 (2C), 127.3, 127.1 (2C), 75.4, 55.5, 52.7, 44.5, 27.0, 25.8, 11.8, 10.4; LCMS (Formic): *t*_R = 1.13 min, [M+H]⁺ = 287, (100% purity); HRMS: (C₁₇H₂₂N₂O₂) [M+H]⁺ requires 287.1754, found [M+H]⁺ 287.1746.

3,5-Dimethyl-4-(3-phenoxy-piperidin-1-yl)isoxazole (149)

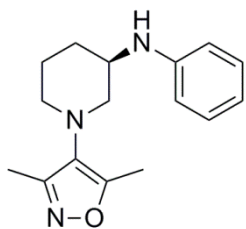
A solution of 3-(3-phenoxy-piperidin-1-yl)pentane-2,4-dione **153** (215 mg, 0.781 mmol) and hydroxylamine hydrochloride (810 mg, 11.7 mmol) in toluene (20 mL) was heated to reflux using Dean Stark apparatus for 16 h. The reaction mixture was allowed to cool before being filtered and washed through with EtOAc (3 x 20 mL). The organics were

combined and the solvent was removed *in vacuo*. The residue was taken up into DCM (3 mL) and purified by normal phase column chromatography (EtOAc in cyclohexane, 0 → 60%, 24 g SiO₂) to provide the titled compound as an orange oil (113 mg, 53% yield). ν_{\max} (neat): 2946(w), 2812(w), 1630(w), 1598(m), 1586(m) cm⁻¹; ¹H NMR (400 MHz, CDCl₃) δ = 7.33 - 7.26 (m, 2H), 7.00 - 6.91 (m, 3H), 4.44 - 4.36 (m, 1H), 3.33 - 3.27 (m, 1H), 3.01 - 2.86 (m, 3H), 2.38 (s, 3H), 2.24 (s, 3H), 2.22 - 2.14 (m, 1H), 1.96 - 1.87 (m, 1H), 1.78 - 1.66 (m, 1H), 1.65 - 1.54 (m, 1H); ¹³C NMR (101 MHz, CDCl₃) δ = 160.9, 158.3, 157.4, 129.6 (2C), 127.6, 121.1, 115.9 (2C), 72.8, 56.5, 52.4, 29.9, 24.0, 11.5, 10.4; LCMS (Formic): t_R = 1.31 min, [M+H]⁺ = 273, (100% purity); HRMS: (C₁₆H₂₀N₂O₂) [M+H]⁺ requires 273.1598, found [M+H]⁺ 273.1593.

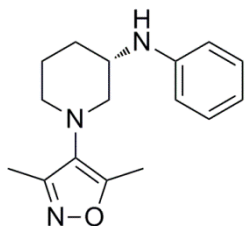
1-(3,5-Dimethylisoxazol-4-yl)-N-phenylpiperidin-3-amine (150)



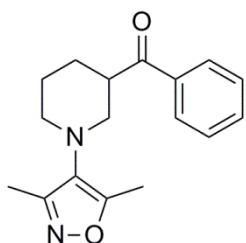
A microwave vial was charged with Pd₂(dba)₃ (70 mg, 0.077 mmol), DavePhos (45 mg, 0.12 mmol), NaO^tBu (207 mg, 2.15 mmol) and toluene (2 mL). The vial was sealed, and evacuated and purged with nitrogen. To this was added a solution of 1-(3,5-dimethylisoxazol-4-yl)piperidin-3-amine **157** (300 mg, 1.54 mmol) and bromobenzene (162 μ L, 1.54 mmol) in toluene (2 mL) and the sealed vial was heated to 130 °C for 15 h. This was allowed to cool and EtOAc (50 mL) was added. The organic phase was washed with 0.2 M HCl (aq, 20 mL), sat. NaHCO₃ (aq, 20 mL), H₂O (20 mL) and brine (20 mL) before being passed through a hydrophobic frit, and the solvent being removed *in vacuo*. The residue was taken up into DCM (3 mL) and purified by normal phase column chromatography (EtOAc in cyclohexane, 0 → 40%, 40 g SiO₂) to provide the titled compound as an orange oil (211 mg, 51% yield). ν_{\max} (neat): 3374(br.), 2937(w), 2809(w), 1601(s) cm⁻¹; ¹H NMR (400 MHz, CDCl₃) δ = 7.24 - 7.16 (m, 2H), 6.74 - 6.69 (m, 1H), 6.68 - 6.62 (m, 2H), 4.08 (br. s., 1H), 3.68 - 3.60 (m, 1H), 3.28 (dd, J = 3.2, 11.1 Hz, 1H), 3.02 - 2.89 (m, 2H), 2.81 (dd, J = 6.3, 11.1 Hz, 1H), 2.39 (s, 3H), 2.26 (s, 3H), 1.92 - 1.79 (m, 2H), 1.75 - 1.56 (m, 2H); ¹³C NMR (101 MHz, CDCl₃) δ = 160.7, 158.2, 146.8, 129.4 (2C), 127.8, 117.5, 113.4 (2C), 57.9, 52.8, 49.0, 29.0, 23.5, 11.6, 10.5; LCMS (Formic): t_R = 1.11 min, [M+H]⁺ = 272, (98% purity); HRMS: (C₁₆H₂₁N₃O) [M+H]⁺ requires 272.1757, found [M+H]⁺ 272.1756.

(+)-1-(3,5-Dimethylisoxazol-4-yl)-*N*-phenylpiperidin-3-amine ((+)-150)

1-(3,5-Dimethylisoxazol-4-yl)-*N*-phenylpiperidin-3-amine **150** (163 mg) was dissolved in EtOH (3 mL) and separated on a 30 mm x 25 cm Chiralcel OJ-H (5 μ m) column, eluting with 30% EtOH in heptane to provide the (-)-enantiomer **(-)-150** (see below) and the titled compound as an orange oil (89 mg). Configuration has been assigned by comparison of biological assay and crystallographic data. e.e. >99.0%; $[\alpha]_D^{25} +24.5^\circ$ (c 0.50, CDCl₃); ν_{\max} (neat): 3365(br.), 2938(w), 2810(w), 1601(s) cm⁻¹; ¹H NMR (400 MHz, CDCl₃) δ = 7.23 - 7.16 (m, 2H), 6.75 - 6.69 (m, 1H), 6.68 - 6.63 (m, 2H), 4.13 (br. s, 1H), 3.67 - 3.61 (m, 1H), 3.28 (dd, J = 3.1, 11.1 Hz, 1H), 3.01 - 2.89 (m, 2H), 2.81 (dd, J = 6.4, 11.0 Hz, 1H), 2.39 (s, 3H), 2.26 (s, 3H), 1.91 - 1.81 (m, 2H), 1.75 - 1.57 (m, 2H); ¹³C NMR (101 MHz, CDCl₃) δ = 160.7, 158.2, 146.7, 129.4 (2C), 127.8, 117.5, 113.4 (2C), 57.9, 52.8, 49.0, 29.0, 23.5, 11.6, 10.5; LCMS (High pH): t_R = 1.23 min, $[M+H]^+$ = 272, (99% purity); HRMS: (C₁₆H₂₁N₃O) $[M+H]^+$ requires 272.1763, found $[M+H]^+$ 272.1770.

(-)-1-(3,5-Dimethylisoxazol-4-yl)-*N*-phenylpiperidin-3-amine ((-)-150)

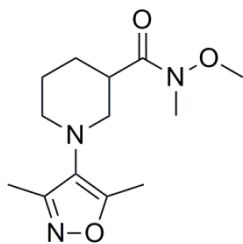
The titled compound was isolated as per the above protocol, as an orange oil (48 mg). Configuration has been assigned by comparison of biological assay and crystallographic data. e.e. = 98.7%; $[\alpha]_D^{25} -1.9^\circ$ (c 0.50, CDCl₃); ν_{\max} (neat): 3366(br.), 2938(w), 2810(w), 1601(s) cm⁻¹; ¹H NMR (400 MHz, CDCl₃) δ = 7.23 - 7.16 (m, 2H), 6.75 - 6.69 (m, 1H), 6.67 - 6.63 (m, 2H), 4.10 (br. s, 1H), 3.67 - 3.61 (m, 1H), 3.28 (dd, J = 3.2, 11.1 Hz, 1H), 3.01 - 2.89 (m, 2H), 2.81 (dd, J = 6.4, 11.0 Hz, 1H), 2.39 (s, 3H), 2.26 (s, 3H), 1.90 - 1.81 (m, 2H), 1.75 - 1.57 (m, 2H); ¹³C NMR (101 MHz, CDCl₃) δ = 160.7, 158.2, 146.7, 129.4 (2C), 127.8, 117.5, 113.4 (2C), 57.9, 52.8, 49.0, 29.0, 23.5, 11.6, 10.5; LCMS (High pH): t_R = 1.23 min, $[M+H]^+$ = 272, (100% purity); HRMS: (C₁₆H₂₁N₃O) $[M+H]^+$ requires 272.1757, found $[M+H]^+$ 272.1748.

(1-(3,5-Dimethylisoxazol-4-yl)piperidin-3-yl)(phenyl)methanone (151)

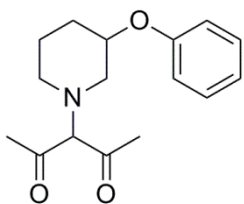
To a solution of 1-(3,5-dimethylisoxazol-4-yl)-*N*-methoxy-*N*-methylpiperidine-3-carboxamide **152** (2.00 g, 7.48 mmol) in THF (40 mL) at 0 °C under a nitrogen atmosphere was added phenylmagnesium bromide, 1 M in THF (22.4 mL, 22.4 mmol) dropwise. The reaction was allowed to warm to RT and stirred for 3 h. The reaction was quenched with 1 M HCl (aq, 60 mL) and extracted with EtOAc (2 x

60 mL). The organic phase was washed with brine (60 mL) and passed through a hydrophobic frit before the solvent was removed *in vacuo*. The residue was taken up into DCM (2 mL) and purified by normal phase column chromatography (EtOAc in cyclohexane, 0 → 50%, 120 g SiO₂) to provide the titled compound as a yellow oil (1.90 g, 89% yield). ν_{\max} (neat): 2942(w), 2818(w), 1676(s), 1630(w), 1597(w), 1580(w) cm⁻¹; ¹H NMR (400 MHz, CDCl₃) δ = 8.00 - 7.94 (m, 2H), 7.62 - 7.55 (m, 1H), 7.53 - 7.47 (m, 2H), 3.67 - 3.57 (m, 1H), 3.21 - 3.13 (m, 2H), 3.05 - 2.98 (m, 1H), 2.91 (dt, J = 3.2, 11.2 Hz, 1H), 2.39 (s, 3H), 2.25 (s, 3H), 2.09 - 2.01 (m, 1H), 1.94 - 1.74 (m, 2H), 1.70 - 1.57 (m, 1H); ¹³C NMR (101 MHz, CDCl₃) δ = 201.7, 160.9, 158.3, 136.0, 133.1, 128.7 (2C), 128.2 (2C), 128.0, 54.8, 52.7, 45.3, 27.6, 25.7, 11.6, 10.4; LCMS (Formic): t_R = 1.22 min, [M+H]⁺ = 285, (100% purity); HRMS: (C₁₇H₂₀N₂O₂) [M+H]⁺ requires 285.1598, found [M+H]⁺ 285.1585.

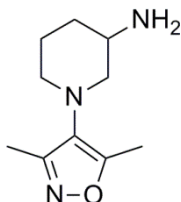
1-(3,5-Dimethylisoxazol-4-yl)-N-methoxy-N-methylpiperidine-3-carboxamide (152)



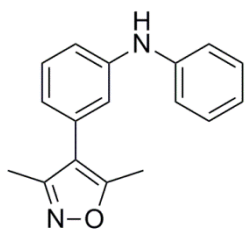
A slurry of methyl 1-(3,5-dimethylisoxazol-4-yl)piperidine-3-carboxylate **131** (2.00 g, 8.39 mmol) and *N,O*-dimethylhydroxylamine hydrochloride (1.23 g, 12.6 mmol) in THF (15 mL) was cooled to -20 °C under a nitrogen atmosphere. A solution of *i*PrMgCl, 2 M in THF (12.6 mL, 25.2 mmol) was added dropwise over 15 min. The mixture was stirred at -10 °C for 30 min before it was quenched with H₂O (10 mL) and sat. NH₄Cl (aq, 10 mL). The product was extracted with TBME (3 x 20 mL), and the combined organics were washed with brine (20 mL) before being passed through a hydrophobic frit. The solvent was removed *in vacuo* to give the titled compound as a yellow oil (2.16 g, 96% yield). ν_{\max} (neat): 2939(m), 2818(w), 1655(s) cm⁻¹; ¹H NMR (400 MHz, CDCl₃) δ = 3.74 (s, 3H), 3.20 (s, 3H), 3.09 - 2.84 (m, 5H), 2.38 (s, 3H), 2.24 (s, 3H), 1.96 - 1.89 (m, 1H), 1.86 - 1.78 (m, 1H), 1.77 - 1.54 (m, 2H); ¹³C NMR (101 MHz, CDCl₃) δ = 174.7, 160.6, 158.3, 128.1, 61.6, 54.5, 52.5, 40.0, 32.2, 26.8, 25.7, 11.6, 10.4; LCMS (Formic): t_R = 0.87 min, [M+H]⁺ = 268, (99% purity); HRMS: (C₁₃H₂₁N₃O₃) [M+H]⁺ requires 268.1656, found [M+H]⁺ 268.1643.

3-(3-Phenoxypiperidin-1-yl)pentane-2,4-dione (153)

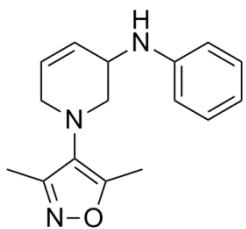
A solution of 3-phenoxy piperidine **155** (250 mg, 1.41 mmol) and NEt_3 (236 μL , 1.69 mmol) in DMF (1.5 mL) was stirred at RT under a nitrogen atmosphere. 3-Chloropentane-2,4-dione **70** (175 μL , 1.55 mmol) was added and the resulting solution stirred at RT under a nitrogen atmosphere for 4.5 h. The reaction was poured into H_2O (40 mL) and the resulting mixture extracted with EtOAc (3 x 30 mL). The combined organics were washed with 5% LiCl (aq, 3 x 10 mL) and brine (10 mL), and passed through a hydrophobic frit. The solvent was removed *in vacuo* and the residue was taken up into cyclohexane (5 mL) and purified by normal phase column chromatography (EtOAc in cyclohexane, 0 \rightarrow 70%, 24 g SiO_2) to provide the titled compound as a colourless oil (228 mg, 59% yield). NMR analysis showed the product to exist mainly in an enol form in CDCl_3 . ^1H NMR (400 MHz, CDCl_3) δ = 15.83 (s, 1H), 7.34 - 7.25 (m, 2H), 6.99 - 6.89 (m, 3H), 4.37 (m, 1H), 3.21 (s, 1H), 3.00 - 2.83 (m, 3H), 2.24 - 2.18 (m, 6H), 2.11 - 2.03 (m, 1H), 1.95 - 1.85 (m, 1H), 1.70 - 1.59 (m, 2H); LCMS (Formic): t_{R} = 0.99 min, $[\text{M}+\text{H}]^+$ = 276, (98% purity).

1-(3,5-Dimethylisoxazol-4-yl)piperidin-3-amine (157)

A solution of *tert*-butyl (1-(3,5-dimethylisoxazol-4-yl)piperidin-3-yl)carbamate **74** (815 mg, 2.76 mmol) in DCM (10 mL) was treated with TFA (6.0 mL, 78 mmol). The mixture was stirred at RT under atmospheric conditions for 3 h. The solvent was removed *in vacuo* and the residue was dissolved in H_2O (10 mL), and 2 M NaOH (aq, 11 mL) was added. The product was extracted with DCM (10 x 25 mL). The combined organics were passed through a hydrophobic frit, and the solvent removed *in vacuo* to give the titled compound as an orange oil (392 mg, 73% yield). ν_{max} (neat): 2931(m), 2854(w), 2807(w), 1629(w) cm^{-1} ; ^1H NMR (400 MHz, CDCl_3) δ = 3.10 - 3.03 (m, 1H), 3.00 - 2.75 (m, 3H), 2.63 (dd, J = 8.0, 10.7 Hz, 1H), 2.40 - 2.33 (m, 3H), 2.24 (s, 3H), 1.94 - 1.75 (m, 2H), 1.71 - 1.57 (m, 1H), 1.31 - 1.21 (m, 1H). Amine protons were not observed; ^{13}C NMR (101 MHz, CDCl_3) δ = 164.5, 162.8, 133.0, 66.1, 57.0, 53.5, 38.4, 29.6, 16.5, 15.1; LCMS (High pH): t_{R} = 0.71 min, $[\text{M}+\text{H}]^+$ = 196, (100% purity); HRMS: ($\text{C}_{10}\text{H}_{17}\text{N}_3\text{O}$) $[\text{M}+\text{H}]^+$ requires 196.1444, found $[\text{M}+\text{H}]^+$ 196.1436.

3-(3,5-Dimethylisoxazol-4-yl)-N-phenylaniline (159)

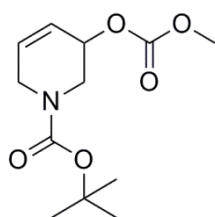
3-Bromo-*N*-phenylaniline **158** (211 mg, 0.851 mmol), (3,5-dimethylisoxazol-4-yl)boronic acid **31** (100 mg, 0.710 mmol), K_2CO_3 (196 mg, 1.419 mmol) and $Pd(PPh_3)_4$ (82 mg, 0.071 mmol) were dissolved in IPA (1.0 mL) and H_2O (1.0 mL). The reaction vessel was sealed and heated in Biotage Initiator reactor at 120 °C for 15 min. After cooling, the reaction was partitioned between H_2O (10 mL) and DCM (20 mL). The aqueous phase was further extracted with DCM (2 x 20 mL). The combined organics were washed with brine (20 mL), passed through a hydrophobic frit, and the solvent was removed *in vacuo*. The residue was taken up into 1:1 MeOH:DMSO (2 mL) and purified by MDAP (High pH) to provide the titled compound as a white solid (41 mg, 22% yield). M.pt.: 123–125 °C; ν_{max} (neat): 3406(w), 3289(m), 3197(w), 3131(w), 3085(w), 1629(w) cm^{-1} ; 1H NMR (400 MHz, $DMSO-d_6$) δ = 8.25 (s, 1H), 7.32 (t, J = 7.8 Hz, 1H), 7.28 - 7.22 (m, 2H), 7.14 - 7.06 (m, 3H), 6.99 (t, J = 1.8 Hz, 1H), 6.86 (t, J = 7.3 Hz, 1H), 6.81 (d, J = 7.8 Hz, 1H), 2.41 (s, 3H), 2.24 (s, 3H); ^{13}C NMR (101 MHz, $DMSO-d_6$) δ = 165.3, 158.5, 144.5, 143.5, 131.2, 130.1, 129.7 (2C), 120.6, 120.4, 117.7 (2C), 117.3, 116.6, 115.8, 11.9, 11.0; LCMS (High pH): t_R = 1.26 min, $[M+H]^+$ = 265, (100% purity); HRMS: ($C_{17}H_{16}N_2O$) $[M+H]^+$ requires 265.1335, found $[M+H]^+$ 265.1330.

1-(3,5-Dimethylisoxazol-4-yl)-N-phenyl-1,2,3,6-tetrahydropyridin-3-amine (160)

A solution of *N*-phenyl-1,2,3,6-tetrahydropyridin-3-amine **165** (248 mg, 1.42 mmol) and NEt_3 (278 μ L, 1.99 mmol) in MeCN (10 mL) was stirred at RT under a nitrogen atmosphere. 3-Chloropentane-2,4-dione **70** (225 μ L, 1.99 mmol) was added and the resulting solution stirred at RT for 19 h. The solvent was removed *in vacuo* and the residue was taken up into EtOAc (20 mL) and filtered. The precipitate was washed with further EtOAc (3 x 5 mL). The organics were combined and the solvent was removed *in vacuo*. The residue was redissolved in EtOH (10 mL), and hydroxylamine, 50 wt% in H_2O (131 μ L, 2.14 mmol) was added. The reaction mixture heated to reflux for 16 h, under atmospheric conditions. At this point a solution of Na_2CO_3 (302 mg, 2.85 mmol) in H_2O (10 mL) was added and the mixture heated to reflux for 4 h under atmospheric conditions. The reaction mixture was allowed to cool and was concentrated *in vacuo* before being neutralised with 2 M HCl (aq, 1.5 mL) and extracted with EtOAc (3 x 100 mL). The combined organics were passed through a hydrophobic frit and the solvent was removed *in vacuo*. The residue was taken up into DCM (4 mL) and purified by normal phase column chromatography (EtOAc in cyclohexane, 0 \rightarrow 50%,

80 g SiO₂) to provide the titled compound as an orange oil (171 mg, 45% yield). ν_{\max} (neat): 3362(br.), 3035(w), 2924(w), 2806(w), 1600(s) cm⁻¹; ¹H NMR (400 MHz, CDCl₃) δ = 7.21 - 7.15 (m, 2H), 6.73 (tt, J = 1.0, 7.3 Hz, 1H), 6.67 - 6.63 (m, 2H), 6.00 - 5.90 (m, 2H), 4.12 (br. s., 1H), 4.02 (br. s., 1H), 3.59 - 3.48 (m, 1H), 3.48 - 3.40 (m, 1H), 3.30 (dd, J = 3.2, 11.2 Hz, 1H), 3.05 (dd, J = 3.8, 11.2 Hz, 1H), 2.35 (s, 3H), 2.22 (s, 3H); ¹³C NMR (101 MHz, CDCl₃) δ = 161.7, 158.4, 146.7, 129.5 (2C), 128.3, 127.1, 126.9, 118.0, 113.7 (2C), 53.9, 51.2, 48.4, 11.5, 10.5; LCMS (High pH): t_R = 1.19 min, [M+H]⁺ = 270, (100% purity); HRMS: (C₁₆H₁₉N₃O) [M+H]⁺ requires 270.1601, found [M+H]⁺ 270.1589.

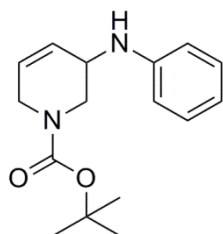
***tert*-Butyl 3-((methoxycarbonyl)oxy)-3,6-dihydropyridine-1(2*H*)-carboxylate (162)**



Adapted from literature procedure. Spectral data matches that reported.¹⁵³

Methyl chloroformate (4.65 mL, 60.2 mmol) was added to a solution of *tert*-butyl 3-hydroxy-3,6-dihydropyridine-1(2*H*)-carboxylate **161** (4.00 g, 20.1 mmol) and pyridine (4.87 mL, 60.2 mmol) in DCM (100 mL) at 0 °C under atmospheric conditions. The reaction was allowed to warm to RT and stirred for 16 h. Brine (100 mL) was added, and the layers separated. The aqueous layer was extracted with DCM (2 x 50 mL) and the combined organics were washed with sat. NaHCO₃ (aq, 50 mL) before being passed through a hydrophobic frit. The solvent was removed *in vacuo* and the residue was taken up into DCM (3 mL) and purified by normal phase column chromatography (EtOAc in cyclohexane, 0 → 20%, 120 g SiO₂) to provide the titled compound as a colourless oil (4.45 g, 86% yield). ¹H NMR (500 MHz, CDCl₃) δ = 6.06 - 5.85 (m, 2H), 5.18 - 4.97 (m, 1H), 4.22 - 3.95 (m, 1H), 3.79 (s, 5H), 3.57 (br. s., 1H), 1.46 (s, 9H); ¹³C NMR (126 MHz, CDCl₃) δ = 155.2, 154.7, 131.1, 123.2, 80.1, 69.2, 54.7, 44.8, 42.7, 28.3 (3C); HRMS: (C₁₂H₁₉NO₅) [M+H]⁺ requires 258.1336, found [M+H]⁺ 258.1335.

***tert*-Butyl 3-(phenylamino)-3,6-dihydropyridine-1(2*H*)-carboxylate (164)**

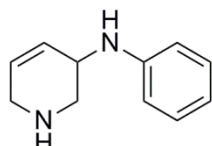


To a solution of *tert*-butyl 3-((methoxycarbonyl)oxy)-3,6-dihydropyridine-1(2*H*)-carboxylate **162** (2.00 g, 7.77 mmol) in 35% NH₃ (aq, 25.0 mL, 452 mmol) and 1,4-dioxane (50 mL) was added Pd(PPh₃)₄ (898 mg, 0.777 mmol). The resulting solution was stirred at RT under atmospheric conditions for 20 h. The reaction mixture was diluted with sat. NaHCO₃ (aq, 50 mL) and extracted with DCM (3 x 50 mL), followed by 10% MeOH in DCM (3 x 50 mL). The combined organics were passed through a hydrophobic frit and the solvent was removed *in vacuo*. The residue was taken up into 1:1 MeOH:DMSO (3 mL) and purified by reverse phase column chromatography (MeCN

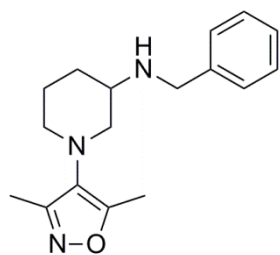
in H₂O + 0.1% (NH₄)₂CO₃, 15 → 55%, 120 g C₁₈) to provide the intermediate amine **163** as a pale yellow gum. LCMS (High pH): t_R = 0.76 min, [M+H]⁺ = 199, (78% purity).

To a microwave vial was added Pd₂(dba)₃ (158 mg, 0.172 mmol), DavePhos (102 mg, 0.259 mmol), NaO^tBu (464 mg, 4.83 mmol) and toluene (6 mL). The vial was sealed, and evacuated and purged with nitrogen. To this was added a solution of the intermediate amine **163** (684 mg, 3.45 mmol) and bromobenzene (545 μL, 5.17 mmol) in toluene (10 mL) and the sealed vial was heated to 130 °C for 15 h. This was allowed to cool and the solvent was removed under a stream of nitrogen. The residue was taken up into EtOAc (300 mL) and filtered through a pad of Celite (10 g). The solvent was removed *in vacuo* and the residue taken up into 1:1 MeOH:DMSO (5 mL) and purified by reverse phase column chromatography (MeCN in H₂O + 0.1% (NH₄)₂CO₃, 50 → 95%, 120 g C₁₈) to provide the titled compound as a brown oil (476 mg, 22% yield). ν_{max} (CDCl₃): 3369(w), 2976(w), 2931(w), 1689(s), 1602(s) cm⁻¹; ¹H NMR (400 MHz, CD₃OD) δ = 7.15 - 7.08 (m, 2H), 6.68 (d, *J* = 7.8 Hz, 2H), 6.64 (tt, *J* = 1.0, 7.3 Hz, 1H), 5.90 (br. s., 2H), 4.17 - 3.69 (m, 4H), 3.42 (br. s., 1H), 1.56 - 1.16 (m, 10H); ¹³C NMR (126 MHz, CD₃OD) δ = 155.3, 147.3, 128.7 (2C), 127.1, 126.8, 117.0, 113.2 (2C), 79.7, 47.0, 44.0, 42.6, 27.0 (3C); LCMS (High pH): t_R = 1.26 min, [M+H]⁺ = 275, (99% purity); HRMS: (C₁₆H₂₂N₂O₂) [M+H]⁺ requires 275.1754, found [M+H]⁺ 275.1751.

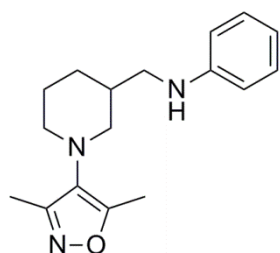
***N*-Phenyl-1,2,3,6-tetrahydropyridin-3-amine (165)**



TFA (3.00 mL, 38.9 mmol) was added to a solution of *tert*-butyl 3-(phenylamino)-3,6-dihydropyridine-1(2*H*)-carboxylate **164** (442 mg, 1.611 mmol) in DCM (6 mL), cooled in an ice bath. The solution was allowed to warm to RT and stirred for 1 h under atmospheric conditions. The solvent was removed under a stream of nitrogen and the residue was taken up into MeOH (5 mL) and loaded onto a pre-equilibrated SCX-2 cartridge (20 g). After 10 minutes the column was flushed with MeOH (140 mL) followed by NH₃, 2 M in MeOH (140 mL). The desired fractions were combined and the solvent removed *in vacuo* to give the titled compound as a brown gum (260 mg, 93% yield). ν_{max} (neat): 3280(m), 3224(m), 3099(w), 3028(w), 2934(w), 2919(w), 2837(w), 1600(s) cm⁻¹; ¹H NMR (400 MHz, DMSO-*d*₆) δ = 7.08 - 7.02 (m, 2H), 6.63 - 6.58 (m, 2H), 6.51 (tt, *J* = 1.0, 7.3 Hz, 1H), 5.87 - 5.81 (m, 1H), 5.79 - 5.73 (m, 1H), 5.39 (d, *J* = 9.0 Hz, 1H), 3.83 (br. s, 1H), 3.24 - 3.09 (m, 3H), 2.97 (dd, *J* = 4.4, 12.2 Hz, 1H), 2.61 (dd, *J* = 5.6, 12.2 Hz, 1H); ¹³C NMR (101 MHz, DMSO-*d*₆) δ = 147.8, 129.6, 128.9 (2C), 127.6, 115.7, 112.5 (2C), 47.7, 46.1, 44.4; LCMS (High pH): t_R = 0.80 min, [M+H]⁺ = 175, (100% purity); HRMS: (C₁₁H₁₄N₂) [M+H]⁺ requires 175.1230, found [M+H]⁺ 175.1227.

N-Benzyl-1-(3,5-dimethylisoxazol-4-yl)piperidin-3-amine (169)

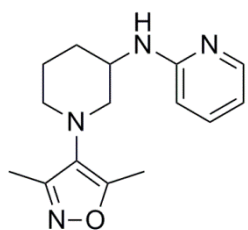
1-(3,5-Dimethylisoxazol-4-yl)piperidin-3-amine **157** (37 mg, 0.19 mmol) was dissolved in MeOH (0.50 mL) and AcOH (56 μ L). Benzaldehyde (19 μ L, 0.19 mmol) was added, followed by picoline borane (20 mg, 0.19 mmol), and the reaction vessel was sealed and stirred at RT for 16 h. The solvent was removed under a stream of nitrogen. The residue was dissolved in 1:1 MeOH:DMSO (1 mL) and purified by MDAP (High pH) to provide the titled compound as a brown oil (34 mg, 63% yield). ν_{\max} (neat): 3027(w), 2932(m), 2808(w), 1629(w) cm^{-1} ; $^1\text{H NMR}$ (400 MHz, DMSO- d_6) δ = 7.38 - 7.25 (m, 4H), 7.20 (tt, J = 1.7, 7.1 Hz, 1H), 3.74 (s, 2H), 3.12 - 3.03 (m, 1H), 2.89 - 2.81 (m, 1H), 2.75 (dt, J = 2.9, 10.6 Hz, 1H), 2.62 - 2.53 (m, 2H), 2.31 (s, 3H), 2.10 (s, 3H), 2.06 (br. s., 1H), 1.90 - 1.79 (m, 1H), 1.73 - 1.63 (m, 1H), 1.54 - 1.42 (m, 1H), 1.25 - 1.12 (m, 1H); $^{13}\text{C NMR}$ (101 MHz, CDCl_3) δ = 160.6, 158.4, 140.6, 128.5 (2C), 128.1, 128.0 (2C), 127.0, 58.2, 54.0, 52.8, 51.2, 30.7, 24.4, 11.5, 10.5; LCMS (High pH): t_{R} = 1.13 min, $[\text{M}+\text{H}]^+$ = 286, (100% purity); HRMS: ($\text{C}_{17}\text{H}_{23}\text{N}_3\text{O}$) $[\text{M}+\text{H}]^+$ requires 286.1914, found $[\text{M}+\text{H}]^+$ 286.1903.

N-((1-(3,5-Dimethylisoxazol-4-yl)piperidin-3-yl)methyl)aniline (170)

A vial was charged with methyl 1-(3,5-dimethylisoxazol-4-yl)piperidine-3-carboxylate **131** (500 mg, 2.10 mmol), TBD (88 mg, 0.63 mmol) and aniline (229 μ L, 2.52 mmol). The vial was sealed, and put under a nitrogen atmosphere before being heated to 95 $^{\circ}\text{C}$ for 15 h. The reaction mixture was allowed to cool before being taken up into MeOH (0.5 mL) and loaded onto a pre-equilibrated SCX-2 cartridge (5 g). After 10 minutes the column was flushed with MeOH (60 mL) followed by NH_3 , 2 M in MeOH (30 mL). The desired fractions were combined and the solvent removed *in vacuo*. The residue was taken up into THF (10 mL). The flask was evacuated and purged with nitrogen before being cooled to 0 $^{\circ}\text{C}$. LiAlH_4 , 2.3 M in 2-MeTHF (9.12 mL, 21.0 mmol) was added dropwise and the resulting solution stirred at 0 $^{\circ}\text{C}$ for 2 h before being allowed to warm to RT and being stirred for a further 16 h. The reaction mixture was quenched with dropwise addition of H_2O (2 mL), followed by 2 M NaOH (aq, 4 mL) and then further H_2O (6 mL). The resulting mixture was filtered and washed through the filter with EtOAc (20 mL). H_2O (25 mL) was added to the filtrate and the phases were separated. The aqueous phase was further extracted with EtOAc (2 x 25 mL). The combined organics were washed with brine (20 mL), passed through a hydrophobic frit, and the solvent was removed *in vacuo*. The residue was taken up into

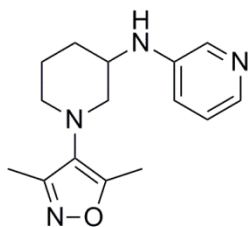
DCM (2.5 mL) and purified by normal phase column chromatography (EtOAc in cyclohexane, 0 → 50%, 40 g SiO₂) to provide the titled compound as a yellow oil (73 mg, 12% yield). ν_{\max} (neat): 3360(w), 2928(m), 2852(w), 2806(w), 1602(s) cm⁻¹; ¹H NMR (400 MHz, CDCl₃) δ = 7.21 - 7.14 (m, 2H), 6.71 (tt, J = 1.0, 7.3 Hz, 1H), 6.65 - 6.56 (m, 2H), 3.82 (br. s, 1H), 3.19 - 3.04 (m, 3H), 2.99 - 2.91 (m, 1H), 2.84 (dt, J = 3.1, 10.6 Hz, 1H), 2.69 (dd, J = 9.0, 11.0 Hz, 1H), 2.35 (s, 3H), 2.22 (s, 3H), 2.04 - 1.93 (m, 1H), 1.92 - 1.84 (m, 1H), 1.82 - 1.73 (m, 1H), 1.71 - 1.58 (m, 1H), 1.29 - 1.15 (m, 1H); ¹³C NMR (101 MHz, CDCl₃) δ = 160.6, 158.4, 148.2, 129.3 (2C), 128.3, 117.4, 112.8 (2C), 56.8, 53.2, 47.6, 36.9, 28.4, 25.4, 11.6, 10.5; LCMS (High pH): t_R = 1.31 min, [M+H]⁺ = 286, (100% purity); HRMS: (C₁₇H₂₃N₃O) [M+H]⁺ requires 286.1914, found [M+H]⁺ 286.1903.

***N*-(1-(3,5-Dimethylisoxazol-4-yl)piperidin-3-yl)pyridin-2-amine (171)**



Prepared using General Procedure B with 2-chloropyridine (29 mg, 24 μ L, 0.26 mmol), heating for 15 h, to provide the titled compound as a brown oil (46 mg, 66% yield). ν_{\max} (CDCl₃): 3335(br.), 2938(w), 2809(w), 1599(s), 1571(m) cm⁻¹; ¹H NMR (400 MHz, CDCl₃) δ = 8.10 (ddd, J = 0.7, 1.7, 5.0 Hz, 1H), 7.42 (ddd, J = 1.7, 7.1, 8.6 Hz, 1H), 6.57 (ddd, J = 1.0, 5.0, 7.1 Hz, 1H), 6.41 (td, J = 0.9, 8.6 Hz, 1H), 4.87 (d, J = 8.3 Hz, 1H), 4.01 - 3.93 (m, 1H), 3.28 (dd, J = 3.2, 11.1 Hz, 1H), 3.01 - 2.89 (m, 2H), 2.83 (dd, J = 6.2, 11.1 Hz, 1H), 2.39 (s, 3H), 2.26 (s, 3H), 1.92 - 1.82 (m, 2H), 1.75 - 1.60 (m, 2H); ¹³C NMR (101 MHz, CDCl₃) δ = 160.6, 158.2, 157.8, 148.4, 137.4, 127.8, 112.9, 107.2, 57.8, 52.8, 47.3, 29.2, 23.4, 11.6, 10.5; LCMS (High pH): t_R = 1.06 min, [M+H]⁺ = 273, (100% purity); HRMS: (C₁₅H₂₀N₄O) [M+H]⁺ requires 273.1710, found [M+H]⁺ 273.1700.

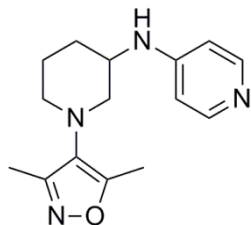
***N*-(1-(3,5-Dimethylisoxazol-4-yl)piperidin-3-yl)pyridin-3-amine (172)**



Prepared using General Procedure B with 3-bromopyridine (41 mg, 0.26 mmol), heating for 15 h, to provide the titled compound as a brown oil (5 mg, 7% yield). ν_{\max} (CDCl₃): 3306(br.), 2931(m), 2855(w), 1587(s) cm⁻¹; ¹H NMR (500 MHz, CDCl₃) δ = 8.07 (d, J = 2.8 Hz, 1H), 7.97 (dd, J = 1.2, 4.7 Hz, 1H), 7.10 (dd, J = 4.7, 8.2 Hz, 1H), 6.91 (ddd, J = 1.2, 2.8, 8.2 Hz, 1H), 4.12 (d, J = 8.2 Hz, 1H), 3.67 - 3.61 (m, 1H), 3.27 (dd, J = 3.0, 11.3 Hz, 1H), 3.01 - 2.93 (m, 2H), 2.83 (dd, J = 6.2, 11.3 Hz, 1H), 2.39 (s, 3H), 2.26 (s, 3H), 1.89 - 1.81 (m, 2H), 1.74 - 1.61 (m, 2H); ¹³C NMR (126 MHz, CDCl₃) δ = 160.9, 158.1, 142.8, 138.9, 136.6, 127.7, 123.8, 119.0, 57.6, 52.8, 48.6, 28.6, 23.2, 11.6, 10.6;

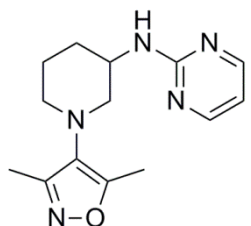
LCMS (High pH): $t_R = 0.98$ min, $[M+H]^+ = 273$, (95% purity); HRMS: ($C_{15}H_{20}N_4O$) $[M+H]^+$ requires 273.1710, found $[M+H]^+ 273.1700$.

***N*-(1-(3,5-Dimethylisoxazol-4-yl)piperidin-3-yl)pyridin-4-amine (173)**

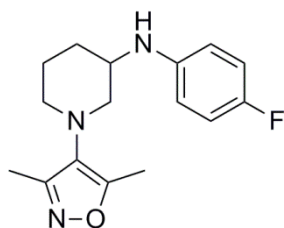


Prepared using General Procedure B with 4-bromopyridine (41 mg, 0.26 mmol), heating for 15 h, to provide the titled compound as a yellow oil (29 mg, 42% yield). ν_{max} ($CDCl_3$): 3242(br.), 2941(w), 1600(s) cm^{-1} ; 1H NMR (400 MHz, $CDCl_3$) $\delta = 8.21$ (d, $J = 6.3$ Hz, 2H), 6.46 (d, $J = 6.3$ Hz, 2H), 4.68 (d, $J = 7.8$ Hz, 1H), 3.69 (s, 1H), 3.26 (dd, $J = 3.0, 11.1$ Hz, 1H), 3.02 - 2.89 (m, 2H), 2.83 (dd, $J = 6.1, 11.1$ Hz, 1H), 2.39 (s, 3H), 2.26 (s, 3H), 1.89 - 1.80 (m, 2H), 1.75 - 1.62 (m, 2H); ^{13}C NMR (101 MHz, $CDCl_3$) $\delta = 160.9, 158.0, 152.1, 150.0$ (2C), 127.6, 107.8 (2C), 57.4, 52.8, 47.9, 28.5, 23.2, 11.6, 10.5; LCMS (Formic): $t_R = 0.50$ min, $[M+H]^+ = 273$, (97% purity); HRMS: ($C_{15}H_{20}N_4O$) $[M+H]^+$ requires 273.1710, found $[M+H]^+ 273.1701$.

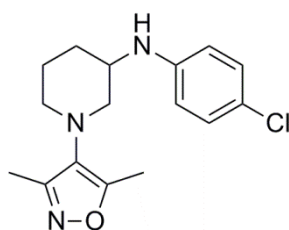
***N*-(1-(3,5-Dimethylisoxazol-4-yl)piperidin-3-yl)pyrimidin-2-amine (174)**



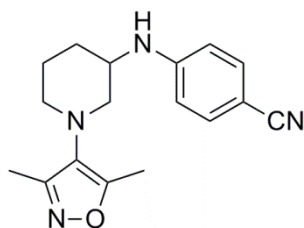
1-(3,5-Dimethylisoxazol-4-yl)piperidin-3-amine **157** (50 mg, 0.26 mmol), 2-fluoropyrimidine **189** (30 mg, 0.31 mmol) and DIPEA (134 μ L, 0.768 mmol) were dissolved in DMF (0.8 mL). The reaction vessel was sealed and heated in a Biotage Initiator reactor at 150 $^{\circ}C$ for 30 min. After cooling the reaction was concentrated under a stream of nitrogen before being diluted with MeOH (0.5 mL) and purified by MDAP (High pH) to provide the titled compound as an off-white solid (57 mg, 81% yield). M.pt.: 120–122 $^{\circ}C$; ν_{max} ($CDCl_3$): 3258(m), 2944(m), 2798(w), 1595(s), 1575(s) cm^{-1} ; 1H NMR (400 MHz, $CDCl_3$) $\delta = 8.29$ (d, $J = 4.9$ Hz, 2H), 6.54 (t, $J = 4.9$ Hz, 1H), 5.56 (d, $J = 7.8$ Hz, 1H), 4.24 - 4.16 (m, 1H), 3.30 (dd, $J = 3.2, 11.2$ Hz, 1H), 2.98 - 2.93 (m, 2H), 2.86 (dd, $J = 6.0, 11.2$ Hz, 1H), 2.39 (s, 3H), 2.26 (s, 3H), 1.92 - 1.81 (m, 2H), 1.76 - 1.64 (m, 2H); ^{13}C NMR (101 MHz, $CDCl_3$) $\delta = 161.6, 160.7, 158.3, 158.1$ (2C), 127.8, 110.6, 57.5, 52.8, 46.9, 29.0, 23.3, 11.6, 10.5; LCMS (High pH): $t_R = 0.96$ min, $[M+H]^+ = 274$, (100% purity); HRMS: ($C_{14}H_{19}N_5O$) $[M+H]^+$ requires 274.1662, found $[M+H]^+ 274.1656$.

1-(3,5-Dimethylisoxazol-4-yl)-N-(4-fluorophenyl)piperidin-3-amine (175)

Prepared using General Procedure B with 1-bromo-4-fluorobenzene (45 mg, 0.26 mmol), heating for 15 h, to provide the titled compound as a brown oil (41 mg, 55% yield). ν_{\max} (neat): 3358(br.), 2939(w), 2811(w), 1614(w) cm^{-1} ; $^1\text{H NMR}$ (400 MHz, CDCl_3) δ = 6.94 - 6.87 (m, 2H), 6.62 - 6.55 (m, 2H), 4.00 (br. s, 1H), 3.60 - 3.53 (m, 1H), 3.25 (dd, J = 3.2, 11.2 Hz, 1H), 3.01 - 2.88 (m, 2H), 2.80 (dd, J = 6.4, 11.2 Hz, 1H), 2.39 (s, 3H), 2.25 (s, 3H), 1.89 - 1.79 (m, 2H), 1.72 - 1.56 (m, 2H); $^{13}\text{C NMR}$ (101 MHz, CDCl_3) δ = 160.7, 158.2, 155.8 (d, $^1J_{\text{C-F}}$ = 235.5 Hz), 143.1, 127.8, 115.8 (d, $^2J_{\text{C-F}}$ = 22.0 Hz, 2C), 114.4 (d, $^3J_{\text{C-F}}$ = 7.3 Hz, 2C), 57.8, 52.8, 49.7, 28.9, 23.4, 11.6, 10.5; $^{19}\text{F NMR}$ (376 MHz, CDCl_3) δ = -127.82 (s); LCMS (High pH): t_{R} = 1.27 min, $[\text{M}+\text{H}]^+$ = 290, (100% purity); HRMS: ($\text{C}_{16}\text{H}_{20}\text{FN}_3\text{O}$) $[\text{M}+\text{H}]^+$ requires 290.1663, found $[\text{M}+\text{H}]^+$ 290.1654.

N-(4-Chlorophenyl)-1-(3,5-dimethylisoxazol-4-yl)piperidin-3-amine (176)

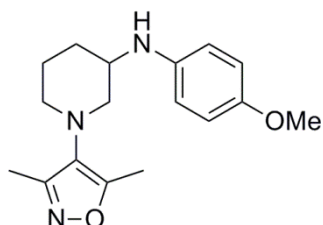
Prepared using General Procedure B with 1-bromo-4-chlorobenzene (49 mg, 0.26 mmol), heating for 4 h, to provide the titled compound as a brown oil (44 mg, 56% yield). ν_{\max} (neat): 3343(br.), 2938(w), 2810(w), 1599(s) cm^{-1} ; $^1\text{H NMR}$ (400 MHz, CDCl_3) δ = 7.13 (d, J = 8.8 Hz, 2H), 6.56 (d, J = 8.8 Hz, 2H), 4.09 (br. s., 1H), 3.63 - 3.54 (m, 1H), 3.25 (dd, J = 3.3, 11.1 Hz, 1H), 3.01 - 2.88 (m, 2H), 2.80 (dd, J = 6.3, 11.1 Hz, 1H), 2.39 (s, 3H), 2.25 (s, 3H), 1.87 - 1.78 (m, 2H), 1.73 - 1.58 (m, 2H); $^{13}\text{C NMR}$ (101 MHz, CDCl_3) δ = 160.8, 158.2, 145.4, 129.2 (2C), 127.8, 121.9, 114.4 (2C), 57.7, 52.8, 49.0, 28.7, 23.3, 11.6, 10.5; LCMS (High pH): t_{R} = 1.36min, $[\text{M}+\text{H}]^+$ = 306, 308, (94% purity); HRMS: ($\text{C}_{16}\text{H}_{20}^{35}\text{ClN}_3\text{O}$) $[\text{M}+\text{H}]^+$ requires 306.1368, found $[\text{M}+\text{H}]^+$ 306.1365.

4-((1-(3,5-Dimethylisoxazol-4-yl)piperidin-3-yl)amino)benzotrile (177)

Prepared using General Procedure B with 4-bromobenzotrile (47 mg, 0.26 mmol), heating for 15 h, to provide the titled compound as a brown oil (37 mg, 49% yield). ν_{\max} (CDCl_3): 3359(br.), 2941(w), 2811(w), 2210(s), 1605 (s) cm^{-1} ; $^1\text{H NMR}$ (400 MHz, CDCl_3) δ = 7.44 (d, J = 8.8 Hz, 2H), 6.59 (d, J = 8.8 Hz, 2H), 4.69 (br. s, 1H), 3.68 (br. s., 1H), 3.26 (dd, J = 3.2, 11.2 Hz, 1H), 3.01 - 2.90 (m, 2H), 2.85 (dd, J = 6.1, 11.2 Hz, 1H), 2.39 (s, 3H), 2.26 (s, 3H), 1.90 -

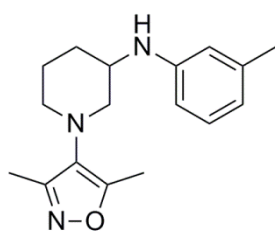
1.79 (m, 2H), 1.74 - 1.63 (m, 2H); ^{13}C NMR (101 MHz, CDCl_3) δ = 160.9, 158.1, 149.9, 133.9 (2C), 127.6, 120.4, 112.5 (2C), 98.7, 57.4, 52.8, 48.2, 28.4, 23.1, 11.7, 10.6; LCMS (High pH): t_{R} = 1.15 min, $[\text{M}+\text{H}]^+$ = 297, (100% purity); HRMS: ($\text{C}_{17}\text{H}_{20}\text{N}_4\text{O}$) $[\text{M}+\text{H}]^+$ requires 297.1710, found $[\text{M}+\text{H}]^+$ 297.1706.

1-(3,5-Dimethylisoxazol-4-yl)-N-(4-methoxyphenyl)piperidin-3-amine (178)

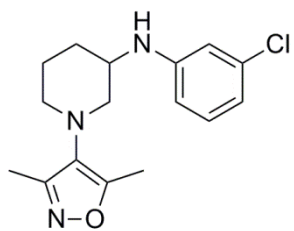


Prepared using General Procedure B (using an alternative purification method) with 1-chloro-4-methoxybenzene (37 mg, 0.26 mmol), heating for 15 h. The Celite-filtered residue was taken up into DCM (1 mL) and purified by normal phase column chromatography (EtOAc in cyclohexane, 0 → 50%, 12 g SiO_2) to provide an impure sample of product which was taken up into 1:1 MeOH:DMSO (1 mL) and purified by MDAP (High pH) to provide the titled compound as a brown oil (38 mg, 49% yield). ν_{max} (neat): 3365 (br.), 2936(m), 2830(w), 1622(w) cm^{-1} ; ^1H NMR (400 MHz, $\text{DMSO}-d_6$) δ = 6.70 (d, J = 9.0 Hz, 2H), 6.57 (d, J = 9.0 Hz, 2H), 4.95 (d, J = 9.0 Hz, 1H), 3.62 (s, 3H), 3.41 - 3.31 (m, 1H), 3.11 (dd, J = 3.4, 11.0 Hz, 1H), 2.96 - 2.88 (m, 1H), 2.86 - 2.77 (m, 1H), 2.62 (dd, J = 8.3, 11.0 Hz, 1H), 2.33 (s, 3H), 2.14 (s, 3H), 1.93 - 1.84 (m, 1H), 1.80 - 1.72 (m, 1H), 1.64 - 1.53 (m, 1H), 1.37 - 1.27 (m, 1H); ^{13}C NMR (101 MHz, CDCl_3) δ = 160.7, 158.2, 152.3, 140.8, 127.9, 115.1 (2C), 115.1 (2C), 57.9, 55.8, 52.8, 50.1, 29.1, 23.5, 11.6, 10.5; LCMS (High pH): t_{R} = 1.18 min, $[\text{M}+\text{H}]^+$ = 302, (100% purity); HRMS: ($\text{C}_{17}\text{H}_{23}\text{N}_3\text{O}_2$) $[\text{M}+\text{H}]^+$ requires 302.1863, found $[\text{M}+\text{H}]^+$ 302.1871.

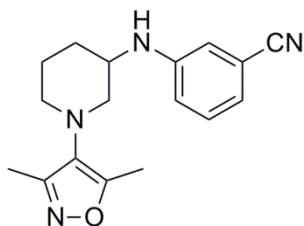
1-(3,5-Dimethylisoxazol-4-yl)-N-(*m*-tolyl)piperidin-3-amine (179)



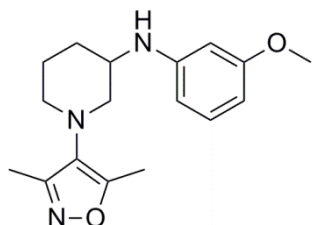
Prepared using General Procedure B with 1-chloro-3-methylbenzene (32 mg, 30 μL , 0.26 mmol), heating for 15 h, to provide the titled compound as a brown oil (18 mg, 25% yield). ν_{max} (CDCl_3): 3350(br.), 2938(m), 2810(w), 1605(s), 1590(m) cm^{-1} ; ^1H NMR (400 MHz, CDCl_3) δ = 7.09 (dt, J = 1.0, 7.3 Hz, 1H), 6.54 (d, J = 7.3 Hz, 1H), 6.49 - 6.44 (m, 2H), 4.00 (br. s., 1H), 3.68 - 3.58 (m, 1H), 3.28 (dd, J = 3.0, 11.1 Hz, 1H), 3.01 - 2.88 (m, 2H), 2.79 (dd, J = 6.3, 11.1 Hz, 1H), 2.40 (s, 3H), 2.30 (s, 3H), 2.27 (s, 3H), 1.90 - 1.80 (m, 2H), 1.73 - 1.57 (m, 2H); ^{13}C NMR (101 MHz, CDCl_3) δ = 160.6, 158.2, 146.8, 139.2, 129.3, 127.9, 118.4, 114.2, 110.5, 58.0, 52.8, 48.9, 29.0, 23.5, 21.6, 11.6, 10.5; LCMS (High pH): t_{R} = 1.34 min, $[\text{M}+\text{H}]^+$ = 286, (100% purity); HRMS: ($\text{C}_{17}\text{H}_{23}\text{N}_3\text{O}$) $[\text{M}+\text{H}]^+$ requires 286.1919, found $[\text{M}+\text{H}]^+$ 286.1930.

***N*-(3-Chlorophenyl)-1-(3,5-dimethylisoxazol-4-yl)piperidin-3-amine (180)**

Prepared using General Procedure B with 1-bromo-3-chlorobenzene (49 mg, 0.26 mmol), heating for 4 h, to provide the titled compound as a brown oil (41 mg, 52% yield). ν_{\max} (CDCl₃): 3349(br.), 2939(w), 2811(w), 1598(s) cm⁻¹; ¹H NMR (400 MHz, CDCl₃) δ = 7.09 (t, J = 7.9 Hz, 1H), 6.69 - 6.64 (m, 1H), 6.61 (t, J = 2.1 Hz, 1H), 6.52 - 6.47 (m, 1H), 4.19 (br. s, 1H), 3.64 - 3.57 (m, 1H), 3.26 (dd, J = 3.1, 11.1 Hz, 1H), 3.01 - 2.88 (m, 2H), 2.80 (dd, J = 6.2, 11.1 Hz, 1H), 2.39 (s, 3H), 2.27 - 2.25 (m, 3H), 1.89 - 1.78 (m, 2H), 1.73 - 1.59 (m, 2H); ¹³C NMR (101 MHz, CDCl₃) δ = 160.8, 158.2, 147.9, 135.2, 130.4, 127.7, 117.2, 112.8, 111.5, 57.7, 52.8, 48.7, 28.6, 23.3, 11.7, 10.6; LCMS (High pH): t_R = 1.33 min, [M+H]⁺ = 306, 308, (100% purity); HRMS: (C₁₆H₂₀³⁵ClN₃O) [M+H]⁺ requires 306.1368, found [M+H]⁺ 306.1357.

***N*-((1-(3,5-Dimethylisoxazol-4-yl)piperidin-3-yl)amino)benzonitrile (181)**

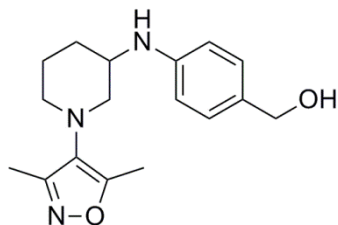
Prepared using General Procedure B with 3-bromobenzonitrile (47 mg, 0.26 mmol), heating for 15 h, to provide the titled compound as a brown oil (28 mg, 37% yield). ν_{\max} (CDCl₃): 3382(br.), 2939(m), 2811(w), 2227(m), 1601(s), 1582(m) cm⁻¹; ¹H NMR (400 MHz, CDCl₃) δ = 7.24 (t, J = 7.8 Hz, 1H), 6.96 (s, 1H), 6.85 - 6.78 (m, 2H), 4.36 (d, J = 8.6 Hz, 1H), 3.67 - 3.59 (m, 1H), 3.26 (dd, J = 3.0, 11.4 Hz, 1H), 3.02 - 2.90 (m, 2H), 2.84 (dd, J = 6.1, 11.4 Hz, 1H), 2.40 (s, 3H), 2.27 (s, 3H), 1.90 - 1.79 (m, 2H), 1.74 - 1.61 (m, 2H); ¹³C NMR (101 MHz, CDCl₃) δ = 160.9, 158.0, 147.1, 130.1, 127.6, 120.7, 119.3, 117.5, 115.4, 113.2, 57.5, 52.8, 48.5, 28.4, 23.1, 11.6, 10.6; LCMS (High pH): t_R = 1.19 min, [M+H]⁺ = 297, (95% purity); HRMS: (C₁₇H₂₀N₄O) [M+H]⁺ requires 297.1710, found [M+H]⁺ 297.1704.

***N*-(3-Methoxyphenyl)-1-(3,5-dimethylisoxazol-4-yl)piperidin-3-amine (182)**

Prepared using General Procedure B with 3-bromoanisole (48 mg, 0.26 mmol), heating for 15 h, to provide the titled compound as a brown oil (31 mg, 40% yield). ν_{\max} (CDCl₃): 3385(br.), 2937(m), 2834(w), 1613(s) cm⁻¹; ¹H NMR (400 MHz, CDCl₃) δ = 7.10 (t, J = 8.1 Hz, 1H), 6.31 - 6.24 (m, 2H), 6.20 (t, J = 2.1 Hz, 1H), 4.06 (br. s, 1H), 3.79 (s, 3H), 3.65 - 3.58 (m, 1H), 3.28 (dd, J = 3.0, 11.1 Hz, 1H), 3.01 - 2.88 (m, 2H), 2.80 (dd, J = 7.1, 11.1 Hz, 1H), 2.39 (s, 3H), 2.26 (s, 3H), 1.90 - 1.80 (m, 2H), 1.73 - 1.58 (m, 2H); ¹³C NMR (101 MHz, CDCl₃) δ = 161.0, 160.7, 158.2,

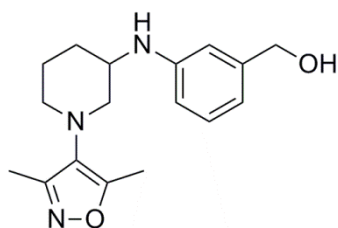
148.2, 130.1, 127.8, 106.5, 102.3, 99.5, 57.9, 55.1, 52.8, 49.0, 29.0, 23.5, 11.6, 10.5; LCMS (High pH): $t_R = 1.24$ min, $[M+H]^+ = 302$, (98% purity); HRMS: ($C_{17}H_{23}N_3O_2$) $[M+H]^+$ requires 302.1863, found $[M+H]^+ 302.1855$.

(4-((1-(3,5-Dimethylisoxazol-4-yl)piperidin-3-yl)amino)phenyl)methanol (183)



A solution of methyl 4-((1-(3,5-dimethylisoxazol-4-yl)piperidin-3-yl)amino)benzoate **190** (50 mg, 0.15 mmol) in THF (2 mL) was added dropwise to $LiAlH_4$, 2.3 M in 2-MeTHF (660 μ L, 1.52 mmol) in THF (2 mL) cooled to 0 °C under a nitrogen atmosphere. The resulting solution was stirred at 0 °C for 16 h before being warmed to 20 °C over 10 min. The reaction mixture was quenched with dropwise addition of H_2O (1 mL), followed by 2 M NaOH (aq, 2 mL) and then further H_2O (3 mL). The resulting mixture was filtered and washed through the filter with EtOAc (20 mL). H_2O (20 mL) was added to the filtrate and the phases were separated. The aqueous phase was further extracted with EtOAc (2 x 20 mL). The combined organics were washed with brine (20 mL), passed through a hydrophobic frit, and the solvent was removed *in vacuo*. The residue was taken up into DCM (1 mL) and purified by normal phase column chromatography (EtOAc in cyclohexane, 0 \rightarrow 80%, 12 g SiO_2) to provide the titled compound as a colourless gum (31 mg, 68% yield). ν_{max} (DCM): 3361(br.), 2937(m), 2855(w), 1614(s) cm^{-1} ; 1H NMR (400 MHz, $DMSO-d_6$) $\delta = 7.02$ (d, $J = 8.1$ Hz, 2H), 6.58 (d, $J = 8.1$ Hz, 2H), 5.42 - 5.21 (m, 1H), 4.30 (s, 2H), 3.44 (br. s., 1H), 3.32 (br. s., 1H), 3.14 (dd, $J = 3.4, 11.0$ Hz, 1H), 2.97 - 2.89 (m, 1H), 2.83 (dt, $J = 2.9, 10.4$ Hz, 1H), 2.64 (dd, $J = 8.3, 11.0$ Hz, 1H), 2.35 (s, 3H), 2.18 - 2.12 (m, 3H), 1.95 - 1.87 (m, 1H), 1.82 - 1.73 (m, 1H), 1.68 - 1.55 (m, 1H), 1.41 - 1.29 (m, 1H); ^{13}C NMR (101 MHz, $CDCl_3$) $\delta = 160.7, 158.2, 146.6, 129.9, 129.0$ (2C), 127.8, 113.4 (2C), 65.3, 57.8, 52.8, 48.9, 28.9, 23.4, 11.6, 10.5; LCMS (High pH): $t_R = 0.97$ min, $[M+H]^+ = 302$, (100% purity); HRMS: ($C_{17}H_{23}N_3O_2$) $[M+H]^+$ requires 302.1863, found $[M+H]^+ 302.1864$.

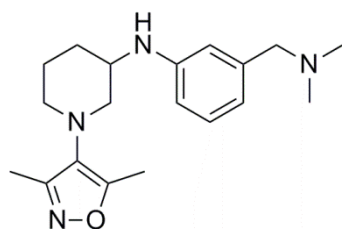
(3-((1-(3,5-Dimethylisoxazol-4-yl)piperidin-3-yl)amino)phenyl)methanol (185)



A solution of *tert*-butyl 3-((1-(3,5-dimethylisoxazol-4-yl)piperidin-3-yl)amino)-benzoate **192** (135 mg, 0.363 mmol) in THF (2 mL) was added dropwise to $LiAlH_4$, 2.3 M in 2-MeTHF (1.58 mL, 3.63 mmol) in THF (2 mL) cooled to 0 °C under a nitrogen atmosphere. The resulting solution was stirred at 0 °C for 2 h, followed by 20 °C for 16 h. The reaction mixture was quenched with dropwise addition of H_2O (1 mL), followed by 2 M NaOH (aq, 2 mL) and then further

H₂O (3 mL). The resulting mixture was filtered and washed through the filter with EtOAc (20 mL). H₂O (20 mL) was added to the filtrate and the phases were separated. The aqueous phase was further extracted with EtOAc (2 x 20 mL). The combined organics were washed with brine (20 mL), passed through a hydrophobic frit, and the solvent was removed *in vacuo*. The residue was taken up into 1:1 MeOH:DMSO (2 mL) and purified by MDAP (High pH) to provide the titled compound as a brown oil (71 mg, 65% yield). ν_{\max} (neat): 3347(br.), 2935(m), 2854(w), 2813(w), 1606(s), 1591(s) cm⁻¹; ¹H NMR (400 MHz, DMSO-*d*₆) δ = 7.00 (t, *J* = 7.7 Hz, 1H), 6.60 (br. s, 1H), 6.50 - 6.44 (m, 2H), 5.36 (d, *J* = 8.6 Hz, 1H), 4.96 (t, *J* = 5.4 Hz, 1H), 4.37 (d, *J* = 4.9 Hz, 2H), 3.49 - 3.39 (m, 1H), 3.15 (dd, *J* = 3.4, 10.9 Hz, 1H), 2.98 - 2.89 (m, 1H), 2.84 (dt, *J* = 2.9, 10.2 Hz, 1H), 2.63 (dd, *J* = 8.4, 10.9 Hz, 1H), 2.35 (s, 3H), 2.16 (s, 3H), 1.97 - 1.87 (m, 1H), 1.83 - 1.72 (m, 1H), 1.68 - 1.55 (m, 1H), 1.41 - 1.29 (m, 1H); ¹³C NMR (101 MHz, CDCl₃) δ = 160.7, 158.2, 147.1, 142.3, 129.6, 127.8, 115.9, 112.6, 111.7, 65.6, 57.9, 52.8, 48.8, 28.9, 23.4, 11.6, 10.5; LCMS (High pH): t_R = 1.01 min, [M+H]⁺ = 302, (100% purity); HRMS: (C₁₇H₂₃N₃O₂) [M+H]⁺ requires 302.1863, found [M+H]⁺ 302.1855.

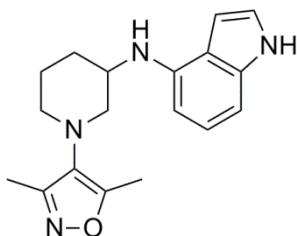
***N*-3-((Dimethylamino)methyl)phenyl)-1-(3,5-dimethylisoxazol-4-yl)piperidin-3-amine (186)**



A solution of 3-((1-(3,5-dimethylisoxazol-4-yl)piperidin-3-yl)amino)-*N,N*-dimethyl-benzamide **193** (47 mg, 0.137 mmol) in THF (2 mL) was added dropwise to LiAlH₄, 2.3 M in 2-MeTHF (597 μ L, 1.37 mmol) in THF (2 mL) cooled to 0 °C under a nitrogen atmosphere. The resulting solution was stirred at 0 °C for 18 h before being allowed to warm to RT. The reaction mixture was quenched with dropwise addition of H₂O (1 mL), followed by 2 M NaOH (aq, 2 mL), and then further H₂O (3 mL). The resulting mixture was filtered and washed through the filter with EtOAc (20 mL). H₂O (20 mL) was added to the filtrate and the phases were separated. The organic phase was washed with brine (20 mL), passed through a hydrophobic frit, and the solvent was removed *in vacuo*. The residue was taken up into 1:1 MeOH:DMSO (1 mL) and purified by MDAP (High pH). The desired fractions were combined and the solvent removed *in vacuo* to give the titled compound as a colourless oil (21 mg, 47% yield). ν_{\max} (neat): 3350(br.), 2938(m), 2854(w), 2812(m), 2769(m), 1605(s), 1590(s) cm⁻¹; ¹H NMR (400 MHz, CDCl₃) δ = 7.12 (t, *J* = 7.9 Hz, 1H), 6.64 - 6.60 (m, 2H), 6.55 - 6.51 (m, 1H), 4.04 (br. s, 1H), 3.65 (br. s, 1H), 3.35 (s, 2H), 3.25 (dd, *J* = 3.2, 11.2 Hz, 1H), 3.00 - 2.87 (m, 2H), 2.78 (dd, *J* = 6.1, 11.2 Hz, 1H), 2.37 (s, 3H), 2.25 (s, 9H), 1.87 - 1.78 (m, 2H), 1.71 - 1.55 (m, 2H); ¹³C NMR (101 MHz, CDCl₃) δ = 160.7, 158.2, 146.9, 140.2, 129.2, 127.9, 118.4, 114.1,

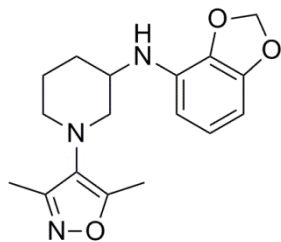
112.0, 64.6, 58.0, 52.8, 48.8, 45.4 (2C), 29.0, 23.5, 11.6, 10.5; LCMS (High pH): $t_R = 1.20$ min, $[M+H]^+ = 329$, (100% purity); HRMS: (C₁₉H₂₈N₄O) $[M+H]^+$ requires 329.2336, found $[M+H]^+ 329.2337$.

***N*-(1-(3,5-Dimethylisoxazol-4-yl)piperidin-3-yl)-1*H*-indol-4-amine (187)**



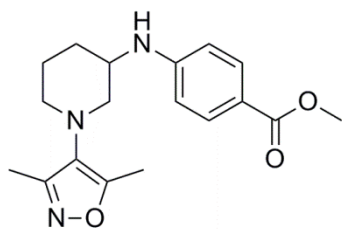
A vial was charged with BrettPhos (8.3 mg, 0.015 mmol) and BrettPhos G1 Precatalyst, TBME adduct (12 mg, 0.015 mmol). The vial was sealed before being evacuated and purged with nitrogen. LiHMDS, 1.0 M in THF (737 μ L, 0.737 mmol) was added, followed by a solution of 1-(3,5-dimethylisoxazol-4-yl)piperidin-3-amine **157** (60 mg, 0.31 mmol) and 4-bromo-1*H*-indole **195** (39 μ L, 0.31 mmol) in THF (0.5 mL). The mixture was heated to 80 °C for 4 h. The solution was allowed to cool to RT and quenched with 1 M HCl (aq, 0.5 mL), diluted with EtOAc (5 mL) and poured into sat. NaHCO₃ (aq, 15 mL). The layers were separated and the aqueous phase was further extracted with EtOAc (3 x 10 mL). The combined organics were washed with brine (5 mL), passed through a hydrophobic frit, and the solvent removed *in vacuo*. The residue was taken up into 1:1 MeOH:DMSO (1 mL) and purified by MDAP (Formic). The desired fractions were concentrated, taken up into 1:1 MeOH:DMSO (1 mL) and purified by MDAP (High pH). The desired fractions were concentrated, taken up into DCM (1 mL) and purified by normal phase column chromatography (EtOAc in cyclohexane, 0 \rightarrow 50%, 12 g SiO₂) to provide the titled compound as a white solid (8 mg, 8% yield). M.pt.: 197–198 °C (colour change to black at 175 °C); ν_{max} (neat): 3248(m), 2922(w), 2846(w), 1594(m) cm⁻¹; ¹H NMR (500 MHz, CDCl₃) $\delta = 8.16$ (br. s., 1H), 7.13 (t, $J = 2.7$ Hz, 1H), 7.09 (t, $J = 8.0$ Hz, 1H), 6.83 (d, $J = 8.0$ Hz, 1H), 6.48 - 6.45 (m, 1H), 6.34 (d, $J = 7.4$ Hz, 1H), 4.47 (br. s, 1H), 3.87 - 3.82 (m, 1H), 3.38 (dd, $J = 2.7, 11.0$ Hz, 1H), 3.03 - 2.90 (m, 3H), 2.42 (s, 3H), 2.30 (s, 3H), 1.94 - 1.85 (m, 2H), 1.84 - 1.76 (m, 1H), 1.73 - 1.64 (m, 1H); ¹³C NMR (126 MHz, CDCl₃) $\delta = 160.8, 158.3, 139.9, 136.6, 127.9, 123.5, 122.0, 116.9, 101.0, 99.9, 98.4, 58.1, 52.9, 48.7, 28.8, 23.5, 11.6, 10.5$; LCMS (Formic): $t_R = 0.84$ min, $[M+H]^+ = 311$, (100% purity); HRMS: (C₁₈H₂₂N₄O) $[M+H]^+$ requires 311.1866, found $[M+H]^+ 311.1875$.

***N*-(Benzo[d][1,3]dioxol-4-yl)-1-(3,5-dimethylisoxazol-4-yl)piperidin-3-amine
(188)**

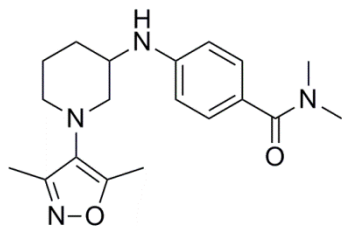


Prepared using General Procedure B (using an alternative purification method) with 4-bromo-1,3-benzodioxole (52 mg, 0.26 mmol), heating for 15 h. The Celite-filtered residue was taken up into DCM (1 mL) and purified by normal phase column chromatography (EtOAc in cyclohexane, 0 → 20%, 12 g SiO₂) to provide the titled compound as a yellow oil (54 mg, 67% yield). ν_{\max} (neat): 3386(br.), 2937(m), 2811(w), 1644(s), 1601(w) cm⁻¹; ¹H NMR (400 MHz, CDCl₃) δ = 6.74 (t, *J* = 8.1 Hz, 1H), 6.35 - 6.30 (m, 2H), 5.94 (d, *J* = 1.5 Hz, 1H), 5.93 (d, *J* = 1.5 Hz, 1H), 4.14 (br. s, 1H), 3.73 - 3.66 (m, 1H), 3.26 (dd, *J* = 2.9, 11.1 Hz, 1H), 3.01 - 2.89 (m, 2H), 2.84 (dd, *J* = 6.0, 11.1 Hz, 1H), 2.39 (s, 3H), 2.26 (s, 3H), 1.91 - 1.76 (m, 2H), 1.72 - 1.61 (m, 2H); ¹³C NMR (101 MHz, CDCl₃) δ = 160.9, 158.3, 147.5, 134.1, 131.5, 127.8, 122.5, 107.3, 100.5, 99.1, 58.0, 52.8, 48.9, 28.9, 23.2, 11.6, 10.5; LCMS (High pH): *t*_R = 1.26 min, [M+H]⁺ = 316, (100% purity); HRMS: (C₁₇H₂₁N₃O₃) [M+H]⁺ requires 316.1656, found [M+H]⁺ 316.1649.

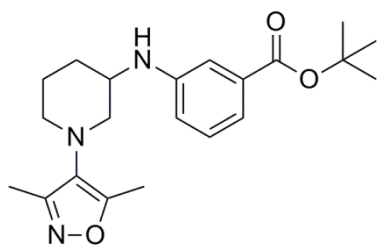
Methyl 4-((1-(3,5-dimethylisoxazol-4-yl)piperidin-3-yl)amino)benzoate (190)



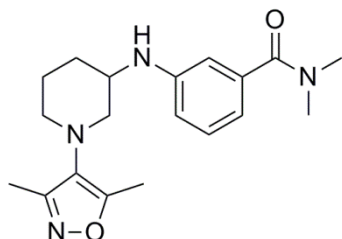
Prepared using General Procedure C with methyl 4-bromobenzoate (110 mg, 0.51 mmol), heating for 4 h, to provide the titled compound as a yellow oil (114 mg, 68% yield). ν_{\max} (CDCl₃): 3367(br.), 2946(w), 2814(w), 1703(m), 1603(s) cm⁻¹; ¹H NMR (500 MHz, CDCl₃) δ = 7.88 (d, *J* = 8.8 Hz, 2H), 6.58 (d, *J* = 8.8 Hz, 2H), 3.87 (s, 3H), 3.74 - 3.69 (m, 1H), 3.27 (dd, *J* = 3.0, 11.3 Hz, 1H), 3.01 - 2.91 (m, 2H), 2.84 (dd, *J* = 6.0, 11.3 Hz, 1H), 2.39 (s, 3H), 2.26 (s, 3H), 1.90 - 1.81 (m, 2H), 1.73 - 1.64 (m, 2H); ¹³C NMR (126 MHz, CDCl₃) δ = 167.2, 160.8, 158.1, 150.6, 131.7 (2C), 127.7, 118.4, 111.8 (2C), 57.6, 52.8, 51.5, 48.3, 28.6, 23.2, 11.6, 10.6; LCMS (High pH): *t*_R = 1.22 min, [M+H]⁺ = 330, (100% purity); HRMS: (C₁₈H₂₃N₃O₃) [M+H]⁺ requires 330.1812, found [M+H]⁺ 330.1804.

4-((1-(3,5-Dimethylisoxazol-4-yl)piperidin-3-yl)amino)-*N,N*-dimethylbenzamide (191)

Prepared using General Procedure C with 4-bromo-*N,N*-dimethylbenzamide (117 mg, 0.51 mmol), heating for 4 h, to provide the titled compound as a yellow oil (118 mg, 67% yield). ν_{\max} (CDCl₃): 3314(br.), 2937(w), 1607(s) cm⁻¹; ¹H NMR (500 MHz, CDCl₃) δ = 7.33 (d, *J* = 8.5 Hz, 2H), 6.60 (d, *J* = 8.5 Hz, 2H), 3.69 - 3.64 (m, 1H), 3.27 (dd, *J* = 3.0, 11.3 Hz, 1H), 3.08 (s, 6H), 3.01 - 2.90 (m, 2H), 2.82 (dd, *J* = 6.2, 11.3 Hz, 1H), 2.39 (s, 3H), 2.26 (s, 3H), 1.89 - 1.81 (m, 2H), 1.72 - 1.61 (m, 2H). Anilinic proton not observed; ¹³C NMR (126 MHz, CDCl₃) δ = 172.0, 160.8, 158.1, 148.1, 129.6 (2C), 127.7, 124.3, 112.2 (2C), 57.7, 52.8, 48.6, 39.7, 34.0, 28.7, 23.3, 11.6, 10.5; LCMS (High pH): *t*_R = 1.03 min, [M+H]⁺ = 343, (100% purity); HRMS: (C₁₉H₂₆N₄O₂) [M+H]⁺ requires 343.2129, found [M+H]⁺ 343.2118.

***tert*-Butyl 3-((1-(3,5-dimethylisoxazol-4-yl)piperidin-3-yl)amino)benzoate (192)**

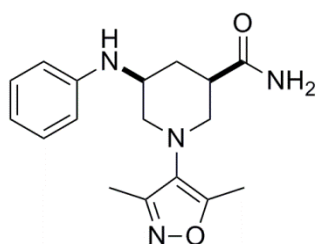
Prepared using General Procedure C with *tert*-butyl-3-bromobenzoate (132 mg, 0.51 mmol), heating for 4 h, to provide the titled compound as a yellow oil (141 mg, 74% yield). ν_{\max} (CDCl₃): 3369(br.), 2975(w), 2937(w), 1709(s), 1605(s), 1587(m) cm⁻¹; ¹H NMR (500 MHz, CDCl₃) δ = 7.34 - 7.31 (m, 1H), 7.28 - 7.26 (m, 1H), 7.22 (t, *J* = 7.8 Hz, 1H), 6.79 (dd, *J* = 1.9, 7.8 Hz, 1H), 3.72 - 3.66 (m, 1H), 3.27 (dd, *J* = 3.0, 11.3 Hz, 1H), 3.01 - 2.90 (m, 2H), 2.81 (dd, *J* = 6.3, 11.3 Hz, 1H), 2.39 (s, 3H), 2.26 (s, 3H), 1.88 - 1.81 (m, 2H), 1.71 - 1.62 (m, 2H), 1.60 (s, 9H). Anilinic proton not observed; ¹³C NMR (126 MHz, CDCl₃) δ = 166.1, 160.8, 158.2, 146.7, 133.1, 129.2, 127.8, 118.5, 117.3, 113.9, 80.8, 57.8, 52.8, 48.8, 28.7, 28.2 (3C), 23.3, 11.6, 10.6; LCMS (High pH): *t*_R = 1.45 min, [M+H]⁺ = 372, (100% purity); HRMS: (C₂₁H₂₉N₃O₃) [M+H]⁺ requires 372.2282, found [M+H]⁺ 372.2275.

3-((1-(3,5-Dimethylisoxazol-4-yl)piperidin-3-yl)amino)-*N,N*-dimethylbenzamide (193)

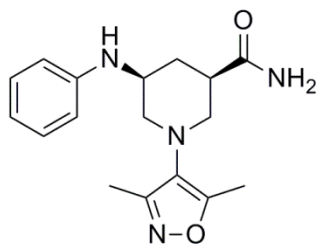
Prepared using General Procedure C with 3-bromo-*N,N*-dimethylbenzamide (117 mg, 0.512 mmol), heating for 15 h, to provide the titled compound as an orange gum (97 mg, 55% yield). ν_{\max} (DCM): 3328 (w), 2936(m), 2810(w), 1623(s), 1603(s), 1582(s) cm⁻¹; ¹H NMR (400 MHz, CDCl₃)

δ = 7.18 (t, J = 7.7 Hz, 1H), 6.71 - 6.61 (m, 3H), 4.20 (br. s., 1H), 3.68 - 3.61 (m, 1H), 3.26 (dd, J = 3.1, 11.1 Hz, 1H), 3.10 (br. s., 3H), 3.00 (br. s., 3H), 2.97 - 2.87 (m, 2H), 2.81 (dd, J = 6.2, 11.1 Hz, 1H), 2.38 (s, 3H), 2.25 (s, 3H), 1.89 - 1.77 (m, 2H), 1.72 - 1.59 (m, 2H); ^{13}C NMR (101 MHz, CDCl_3) δ = 172.0, 160.8, 158.2, 146.9, 137.7, 129.2, 127.8, 115.6, 114.2, 111.7, 57.8, 52.8, 48.7, 39.5, 35.2, 28.7, 23.3, 11.6, 10.5; LCMS (High pH): t_{R} = 1.02 min, $[\text{M}+\text{H}]^+$ = 343, (100% purity); HRMS: ($\text{C}_{19}\text{H}_{26}\text{N}_4\text{O}_2$) $[\text{M}+\text{H}]^+$ requires 343.2129, found $[\text{M}+\text{H}]^+$ 343.2130.

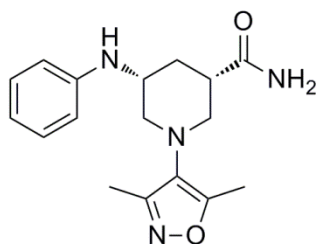
(±)-*cis*-1-(3,5-Dimethylisoxazol-4-yl)-5-(phenylamino)piperidine-3-carboxamide (196)



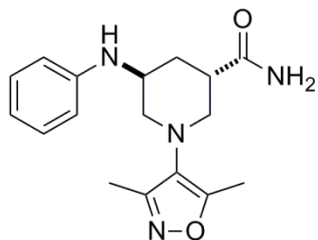
A vial was charged with methyl 1-(3,5-dimethylisoxazol-4-yl)-5-(phenylamino)piperidine-3-carboxylate **198** (124 mg, 0.376 mmol) and MeOH (1.2 mL) and was cooled to 0 °C, with stirring. Magnesium nitride (190 mg, 1.88 mmol) was added and the vial was capped immediately. The mixture was stirred at 0 °C for 1 h, RT for 30 min, and 80 °C for 24 h. The mixture was allowed to cool, MeOH (0.6 mL) was added and the mixture was once again cooled to 0 °C. Another portion of magnesium nitride (114 mg, 1.13 mmol) was added and the mixture was stirred at 0 °C for 1 h, RT for 30 min, and 80 °C for 24 h. The reaction mixture was allowed to cool before being diluted with DCM (25 mL) and H₂O (25 mL). The aqueous layer was neutralised with 2 M HCl (aq, 25 mL) and the layers separated. The aqueous phase was washed with DCM (2 x 25 mL), before being basified with 2 M NaOH (aq, 75 mL) and extracted with DCM (3 x 25 mL). The combined organics were passed through a hydrophobic frit and the solvent was removed *in vacuo*. The residue was taken up into 1:1 MeOH:DMSO (2 mL) and purified by MDAP (Formic) to provide the *trans*-diastereomer **197** (see below) and the titled compound as a light brown oil (43 mg, 36% yield). ν_{max} (CDCl_3): 3343(m), 3196(w), 2940(w), 2819(w), 1670(s), 1602(s) cm^{-1} ; ^1H NMR (400 MHz, CDCl_3) δ = 7.18 (dd, J = 7.3, 8.6 Hz, 2H), 6.72 (t, J = 7.3 Hz, 1H), 6.62 (d, J = 8.6 Hz, 2H), 5.56 (br. s., 1H), 5.51 (br. s., 1H), 3.62 (tt, J = 4.2, 10.0 Hz, 1H), 3.33 (dd, J = 3.9, 11.0 Hz, 1H), 3.17 (dd, J = 4.2, 11.0 Hz, 1H), 3.09 (dd, J = 10.0, 11.5 Hz, 1H), 2.74 - 2.58 (m, 2H), 2.39 - 2.29 (m, 4H), 2.25 (s, 3H), 1.58 (q, J = 11.8 Hz, 1H). Anilinic proton not observed; ^{13}C NMR (101 MHz, CDCl_3) δ = 174.7, 161.4, 158.1, 146.4, 129.5 (2C), 127.1, 117.9, 113.2 (2C), 57.9, 54.4, 49.8, 43.0, 34.1, 11.5, 10.4; LCMS (Formic): t_{R} = 0.74 min, $[\text{M}+\text{H}]^+$ = 315, (99% purity); HRMS: ($\text{C}_{17}\text{H}_{22}\text{N}_4\text{O}_2$) $[\text{M}+\text{H}]^+$ requires 315.1821, found $[\text{M}+\text{H}]^+$ 315.1823.

(3R,5S)-1-(3,5-Dimethylisoxazol-4-yl)-5-(phenylamino)piperidine-3-carboxamide ((-)-196)

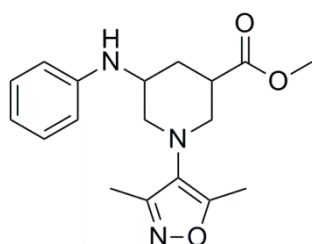
(±)-*cis*-1-(3,5-Dimethylisoxazol-4-yl)-5-(phenylamino)piperidine-3-carboxamide **196** (39 mg) was dissolved in EtOH (2 mL) and separated on a 30 mm x 25 cm Chiralcel OJ-H (5 μm) column, eluting with 50% EtOH + 0.2% *i*PrNH₂ in heptane + 0.2% *i*PrNH₂, to provide the (+)-enantiomer **(+)-196** (see below) and the titled compound as a white solid (15 mg). Identity of enantiomer has been assigned by comparison of biological assay and crystallographic data. e.e. >99.0%; [α]_D²⁰ -12.0° (c 0.25, MeOH); M.pt.: 168–170 °C; ν_{\max} (CDCl₃): 3343(br.), 3191(w), 2950(w), 2819(w), 1668(s), 1602(s) cm⁻¹; ¹H NMR (400 MHz, CDCl₃) δ = 7.18 (dd, *J* = 7.3, 8.6 Hz, 2H), 6.72 (tt, *J* = 1.0, 7.3 Hz, 1H), 6.62 (dd, *J* = 1.0, 8.6 Hz, 2H), 5.59 (br. s., 1H), 5.55 (br. s., 1H), 3.62 (tt, *J* = 4.2, 10.0 Hz, 1H), 3.32 (dd, *J* = 3.7, 11.0 Hz, 1H), 3.16 (dd, *J* = 4.4, 11.0 Hz, 1H), 3.08 (dd, *J* = 10.0, 11.5 Hz, 1H), 2.72 - 2.59 (m, 2H), 2.40 - 2.29 (m, 4H), 2.24 (s, 3H), 1.58 (q, *J* = 11.8 Hz, 1H). Anilinic proton not observed; ¹³C NMR (101 MHz, CDCl₃) δ = 174.7, 161.3, 158.0, 146.4, 129.5 (2C), 127.1, 117.9, 113.2 (2C), 57.8, 54.4, 49.8, 43.0, 34.0, 11.5, 10.4; LCMS (Formic): *t*_R = 0.76 min, [M+H]⁺ = 315, (100% purity); HRMS: (C₁₇H₂₂N₄O₂) [M+H]⁺ requires 315.1821, found [M+H]⁺ 315.1817.

(3S,5R)-1-(3,5-Dimethylisoxazol-4-yl)-5-(phenylamino)piperidine-3-carboxamide ((+)-196)

The titled compound was isolated as per the above protocol, as a white solid (15 mg). Identity of enantiomer has been assigned by comparison of biological assay and crystallographic data. e.e. = 96.6%; [α]_D²⁰ +10.8° (c 0.25, MeOH); M.pt.: 170–171 °C; ν_{\max} (CDCl₃): 3344(br.), 3196(w), 2948(w), 2814(w), 1669(s), 1602(s) cm⁻¹; ¹H NMR (400 MHz, CDCl₃) δ = 7.18 (dd, *J* = 7.3, 8.6 Hz, 2H), 6.72 (tt, *J* = 1.0, 7.3 Hz, 1H), 6.62 (dd, *J* = 1.0, 8.6 Hz, 2H), 5.57 (br. s., 1H), 5.49 (br. s., 1H), 3.62 (tt, *J* = 4.2, 10.0 Hz, 1H), 3.33 (dd, *J* = 3.9, 11.0 Hz, 1H), 3.17 (dd, *J* = 4.4, 11.0 Hz, 1H), 3.09 (dd, *J* = 10.0, 11.5 Hz, 1H), 2.73 - 2.59 (m, 2H), 2.39 - 2.29 (m, 4H), 2.25 (s, 3H), 1.58 (q, *J* = 11.8 Hz, 1H). Anilinic proton not observed; ¹³C NMR (101 MHz, CDCl₃) δ = 174.7, 161.3, 158.0, 146.4, 129.5 (2C), 127.1, 117.9, 113.2 (2C), 57.8, 54.4, 49.8, 43.0, 34.0, 11.5, 10.4; LCMS (Formic): *t*_R = 0.73 min, [M+H]⁺ = 315, (100% purity); HRMS: (C₁₇H₂₂N₄O₂) [M+H]⁺ requires 315.1821, found [M+H]⁺ 315.1824.

(±)-trans-1-(3,5-Dimethylisoxazol-4-yl)-5-(phenylamino)piperidine-3-carboxamide (197)

The titled compound was isolated alongside the *cis*-diastereomer **196** (see above), as a light brown oil (30 mg, 26% yield). ν_{\max} (CDCl₃): 3354(br.), 3196(w), 2940(w), 2825(w), 1668(s), 1602(s) cm⁻¹; ¹H NMR (400 MHz, CDCl₃) δ = 7.20 (dd, J = 7.3, 8.6 Hz, 2H), 6.73 (t, J = 7.3 Hz, 1H), 6.63 (d, J = 8.6 Hz, 2H), 5.82 (br. s, 1H), 5.44 (br. s, 1H), 3.87 - 3.81 (m, 1H), 3.25 (dd, J = 2.8, 11.4 Hz, 1H), 3.21 - 3.15 (m, 2H), 2.93 (dd, J = 4.2, 11.4 Hz, 1H), 2.82 - 2.72 (m, 1H), 2.41 (s, 3H), 2.27 (s, 3H), 2.09 (td, J = 4.2, 13.2 Hz, 1H), 1.96 (ddd, J = 3.2, 10.5, 13.2 Hz, 1H). Anilinic proton not observed; ¹³C NMR (101 MHz, CDCl₃) δ = 175.3, 161.6, 157.9, 146.3, 129.6 (2C), 127.1, 117.8, 113.3 (2C), 57.5, 54.4, 46.8, 39.5, 30.9, 11.7, 10.7; LCMS (Formic): t_R = 0.79 min, [M+H]⁺ = 315, (100% purity); HRMS: (C₁₇H₂₂N₄O₂) [M+H]⁺ requires 315.1821, found [M+H]⁺ 315.1819.

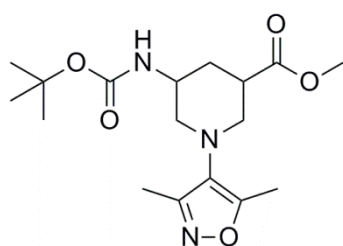
Methyl 1-(3,5-dimethylisoxazol-4-yl)-5-(phenylamino)piperidine-3-carboxylate (198)

A flask containing methyl 5-((*tert*-butoxycarbonyl)amino)-1-(3,5-dimethylisoxazol-4-yl)piperidine-3-carboxylate **200** (608 mg, 1.72 mmol) was evacuated and purged with nitrogen. To this was added DCM (10 mL) and the solution cooled in an ice water bath before being treated with TFA (5.0 mL, 65 mmol). The mixture was stirred at RT under a nitrogen atmosphere for 1.5 h. The solvent was removed *in vacuo* and the residue was taken up into MeOH (2 mL) and loaded onto a pre-equilibrated SCX-2 cartridge (10 g). After 10 minutes the column was flushed with MeOH (100 mL) followed by 2 M NH₃ in MeOH (100 mL). The desired fractions were combined and the solvent removed *in vacuo* to provide the intermediate amine **199** as an orange oil. LCMS (High pH): t_R = 0.69 min, [M+H]⁺ = 254, (63% purity); t_R = 0.71 min, [M+H]⁺ = 254, (28% purity).

To a microwave vial was added Pd₂(dba)₃ (64 mg, 0.070 mmol), DavePhos (41 mg, 0.11 mmol), NaO^tBu (188 mg, 1.96 mmol) and toluene (6 mL). The vial was sealed, and evacuated and purged with nitrogen. To this was added a solution of the amine intermediate **199** (354 mg, 1.40 mmol) and bromobenzene (294 μ L, 2.80 mmol) in toluene (6 mL) and the sealed vial was heated to 130 °C for 4 h. After cooling, the solvent was removed *in vacuo*, and the residue was taken up into EtOAc (25 mL), filtered through

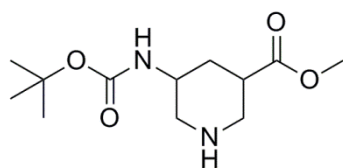
Celite (10 g), and flushed through with further EtOAc (3 x 20 mL). The combined organics were concentrated *in vacuo* and the residue was taken up into DCM (3 mL) and purified by normal phase column chromatography (EtOAc in cyclohexane, 0 → 50%, 80 g SiO₂) to provide the titled compound as an orange gum (124 mg, 22% yield). ¹H NMR suggests the product consists of a 1:1 mixture of diastereomers. ¹H NMR (400 MHz, CDCl₃) δ = 7.23 - 7.14 (m, 2H), 6.75 - 6.58 (m, 3H), 4.20 - 3.79 (m, 1H), 3.73 - 3.65 (m, 3H), 3.36 - 3.14 (m, 3H), 3.03 (dd, *J* = 9.8, 11.2 Hz, 1H), 2.95 - 2.85 (m, 1H), 2.84 - 2.62 (m, 1H), 2.39 - 2.36 (m, 3H), 2.27 - 2.24 (m, 3H), 2.06 - 1.96 (m, 1H), 1.65 - 1.49 (m, 1H); LCMS (Formic): *t_R* = 1.12 min, [M+H]⁺ = 330, (41% purity); *t_R* = 1.14 min, [M+H]⁺ = 330, (59% purity).

Methyl 5-((*tert*-butoxycarbonyl)amino)-1-(3,5-dimethylisoxazol-4-yl)piperidine-3-carboxylate (200)



Methyl 5-((*tert*-butoxycarbonyl)amino)-1-(2,4-dioxopentan-3-yl)piperidine-3-carboxylate **204** (1.41 g, 3.97 mmol) was dissolved in toluene (50 mL) and hydroxylamine hydrochloride (2.76 g, 39.7 mmol) was added. The resulting mixture was heated to reflux using Dean Stark apparatus for 15 h under atmospheric conditions. Further portions of hydroxylamine hydrochloride (1.378 g, 19.94 mmol) were added after 2 h and 10 h. The reaction mixture was allowed to cool to RT, filtered and washed through with EtOAc (3 x 50 mL). The organics were combined washed with water (30 mL), 0.5 M HCl (aq, 30 mL), 0.5 M NaOH (aq, 2 x 30 mL), and brine (30 mL), before being passed through a hydrophobic frit and the solvent being removed *in vacuo*. The residue was taken up into DCM (5 mL) and purified by normal phase column chromatography (EtOAc in cyclohexane, 0 → 50%, 80 g SiO₂) to provide the titled compound as a white solid (718 mg, 51% yield). ¹H NMR suggests the product consists of a 1:1 mixture of diastereomers. ¹H NMR (400 MHz, CDCl₃) δ = 5.14 - 4.60 (m, 1H), 4.04 - 3.73 (m, 1H), 3.71 (s, 3H), 3.23 - 2.95 (m, 3H), 2.84 (dd, *J* = 4.0, 10.9 Hz, 1H), 2.79 - 2.58 (m, 1H), 2.38 - 2.32 (m, 3H), 2.24 - 2.21 (m, 3H), 2.05 - 1.80 (m, 1H), 1.57 - 1.40 (m, 10H); LCMS (Formic): *t_R* = 1.07 min, [M+H]⁺ = 354, (49% purity); *t_R* = 1.08 min, [M+H]⁺ = 354, (51% purity).

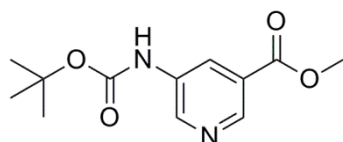
Methyl 5-((*tert*-butoxycarbonyl)amino)piperidine-3-carboxylate (201)



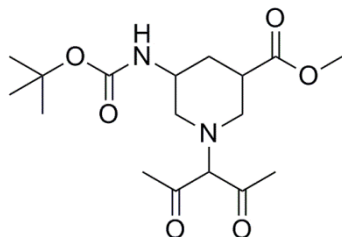
The reaction vessel was purged with nitrogen before being charged with 10 wt% Pd/C (1.62 g, 1.52 mmol), methyl 5-((*tert*-butoxycarbonyl)amino)nicotinate **202** (7.69 g, 30.5 mmol) and MeOH (320 mL). The solution was heated to 65 °C under a 5 bar atmosphere of hydrogen for 18 h. The reaction was allowed to cool

before being purged with nitrogen. The reaction mixture was filtered through a pad of Celite (10 g) and the solvent was removed *in vacuo*. The residue was taken up into 1:1 MeOH:DMSO (10 mL) and purified by reverse phase column chromatography (MeCN in H₂O + 0.1% (NH₄)₂CO₃, 15 → 55%, 400 g C₁₈). The desired fractions were combined and the solvent removed *in vacuo*. The residue was taken up into MeOH (20 mL) and loaded onto a pre-equilibrated aminopropyl cartridge (50 g). After 10 minutes the column was flushed with MeOH (100 mL). The fractions were combined and the solvent removed *in vacuo* to give the titled compound as a white solid (4.47 g, 57% yield). ¹H NMR suggests a 1:1 mixture of diastereomers is present. ¹H NMR (400 MHz, DMSO-*d*₆) δ = 6.82 - 6.64 (m, 1H), 3.60 (s, 1.5H), 3.59 (s, 1.5H), 3.52 - 3.18 (m, 2H), 3.05 - 2.83 (m, 1H), 2.82 - 2.58 (m, 2H), 2.49 - 2.39 (m, 1H), 2.34 - 2.19 (m, 1H), 2.14 - 1.96 (m, 1H), 1.87 - 1.62 (m, 1H), 1.39 (s, 4.5H), 1.38 (s, 4.5H); LCMS (High pH): t_R = 0.76 min, [M+H]⁺ = 259, (54% purity); t_R = 0.78 min, [M+H]⁺ = 259, (46% purity).

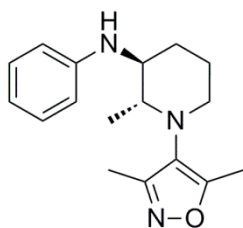
Methyl 5-((*tert*-butoxycarbonyl)amino)nicotinate (**202**)



Methyl 5-aminonicotinate **203** (5.00 g, 32.9 mmol) and Boc anhydride (8.61 g, 39.4 mmol) were dissolved in DCM (100 mL). NEt₃ (6.87 mL, 49.3 mmol) was added, followed by DMAP (803 mg, 6.57 mmol), and the reaction mixture stirred at RT under atmospheric conditions for 15 h. The solvent was removed *in vacuo*. The solid was transferred to a filter with the aid of ice cold water (50 mL) and filtered with further portions of water (3 x 50 mL) and the solid was dried on the filter. The aqueous washings were discarded and the solid was dissolved on the filter in EtOAc (50 mL) and the insoluble solids washed with further EtOAc (3 x 50 mL). The combined organics were concentrated *in vacuo* before being taken up into DMSO (15 mL) and purified by reverse phase column chromatography (MeCN in H₂O + 0.1% (NH₄)₂CO₃, 30 → 70%, 400 g C₁₈). The desired fractions were combined and concentrated *in vacuo*. The remaining aqueous solution was cooled in ice water, filtered, washed on the filter with water (3 x 50 mL) and dried to provide the titled compound as a white solid (4.02 g, 49% yield). M.pt.: 151–153 °C; ν_{max} (neat): 3342(s), 3080(w), 2978(w), 2930(w), 1748(s), 1702(s) cm⁻¹; ¹H NMR (400 MHz, DMSO-*d*₆) δ = 9.84 (s, 1H), 8.78 (d, *J* = 2.7 Hz, 1H), 8.69 (d, *J* = 2.0 Hz, 1H), 8.50 (t, *J* = 2.3 Hz, 1H), 3.89 (s, 3H), 1.50 (s, 9H); ¹³C NMR (101 MHz, DMSO-*d*₆) δ = 165.2, 152.7, 143.5, 143.2, 136.3, 125.3, 124.5, 80.1, 52.4, 28.0 (3C); LCMS (High pH): t_R = 0.96 min, [M+H]⁺ = 253, (100% purity); HRMS: (C₁₂H₁₆N₂O₄) [M+H]⁺ requires 253.1183, found [M+H]⁺ 253.1187.

Methyl 5-((*tert*-butoxycarbonyl)amino)-1-(2,4-dioxopentan-3-yl)piperidine-3-carboxylate (204)

A solution of methyl 5-((*tert*-butoxycarbonyl)amino)-piperidine-3-carboxylate **201** (2.00 g, 7.74 mmol) and NEt_3 (1.51 mL, 10.8 mmol) in MeCN (60 mL) was stirred at RT under a nitrogen atmosphere. 3-Chloropentane-2,4-dione **70** (1.22 mL, 10.8 mmol) was added and the resulting solution was stirred at RT under a nitrogen atmosphere for 19 h. The solvent was removed *in vacuo* and the residue was taken up into EtOAc (200 mL) and washed with H_2O (2 x 50 mL) and brine (50 mL) before being passed through a hydrophobic frit, and the solvent being removed *in vacuo*. The residue was taken up into DCM (5 mL) and purified by normal phase column chromatography (EtOAc in cyclohexane, 0 → 50%, 120 g SiO_2) to provide the titled compound as an orange gum (1.46 g, 53% yield). ^1H NMR suggests product consists of a 1:1 mixture of diastereomers and mainly exists in an enol form in CDCl_3 . ^1H NMR (400 MHz, CDCl_3) δ = 16.11 - 15.79 (m, 1H), 4.81 - 4.60 (m, 1H), 4.10 - 3.84 (m, 1H), 3.76 - 3.65 (m, 3H), 3.19 - 2.91 (m, 2H), 2.82 - 2.54 (m, 2H), 2.51 - 2.28 (m, 1H), 2.27 - 2.16 (m, 3H), 2.13 - 1.96 (m, 3H), 1.87 - 1.58 (m, 1H), 1.56 - 1.48 (m, 1H), 1.45 (s, 9H); LCMS (Formic): t_{R} = 1.04 min, $[\text{M}+\text{H}]^+$ = 357, (100% purity).

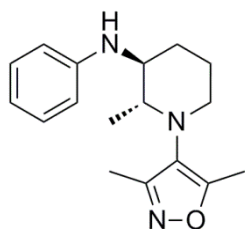
(2*R*,3*S*)-1-(3,5-Dimethylisoxazol-4-yl)-2-methyl-*N*-phenylpiperidin-3-amine (205)

(5*S*,6*R*)-1-(3,5-Dimethylisoxazol-4-yl)-6-methyl-5-(phenylamino)-piperidin-2-one **226** (27 mg, 0.090 mmol) was dissolved in THF (1 mL) and the flask evacuated and purged with nitrogen. $\text{BH}_3\cdot\text{THF}$, 1 M in THF (450 μL , 0.45 mmol) was added and the mixture was stirred at RT for 4 h. After 2 h further $\text{BH}_3\cdot\text{THF}$, 1 M in THF (450 μL , 0.45 mmol) was added. The reaction mixture was quenched with 2 M HCl (aq, 3 mL), dropwise. After 15 minutes the mixture was neutralised with 2 M NaOH (aq, 3 mL) and extracted with DCM (3 x 20 mL). The combined organics were passed through a hydrophobic frit and the solvent was removed *in vacuo*. The residue was taken up into DCM (2 mL) and purified by normal phase column chromatography (EtOAc in cyclohexane, 0 → 30%, 12 g SiO_2) to provide the titled compound as a colourless oil (19 mg, 74%). e.e. = 44.0%; ν_{max} (neat): 3356(br.), 2932(m), 2854(w), 2805(w), 1601(s) cm^{-1} ; ^1H NMR (400 MHz, CDCl_3) δ = 7.21 - 7.15 (m, 2H), 6.69 (tt, J = 1.0, 7.3 Hz, 1H), 6.65 - 6.60 (m, 2H), 3.83 (br. s, 1H), 3.27 (ddd, J = 3.8, 6.4, 8.1 Hz, 1H), 3.09 (ddd, J = 4.0, 6.8, 11.2 Hz, 1H), 2.94 (quin, J = 6.5 Hz, 1H), 2.87 (ddd, J = 3.5, 8.2, 11.2 Hz, 1H), 2.35 (s, 3H),

2.23 (s, 3H), 2.11 - 2.02 (m, 1H), 1.81 - 1.71 (m, 1H), 1.71 - 1.59 (m, 1H), 1.51 - 1.39 (m, 1H), 1.06 (d, $J = 6.5$ Hz, 3H); ^{13}C NMR (151 MHz, CDCl_3) $\delta = 162.5, 158.8, 147.3, 129.4$ (2C), 126.2, 117.2, 113.3 (2C), 60.7, 54.7, 50.3, 28.6, 23.9, 15.5, 11.4, 10.7; LCMS (Formic): $t_{\text{R}} = 1.30$ min, $[\text{M}+\text{H}]^+ = 286$, (100% purity); HRMS: ($\text{C}_{17}\text{H}_{23}\text{N}_3\text{O}$) $[\text{M}+\text{H}]^+$ requires 286.1919, found $[\text{M}+\text{H}]^+ 286.1925$. Diastereomer assigned by examining the 1D ROESY correlation between piperidinyll methine peaks, and comparing the strength of this correlation with that of corresponding interaction in the opposite diastereomer **206**. Irradiation of the peak at 3.27 ppm resulted in a ROESY correlation with the peak at 2.94 ppm that was roughly 50% weaker than the correlation seen for the opposite diastereomer **206**, indicating that the protons are on opposite sides of the ring.

(2R,3S)-1-(3,5-Dimethylisoxazol-4-yl)-2-methyl-N-phenylpiperidin-3-amine

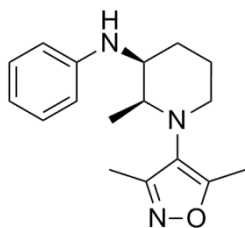
(205a)



Enantioenriched sample **205** (15 mg) was dissolved in EtOH (1 mL) and purified on a 30 mm x 25 cm Chiralcel OJ-H (5 μm) column, eluting with 15% [EtOH + 0.2% *i*PrNH₂] in [Heptane + 0.2% *i*PrNH₂] to provide the 2*S*,3*R*-enantiomer **236** and the titled compound as a colourless oil (9 mg). e.e. = 96.5%; ν_{max} (CDCl_3): 3370(br.), 2935(m), 2858(w), 2812(w), 1602(s) cm^{-1} ; ^1H NMR (400 MHz, CDCl_3) $\delta = 7.21 - 7.15$ (m, 2H), 6.70 (t, $J = 7.3$ Hz, 1H), 6.64 (d, $J = 7.8$ Hz, 2H), 3.31 - 3.24 (m, 1H), 3.13 - 3.05 (m, 1H), 2.95 (quin, $J = 6.4$ Hz, 1H), 2.87 (ddd, $J = 3.4, 8.1, 11.4$ Hz, 1H), 2.35 (s, 3H), 2.23 (s, 3H), 2.11 - 2.02 (m, 1H), 1.81 - 1.71 (m, 1H), 1.71 - 1.60 (m, 1H), 1.51 - 1.40 (m, 1H), 1.06 (d, $J = 6.4$ Hz, 3H); LCMS (High pH): $t_{\text{R}} = 1.32$, $[\text{M}+\text{H}]^+ = 286$, (100% purity); HRMS: ($\text{C}_{17}\text{H}_{23}\text{N}_3\text{O}$) $[\text{M}+\text{H}]^+$ requires 286.1919, found $[\text{M}+\text{H}]^+ 286.1917$.

(2S,3S)-1-(3,5-Dimethylisoxazol-4-yl)-2-methyl-N-phenylpiperidin-3-amine

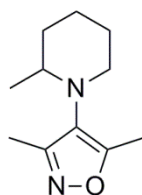
(206)



(5*S*,6*S*)-1-(3,5-Dimethylisoxazol-4-yl)-6-methyl-5-(phenylamino)-piperidin-2-one **227** (127 mg, 0.424 mmol) was dissolved in THF (3 mL) and the flask evacuated and purged with nitrogen. $\text{BH}_3\cdot\text{THF}$, 1 M in THF (2.12 mL, 2.12 mmol) was added and the mixture was stirred at RT for 2 h before being quenched with 2 M HCl (aq, 6 mL), dropwise. After 15 minutes the mixture was neutralised with 2 M NaOH (aq, 6 mL) and extracted with DCM (3 x 25 mL). The combined organics were passed through a hydrophobic frit and the solvent was removed *in vacuo*. The residue was taken up into DCM (2 mL) and purified by normal phase column chromatography (EtOAc in cyclohexane, 0 \rightarrow 30%, 12 g SiO_2) to provide the titled compound as an orange oil (85

mg, 70% yield). e.e. = 44.2%; $[\alpha]_D^{20} +41.2^\circ$ (c 0.25 MeOH); ν_{\max} (neat): 3402(br.), 2933(m), 2854(w), 2816(w), 1600(s) cm^{-1} ; $^1\text{H NMR}$ (400 MHz, CDCl_3) δ = 7.21 - 7.15 (m, 2H), 6.68 (tt, J = 1.0, 7.3 Hz, 1H), 6.65 - 6.60 (m, 2H), 4.32 (br. s, 1H), 3.63 - 3.57 (m, 1H), 3.31 (dq, J = 2.4, 6.6 Hz, 1H), 2.98 (dd, J = 3.1, 7.9 Hz, 2H), 2.38 (s, 3H), 2.29 (s, 3H), 2.11 - 2.01 (m, 1H), 1.91 - 1.76 (m, 1H), 1.60 - 1.48 (m, 2H), 0.92 (d, J = 6.6 Hz, 3H); $^{13}\text{C NMR}$ (151 MHz, CDCl_3) δ = 163.3, 159.0, 147.4, 129.4 (2C), 125.6, 116.8, 113.1 (2C), 58.6, 53.2, 52.2, 27.9, 21.9, 16.3, 11.3, 10.8; LCMS (Formic): t_R = 1.31 min, $[\text{M}+\text{H}]^+$ = 286, (100% purity); HRMS: ($\text{C}_{17}\text{H}_{23}\text{N}_3\text{O}$) $[\text{M}+\text{H}]^+$ requires 286.1919, found $[\text{M}+\text{H}]^+$ 286.1927. Diastereomer assigned by examining the 1D ROESY correlation between piperidinyll methine peaks, and comparing the strength of this correlation with that of corresponding interaction in the opposite diastereomer **205**. Irradiation of the peak at 3.60 ppm resulted in a ROESY correlation with the peak at 3.31 ppm that was roughly twice as strong as the correlation seen for the opposite diastereomer, indicating that the protons are on the same face of the ring.

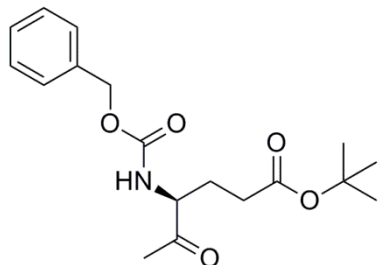
3,5-Dimethyl-4-(2-methylpiperidin-1-yl)isoxazole (208)



4-Amino-3,5-dimethylisoxazole **46** (100 mg, 0.892 mmol) was dissolved in MeOH (2.5 mL) and AcOH (0.278 mL). 6-Chlorohexan-2-one **210** (118 μL , 0.892 mmol) was added, followed by picoline borane (95 mg, 0.89 mmol). The reaction vessel was sealed and stirred at RT for 16 h. The solvent was removed *in vacuo*. 2 M HCl (aq, 5 mL) was added and the mixture was left to stand for 30 min. The solution was then basified with sat. Na_2CO_3 (aq, 10 mL), and extracted with DCM (3 x 20 mL). The organics were passed through a hydrophobic frit and the solvent was removed *in vacuo*. The residue was dissolved in THF (3 mL) and the flask sealed before being evacuated and purged with nitrogen. $t\text{-BuOK}$, 1 M in THF (1.96 mL, 1.96 mmol) was added and the solution was stirred for 2 h at RT. LiHMDS, 1 M in THF (1.96 mL, 1.96 mmol) was added and the reaction mixture stirred for 30 min at RT. The reaction mixture was partitioned between sat. NH_4Cl (aq, 10 mL) and EtOAc (15 mL). The aqueous phase was further extracted with EtOAc (2 x 15 mL) and the combined organics were washed with brine (25 mL) before being passed through a hydrophobic frit. The solvent was removed *in vacuo* and the residue was taken up into DCM (0.5 mL) and purified by normal phase column chromatography (EtOAc in cyclohexane, 0 \rightarrow 20%, 24 g SiO_2) to provide the titled compound as a yellow oil (77 mg, 44% yield). ν_{\max} (neat): 2931(s), 2856(w), 2811(w), 1677(w), 1638(w) cm^{-1} ; $^1\text{H NMR}$ (400 MHz, CDCl_3) δ = 2.98 - 2.83 (m, 3H), 2.31 (s, 3H), 2.23 (s, 3H), 1.82 - 1.56 (m, 4H), 1.44 - 1.22 (m, 2H), 0.85 (d, J = 6.4 Hz, 3H); $^{13}\text{C NMR}$ (101 MHz, CDCl_3) δ = 163.3, 159.2, 126.4, 55.1, 53.9, 35.3, 26.9,

24.6, 20.6, 11.1, 10.7; LCMS (High pH): $t_R = 1.25$ min, $[M+H]^+ = 195$, (100% purity); HRMS: ($C_{11}H_{18}N_2O$) $[M+H]^+$ requires 195.1492, found $[M+H]^+ 195.1493$.

***tert*-Butyl (*S*)-4-(((benzyloxy)carbonyl)amino)-5-oxohexanoate (**217**)**

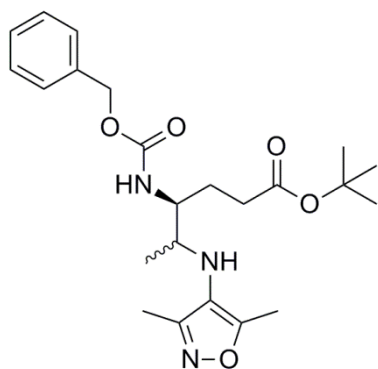


N,O-Dimethylhydroxylamine hydrochloride (867 mg, 8.89 mmol) and DIPEA (4.66 mL, 26.7 mmol) were dissolved in DMF (100 mL) and cooled to 0 °C under a nitrogen atmosphere. (*S*)-2-(((benzyloxy)carbonyl)amino)-5-(*tert*-butoxy)-5-oxopentanoic acid **215** (3.00 g, 8.89 mmol) followed by COMU (3.81 g, 8.89 mmol). The mixture was stirred for 20 min at 0 °C then allowed to warm to RT and stirred for 3 h. The solution was diluted with H₂O (200 mL) and extracted with Et₂O (4 x 100 mL). The combined organics were washed with 1 M HCl (aq, 30 mL), sat. Na₂CO₃ (aq, 3 x 30 mL) and brine (30 mL) before being passed through a hydrophobic frit and the solvent being removed *in vacuo* to provide the Weinreb amide intermediate **216** as a pink oil (3.42 g). Product was taken on to the next step without purification. LCMS (Formic): $t_R = 1.14$ min, $[M+H]^+ = 381$, (83% purity); ¹H NMR (400 MHz, CDCl₃) $\delta = 7.38 - 7.28$ (m, 5H), 5.13 (d, $J = 12.2$ Hz, 1H), 5.08 (d, $J = 12.2$ Hz, 1H), 5.17 - 5.04 (m, 1H), 4.83 - 4.69 (m, 1H), 3.79 (s, 3H), 3.22 (s, 3H), 2.33 (t, $J = 7.6$ Hz, 2H), 2.11 - 2.00 (m, 1H), 1.95 - 1.82 (m, 1H), 1.44 (s, 9H).

The intermediate **216** was dissolved in THF (70 mL) and cooled to -78 °C under a nitrogen atmosphere. MeMgBr, 3 M in Et₂O (8.47 mL, 25.4 mmol) was added dropwise. The reaction mixture was stirred at -78 °C for 1 h before being allowed to warm to 0 °C, stirred for 2 h and then allowed to warm to RT and stirred for 4 h. The reaction mixture was cooled to 0 °C and 0.5 M HCl (aq, 10 mL) was added, dropwise. The reaction mixture was partitioned between 0.5 M HCl (aq, 50 mL) and EtOAc (50 mL). The aqueous phase was further extracted with EtOAc (2 x 75 mL). The combined organics were washed with brine (30 mL), passed through a hydrophobic frit, and the solvent was removed *in vacuo*. The residue was taken up into DCM (5 mL) and purified by normal phase column chromatography (EtOAc in cyclohexane, 0 → 30%, 120 g SiO₂) to provide the titled compound as a colourless oil (1.77 g, 59% yield). e.e. = 47.9%; ν_{max} (neat): 3337(br.), 2978(w), 2931(w), 1717(s) cm⁻¹; ¹H NMR (400 MHz, CDCl₃) $\delta = 7.42 - 7.28$ (m, 5H), 5.63 - 5.47 (m, 1H), 5.11 (s, 2H), 4.48 - 4.37 (m, 1H), 2.45 - 2.11 (m, 6H), 1.89 - 1.76 (m, 1H), 1.44 (s, 9H); ¹³C NMR (101 MHz, CDCl₃) $\delta = 206.2, 172.1, 156.0, 136.3, 128.5$ (2C), 128.2, 128.1 (2C), 80.9, 67.0, 59.7, 30.9, 28.1 (3C), 27.0, 26.5; LCMS (Formic): $t_R = 1.16$ min,

$[M-C_4H_8+H]^+ = 280$, (100% purity); HRMS: $(C_{18}H_{25}NO_5)$ $[M+H]^+$ requires 336.1806, found $[M+H]^+ 336.1800$.

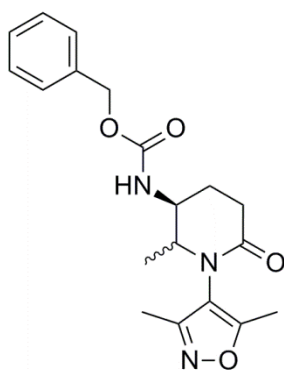
***tert*-Butyl (4*S*)-4-(((benzyloxy)carbonyl)amino)-5-((3,5-dimethylisoxazol-4-yl)amino)hexanoate (218)**



4-Amino-3,5-dimethylisoxazole **46** (584 mg, 5.21 mmol) and *tert*-butyl (*S*)-4-(((benzyloxy)carbonyl)amino)-5-oxohexanoate **217** (1.75 g, 5.21 mmol) were dissolved in MeOH (27 mL) and AcOH (3.0 mL). Picoline borane (557 mg, 5.21 mmol) was added and the reaction vessel was sealed and stirred at RT for 16 h. The reaction mixture was concentrated *in vacuo* and 2 M HCl (aq, 50 mL) was added. The solution was left to

stand for 30 min before being basified with sat. Na_2CO_3 (aq, 50 mL) and extracted with EtOAc (3 x 50 mL). The combined organics were washed with brine (25 mL), passed through a hydrophobic frit, and the solvent was removed *in vacuo*. The residue was taken up into DCM (6 mL) and purified by normal phase column chromatography (3:1 EtOAc:EtOH in cyclohexane, 0 → 40%, 120 g SiO_2) to provide the titled compound as a colourless oil (2.13 g, 94% yield). 1H NMR suggests a 1:3 mixture of diastereomers. Major Diastereomer: 1H NMR (400 MHz, $CDCl_3$) $\delta = 7.40 - 7.32$ (m, 5H), 5.20 - 5.07 (m, 2H), 5.02 - 4.89 (m, 1H), 3.71 - 3.59 (m, 1H), 3.16 - 2.99 (m, 1H), 2.36 (t, $J = 7.6$ Hz, 2H), 2.31 (s, 3H), 2.20 (s, 3H), 2.02 - 1.58 (m, 3H), 1.48 - 1.43 (m, 9H), 1.05 (d, $J = 6.4$ Hz, 3H); Minor Diastereomer: 1H NMR (400 MHz, $CDCl_3$) $\delta = 7.40 - 7.32$ (m, 5H), 5.20 - 5.07 (m, 2H), 5.02 - 4.89 (m, 1H), 3.81 - 3.71 (m, 1H), 3.16 - 2.99 (m, 1H), 2.36 (t, $J = 7.6$ Hz, 2H), 2.26 (s, 3H), 2.14 (s, 3H), 2.02 - 1.58 (m, 3H), 1.48 - 1.43 (m, 9H), 1.07 (d, $J = 6.4$ Hz, 3H); LCMS (High pH): $t_R = 1.25$ min, $[M+H]^+ = 432$, (95% purity).

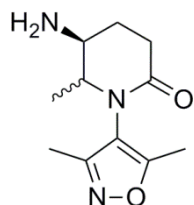
Benzyl ((3*S*)-1-(3,5-dimethylisoxazol-4-yl)-2-methyl-6-oxopiperidin-3-yl)carbamate (224)



TFA (5 mL, 64.9 mmol) was added dropwise to a stirred solution of *tert*-butyl (4*S*)-4-(((benzyloxy)carbonyl)amino)-5-((3,5-dimethylisoxazol-4-yl)amino)hexanoate **218** (953 mg, 2.21 mmol) in DCM (20 mL), using ice water for external cooling. The reaction mixture was allowed to warm to RT and stirred for 2 h, before being heated to 40 °C for 16 h, under atmospheric conditions. The reaction mixture was allowed to cool before being quenched with sat. $NaHCO_3$ (aq, 50 mL) and

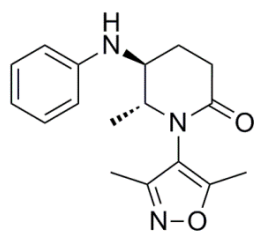
extracted with DCM (3 x 50 mL). The combined organics were washed with brine (25 mL), passed through a hydrophobic frit, and the solvent was removed *in vacuo*. The residue was taken up into DCM (3 mL) and purified by normal phase column chromatography (3:1 EtOAc:EtOH in cyclohexane, 0 → 100%, 40 g SiO₂) to provide the titled compound as a colourless gum (487 mg, 62% yield). ¹H NMR suggests a 1:3 mixture of diastereomers. Major Diastereomer: ¹H NMR (400 MHz, DMSO-*d*₆, 120 °C) δ = 7.49 - 7.29 (m, 6H), 5.15 - 5.02 (m, 2H), 4.16 - 4.03 (m, 1H), 3.84 - 3.58 (m, 1H), 2.68 - 2.39 (m, 2H), 2.24 (s, 3H), 2.06 (s, 3H), 2.05 - 1.97 (m, 1H), 1.95 - 1.81 (m, 1H), 1.05 (d, *J* = 6.6 Hz, 3H); Minor Diastereomer: ¹H NMR (400 MHz, DMSO-*d*₆, 120 °C) δ = 7.49 - 7.29 (m, 6H), 5.15 - 5.02 (m, 2H), 4.16 - 4.03 (m, 1H), 3.84 - 3.58 (m, 1H), 2.68 - 2.39 (m, 2H), 2.20 (s, 3H), 2.02 (s, 3H), 2.05 - 1.97 (m, 1H), 1.95 - 1.81 (m, 1H), 1.11 (d, *J* = 6.6 Hz, 3H); LCMS (High pH): *t*_R = 0.91 min, [M+H]⁺ = 358, (100% purity).

(5*S*)-5-Amino-1-(3,5-dimethylisoxazol-4-yl)-6-methylpiperidin-2-one (225)



A solution of benzyl ((3*S*)-1-(3,5-dimethylisoxazol-4-yl)-2-methyl-6-oxopiperidin-3-yl)carbamate **224** (240 mg, 0.671 mmol) in conc. HCl (6.00 mL, 72.0 mmol) was stirred at RT, under atmospheric conditions, for 4 h. The solvent was removed *in vacuo* and the residue taken up into MeOH (1 mL) and loaded onto a pre-equilibrated SCX-2 cartridge (2 g). After 10 minutes the column was flushed with MeOH (30 mL) followed by NH₃, 2 M in MeOH (30 mL). The desired fractions were combined and the solvent was removed *in vacuo* to give the titled compound as a colourless gum (133 mg, 89% yield). ¹H NMR suggests a 1:3 mixture of diastereomers. Major Diastereomer: ¹H NMR (400 MHz, DMSO-*d*₆, 120 °C) δ = 3.65 - 3.49 (m, 1H), 3.39 - 3.29 (m, 1H), 2.59 - 2.47 (m, 1H), 2.46 - 2.31 (m, 1H), 2.24 (s, 3H), 2.06 (s, 3H), 1.88 - 1.67 (m, 2H), 1.59 (br. s., 2H), 1.05 (d, *J* = 6.6 Hz, 3H); Minor Diastereomer: ¹H NMR (400 MHz, DMSO-*d*₆, 120 °C) δ = 3.39 - 3.29 (m, 1H), 3.00 - 2.90 (m, 1H), 2.59 - 2.47 (m, 1H), 2.46 - 2.31 (m, 1H), 2.25 (s, 3H), 2.07 (s, 3H), 1.88 - 1.67 (m, 2H), 1.59 (br. s., 2H), 1.09 (d, *J* = 6.6 Hz, 3H); LCMS (High pH): *t*_R = 0.44 min, [M+H]⁺ = 224, (74%); *t*_R = 0.48 min, [M+H]⁺ = 224, (26%).

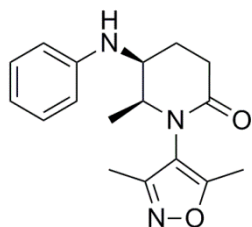
(5*S*,6*R*)-1-(3,5-Dimethylisoxazol-4-yl)-6-methyl-5-(phenylamino)piperidin-2-one (226)



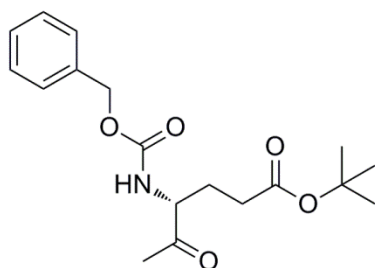
A microwave vial was charged with Pd₂(dba)₃ (25 mg, 0.027 mmol), DavePhos (16 mg, 0.040 mmol), NaO^tBu (72 mg, 0.75 mmol) and toluene (0.5 mL). The vial was sealed before being evacuated and purged with nitrogen. To this was added a solution of (5*S*)-5-amino-1-(3,5-dimethylisoxazol-4-yl)-6-methylpiperidin-2-one

ridin-2-one **225** (120 mg, 0.537 mmol) and bromobenzene (113 μ L, 1.08 mmol) in toluene (0.5 mL) and the sealed vial was heated to 130 $^{\circ}$ C for 15 h. This was allowed to cool and the solvent was removed under a stream of nitrogen. The residue was taken up into EtOAc (10 mL) and filtered through Celite (2.5 g), and flushed through with further EtOAc (3 x 20 mL). The combined organics were concentrated *in vacuo* and the residue was dissolved in DCM (4 mL) and purified by normal phase column chromatography (3:1 EtOAc:EtOH in cyclohexane, 0 \rightarrow 100%, 40 g SiO₂). The fractions were combined in two separate batches which were concentrated *in vacuo* and taken up into 1:1 MeOH:DMSO (3 mL total) and further purified by MDAP (High pH) to provide the major diastereomer **227** (see below) and the titled compound, as a pale yellow solid (24 mg, 15% yield). e.e. = 44.6%; $[\alpha]_D^{20}$ -25.8 $^{\circ}$ (c 0.25, MeOH); M.pt.: 174–177 $^{\circ}$ C; ν_{\max} (neat): 3323(m), 2977(w), 2927(w), 1652(s), 1639(s), 1601(s) cm^{-1} ; $^1\text{H NMR}$ (400 MHz, DMSO-*d*₆, 120 $^{\circ}$ C) δ = 7.15 - 7.08 (m, 2H), 6.74 - 6.68 (m, 2H), 6.59 (tt, J = 1.0, 7.3 Hz, 1H), 5.61 (d, J = 7.6 Hz, 1H), 3.71 - 3.59 (m, 2H), 2.74 - 2.63 (m, 1H), 2.54 - 2.45 (m, 1H), 2.33 - 2.22 (m, 1H), 2.15 (s, 3H), 1.98 (s, 3H), 1.93 - 1.82 (m, 1H), 1.20 (d, J = 6.4 Hz, 3H); $^{13}\text{C NMR}$ (101 MHz, DMSO-*d*₆, 120 $^{\circ}$ C) δ = 168.3, 163.5, 157.5, 146.9, 128.3 (2C), 117.5, 115.9, 112.6 (2C), 59.0, 51.1, 27.7, 22.4, 18.4, 9.7, 8.4; LCMS (High pH): t_R = 0.99 min, $[\text{M}+\text{H}]^+$ = 300, (100% purity); HRMS: (C₁₇H₂₁N₃O₂) $[\text{M}+\text{H}]^+$ requires 300.1712, found $[\text{M}+\text{H}]^+$ 300.1720.

(5*S*,6*S*)-1-(3,5-Dimethylisoxazol-4-yl)-6-methyl-5-(phenylamino)piperidin-2-one (227)



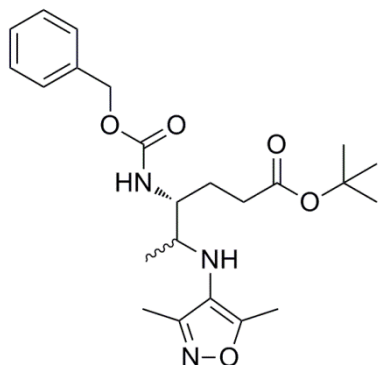
The titled compound was isolated as the major diastereomer of the above protocol **226** as an orange oil (67 mg, 42% yield). e.e. = 46.6%; $[\alpha]_D^{20}$ +8.4 $^{\circ}$ (c 0.25, MeOH); ν_{\max} (neat): 3346(br.), 3057(w), 2975(w), 1655(s), 1638(s), 1601(s) cm^{-1} ; $^1\text{H NMR}$ (400 MHz, DMSO-*d*₆, 120 $^{\circ}$ C) δ = 7.12 - 7.04 (m, 2H), 6.71 (d, J = 7.6 Hz, 2H), 6.56 (t, J = 7.3 Hz, 1H), 5.36 (d, J = 8.6 Hz, 1H), 4.12 - 4.03 (m, 1H), 3.74 (quin, J = 5.9 Hz, 1H), 2.60 - 2.53 (m, 2H), 2.27 (s, 3H), 2.09 (s, 3H), 2.07 - 1.88 (m, 2H), 1.06 (d, J = 6.6 Hz, 3H); $^{13}\text{C NMR}$ (101 MHz, DMSO-*d*₆, 120 $^{\circ}$ C) δ = 168.1, 163.4, 157.3, 146.8, 128.3 (2C), 118.0, 116.0, 112.6 (2C), 56.4, 49.8, 29.3, 22.1, 13.3, 9.9, 8.6; LCMS (High pH): t_R = 0.94 min, $[\text{M}+\text{H}]^+$ = 300, (100% purity); HRMS: (C₁₇H₂₁N₃O₂) $[\text{M}+\text{H}]^+$ requires 300.1712, found $[\text{M}+\text{H}]^+$ 300.1723.

***tert*-Butyl (*R*)-4-(((benzyloxy)carbonyl)amino)-5-oxohexanoate (**228**)**

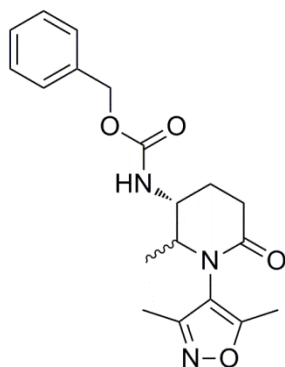
N,O-Dimethylhydroxylamine hydrochloride (867 mg, 8.89 mmol) and DIPEA (4.66 mL, 26.7 mmol) were dissolved in DMF (100 mL) and cooled to 0 °C under a nitrogen atmosphere. (*R*)-2-(((benzyloxy)carbonyl)amino)-5-(*tert*-butoxy)-5-oxopentanoic acid (3.00 g, 8.89 mmol) was added, followed by COMU (3.81 g, 8.89

mmol). The mixture was stirred for 20 min at 0 °C then allowed to warm to RT and stirred for 3 h. The solution was diluted with H₂O (200 mL) and extracted with Et₂O (4 x 100 mL). The combined organics were washed with 1 M HCl (aq, 30 mL), sat. Na₂CO₃ (aq, 3 x 30 mL) and brine (30 mL) before being passed through a hydrophobic frit and the solvent being removed *in vacuo* to provide the Weinreb amide intermediate **229** as an orange oil (3.40 g). Product was taken on to the next step without purification. LCMS (Formic): *t*_R = 1.14 min, [M+H]⁺ = 381, (82% purity); ¹H NMR (400 MHz, CDCl₃) δ = 7.39 - 7.28 (m, 5H), 5.52 (d, *J* = 8.3 Hz, 1H), 5.13 (d, *J* = 12.2 Hz, 1H), 5.08 (d, *J* = 12.2 Hz, 1H), 4.83 - 4.69 (m, 1H), 3.79 (s, 3H), 3.22 (s, 3H), 2.33 (t, *J* = 7.6 Hz, 2H), 2.11 - 2.00 (m, 1H), 1.94 - 1.83 (m, 1H), 1.44 (s, 9H).

The intermediate **229** was dissolved in THF (70 mL) and cooled to -78 °C under a nitrogen atmosphere. MeMgBr, 3 M in Et₂O (8.94 mL, 26.8 mmol) was added dropwise. The reaction mixture was stirred at -78 °C for 1 h before being allowed to warm to 0 °C, stirred for 2 h and then allowed to warm to RT and stirred for 3 h. The reaction mixture was cooled to 0 °C and 0.5 M HCl (aq, 10 mL) was added, dropwise. The reaction mixture was partitioned between 0.5 M HCl (aq, 50 mL) and EtOAc (50 mL). The aqueous phase was further extracted with EtOAc (2 x 75 mL). The combined organics were washed with brine (30 mL), passed through a hydrophobic frit, and the solvent was removed *in vacuo*. The residue was taken up into DCM (5 mL) and purified by normal phase column chromatography (EtOAc in cyclohexane, 0 → 30%, 120 g SiO₂) to provide the titled compound as a colourless oil (1.85 g, 62% yield). ¹H NMR (400 MHz, CDCl₃) δ = 7.42 - 7.28 (m, 5H), 5.57 (d, *J* = 6.6 Hz, 1H), 5.11 (s, 2H), 4.49 - 4.36 (m, 1H), 2.41 - 2.16 (m, 6H), 1.83 (s, 1H), 1.44 (s, 9H); LCMS (Formic): *t*_R = 1.16 min, [M-C₄H₈+H]⁺ = 280, (100% purity).

***tert*-Butyl (4*R*)-4-(((benzyloxy)carbonyl)amino)-5-((3,5-dimethylisoxazol-4-yl)amino)hexanoate (230)**

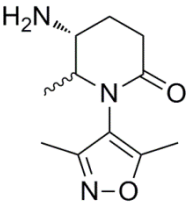
4-Amino-3,5-dimethylisoxazole **46** (352 mg, 3.16 mmol) and *tert*-butyl (*R*)-4-(((benzyloxy)carbonyl)amino)-5-oxohexanoate **228** (1.06 g, 3.16 mmol) were dissolved in MeOH (16 mL) and AcOH (1.8 mL). Picoline borane (338 mg, 3.16 mmol) was added and the reaction vessel was sealed and stirred at RT for 16 h. 2 M HCl (aq, 50 mL) was added to the reaction mixture, which was left to stand for 15 min before being basified with sat. Na₂CO₃ (aq, 50 mL) and extracted with EtOAc (3 x 50 mL). The combined organics were washed with brine (25 mL), passed through a hydrophobic frit, and the solvent was removed *in vacuo*. The residue was taken up into DCM (6 mL) and purified by normal phase column chromatography (3:1 EtOAc:EtOH in cyclohexane, 0 → 40%, 120 g SiO₂) to provide the titled compound as a colourless oil (1.21 g, 88% yield). ¹H NMR suggests a 1:5 mixture of diastereomers. Major Diastereomer: ¹H NMR (400 MHz, CDCl₃) δ = 7.41 - 7.28 (m, 5H), 5.19 - 5.04 (m, 2H), 4.99 - 4.87 (m, 1H), 3.69 - 3.58 (m, 1H), 3.12 - 2.97 (m, 1H), 2.34 (t, *J* = 7.0 Hz, 2H), 2.30 (s, 3H), 2.18 (s, 3H), 2.02 - 1.58 (m, 3H), 1.46 - 1.42 (m, 9H), 1.03 (d, *J* = 6.4 Hz, 3H); Minor Diastereomer: ¹H NMR (400 MHz, CDCl₃) δ = 7.41 - 7.28 (m, 5H), 5.19 - 5.04 (m, 2H), 4.99 - 4.87 (m, 1H), 3.78 - 3.68 (m, 1H), 3.12 - 2.97 (m, 1H), 2.34 (t, *J* = 7.0 Hz, 2H), 2.24 (s, 3H), 2.12 (s, 3H), 2.00 - 1.53 (m, 3H), 1.46 - 1.42 (m, 9H), 1.05 (d, *J* = 6.6 Hz, 3H); LCMS (Formic): *t*_R = 1.28 min, [M+H]⁺ = 432, (100% purity).

Benzyl ((3*R*)-1-(3,5-dimethylisoxazol-4-yl)-2-methyl-6-oxopiperidin-3-yl)carbamate (231)

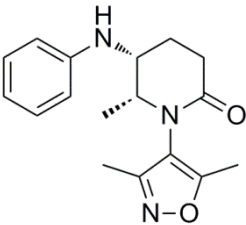
TFA (5 mL, 64.9 mmol) was added dropwise to a stirred solution of *tert*-butyl (4*R*)-4-(((benzyloxy)carbonyl)amino)-5-((3,5-dimethylisoxazol-4-yl)amino)hexanoate **230** (1.20 g, 2.78 mmol) in DCM (20 mL), using ice water for external cooling. The reaction mixture was heated to 40 °C for 20 h, under atmospheric conditions. The reaction mixture was allowed to cool before being quenched with sat. NaHCO₃ (aq, 50 mL) and extracted with DCM (3 x 40 mL). The combined organics were washed with brine (40 mL), passed through a hydrophobic frit, and the solvent was removed *in vacuo*. The residue was taken up into DCM (3 mL) and purified

by normal phase column chromatography (3:1 EtOAc:EtOH in cyclohexane, 0 → 100%, 40 g SiO₂) to provide the titled compound as a colourless gum (601 mg, 61% yield). ¹H NMR suggests a 1:5 mixture of diastereomers. Major Diastereomer: ¹H NMR (400 MHz, CDCl₃) δ = 7.44 - 7.30 (m, 5H), 5.23 - 5.03 (m, 2H), 4.86 (d, *J* = 6.4 Hz, 1H), 3.91 (br. s, 1H), 2.76 - 2.48 (m, 2H), 2.41 - 1.67 (m, 9H), 1.12 (d, *J* = 6.6 Hz, 3H); Minor Diastereomer: ¹H NMR (400 MHz, CDCl₃) δ = 7.44 - 7.30 (m, 5H), 5.23 - 5.03 (m, 2H), 4.27 (br. s., 1H), 3.67 (br. s., 1H), 2.76 - 2.48 (m, 2H), 2.41 - 1.67 (m, 9H), 1.22 (d, *J* = 6.6 Hz, 3H); LCMS (High pH): *t*_R = 0.90 min, [M+H]⁺ = 358, (65% purity), *t*_R = 0.91 min, [M+H]⁺ = 358, (35% purity).

(5*R*)-5-Amino-1-(3,5-dimethylisoxazol-4-yl)-6-methylpiperidin-2-one (232)

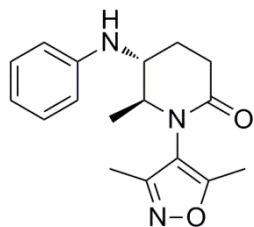
 A solution of benzyl ((3*R*)-1-(3,5-dimethylisoxazol-4-yl)-2-methyl-6-oxopiperidin-3-yl)carbamate **231** (594 mg, 1.662 mmol) in conc. HCl (14.0 mL, 168 mmol) was stirred at RT, under atmospheric conditions, for 4 h. The solvent was removed *in vacuo* and the residue taken up into MeOH (1 mL) and loaded onto a pre-equilibrated SCX-2 cartridge (5 g). After 10 minutes the column was flushed with MeOH (3 CV) followed by NH₃, 2 M in MeOH (3 CV). The desired fractions were combined and the solvent was removed *in vacuo* to give the titled compound as a colourless gum (285 mg, 77% yield). ¹H NMR suggests a 1:3 mixture of diastereomers. Major Diastereomer: ¹H NMR (400 MHz, DMSO-*d*₆, 120 °C) δ = 3.63 - 3.55 (m, 1H), 3.39 - 3.31 (m, 1H), 2.59 - 2.52 (m, 1H), 2.46 - 2.31 (m, 1H), 2.24 (s, 3H), 2.06 (s, 3H), 1.92 - 1.67 (m, 2H), 1.55 (br. s., 2H), 1.07 (d, *J* = 6.6 Hz, 3H); Minor Diastereomer: ¹H NMR (400 MHz, DMSO-*d*₆, 120 °C) δ = 3.39 - 3.31 (m, 1H), 3.00 - 2.95 (m, 1H), 2.59 - 2.52 (m, 1H), 2.46 - 2.31 (m, 1H), 2.25 (s, 3H), 2.07 (s, 3H), 1.92 - 1.67 (m, 2H), 1.55 (br. s., 2H), 1.11 (d, *J* = 6.6 Hz, 3H); LCMS (High pH): *t*_R = 0.46 min, [M+H]⁺ = 224, (69% purity); *t*_R = 0.49 min, [M+H]⁺ = 224, (31% purity).

(5*R*,6*R*)-1-(3,5-Dimethylisoxazol-4-yl)-6-methyl-5-(phenylamino)piperidin-2-one (233)

 A microwave vial was charged with Pd₂(dba)₃ (57 mg, 0.063 mmol), DavePhos (37 mg, 0.094 mmol), NaO^tBu (169 mg, 1.76 mmol) and toluene (3.5 mL). The vial was sealed before being evacuated and purged with nitrogen. To this was added a solution of (5*R*)-5-amino-1-(3,5-dimethylisoxazol-4-yl)-6-methylpiperidin-2-one **232** (280 mg, 1.25 mmol) and bromobenzene (264 μL, 2.51 mmol) in toluene (3.5 mL) and the sealed vial was heated to 130 °C for 15 h. This was allowed to cool and the solvent was removed under a stream of nitrogen. The residue was taken up into EtOAc (10 mL) and filtered through Celite (2.5 g), and flushed through with further

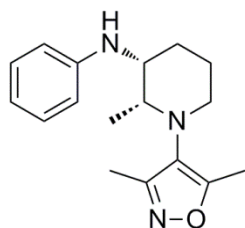
EtOAc (3 x 20 mL). The combined organics were concentrated *in vacuo* and the residue was dissolved in DCM (4 mL) and purified by normal phase column chromatography (3:1 EtOAc:EtOH in cyclohexane, 0 → 100%, 40 g SiO₂). The fractions were combined in two separate batches which were concentrated *in vacuo* and taken up into 1:1 MeOH:DMSO (6 mL total) and further purified by MDAP (High pH) to provide the minor diastereomer **234** (see below) and the titled compound as a pale yellow solid (133 mg, 35% yield). e.e. = 53.7%; $[\alpha]_D^{20}$ -8.6° (c 0.25, MeOH); ¹H NMR (400 MHz, DMSO-*d*₆, 120 °C) δ = 7.15 - 7.08 (m, 2H), 6.75 (d, *J* = 7.8 Hz, 2H), 6.60 (t, *J* = 7.2 Hz, 1H), 5.23 (d, *J* = 8.1 Hz, 1H), 4.13 - 4.05 (m, 1H), 3.83 - 3.76 (m, 1H), 2.63 - 2.57 (m, 2H), 2.30 (s, 3H), 2.12 (s, 3H), 2.11 - 1.95 (m, 2H), 1.11 (d, *J* = 6.6 Hz, 3H); LCMS (High pH): *t*_R = 0.94 min, [M+H]⁺ = 300, (100% purity).

(5*R*,6*S*)-1-(3,5-Dimethylisoxazol-4-yl)-6-methyl-5-(phenylamino)piperidin-2-one (234)



The titled compound was isolated as the minor diastereomer of the above protocol **233**, as a pale yellow gum (90 mg, 24% yield). e.e. = 53.5%; $[\alpha]_D^{20}$ +34.0° (c 0.25, MeOH); ¹H NMR (400 MHz, DMSO-*d*₆, 120 °C) δ = 7.15 - 7.09 (m, 2H), 6.72 (d, *J* = 8.3 Hz, 2H), 6.61 (t, *J* = 7.2 Hz, 1H), 5.46 (d, *J* = 5.9 Hz, 1H), 3.71 - 3.62 (m, 2H), 2.74 - 2.53 (m, 1H), 2.48 (d, *J* = 6.4 Hz, 1H), 2.34 - 2.21 (m, 1H), 2.17 (s, 3H), 2.00 (s, 3H), 1.94 - 1.79 (m, 1H), 1.22 (d, *J* = 6.5 Hz, 3H); LCMS (High pH): *t*_R = 0.98 min, [M+H]⁺ = 300, (100% purity).

(2*R*,3*R*)-1-(3,5-Dimethylisoxazol-4-yl)-2-methyl-*N*-phenylpiperidin-3-amine (235)

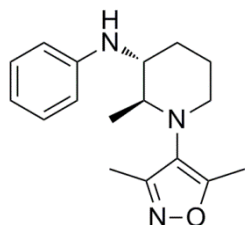


(5*R*,6*R*)-1-(3,5-Dimethylisoxazol-4-yl)-6-methyl-5-(phenylamino)piperidin-2-one **233** (111 mg, 0.371 mmol) was dissolved in THF (3 mL) and the flask evacuated and purged with nitrogen. BH₃.THF, 1 M in THF (1.85 mL, 1.85 mmol) was added and the mixture was stirred at RT for 2 h before being quenched with 2 M HCl (aq, 6 mL), dropwise. After 15 minutes the mixture was neutralised with 2 M NaOH (aq, 6 mL) and extracted with DCM (3 x 25 mL). The combined organics were passed through a hydrophobic frit and the solvent was removed *in vacuo*. The residue was taken up into DCM (2 mL) and purified by normal phase column chromatography (EtOAc in cyclohexane, 0 → 30%, 12 g SiO₂) to provide the titled compound as a colourless oil (86 mg, 81% yield). e.e. = 52.5%; $[\alpha]_D^{20}$ -46.8° (c 0.25, MeOH); ¹H NMR (400 MHz, CDCl₃) δ = 7.22 - 7.16 (m, 2H), 6.69 (tt, *J* = 1.0, 7.3 Hz, 1H), 6.65 (d, *J* = 7.8 Hz, 2H), 4.33 (br. s, 1H),

3.63 - 3.58 (m, 1H), 3.31 (dq, $J = 2.6, 6.5$ Hz, 1H), 3.01 - 2.95 (m, 2H), 2.38 (s, 3H), 2.29 (s, 3H), 2.10 - 2.01 (m, 1H), 1.91 - 1.77 (m, 1H), 1.60 - 1.49 (m, 2H), 0.93 (d, $J = 6.6$ Hz, 3H); LCMS (Formic): $t_R = 1.31$ min, $[M+H]^+ = 286$, (100% purity).

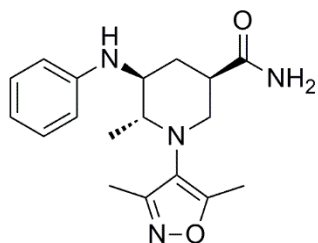
(2*S*,3*R*)-1-(3,5-Dimethylisoxazol-4-yl)-2-methyl-*N*-phenylpiperidin-3-amine

(236)



The titled compound was isolated as the minor component in the chiral separation of *trans*-piperidine **205**, which also provided the 2*R*,3*S*-enantiomer **205a** as the major component. Compound isolated as a colourless oil (3 mg). e.e. = 100%; ν_{max} (CDCl₃): 3365(br.), 2935(m), 2852(w), 2812(w), 1602(s) cm⁻¹; ¹H NMR (400 MHz, CDCl₃) $\delta = 7.21 - 7.15$ (m, 2H), 6.70 (t, $J = 7.3$ Hz, 1H), 6.63 (d, $J = 8.1$ Hz, 2H), 3.31 - 3.24 (m, 1H), 3.13 - 3.05 (m, 1H), 2.95 (quin, $J = 6.4$ Hz, 1H), 2.87 (ddd, $J = 3.5, 8.2, 11.5$ Hz, 1H), 2.35 (s, 3H), 2.23 (s, 3H), 2.11 - 2.02 (m, 1H), 1.81 - 1.71 (m, 1H), 1.71 - 1.60 (m, 1H), 1.50 - 1.40 (m, 1H), 1.06 (d, $J = 6.4$ Hz, 3H); LCMS (High pH): $t_R = 1.33$, $[M+H]^+ = 286$, (100% purity); HRMS: (C₁₇H₂₃N₃O) $[M+H]^+$ requires 286.1919, found $[M+H]^+ = 286.1919$. Data is consistent with that collected for the mixture of enantiomers **205**.

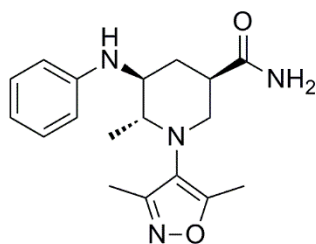
(3*S*,5*S*,6*R*)-1-(3,5-Dimethylisoxazol-4-yl)-6-methyl-5-(phenylamino)piperidine-3-carboxamide (237)



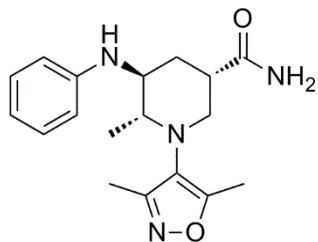
A vial was charged with (5*S*,6*R*)-1-(3,5-dimethylisoxazol-4-yl)-6-methyl-5-(phenylamino)piperidine-3-carboxylic acid **292** (27 mg, 0.082 mmol) and DIPEA (43 μ L, 0.25 mmol). To this was added NH₃, 0.4 M in THF (3.07 mL, 1.23 mmol) followed by COMU (70 mg, 0.16 mmol). The vial was stoppered and stirred at RT for 1 h, before a second portion of COMU (70 mg, 0.16 mmol) was added and the reaction stirred for a further 16 h. The reaction mixture was diluted with EtOAc (50 mL) and washed with sat. Na₂CO₃ (aq, 3 x 15 mL) and brine (15 mL) before being passed through a hydrophobic frit, and the solvent being removed *in vacuo*. The residue was taken up into 1:1 MeOH:DMSO (2 mL) and purified by reverse phase preparative HPLC (MeCN + 0.1% HCO₂H in H₂O + 0.1% HCO₂H, 40 \rightarrow 70%). The mixed fractions were combined, concentrated *in vacuo* and the residue taken up into 1:1 MeOH:DMSO (2 mL) and purified by reverse phase chromatography (MeCN + 0.1% HCO₂H in H₂O + 0.1% HCO₂H, 40 \rightarrow 60%, 60 g C₁₈). The fractions containing mostly the minor diastereomer **240** were combined and concentrated *in vacuo* (see below). The mixed fractions were combined, concentrated *in vacuo* and the residue taken up into 1:1

MeOH:DMSO (1 mL) and purified by MDAP (Formic). All pure fractions of the desired diastereomer from the three purification methods were combined, and the solvent was removed *in vacuo* to provide the titled compound as a white solid (12 mg, 43% yield). e.e. = 60.1%; ν_{\max} (DCM): 3341(br.), 3191(w), 2929(w), 1666(s), 1601(s) cm^{-1} ; $^1\text{H NMR}$ (400 MHz, CD_3OD) δ = 7.13 - 7.06 (m, 2H), 6.65 (d, J = 7.8 Hz, 2H), 6.57 (t, J = 7.3 Hz, 1H), 3.20 (ddd, J = 4.2, 9.3, 11.2 Hz, 1H), 3.15 (t, J = 11.2 Hz, 1H), 3.02 (ddd, J = 1.5, 3.7, 11.2 Hz, 1H), 2.94 (qd, J = 6.1, 9.0 Hz, 1H), 2.79 - 2.69 (m, 1H), 2.37 (s, 3H), 2.31 (dtd, J = 1.7, 3.7, 13.0 Hz, 1H), 2.27 (s, 3H), 1.51 (q, J = 12.5 Hz, 1H), 0.99 (d, J = 6.1 Hz, 3H). Anilinic and primary amide protons not observed; $^{13}\text{C NMR}$ (101 MHz, CD_3OD) δ = 178.8, 166.0, 160.7, 149.8, 130.3 (2C), 127.1, 117.7, 114.2 (2C), 62.3, 57.5, 56.9, 44.4, 36.4, 17.9, 11.1, 10.7; LCMS (Formic): t_{R} = 0.94 min, $[\text{M}+\text{H}]^+$ = 329, (100% purity); HRMS: ($\text{C}_{18}\text{H}_{24}\text{N}_4\text{O}_2$) $[\text{M}+\text{H}]^+$ requires 329.1978, found $[\text{M}+\text{H}]^+$ 329.1974.

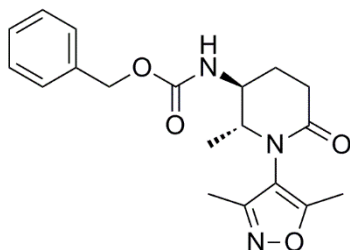
(3*S*,5*S*,6*R*)-1-(3,5-Dimethylisoxazol-4-yl)-6-methyl-5-(phenylamino)piperidine-3-carboxamide (237a)



(3*S*,5*S*,6*R*)-1-(3,5-Dimethylisoxazol-4-yl)-6-methyl-5-(phenylamino)piperidine-3-carboxamide **237** (10 mg) was dissolved in EtOH (1 mL) and purified on a 30 mm x 25 cm Chiralpak AD-H (5 μm) column, eluting with 25% EtOH + 0.2% $i\text{PrNH}_2$ in heptane + 0.2% $i\text{PrNH}_2$ to provide the (3*R*,5*R*,6*S*)-enantiomer **293** and the titled compound as a white solid (6 mg). Identity of enantiomer has been confirmed with reference to the biological assay and crystallographic data. e.e. = 97.8%; M.pt.: 95–99 °C; ν_{\max} (DCM): 3346(br.), 3196(w), 2935(w), 1667(s), 1601(s) cm^{-1} ; $^1\text{H NMR}$ (400 MHz, CD_3OD) δ = 7.11 - 7.04 (m, 2H), 6.65 - 6.61 (m, 2H), 6.56 (tt, J = 1.0, 7.3 Hz, 1H), 3.18 (ddd, J = 4.2, 9.3, 11.2 Hz, 1H), 3.13 (t, J = 11.2 Hz, 1H), 3.01 (ddd, J = 1.5, 3.7, 11.2 Hz, 1H), 2.93 (qd, J = 6.1, 9.0 Hz, 1H), 2.76 - 2.67 (m, 1H), 2.35 (s, 3H), 2.30 (dtd, J = 1.7, 3.7, 13.0 Hz, 1H), 2.25 (s, 3H), 1.49 (q, J = 12.5 Hz, 1H), 0.97 (d, J = 6.1 Hz, 3H). Anilinic and primary amide protons not observed; LCMS (Formic): t_{R} = 0.94 min, $[\text{M}+\text{H}]^+$ = 329, (100% purity); HRMS: ($\text{C}_{18}\text{H}_{24}\text{N}_4\text{O}_2$) $[\text{M}+\text{H}]^+$ requires 329.1978, found $[\text{M}+\text{H}]^+$ 329.1970.

(3R,5S,6R)-1-(3,5-Dimethylisoxazol-4-yl)-6-methyl-5-(phenylamino)piperidine-3-carboxamide (240)

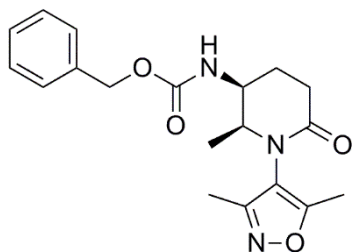
The titled compound was isolated as the minor diastereomer in the synthesis of the (3*S*,5*S*,6*R*)-analogue **237**, as a white solid (6 mg, 22% yield). ¹H NMR indicates that the sample contains 15% of the opposite diastereomer **237**. ν_{\max} (DCM): 3346(br.), 3196(w), 2932(w), 1668(s), 1602(s) cm⁻¹; ¹H NMR (400 MHz, CD₃OD) δ = 7.16 - 7.09 (m, 2H), 6.70 (d, *J* = 7.8 Hz, 2H), 6.61 (t, *J* = 7.3 Hz, 1H), 3.63 - 3.57 (m, 1H), 3.45 (dd, *J* = 7.1, 11.7 Hz, 1H), 3.17 - 3.06 (m, 2H), 2.83 - 2.76 (m, 1H), 2.37 (s, 3H), 2.31 (ddd, *J* = 4.4, 8.1, 13.6 Hz, 1H), 2.17 (s, 3H), 1.72 (ddd, *J* = 4.4, 7.0, 13.6 Hz, 1H), 1.10 (d, *J* = 6.6 Hz, 3H). Anilinic and primary amide protons not observed; ¹³C NMR (101 MHz, CD₃OD) δ = 179.3, 164.2, 160.2, 149.2, 130.4 (2C), 127.6, 118.0, 114.4 (2C), 60.6, 53.3, 52.0, 41.0, 30.5, 14.9, 11.6, 10.6; LCMS (Formic): *t_R* = 0.91 min, [M+H]⁺ = 329, (84% purity); HRMS: (C₁₈H₂₄N₄O₂) [M+H]⁺ requires 329.1978, found [M+H]⁺ 329.1973.

Benzyl ((2*R*,3*S*)-1-(3,5-dimethylisoxazol-4-yl)-2-methyl-6-oxopiperidin-3-yl)carbamate (262)

A mixture of 3,5-dimethylisoxazol-4-amine **46** (1.01 g, 9.01 mmol), *tert*-butyl (*S*)-4-(((benzyloxy) carbonyl)amino)-5-oxohexanoate **217** (2.02 g, 6.01 mmol) and zinc trifluoromethanesulfonate (2.18 g, 6.01 mmol) was dissolved in THF (40 mL), and stirred until the salts had dissolved. PMHS (1.82 mL, 30.0 mmol) was added and the mixture was stirred at 60 °C for 72 h under atmospheric conditions. Further PMHS (1.09 mL, 18.0 mmol) was added and the reaction was heated for a further 24 h. The reaction mixture was allowed to cool to RT before being chilled in an ice-water bath. MeOH (20 mL) was added, followed by slow addition of 2 M NaOH (aq, 40 mL). The reaction was stirred at 0 °C for 2 h, and then heated to 60 °C for 24 h. After being allowed to cool to RT the mixture was acidified with 2 M HCl (aq, 50 mL) before being extracted with DCM (3 x 50 mL). The combined organics were washed with brine (25 mL), passed through a hydrophobic frit, and the solvent was removed *in vacuo*. The residue was taken up into DCM (7 mL) and purified by normal phase column chromatography (3:1 EtOAc:EtOH in cyclohexane, 0 → 50%, 80 g SiO₂) to provide the minor diastereomer **263** (see below) and the titled compound as a yellow gum (901 mg, 42% yield). ν_{\max} (DCM): 3302(br.), 2970(w),

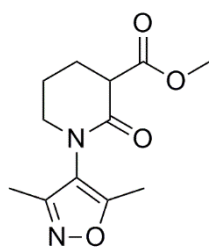
1697(m), 1636(s), 1534(m) cm^{-1} ; ^1H NMR (400 MHz, $\text{DMSO-}d_6$, 120 $^\circ\text{C}$) δ = 7.74 (br. s., 1H), 7.46 - 7.29 (m, 5H), 5.10 (d, J = 12.5 Hz, 1H), 5.04 (d, J = 12.5 Hz, 1H), 3.75 - 3.67 (m, 1H), 3.63 - 3.54 (m, 1H), 2.69 - 2.56 (m, 1H), 2.47 - 2.37 (m, 1H), 2.17 (s, 3H), 2.15 - 2.08 (m, 1H), 1.98 (s, 3H), 1.80 (qd, J = 6.4, 13.4 Hz, 1H), 1.09 (d, J = 6.4 Hz, 3H); ^{13}C NMR (101 MHz, $\text{DMSO-}d_6$, 120 $^\circ\text{C}$) δ = 168.1, 155.3, 143.9, 140.8, 136.5, 127.6 (2C), 127.1, 127.0 (2C), 110.9, 65.0, 59.0, 50.3, 28.0, 22.7, 18.2, 9.7, 8.4; LCMS (Formic): t_R = 0.88 min, $[\text{M}+\text{H}]^+$ = 358, (100% purity); HRMS: ($\text{C}_{19}\text{H}_{23}\text{N}_3\text{O}_4$) $[\text{M}+\text{H}]^+$ requires 358.1767, found $[\text{M}+\text{H}]^+$ 358.1766.

Benzyl ((2*S*,3*S*)-1-(3,5-dimethylisoxazol-4-yl)-2-methyl-6-oxopiperidin-3-yl)carbamate (263)



Isolated as the byproduct in the synthesis of the *trans*-diastereomer **262** (see above), as an orange gum (245 mg, 11% yield). NMR indicates this material contains ~10% of the *trans*-diastereomer **262**. ν_{max} (DCM): 3282(br.), 2973(w), 1715(s), 1657(m), 1637(s) cm^{-1} ; ^1H NMR (400 MHz, $\text{DMSO-}d_6$, 120 $^\circ\text{C}$) δ = 7.39 - 7.27 (m, 5H), 7.17 (d, J = 5.9 Hz, 1H), 5.10 (d, J = 12.5 Hz, 1H), 5.06 (d, J = 12.5 Hz, 1H), 4.16 - 4.07 (m, 1H), 3.84 - 3.75 (m, 1H), 2.63 - 2.52 (m, 1H), 2.48 - 2.43 (m, 1H), 2.23 (s, 3H), 2.06 (s, 3H), 2.04 - 1.87 (m, 2H), 1.06 (d, J = 6.6 Hz, 3H); ^{13}C NMR (101 MHz, $\text{DMSO-}d_6$, 120 $^\circ\text{C}$) δ = 167.8, 163.5, 157.3, 155.1, 136.5, 127.6 (2C), 127.1, 127.0 (2C), 110.9, 65.1, 56.6, 48.7, 28.7, 21.5, 13.4, 9.8, 8.4; LCMS (Formic): t_R = 0.87 min, $[\text{M}+\text{H}]^+$ = 358, (100% purity); HRMS: ($\text{C}_{19}\text{H}_{23}\text{N}_3\text{O}_4$) $[\text{M}+\text{H}]^+$ requires 358.1767, found $[\text{M}+\text{H}]^+$ 358.1761.

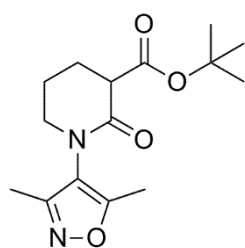
Methyl 1-(3,5-dimethylisoxazol-4-yl)-2-oxopiperidine-3-carboxylate (264)



To a solution of 1-(3,5-dimethylisoxazol-4-yl)piperidin-2-one **89** (500 mg, 2.57 mmol) in THF (15 mL), at -78 $^\circ\text{C}$ under a nitrogen atmosphere, was added LiHMDS, 1.0 M in THF (5.15 mL, 5.15 mmol). The mixture was stirred for 15 min before a solution of methyl chloroformate (240 μL , 3.1 mmol) in THF (5 mL) was added, and the mixture was stirred at -78 $^\circ\text{C}$ for a further 2 h. The reaction was quenched with sat. NH_4Cl (aq, 10 mL) and allowed to warm to RT. The mixture was diluted with H_2O (15 mL) and extracted with DCM (3 x 25 mL). The combined organics were washed with brine (25 mL) before being passed through a hydrophobic frit, and the solvent being removed *in vacuo*. The residue was taken up into DCM (2 mL) and purified by normal phase column chromatography (3:1 EtOAc:EtOH in cyclohexane, 0 \rightarrow 50%, 40 g SiO_2) to provide the

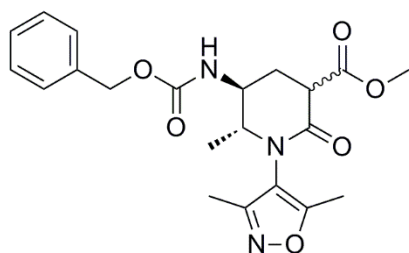
titled compound as a pale yellow oil (568 mg, 87% yield). ν_{\max} (CDCl₃): 3500(br.), 2954(w), 1738(s), 1663(s), 1645(s) cm⁻¹; ¹H NMR (400 MHz, CDCl₃) δ = 3.78 (s, 3H), 3.59 (t, J = 6.7 Hz, 1H), 3.56 - 3.44 (m, 2H), 2.31 (s, 3H), 2.30 - 2.20 (m, 2H), 2.18 (s, 3H), 2.14 - 2.03 (m, 1H), 1.99 - 1.88 (m, 1H); ¹³C NMR (101 MHz, CDCl₃) δ = 171.0, 166.1, 164.0, 157.6, 119.2, 52.6, 51.1, 49.1, 25.2, 21.2, 11.0, 9.7; LCMS (Formic): t_R = 0.62 min, [M+H]⁺ = 253, (95% purity); HRMS: (C₁₂H₁₆N₂O₄) [M+H]⁺ requires 253.1188, found [M+H]⁺ 253.1192.

tert-Butyl 1-(3,5-dimethylisoxazol-4-yl)-2-oxopiperidine-3-carboxylate (265)



To a solution of 1-(3,5-dimethylisoxazol-4-yl)piperidin-2-one **89** (500 mg, 2.57 mmol) in THF (2 mL), at -78 °C under a nitrogen atmosphere, was added LiHMDS, 1.0 M in THF (5.15 mL, 5.15 mmol). The mixture was stirred for 1 h before a solution of Boc-anhydride (674 mg, 3.09 mmol) in THF (2 mL) was added, and the mixture was stirred at -78 °C for a further 2 h. The reaction was quenched with sat. NH₄Cl (aq, 10 mL) and allowed to warm to RT. The mixture was diluted with H₂O (15 mL) and extracted with DCM (3 x 25 mL). The combined organics were washed with brine (25 mL) before being passed through a hydrophobic frit, and the solvent being removed *in vacuo*. The residue was taken up into DCM (2 mL) and purified by normal phase column chromatography (3:1 EtOAc:EtOH in cyclohexane, 0 → 50%, 40 g SiO₂) to provide the titled compound as a yellow oil (623 mg, 82% yield). ν_{\max} (CDCl₃): 3500(br.), 2977(w), 2935(w), 1728(s), 1665(s), 1646(s) cm⁻¹; ¹H NMR (400 MHz, CDCl₃) δ = 3.55 - 3.41 (m, 3H), 2.31 (s, 3H), 2.28 - 2.19 (m, 2H), 2.18 (s, 3H), 2.12 - 2.01 (m, 1H), 1.96 - 1.85 (m, 1H), 1.49 (s, 9H); ¹³C NMR (101 MHz, CDCl₃) δ = 169.6, 166.6, 164.0, 157.6, 119.3, 82.0, 51.0, 50.3, 28.0 (3C), 25.3, 21.1, 11.0, 9.8; LCMS (Formic): t_R = 0.89 min, [M-C₄H₈+H]⁺ = 239, (96% purity); HRMS: (C₁₅H₂₂N₂O₄) [M-C₄H₈+H]⁺ requires 239.1032, found [M-C₄H₈+H]⁺ 239.1036.

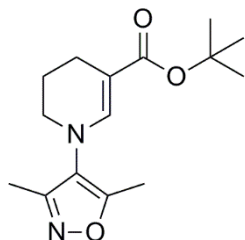
Methyl (5S,6R)-5-(((benzyloxy)carbonyl)amino)-1-(3,5-dimethylisoxazol-4-yl)-6-methyl-2-oxopiperidine-3-carboxylate (269)



To a solution of benzyl ((2R,3S)-1-(3,5-dimethylisoxazol-4-yl)-2-methyl-6-oxopiperidin-3-yl)carbamate **262** (743 mg, 2.08 mmol) in THF (10 mL), at -78 °C under a nitrogen atmosphere, was added LiHMDS, 1.0 M in THF (6.24 mL, 6.24 mmol). After 5 min at -78 °C the reaction was warmed to -42 °C and stirred for 4 h. The reaction

was once again cooled to $-78\text{ }^{\circ}\text{C}$ and a solution of methyl chloroformate (177 μL , 2.29 mmol) in THF (0.5 mL) was added, and the mixture stirred at $-78\text{ }^{\circ}\text{C}$ for 30 min before being quenched with sat. NH_4Cl (aq, 5 mL). The mixture was allowed to warm to RT and was partitioned between H_2O (20 mL) and DCM (25 mL). The aqueous phase was further extracted with DCM (2 x 25 mL), and the combined organics were washed with brine (25 mL), passed through a hydrophobic frit, and the solvent removed *in vacuo*. The residue was taken up into DCM (7 mL) and purified by normal phase column chromatography (3:1 TBME:EtOH in cyclohexane, 0 \rightarrow 50%, 80 g SiO_2) to provide the titled compound as an off-white solid (437 mg, 51% yield). Major Diastereomer: ^1H NMR (400 MHz, $\text{DMSO-}d_6$, $120\text{ }^{\circ}\text{C}$) δ = 7.44 - 7.28 (m, 5H), 5.14 - 5.05 (m, 2H), 3.89 - 3.60 (m, 3H), 3.72 (s, 3H), 2.44 - 2.25 (m, 2H), 2.20 (s, 3H), 2.03 (s, 3H), 1.16 (d, J = 6.4 Hz, 3H); Minor Diastereomer: ^1H NMR (400 MHz, $\text{DMSO-}d_6$, $120\text{ }^{\circ}\text{C}$) δ = 7.44 - 7.28 (m, 5H), 5.14 - 5.05 (m, 2H), 3.89 - 3.60 (m, 3H), 3.68 (s, 3H), 2.44 - 2.25 (m, 2H), 2.24 (s, 3H), 2.05 (s, 3H), 1.10 (d, J = 6.6 Hz, 3H). Carbamate proton not observed; LCMS (Formic): t_{R} = 0.97 min, $[\text{M}+\text{H}]^+$ = 416, (94% purity).

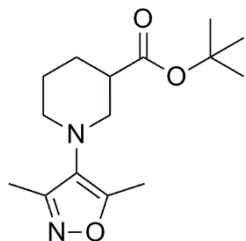
***tert*-Butyl 1-(3,5-dimethylisoxazol-4-yl)-1,4,5,6-tetrahydropyridine-3-carboxylate (273)**



A flask was charged with $\text{Zn}(\text{OAc})_2$ (26 mg, 0.14 mmol) before being evacuated and purged with nitrogen. THF (3 mL) was added, followed by triethoxysilane (770 μL , 4.2 mmol), and the mixture was stirred at RT for 30 min. *tert*-butyl 1-(3,5-dimethylisoxazol-4-yl)-2-oxopiperidine-3-carboxylate **265** (410 mg, 1.39 mmol) was added as a solution in THF (7 mL) and the mixture was stirred for 3 days at RT. Further triethoxysilane (770 μL , 4.2 mmol) was added and the mixture was stirred for 2 days. The reaction was quenched with 1 M NaOH (aq, 10 mL) and stirred for 1 h before being extracted with EtOAc (3 x 20 mL). The combined organics were washed with brine (20 mL), passed through a hydrophobic frit, and the solvent was removed *in vacuo*. The residue was taken up into DCM (2 mL) and purified by normal phase column chromatography (EtOAc in cyclohexane, 0 \rightarrow 50%, 40 g SiO_2) to provide the titled compound as a colourless oil (108 mg, 28% yield). ν_{max} (CDCl_3): 2972(w), 2930(w), 2855(w), 1680(s), 1623(s) cm^{-1} ; ^1H NMR (400 MHz, CDCl_3) δ = 7.15 (t, J = 1.0 Hz, 1H), 3.30 (t, J = 5.6 Hz, 2H), 2.37 - 2.32 (m, 5H), 2.22 (s, 3H), 1.95 (quin, J = 5.6 Hz, 2H), 1.48 (s, 9H); ^{13}C NMR (101 MHz, CDCl_3) δ = 167.7, 163.1, 157.5, 143.1, 124.4, 101.1, 78.7, 48.8, 28.5 (3C), 21.8, 20.2, 10.7, 9.7; LCMS (Formic): t_{R} = 1.17 min, $[\text{M}-\text{C}_4\text{H}_8+\text{H}]^+$ = 223, $[\text{M}+\text{H}]^+$

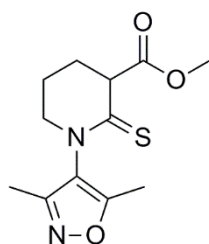
= 279, (100% purity); HRMS: (C₁₅H₂₂N₂O₃) [M–C₄H₈+H]⁺ requires 223.1083, found [M–C₄H₈+H]⁺ 223.1089.

***tert*-Butyl 1-(3,5-dimethylisoxazol-4-yl)piperidine-3-carboxylate (274)**



To a vial containing *tert*-butyl 1-(3,5-dimethylisoxazol-4-yl)-1,4,5,6-tetrahydropyridine-3-carboxylate **273** (101 mg, 0.363 mmol) was added AcOH (2.00 mL, 34.9 mmol) followed by sodium triacetoxyborohydride (231 mg, 1.09 mmol). After 15 min the reaction was cooled in an ice-water bath and quenched with sat. NaHCO₃ (aq, 30 mL), before being extracted with EtOAc (3 x 25 mL). The combined organics were washed with brine (25 mL), passed through a hydrophobic frit, and the solvent was removed *in vacuo* to provide the titled compound as a colourless oil (102 mg, 100% yield). ν_{\max} (CDCl₃): 2935(w), 2814(w), 1724(s), 1629(w) cm⁻¹; ¹H NMR (400 MHz, CDCl₃) δ = 3.16 - 3.09 (m, 1H), 3.00 (dd, *J* = 9.2, 11.1 Hz, 1H), 2.95 - 2.87 (m, 1H), 2.87 - 2.79 (m, 1H), 2.57 - 2.49 (m, 1H), 2.36 (s, 3H), 2.23 (s, 3H), 1.97 - 1.89 (m, 1H), 1.84 - 1.76 (m, 1H), 1.69 - 1.51 (m, 2H), 1.45 (s, 9H); ¹³C NMR (101 MHz, CDCl₃) δ = 173.1, 161.0, 158.4, 128.0, 80.4, 54.4, 52.6, 43.2, 28.1 (3C), 26.5, 25.3, 11.5, 10.5; LCMS (Formic): *t_R* = 1.28 min, [M+H]⁺ = 281, (100% purity); HRMS: (C₁₅H₂₄N₂O₃) [M+H]⁺ requires 281.1865, found [M+H]⁺ 281.1864.

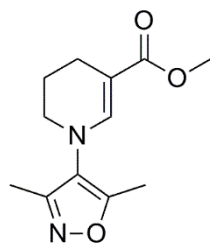
Methyl 1-(3,5-dimethylisoxazol-4-yl)-2-thioxopiperidine-3-carboxylate (279)



A mixture of methyl 1-(3,5-dimethylisoxazol-4-yl)-2-oxopiperidine-3-carboxylate **264** (415 mg, 1.65 mmol), Lawesson's Reagent (732 mg, 1.81 mmol), and toluene (10 mL) was heated to 110 °C for 2 h. The reaction mixture was allowed to cool before being diluted with sat. NaHCO₃ (aq, 60 mL) and extracted with EtOAc (2 x 60 mL). The combined organics were washed with brine (50 mL) and passed through a hydrophobic frit before the solvent was removed *in vacuo*. The residue was taken up into DCM (4 mL) and purified by normal phase column chromatography (3:1 TBME:EtOH in cyclohexane, 0 → 75%, 80 g SiO₂) to provide the titled compound as a yellow solid (385 mg, 87% yield). Rotamers were apparent in ¹H and ¹³C NMR, which only partially coalesced at 120°C. M.pt.: 117–119 °C; ν_{\max} (neat): 2949(w), 1735(s), 1652(w) cm⁻¹; ¹H NMR (400 MHz, DMSO-*d*₆) δ = 4.12 - 4.02 (m, 1H), 3.67 (s, 3H), 3.66 - 3.59 (m, 2H), 2.28 (s, 1.5H), 2.25 (s, 1.5H), 2.20 - 2.12 (m, 1H), 2.10 (s, 1.5H), 2.09 (s, 1.5H), 2.07 - 1.92 (m, 3H); ¹H NMR (400 MHz, DMSO-*d*₆, 120 °C) δ = 4.09 (q, *J* = 6.1 Hz, 1H), 3.71 (s, 3H), 3.65 (t, *J* = 6.0 Hz, 2H), 2.28 (s, 1.5H), 2.26 (s, 1.5H), 2.20 - 2.13 (m, 1H), 2.11 (s, 1.5H), 2.11 (s, 1.5H), 2.10 - 1.95

(m, 3H); ^{13}C NMR (101 MHz, $\text{DMSO-}d_6$) δ = 199.0, 198.9, 171.0, 171.0, 163.7, 163.2, 157.1, 156.7, 122.9, 122.9, 55.6, 55.6, 53.4, 53.4, 52.1, 52.1, 23.7, 23.7, 19.9, 19.8, 10.6, 10.5, 9.5, 9.3; LCMS (High pH): t_{R} = 0.84 min, $[\text{M}+\text{H}]^+$ = 269, (100% purity); HRMS: ($\text{C}_{12}\text{H}_{16}\text{N}_2\text{O}_3\text{S}$) $[\text{M}+\text{H}]^+$ requires 269.0960, found $[\text{M}+\text{H}]^+$ 269.0959.

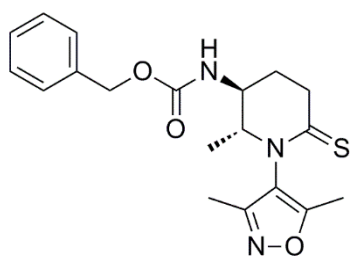
Methyl 1-(3,5-dimethylisoxazol-4-yl)-1,4,5,6-tetrahydropyridine-3-carboxylate (281)



To a solution of methyl 1-(3,5-dimethylisoxazol-4-yl)-2-thioxopiperidine-3-carboxylate **279** (100 mg, 0.373 mmol) in MeCN (2 mL), under a nitrogen atmosphere, was added MeI (233 μL , 3.73 mmol). The vial was sealed and heated to 40 $^{\circ}\text{C}$ for 16 h. The mixture was allowed to cool to RT before the solvent was removed *in vacuo*.

The residue was taken up into MeOH (2 mL) and cooled to -78 $^{\circ}\text{C}$. NaBH_4 (28 mg, 0.75 mmol) was added and the reaction was stirred at -78 $^{\circ}\text{C}$ for 2 h. 2M HCl (aq, 5 mL) was added, and the mixture was allowed to warm to RT. The mixture was basified with 1 M NaOH (aq, 15 mL) and extracted with DCM (3 x 20 mL). The combined organics were washed with brine (20 mL), passed through a hydrophobic frit, and the solvent was removed *in vacuo*. The residue was taken up into DCM (2 mL) and purified by normal phase column chromatography (EtOAc in cyclohexane, 0 \rightarrow 70%, 24 g SiO_2) to provide the titled compound as a colourless gum (76 mg, 86% yield). ν_{max} (CDCl_3): 2948(w), 2851(w), 1688(m), 1621(s) cm^{-1} ; ^1H NMR (400 MHz, CDCl_3) δ = 7.25 (t, J = 1.2 Hz, 1H), 3.69 (s, 3H), 3.32 (t, J = 5.6 Hz, 2H), 2.38 (t, J = 6.2 Hz, 2H), 2.34 (s, 3H), 2.21 (s, 3H), 1.96 (quin, J = 5.9 Hz, 2H); ^{13}C NMR (101 MHz, CDCl_3) δ = 168.5, 163.3, 157.4, 144.0, 124.2, 99.2, 50.8, 48.9, 21.7, 20.1, 10.7, 9.6; LCMS (Formic): t_{R} = 0.91 min, $[\text{M}+\text{H}]^+$ = 237, (99% purity); HRMS: ($\text{C}_{12}\text{H}_{16}\text{N}_2\text{O}_3$) $[\text{M}+\text{H}]^+$ requires 237.1239, found $[\text{M}+\text{H}]^+$ 237.1240.

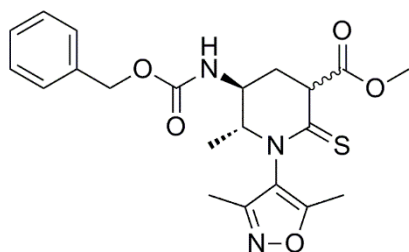
Benzyl ((2R,3S)-1-(3,5-dimethylisoxazol-4-yl)-2-methyl-6-thioxopiperidin-3-yl)carbamate (282)



A mixture of benzyl ((2R,3S)-1-(3,5-dimethylisoxazol-4-yl)-2-methyl-6-oxopiperidin-3-yl)carbamate **262** (50 mg, 0.14 mmol), Lawesson's Reagent (62 mg, 0.15 mmol), and toluene (1 mL) was heated to 110 $^{\circ}\text{C}$ for 90 min. The reaction mixture was allowed to cool before being diluted with sat. NaHCO_3 (aq, 20 mL) and extracted with EtOAc (2 x 20 mL). The combined organics were washed with brine (20 mL), passed through a hydrophobic frit, and the solvent was removed *in vacuo*. The residue was taken up into DCM (4 mL) and purified

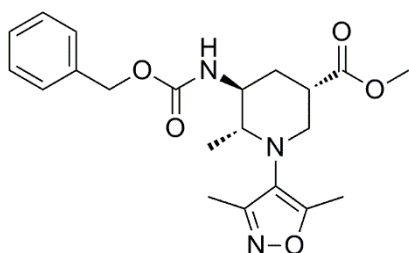
by normal phase column chromatography (3:1 TBME:EtOH in cyclohexane, 0 → 50%, 12 g SiO₂) to provide the titled compound as a yellow gum (39 mg, 75% yield). ν_{\max} (CDCl₃): 3316(br.), 2950(w), 1697(s) cm⁻¹; ¹H NMR (400 MHz, CDCl₃) δ = 7.45 - 7.31 (m, 5H), 5.22 - 5.06 (m, 3H), 4.06 - 3.94 (m, 1H), 3.81 (br. s., 1H), 3.35 - 3.12 (m, 2H), 2.31 - 2.18 (m, 4H), 2.12 - 1.96 (m, 3H), 1.93 - 1.79 (m, 1H), 1.31 (d, J = 6.6 Hz, 3H); ¹³C NMR (101 MHz, CDCl₃) δ = 202.3, 202.2, 165.7, 162.8, 158.5, 156.3, 155.8, 135.8, 135.8, 128.7, 128.5, 128.5, 128.4, 122.6, 121.1, 67.3, 64.1, 63.0, 50.2, 50.0, 37.1, 37.1, 22.1, 18.8, 18.7, 12.0, 10.9, 10.4, 9.2. Rotamers are apparent in ¹H and ¹³C NMR spectra; LCMS (High pH): t_R = 1.07 min, [M+H]⁺ = 374, (100% purity); HRMS: (C₁₉H₂₃N₃O₃S) [M+H]⁺ requires 374.1538, found [M+H]⁺ 374.1538.

Methyl (5*S*,6*R*)-5-(((benzyloxy)carbonyl)amino)-1-(3,5-dimethylisoxazol-4-yl)-6-methyl-2-thioxopiperidine-3-carboxylate (283)



A mixture of methyl (5*S*,6*R*)-5-(((benzyloxy)carbonyl)amino)-1-(3,5-dimethylisoxazol-4-yl)-6-methyl-2-oxopiperidine-3-carboxylate **269** (299 mg, 0.720 mmol), Lawesson's Reagent (640 mg, 1.58 mmol), and toluene (10 mL) was heated to 110 °C for 6 h. The reaction mixture was allowed to cool before being diluted with sat. NaHCO₃ (aq, 60 mL) and extracted with EtOAc (3 x 40 mL). The combined organics were washed with brine (40 mL) and passed through a hydrophobic frit, before the solvent was removed *in vacuo*. The residue was taken up into DCM (6 mL) and purified by normal phase column chromatography (EtOAc in cyclohexane, 0 → 50%, 80 g SiO₂) to provide the titled compound as a yellow gum (187 mg, 60% yield). ¹H NMR (400 MHz, CDCl₃) δ = 7.47 - 7.31 (m, 5H), 5.23 - 5.14 (m, 1H), 5.13 - 5.02 (m, 1H), 4.26 - 4.15 (m, 1H), 4.11 - 3.98 (m, 1H), 3.95 - 3.74 (m, 4H), 2.61 - 2.43 (m, 1H), 2.31 - 1.91 (m, 7H), 1.41 - 1.28 (m, 3H). Carbamate proton not observed; LCMS (Formic): t_R = 1.07, [M+H]⁺ = 432, (63% purity); t_R = 1.09 min, [M+H]⁺ = 432, (25% purity).

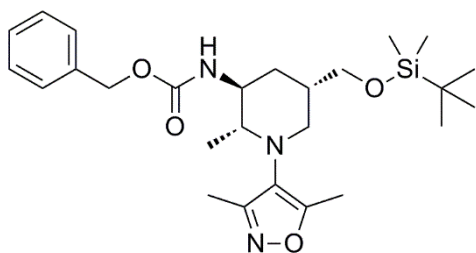
Methyl (3*S*,5*S*,6*R*)-5-(((benzyloxy)carbonyl)amino)-1-(3,5-dimethylisoxazol-4-yl)-6-methylpiperidine-3-carboxylate (285)



To a solution of methyl (5*S*,6*R*)-5-(((benzyloxy)carbonyl)amino)-1-(3,5-dimethylisoxazol-4-yl)-6-methyl-2-thioxopiperidine-3-carboxylate **283** (185 mg, 0.429 mmol) in MeCN (2 mL) was added MeI (536 μ L, 8.57 mmol). The vial was sealed

and heated to 40 °C for 16 h before being allowed to cool to RT and the solvent being removed *in vacuo*. The residue was dissolved in MeOH (2 mL) and AcOH (2 mL). To this was added 5 portions of NaBH₃CN (54 mg, 0.86 mmol) at half hour intervals, and the mixture subsequently stirred for a further 1 h. The reaction mixture was slowly transferred to an ice-cold solution of sat. NaHCO₃ (aq, 60 mL) and the mixture stirred until effervescence had diminished (~15 min). The mixture was extracted with DCM (3 x 40 mL). The combined organics were washed with brine (40 mL), before being passed through a hydrophobic frit and the solvent being removed *in vacuo*. The residue was taken up into DCM (2 mL) and purified by normal phase column chromatography (3:1 TBME:EtOH + 1% NEt₃ in cyclohexane, 0 → 75%, 40 g SiO₂) to provide the titled compound as a white gum (69 mg, 40% yield). ν_{\max} (CDCl₃): 3328(br.), 2953(w), 2822(w), 1723(s), 1641(w) cm⁻¹; ¹H NMR (400 MHz, CDCl₃) δ = 7.45 - 7.30 (m, 5H), 5.23 - 5.06 (m, 3H), 3.74 (s, 3H), 3.44 (dd, *J* = 7.1, 11.6 Hz, 1H), 3.06 (dd, *J* = 3.8, 11.6 Hz, 1H), 2.95 (quin, *J* = 6.4 Hz, 1H), 2.80 - 2.71 (m, 1H), 2.32 (s, 3H), 2.30 - 2.21 (m, 1H), 2.19 (s, 3H), 1.82 (td, *J* = 6.1, 12.2 Hz, 1H), 1.03 (d, *J* = 6.4 Hz, 3H). Carbamate proton not observed; ¹³C NMR (101 MHz, CDCl₃) δ = 173.3, 158.4, 155.6, 136.4, 128.5 (2C), 128.2 (2C), 128.2, 126.7, 125.5, 66.8, 59.8, 51.9, 50.6, 50.0, 39.1, 29.2, 14.0, 11.4, 10.5; LCMS (Formic): *t*_R = 1.11 min, [M+H]⁺ = 402, (86% purity); HRMS: (C₂₁H₂₇N₃O₅) [M+H]⁺ requires 402.2029, found [M+H]⁺ 402.2022.

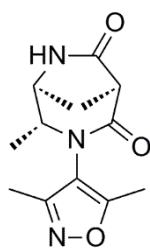
Benzyl ((2*R*,3*S*,5*S*)-5-(((*tert*-butyldimethylsilyl)oxy)methyl)-1-(3,5-dimethylisoxazol-4-yl)-2-methylpiperidin-3-yl)carbamate (287)



A vial containing methyl (5*S*,6*R*)-5-(((benzyl-oxy)carbonyl)amino)-1-(3,5-dimethylisoxazol-4-yl)-6-methyl-2-oxopiperidine-3-carboxylate **269** (20 mg, 0.048 mmol) was sealed, and evacuated and purged with nitrogen, before THF (1 mL) was added. To this was added BH₃.THF, 1 M in THF (290 μ L, 0.29 mmol) dropwise, and the solution stirred for 24 h at RT. The reaction was quenched with H₂O (0.5 mL) followed by 2 M HCl (aq, 4 mL). The mixture was basified with 2 M NaOH (aq, 5 mL) and extracted with DCM (3 x 20 mL). The combined organics were washed with brine (20 mL), passed through a hydrophobic frit and the solvent was removed *in vacuo* to provide the intermediate **286** as a colourless gum. LCMS (Formic): *t*_R = 0.98 min, [M+H]⁺ = 374, (86% purity).

The residue was taken up into DMF (1 mL), and imidazole (7 mg, 0.1 mmol) was added, followed by TBDMSCl (15 mg, 0.1 mmol), and the reaction was stirred at RT for 16 h. The reaction mixture was partitioned between H₂O (10 mL) and DCM (10 mL), and the layers separated. The aqueous phase was further extracted with DCM (2 x 10 mL). The combined organics were washed with brine (10 mL), passed through a hydrophobic frit, and the solvent was removed *in vacuo*. The residue was taken up into DCM (1 mL) and purified by normal phase column chromatography (EtOAc in cyclohexane, 0 → 50%, 12 g SiO₂) to provide the titled compound as a colourless gum (13 mg, 55% yield). ν_{\max} (neat): 3322(br.), 2953(m), 2929(m), 2856(m), 1717(s) cm⁻¹; ¹H NMR (400 MHz, CDCl₃) δ = 7.39 - 7.31 (m, 5H), 5.41 (d, *J* = 9.0 Hz, 1H), 5.15 (d, *J* = 12.2 Hz, 1H), 5.10 (d, *J* = 12.2 Hz, 1H), 3.80 - 3.69 (m, 1H), 3.58 (d, *J* = 5.9 Hz, 2H), 3.11 (dd, *J* = 9.0, 11.2 Hz, 1H), 3.01 - 2.93 (m, 1H), 2.90 (dd, *J* = 3.9, 11.2 Hz, 1H), 2.33 (s, 3H), 2.17 (s, 3H), 2.00 - 1.87 (m, 1H), 1.70 (ddd, *J* = 3.7, 10.3, 13.7 Hz, 1H), 1.60 (td, *J* = 4.9, 13.7 Hz, 1H), 1.04 (d, *J* = 6.6 Hz, 3H), 0.89 (s, 9H), 0.05 (s, 6H). Carbamate proton not observed; ¹³C NMR (101 MHz, CDCl₃) δ = 161.2, 158.3, 155.6, 136.6, 128.5 (2C), 128.2 (2C), 128.1, 126.1, 66.7, 65.0, 59.5, 50.2, 49.0, 35.4, 27.9, 25.9 (3C), 18.2, 12.7, 11.7, 10.5, -5.4, -5.5; LCMS (High pH): *t*_R = 1.63 min, [M+H]⁺ = 488, (94% purity); HRMS: (C₂₆H₄₁N₃O₄Si) [M+H]⁺ requires 488.2945, found [M+H]⁺ 488.2944.

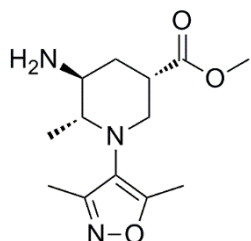
(1*S*,4*R*,5*S*)-3-(3,5-Dimethylisoxazol-4-yl)-4-methyl-3,6-diazabicyclo[3.2.1]octane-2,7-dione (289)



A vial was charged methyl (5*S*,6*R*)-5-(((benzyloxy)carbonyl)amino)-1-(3,5-dimethylisoxazol-4-yl)-6-methyl-2-oxopiperidine-3-carboxylate **269** (25 mg, 0.060 mmol) and NaI (45 mg, 0.30 mmol). The vial was sealed and evacuated and purged with nitrogen, before MeCN (0.5 mL) was added. This was cooled to 0 °C and TMSCl (38 μ L, 0.30 mmol) was added. This was stirred at 0 °C for 10 min before being allowed to warm to RT and stirred for 2 h. The reaction was quenched with MeOH (2 mL) and stirred for 1 min before the solvent was removed *in vacuo*. The residue was taken up into MeOH (0.5 mL) and loaded onto a pre-equilibrated SCX-2 cartridge (1 g). After 15 min, the column was flushed with MeOH (5 CV) before being eluted with 2 M NH₃ in MeOH (5 CV). The ammonia fractions were combined and the solvent was removed *in vacuo* to provide the titled compound as a colourless gum (14 mg, 93% yield). ν_{\max} (neat): 3260(br.), 2978(w), 1704(s), 1666(s), 1643(s) cm⁻¹; ¹H NMR (400 MHz, DMSO-*d*₆, 120 °C) δ = 8.02 (br. s., 1H), 3.80 - 3.74 (m, 1H), 3.60 (q, *J* = 6.5 Hz, 1H), 2.92 (d, *J* = 4.8 Hz, 1H), 2.45 (d, *J* = 11.7 Hz, 1H), 2.33 (td, *J* = 4.8, 11.7 Hz, 1H), 2.23 (s, 3H), 2.03 (s, 3H), 1.15 (d, *J* = 6.5 Hz, 3H); ¹³C NMR (101 MHz,

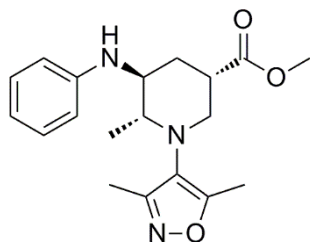
DMSO-*d*₆, 120 °C) δ = 172.3, 166.1, 146.0, 145.8, 136.0, 60.9, 53.2, 49.4, 27.3, 17.1, 9.7, 8.2; LCMS (Formic): t_R = 0.47 min, $[M+H]^+$ = 250, (100% purity); HRMS: (C₁₂H₁₅N₃O₃) $[M+H]^+$ requires 250.1192, found $[M+H]^+$ 250.1189.

Methyl (3*S*,5*S*,6*R*)-5-amino-1-(3,5-dimethylisoxazol-4-yl)-6-methylpiperidine-3-carboxylate (290)



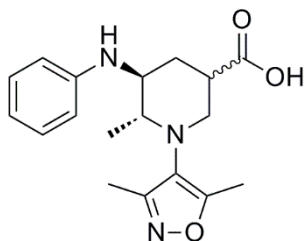
A vial was charged methyl (3*S*,5*S*,6*R*)-5-(((benzyloxy)carbonyl)amino)-1-(3,5-dimethylisoxazol-4-yl)-6-methylpiperidine-3-carboxylate **285** (78 mg, 0.19 mmol) and NaI (291 mg, 1.94 mmol). The vial was sealed and evacuated and purged with nitrogen, before MeCN (1 mL) was added. This was cooled to 0 °C and TMSCl (248 μ L, 1.94 mmol) was added, dropwise. This was stirred at 0 °C for 10 min before being allowed to warm to RT and stirred for 2 h. Three further portions of TMSCl (248 μ L, 1.94 mmol) were added at 30 min intervals, and the reaction stirred for a final 30 min. The reaction was quenched with MeOH (3 mL) and stirred for 1 min before being transferred to a flask with MeOH (40 mL) and the solvent being removed *in vacuo*. The residue was taken up into MeOH (0.5 mL) and loaded onto a pre-equilibrated SCX-2 cartridge (10 g). After 15 min, the column was flushed with MeOH (5 CV) before being eluted with 2 M NH₃ in MeOH (5 CV). The ammonia fractions were combined and the solvent removed *in vacuo*. The residue was taken up into MeOH (0.5 mL) and loaded onto a second pre-equilibrated SCX-2 cartridge (5 g). After 15 min, the column was flushed with MeOH (5 CV) before being eluted with 2 M NH₃ in MeOH (5 CV). The ammonia fractions were combined and the solvent removed *in vacuo* to provide the titled compound as a yellow gum (41 mg, 79% yield). ν_{max} (CDCl₃): 3366(br.), 2929(m), 2825(w), 1761(s), 1676(m) cm⁻¹; ¹H NMR (400 MHz, CD₃OD) δ = 3.68 (s, 3H), 3.34 - 3.29 (m, 1H), 3.13 (dd, J = 3.4, 11.7 Hz, 1H), 2.78 - 2.70 (m, 2H), 2.64 (ddd, J = 4.2, 7.6, 10.5 Hz, 1H), 2.33 (dtd, J = 1.7, 4.2, 13.2 Hz, 1H), 2.24 (s, 3H), 2.14 (s, 3H), 1.49 (ddd, J = 4.6, 10.5, 13.2 Hz, 1H), 0.90 (d, J = 6.1 Hz, 3H). Amine protons not observed; ¹³C NMR (101 MHz, CD₃OD) δ = 175.7, 165.6, 160.6, 127.0, 63.4, 54.8, 52.9, 52.4, 41.1, 34.1, 16.5, 11.1, 10.6; LCMS (High pH): t_R = 0.74 min, $[M+H]^+$ = 268, (98% purity); HRMS: (C₁₃H₂₁N₃O₃) $[M+H]^+$ requires 268.1661, found $[M+H]^+$ 268.1660.

Methyl (3*S*,5*S*,6*R*)-1-(3,5-dimethylisoxazol-4-yl)-6-methyl-5-(phenylamino)piperidine-3-carboxylate (291)



A vial was charged with Pd₂(dba)₃ (14. mg, 0.015 mmol), DavePhos (12 mg, 0.031 mmol) and NaO^tBu (21 mg, 0.22 mmol). The vial was sealed, evacuated and purged with nitrogen before toluene (0.5 mL) was added, and the mixture was stirred at RT for 5 min. To this was added a solution of methyl (3*S*,5*S*,6*R*)-5-amino-1-(3,5-dimethylisoxazol-4-yl)-6-methylpiperidine-3-carboxylate **290** (41 mg, 0.15 mmol) and bromobenzene (32 μL, 0.31 mmol) in toluene (1.5 mL) and the sealed vial was heated to 130 °C for 16 h. This was allowed to cool and the solvent was removed *in vacuo*. The residue was taken up into EtOAc (5 mL) and filtered through Celite (2.5 g), and flushed through with further EtOAc (3 x 10 mL). The combined organics were concentrated *in vacuo* and the residue was taken up into DCM (2 mL) and purified by normal phase column chromatography (EtOAc in cyclohexane, 0 → 50%, 24 g SiO₂) to provide the titled compound as a yellow gum (29 mg, 55% yield). ν_{\max} (CDCl₃): 3383(br.), 2929(m), 2856(w), 1732(s), 1602(s) cm⁻¹; ¹H NMR (400 MHz, CDCl₃) δ = 7.23 - 7.17 (m, 2H), 6.71 (tt, *J* = 1.0, 7.3 Hz, 1H), 6.68 - 6.65 (m, 2H), 3.86 (br. s, 1H), 3.74 (s, 3H), 3.58 - 3.52 (m, 1H), 3.45 (dd, *J* = 6.4, 11.5 Hz, 1H), 3.12 (dd, *J* = 3.7, 11.5 Hz, 1H), 2.99 (quin, *J* = 6.4 Hz, 1H), 2.84 - 2.77 (m, 1H), 2.38 (ddd, *J* = 3.7, 7.1, 13.4 Hz, 1H), 2.34 (s, 3H), 2.22 (s, 3H), 1.70 (ddd, *J* = 4.4, 7.6, 13.4 Hz, 1H), 1.07 (d, *J* = 6.4 Hz, 3H); ¹³C NMR (101 MHz, CDCl₃) δ = 173.8, 162.7, 158.5, 146.9, 129.5 (2C), 125.6, 117.4, 113.1 (2C), 60.2, 52.2, 51.8, 51.1, 39.2, 29.2, 14.9, 11.3, 10.5; LCMS (High pH): *t*_R = 1.20 min, [M+H]⁺ = 344, (93% purity); HRMS: (C₁₉H₂₅N₃O₃) [M+H]⁺ requires 344.1974, found [M+H]⁺ 344.1968.

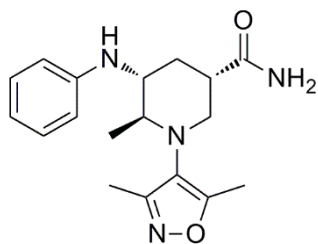
(5*S*,6*R*)-1-(3,5-Dimethylisoxazol-4-yl)-6-methyl-5-(phenylamino)piperidine-3-carboxylic acid (292)



To a vial containing methyl (3*S*,5*S*,6*R*)-1-(3,5-dimethylisoxazol-4-yl)-6-methyl-5-(phenylamino)piperidine-3-carboxylate **291** (28 mg, 0.082 mmol) was added a solution of NaOMe, 0.25 wt% in MeOH (3.73 mL, 0.163 mmol), under a nitrogen atmosphere. The vial was heated at 65 °C for 16 h, before being allowed to cool to RT. 1 M NaOH (aq, 408 μL, 0.408 mmol) was added and the reaction was heated at 65 °C for a further 2 h before being allowed to cool to RT. The reaction mixture was diluted with H₂O (30 mL) and washed with DCM (10 mL). The

aqueous phase was then acidified to ~pH 5 with 2 M HCl (aq, 0.3 mL) and extracted with DCM (3 x 20 mL). The combined organics were washed with brine (10 mL), passed through a hydrophobic frit, and the solvent was removed *in vacuo* to provide the titled compound as a yellow oil (27 mg, 101% yield). ¹H NMR suggests a 1.4:1 mixture of diastereomers, with the all-equatorial arrangement being the major component. Major Diastereomer: ¹H NMR (400 MHz, CDCl₃) δ = 7.23 - 7.15 (m, 2H), 6.72 (t, *J* = 7.3 Hz, 1H), 6.68 - 6.60 (m, 2H), 3.26 - 3.14 (m, 2H), 3.09 (t, *J* = 11.0 Hz, 1H), 2.89 - 2.78 (m, 2H), 2.61 - 2.52 (m, 1H), 2.34 (s, 3H), 2.26 (s, 3H), 1.46 (q, *J* = 12.2 Hz, 1H), 1.03 (d, *J* = 6.1 Hz, 3H); Minor Diastereomer: ¹H NMR (400 MHz, CDCl₃) δ = 7.23 - 7.15 (m, 2H), 6.72 (t, *J* = 7.3 Hz, 1H), 6.68 - 6.60 (m, 2H), 3.54 (ddd, *J* = 4.2, 6.6, 8.1 Hz, 1H), 3.45 (dd, *J* = 5.9, 11.7 Hz, 1H), 3.26 - 3.14 (m, 1H), 2.89 - 2.78 (m, 2H), 2.47 - 2.39 (m, 1H), 2.34 (s, 3H), 2.24 (s, 3H), 1.70 (ddd, *J* = 4.4, 8.3, 13.4 Hz, 1H), 1.08 (d, *J* = 6.4 Hz, 3H). Anilinic and carboxylic acid protons not observed; LCMS (Formic): *t_R* = 1.03, [M+H]⁺ = 330, (38% purity); *t_R* = 1.08 min, [M+H]⁺ = 330, (56% purity).

(3*S*,5*R*,6*S*)-1-(3,5-Dimethylisoxazol-4-yl)-6-methyl-5-(phenylamino)piperidine-3-carboxamide (293)



The titled compound was isolated as the minor enantiomer in the chiral separation of (3*S*,5*S*,6*R*)-1-(3,5-Dimethylisoxazol-4-yl)-6-methyl-5-(phenylamino)piperidine-3-carboxamide **237**, as a colourless oil (1.5 mg). Identity of enantiomer has been assigned with reference to the biological assay data. e.e. > 99.0%; *v*_{max} (DCM): 3348(br.), 3202(w), 2935(w), 1667(s), 1602(s) cm⁻¹; ¹H NMR (400 MHz, CD₃OD) δ = 7.10 - 7.05 (m, 2H), 6.65 - 6.60 (m, 2H), 6.56 (tt, *J* = 1.0, 7.3 Hz, 1H), 3.18 (ddd, *J* = 4.2, 9.3, 11.2 Hz, 1H), 3.13 (t, *J* = 11.2 Hz, 1H), 3.01 (ddd, *J* = 1.5, 3.7, 11.2 Hz, 1H), 2.93 (qd, *J* = 6.1, 9.0 Hz, 1H), 2.77 - 2.67 (m, 1H), 2.35 (s, 3H), 2.30 (dtd, *J* = 1.7, 3.7, 13.0 Hz, 1H), 2.25 (s, 3H), 1.49 (q, *J* = 12.5 Hz, 1H), 0.97 (d, *J* = 6.1 Hz, 3H). Anilinic and primary amide protons not observed; LCMS (Formic): *t_R* = 0.94 min, [M+H]⁺ = 329, (94% purity); HRMS: (C₁₈H₂₄N₄O₂) [M+H]⁺ requires 329.1978, found [M+H]⁺ 329.1971.

9.3 Supplementary Protocols

Artificial Membrane Permeability

An artificial membrane was prepared by applying 1.8% egg phosphatidyl choline and 1% cholesterol n-decane solution to the bottom of a microfiltration insert in a Transwell plate. To both the top (acceptor) and bottom (donor) wells of the plate was added 50 mM phosphate buffer (pH 7.4) containing 0.5% 2-hydroxypropyl- β -cyclodextrin, and the lipids formed bilayers across the small holes in the filter. The compound solution was added to the donor well and the plate was allowed to incubate at RT for 3 h.^{190,191} The sample concentration in both the donor and acceptor compartments was determined by HPLC and the rate of permeation calculated, and expressed in nm/s.

BRD4 FRET Assays

Unless otherwise stated, compounds are reported from three or more test occasions ($n \geq 3$) in these FRET assays.

BRD4 proteins were produced using the published protocols.¹⁹² Compounds were screened against *N*-terminal 6His-tagged single mutant tandem bromodomain proteins: BRD4 (1-477) Y390A (mutated in BD2 to monitor compound binding to BD1) or BRD4 (1-477) Y97A (mutated in BD1 to monitor compound binding to BD2), in a dose-response format using an Alexa Fluor 647 derivative of I-BET762 **300** (Figure 82).

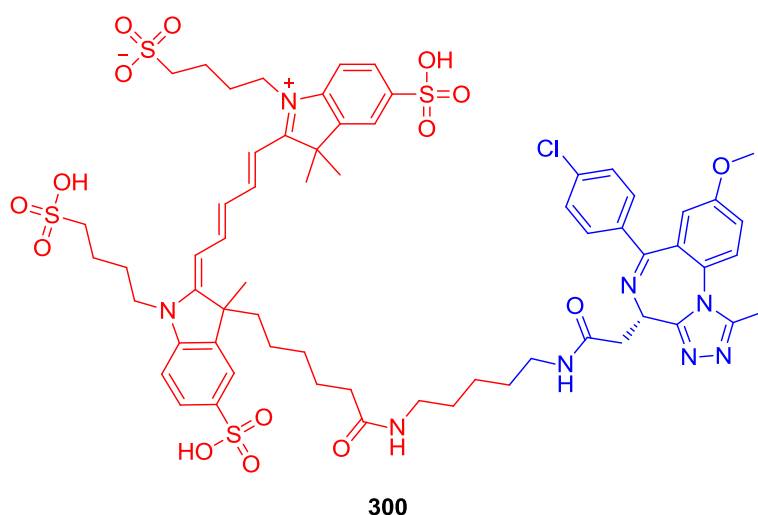


Figure 82. Fluorophore tagged derivative of I-BET762 **300 used in the mutant BRD4 FRET assays. The portion derived from I-BET762 is coloured blue and the portion derived from Alexa Fluor 647 is coloured red.**

Compounds were titrated from either 10 mM or 100 mM (the latter being referred to as the “high concentration” assay in the text, giving a lower pIC_{50} limit of 3.3, as opposed to 4.3) in 100% DMSO and 100 nL transferred to a low volume black 384 well micro titre

plate using a Labcyte Echo 555. A Thermo Scientific Multidrop Micro were used to dispense 5 μ L of 10 nM protein in 50 mM HEPES, 50 mM NaCl and 1 mM CHAPS, pH 7.4, in the presence of 50 nM fluorophore compound **300** ($\sim K_d$ concentration for the interaction between all BET single mutant tandem bromodomain proteins and **300**). After equilibrating for 1 h in the dark at RT, the bromodomain protein:fluorescent ligand interaction was detected using TR-FRET following a 5 μ L addition of 1.5 nM europium chelate labelled anti-6His antibody (Perkin Elmer, W1024, AD0111) in assay buffer. Time resolved fluorescence (TRF) was then detected on a TRF laser equipped Perkin Elmer Envision multimode plate reader (excitation = 337 nm; emission 1 = 615 nm; emission 2 = 665 nm; dual wavelength bias dichroic = 400 nm, 630 nm). TR-FRET ratio was calculated using the following equation: Ratio = ((Acceptor fluorescence at 665 nm) / (Donor fluorescence at 615 nm)) * 1000. TR-FRET ratio data was normalised to a mean of 16 replicates per micro titre plate of both 10 μ M I-BET151 **12** and 1% DMSO controls and IC_{50} values determined for each of the compounds tested by fitting the fluorescence ratio data to a four parameter model: $y = a + ((b - a) / (1 + (10^x / 10^c)^d))$ where 'a' is the minimum, 'b' is the Hill slope, 'c' is the IC_{50} and 'd' is the maximum.

BROMOscan® Bromodomain Profiling

BROMOscan® bromodomain profiling was provided by DiscoverX Corp. (Fremont, CA, USA, <http://www.discoverx.com>). Determination of the percent inhibition of DNA tagged bromodomains by test compounds was achieved through binding competition against a proprietary reference immobilized ligand. For each protein, two readings were made and an average taken.

CAD Solubility

GSK in-house kinetic solubility assay: A 5 μ L aliquot of a 10 mM solution of compound in DMSO was diluted to 100 μ L with phosphate buffered saline (pH 7.4) and equilibrated for 1 h at RT. The mixture was filtered through a Millipore Multiscreen_{HTS}-PCF filter plate (MSSL BPC). The filtrate was quantified by suitably calibrated Charged Aerosol Detector (CAD).¹⁹³

ChromLogD_{pH7.4}

The Chromatographic Hydrophobicity Index (CHI)¹⁹⁴ values were measured using a reverse phase HPLC column (50 x 2 mm 3 μ M Gemini NX C₁₈, Phenomenex, UK) with fast acetonitrile gradient and an aqueous mobile phase adjusted to pH 7.4. CHI values were derived directly from the gradient retention times by using a calibration line obtained for standard compounds. The CHI value approximates to the volume % organic

concentration when the compound elutes. CHI is linearly transformed into ChromLogD by least-squares fitting of experimental CHI values to calculated ClogP values for over 20 thousand research compounds using the following formula: $\text{ChromLogD} = 0.0857\text{CHI} - 2.00$.¹⁶¹

CLND Solubility

GSK in-house kinetic solubility assay: A 5 μL aliquot of a 10 mM solution of compound in DMSO was diluted to 100 μL with phosphate buffered saline (pH 7.4) and equilibrated for 1 h at RT. The mixture was filtered through a Millipore Multiscreen_{HTS}-PCF filter plate (MSSL BPC). The filtrate was quantified by suitably calibrated flow injection Chemiluminescent Nitrogen Detection (CLND).¹⁹⁵

FaSSIF Solubility

This experiment determines the solubility of solid compounds in Fasted Simulated Intestinal Fluid (FaSSIF) at pH 6.5 after 4 h equilibration at RT. 1 mL of FaSSIF buffer (3 mM sodium taurocholate, 0.75 mM lecithin in sodium phosphate buffer at pH 6.5) is added to manually weighed 1 mg of solid compound in a 2 mL HPLC autosampler vial. The resulting suspension is shaken at 900 rpm for 4 h at RT and then transferred to a Multiscreen HTS, 96-well solubility filter plate. The residual solid is removed by filtration. The supernatant solution is quantified by HPLC-UV using single point calibration of a known concentration of the compound in DMSO. The dynamic range of the assay is 1-1000 $\mu\text{g}/\text{mL}$.

PBMC Assay

Blood containing 15% v/v ACD-A anticoagulant (Baxter Healthcare) was collected and 30 mL poured into 50 mL Leucosep tubes (Greiner Bio-one) pre-filled with Ficoll. The tubes were centrifuged for 15 min at 800 x g (RT). The enriched cell fractions from each Leucosep tube were pooled in a 500 mL centrifuge tube. The pooled fractions were centrifuged at RT for 10 min at 400 x g, and the supernatant discarded. The cell pellet was resuspended in 40 mL PBS and the cells counted on a Nucleocounter (Chemometec). The cells were centrifuged at 300 x g for 10 min at r.t., the supernatant discarded, and the cell pellet resuspended in freezing medium (90% heat-inactivated FBS, 10% DMSO) to make a final concentration of 4×10^7 cells/mL. The cells were aliquoted and cryopreserved using a controlled-rate freezer (Planer). Compound plates containing 0.5 μL test sample in 100% DMSO were prepared (two replicates on account of PBMC donor variability). PBMCs were thawed from frozen stocks and resuspended in warm media (500 mL RPMI, 50 mL Heat Inactivated Australian Foetal Bovine Serum, 5 mL

Penicillin/Streptomycin, 5 mL Glutamax) at a concentration of 0.32×10^6 cells/mL. 10 μ L of lipopolysaccharide (1 ng/mL final assay concentration) was added to each well of the compound plates. The seeded plates were then lidded and placed in the humidified primary cell incubator for 18–24 h at 37 °C, 5% CO₂. 20 μ L of cell supernatant was placed in a 96-well MSD plate pre-coated with human MCP-1 capture antibody. The plates were sealed and placed on a shaker at 600 rpm for 2 h at RT. 20 μ L of Anti-human MCP-1 antibody labelled with MSD SULFO-TAG™ reagent was added to each well of the MSD plate (stock 50X was diluted 1:50 with Diluent 100, final assay concentration is 1 μ g/mL). The plates were then re-sealed and shaken for 1 h before washing with PBS. 150 μ L of 2X MSD Read Buffer T (stock 4X MSD Read Buffer T was diluted 50:50 with de-ionised water) was then added to each well and the plates read (electrochemiluminescence detection) on the MSD Sector Imager 6000.

The human biological samples were sourced ethically and their research use was in accord with the terms of the informed consents under an IRB/EC approved protocol.

pK_a Determination

Sirius T3 (Sirius Analytical Inc, UK) instrument is used for pK_a determination of compounds. The pK_a determination is based on acid-base titration and the protonation/deprotonation of the molecule is measured either by UV spectroscopy or potentiometrically. The pK_a value is calculated from the pH where 50% of the protonated and unprotonated form of the molecules are present. The UV-metric method provides pK_a results for samples with chromophores whose UV absorbance changes as a function of pH. It typically requires 5 μ L of a 10 mM solution of the samples and the UV absorbance is monitored over 54 pH values in a buffered solution in about 5 min. When the ionization centre is far from the UV chromophore pH-metric method based on potentiometric acid-base titration is used. The pH of each point in the titration curve is calculated using equations that contain pK_a, and the calculated points are fitted to the measured curve by manipulating the pK_a. The pK_a that provides the best fit is taken to be the measured pK_a. Usually 0.5–1 mg of solid material is required for the measurements. When the compound precipitates at some point during the pH titration, co-solvent method using methanol is applied using various concentration of co-solvent. The pK_a in water is calculated using the Yasuda-Shedlovsky extrapolation method.

10. References

1. Prieto-Martínez, F. D.; Gortari, E. F.; Méndez-Lucio, O.; Medina-Franco, J. L. *RSC Adv.* **2016**, *6*, 56225–56239.
2. Lovering, F.; Bikker, J.; Humblet, C. *J. Med. Chem.* **2009**, *52*, 6752–6756.
3. Lovering, F. *Med. Chem. Commun.* **2013**, *4*, 515–519.
4. Berg, J. M.; Tymoczko, J. L.; Stryer, L. *Biochemistry*, 7th ed., W. H. Freeman and Company: New York, 2012, p. 973-993.
5. Li, G.; Reinberg, D. *Curr. Opin. Genet. Dev.* **2011**, *21*, 175–186.
6. Paweletz, N. *Nat. Rev. Mol. Cell Biol.* **2001**, *2*, 72–75.
7. Luger, K.; Mäder, A. W.; Richmond, R. K.; Sargent, D. F.; Richmond, T. J. *Nature* **1997**, *389*, 251–260.
8. National Human Genome Research Institute.
<http://genome.nhgri.nih.gov/histones/complete.shtml> (accessed Jun 28, 2015).
9. Watson, J. D.; Crick, F. H. C. *Nature* **1953**, *171*, 737–738.
10. Olins, D. E.; Olins, A. L. *Nat. Rev. Mol. Cell Biol.* **2003**, *4*, 809–814.
11. Porter, I. M.; Khoudoli, G. A.; Swedlow, J. R. *Curr. Biol.* **2004**, *14*, R554–R556.
12. Pines, J.; Rieder, C. L. *Nat. Cell Biol.* **2001**, *3*, E3–E6.
13. Leja, D. National Human Genome Research Institute.
<http://www.genome.gov/Glossary/resources/chromatin.pdf> (accessed Jun 28, 2015).
14. Orphanides, G.; Reinberg, D. *Cell* **2002**, *108*, 439–451.
15. Richards, E. J.; Elgin, S. C. R. *Cell* **2002**, *108*, 489–500.
16. Jaenisch, R.; Bird, A. *Nat. Genet. Suppl.* **2003**, *33*, 245–254.
17. López-Maury, L.; Marguerat, S.; Bähler, J. *Nat. Rev. Genet.* **2008**, *9*, 583–593.
18. Arrowsmith, C. H.; Bountra, C.; Fish, P. V.; Lee, K.; Schapira, M. *Nat. Rev. Drug Discov.* **2012**, *11*, 384–400.
19. Bernstein, B. E.; Meissner, A.; Lander, E. S. *Cell* **2007**, *128*, 669–681.
20. Severin, P. M. D.; Zou, X.; Gaub, H. E.; Schulten, K. *Nucleic Acids Res.* **2011**, *39*, 8740–8751.
21. Severin, P. M. D.; Zou, X.; Schulten, K.; Gaub, H. E. *Biophys. J.* **2013**, *104*, 208–215.

22. Curradi, M.; Izzo, A.; Badaracco, G.; Landsberger, N. *Mol. Cell. Biol.* **2002**, *22*, 3157–3173.
23. Bannister, A. J.; Kouzarides, T. *Cell Res.* **2011**, *21*, 381–395.
24. Grunstein, M. *Nature* **1997**, *389*, 349–352.
25. Berg, J. M.; Tymoczko, J. L.; Stryer, L. *Biochemistry*, 7th ed., W. H. Freeman and Company: New York, 2012, p. 898-899.
26. Josling, G. A.; Selvarajah, S. A.; Petter, M.; Duffy, M. F. *Genes* **2012**, *3*, 320–343.
27. Agalioti, T.; Chen, G.; Thanos, D. *Cell* **2002**, *111*, 381–392.
28. Ruthenburg, A. J.; Li, H.; Milne, T. A.; Dewell, S.; McGinty, R. K.; Yuen, M.; Ueberheide, B.; Dou, Y.; Muir, T. W.; Patel, D. J.; Allis, C. D. *Cell* **2011**, *145*, 692–706.
29. Filippakopoulos, P.; Knapp, S. *Nat. Rev. Drug Discov.* **2014**, *13*, 337–356.
30. Kennison, J. A.; Tamkunt, J. W. *Proc. Natl. Acad. Sci. USA* **1988**, *85*, 8136–8140.
31. Thompson, M. *Biochimie* **2009**, *91*, 309–319.
32. Filippakopoulos, P.; Picaud, S.; Mangos, M.; Keates, T.; Lambert, J.-P.; Barsyte-Lovejoy, D.; Felletar, I.; Volkmer, R.; Müller, S.; Pawson, T.; Gingras, A.-C.; Arrowsmith, C. H.; Knapp, S. *Cell* **2012**, *149*, 214–231.
33. Chung, C.-W.; Dean, A. W.; Woolven, J. M.; Bamborough, P. *J. Med. Chem.* **2012**, *55*, 576–586.
34. Chung, C.-W.; Tough, D. F. *Drug Discov. Today Ther. Strateg.* **2012**, *9*, e111–e120.
35. Duvic, M.; Vu, J. *Expert Opin. Investig. Drugs* **2007**, *16*, 1111–1120.
36. Bertino, E. M.; Otterson, G. A. *Expert Opin. Investig. Drugs* **2011**, *20*, 1151–1158.
37. FDA list of approved drugs categorised by Established Pharmacologic Class <https://www.fda.gov/downloads/drugs/guidancecomplianceregulatoryinformation/lawsactsandrules/ucm428333.pdf> (accessed Mar 16, 2017).
38. <https://www.drugs.com/drug-class/histone-deacetylase-inhibitors.html> (accessed Mar 16, 2017).
39. Fedorov, O. *Future Med. Chem.* **2014**, *6*, 1101–1103.
40. Muller, S.; Filippakopoulos, P.; Knapp, S. *Expert Rev. Mol. Med.* **2011**, *13*, e29.
41. Filippakopoulos, P.; Qi, J.; Picaud, S.; Shen, Y.; Smith, W. B.; Fedorov, O.; Morse, E. M.; Keates, T.; Hickman, T. T.; Felletar, I.; Philpott, M.; Munro, S.; McKeown, M. R.;

- Wang, Y.; Christie, A. L.; West, N.; Cameron, M. J.; Schwartz, B.; Heightman, T. D.; La Thangue, N.; French, C. A.; Wiest, O.; Kung, A. L.; Knapp, S.; Bradner, J. E. *Nature* **2010**, *468*, 1067–1073.
42. Rahman, S.; Sowa, M. E.; Ottinger, M.; Smith, J. A.; Shi, Y.; Harper, J. W.; Howley, P. *M. Mol. Cell. Biol.* **2011**, *31*, 2641–2652.
43. Liu, L.; Zhen, X. T.; Denton, E.; Marsden, B. D.; Schapira, M. *Bioinformatics* **2012**, *28*, 2205–2206.
44. Shi, J.; Vakoc, C. R. *Mol. Cell* **2014**, *54*, 728–736.
45. Dey, A.; Ellenberg, J.; Farina, A.; Coleman, A. E.; Maruyama, T.; Sciortino, S.; Lippincott-Schwartz, J.; Ozato, K. *Mol. Cell. Biol.* **2000**, *20*, 6537–6549.
46. Belkina, A. C.; Denis, G. V. *Nat. Rev. Cancer* **2012**, *12*, 465–477.
47. Andrieu, G.; Belkina, A. C.; Denis, G. V. *Drug Discov. Today Technol.* **2016**, *19*, 45–50.
48. French, C. A. *Cancer Genet.* **2010**, *203*, 16–20.
49. Grunwald, C.; Koslowski, M.; Arsiray, T.; Dhaene, K.; Praet, M.; Victor, A.; Morresi-Hauf, A.; Lindner, M.; Passlick, B.; Lehr, H.-A.; Schäfer, S. C.; Seitz, G.; Huber, C.; Sahin, U.; Türeci, O. *Int. J. Cancer* **2006**, *118*, 2522–2528.
50. Scanlan, M. J.; Altorki, N. K.; Gure, A. O.; Williamson, B.; Jungbluth, A.; Chen, Y.; Old, L. J. *Cancer Lett.* **2000**, *150*, 155–164.
51. Crawford, N. P. S.; Alsarraj, J.; Lukes, L.; Walker, R. C.; Officewala, J. S.; Yang, H. H.; Lee, M. P.; Ozato, K.; Hunter, K. W. *Proc. Natl. Acad. Sci. USA* **2008**, *105*, 6380–6385.
52. You, J.; Srinivasan, V.; Denis, G. V.; Harrington, W. J.; Ballestas, M. E.; Kaye, K. M.; Howley, P. M. *J. Virol.* **2006**, *80*, 8909–8919.
53. Weidner-Glunde, M.; Ottinger, M.; Schulz, T. F. *Front. Biosci.* **2010**, *15*, 537–549.
54. Lin, A.; Wang, S.; Nguyen, T.; Shire, K.; Frappier, L. *J. Virol.* **2008**, *82*, 12009–12019.
55. Karelis, A. D.; Faraj, M.; Bastard, J. P.; St-Pierre, D. H.; Brochu, M.; Prud'homme, D.; Rabasa-Lhoret, R. *J. Clin. Endocrinol. Metab.* **2005**, *90*, 4145–4150.
56. Wang, F.; Liu, H.; Blanton, W. P.; Belkina, A.; Nathan, K.; Denis, G. V. *Biochem. J.* **2011**, *425*, 71–83.
57. Mahdi, H.; Fisher, B. A.; Källberg, H.; Plant, D.; Malmström, V.; Rönnelid, J.;

- Charles, P.; Ding, B.; Alfredsson, L.; Padyukov, L.; Symmons, D. P. M.; Venables, P. J.; Klareskog, L.; Lundberg, K. *Nat. Genet.* **2009**, *41*, 1319–1324.
58. Jones, M. H.; Numata, M.; Shimane, M. *Genomics* **1997**, *45*, 529–534.
59. Berkovits, B. D.; Wolgemuth, D. J. In *Current Topics in Developmental Biology*; Elsevier Inc., 2013; Vol. 102, pp. 293–326.
60. Plaseski, T.; Noveski, P.; Popeska, Z.; Efremov, G. D.; Plaseska-Karanfilska, D. *J. Androl.* **2012**, *33*, 675–683.
61. Nicodème, E.; Jeffrey, K. L.; Schaefer, U.; Beinke, S.; Dewell, S.; Chung, C.-W.; Chandwani, R.; Marazzi, I.; Wilson, P.; Coste, H.; White, J.; Kirilovsky, J.; Rice, C. M.; Lora, J. M.; Prinjha, R. K.; Lee, K.; Tarakhovsky, A. *Nature* **2010**, *468*, 1119–1123.
62. Vidler, L. R.; Filippakopoulos, P.; Fedorov, O.; Picaud, S.; Martin, S.; Tomsett, M.; Woodward, H.; Brown, N.; Knapp, S.; Hoelder, S. *J. Med. Chem.* **2013**, *56*, 8073–8088.
63. Bamborough, P.; Diallo, H.; Goodacre, J. D.; Gordon, L.; Lewis, A.; Seal, J. T.; Wilson, D. M.; Woodrow, M. D.; Chung, C. W. *J. Med. Chem.* **2012**, *55*, 587–596.
64. Hewings, D. S.; Fedorov, O.; Filippakopoulos, P.; Martin, S.; Picaud, S.; Tumber, A.; Wells, C.; Olcina, M. M.; Freeman, K.; Gill, A.; Ritchie, A. J.; Sheppard, D. W.; Russell, A. J.; Hammond, E. M.; Knapp, S.; Brennan, P. E.; Conway, S. J. *J. Med. Chem.* **2013**, *56*, 3217–3227.
65. Picaud, S.; Da Costa, D.; Thanasopoulou, A.; Filippakopoulos, P.; Fish, P. V.; Philpott, M.; Fedorov, O.; Brennan, P.; Bunnage, M. E.; Owen, D. R.; Bradner, J. E.; Tanriere, P.; O’Sullivan, B.; Müller, S.; Schwaller, J.; Stankovic, T.; Knapp, S. *Cancer Res.* **2013**, *73*, 3336–3346.
66. Zhao, L.; Cao, D.; Chen, T.; Wang, Y.; Miao, Z.; Xu, Y.; Chen, W.; Wang, X.; Li, Y.; Du, Z.; Xiong, B.; Li, J.; Xu, C.; Zhang, N.; He, J.; Shen, J. *J. Med. Chem.* **2013**, *56*, 3833–3851.
67. Lucas, X.; Wohlwend, D.; Hügler, M.; Schmidtkunz, K.; Gerhardt, S.; Schüle, R.; Jung, M.; Einsle, O.; Günther, S. *Angew. Chem. Int. Ed.* **2013**, *52*, 14055–14059.
68. www.chemspider.com/Chemical-Structure.58828664.html (accessed Oct 6, 2017).
69. www.chemspider.com/Chemical-Structure.58172612.html (accessed Oct 6, 2017).

70. Albrecht, B. K.; Gehling, V. S.; Hewitt, M. C.; Vaswani, R. G.; Côté, A.; Leblanc, Y.; Nasveschuk, C. G.; Bellon, S.; Bergeron, L.; Campbell, R.; Cantone, N.; Cooper, M. R.; Cummings, R. T.; Jayaram, H.; Joshi, S.; Mertz, J. A.; Neiss, A.; Normant, E.; O'Meara, M.; Pardo, E.; Poy, F.; Sandy, P.; Supko, J.; Sims, R. J.; Harmange, J. C.; Taylor, A. M.; Audia, J. E. *J. Med. Chem.* **2016**, *59*, 1330–1339.
71. Seal, J.; Lamotte, Y.; Donche, F.; Bouillot, A.; Mirguet, O.; Gellibert, F.; Nicodeme, E.; Krysa, G.; Kirilovsky, J.; Beinke, S.; McCleary, S.; Rioja, I.; Bamborough, P.; Chung, C. W.; Gordon, L.; Lewis, T.; Walker, A. L.; Cutler, L.; Lugo, D.; Wilson, D. M.; Witherington, J.; Lee, K.; Prinjha, R. K. *Bioorg. Med. Chem. Lett.* **2012**, *22*, 2968–2972.
72. Gosmani, R.; Nguyen, V. L.; Toum, J.; Simon, C.; Brusq, J.-M. G.; Krysa, G.; Mirguet, O.; Riou-Eymard, A. M.; Boursier, E. V.; Trottet, L.; Bamborough, P.; Clark, H.; Chung, C.; Cutler, L.; Demont, E. H.; Kaur, R.; Lewis, A. J.; Schilling, M. B.; Soden, P. E.; Taylor, S.; Walker, A. L.; Walker, M. D.; Prinjha, R. K.; Nicodème, E. *J. Med. Chem.* **2014**, *726*, 8111–8131.
73. Lu, P.; Qu, X.; Shen, Y.; Jiang, Z.; Wang, P.; Zeng, H.; Ji, H.; Deng, J.; Yang, X.; Li, X.; Lu, H.; Zhu, H. *Sci. Rep.* **2016**, *6*, 24100.
74. www.clinicaltrials.gov (accessed Oct 5, 2017).
75. Delmore, J. E.; Issa, G. C.; Lemieux, M. E.; Rahl, P. B.; Shi, J.; Jacobs, H. M.; Kastritis, E.; Gilpatrick, T.; Paranal, R. M.; Qi, J.; Chesi, M.; Schinzel, A. C.; McKeown, M. R.; Heffernan, T. P.; Vakoc, C. R.; Bergsagel, P. L.; Ghobrial, I. M.; Richardson, P. G.; Young, R. A.; Hahn, W. C.; Anderson, K. C.; Kung, A. L.; Bradner, J. E.; Mitsiades, C. S. *Cell* **2011**, *146*, 904–917.
76. Patel, J. H.; Loboda, A. P.; Showe, M. K.; Showe, L. C.; McMahon, S. B. *Nat. Rev. Cancer* **2004**, *4*, 562–568.
77. Taub, R.; Kirsch, I.; Morton, C.; Lenoir, G.; Swan, D.; Tronick, S.; Aaronson, S.; Leder, P. *Proc. Natl. Acad. Sci. USA* **1982**, *79*, 7837–7841.
78. Dalla-favera, R.; Bregni, M.; Eriksont, J. A. N.; Patterson, D.; Gallo, R. C.; Crocetti, C. M. *Proc. Natl. Acad. Sci. USA* **1982**, *79*, 7824–7827.
79. Nesbit, C. E.; Tersak, J. M.; Prochownik, E. V. *Oncogene* **1999**, *18*, 3004–3016.
80. Mertz, J. A.; Conery, A. R.; Bryant, B. M.; Sandy, P.; Balasubramanian, S.; Mele, D. A.; Bergeron, L.; Sims, R. J. *Proc. Natl. Acad. Sci.* **2011**, *108*, 16669–16674.
81. Banerjee, C.; Archin, N.; Michaels, D.; Belkina, A. C.; Denis, G. V.; Bradner, J.;

- Sebastiani, P.; Margolis, D. M.; Montano, M. J. *Leukoc. Biol.* **2012**, *92*, 1147–1154.
82. Bisgrove, D. A.; Mahmoudi, T.; Henklein, P.; Verdin, E. *Proc. Natl. Acad. Sci. USA* **2007**, *104*, 13690–13695.
83. Galdeano, C.; Ciulli, A. *Future Med. Chem.* **2016**, *8*, 1655–1680.
84. Gamsjaeger, R.; Webb, S. R.; Lamonica, J. M.; Billin, A.; Blobel, G. A.; Mackay, J. P. *Mol. Cell. Biol.* **2011**, *31*, 2632–2640.
85. Baud, M. G. J.; Lin-shiao, E.; Cardote, T.; Tallant, C.; Pschibul, A.; Chan, K.; Zengerle, M.; Garcia, J. R.; Kwan, T. T.; Ferguson, F. M.; Ciulli, A. *Science* **2014**, *346*, 638–641.
86. Baud, M. G. J.; Lin-Shiao, E.; Zengerle, M.; Tallant, C.; Ciulli, A. *J. Med. Chem.* **2015**, *59*, 1492–1500.
87. Gacias, M.; Gerona-Navarro, G.; Plotnikov, A. N.; Zhang, G.; Zeng, L.; Kaur, J.; Moy, G.; Rusinova, E.; Rodriguez, Y.; Matikainen, B.; Vincek, A.; Joshua, J.; Casaccia, P.; Zhou, M. M. *Chem. Biol.* **2014**, *21*, 841–854.
88. Hewings, D. S.; Rooney, T. P. C.; Jennings, L. E.; Hay, D. A.; Schofield, C. J.; Brennan, P. E.; Knapp, S.; Conway, S. J. *J. Med. Chem.* **2012**, *55*, 9393–9413.
89. Unzue, A.; Zhao, H.; Lolli, G.; Dong, J.; Zhu, J.; Zechner, M.; Dolbois, A.; Caflich, A.; Nevado, C. *J. Med. Chem.* **2016**, *59*, 3087–3097.
90. Leeson, P. D.; Springthorpe, B. *Nat. Rev. Drug Discov.* **2007**, *6*, 881–890.
91. ChEMBL: <https://www.ebi.ac.uk/chembl/>.
92. Binding Database: <https://www.bindingdb.org/>.
93. Prieto-Martínez, F. D.; Medina-Franco, J. L. Department of Pharmacy, School of Chemistry, Universidad Nacional Autónoma de México, Personal communication (correction to Table S9), November 2016.
94. *Handbook of Chemistry and Physics*; Lide, D. R.; Haynes, W. M., Eds.; 95th ed.; CRC Press, 2014.
95. Yalkowsky, S. H.; Valvani, S. C. *J. Pharm. Sci.* **1980**, *69*, 912–922.
96. Jain, N.; Yalkowsky, S. H. *J. Pharm. Sci.* **2001**, *90*, 234–252.
97. Lamanna, C.; Bellini, M.; Padova, A.; Westerberg, G.; Maccari, L. *J. Med. Chem.* **2008**, *51*, 2891–2897.
98. Hewings, D. S.; Wang, M.; Philpott, M.; Fedorov, O.; Uttarkar, S.; Filippakopoulos,

- P.; Picaud, S.; Vuppusetty, C.; Marsden, B.; Knapp, S.; Conway, S. J.; Heightman, T. *D. J. Med. Chem.* **2011**, *54*, 6761–6770.
99. Bamborough, P.; Diallo, H.; Goodacre, J. D.; Gordon, L.; Lewis, A.; Seal, J. T.; Wilson, D. M.; Woodrow, M. D.; Chung, C.-W. *J. Med. Chem.* **2012**, *55*, 587–596.
100. Molecular Operating Environment (MOE) 2014. Energy minimised using Amber12:EHT force field and search implemented using the LowModeMD sampling algorithm.
101. Calculated using ChemAxon.
102. Teague, S. J.; Davis, A. M.; Leeson, P. D.; Oprea, T. *Angew. Chem. Int. Ed.* **1999**, *38*, 3743–3748.
103. Dawson, M. A.; Prinjha, R. K.; Dittmann, A.; Giotopoulos, G.; Bantscheff, M.; Chan, W.-I.; Robson, S. C.; Chung, C.; Hopf, C.; Savitski, M. M.; Huthmacher, C.; Gudgin, E.; Lugo, D.; Beinke, S.; Chapman, T. D.; Roberts, E. J.; Soden, P. E.; Auger, K. R.; Mirguet, O.; Doehner, K.; Delwel, R.; Burnett, A. K.; Jeffrey, P.; Drewes, G.; Lee, K.; Huntly, B. J. P.; Kouzarides, T. *Nature* **2011**, *478*, 529–533.
104. Ran, X.; Zhao, Y.; Liu, L.; Bai, L.; Yang, C. Y.; Zhou, B.; Meagher, J. L.; Chinnaswamy, K.; Stuckey, J. A.; Wang, S. *J. Med. Chem.* **2015**, *58*, 4927–4939.
105. Hay, D.; Fedorov, O.; Filippakopoulos, P.; Martin, S.; Philpott, M.; Picaud, S.; Hewings, D. S.; Uttakar, S.; Heightman, T. D.; Conway, S. J.; Knapp, S.; Brennan, P. *E. Med. Chem. Commun.* **2013**, *4*, 140–144.
106. Zhang, Z.; Hou, S.; Chen, H.; Ran, T.; Jiang, F.; Bian, Y.; Zhang, D.; Zhi, Y.; Wang, L.; Zhang, L.; Li, H.; Zhang, Y.; Tang, W.; Lu, T.; Chen, Y. *Bioorg. Med. Chem. Lett.* **2016**, *26*, 2931–2935.
107. Fall, Y.; Reynaud, C.; Doucet, H.; Santelli, M. *European J. Org. Chem.* **2009**, 4041–4050.
108. Moccia, M.; Cortigiani, M.; Monasterolo, C.; Torri, F.; Del Fiandra, C.; Fuller, G.; Kelly, B.; Adamo, M. F. A. *Org. Process Res. Dev.* **2015**, *19*, 1274–1281.
109. Iglesias, M.; Schuster, O.; Albrecht, M. *Tetrahedron Lett.* **2010**, *51*, 5423–5425.
110. Ranganath Rao, J. G.; Arumugam, N.; Ansari, M. M.; Gudla, C.; Pachiyapan, S.; Ramalingam, M.; George, J.; Arul, G. F.; Bommegowda, Y. K.; Angupillai, S. K.; Kottamalai, R.; Jidugu, P.; Rao, D. S. PCT/IN2011/000479 (WO 2012/011125), 2012.

111. Gutierrez, C. D.; Bavetsias, V.; Mcdonald, E. *J. Comb. Chem.* **2008**, *10*, 280–284.
112. Coleman, J. D.; Dhar, T. G. M. PCT/US99/05981 (WO 99/48890), 1999.
113. Kienle, M.; Dunst, C.; Knochel, P. *Org. Lett.* **2009**, *11*, 5158–5161.
114. Yuan, Y.; Hou, W.; Zhang-Negrerie, D.; Zhao, K.; Du, Y. *Org. Lett.* **2014**, *16*, 5410–5413.
115. Bustos, C.; Schott, E.; Rios, M.; Sanchez, C.; Cárcamo, J. *J. Chil. Chem. Soc.* **2009**, *54*, 267–268.
116. Bustos, C.; Molins, E.; Cárcamo, J.-G.; Aguilar, M. N.; Sánchez, C.; Moreno-Villoslada, I.; Nishide, H.; Mesías-Salazar, A.; Zarate, X.; Schott, E. *New J. Chem.* **2015**, *39*, 4295–4307.
117. Surry, D. S.; Buchwald, S. L. *Chem. Sci.* **2011**, *2*, 27–50.
118. Jiang, L.; Lu, X.; Zhang, H.; Jiang, Y.; Ma, D. *J. Org. Chem.* **2009**, *74*, 4542–4546.
119. Ma, D.; Cai, Q.; Zhang, H. *Org. Lett.* **2003**, *5*, 2453–2455.
120. Qiao, J.; Lam, P. *Synthesis* **2011**, *6*, 829–856.
121. Chan, D. M. T.; Wang, R.; Winters, M. P. *Tetrahedron Lett.* **1998**, *39*, 2933–2936.
122. Jitender, B.; Van der Eycken, E. *Chem. Soc. Rev.* **2013**, *42*, 9283–9303.
123. Takasu, N.; Oisaki, K.; Kanai, M. *Org. Lett.* **2013**, *15*, 1918–1921.
124. Ladouceur, G. H.; Velthuisen, E.; Choi, S.; Wang, Y.; Baryza, J. L.; Coish, P.; Bullock, W.; Smith, R.; Chen, M. PCT/US02/41634 (WO 03/057673), 2002.
125. Ahmed, Z.; Langer, P. *Tetrahedron Lett.* **2006**, *47*, 417–419.
126. Sher, M.; Ahmed, Z.; Rashid, M. A.; Fischer, C.; Spannenberg, A.; Langer, P. *Tetrahedron* **2007**, *63*, 4929–4936.
127. Elliott, R. L.; Kopecka, H.; Lin, N.-H.; He, Y.; Garvey, D. S. *Synthesis* **1995**, 772–774.
128. Felix, C. P.; Khatimi, N.; Laurent, A. *J. Org. Chem.* **1995**, *60*, 3907–3909.
129. Flores, A. F. C.; Piovesan, L. A.; Souto, A. A.; Pereira, M. A.; Martins, M. A. P.; Balliano, T. L.; da Silva, G. S. *Synth. Commun.* **2013**, *43*, 2326–2336.
130. Di Nunno, L.; Scilimato, A.; Vitale, P. *Tetrahedron* **2002**, *58*, 2659–2665.
131. Tang, S.; He, J.; Sun, Y.; He, L.; She, X. *J. Org. Chem.* **2010**, *75*, 1961–1966.
132. Tortolani, D. R.; Poss, M. A. *Org. Lett.* **1999**, *1*, 1261–1262.
133. Chandrasekhar, S.; Raji Reddy, C.; Nagendra Babu, B. *J. Org. Chem.* **2002**, *67*,

9080–9082.

134. Hopkins, A. L.; Groom, C. R.; Alex, A. *Drug Discov. Today* **2004**, *9*, 430–431.
135. Murray, C. W.; Erlanson, D. a.; Hopkins, A. L.; Keserü, G. M.; Leeson, P. D.; Rees, D. C.; Reynolds, C. H.; Richmond, N. J. *ACS Med. Chem. Lett.* **2014**, *5*, 616–618.
136. Docking experiments performed by Armelle Le Gall.
137. Evans pKa table http://evans.rc.fas.harvard.edu/pdf/evans_pKa_table.pdf.
138. Kim, S.; Oh, C. H.; Ko, J. S.; Ahn, K. H.; Kim, Y. J. *J. Org. Chem.* **1985**, *50*, 1927–1932.
139. Leonard, N. J.; Fox, R. C.; Oki, M. *J. Am. Chem. Soc.* **1954**, *76*, 5708–5714.
140. Pletsas, D.; Garelnabi, E. A. E.; Li, L.; Phillips, R. M.; Wheelhouse, R. T. *J. Med. Chem.* **2013**, *56*, 7120–7132.
141. De, K.; Legros, J.; Crousse, B.; Bonnet-Delpon, D. *J. Org. Chem.* **2009**, *74*, 6260–6265.
142. Gelin, C.; Flyer, A.; Adams, C. M.; Darsigny, V.; Hurley, T. B.; Karki, R. G.; Ji, N.; Kawanami, T.; Meredith, E.; Ser-Rano-Wi, M. H.; Rao, C.; Solovay, C.; Lee, G. T.; Towler, C.; Har, D.; Shen, L.; Hu, B.; Jiang, X.; Cap-Paci-Daniel, C. PST/US2012/047617 (WO 2013/016197), 2013.
143. Damera, K.; Reddy, K. L.; Sharma, G. V. M. *Lett. Org. Chem.* **2009**, *6*, 151–155.
144. Wang, J.; Meng, W.; Ni, Z.; Xue, S. *Chinese J. Chem.* **2011**, *29*, 2109–2113.
145. Chen, P.; Cao, L.; Tian, W.; Wang, X.; Li, C. *Chem. Commun.* **2010**, *46*, 8436–8438.
146. Within GSK laboratories.
147. Veitch, G. E.; Bridgwood, K. L.; Ley, S. V. *Org. Lett.* **2008**, *10*, 3623–3625.
148. Valeur, E.; Bradley, M. *Chem. Soc. Rev.* **2009**, *38*, 606–631.
149. Sabot, C.; Kumar, K. A.; Meunier, S.; Mioskowski, C. *Tetrahedron Lett.* **2007**, *48*, 3863–3866.
150. Williams, M. J.; Jobson, R. B.; Yasuda, N.; Marchesini, G.; Dolling, U.-H.; Grabowski, E. J. *J. Tetrahedron Lett.* **1995**, *36*, 5461–5464.
151. Jean, L.; Rouden, J.; Maddaluno, J.; Lasne, M. C. *J. Org. Chem.* **2004**, *69*, 8893–8902.
152. Jones, K. *Unpublished Results*.
153. Takahata, H.; Suto, Y.; Kato, E.; Yoshimura, Y.; Ouchi, H. *Adv. Synth. Catal.* **2007**, *349*, 685–693.

154. Nagano, T.; Kobayashi, S. *J. Am. Chem. Soc.* **2009**, *131*, 4200–4201.
155. Picaud, S.; Wells, C.; Felletar, I.; Brotherton, D.; Martin, S.; Savitsky, P.; Diez-Dacal, B.; Philpott, M.; Bountra, C.; Lingard, H.; Fedorov, O.; Müller, S.; Brennan, P. E.; Knapp, S.; Filippakopoulos, P. *Proc. Natl. Acad. Sci. USA* **2013**, *110*, 19754–19759.
156. McLure, K. G.; Gesner, E. M.; Tsujikawa, L.; Kharenko, O. A.; Attwell, S.; Campeau, E.; Wasiak, S.; Stein, A.; White, A.; Fontano, E.; Suto, R. K.; Wong, N. C. W.; Wagner, G. S.; Hansen, H. C.; Young, P. R. *PLoS One* **2013**, *8*, e83190.
157. Kharenko, O. A.; Gesner, E. M.; Patel, R. G.; Norek, K.; White, A.; Fontano, E.; Suto, R. K.; Young, P. R.; McLure, K. G.; Hansen, H. C. *Biochem. Biophys. Res. Commun.* **2016**, *477*, 62–67.
158. Cheng, C.; Diao, H.; Zhang, F.; Wang, Y.; Wang, K.; Wu, R. *Phys. Chem. Chem. Phys.* **2017**, *19*, 23934–23941.
159. Sato, S.; Sakamoto, T.; Miyazawa, E.; Kikugawa, Y. *Tetrahedron* **2004**, *60*, 7899–7906.
160. Bayliss, M. K.; Butler, J.; Feldman, P. L.; Green, D. V. S.; Leeson, P. D.; Palovich, M. R.; Taylor, A. J. *Drug Discov. Today* **2016**, *21*, 1719–1727.
161. Young, R. J.; Green, D. V. S.; Luscombe, C. N.; Hill, A. P. *Drug Discov. Today* **2011**, *16*, 822–830.
162. Rianjongdee, F. *Unpublished Results*.
163. Kugler-Steigmeier, M. E.; Friederich, U.; Graf, U.; Lutz, W. K.; Maier, P.; Schlatter, C. *Mutat. Res.* **1989**, *211*, 279–289.
164. Erez, R.; Shabat, D. *Org. Biomol. Chem.* **2008**, *6*, 2669–2672.
165. Henderson, J. L.; Buchwald, S. L. *Org. Lett.* **2010**, *12*, 4442–4445.
166. Mack, J. *Unpublished Results*.
167. Tyrrell, E.; Brawn, P.; Carew, M.; Greenwood, I. *Tetrahedron Lett.* **2011**, *52*, 369–372.
168. Jiang, S.; Li, P.; Lai, C. C.; Kelley, J. A.; Roller, P. P. *J. Org. Chem.* **2006**, *71*, 7307–7314.
169. Clayden, J.; Greeves, N.; Warren, S. *Organic Chemistry*, 2nd ed., Oxford University Press, 2012, p. 861-865.
170. Reetz, M. T.; Schmitz, A. *Tetrahedron Lett.* **1999**, *40*, 2741–2742.

171. Reetz, M. T.; Jaeger, R.; Drewlies, R.; Hübel, M. *Angew. Chemie Int. Ed. English* **1991**, *30*, 103–106.
172. Hughes, G.; Devine, P. N.; Naber, J. R.; O'Shea, P. D.; Foster, B. S.; McKay, D. J.; Volante, R. P. *Angew. Chem. Int. Ed.* **2007**, *46*, 1839–1842.
173. Jiang, Y.; Chen, X.; Hu, X. Y.; Shu, C.; Zhang, Y. H.; Zheng, Y. S.; Lian, C. X.; Yuan, W. C.; Zhang, X. M. *Adv. Synth. Catal.* **2013**, *355*, 1931–1936.
174. Enthaler, S. *Catal. Letters* **2011**, *141*, 55–61.
175. Cossy, J.; Mirguet, O.; Pardo, D. G.; Desmurs, J.-R. *Tetrahedron Lett.* **2001**, *42*, 7805–7807.
176. Park, Y.; Lee, Y. J.; Hong, S.; Lee, M.; Park, H. *Org. Lett.* **2012**, *14*, 852–854.
177. Das, S.; Addis, D.; Zhou, S.; Junge, K.; Beller, M. *J. Am. Chem. Soc.* **2010**, *132*, 1770–1771.
178. Kuehne, M. E.; Cowen, S. D.; Xu, F.; Borman, L. S. *J. Org. Chem.* **2001**, *66*, 5303–5316.
179. Sundberg, R. J.; Powers Walters, C.; Bloom, J. D. *J. Org. Chem.* **1981**, *46*, 3730–3732.
180. Maligres, P. E.; Chartrain, M. M.; Upadhyay, V.; Cohen, D.; Reamer, R. A.; Askin, D.; Volante, R. P.; Reider, P. J. *J. Org. Chem.* **1998**, *63*, 9548–9551.
181. Liu, Z.; Mehta, S. J.; Lee, K.-S.; Grossman, B.; Qu, H.; Gu, X.; Nichol, G. S.; Hrubby, V. J. *J. Org. Chem.* **2012**, *77*, 1289–1300.
182. Mirguet, O.; Gosmini, R.; Toum, J.; Clément, C. A.; Barnathan, M.; Brusq, J.-M.; Mordaunt, J. E.; Grimes, R. M.; Crowe, M.; Pineau, O.; Ajakane, M.; Daugan, A.; Jeffrey, P.; Cutler, L.; Haynes, A. C.; Smithers, N. N.; Chung, C.; Bamborough, P.; Uings, I. J.; Lewis, A.; Witherington, J.; Parr, N.; Prinjha, R. K.; Nicodème, E. *J. Med. Chem.* **2013**, *56*, 7501–7515.
183. Tanimori, S.; Fukubayashi, K.; Kiriata, M. *Tetrahedron Lett.* **2001**, *42*, 4013–4016.
184. Honda, T.; Takahashi, R.; Namiki, H. *J. Org. Chem.* **2005**, *70*, 499–504.
185. Girardin, M.; Ouellet, S. G.; Gauvreau, D.; Moore, J. C.; Hughes, G.; Devine, P. N.; O'Shea, P. D.; Campeau, L. C. *Org. Process Res. Dev.* **2013**, *17*, 61–68.
186. Chung, J. Y. L.; Marcune, B.; Strotman, H. R.; Petrova, R. I.; Moore, J. C.; Dormer, P. G. *Org. Process Res. Dev.* **2015**, *19*, 1418–1423.

187. Singh, R. K.; Jain, S.; Sinha, N.; Mehta, A.; Naqvi, F.; Anand, N. *Tetrahedron* **2006**, *62*, 4011–4017.
188. Gurjar, M. K.; Bera, S.; Joshi, R. R.; Joshi, R. A. *Heterocycles* **2003**, *60*, 2293–2303.
189. Yamagami, C.; Sigiura, M.; Takao, N. *Chem. Pharm. Bull.* **1980**, *28*, 3665–3669.
190. Kansy, M.; Senner, F.; Gubernator, K. *J. Med. Chem.* **1998**, *41*, 1007–1010.
191. Veber, D. F.; Johnson, S. R.; Cheng, H. Y.; Smith, B. R.; Ward, K. W.; Kopple, K. D. *J. Med. Chem.* **2002**, *45*, 2615–2623.
192. Chung, C.; Coste, H.; White, J. H.; Mirguet, O.; Wilde, J.; Gosmini, R. L.; Delves, C.; Magny, S. M.; Woodward, R.; Hughes, S. A.; Boursier, E. V.; Flynn, H.; Bouillot, A. M.; Bamborough, P.; Brusq, J.-M. G.; Gellibert, F. J.; Jones, E. J.; Riou, A. M.; Homes, P.; Martin, S. L.; Uings, I. J.; Toum, J.; Clément, C. A.; Boullay, A.-B.; Grimley, R. L.; Blandel, F. M.; Prinjha, R. K.; Lee, K.; Kirilovsky, J.; Nicodeme, E. *J. Med. Chem.* **2011**, *54*, 3827–3838.
193. Robinson, M. W.; Hill, A. P.; Readshaw, S. A.; Hollerton, J. C.; Upton, R. J.; Lynn, S. M.; Besley, S. C.; Boughtflower, B. J. *Anal. Chem.* **2017**, *89*, 1772–1777.
194. Valkó, K.; Bevan, C.; Reynolds, D. *Anal. Chem.* **1997**, *69*, 2022–2029.
195. Bhattachar, S. N.; Wesley, J. A.; Seadeek, C. *J. Pharm. Biomed. Anal.* **2006**, *41*, 152–157.